https://doi.org/10.25923/6x63-2422

A Retrospective Assessment and Characterization of Per- and Polyfluoroalkyl Substances (PFASs) in the Great Lakes.

Authors

Michael A. Edwards

Andrea Pugh

Erik D. Davenport

W. Edward Johnson

November 2024

NOAA TECHNICAL MEMORANDUM NOS NCCOS 345

NOAA NCCOS Monitoring and Assessment Branch

Citation
Edwards, M. A., Pugh, A., Davenport, E, D., and Johnson W. E. 2024. A Retrospective Assessment and Characterization of Per- and Polyfluoroalkyl Substances (PFASs) in the Great Lakes. NOAA Technical Memorandum NOS NCCOS 345. Silver Spring, MD. 182 pp. https://doi.org/10.25923/6x63-2422.

Acknowledgements

The production of this report would not have been possible without the cooperative effort, input and participation of many. The Great Lakes Mussel Watch Program wishes to acknowledge and express sincere thanks to our NOAA GLERL partners and other Great Lakes state and federal collaborators for their assistance with fieldwork and sample collection, which resulted in the data provided in this report. We would also like to thank the laboratory researchers and partners at the TDI-Brooks International (College Station, TX), and the NOAA/ National Centers for Coastal Ocean Science (NCCOS) Ecotoxicology Branch/Hollings Marine Laboratory (Charleston, SC), for their contributions to this project. Equally important, we would like to express our sincere thanks to the Great Lakes Restoration Initiative (GLRI) and NOAA/NCCOS for supporting and providing funding for research and data included in this report. Finally, we would like to thank all the reviewers who devoted their time and effort with the review of this report. Your collective insight and input has resulted in a document which is far superior to that which we originally envisioned.

Cover photo credits: NOAA, Great Lakes MWP
Back cover photo credit: NOAA ,Great Lakes MWP

Disclaimer
This report has been reviewed and approved for publication according to the NOAA's Scientific Integrity Policy and Fundamental Research Communications (FRC) framework, and the National Ocean Service (NOS) process for FRC review. The opinions, findings, conclusions, and recommendations expressed in this report are those of the authors, and they do not necessarily reflect those of NOAA. Any use of trade, firm, or product names is for descriptive purposes only and does not imply endorsement by the U.S. Government.

Mention of trade names or commercial products does not constitute endorsement or recommendation for their use by the United States government.

A Retrospective Assessment and Characterization of Per- and Polyfluoroalkyl Substances (PFASs) in the Great Lakes.

November 2024

Authors:

Michael A. Edwards[1,], Andrea Pugh[1,], Erik D. Davenport[1], and W. Edward Johnson[1]

[1] NOAA National Ocean Service, National Centers for Coastal Ocean Science, Stressor Detection and Impacts Division, Silver Spring, MD

NOAA Technical Memorandum NOS NCCOS 345

United States Department of Commerce	National Oceanic and Atmospheric Administration	National Ocean Service
Gina M. Raimondo Secretary	Richard W. Spinrad Under Secretary	Nicole LeBoeuf Assistant Administrator

EXECUTIVE SUMMARY

This report provides a retrospective assessment of per- and polyfluoroalkyl substances (PFAS) in the Laurentian Great Lakes, based on samples collected from 2013 to 2018. PFAS are a group of synthetic, fluorine-containing compounds—over 12,000 variations of which are used in consumer and industrial applications including surface coatings, fire-fighting foams, insecticides, and polymer manufacturing. These compounds are highly persistent, resistant to biodegradation, and can bioaccumulate in ecosystems, posing risks to both wildlife and humans. The Binational Lakewide Action and Management Plans (LAMPs), established under the Great Lakes Water Quality Agreement (GLWQA), recognize a significant data gap in the environmental occurrence and concentration of PFAS compounds in the Great Lakes Basin to make sound decisions. While some studies have documented PFAS in lower-trophic-level organisms like dreissenid mussels, overall data remains limited. The NOAA-NCCOS Mussel Watch Program (MWP) provides the largest contaminant database from bivalves in the Great Lakes, offering a valuable resource for understanding PFAS distribution. This study leverages monitoring data collected from 2013 to 2018 to assess the magnitude, environmental occurrence, and spatial distribution of PFAS across the Great Lakes Basin. The findings aim to inform future management and policy decisions, support the International Joint Commission's (IJC's) efforts to address harmful substances affecting water quality and human health, and guide future binational actions between the U.S. and Canada.

The findings of this study revealed, PFAS compounds measured in mussel tissue basin-wide were mainly detected as complex mixtures, with 2 to 8 compounds detected above method detection limit (> MDLs) in mussels at one or more sampling location during the 2013 and 2018 sampling event. Compositionally, perfluoroalkyl carboxylic acid (PFCA: $C_nF_{2n+1}COOH$) and perfluoroalkane sulfonic acid (PFSA: $C_nF_{2n+1}SO_3H$) compound groups accounted for 42.1% and 36.8% of the total PFAS measured (> MDLs) in mussel tissue samples. The highest PFAS levels were consistently detected in mussels from river, tributary, and harbor sites, relative to offshore (nearshore and open-lake zones) sampling locations. Similar to previous studies, this basin-wide results showed patterns in elevated mussel PFAS contaminant levels closely matched sites sampled adjacent to developed/urban land-use gradients and riverine systems, with larger population densities and industrial centers in Lakes Michigan, Erie, Ontario, and the Detroit and Niagara River connecting channels, compared to other sites sampled basin-wide. PFAS composition was highest in mussels from non-wastewater treatment plant (non-WWTP) sampling locations, relative to other discharge-types assessed in this study, thus confirming the importance of non-point/diffuse emission sources as significant environmental pathways for PFAS compounds detected within the Great Lakes Basin. Between-lakes and connecting channels comparison revealed summed ∑PFAS concentrations varied by several orders of magnitude between mussel sampling locations, with elevated PFAS concentrations primarily detected in mussels from sites sampled in Lake Michigan, compared to mussels sampled from other Great Lakes and connecting channels assessed in this study. Equally noteworthy, significant correlations were observed between several long and short-chained PFAS compounds and mussel sampling locations dominant land-use categories, site population estimates, point source, and wastewater parameters.

Taken together, the findings from our PFAS ecological risk assessment suggest, for ∑PFAS compounds assessed in this study with tissue threshold exceedances above hazard quotient (HQ); HQ > 0.1 and HQ > 1, these compounds might pose moderate to high risk, and the possibility of sub-lethal and adverse biological effects to Great Lakes aquatic biota. Of equal importance, despite some ∑PFAS compounds quantified in mussels at environmentally low concentrations, with these contaminants currently detected as complex mixtures in mussels across Great Lakes sampling locations, the cumulative risk of long-term PFAS exposure to both lower and upper trophic-level organisms cannot be ignored. Hence, from a management perspective, with bivalves being shown to act as transfer vectors of various contaminants including PFAS to higher trophic-level organisms (i.e., fish) across the Great Lakes Basin food-web, the toxicological effects and endpoints on reproduction, development, growth, and survival resulting from PFASs long-term low-level exposures (i.e., chronic exposure at individual, population, and community levels), may warrant additional consideration including continued monitoring and assessment of these contaminants. The findings of this study will help in identifying and contextualizing the relationship between detected PFAS compounds and their environmental pathways, discharge-types, land-use gradients, as well as their likely "sinks" and "hot spots" in the Great Lakes Basin. These efforts will further aid in prioritizing PFAS compounds to be monitored, thus making the most efficient use of resources and funds, while identifying the Best Management Action and Practices (BMAPs) that can be used to support measures in reducing and abating the continued occurrence of legacy, as well as emerging chemicals of mutual concern (CMCs) in the Great Lakes Basin.

KEY FINDINGS

- Twenty eight PFAS were targeted in this study and $\sum_{19}$PFAS were quantified at least once in dreissenid mussel above method detection limit (> MDLs), with a $\sum$PFAS concentration ranging from 0.064 to 4.73 ng/g (wet weight).
- PFAS compounds were detected (> MDLs) in dreissenid mussels at 106 Great Lakes sites (out of 120), mainly as complex mixtures, with 2 to 8 compounds detected at one or more mussel sampling location.
- Elevated $\sum$PFAS concentration levels (> MDLs) measured in dreissenid mussels were typically associated with PFBA, PFPeA, PFDS, PFDoA, PFTreA, PFOSA, and PFOS compounds.
- Elevated mussel PFAS contaminant levels closely matched sites adjacent to urban rivers and tributaries, with larger population densities and industrial centers in Lakes Michigan, Erie, Ontario, and the Detroit and Niagara River connecting channels.
- Compositionally, PFCA ($C_nF_{2n+1}COOH$) and PFSA ($C_nF_{2n+1}SO_3H$) compound groups accounted for 42.1% and 36.8% of the total PFAS measured (> MDLs) in mussel tissue samples.
- Basin-wide, the highest mean $\sum_{19}$PFAS concentrations were measured in mussels from sites sampled in Lake Michigan, followed by sites sampled in Niagara River, Lake Erie, Lake Ontario, and Detroit River.
- Long-chained PFAS compounds were more persistent and more widely detected across mussel sampling locations major discharge-types, and predominant land-use types.
- Short-chained ($C_4 \geq n \leq C_7$) $\sum$PFAS concentrations measured in mussels across basin-wide sampling locations were < 3 times lower, when compared to long-chained ($n \geq C_7$–C_{14}) $\sum$PFAS compounds concentration.
- Several short-chained compounds including PFBS, PFBA, PFPeS, PFPeA, PFHxS, PFHpS, and PFHpA were readily detected in mussel tissue, thus highlighting the bioaccumulation potential of some short-chained PFAS compounds in Great Lakes aquatic biota.
- PFAS concentrations measured across mussel reference sites decreased in order of: Lake Michigan > Niagara River > Lake Erie > Lake Huron.
- A river to offshore gradient was observed for several long -and- short-chained PFAS compounds (PFHxS, PFBS, PFOA, PFHpA, PFNS, PFPeA, PFPeS, PFOSA, PFDoA, PFBA, PFOS) measured in mussels across inshore river and offshore/open-lake sampling locations.
- Significant relationship was found between several PFAS group concentrations, and mussel sampling locations dominant land-use categories, site population estimates, point source, and wastewater parameters.
- Overall $\sum_{19}$PFAS composition was highest in mussels from non-WWTP sampling locations, compared to other site discharge-types including sites sampled downstream and along wastewater discharge zones, sites sampled proximate to wastewater treatment plants/combined sewer overflows (WWTPs/CSOs), and wastewater treatment plants (WTTPs) assessed in this study.
- An environmental gradient was observed for several PFAS compounds including PFTreA, PFDoA, PFNS, PFPeA, PFOA, and PFHxS examined across mussel sites sampled proximate to WWTPs/CSOs and sites sampled downstream and along wastewater discharge zones.
- To the best of our knowledge, this study is the first to report the detection of novel PFAS alternatives N-MeFOSAA (C_{11}), 8:2 FTS (C_{10}), and 11Cl-PF3OUdS (C_{10}) PFAS compounds in Great Lakes dreissenid mussels.
- The results of this study serves as an early warning of emerging replacement short-chained PFAS compounds and precursor's that are currently detected in Great Lakes lower trophic-level organisms (i.e., dreissenid mussels), and which PFAS compounds may require further consideration and investigation.

Table of Contents

COMMONLY USED ACRONYMS

ADONA	4,8-dioxa-3H-perfluorononanoic acid
AOC	Area of Concern
CASRN	Chemical Abstracts Service Registry Number
CECs	Chemicals of Emerging Concern
CMCs	Chemicals of Mutual Concern
CSOs	Combined Sewer Overflows
FTS	Fluorotelomer sulfonic acid
GLRI	Great Lakes Restoration Initiative
HFPO-DA	Hexafluoropropylene oxide dimer acid (Gen-X)
HQs	Hazard quotients
Log Kow	octanol–water partition coefficient
LC-PFASs	Long-chained Per-/polyfluoroalkyl substances
MWP	Mussel Watch Program
MDL	Method Detection Limit
NCCOS	National Centers for Coastal Ocean Science
NOAA	National Oceanic and Atmospheric Administration
NS&T	National Status & Trends
N-EtFOSAA	N-Ethyl perfluorooctane sulfonamido acetic acid
N-MeFOSAA	N-Methyl perfluorooctane sulfonamido acetic acid
PFAS	Per-/polyfluoroalkyl substances
PFBA	Perfluoro-n-butanoic acid
PFBS	Perfluoro-1-butanesulfonate
PFCA	Perfluoroalkyl carboxylic acid
PFDA	Perfluoro-n-decanoic acid
PFDoA	Perfluoro-n-dodecanoic acid
PFDS	Perfluoro-1-decanesulfonic acid
PFHpA	Perfluoro-n-heptanoic acid
PFHpS	Perfluoro-1-heptanesulfonic acid
PFHxA	Perfluoro-n-hexanoic acid
PFHxS	Perfluoro-1-hexanesulfonic acid
PFNA	Perfluoro-n-nonanoic acid
PFNS	Perfluoro-1-nonanesulfonic acid
PFOA	Perfluoro-n-octanoic acid
PFOS	Perfluoro-1-octanesulfonic acid
PFOSA	Perfluorooctane sulfonamide
PFPeA	Perfluoro-n-pentanoic acid
PFPeS	Perfluoro-1-pentanesulfonic acid
PFSA	Perfluoroalkane sulfonic acid
PFTreA	Perfluoro-n-tetradecanoic acid
PFTriA	Perfluoro-n-tridecanoic acid
PFUnA	Perfluoro-n-undecanoic acid
PNEC	predicted no-effect concentration value
SC-PFASs	Short-chained Per-/polyfluoroalkyl substances
vPvB	very persistent and very bio-accumulative
ww	wet weight
WWTPs	Wastewater Treatment Plants
9Cl-PF3ONS	9-chlorohexadecafluoro-3-oxanone-1-sulfonic acid
11Cl-PF3OUdS	11-chloroeicosafluoro-3-oxaundecane-1-sulfonic acid
4:2 FTS	1H,1H,2H,2H-perfluoro-1-hexanesulfonic acid (4:2 fluorotelomer sulfonic acid)
6:2 FTS	1H,1H,2H,2H-perfluoro-1-octanesulfonic acid (6:2 fluorotelomer sulfonic acid)
8:2 FTS	1H,1H,2H,2H-perfluoro-1-decanesulfonic acid (8:2 fluorotelomer sulfonic acid)

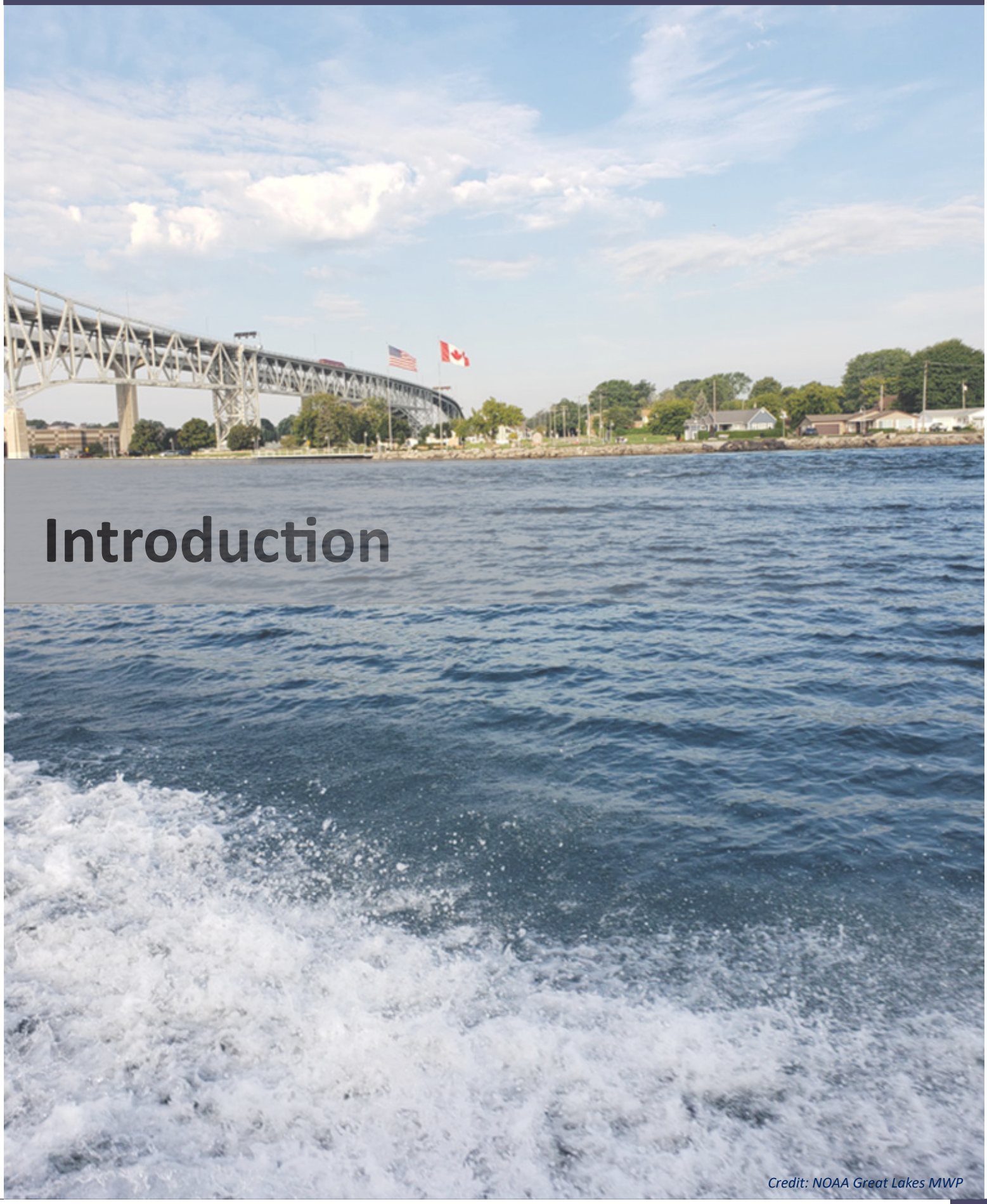

Introduction

Credit: NOAA Great Lakes MWP

Introduction

1.0. INTRODUCTION

Per- and polyfluoroalkyl substances (PFASs) are a group of over 12,000 short -and- long-chained synthetic fluorine-containing compounds (Salvatore et al., 2022), which are produced and used in consumer and industrial applications related to surface protection/coatings, fire-fighting aqueous film-forming foams (AFFF), insecticides, and commercial polymer manufacturing (Sinclair et al., 2020). As shown in numerous studies, PFAS compounds are remarkably persistent (Sinclair et al., 2020), and resist biodegradation due to their physicochemical properties and stable structures, thus allowing their persistence in aquatic environment for extended periods, usually from days (e.g., PFBS: half-life [$t_{1/2}$] water = 39 days; United States Environmental Protection Agency's Estimation Program Interface [EPI Suite ™ v4.1] software), to years (e.g., PFOA: half-life [$t_{1/2}$] water = 40 years, and PFOS: half-life [$t_{1/2}$] water = 90 years; Savoca and Pace, 2021; Sinclair et al., 2020). Hence, PFASs are ubiquitous environmental contaminants with the potential to bioaccumulate in lower-trophic level organisms and humans across the food web. PFAS compounds typically enter aquatic environments from mixed sources such as fire training/fire response sites, industrial/urban sites, wastewater treatment systems, leaching from landfills, and agricultural runoff from land applied contaminated biosolids (Pepper, et al., 2023). Due to their widespread use and high environmental stability and resistance to degradation, these particular chemicals of mutual concern (CMCs) are becoming ubiquitous in sediment and tissue samples (Remucal, 2019; Swam et al., 2023).

Although thousands of PFAS compounds (over 12,000 variations; Pizzorno, 2024; Spyrakis and Dragani, 2023) are released in both aquatic and terrestrial matrices, there is little or no information available on the environmental and toxicological impacts for most of these compounds. Currently, only a few are becoming more routinely monitored in aquatic environments (Swam et al., 2023). Among the thousands of known PFAS compounds, the long-chained perfluoro-n-octanoic acid (PFOA) and perfluoro-1-octanesulfonic acid (PFOS) compounds are among the most documented and studied (Cordner et al., 2019). Mounting evidence have revealed these compounds are linked to various deleterious and toxicological endpoints such as liver damage, cancer, developmental toxicity, immune system suppression, tumor induction, endocrine disruption, and obesity as reported in human models (Di Nisio et al., 2018; Fenton et al., 2020; Mokra, 2021). In addition, previous studies have also revealed exposure to these PFAS compounds could cause adverse health effects including lower semen quality in young males, elevated infertility and reduced birth weight, the onset of early menopause in women, and delayed puberty in children (Grun and Blumberg, 2009; Joensen et al., 2009; Knox et al., 2011; Li et al., 2020). Hence, these PFAS compounds have garnered interest in the past 10-15 years.

While the manufacturing of various long-chained PFAS compounds including PFOS and PFOA has been phased out in the United States and replaced with newer short-chained compounds beginning in 2006 (Cordner et al., 2019 ; Westreich et al., 2018), the United States Environmental Protection Agency (USEPA) and several states have started issuing health advisory, as well as the development of drinking water guidelines and regulatory limits for several PFAS compounds (Cordner et al., 2019; USEPA, 2020), including PFOS (estimated serum half-life [$t_{1/2}$]: 7.8 - 8.5 years; Nilsson et at., 2022; Olsen et al., 2007), and PFOA (estimated serum half-life [$t_{1/2}$]: 3.5 - 5 years; Nilsson et at., 2022; Olsen et al., 2007). In addition, among the PFAS compounds for which the USEPA have established legally enforceable levels (MCLs) in drinking water (e.g., PFOA, PFOS, PFHxS, PFNA, and HFPO-DA; Rosenblum et al., 2024), guidelines have also been developed and established for PFAS mixtures containing two or more compounds including PFHxS (estimated serum half-life [$t_{1/2}$]: 15.5 years; Worley et al., 2017), PFNA (estimated serum half-life [$t_{1/2}$]: 3.5 years; Yu et at., 2021), HFPO-DA, and PFBS (estimated serum half-life [$t_{1/2}$]: 25.8 years; Olsen et al., 2009).

Within the Laurentian Great Lakes, PFASs are listed as CMCs under the 2012 Annex 3 Great Lakes Water Quality Agreement (GLWQA; Barbiero et al., 2018; Jetoo and Krantzberg, 2014; VanNijnatten and Johns, 2020). These contaminants are also subjected to binational monitoring and prevention efforts within the Great Lakes basin. Despite this, limited baseline data exists on the environmental distribution and concentration of PFAS in lower trophic-level organisms in the Great Lakes, compared to other CMC groups (e.g., mercury, flame retardants like hexabromocyclododecane [HBCDs] and polybrominated diphenyl ethers [PBDEs], polychlorinated biphenyls [PCBs], and short-chained chlorinated paraffins [SCCPs]; Jetoo and Krantzberg, 2014). Currently, PFASs and other chemicals of emerging and mutual concern are outpacing agencies' resources to monitor and assess these contaminants in upper trophic-level organisms and surface water across the Laurentian Great Lakes (Ankley et al., 2020; Cordner et al., 2021; Klečka et al., 2010; Kwiatkowski et al., 2020; Wattigney et al., 2019). While there is a relative abundance of PFAS information on upper trophic-level organisms (e.g., fish), data and information on the environmental occurrence, magnitude, and spatial distribution of PFAS compounds in Great Lakes lower trophic-level aquatic organisms and food-web remain limited.

Introduction

As part of the NOAA/NCCOS National Mussel Watch Program (MWP), a suite of nearly 150 chemical contaminants are measured on an annual basis since 1986 (Kimbrough et al., 2013). The monitoring of these contaminants involves sampling filter-feeding bivalve species for contaminant loads. The NOAA/NCCOS MWP have used this successful model organism to monitor and assess the status and trends of chemical contaminants in tissue across the U.S. coastal waters, including Alaska, Hawaii, Puerto Rico, and the Great Lakes. Since 1992, the NOAA/NCCOS MWP has used dreissenid mussels (zebra/quagga; *Dreissena spp*.) to monitor the environmental occurrence and magnitude of a wide suite of organic pollutants in the Laurentian Great Lakes, establishing one of the most spatially robust biomonitoring data sets in the region (Edwards et al., 2016; Edwards et al., 2024; Kimbrough et al., 2018). Dreissenid mussels are extensively used as bioindicator organisms due to their sessile and sedentary nature, high population density (≥700,000 specimens/m^2; Carvalho et al., 2021), and their quick response to contamination changes in aquatic systems. Other attributes which enable dreissenid mussels as excellent bioindicators, include their ability to sequester and bioaccumulate contaminants from water and suspended sediments, thus reflecting ambient contamination levels in surrounding aquatic systems (Edwards et al., 2024; Kimbrough et al., 2014).

This report serves to collate PFAS tissue concentrations from various Great Lakes studies and monitoring objectives between 2013 and 2018. This dataset focuses on data collected from a variety of projects including dreissenid mussel surveillance and temporal sampling, basin-wide retrospective analyses, priority contaminant mixtures (PCM) studies, place-based contaminant assessment, and integrated assessment case studies (IACS). Specific objectives of this report include; 1) assess and characterize the environmental occurrence, magnitude, and spatial distribution of PFAS compounds detected in dreissenid mussels at basin-wide Great Lakes inshore (tributaries rivers, and harbors), nearshore, and offshore (open-lake) sampling locations; (2) identify and assess potential drivers, and environmental pathways behind the distribution of PFAS compounds detected in dreissenid mussels; (3) explore the relationship between various land-use gradients, and PFAS compounds detected in dreissenid mussels; and (4) assess sites proximal location to point -and- non-point/diffuse source discharge-types effect on PFAS concentration and composition profile.

The results summarized in this report, are intended to inform NOAA/NCCOS MWP management, Great Lakes resource managers, stakeholders, water/watershed managers, and the larger Great Lakes community on the magnitude and environmental occurrence of PFAS compounds detected in dreissenid mussels within the Great Lakes Basin. The results from this study was also designed to augment and provide much-needed tissue data on the magnitude and environmental occurrence of PFAS compounds in the Great Lakes, in addition to comparing PFAS tissue body burden levels across Great Lakes states and federal monitoring programs. Specifically, groups and programs such as the Great Lakes Regional Pollution Working Group and Lake-wide Action Monitoring Programs (LAMPs) for Great Lakes ecosystem restoration can use this information in regional assessment and restoration efforts. This information is important in developing integrated approaches for PFAS source identification, development of mitigation strategies, ecological risk assessment, and suitable mechanisms including Best Management Action and Practices (BMAPs) for identifying and prioritizing PFAS compounds of interest, and their likely “hotspots” within the Great Lakes Basin.

Credit: NOAA Great Lakes MWP

Methods

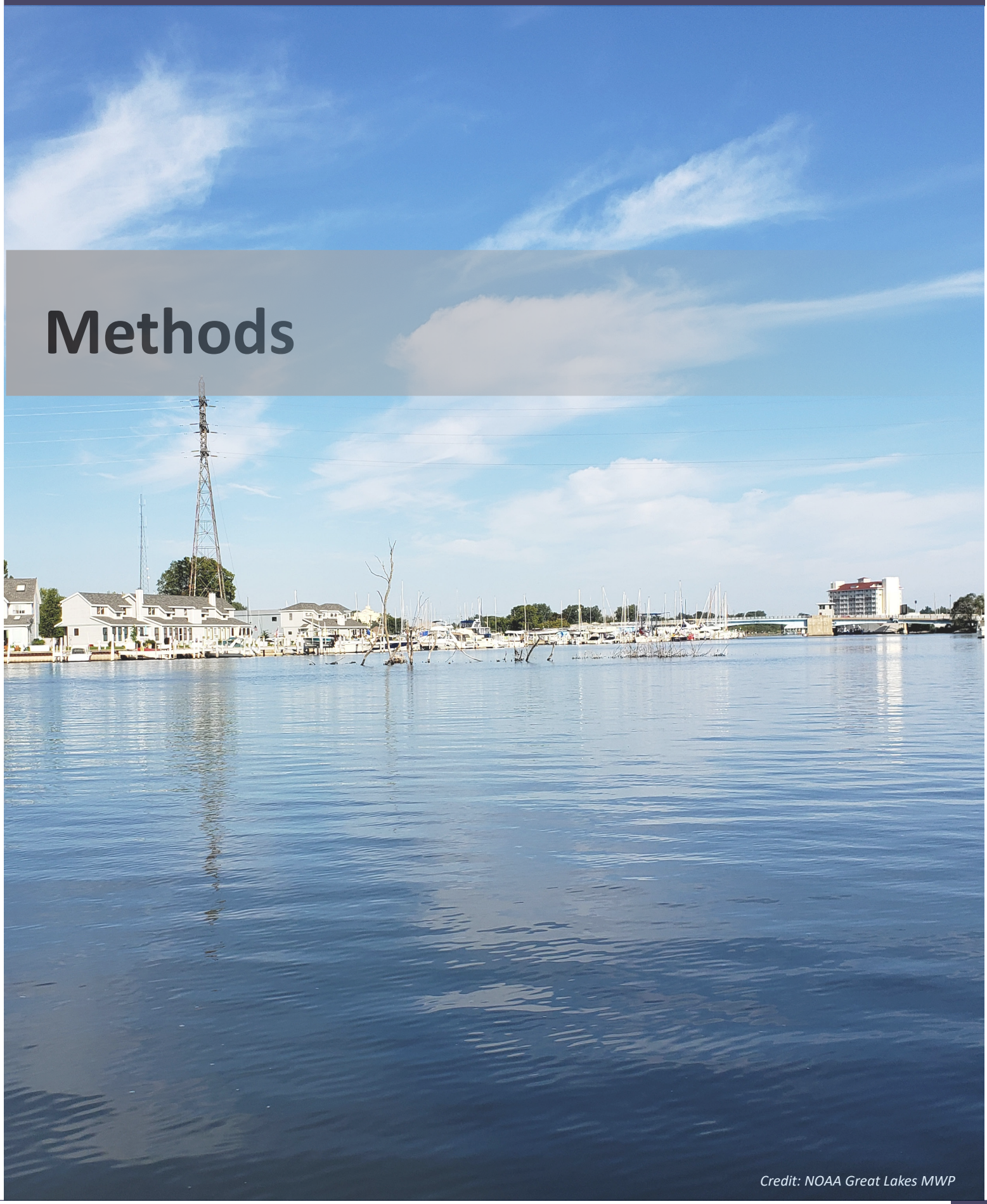

Credit: NOAA Great Lakes MWP

2.0. METHODS

2.1 Study Region

The Laurentian Great Lakes constitutes the largest freshwater system in the world, containing an estimated 21% of the Earth's surface freshwater (~ 90% of United States freshwater; Fields, 2005; Sponberg, 2009). With an estimated gross domestic product (GDP) of approximately $5.8 trillion (Hartig et al., 2020), the Great Lakes Basin covers a total area of 244,000 km² (94,000 mi²), and is home to over 35 million people (Breffle et al., 2013; Danz et al., 2007). The region watersheds which drain almost 518,000 km² (200,000 mi²), support numerous economic industries, including manufacturing, agriculture, and commercial fisheries, with areas of intense urbanization and industrialization occurring along its coastal zone (Wolter et al., 2006). Across the Great Lakes Basin, land-use and land cover differs between eco-regions and eco-provinces, with predominantly forested areas in the northern and southeastern sections, and agricultural activities more pronounced in the western and central sections of the Basin (Morrice et al., 2008). Over the years, increased anthropogenic and environmental stressors including rapid urban growth, and municipal and industrial wastewater discharge, have led to loss of fish and wildlife habitat, increased water quality and beneficial use impairments (BUIs) within the Great Lakes Basin, and adjacent sub-watersheds (Elliot et al., 2017; Kiesling et al., 2022). Specifically, the continuous loading of organic pollutants from point and diffuse/fugitive sources are identified as important environmental drivers behind coastal water quality and ecosystem impairment within the Laurentian Great Lakes (Baldwin et al., 2016; Kiesling et al., 2019).

2.2 Site Designation and Categorization

A total of 120 sites, representing inshore (tributary, rivers, harbors), nearshore, and offshore lake sites were sampled between 2013 and 2018 (Fig. 1). A detailed description of the Great Lakes MWP PFAS sampling locations including designated reference sites is provided in Table A1, and described elsewhere (Edwards et al., 2016; Edwards et al., 2024; Kimbrough et al., 2018). Collectively, between the 2013-2018 study period, 13 sites were sampled in 2013, 29 sites were sampled in 2014, 15 sites were sampled in 2015, 11 sites were sampled in 2016, 18 sites were sampled in 2017, and 34 sites were sampled in 2018. Additional information on Great Lakes mussel PFAS sites location and adjacent sub-watersheds (Hydrologic Unit Code 10, HUC-10) are provided in Figures 2 A-Y. PFAS data derived from dreissenid mussel tissue were generated from multiple contamination assessment studies conducted under the Great Lakes Restoration Initiative (GLRI) Action Plan I (2010-2014), and GLRI Action Plan II (2015-2019), and the Great Lakes MWP basin-wide assessment and contaminant monitoring studies (Edwards et al., 2024; Kimbrough et al., 2018). To increase the likelihood of finding various contaminants including PFAS compounds, mussel sampling locations were preferentially selected based on: 1) riverine systems and tributaries known for high contamination, and 2) pollution gradients influenced by urban and sub-urban centers that receive high volume of pollutants from point-source discharge including CSOs and urban storm-water runoff.

Sampling locations previously established by the MWP in Great Lakes Areas of Concern (AOC; areas designated for restoration due in part to historical environmental contamination; Hartig et al., 2020) and other priority urban areas, including Milwaukee, Niagara, Toledo, Cleveland and Detroit, were also targeted during placed-based and basin-wide surveillance monitoring, with the objective of providing a more robust measure of bioavailable contaminants including PFAS compounds that would be generated from municipal, industrial and fugitive/non-point sources. Tissue samples from basin-wide surveillance and place-based/caged mussel contamination assessments including contaminant source tracking at inshore riverine and nearshore sampling locations (e.g., shoreline-related region reaching a 30-m depth contour or a distance of 5-km from shore, Yurista et al., 2016), were also used to generate bioavailable contaminants including PFAS compounds during the 2013-2018 sampling period. Mussels sampled at designated offshore sampling locations included all lake sites (nearshore lake and deep-water lake sites). Inshore mussel sampling locations included sites sampled at harbor, river, and tributary locations. Overall, most sampling locations have 1-3 sites, except for sampling locations in the Maumee River, Detroit River, Muskegon, Milwaukee Estuary and Niagara River (Table A1).

Methods

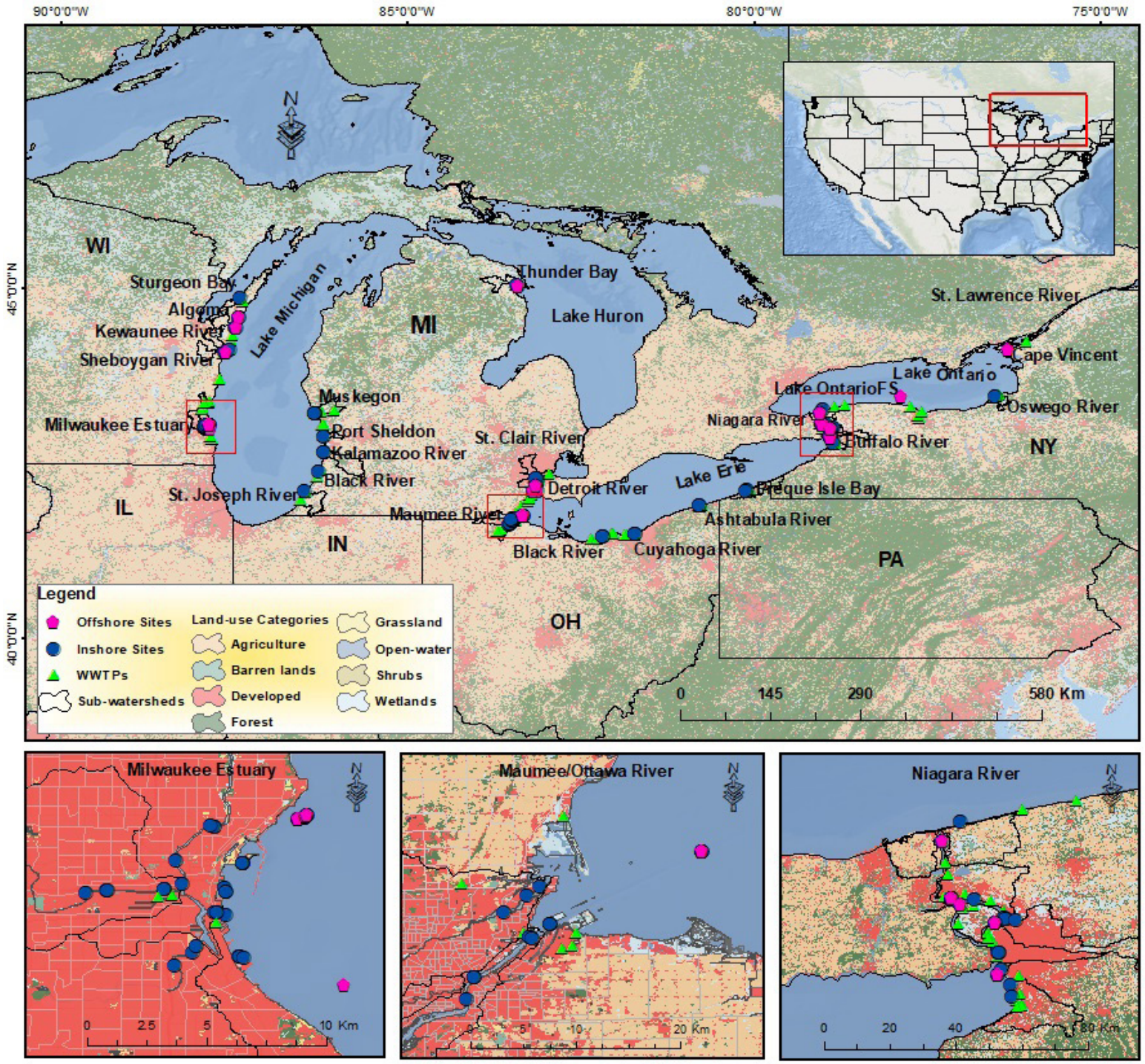

Fig. 1. Map showing the location of Great Lakes inshore (rivers, harbors, and tributaries) and offshore (nearshore lake and deep-water lake) 2013-2018 dreissenid mussel PFAS sampling locations. Most sampling locations have between 1-3 sites, except Maumee River (8 sites), Muskegon (9 temporal sites), Milwaukee Estuary (29 + sites) and Niagara River (28 sites). Where applicable, wastewater treatment plants (WWTPs) (▲) and their proximity to MWP sampling locations are identified on the map. Additional information on MWP site codes and acronyms used in this study is provided in Figures 2A-Y, Table A1 and Table A3 (Appendix).

Methods

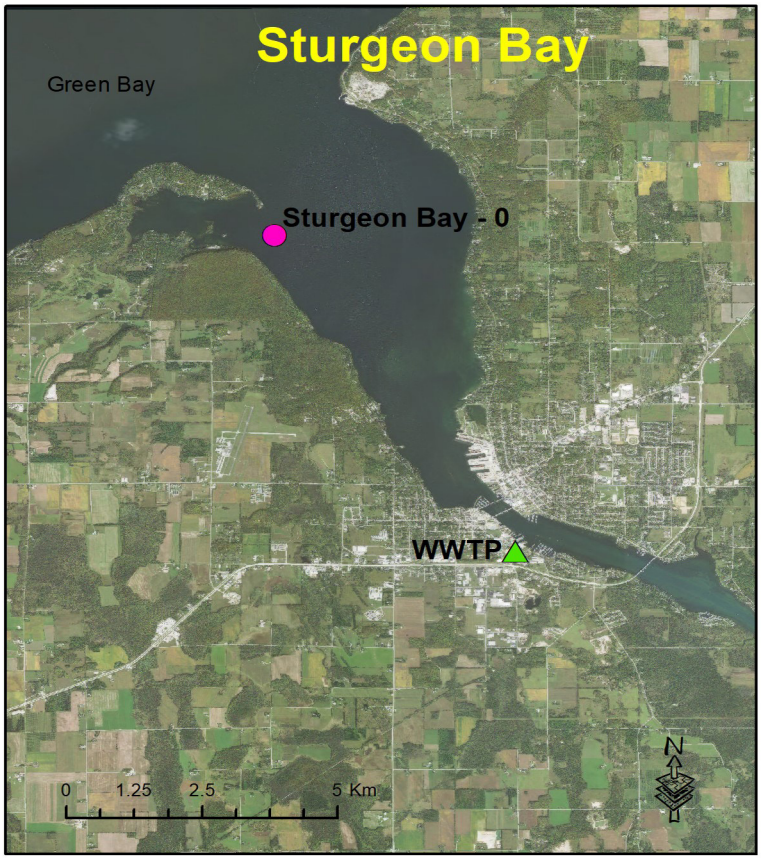

Site Name	Site Code	State	Latitude	Longitude
Sturgeon Bay-0	LMSB-0	WI	44.8798	-87.4170

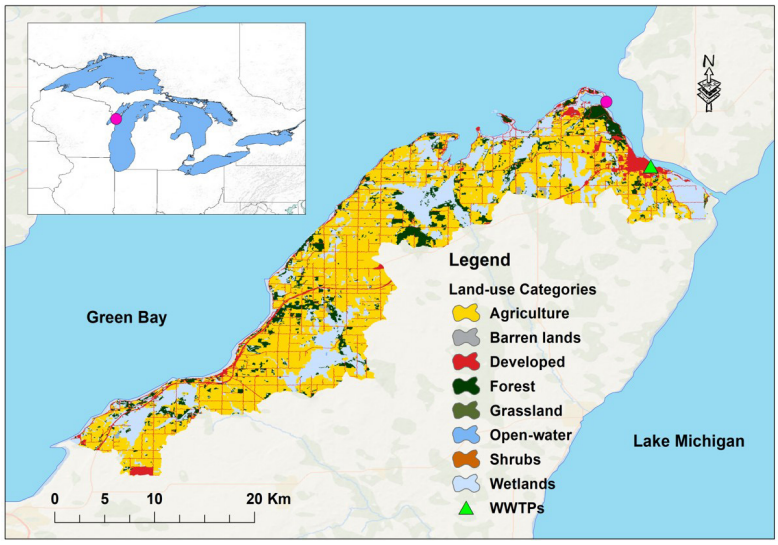

Watershed	HUC-10	SqKm
Red River-Frontal Green Bay	0403010204	375.6

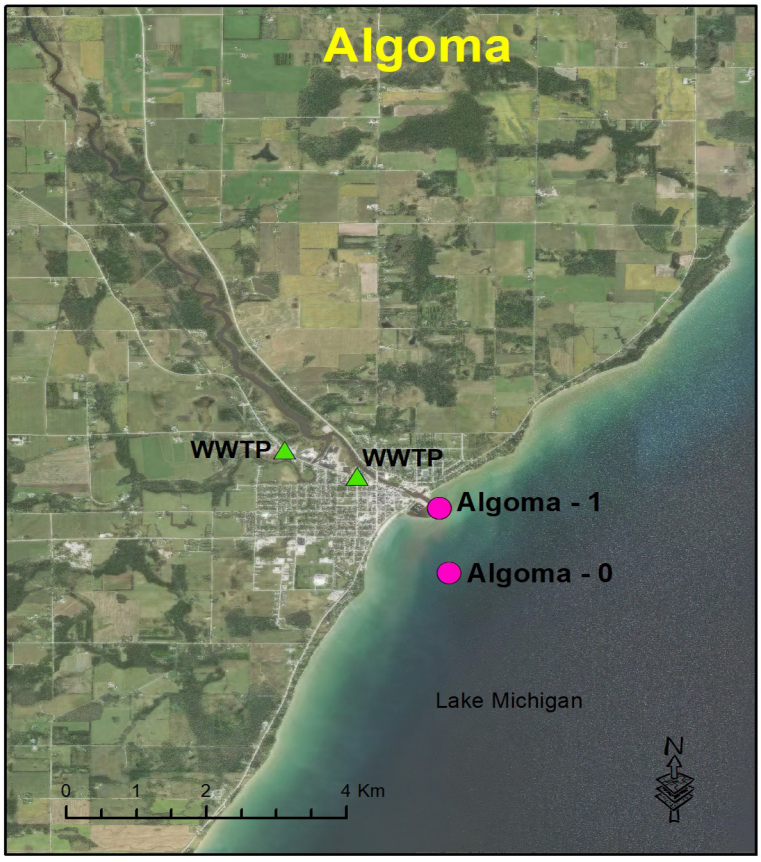

Site Name	Site Code	State	Latitude	Longitude
Algoma-0	LMAG-0	WI	44.5982	-87.4290
Algoma-1	LMAG-1	WI	44.6072	-87.4310

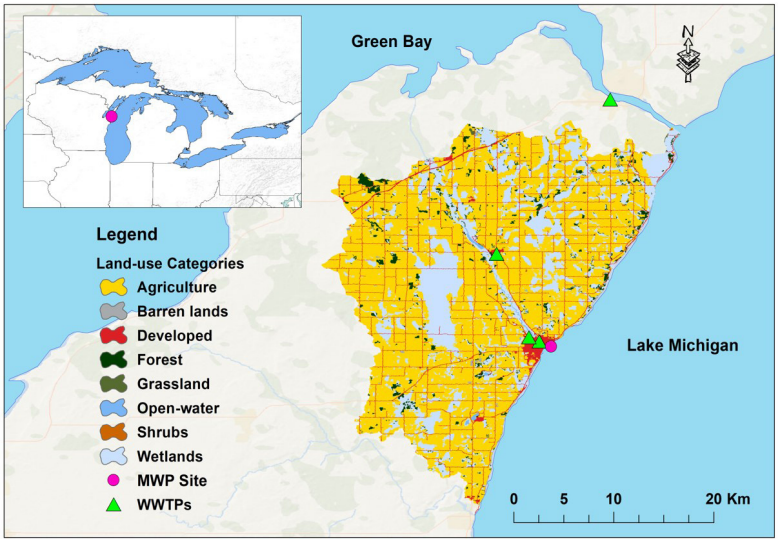

Watershed	HUC-10	SqKm
Ahnapee River-Frontal Lake Michigan	0403010202	498.5

Fig. 2A-B. Great Lakes Mussel Watch PFAS study site locations (●), and adjacent sub-watersheds (HUC-10). Site table provides information on MWP site name, site code, and approximate nominal latitude and longitude for each site. Where applicable, wastewater treatment plants (▲) and reference sites (*) are identified on the map.

Methods

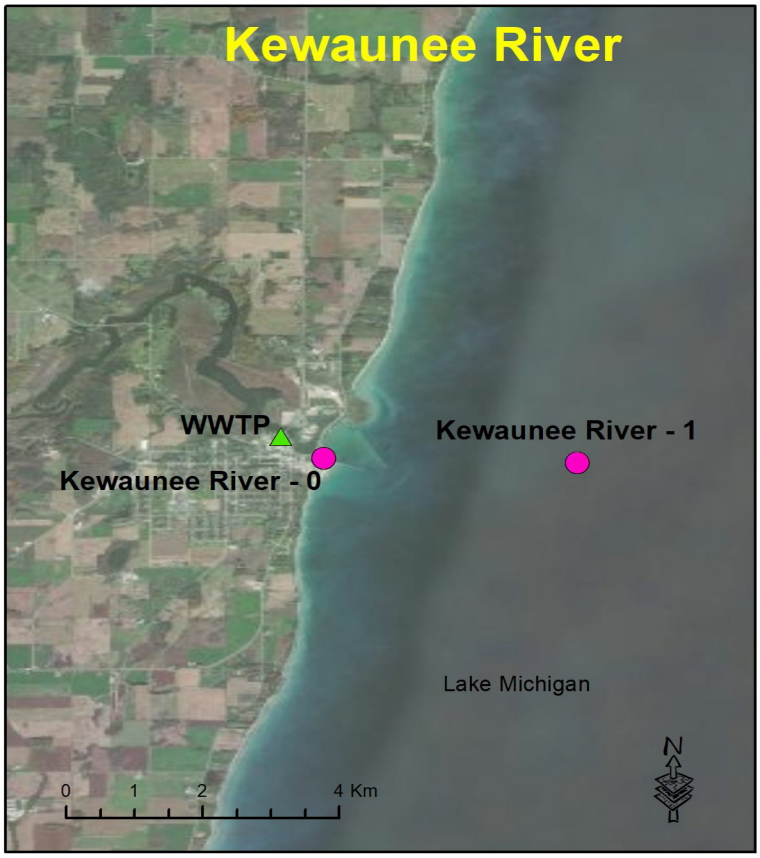

Site Name	Site Code	State	Latitude	Longitude
Kewaunee River-0	LMKW-0	WI	44.4590	-87.4990
Kewaunee River-1	LMKW-1	WI	44.4584	-87.4650

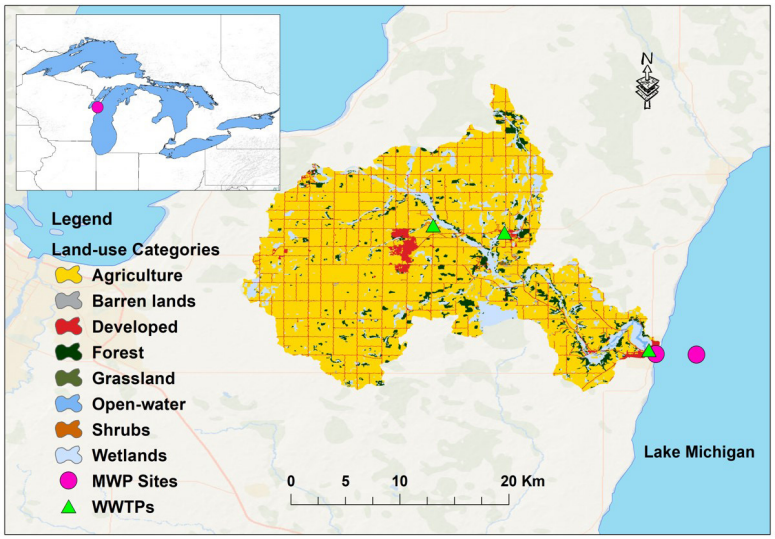

Watershed	HUC-10	SqKm
Kewaunee River	0403010203	367.2

Site Name	Site Code	State	Latitude	Longitude
Two Rivers-0	LMTR-0	WI	44.1431	-87.5620

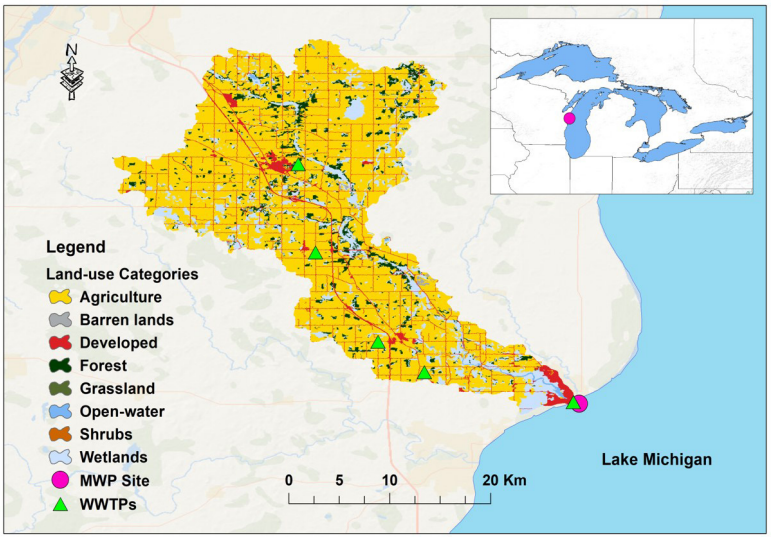

Watershed	HUC-10	SqKm
West Twin River	0403010102	453.4

Fig. 2C-D. Great Lakes Mussel Watch PFAS study site locations (●), and adjacent sub-watersheds (HUC-10). Site table provides information on MWP site name, site code, and approximate nominal latitude and longitude for each site. Where applicable, wastewater treatment plants (▲) and reference sites (*) are identified on the map.

Methods

Site Name	Site Code	State	Latitude	Longitude
Manitowoc-0	LMMW-0	WI	44.0933	-87.6450
Manitowoc-1	LMMW-1	WI	44.1037	-87.6270

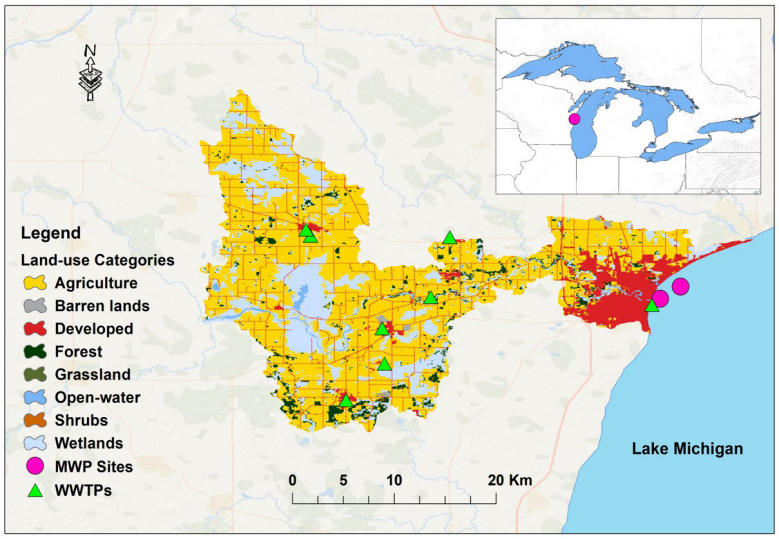

Watershed	HUC-10	SqKm
Red River-Frontal Green Bay	0403010204	375.6

Fig. 2E. Great Lakes Mussel Watch PFAS study site locations (●), and adjacent sub-watersheds (HUC-10). Site table provides information on MWP site name, site code, and approximate nominal latitude and longitude for each site. Where applicable, wastewater treatment plants (▲) and reference sites (*) are identified on the map.

Credit: NOAA Great Lakes MWP

Methods

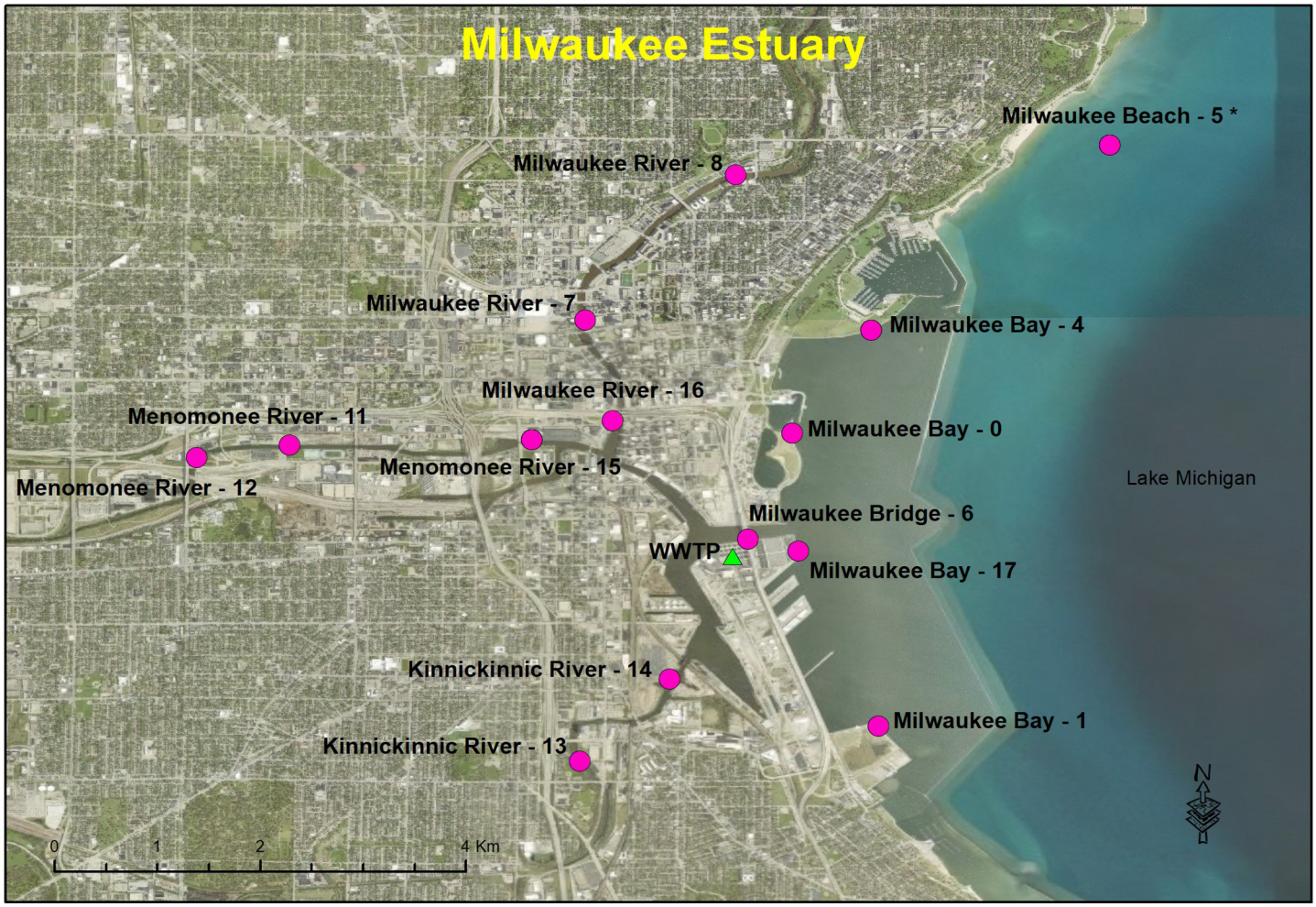

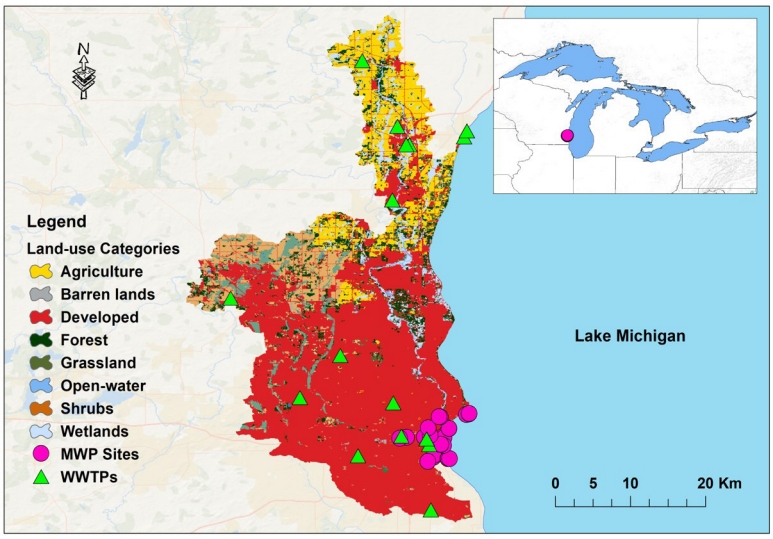

Watersheds	HUC-10	SqKm
Lower Milwaukee River-Frontal Lake Michigan	0404000306	430.4
Menomonee River	0404000304	361.4
Kinnickinnic River	0404000305	64.5

Site Name	Site Code	State	Latitude	Longitude
Milwaukee Bay-0	LMMB-0	WI	43.0325	-87.8940
Milwaukee Bay-1	LMMB-1	WI	43.0078	-87.8872
Milwaukee Bay-4	LMMB-4	WI	43.0432	-87.8878
Milwaukee Bay-17	LMMB-17	WI	43.0234	-87.8943
Milwaukee Beach-5*	LMMB-5*	WI	43.0596	-87.8670
Milwaukee Bridge-6	LMMB-6	WI	43.0245	-87.8987
Milwaukee River-7	LMMB-7	WI	43.0440	-87.9129
Milwaukee River-8	LMMB-8	WI	43.0570	-87.8998
Milwaukee River-16	LMMB-16	WI	43.0351	-87.9105
Kinnickinnic River-13	LMMB-13	WI	43.0095	-87.9067
Kinnickinnic River-14	LMMB-14	WI	43.0120	-87.9055
Menomonee River-11	LMMB-11	WI	43.0329	-87.9391
Menomonee River-12	LMMB-12	WI	43.0318	-87.9469
Menomonee River-15	LMMB-15	WI	43.0334	-87.9176

Fig. 2F. Great Lakes Mussel Watch PFAS study site locations (●), and adjacent sub-watersheds (HUC10). Site table provides information on MWP site name, site code, and approximate nominal latitude and longitude for each site. Where applicable, wastewater treatment plants (▲) and reference sites (*) are identified on the map.

Methods

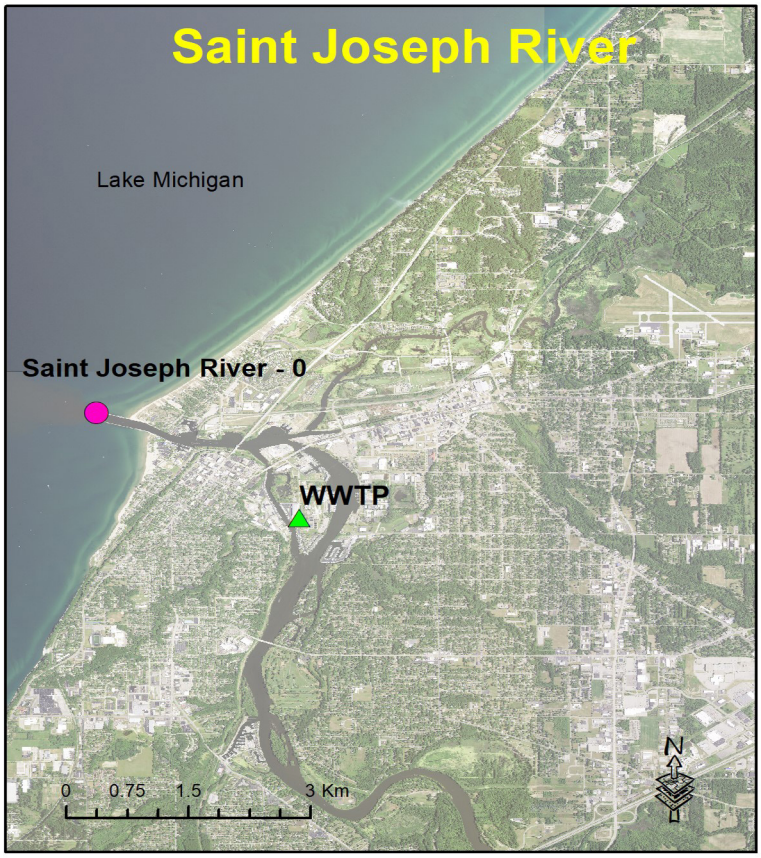

Site Name	Site Code	State	Latitude	Longitude
St. Joseph River-0	LMSJ-0	MI	42.1160	-86.4940

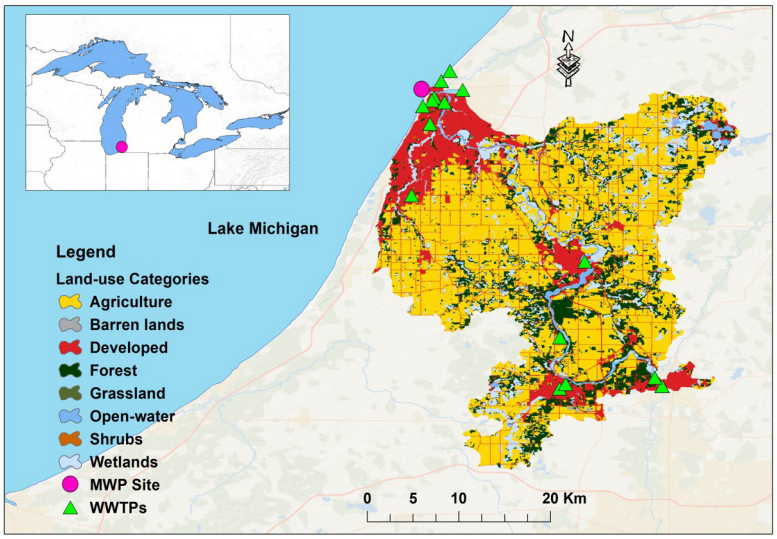

Watershed	HUC-10	SqKm
Saint Joseph River	0405000126	688.1

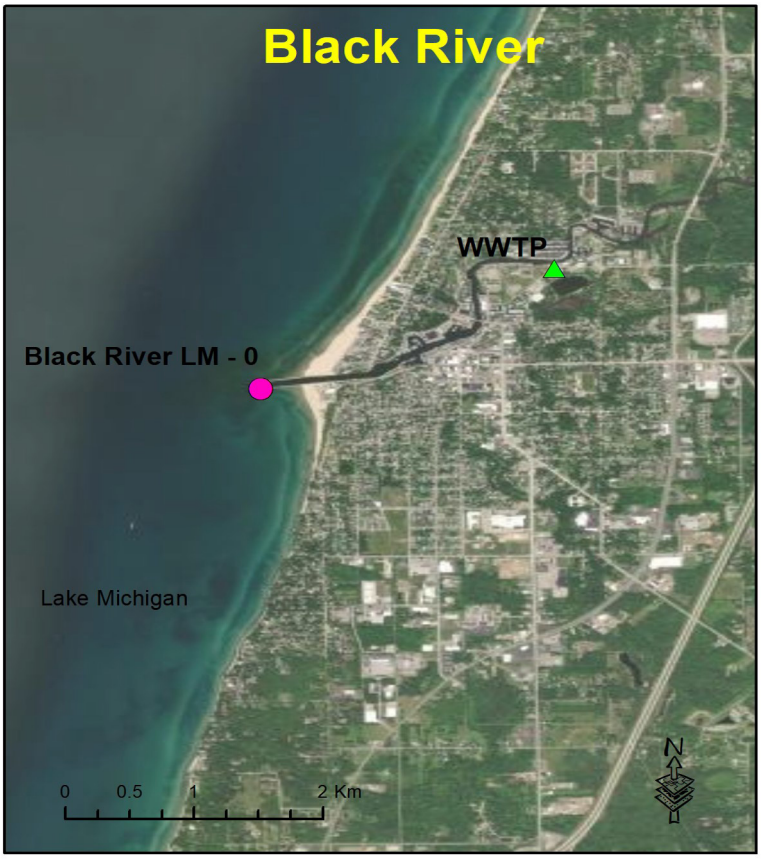

Site Name	Site Code	State	Latitude	Longitude
Black River LM-0	LMMB-0	WI	42.4014	-86.2880

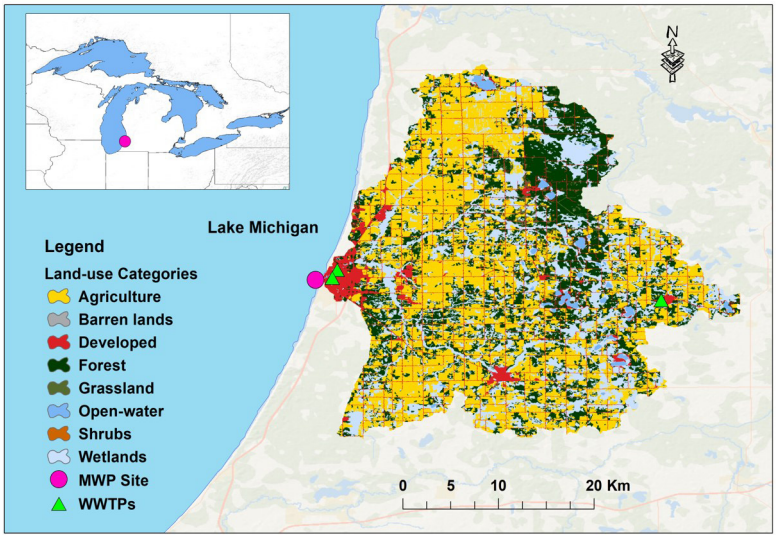

Watershed	HUC-10	SqKm
Black River	0405000202	742.3

Fig. 2G.H. Great Lakes Mussel Watch PFAS study site locations (●), and adjacent sub-watersheds (HUC-10). Site table provides information on MWP site name, site code, and approximate nominal latitude and longitude for each site. Where applicable, wastewater treatment plants (▲) and reference sites (*) are identified on the map.

Methods

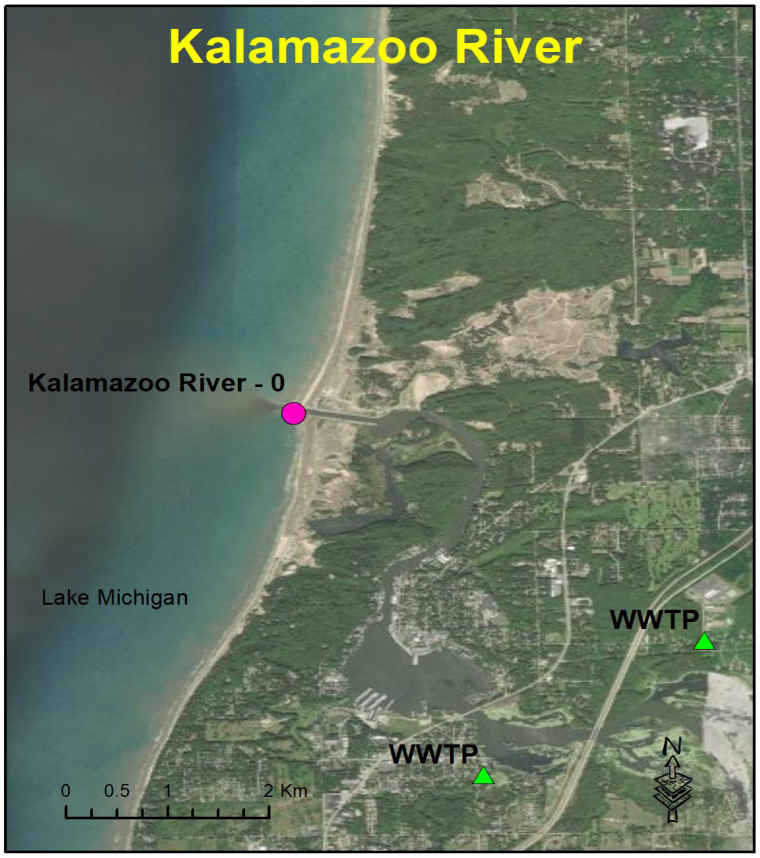

Site Name	Site Code	State	Latitude	Longitude
Kalamazoo River-0	LMKZ-0	WI	42.6766	-86.2150

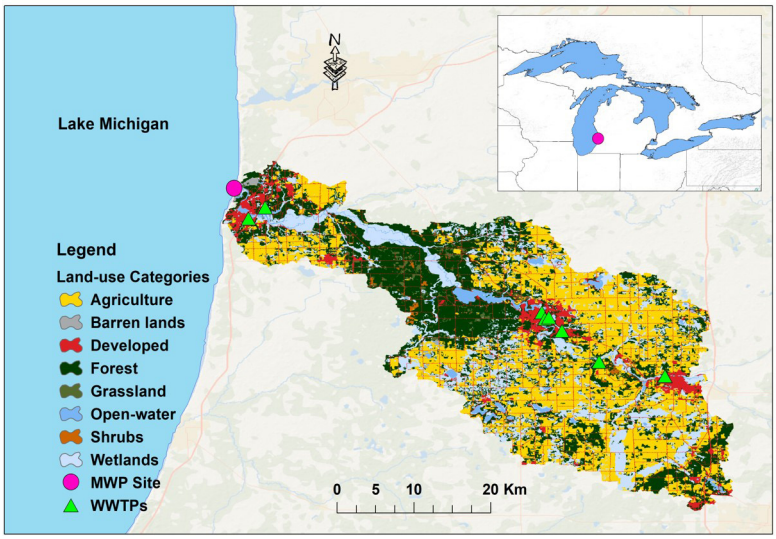

Watershed	HUC-10	SqKm
Kalamazoo River	0405000309	929.7

Site Name	Site Code	State	Latitude	Longitude
Port Sheldon-0	LMPS-0	MI	42.9016	-86.2160

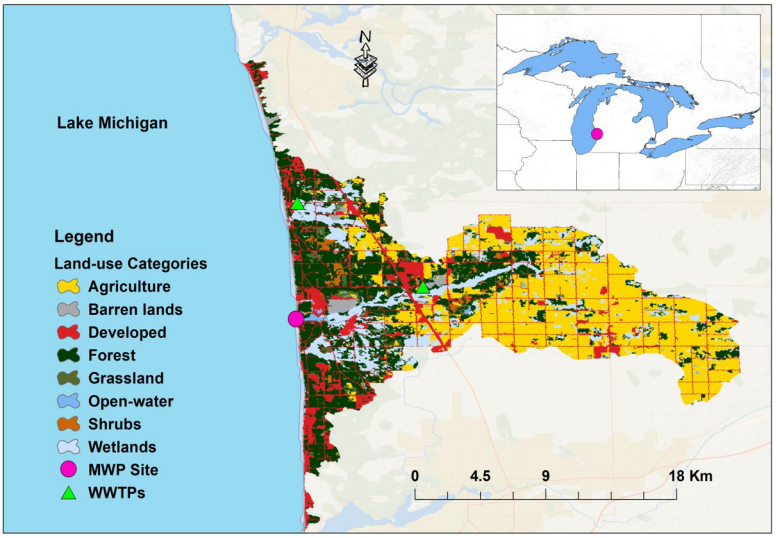

Watershed	HUC-10	SqKm
Pigeon River-Frontal Lake Michigan	0405000203	216.4

Fig. 2I-J. Great Lakes Mussel Watch PFAS study site locations (●), and adjacent sub-watersheds (HUC-10). Site table provides information on MWP site name, site code, and approximate nominal latitude and longitude for each site. Where applicable, wastewater treatment plants (▲) and reference sites (*) are identified on the map.

Methods

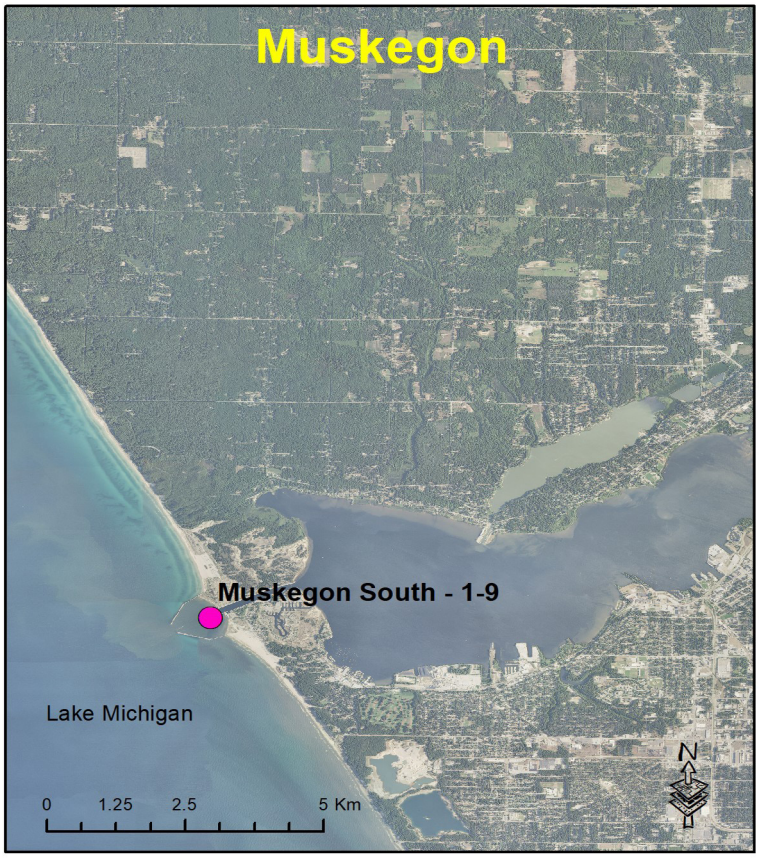

Site Name	Site Code	State	Latitude	Longitude
MuskegonLight-5.2-29.18	MUS-1-3	MI	43.2266	-86.3416
MuskegonLight-6.15-26.18	MUS-4-5	MI	43.2266	-86.3416
MuskegonLight-7.18	MUS-6	MI	43.2266	-86.3416
MuskegonLight-8-9.18	MUS-8	MI	43.2266	-86.3416
MuskegonLight-11.2718	MUS-9	MI	43.2266	-86.3416

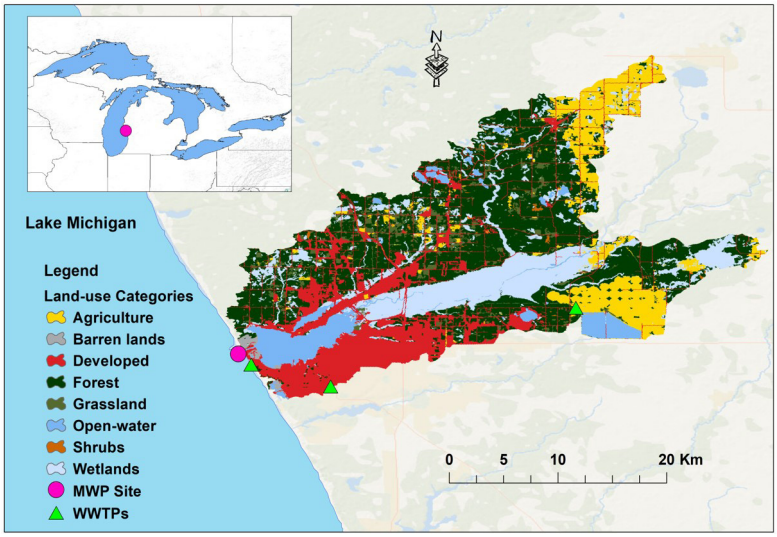

Watershed	HUC-10	SqKm
Muskegon River	0406010210	483.6

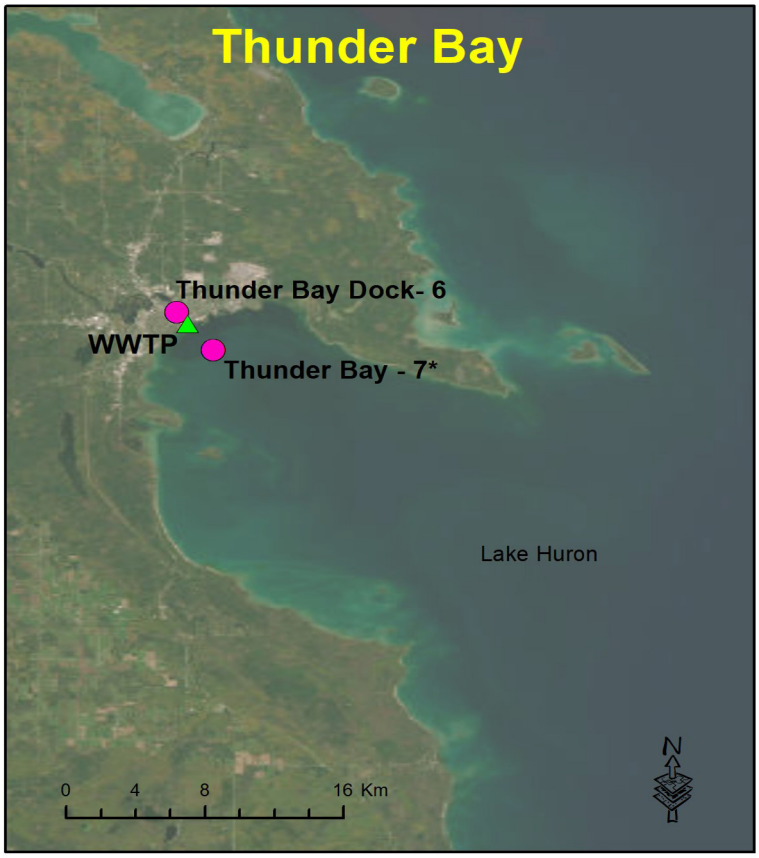

Site Name	Site Code	State	Latitude	Longitude
Thunder Bay Dock-6	TBRD-6	MI	45.0671	-83.4350
Thunder Bay-7*	TBHS5-7*	MI	45.0461	-83.4160

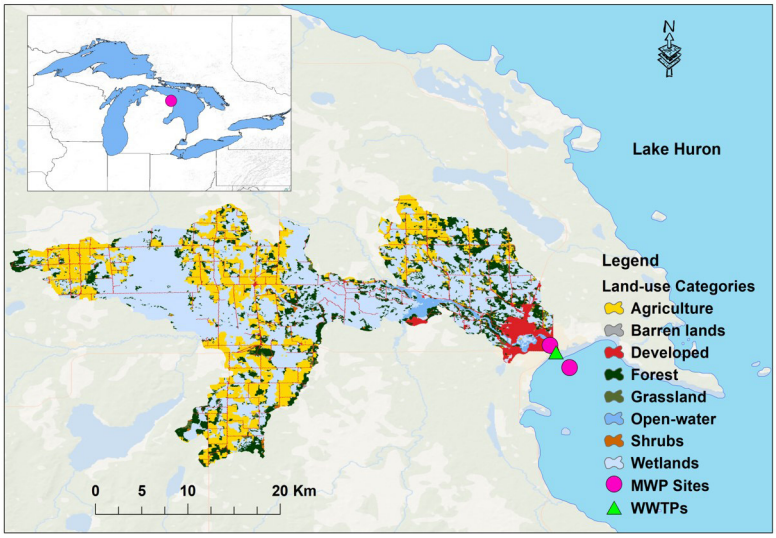

Watershed	HUC-10	SqKm
Black River	0405000202	742.3

Fig. 2K-L. Great Lakes Mussel Watch PFAS study site locations (●), and adjacent sub-watersheds (HUC-10). Site table provides information on MWP site name, site code, and approximate nominal latitude and longitude for each site. Where applicable, wastewater treatment plants (▲) and reference sites (*) are identified on the map.

Methods

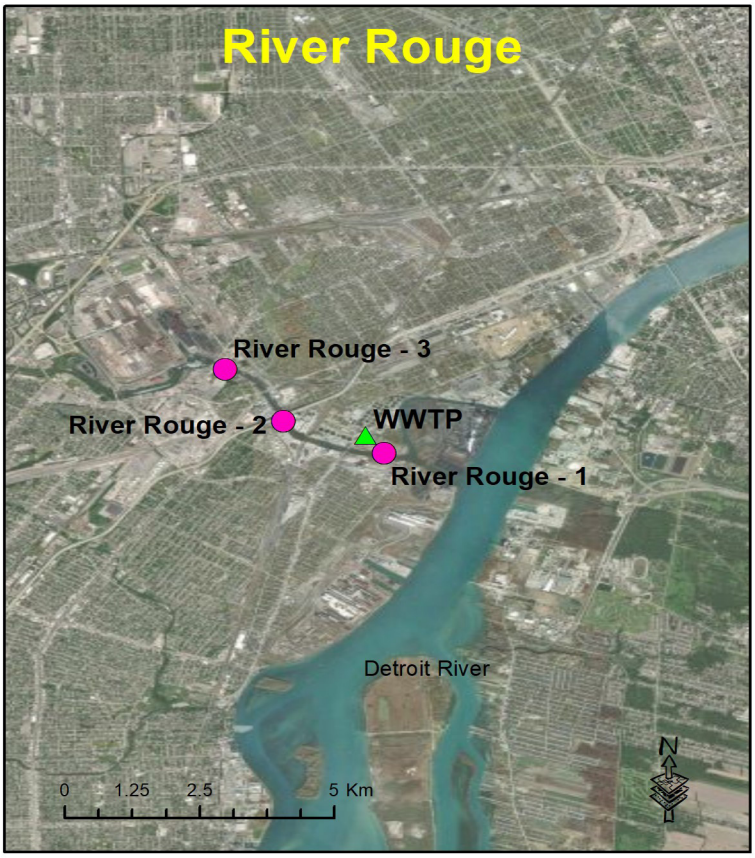

Site Name	Site Code	State	Latitude	Longitude
River Rouge-1	DRRR-1	MI	42.2801	-83.1230
River Rouge-2	DRRR-2	MI	42.2859	-83.1390
River Rouge-3	DRRR-3	MI	42.2951	-83.1490

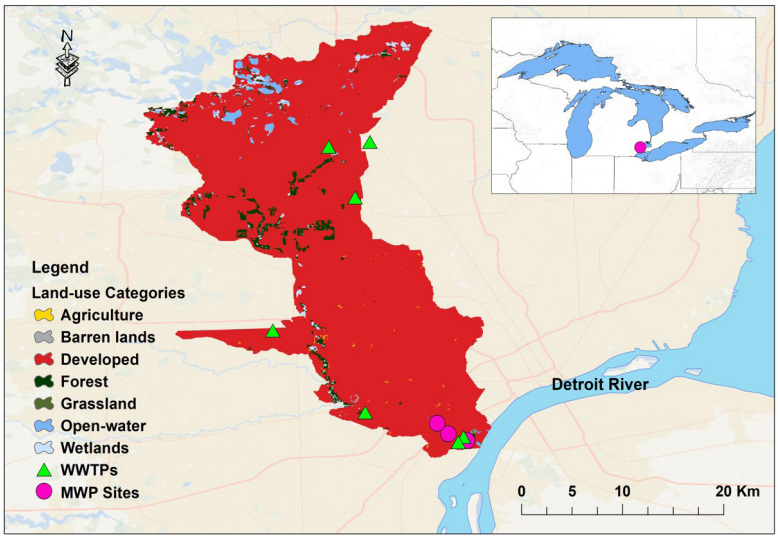

Watershed	HUC-10	SqKm
River Rouge	0409000404	487.0

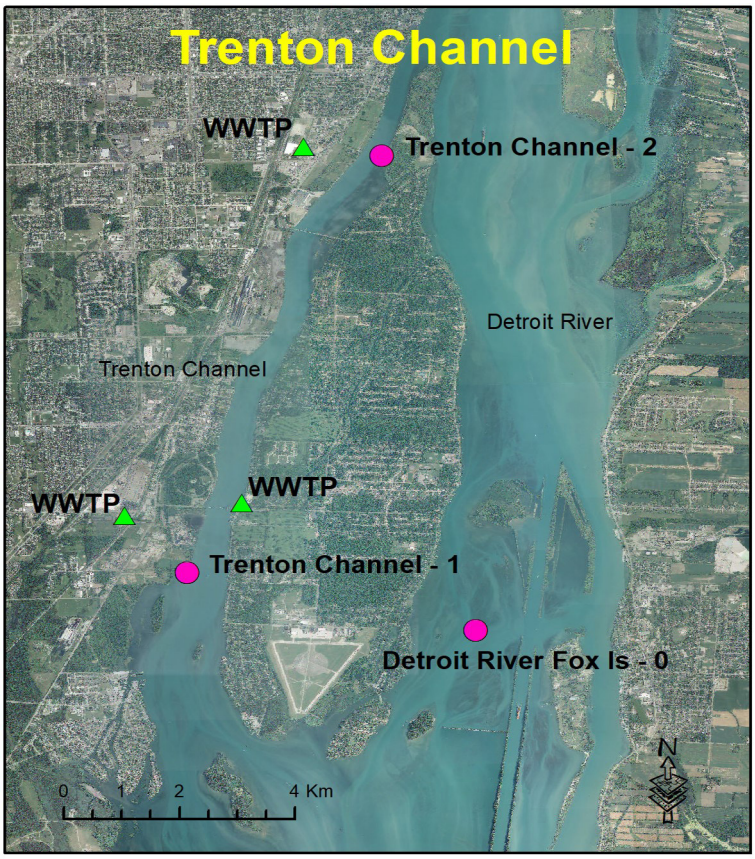

Site Name	Site Code	State	Latitude	Longitude
Detroit River Fox Is-0	DRSE-0	MI	42.1069	-83.1360
Trenton Channel-1	DRTC-1	MI	42.1165	-83.1810
Trenton Channel-2	DRTC-2	MI	42.1861	-83.1500

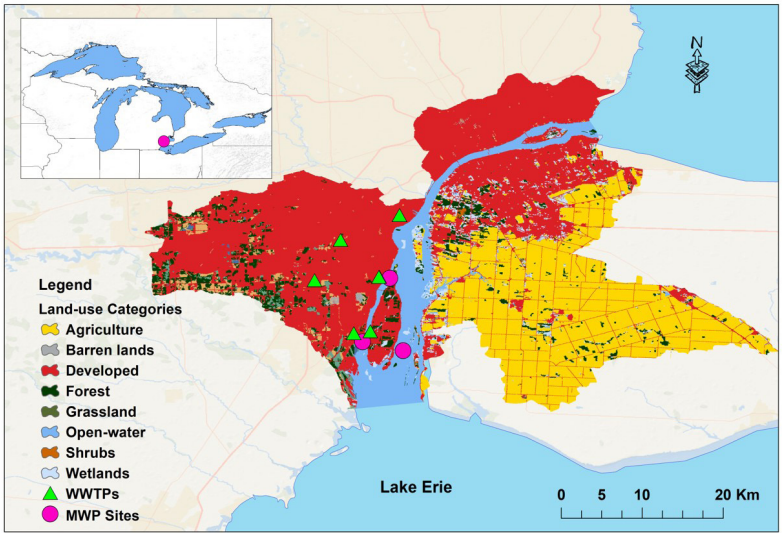

Watershed	HUC-10	SqKm
Detroit	0409000400	676.7

Fig. 2M-N. Great Lakes Mussel Watch PFAS study site locations (●), and adjacent sub-watersheds (HUC-10). Site table provides information on MWP site name, site code, and approximate nominal latitude and longitude for each site. Where applicable, wastewater treatment plants (▲) and reference sites (*) are identified on the map.

Methods

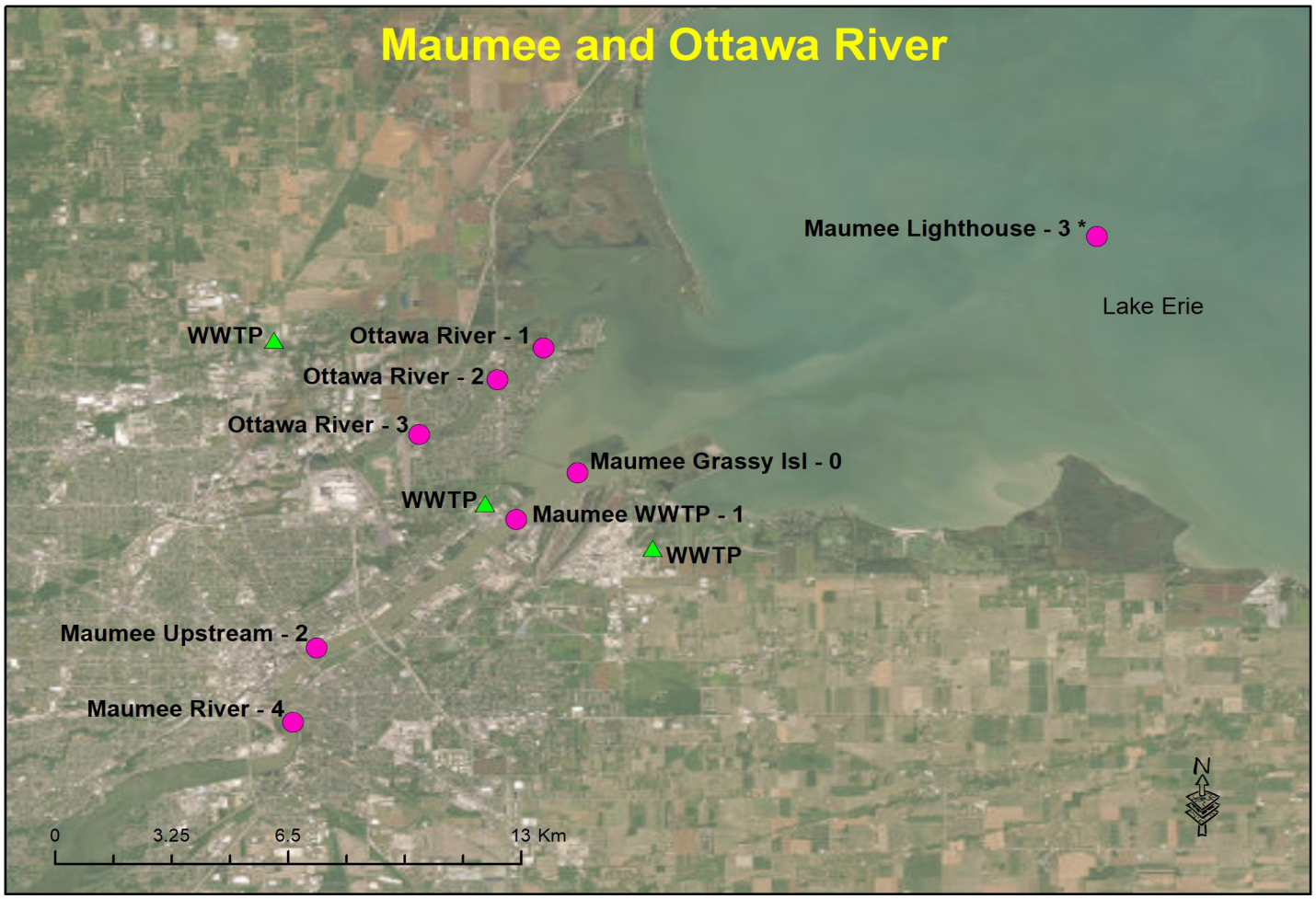

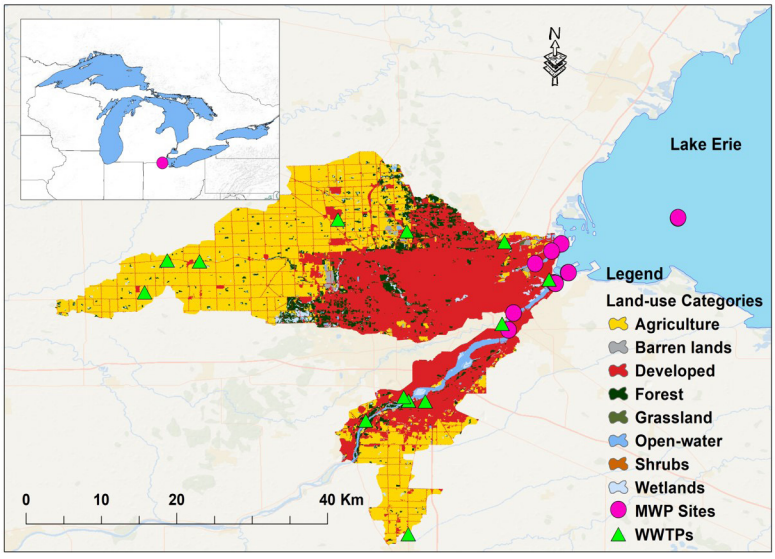

Site Name	Site Code	State	Latitude	Longitude
Maumee Lighthouse-3*	LEMR-3	OH	41.7617	-83.3292
Maumee Grassy Isl-0	LEMR-0	OH	41.7006	-83.4597
Maumee WWTP-1	LEMR-1	OH	41.6891	-83.4768
Maumee Upstream -2	LEMR-2	OH	41.6553	-83.5251
Maumee River-4	LEMR-4	OH	41.6361	-83.5311
Ottawa River-1	LEOT-1	OH	41.7329	-83.4682
Ottawa River-2	LEOT-2	OH	41.7247	-83.4798
Ottawa River-3	LEOT-3	OH	41.7106	-83.4994

Watersheds	HUC-10	SqKm
Ottawa River-Frontal Lake Erie	0410000103	608.2
Grassy Creek-Maumee River	0410000909	191.2

Fig. 2O. Great Lakes Mussel Watch PFAS study site locations (●), and adjacent sub-watersheds (HUC-10). Site table provides information on MWP site name, site code, and approximate nominal latitude and longitude for each site. Where applicable, wastewater treatment plants (▲) and reference sites (*) are identified on the map.

Methods

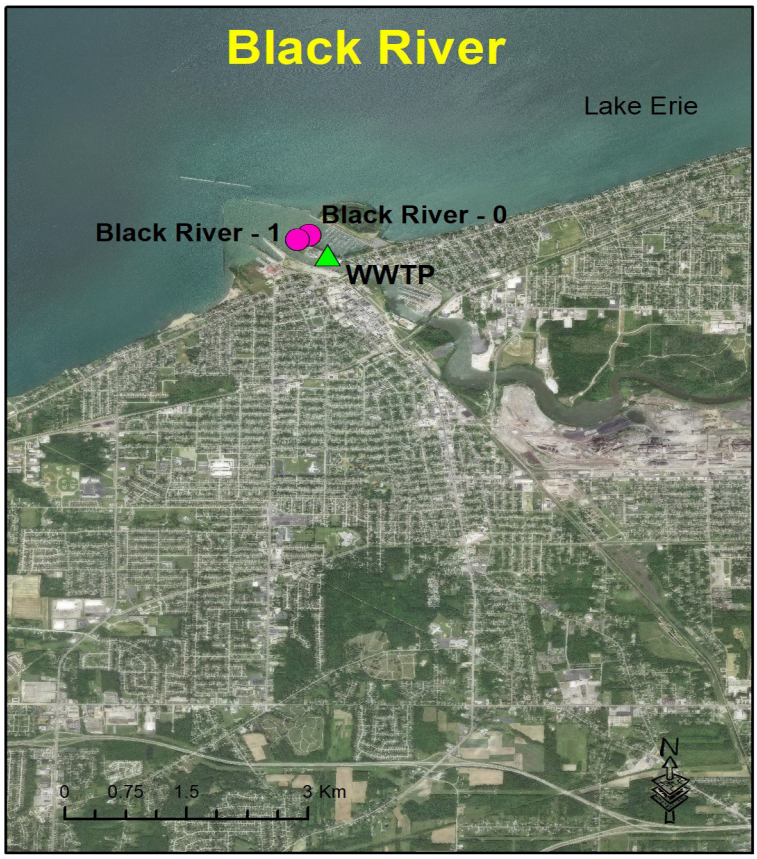

Site Name	Site Code	State	Latitude	Longitude
Black River-0	LEBR-0	OH	41.4741	-82.1810
Black River-1	LEBR-1	OH	41.4736	-82.1820

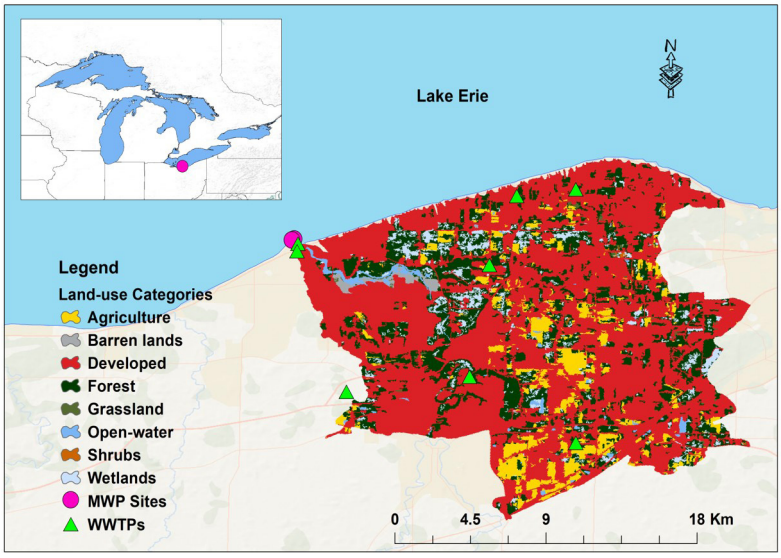

Watershed	HUC-10	SqKm
Black River-Frontal Lake Erie	0411000106	256.0

Site Name	Site Code	State	Latitude	Longitude
Cuyahoga River-5	LECR-5	OH	41.5042	-81.7110
Cuyahoga River-9	LECR-9	OH	41.4984	-81.7200

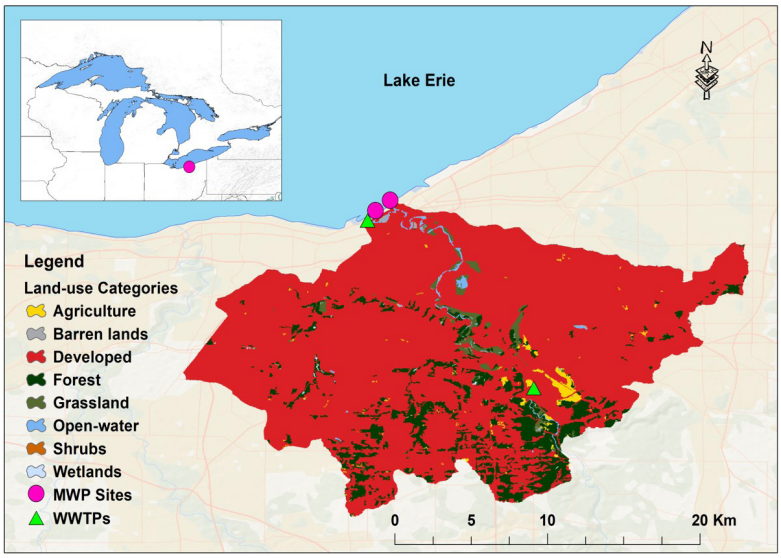

Watershed	HUC-10	SqKm
Big Creek-Cuyahoga River	0411000206	300.8

Fig. 2P-Q. Great Lakes Mussel Watch PFAS study site locations (●), and adjacent sub-watersheds (HUC-10). Site table provides information on MWP site name, site code, and approximate nominal latitude and longitude for each site. Where applicable, wastewater treatment plants (▲) and reference sites (*) are identified on the map.

Methods

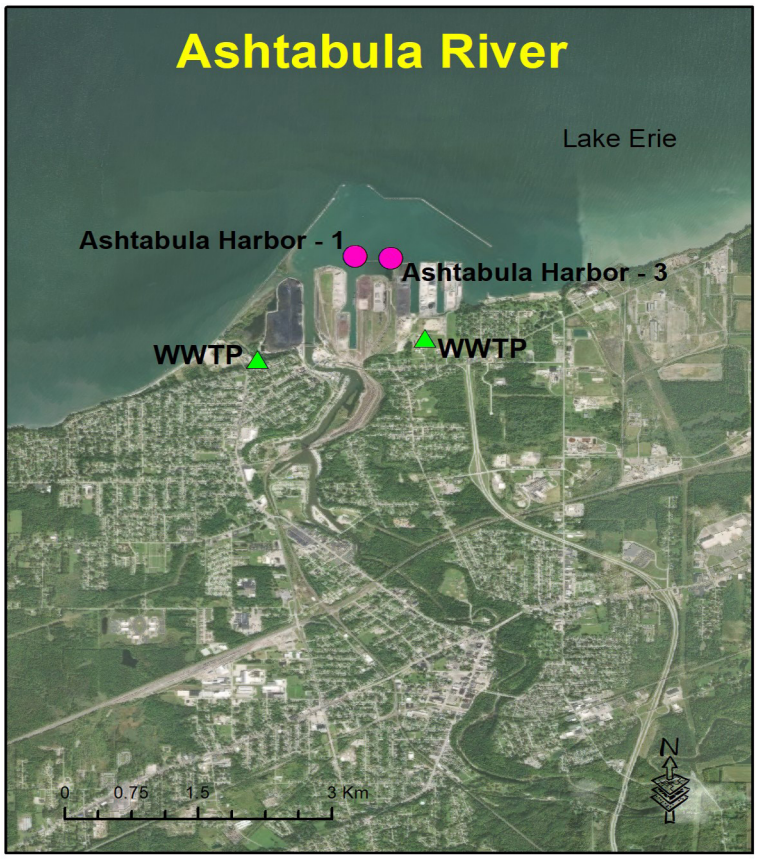

Site Name	Site Code	State	Latitude	Longitude
Ashtabula River-1	LEAR-1	OH	41.9123	-80.7940
Ashtabula River-3	LEAR-3	OH	41.9120	-80.7900

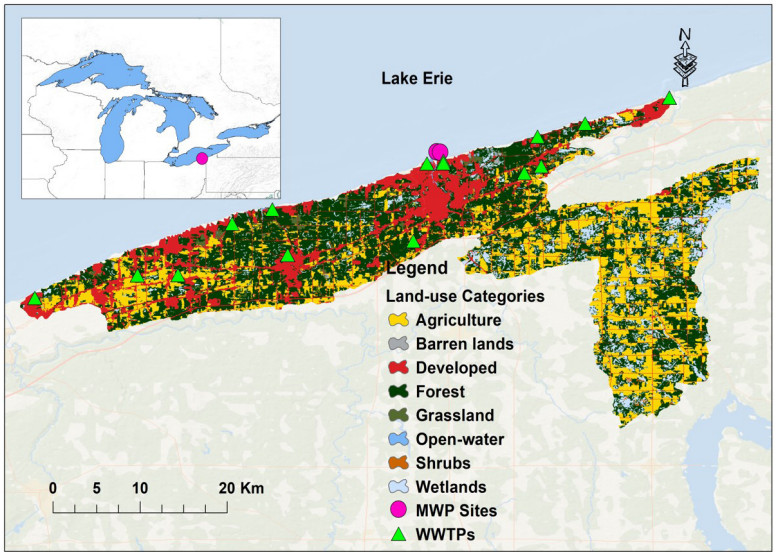

Watersheds	HUC-10	SqKm
Ashtabula River	0411000301	354.0
Crooked Creek-Frontal Lake Erie	0412010107	179.9

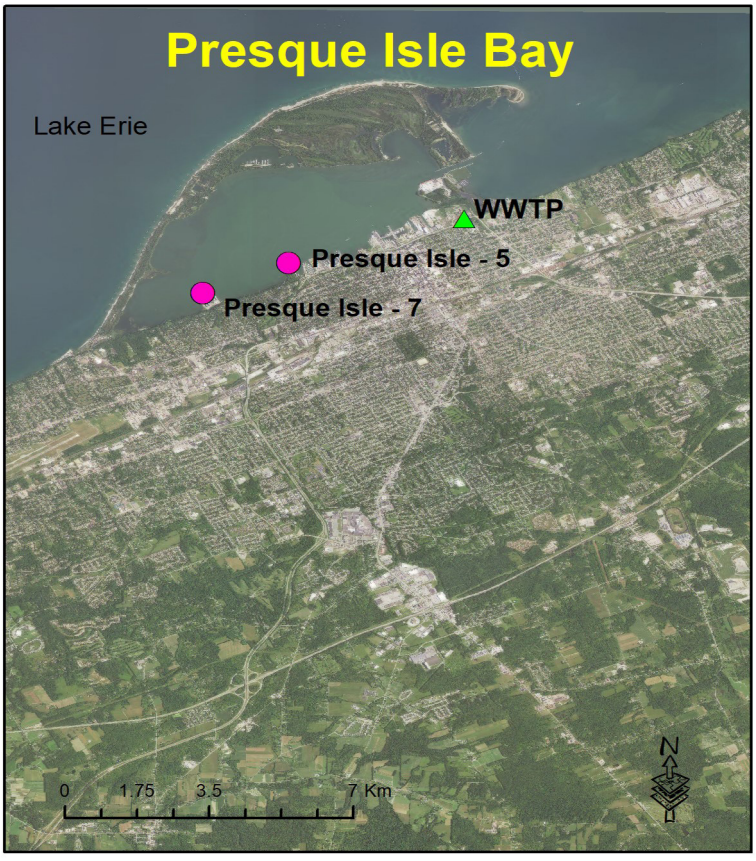

Site Name	Site Code	State	Latitude	Longitude
Presque Isle-5	LEPB-5	PA	42.1304	-80.1130
Presque Isle-7	LEPB-7	PA	42.1233	-80.1320

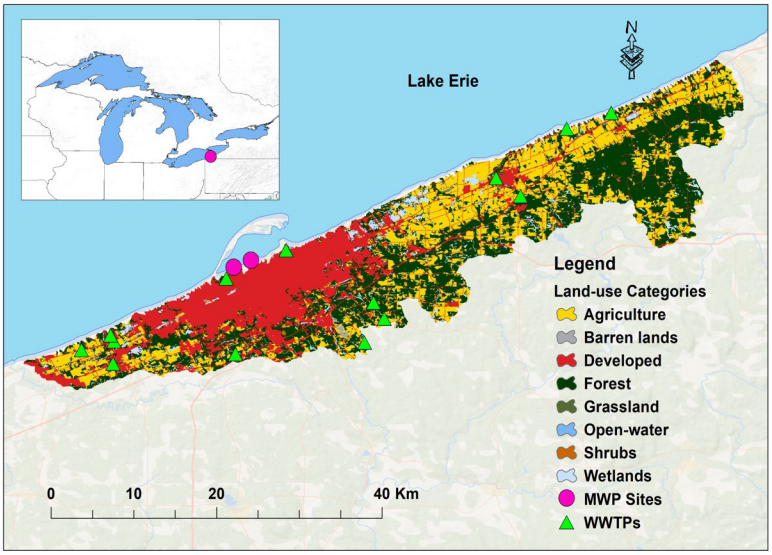

Watershed	HUC-10	SqKm
Six-mile Creek-Frontal Lake Erie	0412010104	677.5

Fig. 2R-S. Great Lakes Mussel Watch PFAS study site locations (●), and adjacent sub-watersheds (HUC-10). Site table provides information on MWP site name, site code, and approximate nominal latitude and longitude for each site. Where applicable, wastewater treatment plants (▲) and reference sites (*) are identified on the map.

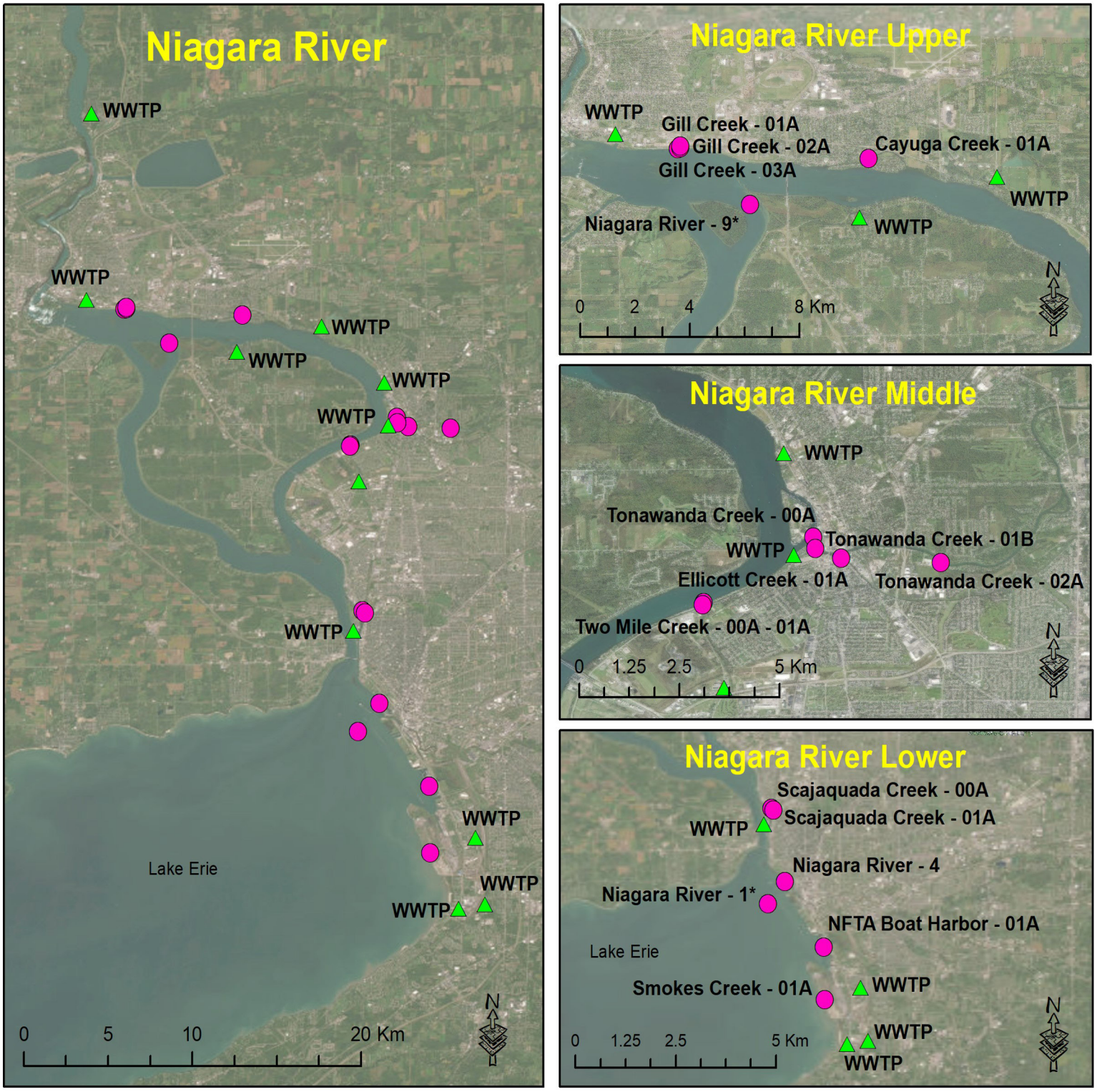

Fig. 2T. Great Lakes Mussel Watch PFAS study site locations (●), and adjacent sub-watersheds (HUC-10). Site table provides information on MWP site name, site code, and approximate nominal latitude and longitude for each site. Where applicable, wastewater treatment plants (▲) and reference sites (*) are identified on the map.

Methods

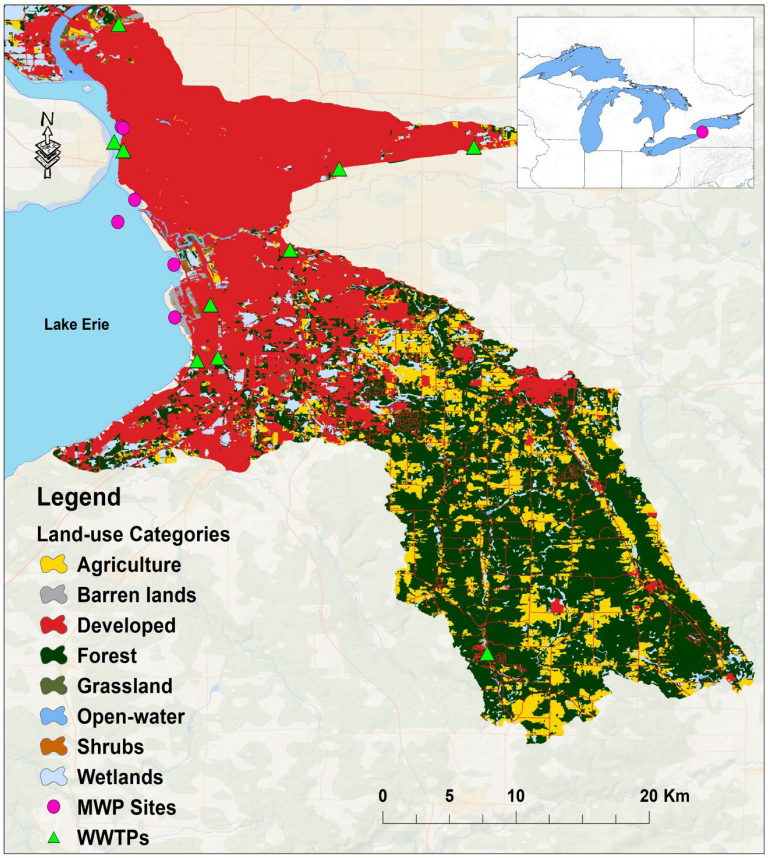

Site Name	Site Code	State	Latitude	Longitude
NFTA Boat Harbor-01A	NRHP-01A	NY	42.8442	-78.8644
Niagara River-1*	NRNF-1*	NY	42.8708	-78.9022
Niagara River-4-6.14	NRNF-4	NY	42.8845	-78.8908
Niagara River-9-6.14*	NRNF-9	NY	43.0612	-79.0028
Scajaquada Creek-00A	NRSC-00A	NY	42.9300	-78.8999
Scajaquada Creek-01A	NRSC-01A	NY	42.9291	-78.8985
Smokes Creek-01A	NRSM-01A	NY	42.8113	-78.8637
Times Beach-01B	NRTB-01B	NY	43.0112	-78.9062

Watersheds	HUC-10	SqKm
Smoke Creek-Frontal Lake Erie	0412010304	174.7
Buffalo River	0412010303	410.2
Niagara River	0412010406	412.8

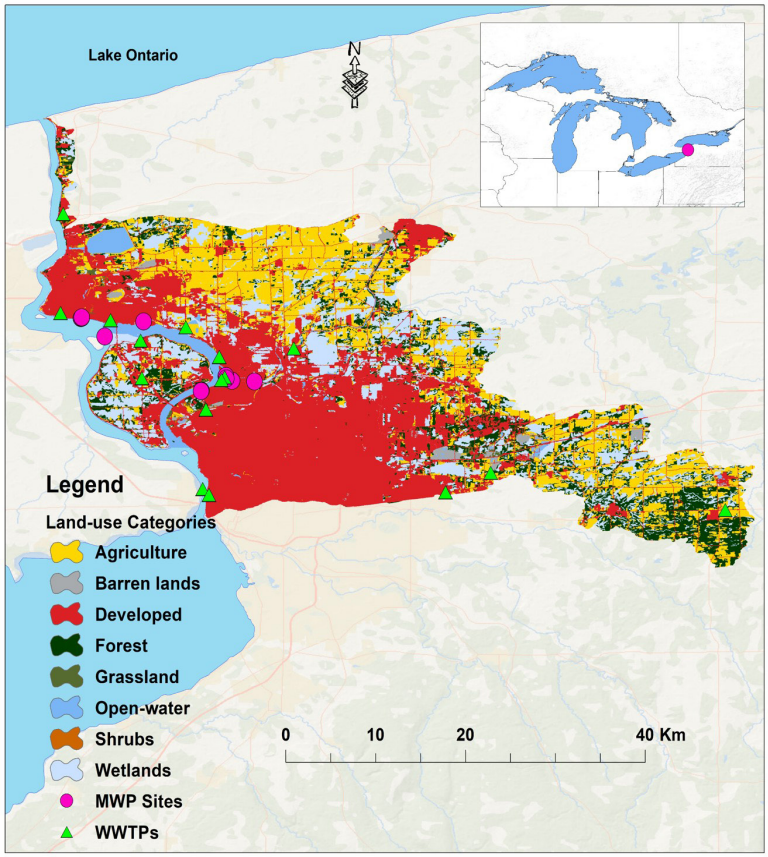

Site Name	Site Code	State	Latitude	Longitude
Cayuga Creek-01A	NRCY-01A	NY	43.0750	-78.9639
Ellicott Creek-01A	NREL-01A	NY	43.0203	-78.8754
Gill Creek-01A-7.14	NRGL-01A	NY	43.0781	-79.0267
Gill Creek-02A-7.14	NRGL-02A	NY	43.0783	-79.0259
Gill Creek-03A-7.14	NRGL-03A	NY	43.0788	-79.0258
Tonawanda Creek-00A	NRTW-00A	NY	43.0247	-78.8816
Tonawanda Creek-01B	NRTW-01B	NY	43.0223	-78.8812
Tonawanda Creek-02A	NRTW-02A	NY	43.0195	-78.8530
Two Mile Creek-00A	NRTM-00A	NY	43.0112	-78.9062
Two Mile Creek-01A	NRTM-01A	NY	43.0108	-78.9064

Watersheds	HUC-10	SqKm
Niagara River	0412010406	412.8
Ellicott Creek	0412010404	310.9

Fig. 2T1-T2. Great Lakes Mussel Watch PFAS study site locations (●), and adjacent sub-watersheds (HUC-10). Site table provides information on MWP site name, site code, and approximate nominal latitude and longitude for each site. Where applicable, wastewater treatment plants (▲) and reference sites (*) are identified on the map.

Methods

Site Name	Site Code	State	Latitude	Longitude
Youngstown-0	NRYT-0	NY	43.2313	-79.0520

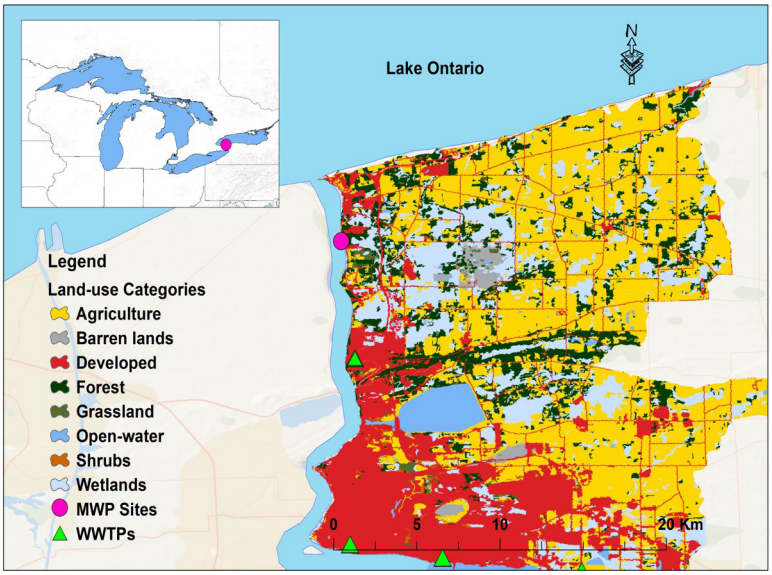

Watersheds	HUC-10	SqKm
Niagara River	0412010406	412.8
Twelvemile Creek-Frontal Lake Ontario	0413000109	307.4

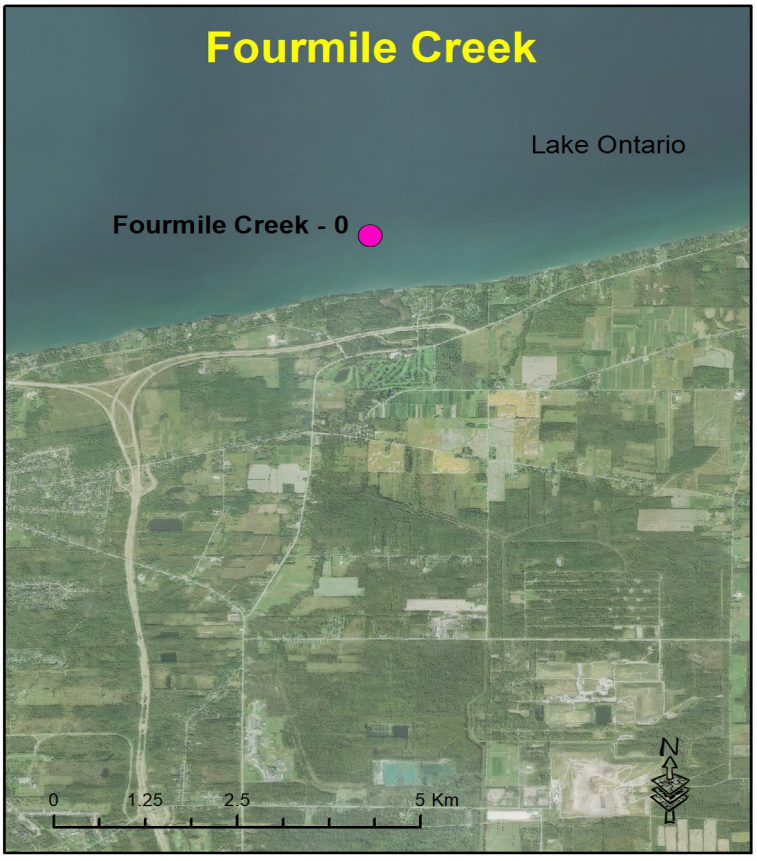

Site Name	Site Code	State	Latitude	Longitude
Fourmile Creek-0	LOFC-0	NY	43.2840	-79.0020

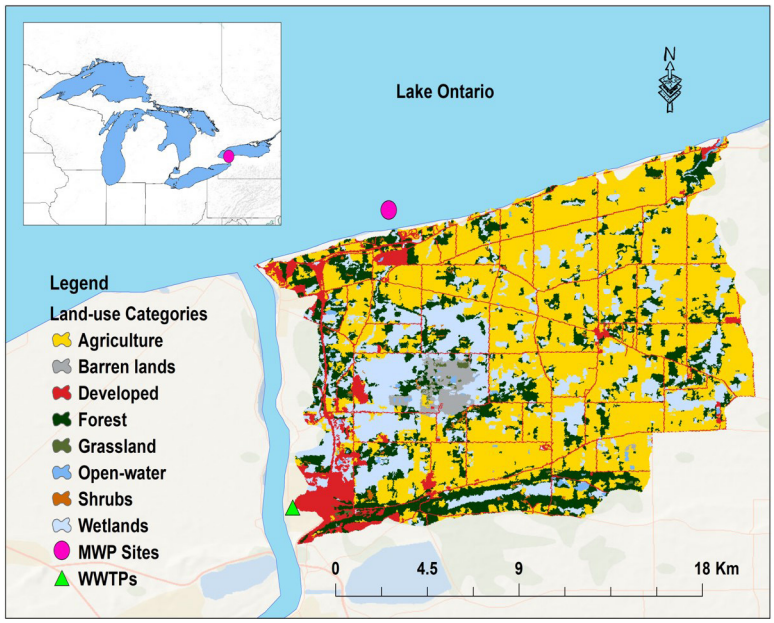

Watershed	HUC-10	SqKm
Twelvemile Creek-Frontal Lake Ontario	0413000109	307.4

Fig. 2U-V. Great Lakes Mussel Watch PFAS study site locations (●), and adjacent sub-watersheds (HUC-10). Site table provides information on MWP site name, site code, and approximate nominal latitude and longitude for each site. Where applicable, wastewater treatment plants (▲) and reference sites (*) are identified on the map.

Methods

Site Name	Site Code	State	Latitude	Longitude
Lake OntarioFS-0	LOFO-0	NY	43.4684	-77.8820

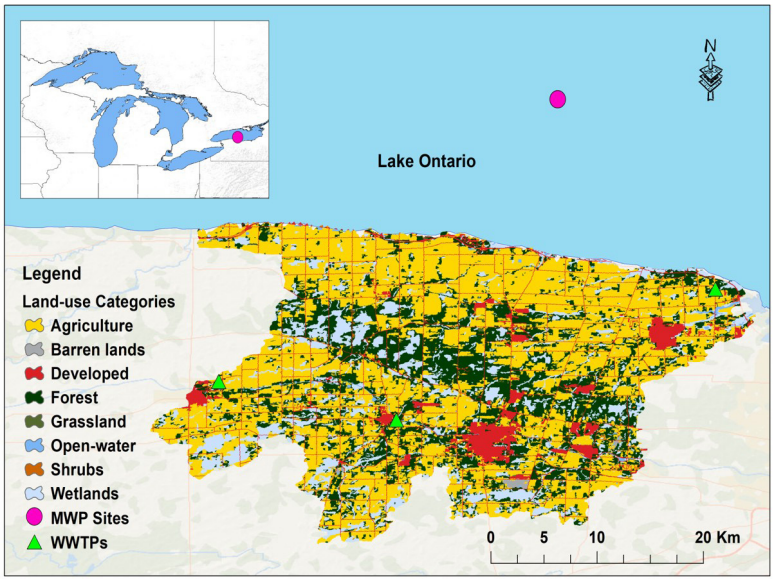

Watersheds	HUC-10	SqKm
Sandy Creek-Frontal Lake Ontario	0413000103	353.8
Salmon Creek-Frontal Lake Ontario	0413000102	316.1

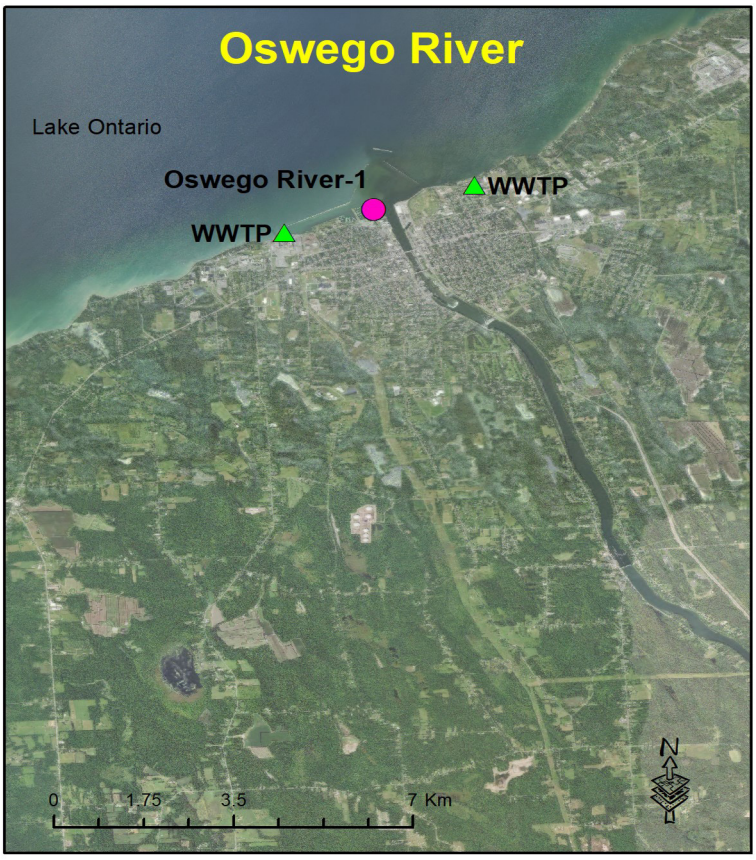

Site Name	Site Code	State	Latitude	Longitude
Oswego River-1	LOOR-1	NY	43.4649	-76.5160

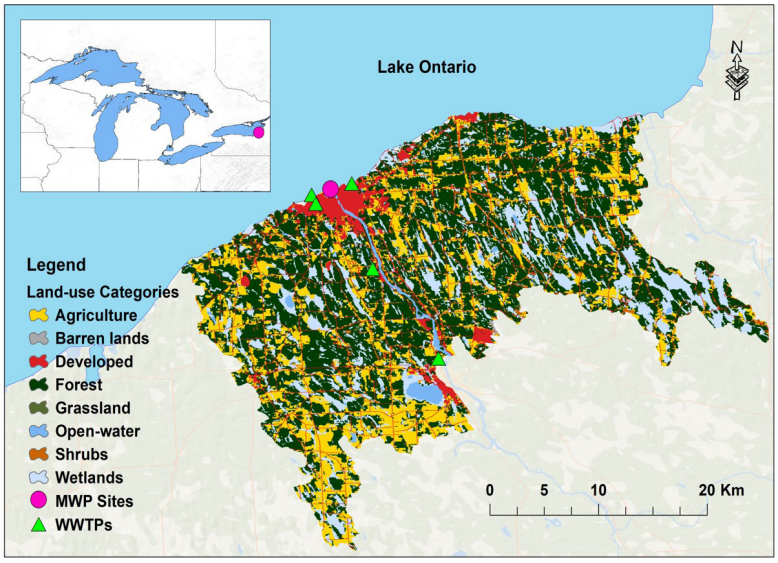

Watersheds	HUC-10	SqKm
Oswego River	0414020302	179.9
Catfish Creek-Frontal Lake Ontario	0414010210	225.5
Ninemile Creek-Frontal Lake Ontario	0414010101	206.4

Fig. 2W-X. Great Lakes Mussel Watch PFAS study site locations (●), and adjacent sub-watersheds (HUC-10). Site table provides information on MWP site name, site code, and approximate nominal latitude and longitude for each site. Where applicable, wastewater treatment plants (▲) and reference sites (*) are identified on the map.

Methods

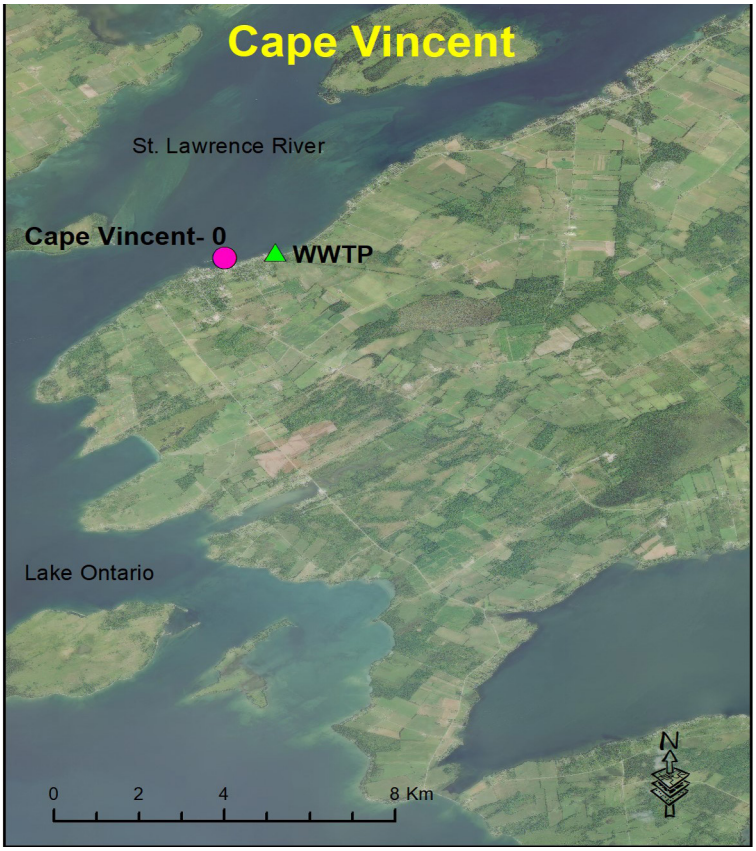

Site Name	Site Code	State	Latitude	Longitude
Cape Vincent-0	LOCV-0	NY	44.1323	-76.3310

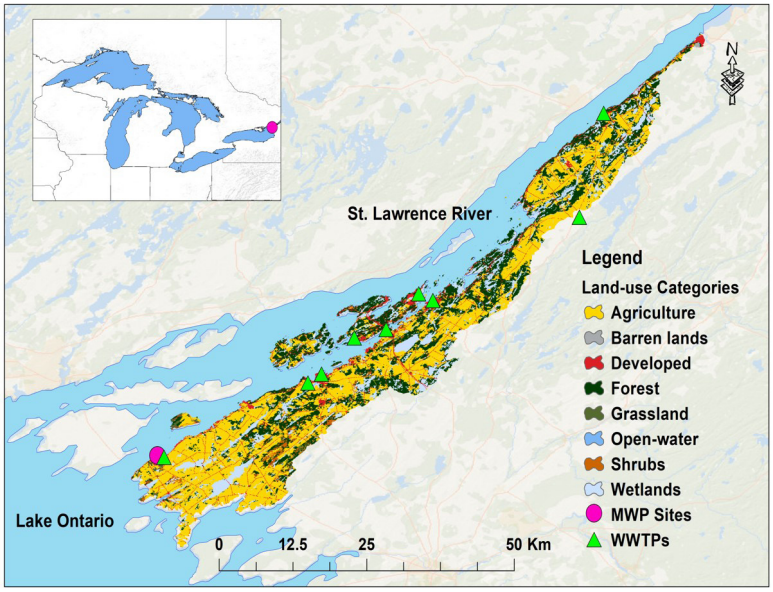

Watersheds	HUC-10	SqKm
Kents Creek-Frontal Lake Ontario	0415010201	184.1
Chippewa Creek-Frontal Saint Lawrence River	0415030901	554.6

Fig. 2Y. Great Lakes Mussel Watch PFAS study site locations (●), and adjacent sub-watersheds (HUC-10). Site table provides information on MWP site name, site code, and approximate nominal latitude and longitude for each site. Where applicable, wastewater treatment plants (▲) and reference sites (*) are identified on the map.

Credit: NOAA Great Lakes MWP

2.3. Sampling Procedures

PFAS sampling procedures utilized both *in-situ* and caged dreissenid mussels for basin-wide surveillance monitoring and place-based contaminant assessments across the 2013 - 2018 sampling period. Mussels were collected between mid-May and Mid-September each year. When available, divers harvested in situ dreissenid mussels from outer harbor stone breakwaters, near-shore lake zone, or in open lake. For sampling locations and place-based contaminant assessment sites where in situ mussels were unavailable, mussels were harvested by divers from nearshore harbor and stone breakwaters, placed in cages (e.g., minnow traps; approximately 300 - 500 mussels per cage) and deployed at selected sampling locations. Mussels were caged from 2-55 days, depending upon the study. For temporal studies (e.g., assessment of metabolomic profiles and DNA damage in mussels; Elgin et al., 2023), mussels were caged for up to 55 days. Dreissenid mussels collected from in situ and place-based/caged deployment was rinsed with site water to remove debris, placed in labeled freezer bags, packed in ice containers and shipped to contract laboratories within two days of collection for analysis. Homogenates with more than 100 individuals were used for chemical analysis. Tissue sample collection and processing were consistent with NOAA methods and procedures for bivalve tissue assessment (Kimbrough et al., 2013).

2.4. Chemical Analysis

A total of 28 PFAS compounds were analyzed in dreissenid mussel tissue (Table 1). Of the 28 PFAS compounds compounds analyzed in this study, 27 compounds were detected in mussel tissue. All 27 $\sum_{27}$PFAS compounds quantified in dreissenid mussels during the 2013-2018 study period were prioritized and grouped into 7 primary compound groups namely (USEPA, 2021); perfluoroalkyl carboxylic acids (PFCAs; $C_nF_{2n+1}COO–$), perfluoroalkane sulfonic acids (PFSAs; $C_nF_{2n+1}SO_3–$), fluorotelomer sulfonic acids (FTSAs; $C_nF_{2n+1}CH_2CH_2SO_3–$), per- and polyfluoroalkyl ether acids (PFESAs; $C_7F_{14}HSO_5–$), per- and polyfluoroalkyl ether carboxylic acids (PFECAs; $CF_3OCF_2CF_2CF_2OCHFCF_2COOH$), perfluoroalkane sulfonamido acetic acids (FOSAAs; $C_nF_{2n+1}SO_2NHCH_2COOH$), and perfluoroalkane sulfonamide (FASAs; $C_nF_{2n+1}SO_2NH_2$). The 27 PFAS compounds quantified in dreissenid mussels were further grouped as follows; 11 PFCAs ([C_4–C_{14}]; PFBA, PFDA, PFDoA, PFHpA, PFHxA, PFNA, PFOA, PFPeA, PFTreA, PFTriA, PFUnA); 7 PFSAs ([C_4–C_{10}]; PFBS, PFDS, PFHpS, PFHxS, PFNS, PFOS, PFPeS); 3 FTSAs ([C_6–C_{10}]; 4:2 FTS, 6:2 FTS, 8:2 FTS); 2 (PFESAs [C_8–C_{10}]; 9Cl-PF3ONS, 11Cl-PF3OUdS); 2 novel PFECAs ([C_6–C_7]; ADONA, HFPO-DA/Gen-X); 2 FOSAAs ([C_{11}–C_{12}]; N-EtFOSAA, N-MeFOSAA); and 1 FASAs ([C_8]; PFOSA). Overall, among the 27 $\sum_{27}$PFAS compounds quantified in this study, 19 compounds namely: 8 PFCAs (PFBA, PFDA, PFDoA, PFHpA, PFOA, PFPeA, PFTreA, PFTriA); 7 PFSAs (PFBS, PFDS, PFHpS, PFHxS, PFNS, PFOS, PFPeS); 1 FTSA (8:2 FTS); 1 PFESA (11Cl-PF3OUdS), 1 FOSAAs (N-MeFOSAA), and 1 FASAs (PFOSA; Table 1), were found in at least one or more mussel tissue samples with concentrations above the method detection limit (> MDLs). These PFAS compounds were further compiled and summarized in this report.

All PFAS tissue samples were analyzed by TDI Brooks in College Station, Texas. TDI Brooks PFAS methods are proprietary and confidential. Hence, in this report, we will refer to the name of the method provided. All PFAS compounds were grouped by analytical method B&B SOP 1104 to simplify detected PFAS presentation and results. Overall, a liberal format was used to record the presence/absence of all $\sum_{27}$PFAS compounds detected in mussel tissue (heat map; Fig. 3). Method detection limit (MDLs) for PFAS compounds analyzed in this study were in the range of 0.002 - 0.05 ng/g wet weight (ww) for mussel tissue samples. The concentration for all PFAS compounds detected in mussel tissue were blank corrected. Specifically, blank corrected samples with concentrations below method detection limit (< MDL) were recorded as zero (0), while blank corrected concentrations above > MDLs were recorded as present, and used in PFAS contaminant concentration summaries, contaminant concentration heatmaps, and statistical comparisons where applicable. The PFAS compounds found in mussel tissue samples with blank corrected concentrations above the method detection limit (> MDLs), were also used in random forest classification, cluster analysis, other pattern recognition and multivariate techniques.

Methods

Table 1. List of ∑28PFAS compounds and compound groups analyzed in dreissenid mussels (zebra/quagga; Dreissena spp.) during the 2013 - 2018 study period, based on TDI Brooks analytical method B&B SOP 1104. Chemical names in black identify PFAS compounds detected with concentrations above the method detection limit (> MDLs), and found in at least one or more mussel tissue samples during the 2013-2018 study period. Chemical names in red signifies PFAS compounds not detected (⊕), or compounds quantified below the method detection limit (< MDLs) in dreissenid mussels during the 2013 – 2018 sampling event. Additional information on ∑28PFAS compounds and compound groups analyzed for dreissenid mussels used in this study is provided in Table A2 (Appendix).

Chemical Name	Acronym	CASRN #	Carbon #	PFAS Group
4,8-dioxa-3H-perfluorononanoic acid	ADONA	958445-44-8	C7	Per- and polyfluoroalkyl ether carboxylic acids (PFECAs)
Hexafluoropropylene oxide dimer acid (Gen-X) (⊕)	HFPO-DA	13252-13-6	C6	Per- and polyfluoroalkyl ether carboxylic acids (PFECAs)
N-Ethylperfluorooctanesulfonamidoacetic acid	N-EtFOSAA	2991-50-6	C12	Perfluoroalkane sulfonamido acetic acids (FASAAs)
N-Methylperfluorooctanesulfonamidoacetic acid	N-MeFOSAA	2355-31-9	C11	Perfluoroalkane sulfonamido acetic acids (FASAAs)
Perfluoro-n-butanoic acid	PFBA	375-22-4	C4	Perfluoroalkyl carboxylic acids (PFCAs)
Perfluoro-1-butanesulfonic acid	PFBS	375-73-5	C4	Perfluoroalkane sulfonic acids (PFSAs)
Perfluoro-n-decanoic acid	PFDA	335-76-2	C10	Perfluoroalkyl carboxylic acids (PFCAs)
Perfluoro-n-dodecanoic acid	PFDoA	307-55-1	C12	Perfluoroalkyl carboxylic acids (PFCAs)
Perfluoro-1-decanesulfonic acid	PFDS	2806-15-7	C10	Perfluoroalkane sulfonic acids (PFSAs)
Perfluoro-n-heptanoic acid	PFHpA	375-85-9	C7	Perfluoroalkyl carboxylic acids (PFCAs)
Perfluoro-1-heptanesulfonic acid	PFHpS	375-92-8	C7	Perfluoroalkane sulfonic acids (PFSAs)
Perfluoro-n-hexanoic acid	PFHxA	307-24-4	C6	Perfluoroalkyl carboxylic acids (PFCAs)
Perfluoro-1-hexanesulfonic acid	PFHxS	3871-99-6	C6	Perfluoroalkane sulfonic acids (PFSAs)
Perfluoro-n-nonanoic acid	PFNA	375-95-1	C9	Perfluoroalkyl carboxylic acids (PFCAs)
Perfluoro-1-nonanesulfonic acid	PFNS	98789-57-2	C9	Perfluoroalkane sulfonic acids (PFSAs)
Perfluoro-n-octanoic acid	PFOA	335-67-1	C8	Perfluoroalkyl carboxylic acids (PFCAs)
Perfluoro-1-octanesulfonic acid	PFOS	1763-23-1	C8	Perfluoroalkane sulfonic acids (PFSAs)
Perfluorooctane sulfonamide	PFOSA	754-91-6	C8	Perfluoroalkane sulfonamides (FASAs)
Perfluoro-n-pentanoic acid	PFPeA	2706-90-3	C5	Perfluoroalkyl carboxylic acids (PFCAs)
Perfluoro-1-pentanesulfonic acid	PFPeS	630402-22-1	C5	Perfluoroalkane sulfonic acids (PFSAs)
Perfluoro-n-tetradecanoic acid	PFTreA	376-06-7	C14	Perfluoroalkyl carboxylic acids (PFCAs)
Perfluoro-n-tridecanoic acid	PFTriA	72629-94-8	C13	Perfluoroalkyl carboxylic acids (PFCAs)
Perfluoro-n-undecanoic acid	PFUnA	2058-94-8	C11	Perfluoroalkyl carboxylic acids (PFCAs)
11-chloroeicosafluoro-3-oxaundecane-1-sulfonic acid	11Cl-PF3OUdS	83329-89-9	C10	Per- and polyfluoroalkyl ether acids (PFEAs)
1H,1H,2H,2H-perfluoro-1-hexanesulfonic acid	4:2 FTS	27619-93-8	C6	Fluorotelomer sulfonic acids (FTSAs)
1H,1H,2H,2H-perfluoro-1-octanesulfonic acid	6:2 FTS	27619-94-9	C8	Fluorotelomer sulfonic acids (FTSAs)
1H,1H,2H,2H-perfluoro-1-decanesulfonic acid	8:2 FTS	27619-96-1	C10	Fluorotelomer sulfonic acids (FTSAs)
9-chlorohexadecafluoro-3-oxanone-1-sulfonic acid	9Cl-PF3ONS	73606-19-6	C8	Per- and polyfluoroalkyl ether acids (PFEAs)

Methods

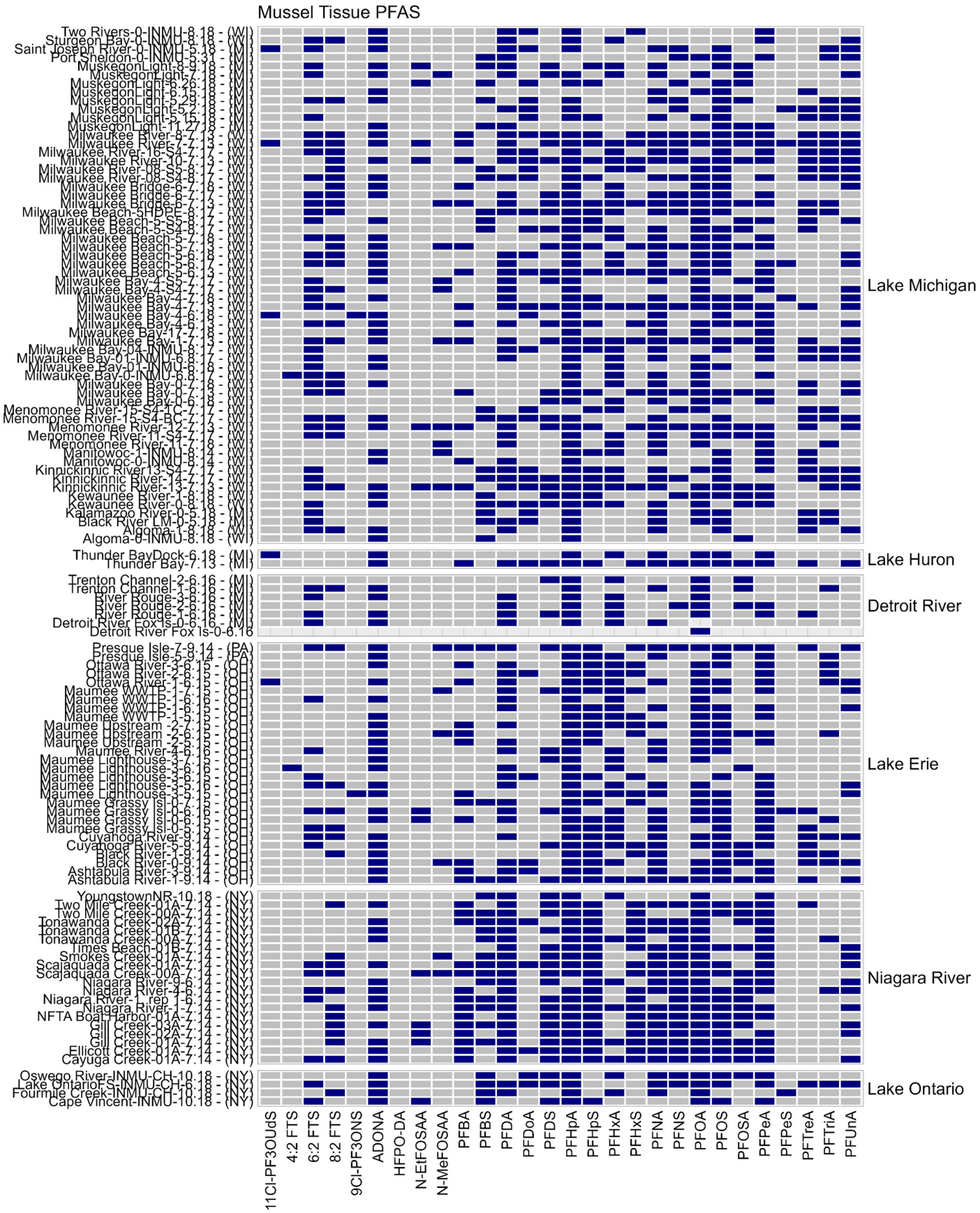

Fig. 3. Heat map depicting the presence ( ) and absence ( ) of all $\sum_{27}$PFAS compounds found in mussel tissue across the Great Lakes sampling locations during the 2013 - 2018 sampling period. Mussel sampling locations are arranged from west (Lake Michigan) to east (Lake Ontario), and are listed by their general location (associated riverine/lake region), state and month/year sampled.

2.5. Data Analysis

2.5.1. Land-use and point-source data

Due to differences in both US and Canadian land-use and land cover (LULC) spatial coverages, specifically for mussel sampling locations near the US and Canadian portion of the Great Lakes Basin, LULC estimates were created from the 2015 North American Land Change Monitoring System (NALCMS; https://www.mrlc.gov/data/north-american-land-change-monitoring-system) land cover raster layer at 30-meter. Generally, mussel sampling locations land-use estimates (percentages) were calculated by identifying and delineating appropriate study sites sub-watersheds/catchments based on the U.S. Geologic Survey (USGS) hydrologic unit code 10-digit watershed (HUC-10; http://water.usgs.gov/GIS/huc.html) classification system (Choy et al., 2017; Scully-Engelmeyer and Granek, 2022b; Siddiqui et al., 2020). Delineated study sites sub-watersheds/catchments (HUC-10) were then used to clip and extract LULC estimates from the NALCMS 30-meter raster layer for each study site. For simplification purposes, the NALCMS LULC classes were reclassified and aggregated into eight generic land-use categories (i.e., developed, agriculture, shrubs, barren lands, grassland, forest, wetlands and open-water; Fig. 4 and Table 2), following the Anderson Level I land-use classification scheme (Anderson et al., 1976). The reclassified land-use categories were further used to sort MWP sites into 5 exclusive land-use categories (i.e., undeveloped [0.2% - 46.7%], wetlands [0.27% - 51.5%], agriculture [0.12% - 59.7%], developed [0.07% - 97.8%], and open-water [0.18% - 100%]) based on each site dominant land-use categories (Table 2 and Table A3 [Appendix]).

The hydraulic unit code 10 (HUC-10) for sub-watersheds adjacent to mussel sampling locations, along with digital maps and orthoimagery datasets were also used to identify appropriate U.S. Environmental Protection Agency (USEPA) National Pollution Discharge Elimination System (NPDES) major and minor permitted WWTPs, CSOs, and 2010 U.S. Census Bureau population and demographic data at the block-group level. Additional site and sub-watershed WWTP and CSO data were generated from existing International Joint Commission (IJC) information on Great Lakes WWTPs (Laitta, 2016), and the USEPA's Enforcement and Compliance History Online (ECHO) facility program (ECHO, 2022). Study site location and proximity to individual USEPA non-permitted and permitted NPDES facilities were determined through Geographic Information System (GIS) analysis using ArcMap 10.8 software (ESRI, Inc).

Table 2. Great Lakes mussel study sites NALCMS land-use and land cover classification scheme, and designated land-use categories. Additional information on mussel sampling locations land-use category estimates (%) is provided in Table A3 (Appendix).

North American Land-use Classification (Groups)	Reclassified NALCMS Land-use and land cover categories	MWP Site Land-use and land cover categories
17 - Urban and Built-up	Developed	Developed
8 - Temperate or sub-polar shrubland 11 - Sub-polar or polar shrubland-lichen-moss	Shrubs	Undeveloped
10 - Temperate or sub-polar grassland 12 - Sub-polar or polar grassland-lichen-moss	Grassland	Undeveloped
15 - Cropland	Agriculture	Agriculture
16 - Barren lands	Barren Lands	Undeveloped
1 - Temperate or sub-polar needleleaf forest 5 - Temperate or sub-polar broadleaf deciduous forest 6 - Mixed Forest	Forest	Undeveloped
14 - Wetland	Wetlands	Wetlands
18 - Water	Open-water	Open-water

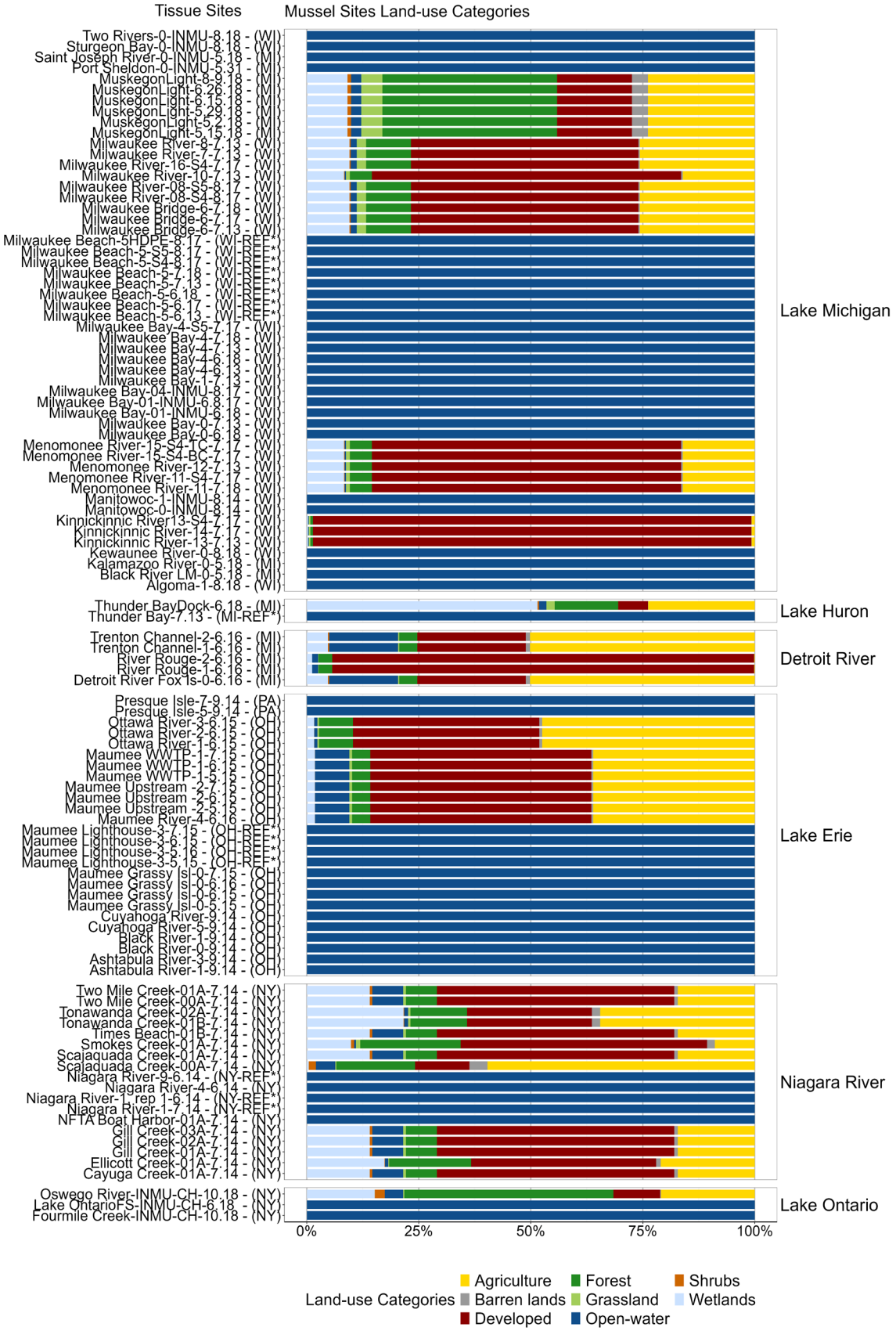

Fig. 4. Great Lakes mussel sampling locations predominant NALCMS land-use category (agriculture, barren, developed, grassland, forest, shrubs, wetlands and open-water) estimates (%). Sampling locations including sampled reference sites (e.g., REF*) are arranged from west (Lake Michigan) to east (Lake Ontario), and are listed by their general location (associated riverine/lake region), state and month/year sampled, which corresponds with mussel study sites information provided in Table A1 (Appendix). Additional information on MWP sites and their adjacent HUC-10 sub-watersheds land-use categories and estimates are provided in Table A3 (Appendix).

2.6. Statistical Analysis

Statistical analyses were conducted using non-parametric Kruskal-Wallis tests, followed by pairwise comparisons using Wilcoxon rank sum test and Dunn Kruskal-Wallis multiple comparison post hoc test ($p < 0.05$), with Benjamini-Hochberg (BH) method. Spearman's (non-parametric) rank correlation (ρ) analysis was used to explore and investigate the relationship among individual PFAS compounds, as well as between PFAS compound concentrations and other study sites environmental variables including site land-use categories, site population estimates, point-sources (WWTPs and CSOs), and site wastewater parameters. Spearman's (non-parametric) rank correlation (ρ) analyses were conducted using the R statistical software (R version 4.0.2; RCore Team, 2020). Random forest (RF) unsupervised classification was used to find patterns in PFAS presence/absence data, as well as characterize the relationship between PFAS concentration and study sites land-use and land cover estimates. RF classification techniques were conducted using the R statistical software (R version 4.0.2; RCore Team, 2020), with the "*randomForest*" package for unsupervised RF classification, followed by cluster analysis which was used to group the RF classification results into distinct clusters. The number of clusters were determined using the gap statistic and Mclust package (Fraley et al., 2012). In addition, principal components analysis (PCA) and hierarchical clustering were also used to group mussel sampling locations with statistically distinct PFAS composition and concentration profiles. Finally, data summaries including descriptive statistics for PFAS compounds measured in dreissenid mussel tissue are provided and organized by compounds magnitude and environmental occurrence, sampling location (inshore and offshore), major discharge-types, and land-use categories.

2.7. PFAS Ecological Risk

The ecological risks posed by PFAS compounds measured in dreissenid mussels (> MDLs) were evaluated using ecotoxicity data and tissue threshold values including predicted no-effect concentration (PNEC) for aquatic biota (e.g., mollusc), and the hazard quotient (HQs) method. As shown in several studies (Barron et al., 2021; Carere et al., 2021; Sardiña et al., 2019b; Sinclair et al., 2020; Wang et al., 2021), PNEC threshold values are widely used in ecological risk assessment to characterize contaminant concentration levels in various environmental matrices. Information on PFAS toxicity and $PNEC_{Tissue}$ threshold values were obtained from the NORMAN ECOTOX database (https://www.norman-network.com/nds/ecotox/lowestPnecsIndex.php), the USEPA ECOTOXicology knowledgebase (ECOTOX) database (https://cfpub.epa.gov/ecotox), PFAS-Tox Database (https://pfastoxdatabase.org/), the Ecological Structure Activity Relationships (ECOSAR) Predictive Model, and published sources. The NORMAN ECOTOX database PFAS $PNEC_{Tissue}$ values for freshwater biota is summarized in Table A6 (Appendix). The hazard quotient (HQs) values used in this study to evaluate the ecological risks posed by individual PFAS compounds measured in dreissenid mussels (> MDLs) were derived using the following Equation (1);

$$HQ = \frac{MEC_{Tissue}}{PNEC_{Tissue}} \quad (1)$$

where; the PFAS environmental concentration (MEC_{Tissue}; ng/g wet weight) was divided by the predicted no-effect concentration value ($PNEC_{Tissue}$; µg/kg wet weight; Table A6 [Appendix]), to obtain the HQ threshold values for PFAS compounds measured in mussels at each Great Lakes sampling location. The ecological risks associated with PFAS compounds measured in dreissenid mussels were categorized as follows; HQ < 0.01, unlikely to pose risk or very low risk; HQ < 0.1, low risk or pose minimal adverse effects; HQ > 0.1, medium or moderate risk; HQ > 1, high risk or elevated adverse effects (e.g., sublethal effects and apical endpoints; Sardiña et al., 2019b). The methods used in the present study to establish mussel tissue PFAS $PNEC_{Tissue}$ threshold values and PFAS HQ risk scores, follows those from previously published studies (Blair et al., 2013; Carere et al., 2021b; Hull et al., 2015; Ng et al., 2022; Zhang et al., 2023).

Methods

Credit: NOAA Great Lakes MWP


Credit: NOAA Great Lakes MWP


Credit: NOAA Great Lakes MWP

Credit: NOAA Great Lakes MWP

Results & Discussion

Credit: NOAA Great Lakes MWP

3.0. Results & Discussion

Comprehensive PFAS measurements within the Great Lakes inshore river-tributary-harbor complexes, lake nearshore, and lake offshore zones were conducted to aid in identifying land-use gradients, and other important environmental pathways controlling PFAS loading and distribution at Great Lakes MWP sampling locations. This study also addresses the magnitude and environmental occurrence of PFAS compounds measured in dreissenid mussels, with the aim of highlighting the complex nature of these contaminants detected in the Great Lakes Basin. We further discuss the spatial distribution and composition profile of these compounds as they are detected in mussel tissue basin-wide, at various point and non-point/diffuse sources, and at predominant MWP site land-use categories/gradients. PFAS compound concentrations are provided in summary tables, bar charts, and site concentration tables. The results presented in this report also serves as an initial assessment to characterize various parent PFAS compounds, their precursors, and compound groups that had the highest probability of being detected in dreissenid mussel tissue basin-wide during the 2013-2018 sampling period. Follow-up and comparative studies are also discussed in this report, in an effort to prioritize and identify appropriate PFAS congeners, and PFAS groups to be monitored in the future. Thus, the results and information provided in this report, is presented with the objective of providing the most efficient use of resources that can be used to support NOAA/NCCOS and Great Lakes management decisions and measures in reducing and abating the continued occurrence of PFAS compounds in stressed Great Lakes aquatic environments.

3.1. PFAS Occurrence and Concentration

The concentrations (min, median, mean, and max) and detection frequency (DF) of individual ∑PFAS analytes measured in mussel tissue is summarized in Table 3. Of the 28 $\sum_{28}$PFAS analyzed in this study, 19 compounds were detected at least once in dreissenid mussels above their method detection limit (> MDLs), with $\sum_{19}$PFAS concentrations ranging from 0.064 to 4.73 ng/g (wet weight). PFAS compounds quantified in mussel tissue with concentrations below method detection limit (< MDLs) were recorded as zero (0), and removed from further discussion in this study. As shown in Fig 5A and table 3, among the $\sum_{19}$PFAS compounds measured above > MDLs, perfluoro-n-tetradecanoic acid (C_{14}-PFTreA) was detected at the highest mean concentration in mussel tissue (mean: 1.31 ng/g wet weight). Perfluorooctane sulfonamide (C_8-PFOSA), a long-chained perfluoroalkane sulfonamide (FASAs) compound (a perfluorooctane sulfonate [PFOS] precursor; Xuan et al., 2024), was also detected at high mean concentration in mussel tissue (1.28 ng/g wet weight), followed by PFBA (0.763 ng/g wet weight), PFDoA (0.75 ng/g wet weight), PFTriA (0.722 ng/g wet weight), PFPeS (0.682 ng/g wet weight), PFOS (0.671 ng/g wet weight), and the precursor N-MeFOSAA (0.516 ng/g wet weight; Fig. 5A). Similar or higher concentrations were observed in our study, compared to PFAS results detected in tree swallows (*Tachycineta bicolor*) from northeastern Michigan and Milwaukee estuary, Wisconsin (Custer et al., 2019; Custer et al, 2024), oysters in a temperate macrotidal estuary (Gironde, SW France; Munoz et al., 2017), bivalves along the Korean coast (Lee et al., 2020), and shellfish collected along the English Channel, Atlantic and Mediterranean coasts of France (Munschy et al., 2019). Interestingly, of the two most common and studied PFAS compounds, PFOS (4.73 ng/g wet weight) was detected several magnitudes higher than PFOA (0.208 ng/g wet weight) in mussel tissue. Equally important, PFOS concentrations reported in this study (0.078 - 4.73 ng/g wet weight), were shown to be higher than previously reported for zebra mussels in the Great Lakes (2.4 - 3.1 ng/g wet weight; Kannan et al., 2005).

Overall, approximately 58% of the PFAS compounds quantified in mussel tissue were measured at mean concentrations ranging from 0.09 - 0.441 ng/g wet weight (Table 3), which is indicative of either low uptake or low bioaccumulation potential of these contaminants, likely resulting from low affinity binding (e.g., reversible uptake) occurring in dreissenid mussels (Barber et al., 2023; Munoz et al., 2017). Interestingly, two long-chained ($n \geq C_{10}$–C_{11}) PFAS compounds, 8:2 FTS (Fluorotelomer sulfonic acid), and 11Cl-PF3OUdS (a replacement compound, and a minor component of F-53BS; also known as 8:2 Cl-PFESA; Awad et al, 2020), were also measured in mussel tissue at low concentrations (range, 0.136 - 0.347 ng/g wet weight; Table 3). The detection of the 8:2 FTS precursor compound was recently reported in Great Lakes Bald Eagle eggs (*Haliaeetus leucocephalus*; Wu et al., 2020), at concentrations similar or higher than those detected in mussel tissue. However, to date, limited information exists on the concentrations of 8:2 FTS, and 11Cl-PF3OUdS detection in lower aquatic organisms (i.e., dreissenid mussels) in the Laurentian Great Lakes. To the best of our knowledge, this study is the first to report the detection of the emerging novel PFAS alternatives N-MeFOSAA (C_{11}), 8:2 FTS (C_{10}), and 11Cl-PF3OUdS (C_{10}) PFAS compounds in Great Lakes dreissenid mussels.

In regards to PFAS environmental occurrence, PFDoA (34%) > PFBA (38%) > PFDS (44%) > PFOS (76%) were among the PFAS compounds detected frequently (DF > 30%) in mussel tissue during the 2013-2018 sampling event (Table 3). Our results were consistent with prior studies (George et al., 2023c; Kannan et al., 2005; Stahl et al., 2014), which found PFOS to be the most frequently detected PFAS in Great Lakes aquatic biota (e.g., fish). The frequent detection of these PFAS contaminants in mussel tissue might reflect their historical use, as well as the high uptake and bioaccumulation of these

legacy and long-chained PFAS homologues in mussels (Gomis et al., 2015; Koch et al., 2019). Compositionally, among the PFAS groups assessed in mussel tissue samples, the composition profile for PFCA compounds ($C_nF_{2n+1}COOH$) were higher in mussel tissue, compared to PFSA compounds ($C_nF_{2n+1}SO_3H$). Overall, both PFAS groups accounted for 42.1% and 36.8% of the total PFAS measured (> MDLs) in mussel tissue samples (Fig. 6 and Table 3). These PFAS groups (PFCA and PFSA) were followed by perfluoroalkane sulfonamido acetic acids (FOSAAs), per- and polyfluoroalkyl ether acids (PFESAs), perfluoroalkane sulfonamide (FASAs), and fluorotelomer sulfonic acid (FTSAs) PFAS groups. As shown in Fig. 5B, FASAs (used primarily in raw materials for surfactant and surface protection products; Buck et al., 2011) and PFCAs (primarily used as water, oil, and grease repellents, and also as surfactants and surface treatment agents; Longpré et al., 2020), were among the PFAS groups observed at the highest mean concentration in mussel tissue (1.28 ng/g wet weight and 0.681 ng/g wet weight).

Overall, long-chained ($n \geq C_7$–C_{11}, C_{12}, C_{13} and C_{14}) PFAS homologues were detected ≈ 2 times higher in mussel tissue, compared to short-chained ($n \geq C_4$–C_5, and C_7) PFAS homologues assessed in this study. In particular, long-chained PFCAs ($n \geq 7$; Li et al., 2021) and long-chained PFSAs ($n \geq 6$; Li et al., 2021) accounted for 31.6% and 21.1% of the total PFAS compounds measured (> MDLs) in mussel tissue, with mean concentrations ranging from 0.132 - 1.31 ng/g (wet weight) to 0.106 - 0.671 ng/g (wet weight), respectively. As shown in similar studies, long-chained PFAS compounds dominance in mussels could be attributed to PFCAs and PFSAs bioaccumulation capacity (i.e., rate of uptake exceeds the rate of depuration; BAF > 1 if $K_{uptake} > K_{depuration}$; Giesy et al., 2006), and the binding potential of long-chained PFAS, compared to short-chained PFAS compounds (Byns et al., 2024; Goodrow et al., 2020). Comparatively, with the exception of PFBA (C_4; perfluoro-n-butanoic acid), short-chained PFAS groups were also detected less frequently in mussel tissue samples. This is likely attributed to the physico-chemical properties of short-chained PFAS compounds (Lee et al., 2020; Li et al., 2020), as evidenced by their high-water solubility and relatively low Log K_{OW} values (≤ 4; Table A2, Appendix).

Of the short-chained PFAS groups assessed in this study, the short-chained PFCA homologues ($C_4 \geq n \leq C_7$) were detected at higher mean concentrations in mussel tissue (mean range; 0.199 - 0.763 ng/g wet weight), compared to short-chained PFSA homologues ($C_4 \geq n \leq C_5$; mean range: 0.09 - 0.682 ng/g wet weight; Table 3). Elevated short-chained PFCA and PFSA composition and concentration levels detected in mussel tissue in this study, likely reflects the production/voluntary phase-out and transition from long-chained PFAS compounds (Brendel et al., 2018), resulting in increased use and emission of short-chained replacement compounds within the Great Lakes aquatic systems. Increased short-chained PFAS compounds use and emission within the Great Lakes aquatic environments, could eventually translate into elevated short-chained PFAS levels detected at surrounding mussel sampling locations, and in mussel tissue (Koban et al., 2024b). Similar to our study, prior bivalve studies have suggested the bioaccumulation of short-chained PFAS compounds in mussel tissue, was attributed to elevated PFAS composition and concentrations in surrounding surface water column (Teunen et al., 2021b). Overall, of the short-chained PFCAs detected in mussel tissue, PFBA (C_4: a replacement PFAS compound; Giffard et al., 2022), was measured at the highest mean concentration (0.763 ng/g wet weight), followed by PFPeS (C_5: 0.682 ng/g wet weight; Table 3). Of equal importance, even-carbon chain (C_4–C_8, and C_{10}) PFSA compounds concentration was higher in mussel tissue (range; 0.126 - 4.73 ng/g wet weight), compared to even-carbon chain (C_4–C_8, C_{12}, and C_{14}) PFCA compounds concentration (range; 0.208 - 3.02 ng/g wet weight) measured in mussels during the 2013-2018 sampling period.

To date, information and data on the bioaccumulation potential of short-chained PFCA and PFSA compounds in the Great Lakes lower trophic-level aquatic organisms are limited. The threat of these new and emerging short-chained replacement compounds necessitates a full understanding of their environmental fate and apical endpoints before population effects becomes apparent across the Great Lakes food-web (Kimbrough et al., 2013). Given this, further research is required to determine the bioaccumulation potential of these PFAS compounds to lower trophic-level benthic organisms and communities across the Great Lakes food-web.

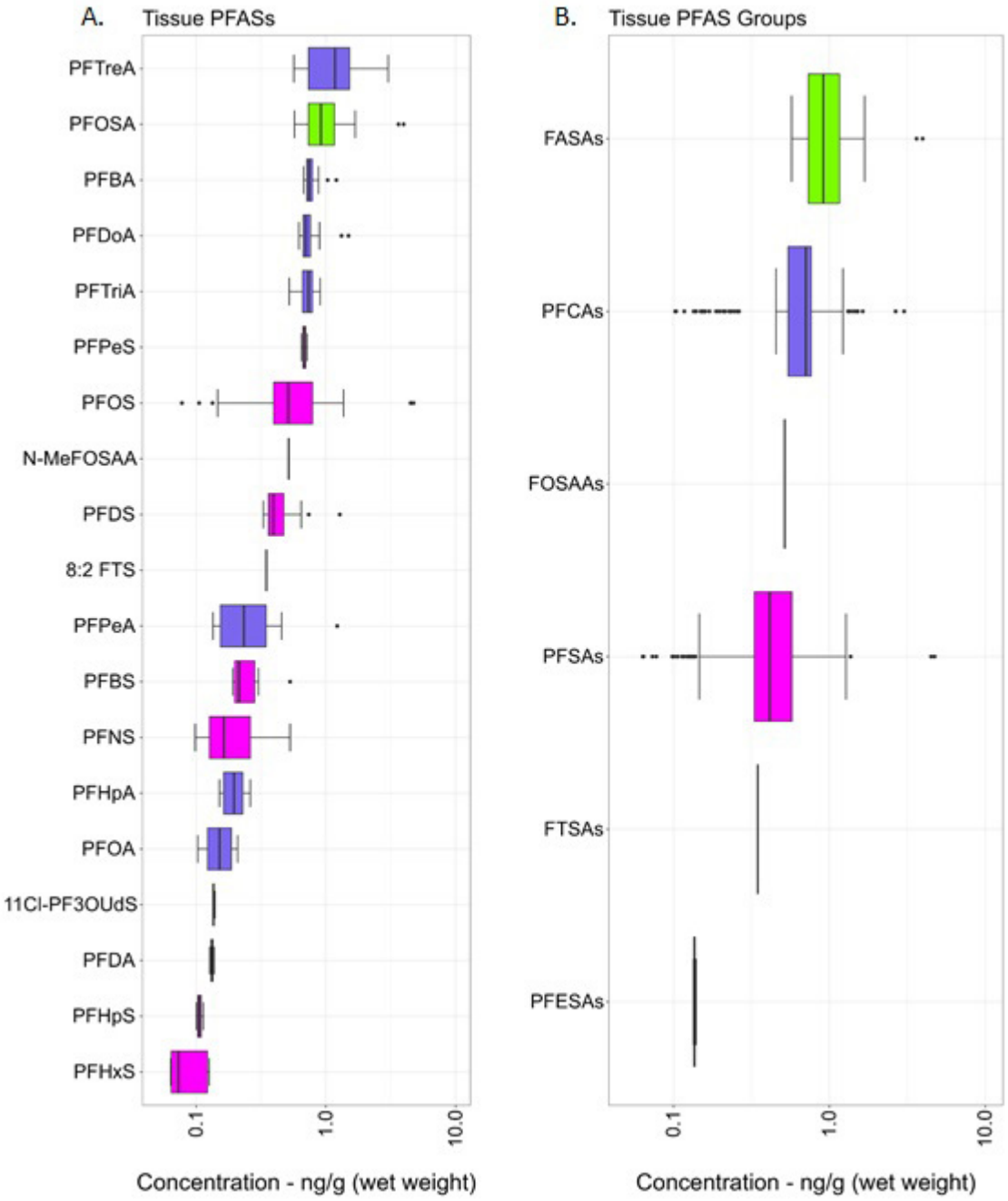

Fig. 5. Boxplots showing $\sum_{19}$PFAS compound concentrations (log ng/g wet weight) measured (> MDLs) in dreissenid mussels sampled between 2013-2018. Figure A. depicts concentrations for individual compounds in descending order based on highest to lowest mean concentrations, while Figure B. groups the same compounds and depicts PFAS concentration summarized by PFAS groups in descending order based on highest to lowest mean concentrations. The x axis represents difference in $\sum_{19}$PFAS compounds, and $\sum_{6}$PFAS compound groups concentration measured in dreissenid mussel tissue. Compounds detected below < MDLs in mussel tissue include: ADONA (4,8-dioxa-3H-perfluorononanoic acid), PFHxA (Perfluoro-n-hexanoic acid), PFNA (perfluorononanoic acid), N-EtFOSAA (N-Ethylperfluorooctanesulfonamidoacetic acid), PFUnA (Perfluoro-n-undecanoic acid), 4:2 FTS (1H,1H,2H,2H-perfluoro-1-hexanesulfonic acid), 6:2 FTS (1H,1H,2H,2H-perfluoro-1-octanesulfonic acid), and 9Cl-PF3ONS (9-chlorohexadecafluoro-3-oxanone-1-sulfonic acid).

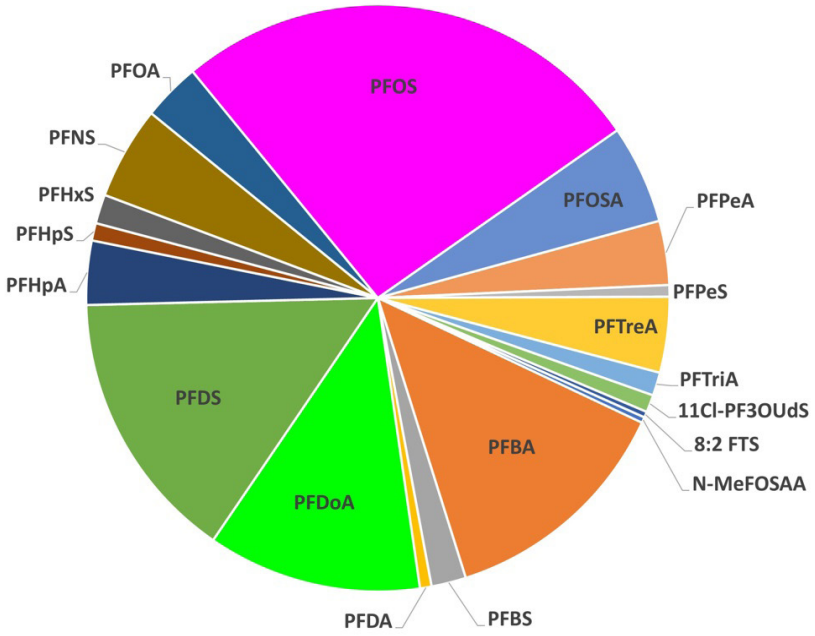

Fig. 6. Relative distribution of $\sum_{19}$PFAS compounds recorded in mussel tissue samples above detection limit (> MDL) between 2013-2018 sampling period.

Table 3. Summary statistics for $\sum_{19}$PFAS compounds and their concentrations (frequency, standard deviation [stdev], minimum, median, mean, and maximum; ng/g wet weight [ww]) measured in dreissenid mussels (quagga/zebra; *Dreissena spp.*) tissue above method detection limit (> MDLs) across Great Lakes MWP sites between 2013-2018. Concentrations below < MDLs were changed to zero.

PFAS Analytes	CASRN #	(n)	Stdev	Frequency	MDL	Min	Median	Mean	Max
				(%)	ng/g ww	ng/g ww	ng/g ww	ng/g ww	ng/g ww
N-MeFOSAA	2355-31-9	1	0	1	0.5	0.516	0.516	0.516	0.516
PFBA	375-22-4	41	0.096	38	0.093	0.673	0.741	0.763	1.20
PFBS	375-73-5	6	0.131	6	0.168	0.192	0.214	0.275	0.529
PFDA	335-76-2	2	0.007	2	0.124	0.128	0.132	0.132	0.137
PFDoA	307-55-1	37	0.174	34	0.127	0.62	0.703	0.75	1.49
PFDS	2806-15-7	47	0.152	44	0.093	0.329	0.394	0.441	1.28
PFHpA	375-85-9	11	0.039	10	0.15	0.151	0.196	0.199	0.261
PFHpS	375-92-8	3	0.007	3	0.088	0.1	0.105	0.106	0.113
PFHxS	3871-99-6	5	0.032	5	0.063	0.064	0.073	0.09	0.126
PFNS	98789-57-2	16	0.143	15	0.098	0.098	0.163	0.223	0.529
PFOA	335-67-1	10	0.039	8	0.094	0.103	0.151	0.153	0.208
PFOS	1763-23-1	82	0.685	76	0.066	0.078	0.513	0.671	4.73
PFOSA	754-91-6	17	0.995	16	0.5	0.573	0.914	1.28	3.97
PFPeA	2706-90-3	11	0.315	10	0.13	0.135	0.234	0.336	1.22
PFPeS	630402-22-1	2	0.05	2	0.5	0.647	0.682	0.682	0.718
PFTreA	376-06-7	13	0.771	12	0.5	0.566	1.18	1.31	3.02
PFTriA	72629-94-8	4	0.157	3	0.5	0.522	0.731	0.722	0.903
11Cl-PF3OUdS	83329-89-9	3	0.003	3	0.133	0.134	0.136	0.136	0.139
8:2 FTS	27619-96-1	1	0	1	0.21	0.347	0.347	0.347	0.347

3.2. Basin-wide PFAS Summary

A summary of $\sum_{19}$PFAS compounds environmental occurrence and magnitude measured (> MDLs) in mussel tissue basin-wide from sampling locations in Lakes Michigan, Huron, Erie, Ontario, and Detroit and Niagara River connecting channels are provided in Table 4 and Fig. 7. Of the 120 sampling locations examined in this study, PFAS was detected in dreissenid mussels above > MDLs at 106 sites. In addition, as shown in Figure 7, PFAS compounds basin-wide were mainly detected as complex mixtures, with 2 to 8 compounds detected in mussels at 76.4% (81/106) of the sites sampled between 2013 and 2018 (Table A4; Appendix). Similar to our study, several comparative studies have also shown PFAS compounds are occurring as complex mixtures in WWTP effluent (Baker et al., 2022b; George et al., 2023), sediment (Codling et al., 2018c; Xia et al., 2024), surface water (Baker et al., 2022b; Kleywegt et al., 2020), fish (George et al., 2023; Ren et al., 2023c), and bird tissue samples (e.g., tree swallows [*Tachycineta bicolor*]; peregrine falcon [*Falco peregrinus*]; Custer et al, 2024; Sun et al., 2020) across the Great Lakes region.

As shown in Fig. 7A and Table 4, the highest mean $\sum_{19}$PFAS concentrations were measured in mussels from sites sampled in Lake Michigan (mean; 0.719 ng/g wet weight), followed by sites sampled in the Niagara River (mean; 0.572 ng/g wet weight), Lake Erie (mean; 0.563 ng/g wet weight), Lake Ontario (mean; 0.536 ng/g wet weight), and the Detroit River (mean; 0.528 ng/g wet weight). However, concentration differences between the respective lakes and connecting channels were not statistically significant (Kruskal-Wallis; $p > 0.05$). Also shown in Fig 7B and Fig. 8, mussel tissue $\sum_{19}$PFAS composition followed similar patterns basin-wide, with the composition profile for sites sampled in Lake Michigan dominated by PFOS (26%), followed by PFDoA (17%), PFDS (12%), and PFBA (9.4%). Similarly, the composition profile for mussels sampled from sites in Lake Erie was dominated by PFOS (33%), followed by PFBA (15.7%), PFDS (11.4%), and PFPeA (8.57%). Mussels from other Great Lakes sampling locations including Lakes Huron and Ontario were primarily dominated by PFOS (40%), PFBS (28.6%), and PFDoA (28.6%). Likewise, PFDS (25%), PFBA (21.9%), PFOS (21.9%), and PFOSA (9.38%), were among the predominant $\sum_{19}$PFAS compounds examined in mussels from the Niagara and Detroit River connecting channels. Similar to our findings, studies conducted by De a Miranda et al. (2023b), and Ren et al. (2023), have also shown where PFOS was among the dominant fluorinated compound detected in Lake Michigan fishes (≈ 45 % in predator fish; ≈ 97 % in prey fish), and Lake Erie fishes (Yellow Perch: [*Perca flavescens*]; range: ≈ 50 - 90%). Overall, PFTreA, PFPeA, PFOSA, PFDoA, PFDS, PFBA, and PFOS were among the largest contributors to the total $\sum_{19}$PFAS composition measured in mussel tissue basin-wide (Fig 7B and Fig. 8). These seven $\sum_{7}$PFAS compounds also comprised approximately 36.8% (7/19) of the total $\sum_{19}$PFAS compounds detected (> MDL) in mussel tissue during the 2013-2018 study period.

In regards to individual $\sum_{19}$PFAS compounds frequency and magnitude, five $\sum_{5}$PFAS compounds namely PFBA (range: 0.724 - 1.20 ng/g wet weight), PFDS (range: 0.358 - 1.28 ng/g wet weight), PFDoA (range: 0.686 - 1.49 ng/g wet weight), PFTreA (range: 0.893 - 3.02 ng/g wet weight), PFOSA (range: 0.664 - 3.97 ng/g wet weight), and PFOS (range: 0.238 - 4.73 ng/g wet weight), were consistently measured at higher concentrations in mussel tissue basin-wide. Similar to our results, studies conducted by De Silva et al. (2011) and Point et al. (2021) also revealed PFOS was more bio-accumulative than other PFAS compounds assessed in Great Lakes tissue (i.e., fish) samples. Unlike the findings of De a Miranda et al. (2023b), and Ren et al. (2022a), lower PFOA composition and concentration (0.103 - 0.197 ng/g wet weight) was detected in mussels from sites sampled in Lake Michigan and Lake Ontario. Previous studies suggest, low PFOA detection and concentration detected in mussels is likely attributed to low to moderate PFOA input and entrainment of residual sediment (Remucal, 2019; Ren et al., 2022a), as well as PFOA low bioaccumulation potential and higher depuration rates in lower-trophic level organisms (De a Miranda et al., 2023b; Dong et al., 2023; Remucal, 2019 ; Ren et al., 2022a). Overall, our results for individual $\sum_{19}$PFAS mussel concentrations were similar or higher than concentrations measured in bivalves collected along the Korean coast (Lee et al., 2020), mussels and oysters from the Antifer, Seine estuary, and the Loire estuary and Gulf of Fos, France (Munschy et al., 2013; Munschy et al., 2019), oysters and mussels from the Pearl River Delta and Hong Kong (Zhao et al., 2014), and PFAS analyzed in marine organism tissues from Narragansett Bay, Rhode Island, and surrounding waters (Hedgespeth et al., 2023).

On average, short-chained ($C_4 \geq n \leq C_7$) $\sum_{5}$PFAS compounds concentration were detected < 3 times lower (range; 0.529 - 1.22 ng/g wet weight; Kruskal-Wallis; p-value < 0.05), when compared to long-chained ($n \geq C_7$–C_{14}) $\sum_{14}$PFAS concentrations measured in mussels basin-wide (0.347 – 4.73 ng/g wet weight; Fig. 10C). Our results suggest, the uptake and bioaccumulation capacity of short-chained ($C_4 \geq n \leq C_7$) PFAS homologues in mussel tissue might be slower, compared to long-chained ($n \geq C_7$–C_{14}) PFAS homologues uptake and bioaccumulation in mussel tissue. Studies conducted by Ren et al. (2022) and Wen et al. (2023) have suggested, short-chained PFAS compounds slow bioaccumulation capacity and uptake in aquatic biota, might be attributable to weaker interaction and bioaccumulation of short-chained PFAS homologues (i.e., decrease in PFAS uptake and attachment to biological molecules including proteins and phospholipids), relative to long-chained PFAS homologues uptake and attachment to biological molecules

in aquatic biota. George et al. (2023) and Wen et al. (2023) further demonstrated in their studies, unlike most persistent organic pollutants which are generally lipophilic, PFAS compounds are proteinophilic, with longer-chained PFAS homologues out competing shorter-chained PFAS homologues for transporters or peptides, thus developing stronger binding capacity with beta-lipoproteins (e.g., strong binding affinities and attraction for albumin in the blood), and liver fatty acid-binding proteins (e.g., strong protein-binding affinities, with fatty acid binding protein [FABP] potential in the liver; Ren et al., 2023). The above results further highlight the potential of long-chained and some short-chained PFAS compounds detected in mussel tissue to biomagnify through the Great Lakes food web, which is consistent with prior studies in the Great Lakes region (De a Miranda et al., 2023; George et al., 2023; Ren et al., 2022a).

Additional in-lake assessment revealed, the mean concentrations for PFAS compound groups measured (> MDLs) in mussels from sampling locations in Lake Michigan, were higher for long-chained C_{13}–C_{14} PFCA compounds (mean: 1.38 ng/g wet weight), compared to C_8-FASAs (mean: 1.10 ng/g wet weight), C_8–C_{12}-PFCAs (mean: 0.664 ng/g wet weight), C_8–C_{10}-PFSAs (mean: 0.645 ng/g wet weight), C_4–C_7-PFCAs (mean: 0.546 ng/g wet weight), and C_4–C_7-PFSAs (mean: 0.258 ng/g wet weight) PFAS groups (Table 5). Similar patterns were also observed for mussels sampled in Lake Erie, in which lake-wide mean concentrations were higher for C_8-FASAs (mean: 2.50 ng/g wet weight), compared to C_{13}–C_{14}-PFCAs (mean: 0.685 ng/g wet weight), C_4–C_7-PFCAs (mean: 0.551 ng/g wet weight), C_8–C_{12}-PFCAs (mean: 0.509 ng/g wet weight), C_8–C_{10}-PFSAs (mean: 0.479 ng/g wet weight), and C_4–C_7-PFSAs (mean: 0.221 ng/g wet weight) compound groups. For other Great Lakes assessed in this study, C_4–C_7-PFCAs (mean: 0.747 ng/g wet weight), and C_8-FASAs (mean: 1.20 ng/g wet weight) were elevated in mussels from Lake Huron, while C_8–C_{10}-PFSA mean concentrations (mean: 0.682 ng/g wet weight) were elevated in mussels from Detroit River. For mussels sampled in the eastern Great Lakes region (i.e., Niagara River, and Lake Ontario), C_4–C_7-PFCAs (mean: 0.747 ng/g wet weight) and C_8-FASAs (mean: 1.20 ng/g wet weight) were detected at elevated mean concentrations in mussels from Niagara River, while C_8–C_{12}-PFCAs (mean: 0.533 ng/g wet weight), and C_8–C_{10}-PFSAs (mean: 0.863 ng/g wet weight) were greater in mussels from Lake Ontario (Table 5).

Between-lakes and connecting channels comparison revealed, summed $\sum_{19}$PFAS concentrations remained spatially heterogenous across mussel sampling locations (> MDLs = 106 sites), with summed $\sum_{19}$PFAS concentrations varying by several orders of magnitude between some sampling locations (range: 0.073 -9.83 ng/g wet weight; Fig 10B and Table A4 [Appendix]). Also shown in Fig. 9, and Fig. 10B, elevated $\sum_{19}$PFAS concentrations were primarily detected in mussels from sites sampled in Lake Michigan, compared to mussels sampled from other Great Lakes and connecting channels assessed in this study. In addition, as shown in Fig. 10B and Table A4 (Appendix), cumulative $\sum_{19}$PFAS concentrations observed in mussel tissue basin-wide decreased in order of: Lake Michigan (range: 0.156 - 9.83 ng/g wet weight) > Lake Erie (range: 0.073 - 6.34 ng/g wet weight) > Niagara River (range: 0.399 - 5.38 ng/g wet weight) > Lake Ontario (0.229 - 2.54 ng/g wet weight) > Lake Huron (range: 0.238 - 1.92 ng/g wet weight) > Detroit River (range: 0.196 - 1.28 ng/g wet weight). Overall, mussels sampled in Lake Michigan (Kinnickinnic River: LMMB-13-S4-7.17, and Kalamazoo River: LMKZ-0-5.18), Lake Erie (Presque Isle: LEPB-7-9.14, and Black River: LEBR-0-9.14), and Niagara River (Two Mile Creek: NRTM-01A-7.14; Refer to Table A1 for definition and additional information on mussel site codes and acronyms), which are closer to larger population/urban centers, depicted the highest summed $\sum_{19}$PFAS concentrations (> 4.46 ng/g wet weight) across the 2013-2018 sampling period.

Similar to previous studies (Codling et al., 2018; Custer et al, 2024; Stahl et al., 2014; Ren et al., 2022), our basin-wide results depicted where patterns in elevated mussel PFAS contaminant body burden levels closely matched sites adjacent to urban rivers and tributaries, with larger population densities and industrial centers in Lakes Michigan, Erie, Ontario, and the Detroit and Niagara River connecting channels, compared to other sites sampled basin-wide in this study. Our results further suggest, input from local sources influenced by urban and industrial activities, are dominant emission sources and primary drivers of PFAS contamination at these sampling locations (Balgooyen and Remucal, 2022; Custer et al., 2024; Lin et al., 2021c; Remucal et al., 2019). Spearman's (ρ) rank correlation results further revealed several long-chained PFAS groups including $\sum_4$PFCAs (PFDA, PFTreA, PFDoA, PFOA, and PFTriA; Spearman's rho (ρ) = 0.371 – 0.888, $p < 0.05$), and $\sum_3$PFSAs (PFOS, and PFNS; Spearman's rho (ρ) = 0.373 – 0.540, $p < 0.05$) concentrations, were significantly correlated with mussel sampling locations population estimate (Fig. 11). Similarly, significant associations were found between the emerging PFAS long-chained C_{10}-8:2 FTS precursor (Spearman's rho (ρ) = 0.695; $p < 0.001$), and the short-chained C_7-PFHpA concentrations (Spearman's rho (ρ) = 0.720; $p < 0.001$), and mussel site population estimates (Fig. 11).

Results & Discussion

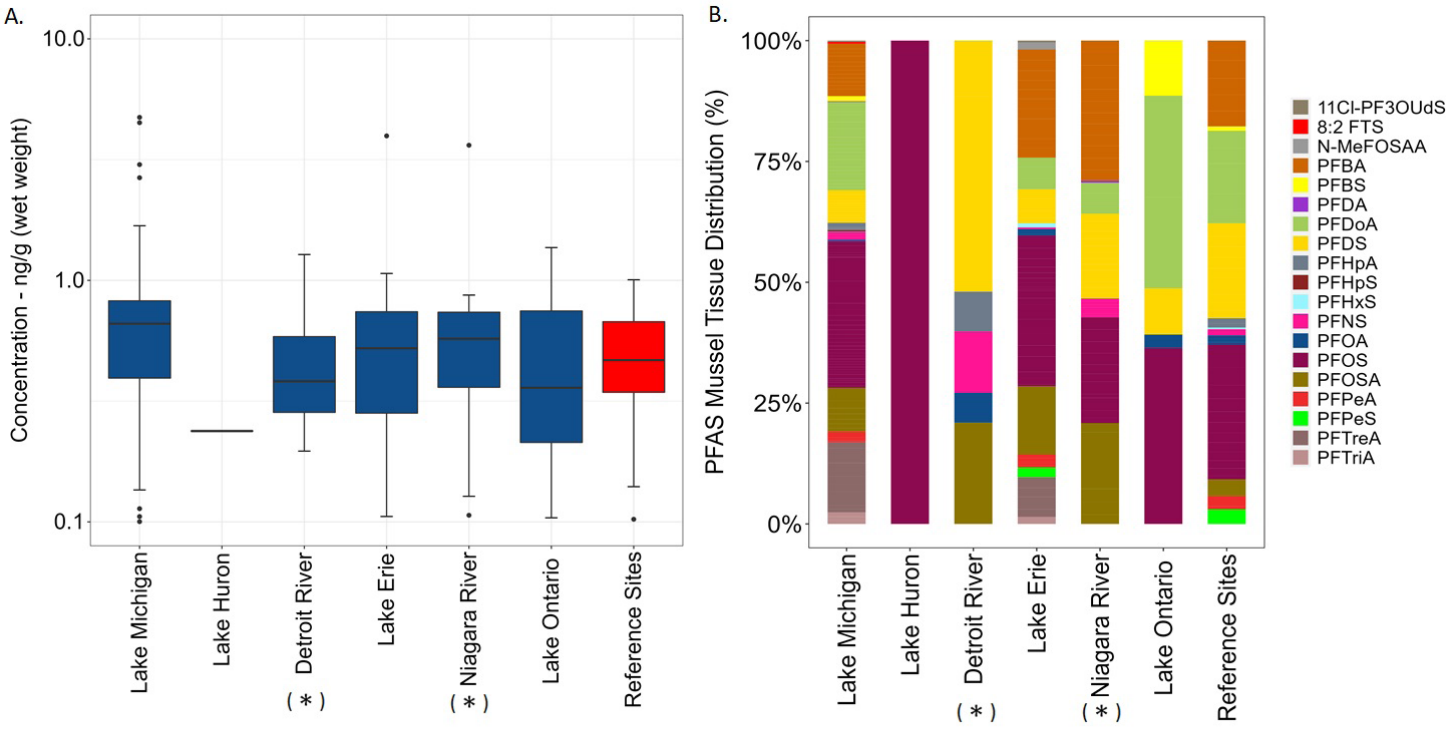

Fig. 7. A). Boxplots depicting ∑19PFAS concentration profile (ng/g wet weight) measured (> MDLs) in dreissenid mussels across Lakes Michigan, Huron, Erie, Ontario, and Detroit and Niagara River connecting channels (*) sampling locations between 2013-2018, and B). The percent composition (%) and relative distribution of ∑19PFAS compounds recorded basin-wide in mussel tissue during the 2013-2018 sampling event. On the x-axes, the corresponding lakes and connecting channels are ordered from left to right based on their geographical location within the Great Lakes Basin. Reference sites provides perspective to the relative ∑PFAS concentrations measured in mussel tissue during the 2013-2018 sampling event.

Table 4. Summary of ∑19PFAS concentrations (ng/g wet weight) measured (> MDLs) in dreissenid mussel tissue from Lakes Michigan, Huron, Erie, Ontario, and Detroit and Niagara River connecting channels (*) mussel sampling locations between 2013-2018. ∑19PFAS concentration (ng/g wet weight) summary also includes ∑19PFAS compounds measured in mussels from reference sites in Lakes Michigan, Huron, and reference sites sampled in western and eastern Lake Erie/Niagara River Basin. Reference sites provides perspective to the relative PFAS concentrations measured in mussel tissue sampled across Great Lakes mussel sampling locations during 2013-2018.

Category	(n)	Stdev	Min	Median	Mean	Max
Location			ng/g (ww)	ng/g (ww)	ng/g (ww)	ng/g (ww)
Lake Michigan	136	0.651	0.064	0.654	0.719	4.73
Lake Huron	1	0	0.238	0.238	0.238	0.238
Detroit River (*)	6	0.402	0.196	0.383	0.528	1.28
Lake Erie	63	0.519	0.064	0.522	0.563	3.97
Niagara River (*)	54	0.483	0.098	0.54	0.572	3.63
Lake Ontario	7	0.449	0.104	0.359	0.536	1.37
Reference Sites	45	0.23	0.073	0.46	0.477	1.01

Table 5. Summary of $\sum_{19}$PFAS compound group concentrations (ng/g wet weight) measured (> MDLs) in dreissenid mussels from Lakes Michigan, Huron, Erie, Ontario, and Detroit and Niagara River connecting channels (*) MWP sampling locations between 2013-2018. Mussel $\sum_{19}$PFAS group concentrations (ng/g wet weight) are arranged by lakes and connecting channels sampled basin-wide from west (Lake Michigan) to east (Lake Ontario).

				Min	Median	Mean	Max
Basin-wide Locations	PFAS Groups	(n)	Stdev	ng/g (ww)	ng/g (ww)	ng/g (ww)	ng/g (ww)
Lake Michigan	C10 – PFESAs	2	0.003	0.136	0.138	0.138	0.139
	C4–C7 PFSAs	8	0.219	0.064	0.156	0.258	0.647
	C10 – FTSAs	1	0	0.347	0.347	0.347	0.347
	C4–C7 PFCAs	30	0.343	0.14	0.687	0.546	1.22
	C8–C10 PFSAs	67	0.742	0.1	0.461	0.645	4.73
	C8–C12 PFCAs	32	0.29	0.103	0.676	0.664	1.49
	C8 – FASAs	8	0.323	0.695	1.01	1.10	1.68
	C13–C14 PFCAs	12	0.768	0.638	1.27	1.38	3.02
Lake Huron	C8–C10 PFSAs	3	0.103	0.152	0.238	0.249	0.358
	C8–C12 PFCAs	1	0	0.686	0.686	0.686	0.686
	C4–C7 PFCAs	1	0	0.724	0.724	0.724	0.724
Detroit River (*)	C8–C12 PFCAs	1	0	0.196	0.196	0.196	0.196
	C4–C7 PFCAs	1	0	0.261	0.261	0.261	0.261
	C8 – FASAs	1	0	0.664	0.664	0.664	0.664
	C8–C10 PFSAs	3	0.518	0.365	0.4	0.682	1.28
Lake Erie	C10 – PFESAs	1	0	0.134	0.134	0.134	0.134
	C4–C7 PFSAs	5	0.279	0.064	0.122	0.221	0.718
	C8–C10 PFSAs	32	0.261	0.078	0.45	0.479	1.07
	C8–C12 PFCAs	7	0.331	0.117	0.686	0.509	0.885
	C11 – FOSAAs	1	0	0.516	0.516	0.516	0.516
	C4–C7 PFCAs	17	0.251	0.135	0.69	0.551	0.789
	C13–C14 PFCAs	5	0.152	0.522	0.666	0.685	0.893
	C8 – FASAs	2	2.07	1.04	2.50	2.50	3.97
Niagara River (*)	C4–C7 PFSAs	1	0	0.192	0.192	0.192	0.192
	C8 – C10 PFSAs	40	0.205	0.098	0.387	0.412	0.818
	C8–C12 PFCAs	3	0.034	0.627	0.666	0.663	0.695
	C4–C7 PFCAs	14	0.047	0.693	0.744	0.747	0.859
	C8 – FASAs	6	1.20	0.573	0.749	1.20	3.63
Lake Ontario	C4–C7 PFSAs	2	0.022	0.199	0.214	0.214	0.229
	C8–C12 PFCAs	3	0.374	0.104	0.707	0.533	0.789
	C8–C10 PFSAs	2	0.713	0.359	0.863	0.863	1.37

Results & Discussion

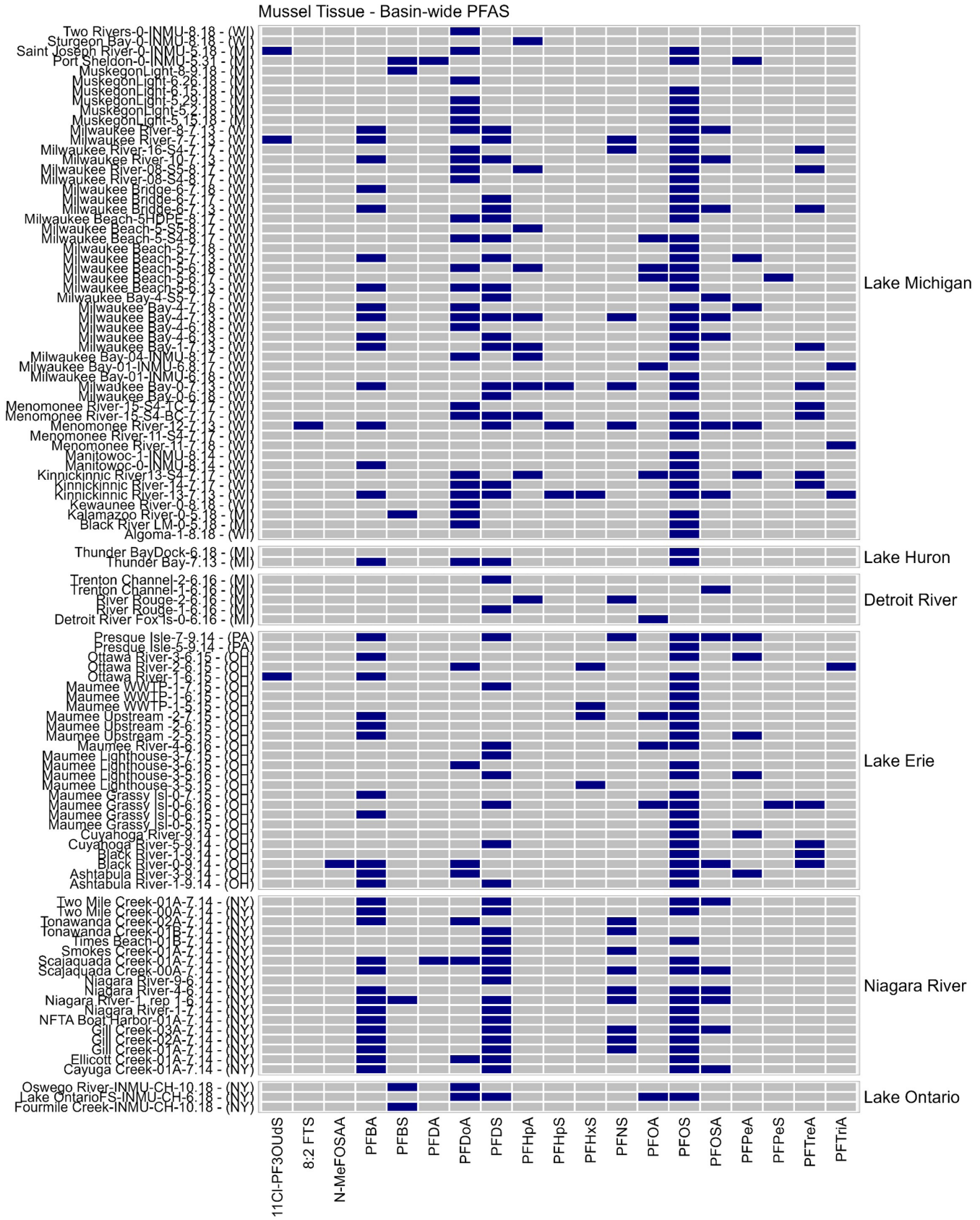

Fig. 8. Heat map depicting presence (■) and absence (■) for $\sum_{19}$PFAS compounds found in mussel tissue above detection limit (> MDLs) across basin-wide mussel sampling locations (Lakes Michigan, Huron, Erie, Ontario, and the Detroit and Niagara River connecting channels) during the 2013-2018 sampling period. Mussel sampling locations are arranged from west (Lake Michigan) to east (Lake Ontario), and are listed by their general location (associated riverine/lake region), state and month/year sampled.

Results & Discussion

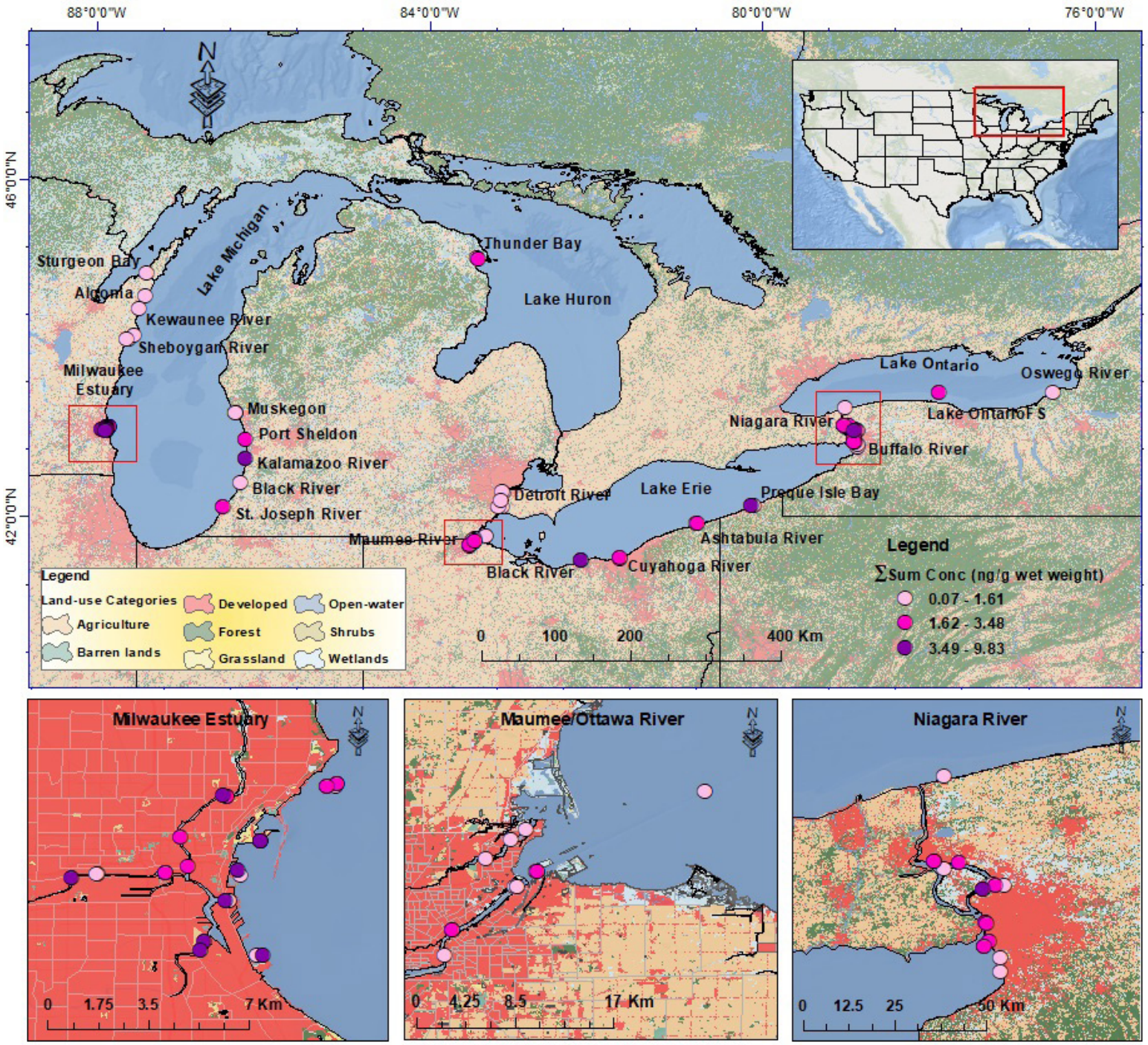

Fig. 9. Map depicting the spatial variation and distribution of mussel sampling locations with low (●), medium (●), and high (●) summed concentrations for $\sum_{19}$PFAS compounds measured in mussel tissue (> MDLs) across Lakes Michigan, Huron, Erie, Ontario, and Detroit and Niagara River connecting channel mussel sampling locations between 2013-2018. Some mussel sampling locations are shown to overlap due to the size of the circles. Additional information on summed $\sum_{19}$PFAS concentrations (ng/g wet weight) measured in mussel tissue across all sampled lakes and connecting channels (Michigan, Huron, Erie, Ontario, and Detroit and Niagara River) is provided in figure 9B, and Table A3 (Appendix).

Results & Discussion

Fig. 10. Barplots depicting A). mussel sampling locations predominant land-use category estimates (%), B), sum total $\sum_{19}$PFAS concentration (ng/g wet weight) measured (> MDL) in mussel tissue across the Great Lakes MWP sampling locations, and C), the concentration profile (%) and relative distribution of predominant $\sum_{19}$PFAS groups (long and short-chained homologues) detected in mussels from basin-wide Great Lakes and connecting channel sampling locations during 2013-2018 sampling event. Clusters 1-3 represents sites with low ( ), medium ( ), and high ( ) summed $\sum_{19}$PFAS concentrations. Mussel sampling locations are arranged from west (Lake Michigan) to east (Lake Ontario), and are listed by their general location (associated riverine/lake region), state and month/year sampled.

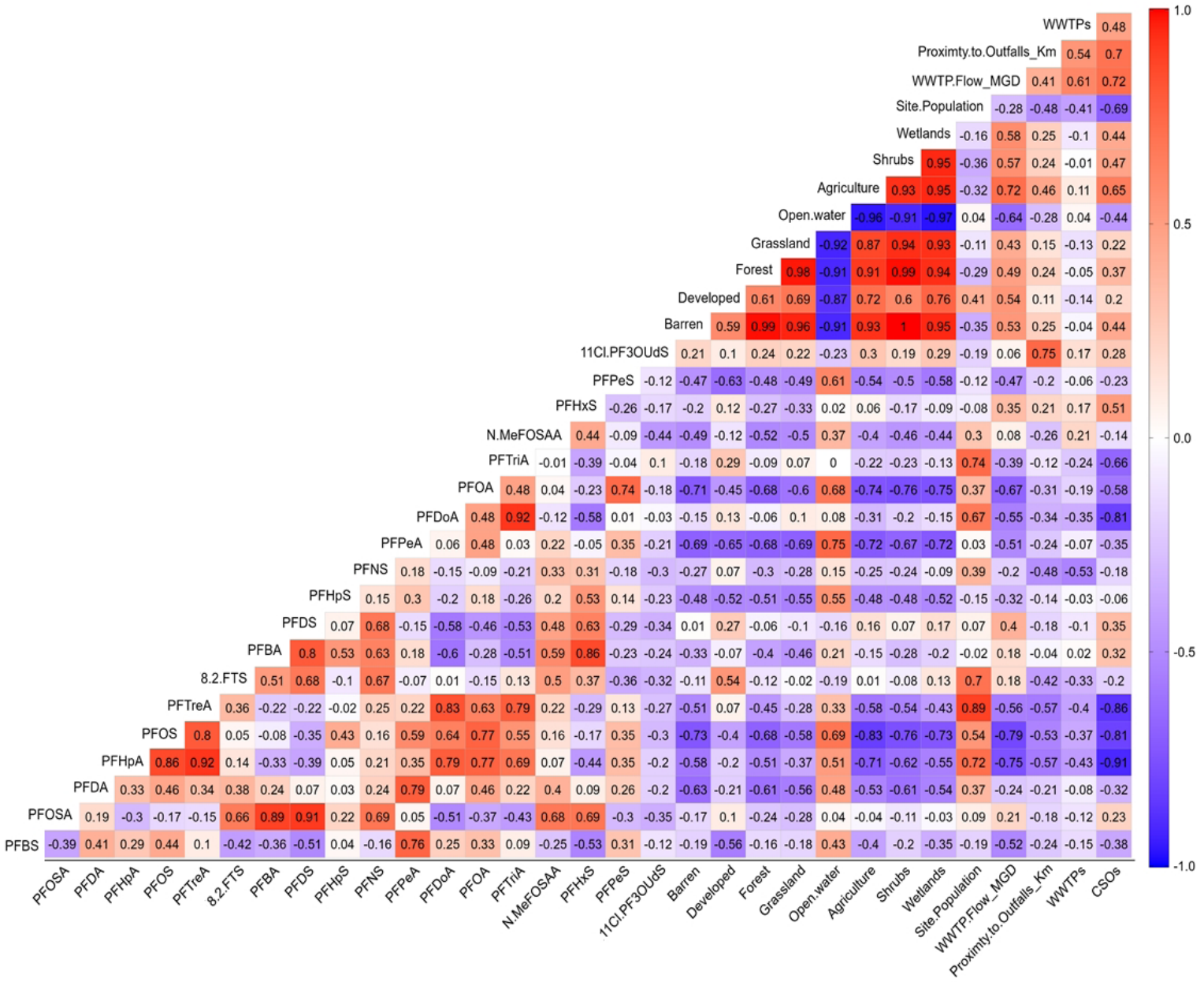

Fig. 11. Spearman's (ρ) correlation matrix depicting correlation coefficients measured between $\sum_{19}$PFAS compounds concentration (> MDL; ng/g wet weight), and mussel sampling locations land-use, and point source/wastewater parameters. High correlation between covariates is represented by the intense colors (e.g., red and blue colors), which indicates either strong positive or strong negative correlation ($p < 0.05$), between PFAS concentrations and mussel sampling locations environmental parameters. Additional information is provided in Table A5 (Appendix).

3.3. Basin-wide vs. Reference Sites PFAS Summary

Of the 19 $\sum_{19}$PFAS compounds measured above > MDLs, 12 $\sum_{12}$PFAS compounds (PFBA[C_4], PFBS[C_4], PFDoA[C_{12}], PFDS[C_{10}], PFHpA[C_7], PFHxS[C_6], PFNS[C_9], PFOA[C_8], PFOS[C_8], PFOSA[C_8], PFPeA[C_5], and PFPeS[C_5]) were detected in mussels from designated Great Lakes reference sites during the 2013-2018 sampling period (Fig. 12 and Table 6A). Overall, PFBA (DF = 28%), PFDoA (DF = 33%), PFDS (DF = 56%), and PFOS (DF= 67%), were among the $\sum_{12}$PFAS compounds frequently detected in mussels from offshore reference sites. The frequent detection of these PFAS compounds in mussels from offshore reference sites is indicative of several factors including PFAS continued input from localized urban water cycle and industrial sources (Lin et al., 2021; Remucal et al., 2019), PFAS compounds environmental physicochemical properties (e.g., high adsorption and aqueous solubility potentials; Point et al., 2021; Remucal et al., 2019), PFAS long range atmospheric transport and deposition (e.g., air–water exchange, wet deposition, and dry deposition; Cousins et al., 2022; Lin et al., 2021; Pfotenhauer et al., 2022; Xia et al., 2024), and the respective Great Lakes long hydraulic residence time, which act as important reservoirs and sinks for these PFAS compounds (Gewurtz et al., 2019; Lin et al., 2021; Remucal et al., 2019).

On average, $\sum_{12}$PFAS concentrations measured in mussels across sampled reference sites ranged from 0.073 to 1.01 ng/g (wet weight), with the short-chained C_4-PFBA compound measured at the highest mean concentration (0.762 ng/g wet weight), followed by PFOSA (0.733 ng/g wet weight), PFDoA (0.683 ng/g wet weight), PFPeS (0.647 ng/g wet weight), PFOS (0.499 ng/g wet weight), and PFDS (0.422 ng/g wet weight; Fig. 12 and Table 6A), respectively. However, differences in PFAS concentrations measured across mussel reference sites were not statistically significant (Kruskal-Wallis; $p > 0.05$). Overall, approximately 50% (6/12) of the PFAS compounds measured in mussels from designated reference sites were measured at relatively low concentrations (< 0.297 ng/g wet weight). The detection of PFAS compounds in mussels and other lower trophic-level organisms at environmentally low concentrations, and also as complex mixtures at Great Lakes off-shore zones remains poorly understood (Blair et al., 2013). Thus, the sub-lethal effects and biological endpoints resulting from PFAS low-level exposures in dreissenid mussels and other aquatic biota, may warrant additional monitoring and assessment of these emerging contaminants at offshore Great Lakes complexes.

Differences between basin-wide and reference sites PFAS concentrations were assessed to find spatial patterns and variation in mussel tissue magnitude and distribution. On average, mussel tissue PFAS concentrations varied between basin-wide and reference sites assessed in this study (Fig. 13; Table 6A and Table 6B), with some PFAS compounds varying between 1 and > 3 orders of magnitude. Interestingly, PFHpA, PFHxS, PFOA, PFBA, and PFPeS mean concentrations measured in mussels from designated offshore reference sites, were similar to chemical signatures observed in mussels from some inshore sampling locations. Overall, mussel tissue $\sum_{12}$PFAS concentrations measured across all designated reference sites decreased in order of: Lake Michigan (range: 0.103 - 1.01 ng/g wet weight) > Niagara River (range: 0.192 - 0.794 ng/g wet weight) > Lake Erie (range: 0.073 - 0.761 ng/g wet weight) > Lake Huron (range: 0.152 - 0.724 ng/g wet weight; Table 7). However, differences in PFAS concentrations measured in mussels from all sampled reference sites (Lake Michigan, Niagara River, Lake Erie, and Lake Huron) were not statistically significant (Kruskal–Wallis; $p > 0.05$). Additional reference site assessment revealed, the highest total $\sum_{12}$PFAS concentrations were measured in mussels from reference sites sampled in the eastern Lake Erie basin/Niagara River (Niagara River-1: [NRNF-1, rep 1-6.14] and Niagara River-1-7.14: [NRNF-1-7.14], followed by sites sampled in Lake Michigan/Milwaukee Estuary (LMMB-5-6.13, LMMB-5-6.18, and LMMB-5-S4-8.17) and western Lake Erie basin (Maumee Lighthouse: LEMR-3-5.16, and LEMR-3-6.15; Fig. 9 and Table A4 [Appendix]).

Overall, our results confirm PFAS compounds detected in mussels from lake nearshore and offshore (open lake) reference sites are similar in complexity and occurrence to other comparative studies (e.g., the USEPA's Great Lakes Fish Monitoring and Surveillance Program [GLFMSP]), that have targeted and examined PFAS compounds in offshore upper trophic-level fish populations throughout the Great Lakes Basin (Point et al., 2021). Our results further highlight the importance of biomonitoring programs such as the MWP, in sampling and detecting both legacy and emerging contaminants on a larger spatial scale at nearshore and offshore lake complexes. Despite some PFAS compound groups being detected at environmentally low concentrations across mussel reference sites, our data showed that these compounds are still measurable, and are bioaccumulating in the tissue of lower trophic-level organisms across the Great Lakes. Equally important, this study provides insight into the persistent nature of PFAS compounds detected in mussel tissue, and the level of contamination occurring at nearshore and offshore Great Lakes mussel sampling locations. From a biomonitoring perspective, our mussel PFAS data from lake nearshore and offshore reference sites, in conjunction with PFAS tissue data from other Great Lakes biomonitoring programs, can provide a better understanding of the trophic transfer of these legacy and emerging contaminants across the Great Lakes food-web (Edwards et al., 2024; Kimbrough et al., 2013).

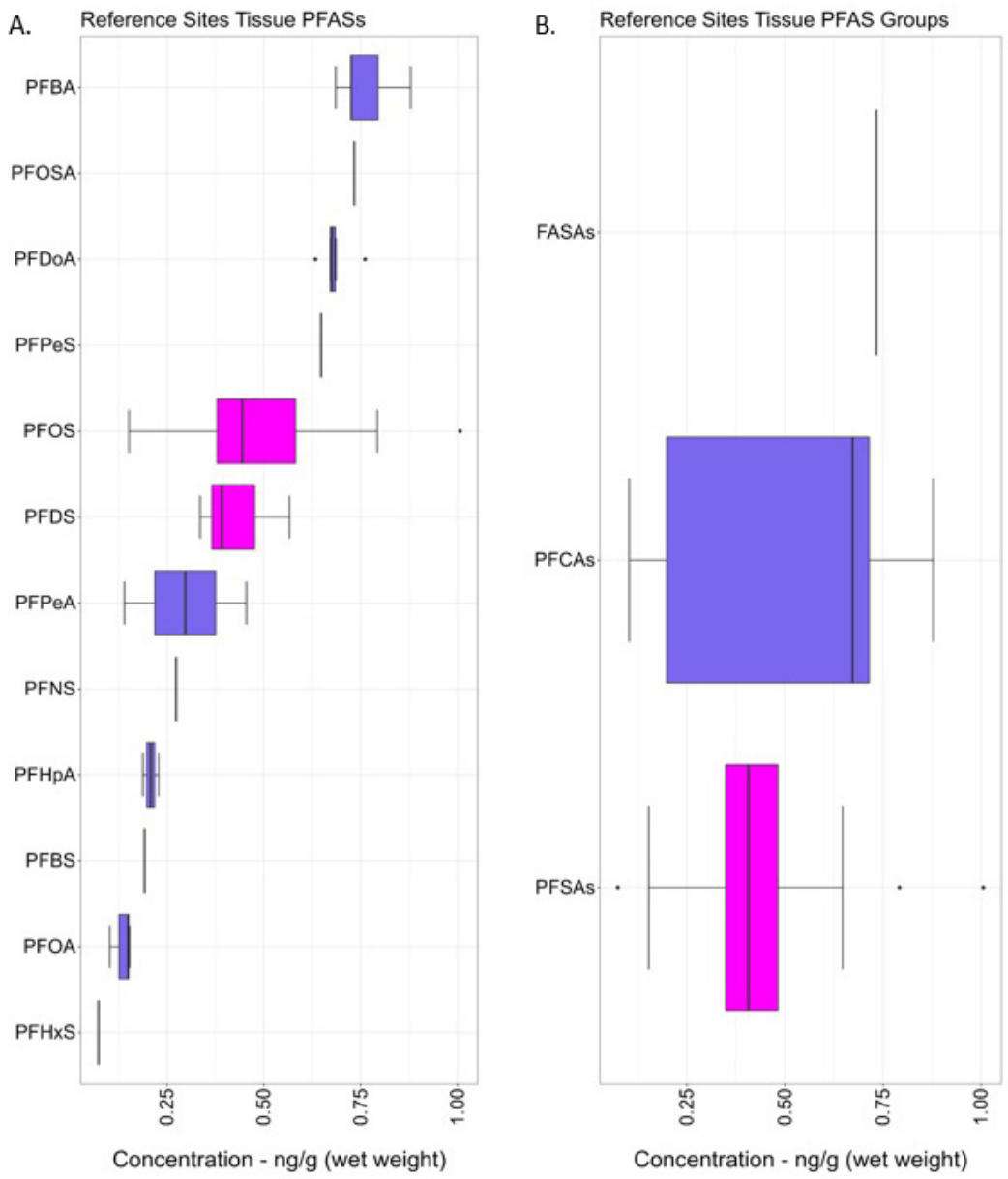

Fig. 12. Boxplots showing $\sum_{12}$PFAS compound concentrations (ng/g wet weight) measured (> MDLs) in dreissenid mussels sampled at designated reference sites between 2013 - 2018. Figure A) depicts mussel reference sites $\sum_{12}$PFAS concentrations summarized by individual compounds in descending order based on highest to lowest mean concentrations, while Figure B), groups the same compounds and depicts PFAS concentration summarized by PFAS groups in descending order based on highest to lowest mean concentrations. The x axis represents difference in $\sum_{12}$PFAS compounds and compound group concentrations quantified in dreissenid mussel tissue samples.

Table 6A. Summary of ∑12PFAS concentrations (ng/g wet weight) measured (> MDLs) in dreissenid mussel tissue from designated MWP reference sites between 2013-2018.

Compounds	(n)	Stdev	Min	Median	Mean	Max
			ng/g (ww)	ng/g (ww)	ng/g (ww)	ng/g (ww)
PFBA	5	0.076	0.686	0.725	0.762	0.879
PFBS	1	0	0.192	0.192	0.192	0.192
PFDoA	6	0.042	0.633	0.676	0.683	0.761
PFDS	10	0.074	0.336	0.391	0.422	0.566
PFHpA	2	0.029	0.188	0.208	0.208	0.228
PFHxS	1	0	0.073	0.073	0.073	0.073
PFNS	1	0	0.273	0.273	0.273	0.273
PFOA	3	0.028	0.103	0.149	0.135	0.153
PFOS	12	0.225	0.152	0.444	0.499	1.01
PFOSA	1	0	0.733	0.733	0.733	0.733
PFPeA	2	0.222	0.14	0.297	0.297	0.454
PFPeS	1	0	0.647	0.647	0.647	0.647

Table 6B. Summary of similar ∑12PFAS concentrations (ng/g wet weight) measured (> MDLs) in dreissenid mussel tissue from basin-wide MWP sites between 2013-2018.

Category	(n)	Stdev	Min	Median	Mean	Max
			ng/g (ww)	ng/g (ww)	ng/g (ww)	ng/g (ww)
PFBA	36	0.1	0.673	0.742	0.764	1.20
PFBS	5	0.139	0.199	0.229	0.292	0.529
PFDoA	31	0.187	0.62	0.712	0.763	1.49
PFDS	37	0.167	0.329	0.394	0.446	1.28
PFHpA	9	0.042	0.151	0.196	0.197	0.261
PFHxS	4	0.035	0.064	0.093	0.094	0.126
PFNS	15	0.147	0.098	0.154	0.22	0.529
PFOA	7	0.042	0.104	0.16	0.16	0.208
PFOS	70	0.733	0.078	0.536	0.7	4.73
PFOSA	16	1.02	0.573	0.927	1.31	3.97
PFPeA	9	0.342	0.135	0.234	0.345	1.22
PFPeS	1	0	0.718	0.718	0.718	0.718

Table 7. Summary of ∑12PFAS concentrations (ng/g wet weight) measured (> MDLs) in dreissenid mussel tissue from sampled Great Lakes MWP reference sites between 2013-2018.

Category	(n)	Stdev	Min	Median	Mean	Max
Location			ng/g (ww)	ng/g (ww)	ng/g (ww)	ng/g (ww)
Lake Erie	7	0.205	0.073	0.454	0.422	0.761
Lake Huron	4	0.274	0.152	0.522	0.48	0.724
Lake Michigan	24	0.243	0.103	0.421	0.464	1.01
Niagara River	10	0.216	0.192	0.522	0.543	0.794

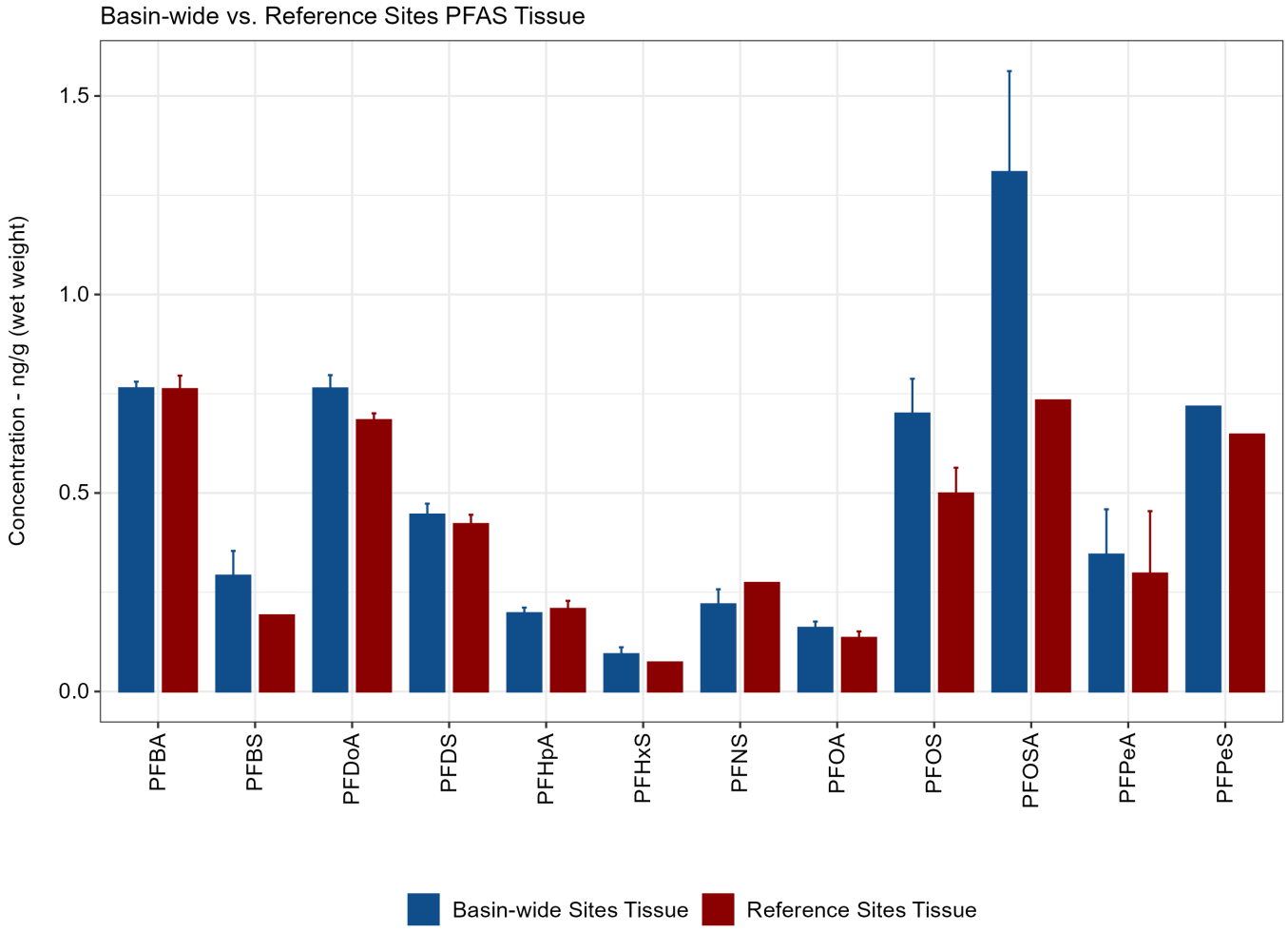

Fig. 13. Barplots depicting comparison between basin-wide lakes/connecting channels (Lake Michigan, Lake Huron, Detroit River, Lake Erie, Niagara River, and Lake Ontario) and reference sites tissue ∑12PFAS compound concentrations (ng/g wet weight) measured between 2013-2018. Additional information is provided in Table 6A and Table 6B.

3.4. PFAS Inshore and Offshore Summary

PFAS concentrations measured (> MDL) in dreissenid mussels across inshore (e.g., tributary, river, and harbor), and offshore sampling locations (nearshore lake, and open lake zone) are summarized in Fig. 14, and Table 8. An assessment of $\sum_{19}$PFAS concentrations revealed, tributary (mean; 0.668 ng/g wet weight), and riverine (mean; 0.662 ng/g wet weight) mussel mean PFAS concentrations were practically similar across inshore and offshore/open-lake sampling locations. However, inshore tributary and riverine mussel mean $\sum_{19}$PFAS concentrations were higher, when compared to harbor (mean; 0.627 ng/g wet weight), and offshore sampling location concentrations (mean; 0.545 ng/g wet weight; Fig. 14; Table 8). Differences in inshore and offshore sampling locations $\sum_{19}$PFAS concentrations were not statistically significant (Kruskal-Wallis; $p > 0.05$). Consistent with our findings, prior studies have also highlighted elevated PFAS concentrations detected in tributaries sampled in Lake Michigan (Balgooyen and Remucal, 2022), Lake Huron (Giesy et al., 2006; Kannan et al., 2005), the Detroit riverine system (Kannan et al., 2005), western Lake Erie basin (Custer et al., 2020; Kannan et al., 2005), Niagara riverine system (Myers et al., 2012), and Lake Ontario (Myers et al., 2012).

Among the PFAS compounds assessed across inshore and offshore sampling locations, PFDS (mean range; 0.409 - 0.468 ng/g wet weight), PFBA (mean range; 0.754 - 0.781 ng/g wet weight), PFDoA (mean range; 0.687 - 0.803 ng/g wet weight), PFOS (mean range; 0.534 - 0.851 ng/g wet weight), PFTreA (mean range; 1.06 - 1.47 ng/g wet weight), and PFOSA (mean range; 0.698 - 1.7 ng/g wet weight) were measured at the highest mean concentrations in mussel tissue. Similarly, PFDS, PFBA, PFDoA, and PFOS were also among the $\sum_{19}$PFAS compounds detected frequently (DF > 25%) in mussels across tributary (DF = 86%, 71%, 29%, and 86%), river (DF = 35%, 37%, 42%, and 77%), harbor (DF = 34%, 34%, 31%, and 75%), and offshore (DF = 56%, 33%, 26%, and 70%) sampling locations, respectively. Overall, PFAS environmental occurrence observed in mussels from inshore Great Lakes sampling locations, were shown to be similar or higher, compared to results reported in zebra mussels and invertebrates from the Llobregat River basin (NE Spain; Campo et al., 2015), and from small rivers and streams across Flanders, Belgium (Byns et al., 2024).

A heatmap depicting the presence and absence of $\sum_{19}$PFAS compounds and their composition in mussels from inshore and offshore sampling locations are shown in Fig. 15. Of the $\sum_{19}$PFAS compounds measured above > MDLs, approximately 94.7% (18/19) were detected in mussels from river sampling locations, followed by harbor (14/19 = 73.7%), offshore (12/19 = 63.2%), and tributary (7/19 = 36.8%) sampling locations. With the exception of mussels sampled from tributary sites, compositionally, PFOS was the dominant compound detected in mussels across all sampled inshore and offshore sites assessed in this study (Fig. 14B and Fig. 15). Elevated PFOS composition were mainly detected in mussels from riverine sampling locations, followed by harbor, and offshore sites. For other $\sum_{19}$PFAS compounds quantified in this study, PFOSA > PFTreA > PFDS > PFBA > PFDoA; were also among the predominant compounds detected in mussels across inshore river and harbor sampling locations. The composition profile observed in mussels from inshore river and tributary sampling locations in this study, further demonstrates and highlight riverine and tributary PFAS discharge, as important transport and environmental pathways for these contaminants within the Great Lakes aquatic environment.

The total concentrations for $\sum_{19}$PFAS compounds measured in mussels across inshore and offshore sampling locations are shown in Fig. 16A. The highest summed $\sum_{19}$PFAS concentrations were detected in mussels from riverine sites sampled in this study. On average, cumulative $\sum_{19}$PFAS concentrations measured in mussels across inshore and offshore sampling locations decreased in the order of; riverine sites (0.260 - 9.83 ng/g wet weight) > harbor (0.156 - 6.34 ng/g wet weight) > tributary (0.238 - 5.38 ng/g wet weight) > offshore sampling locations (0.073 - 3.351 ng/g wet weight), respectively. In general, total $\sum_{19}$PFAS concentrations were higher in mussels from riverine sites sampled in Lake Michigan (Kinnickinnic River: [LMMB-13-7.13], and Kalamazoo River: [LMKZ-0-5.18]). Likewise, elevated PFAS concentrations were detected in mussels from harbor sites sampled in Lake Michigan (Milwaukee Bay [LMMB-4-7.13, and LMMB-0-7.13]), and Lake Erie (Presque Isle [LEPB-7-9.14], and Black River [LEBR-0-9.14]). Interestingly, elevated $\sum_{19}$PFAS concentrations were mainly detected in mussels from tributary sites sampled in western Lake Erie Basin (Gill Creek-03A [NRGL-03A-7.14], Scajaquada Creek: [NRSC-01A-7.14], Two Mile Creek: [NRTM-01A-7.14]), compared to other mussel tributary sites sampled in this study. Similar to our study, elevated PFAS concentrations were also detected in aquatic organisms from Kalamazoo River (Kannan et al., 2005), tree swallow (*Tachycineta bicolor*) nestling carcass samples from Kinnickinnic River (Milwaukee estuary, Wisconsin, USA; Custer et al., 2024), in fish samples from Black River, OH (Lin et al., 2021), and fish sampled from sites in the Niagara riverine system (Sinclair et al., 2006). In regards to offshore sites sampled in this study, elevated $\sum$PFAS concentrations were measured in mussels from sites sampled in western Lake Erie Basin and Lake Michigan (Niagara River: [NRNF-1, rep 1-6.14], and Milwaukee Beach: [LMMB-5-6.13]; Fig. 16A).

Results & Discussion

In regards to PFAS groups distribution, long -and- short-chained PFAS compounds distribution across inshore and offshore sampling locations are shown in Fig. 16B. On average, long-chained PFAS groups were among the dominant compounds measured in mussels across inshore and offshore/open-lake sampling locations. As shown in Fig. 16B and Table 9, with the exception of long-chained ($n \geq C_{13}$–C_{14}) PFCA compounds measured in mussels from river sampling locations, higher mean concentrations were measured for long-chained C_8-FASA compounds measured in mussels across tributary (1.7 ng/g wet weight), harbor (1.59 ng/g wet weight), and offshore sites (0.698 ng/g wet weight), respectively. Results from prior studies suggest the emission profile for long -and- short-chained PFCA groups are primarily driven by industrial sources (Point et al., 2021), whereas the emission profile for long -and- short-chained PFSA compound groups and their precursors (short-chained acids; $-C_nF_{2n+1}$, $n \leq 6$) are primarily influenced and driven by various anthropogenic pressures. Important of these anthropogenic drivers are contribution and input from urban sources (e.g., urban runoff, stormwater runoff, municipal sewage discharge; Langberg et al., 2021), and domestic/human-based consumer products (e.g., carpet/carpet-backing products, paper packaging products, surfactants, pesticide use in urban settings, cookware and food packaging products; Kurwadkar et al., 2022). Therefore, it is plausible that elevated long -and- short-chained PFAS concentration levels detected in mussels across some Great Lakes inshore and offshore sampling locations assessed in this study, is indicative of continuous PFAS loadings that are influenced by input from a mix of adjacent local urban (e.g., wastewater discharge, and urban stormwater runoff) and industrial sources (Lin et al., 2021b; Remucal, 2019).

Additional assessment revealed a river to offshore gradient for several long -and- short-chained $\sum_{11}$PFAS compounds (PFHxS [C_6], PFBS [C_4], PFOA [C_8], PFHpA [C_7], PFNS [C_9], PFPeA [C_5], PFPeS [C_5], PFOSA [C_8], PFDoA [C_{12}], PFBA [C_4], PFOS [C_8]), measured in mussels across inshore river and offshore/open-lake sampling locations (Fig. 17; Table 10A and Table 10B). As shown in Fig. 17, the largest transitory decrease/decline in $\sum_{11}$PFAS concentration across the mussel river-offshore gradient was observed for PFOS (decrease [71.1%]; 1.37 - 4.73 ng/g wet weight), followed by PFBS (decrease [63.7%]; 0.192 - 0.529 ng/g wet weight), PFPeA (decrease [62.8%]; 0.454 - 1.22 ng/g wet weight), PFOSA (decrease [49.5%]; 0.733 - 1.45 ng/g wet weight), PFDoA (decrease [49.0%]; 0.761 - 1.49 ng/g wet weight), PFHxS (decrease [42.1%]; 0.073 - 0.126 ng/g wet weight), and PFNS (decrease [31.8%]; 0.273 - 0.4). On average, the transitory decrease for short-chained ($n \geq C_4$–C_7) $\sum_6$PFAS concentrations across the river-offshore gradient were marginally lower (decrease [92.9%]; 0.073 - 1.03 ng/g wet weight), compared to long-chained PFAS ($n \geq C_7$–C_{12}) $\sum_5$PFAS (decrease [95.9%]; 0.196 - 4.73 ng/g wet weight). As shown in prior studies, contaminant concentration decrease across the Great Lakes inshore and offshore zones are indicative of several factors, important of which are increased in-river retention and downstream river dilution/attenuation (Hladik et al., 2018b; Ogunbiyi et al., 2024), strong lake seiche effect and backwater/back-flushing along river mouth and nearshore-offshore zones (Larson et al., 2013), and active nearshore-offshore surface water dynamics and circulation patterns (e.g., contaminants upwelling and down-welling along nearshore-offshore zones due to prevailing currents; Blagrave et al., 2023; Khairy et al., 2014; Point et al., 2021; Rao and Schwab, 2007). The results presented here fill an important knowledge gap for PFAS compounds partitioning across the Great Lakes river- offshore zones. Our results also provides further evidence of the strong variation that can occur between PFAS compounds concentration across the Great Lakes inshore and offshore complexes. However, the fate of these compounds across the Great Lakes river- offshore zones is not well understood and warrants further investigation.

Credit: NOAA Great Lakes MWP

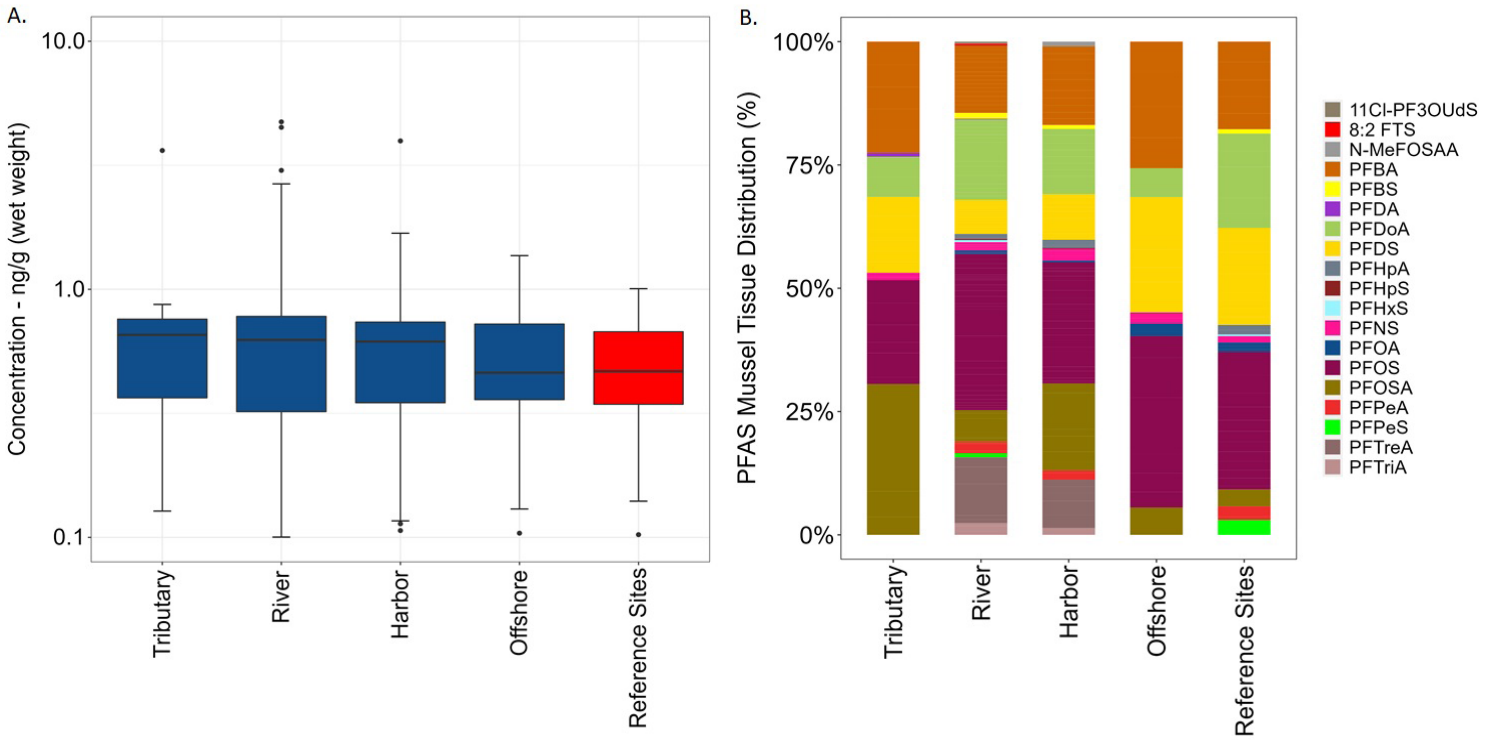

Fig. 14. A). Boxplots depicting ∑19PFAS concentration profile (ng/g wet weight) measured (> MDLs) in dreissenid mussels basin-wide from inshore [harbor, rivers and tributaries] and offshore (near-shore and open-lake) MWP sampling locations between 2013 - 2018, and B), the percent composition (%) and distribution of ∑19PFAS recorded in mussel tissue from inshore [harbor, rivers and tributaries] and offshore (near-shore and open-lake) MWP sampling locations during the 2013 - 2018 sampling event. Reference sites provides perspective to the relative PFAS concentrations measured in mussel tissue from inshore and offshore MWP sampling locations.

Table 8. Summary of ∑19PFAS concentrations (ng/g wet weight) measured (> MDLs) in dreissenid mussels from inshore (harbor, river, tributaries), and offshore (nearshore lake, and open lake zone) MWP sampling locations between 2013-2018. Reference sites provides perspective to the relative PFAS concentrations measured in mussel tissue from inshore and offshore MWP sampling locations during the 2013-2018 sampling period.

Category	(n)	Stdev	Min	Median	Mean	Max
Location			ng/g (ww)	ng/g (ww)	ng/g (ww)	ng/g (ww)
Tributary	25	0.66	0.098	0.645	0.668	3.63
River	134	0.656	0.064	0.576	0.662	4.73
Harbor	86	0.482	0.078	0.597	0.627	3.97
Offshore	22	0.338	0.104	0.461	0.545	1.37
Reference Sites	45	0.23	0.073	0.46	0.477	1.01

Table 9. Summary of ∑19PFAS compound group concentrations (ng/g wet weight) measured (> MDLs) in dreissenid mussels from inshore (harbor, river, tributaries), and offshore (nearshore lake, and open lake zone) MWP sampling locations between 2013-2018.

				Min	**Median**	**Mean**	**Max**
Class-types	PFAS Groups	(n)	Stdev	ng/g (ww)	ng/g (ww)	ng/g (ww)	ng/g (ww)
Tributary	C8–C10 PFSAs	15	0.236	0.098	0.366	0.431	0.818
	C8–C12 PFCAs	2	0.02	0.666	0.681	0.681	0.695
	C4–C7 PFCAs	5	0.04	0.693	0.752	0.754	0.793
	C8 - FASAs	3	1.67	0.605	0.869	1.7	3.63
River	C10 - PFESAs	3	0.003	0.134	0.136	0.136	0.139
	C4–C7 PFSAs	10	0.222	0.064	0.124	0.233	0.718
	C10 - FTSAs	1	0	0.347	0.347	0.347	0.347
	C4–C7 PFCAs	25	0.29	0.157	0.711	0.602	1.22
	C8–C10 PFSAs	56	0.823	0.1	0.42	0.64	4.73
	C8–C12 PFCAs	22	0.331	0.117	0.717	0.686	1.49
	C8 - FASAs	6	0.309	0.573	0.927	0.943	1.45
	C13–C14 PFCAs	11	0.855	0.522	0.903	1.27	3.02
Harbor	C4–C7 PFSAs	3	0.06	0.113	0.199	0.181	0.229
	C8–C10 PFSAs	39	0.213	0.078	0.507	0.5	1.07
	C11 - FOSAAs	1	0	0.516	0.516	0.516	0.516
	C4–C7 PFCAs	20	0.318	0.135	0.681	0.524	1.20
	C8–C12 PFCAs	11	0.169	0.197	0.703	0.667	0.885
	C13–C14 PFCAs	6	0.372	0.666	0.834	1.01	1.52
	C8 - FASAs	6	1.21	0.764	1.099	1.59	3.97
Offshore	C4–C7 PFSAs	3	0.303	0.073	0.192	0.304	0.647
	C8–C12 PFCAs	12	0.283	0.103	0.652	0.459	0.761
	C8–C10 PFSAs	37	0.265	0.13	0.414	0.479	1.37
	C4–C7 PFCAs	13	0.261	0.14	0.724	0.607	0.879
	C8 - FASAs	2	0.049	0.664	0.698	0.698	0.733

Results & Discussion

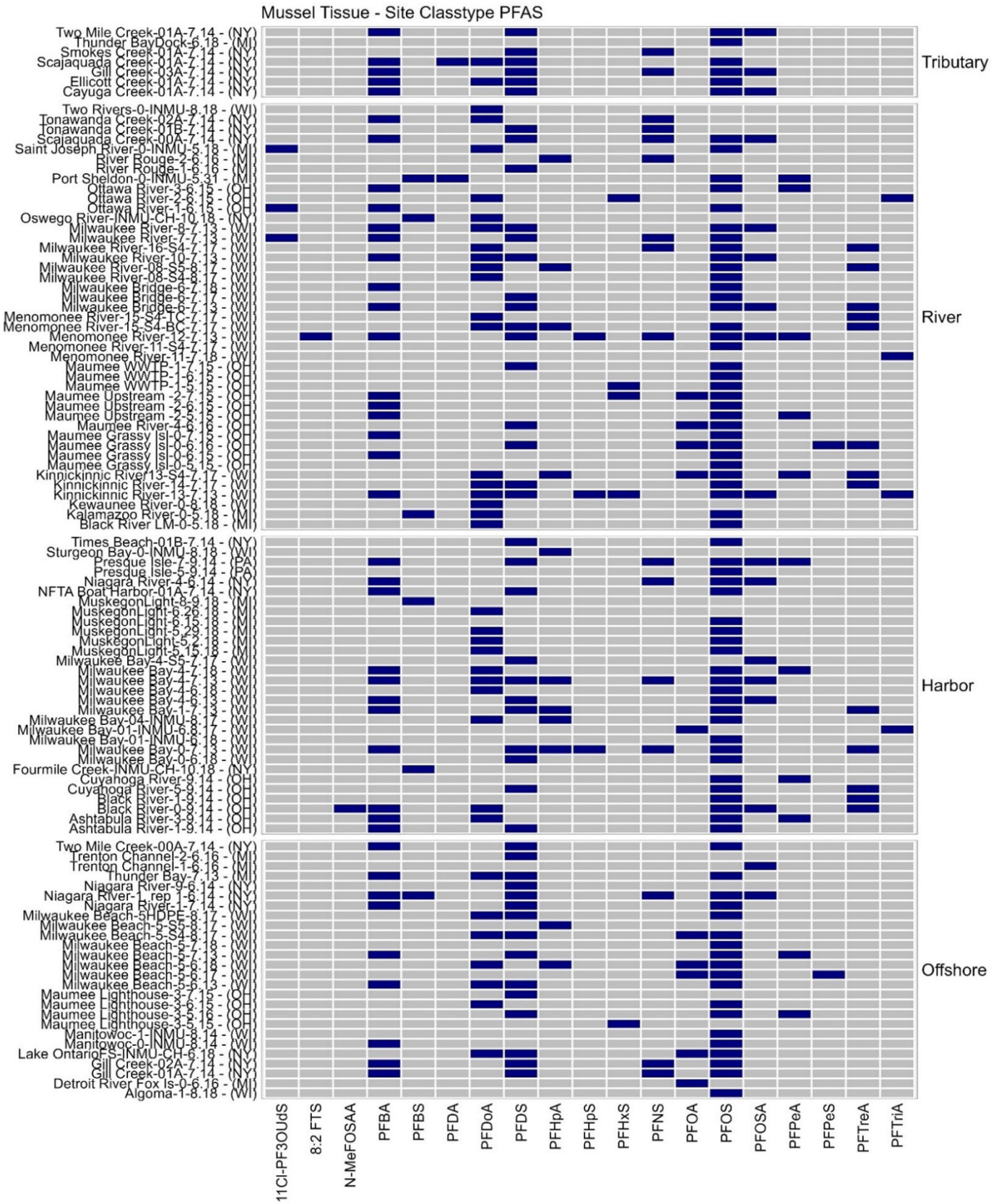

Fig. 15. Heat map depicting presence ( ) and absence ( ) of all $\sum_{19}$PFAS compounds measured in mussel tissue above the detection limit (> MDLs) from inshore (Tributaries, River, Harbor) and offshore (nearshore and open-lake zones) MWP sites during the 2013 - 2018 sampling period. Individual sites are listed by their general location (associated riverine/lake region), state and month/ year sampled.

Results & Discussion

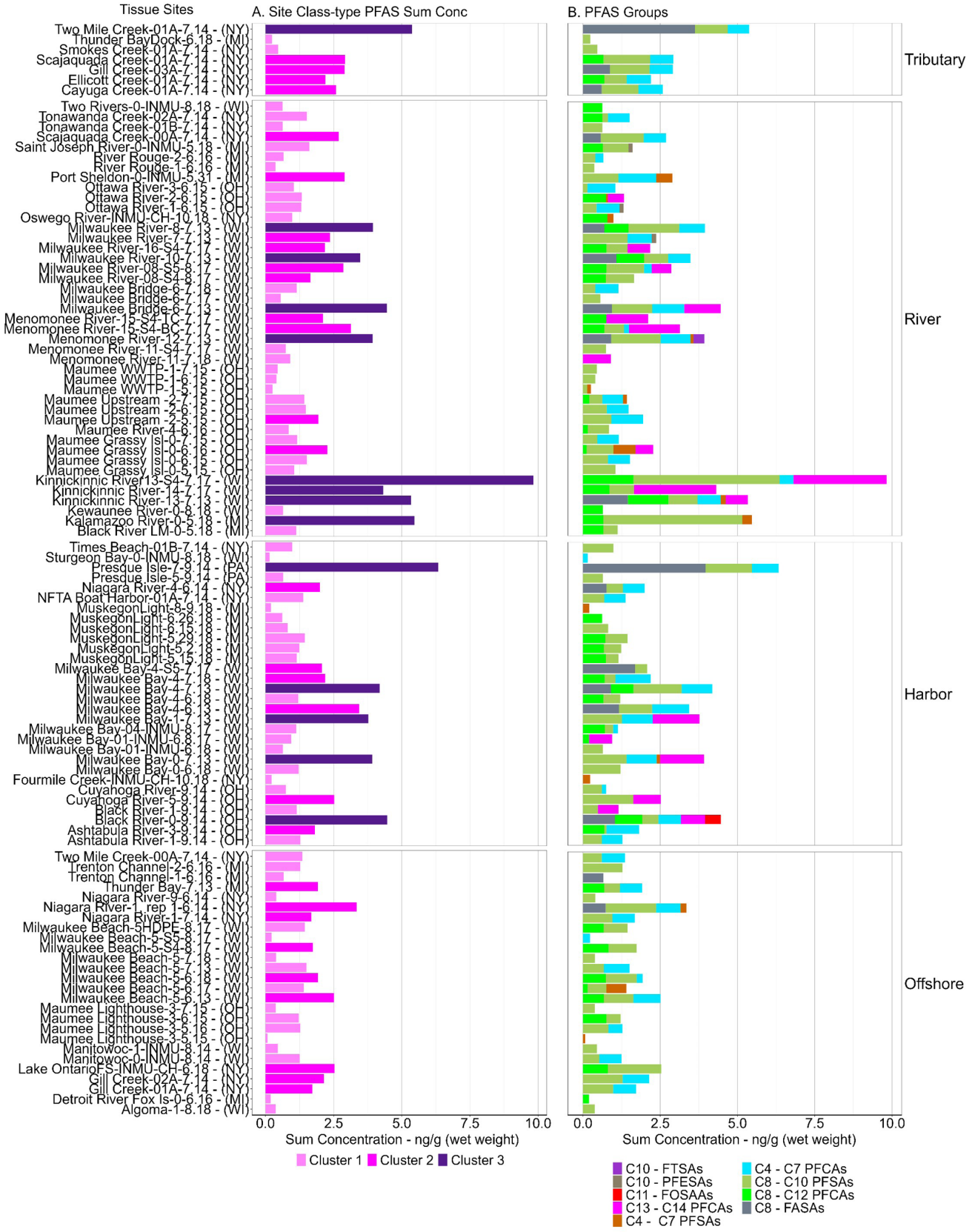

Fig. 16. Barplots depicting A). summed $\sum_{19}$PFAS concentration (ng/g wet weight) measured (> MDL) in mussel tissue across inshore (Tributary, River, and Harbor), and offshore (Nearshore Lake and Open-lake) MWP sampling locations, and B), the composition profile (%) and relative distribution of predominant $\sum_{19}$PFAS groups (long and short-chained homologues) concentration detected in mussels from nearshore and offshore Great Lakes sampling locations during 2013 - 2018 sampling event. Clusters 1-3 represents mussel sampling locations with low ( ), medium ( ), and high ( ) summed $\sum_{19}$PFAS concentrations. $\sum_{19}$PFAS sum concentrations. Individual sites are listed by their general location (associated riverine/lake region), state and month/year sampled.

Table 10A. Summary of ∑11PFAS concentrations (ng/g wet weight) measured in dreissenid mussel tissue from designated MWP river gradient sites between 2013-2018.

Compounds	(n)	Stdev	Min	Median	Mean	Max
			ng/g (ww)	ng/g (ww)	ng/g (ww)	ng/g (ww)
PFOS - (C8)	33	1.02	0.105	0.58	0.851	4.73
PFDoA - (C12)	18	0.234	0.625	0.753	0.803	1.49
PFOSA - (C8)	6	0.309	0.573	0.927	0.943	1.45
PFPeA - (C5)	5	0.449	0.157	0.234	0.42	1.22
PFBA - (C4)	16	0.083	0.676	0.739	0.754	1.03
PFPeS - (C5)	1	0	0.718	0.718	0.718	0.718
PFBS - (C4)	3	0.169	0.199	0.302	0.343	0.529
PFNS - (C9)	7	0.097	0.1	0.185	0.215	0.4
PFHpA - (C7)	4	0.04	0.17	0.23	0.223	0.261
PFOA - (C8)	4	0.039	0.117	0.15	0.156	0.208
PFHxS - (C6)	4	0.035	0.064	0.093	0.094	0.126

Table 10B. Summary of similar ∑11PFAS concentrations (ng/g wet weight) measured (> MDLs) in dreissenid mussel tissue from MWP offshore gradient sites between 2013-2018.

Category	(n)	Stdev	Min	Median	Mean	Max
			ng/g (ww)	ng/g (ww)	ng/g (ww)	ng/g (ww)
PFOS - (C8)	19	0.281	0.152	0.46	0.534	1.37
PFDoA - (C12)	7	0.039	0.633	0.677	0.687	0.761
PFOSA - (C8)	2	0.049	0.664	0.698	0.698	0.733
PFPeA - (C5)	2	0.222	0.14	0.297	0.297	0.454
PFBA - (C4)	9	0.066	0.686	0.741	0.765	0.879
PFPeS - (C5)	1	0	0.647	0.647	0.647	0.647
PFBS - (C4)	1	0	0.192	0.192	0.192	0.192
PFNS - (C9)	3	0.08	0.13	0.138	0.181	0.273
PFHpA - (C7)	2	0.029	0.188	0.208	0.208	0.228
PFOA - (C8)	5	0.039	0.103	0.149	0.141	0.196
PFHxS - (C6)	1	0	0.073	0.073	0.073	0.073

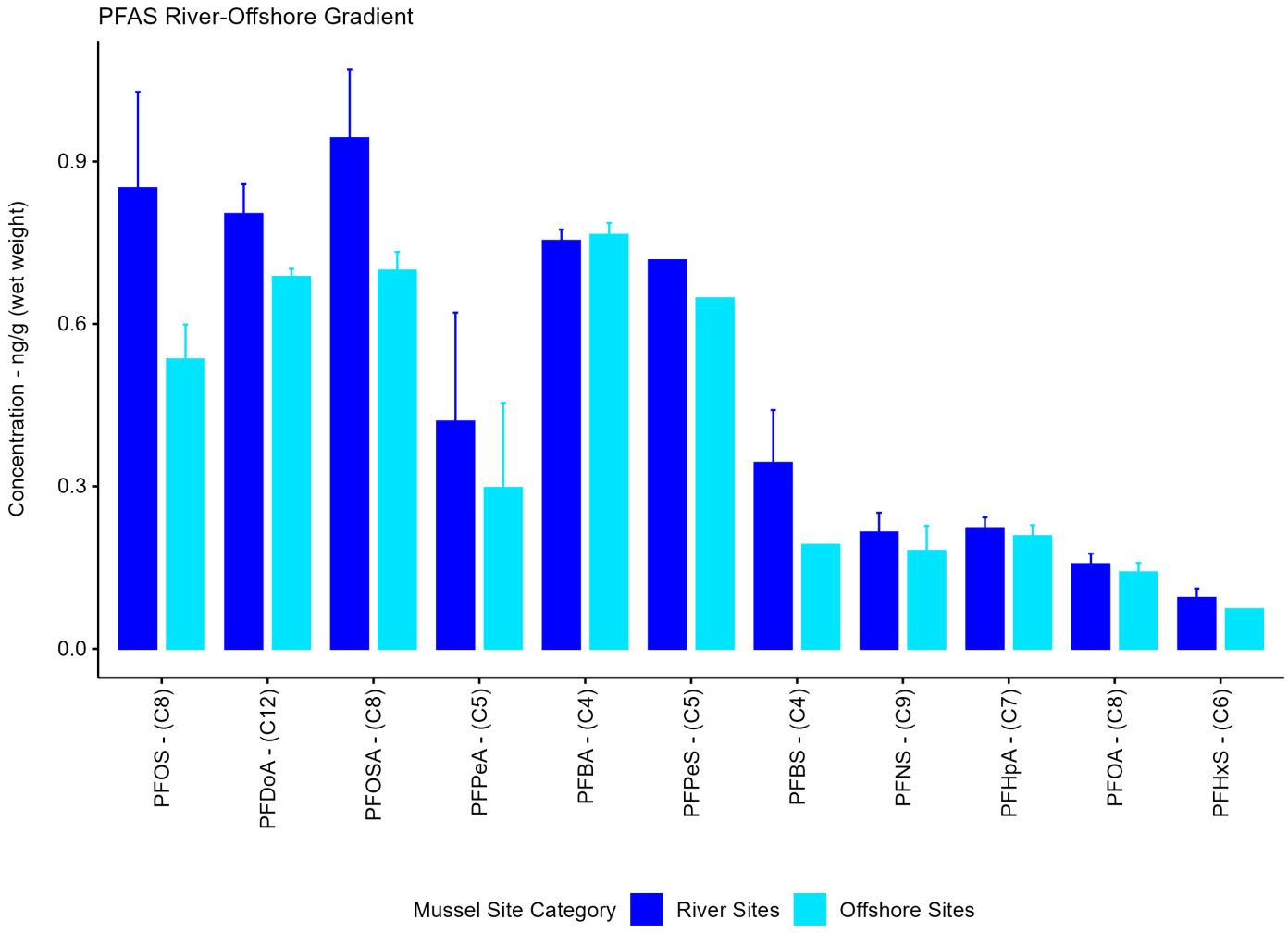

Fig. 17. Barplot depicting the transitory decrease/decline for individual long -and- short-chained $\sum_{11}$PFAS concentrations (ng/g wet weight) measured (> MDL) in mussels across river-offshore gradient (in order of decreasing $\sum_{11}$PFAS concentration, left to right) between 2013 - 2018. The number between brackets represents individual $\sum_{11}$PFAS compounds carbon atom number. Collectively, the largest transitory decrease/decline in PFAS concentration across sampled mussel river-offshore gradient was observed for PFOS (decrease: 71.1%), followed by PFBS (decrease: 63.7%), PFPeA (decrease: 62.8%), PFOSA (decrease: 49.5%), PFDoA (decrease: 49.0%), PFHxS (decrease: 42.1%), PFNS (decrease: 31.8%), PFBA (decrease: 14.7%), PFHpA (decrease: 12.6%), PFPeS (decrease: 9.89%), and PFOA (decrease: 5.77%), respectively. Additional information is provided in Table 10A and Table 10B.

3.5. Site Discharge-types PFAS Summary

PFAS composition and concentration profile measured (> MDL) in mussels at designated discharge-types including sites sampled proximate to WWTPs only, sites proximate to both WWTP and CSO discharge (WWTPs/CSOs), sites sampled downstream and along wastewater discharge zones/gradient, and at sampling locations not influenced by either WWTP or CSO discharge (i.e., non-WWTPs) are displayed and summarized in Fig. 18, and Table 11. Despite being marginally similar, slightly higher mean concentrations were observed in mussels from non-WWTP sites (mean; 0.697 ng/g wet weight), compared to sites sampled in proximity to WTTPs (mean; 0.671 ng/g wet weight), sites sampled downstream and along wastewater discharge (mean; 0.638 ng/g wet weight), and sites sampled proximate to WWTPs/CSOs (mean; 0.435 ng/g wet weight; Fig. 18A. and Table 11). Differences in sampled mussel discharge-types mean $\sum_{19}$PFAS concentration were not statistically significant (Kruskal-Wallis; $p > 0.05$). As shown in Fig. 18B, compared to other major discharge-types assessed in this study, PFAS composition were also higher in mussels from non-WWTP sites (97.4%; 18/19), followed by sites sampled downstream and along wastewater discharge zone/gradient (73.7%; 14/19), sites sampled proximate to WWTPs/CSOs (63.2%; 12/19), and WTTPs (36.8%; 7/19), thus highlighting non-point/diffuse sources as important transport and environmental pathways for PFAS compounds detected within the Great Lakes.

On average, the highest $\sum_{19}$PFAS composition and concentrations were measured in mussels from non-WTTP sites sampled in Lake Michigan (Menomonee River: [LMMB-12-7.13]; Kinnickinnic River: [LMMB-13-7.13 and LMMB-13-S4-7.17]; Milwaukee Bay: [LMMB-0-7.13 and LMMB-4-7.13]), compared to sites sampled in Lake Erie (Presque Isle: LEPB-7-9.14), and Niagara River (Niagara River: NRNF-1, rep 1-6.14; Fig. 19 and Fig. 20). Prior studies have also shown non-point/diffuse sources are also considered significant contributors of PFAS distribution and contamination in freshwater aquatic systems. Results from these studies have shown that this is largely influenced by local anthropogenic sources including PFAS emission from urban surface runoff and input in urban streams and surface water (Lin et al., 2021), runoff from firefighting training facilities (Panieri et al., 2022; Point et al., 2021), and waste streams generated from manufacturing processes including runoff from municipal solid-waste and landfill leachate (Masoner et al., 2020; Point et al., 2021). Similarly, runoff from amended agricultural fields with land applied biosolids (Johnson, 2022; Rafiei and Nejadhashemi, 2023), runoff from civilian airports, and military installations (Capozzi et al., 2023; Christensen et al., 2022), and atmospheric deposition (e.g., air–water exchange, wet deposition, and dry deposition; Gewurtz et al., 2019; Lin et al., 2021; Pfotenhauer et al., 2022; Xia et al., 2024), are also considered significant non-point/diffuse source contributors of PFAS distribution and contamination in freshwater systems. Taken together, these pollution vectors can be considered important mechanisms of PFAS surface water contamination across sampled Great Lakes mussel non-WTTP discharge-type sampling locations.

Of the 19 $\sum_{19}$PFAS compounds measured (> MDL) in mussel tissue samples, 5 compounds (PFDS[C_{10}], PFOSA [C_8], PFDoA[C_{12}], PFBA[C_4], and PFOS[C_8]) were consistently detected in mussels across all discharge-types assessed in this study. Similarly, among these PFAS compounds, PFDS (mean range; 0.37 - 0.519 ng/g wet weight), PFOS (mean range; 0.472 - 0.773 ng/g wet weight), PFDoA (mean range; 0.684 - 0.773 ng/g wet weight), PFBA (mean range; 0.723 - 0.809 ng/g wet weight), and PFOSA (mean range; 0.573 - 1.98 ng/g wet weight), were consistently measured at higher mean concentrations. In addition, the concentration for several PFAS compounds including PFTriA (0.903 ng/g wet weight), PFBA (1.21 ng/g wet weight), PFPeA (1.22 ng/g wet weight), PFDoA (1.49 ng/g wet weight), PFTreA (3.02 ng/g wet weight), and PFOS (4.732 ng/g wet weight), were higher in mussels from non-WWTP sites, compared to the other discharge-types assessed in this study (Kruskal-Wallis; $p > 0.05$). With the exception of PFDS and PFOS, the concentrations for PFDoA (0.885 ng/g wet weight), PFBA (1.03 ng/g wet weight), and PFOSA (1.04 ng/g wet weight), were higher in mussels from sites sampled proximate to WWTPs only, compared to sites sampled in proximity to WWTP/CSO discharge-types. However, no statistically significant difference was observed between PFDoA, PFBA, and PFOSA concentrations measured in mussels from the above sampled discharge-types (Kruskal-Wallis; $p > 0.05$).

Overall, PFOS (DF range; 74 - 80%) was among the $\sum_{19}$PFAS compounds most frequently detected (DF > 30%) in mussels across the major discharge-types examined in this study, followed by PFBA (DF range; 40 - 57%), PFDS (DF range; 33 - 52.2%), and PFDoA (DF range; 42 - 44%). Interestingly, we found that PFOS detections were observed to be mainly elevated in mussels from sites sampled proximate to WWTP/CSOs (DF = 80%) and WWTPs (DF = 78%). PFOS and other PFAS compounds, including their precursors, are introduced into conventional wastewater systems via domestic and commercial wastes including discharges arising from municipal solid waste landfills (MSWLF), hospital waste stream, industrial and sanitation discharge, from personal care products (PCPs) such as sunscreens, shampoos and conditioners, cosmetic products (e.g., foundation/BB creams, exfoliator, concealer, lip liners, and eyeshadow; Pütz et al., 2022), personal hygiene products (Zhou et al., 2023), and cleaning products containing fluorochemicals (Sinclair and Kannan, 2006). Thus, from an environmental standpoint, it plausible that PFOS and other PFAS compounds frequent detection

and elevated concentrations observed in mussels from sites proximate to WWTP discharge in Lake Michigan (Milwaukee Bridge: LMMB-6-7.13), Lake Erie (Black-River: LEBR-0- 9.14), and the Niagara riverine system (Scajaquada Creek: NRSC-00A-7.14), could be attributed to their use and emission into urban and residential water cycle (Houtz, et al., 2012; Kolpin et al., 2021; Lin et al., 2021; Nguyen et al., 2016), resulting in their transformation and incomplete elimination during conventional and engineered wastewater treatment processes (Helmer et al., 2022; Leung et al., 2022).

A broader look at long -and- short-chained PFAS compounds revealed, the distribution and composition profile for some long -and- short-chained PFAS groups detected in mussels, followed similar spatial patterns across assessed mussel site discharge-types (Fig. 20B and Table 12). For example, long-chained PFSA (n ≥ C_8–C_{10}: 33.3% [6/18]) and PFCA groups (n ≥ C_8–C_{12}, and n ≥ C_{13}–C_{14}: 27.8% [5/18]), were more predominant in mussels sampled at non-WWTP sites. Similar patterns in long-chained ∑PFSA and ∑PFCA compounds dominance were also observed in mussels from sites sampled downstream and along wastewater gradient/discharge zones (PFSA: 35.7%; PFCA: 28.6%), sites proximate to WWTPs/CSOs (PFSA: 36.4%; PFCA: 27.3%), and WWTPs (PFSA: 28.6%; PFCA: 28.6%), respectively. Interestingly, long-chained PFSA and PFCA groups dominance observed in mussels across sampled wastewater impacted sites, reflects similar long-chained PFSA and PFCA compounds dominance in fish from a Great Lakes wastewater-dominant aquatic system (George et al., 2023).With the exception of the long-chained perfluoroalkane sulfonamide (FASAs: C_8) compound (mean range: 0.573 - 1.98 ng/g wet weight), long-chained PFCA (n ≥ C_8–C_{12}, C_{13}–C_{14}: mean range: 0.498 - 1.39 ng/g wet weight) and short-chained PFCA compounds (n ≥ C_4–C_7: mean range: 0.525 - 0.809 ng/g wet weight) were consistently detected at higher mean concentrations in mussels across sampled site discharge-types. This pattern was also consistent with even-chain PFCA groups, which were also measured at higher mean concentrations, compared to even-chain PFSAs groups assessed in mussels across designated site discharge-types.

Spearman's (ρ) rank correlation coefficient results revealed moderate to significant ($p < 0.05$) association between PFDS (C_{10}: PFSAs), PFHxS (C_6: PFSAs), 11Cl-PF3OUdS (C_{10}: PFESAs) concentrations, and mussel sampling location point source/wastewater parameters (Spearman's rho (ρ) = 0.352 - 0.755, $p < 0.05$; Fig. 11). In contrast, moderate to significant ($p < 0.05$) negative relationships were observed between several $\sum_{11}$PFAS concentration (PFBS, PFHpA, PFOS, PFTreA, 8:2 FTS, PFNS, PFPeA, PFDoA, PFOA, PFTriA, and PFPeS), and mussel site point source/wastewater parameters (Spearman's rho (ρ) = -0.350 to -0.911, $p < 0.05$). Similarly, PFHpA (Spearman's rho (ρ) = -0.435 to -0.911, $p < 0.05$) depicted significant negative correlation across mussel sites point source/wastewater parameters, followed by PFTreA (Spearman's rho (ρ) = -0.402 to -0.864, $p < 0.05$), PFDoA (Spearman's rho (ρ) = -0.341 to -0.813, $p < 0.05$), PFOS (Spearman's rho (ρ) = -0.374 to -0.809, $p < 0.05$), PFOA (Spearman's rho (ρ) = -0.31 to -0.673, $p < 0.05$), and PFTriA (Spearman's rho (ρ) = -0.390 to -0.663, $p < 0.05$; Fig. 11). Results from the correlation analysis further supports our findings from the river-offshore PFAS assessment, in which a transitory decrease/decline was observed for several $\sum_{11}$PFAS compounds including PFBS, PFOA, PFHpA, PFNS, PFPeA, PFPeS, PFDoA, and PFOS across sampled river-offshore sites (Fig. 17). Recent studies suggest, the negative association observed between ∑PFAS homologues and mussel sampling locations wastewater parameters, are likely indicative of net losses of PFAS homologues and precursor compounds across engineered conventional wastewater treatment systems (Helmer et al., 2022), and along downstream wastewater discharge zones (Desgens-Martin et al., 2023), resulting from parental and precursor PFAS compounds transformation via these degradation pathways (Desgens-Martin et al., 2023; Eriksson et al., 2017; Helmer et al., 2022, Thompson et al., 2022).

Additional assessment revealed an environmental gradient across mussel sites sampled proximate to WWTPs/CSOs and sites sampled downstream and along wastewater discharge zones for several $\sum_6$PFAS compounds including PFTreA (C_{14}), PFDoA (C_{12}), PFNS (C_9), PFPeA (C_5), PFOA (C_8), and PFHxS (C_6; Fig. 21; Table 13A and Table 13B). For $\sum_6$PFAS compounds examined across the WWTPs/CSOs - downstream/wastewater gradient, their concentration levels decreased in the order of; PFHxS (decrease [49.2%]; 0.064 - 0.126 ng/g wet weight) > PFNS (decrease [41.5%]; 0.234 - 0.4 ng/g wet weight) > PFPeA (decrease [40.3%]; 0.157 - 0.263 ng/g wet weight) > PFTreA (decrease [24.1%]; 0.893 - 1.18 ng/g wet weight) > PFDoA (decrease [15.6%]; 0.747 - 0.885 ng/g wet weight) > PFOA (decrease [5.77%]; 0.196 - 0.208 ng/g wet weight), respectively. Overall, with the exception of PFPeA (C_5), long-chained PFCAs were the dominant compounds measured in mussels across this gradient. In addition, although marginally similar, the transitory decrease/decline for $\sum_2$PFSA compounds (i.e., PFNS, and PFHxS) concentration (84%; 0.064 - 0.40 ng/g wet weight) were lower in mussels across WWTPs/CSOs-downstream river/wastewater discharge zones (Kruskal-Wallis; $p > 0.05$), compared to $\sum_4$PFCA (i.e., PFTreA, PFDoA, PFPeA, and PFOA) concentrations transitory decrease (86.7%; 0.157 - 1.18 ng/g wet weight). Results from our correlation analysis further suggest, the transitory decrease/decline observed for $\sum_6$PFAS concentration levels measured across WWTPs/CSOs and along downstream/wastewater discharge gradient, is also indicative of increased dilution (e.g., stream-water and discharged effluent mixing), and attenuation (e.g., partition and sorption of PFAS compounds to dissolved organic carbon, suspended particles and sediment) occurring at these mussel sampling locations (Kolpin et al., 2021).

Results & Discussion

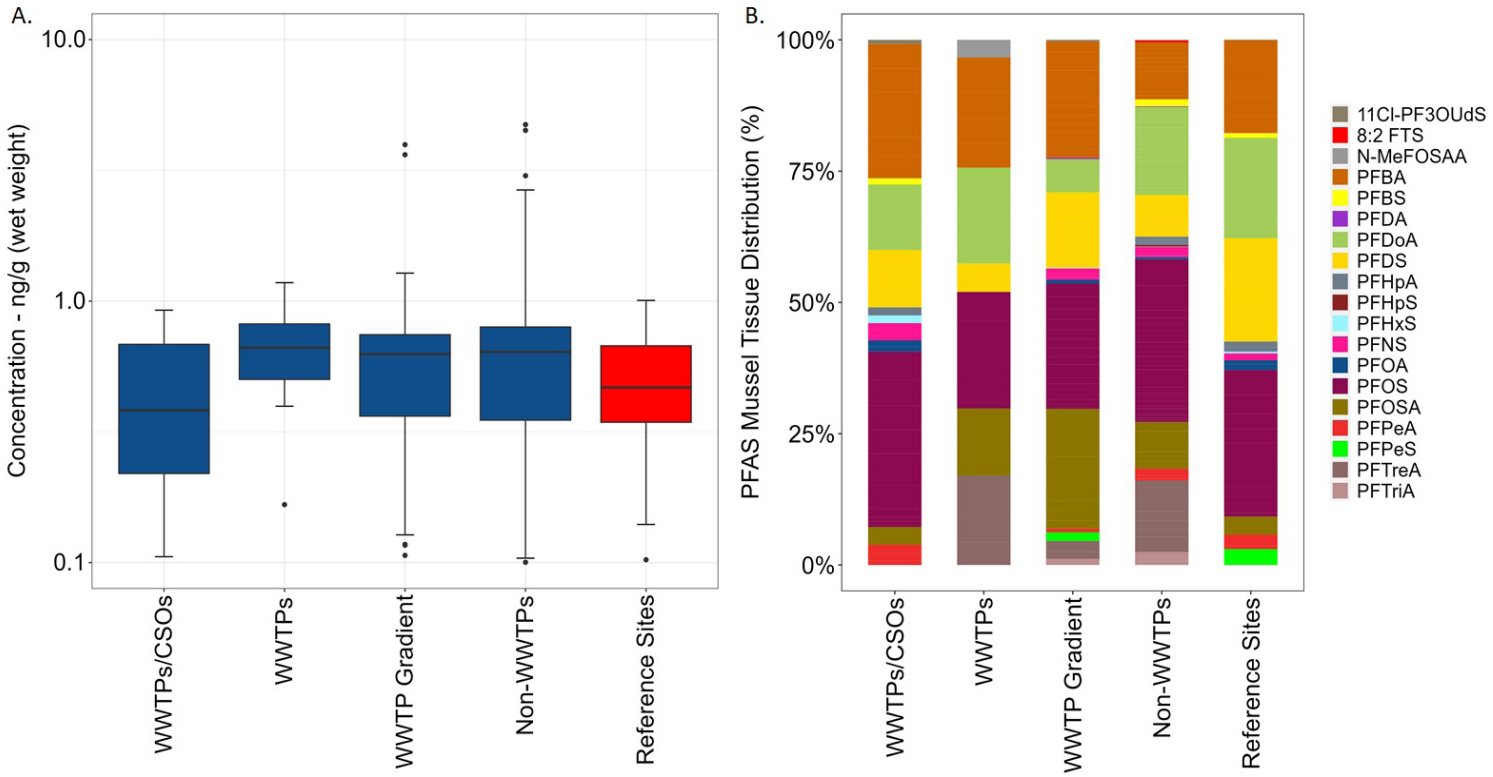

Fig. 18. A). Boxplots depicting overall $\sum_{19}$PFAS concentrations (ng/g wet weight) measured (> MDLs) in dreissenid mussels from sampling locations proximate to point source discharge (WWTPs and WWTPs/CSOs), sites downstream and along gradients of wastewater discharge (WWTP Gradient), and non-WWTP sites (sites not influenced by WWTPs or CSOs) during the 2013-2018 sampling period, and B), the percent composition (%) and relative distribution of $\sum_{19}$PFAS recorded in mussel tissue from designated MWP sampling discharge-types during 2013 - 2018. Reference sites provides perspective to the relative PFAS concentrations measured in mussel tissue from designated MWP discharge-types.

Table 11. Summary of $\sum_{19}$PFAS concentrations (ng/g wet weight) measured (> MDLs) in dreissenid mussels from designated MWP discharge-types including sites sampled proximate to point source discharge (i.e., WWTPs and CSOs), sites downstream and along gradients of wastewater discharge, and sites without wastewater influence (non-WWTPs) during the 2013-2018 sampling period. Reference sites provides perspective to the relative PFAS concentrations measured in mussel tissue from designated MWP discharge-types.

Category	(n)	Stdev	Min	Median	Mean	Max
Sampling Location			ng/g (ww)	ng/g (ww)	ng/g (ww)	ng/g (ww)
WWTPs	23	0.243	0.167	0.663	0.671	1.18
WWTPs/CSOs	39	0.258	0.078	0.365	0.435	0.923
WWTP Gradient	68	0.617	0.064	0.608	0.638	3.97
Non-WWTPs	137	0.657	0.064	0.62	0.697	4.73
Reference Sites	45	0.23	0.073	0.46	0.477	1.01

Table 12. Summary of $\sum_{19}$PFAS compound group concentrations (ng/g wet weight) measured (> MDLs) in dreissenid mussels from designated MWP discharge-types including sites sampled proximate to point source discharge (i.e., WWTPs and CSOs), sites downstream and along wastewater discharge gradients/zones, and sites without wastewater influence (non-WWTPs) during the 2013-2018 sampling period.

				Min	**Median**	**Mean**	**Max**
Discharge-types	PFAS Groups	(n)	Stdev	ng/g (ww)	ng/g (ww)	ng/g (ww)	ng/g (ww)
Non-WWTPs	C10 - PFESAs	1	0	0.139	0.139	0.139	0.139
	C4–C7 PFSAs	11	0.192	0.064	0.192	0.232	0.647
	C10 - FTSAs	1	0	0.347	0.347	0.347	0.347
	C4–C7 PFCAs	34	0.319	0.14	0.693	0.553	1.22
	C8–C10 PFSAs	83	0.683	0.098	0.438	0.597	4.73
	C8–C12 PFCAs	32	0.307	0.103	0.7	0.654	1.49
	C8 - FASAs	9	0.36	0.605	0.914	1.025	1.68
	C13–C14 PFCAs	11	0.803	0.638	1.354	1.396	3.02
WWTP Gradient	C10 - PFESAs	1	0	0.134	0.134	0.134	0.134
	C4–C7 PFSAs	2	0.463	0.064	0.391	0.391	0.718
	C8–C10 PFSAs	36	0.287	0.107	0.454	0.49	1.28
	C8–C12 PFCAs	6	0.276	0.117	0.647	0.508	0.747
	C13–C14 PFCAs	3	0.203	0.522	0.566	0.66	0.893
	C4–C7 PFCAs	15	0.21	0.151	0.719	0.66	0.859
	C8 - FASAs	5	1.666	0.664	0.869	1.978	3.97
WWTPs/CSOs	C10 - PFESAs	1	0	0.136	0.136	0.136	0.136
	C4–C7 PFSAs	3	0.043	0.122	0.126	0.149	0.199
	C8–C10 PFSAs	19	0.25	0.078	0.365	0.425	0.923
	C8–C12 PFCAs	5	0.292	0.16	0.646	0.498	0.789
	C4–C7 PFCAs	10	0.26	0.135	0.674	0.525	0.789
	C8 - FASAs	1	0	0.573	0.573	0.573	0.573
WWTPs	C8–C10 PFSAs	9	0.182	0.167	0.461	0.474	0.863
	C11 - FOSAAs	1	0	0.516	0.516	0.516	0.516
	C8–C12 PFCAs	4	0.122	0.625	0.653	0.704	0.885
	C4–C7 PFCAs	4	0.148	0.722	0.742	0.809	1.03
	C13–C14 PFCAs	3	0.268	0.666	0.775	0.872	1.18
	C8 - FASAs	2	0.069	0.94	0.989	0.989	1.04

Results & Discussion

Fig. 19. Heat map depicting presence ( ) and absence ( ) of all $\sum_{19}$PFAS compounds measured in mussel tissue above the detection limit (> MDLs) from designated MWP site discharge-types (WWTPs, WWTPs/CSOs, WWTP Gradient, Non-WWTPs) during the 2013 - 2018 sampling period. Individual sites are listed by their general location (associated riverine/lake region), state and month/year sampled.

Fig. 20. Barplots depicting A). summed $\sum_{19}$PFAS concentration (ng/g wet weight) measured (> MDL) in mussel tissue from sites sampled proximate to point source discharge (WWTPs and WWTPs/CSOs), sites downstream and along wastewater discharge (WWTP Gradient) zone, and non-WWTP sites during 2013 - 2018, and B), the relative distribution and sum $\sum_{19}$PFAS concentration of predominant PFAS compounds groups (long and short-chained homologues) detected in mussels from sampled major discharge-types. Clusters 1-3 represents mussel sampling locations with low ( ), medium ( ), and high ( ) summed $\sum_{19}$PFAS concentrations. Individual sites are listed by their general location (associated riverine/lake region), state and month/year sampled.

Table 13A. Summary of ∑6PFAS concentrations (ng/g wet weight) measured in dreissenid mussel tissue from designated MWP WWTP/CSO gradient sites between 2013-2018.

Compounds	(n)	Stdev	Min	Median	Mean	Max
			ng/g (ww)	ng/g (ww)	ng/g (ww)	ng/g (ww)
PFTreA - (C14)	3	0.268	0.666	0.775	0.872	1.18
PFDoA - (C12)	7	0.096	0.625	0.663	0.705	0.885
PFNS - (C9)	2	0.174	0.154	0.277	0.277	0.4
PFPeA - (C5)	3	0.072	0.135	0.255	0.218	0.263
PFOA - (C8)	2	0.034	0.16	0.184	0.184	0.208
PFHxS - (C6)	2	0.003	0.122	0.124	0.124	0.126

Table 13B. Summary of similar ∑6PFAS concentrations (ng/g wet weight) measured (> MDLs) in dreissenid mussel tissue from MWP WWTP/CSO - downstream gradient sites between 2013-2018.

Category	(n)	Stdev	Min	Median	Mean	Max
			ng/g (ww)	ng/g (ww)	ng/g (ww)	ng/g (ww)
PFTreA - (C14)	2	0.232	0.566	0.73	0.73	0.893
PFDoA - (C12)	4	0.05	0.627	0.681	0.684	0.747
PFNS - (C9)	6	0.047	0.107	0.143	0.155	0.234
PFPeA - (C5)	2	0.004	0.151	0.154	0.154	0.157
PFOA - (C8)	2	0.056	0.117	0.157	0.157	0.196
PFHxS - (C6)	1	0	0.064	0.064	0.064	0.064

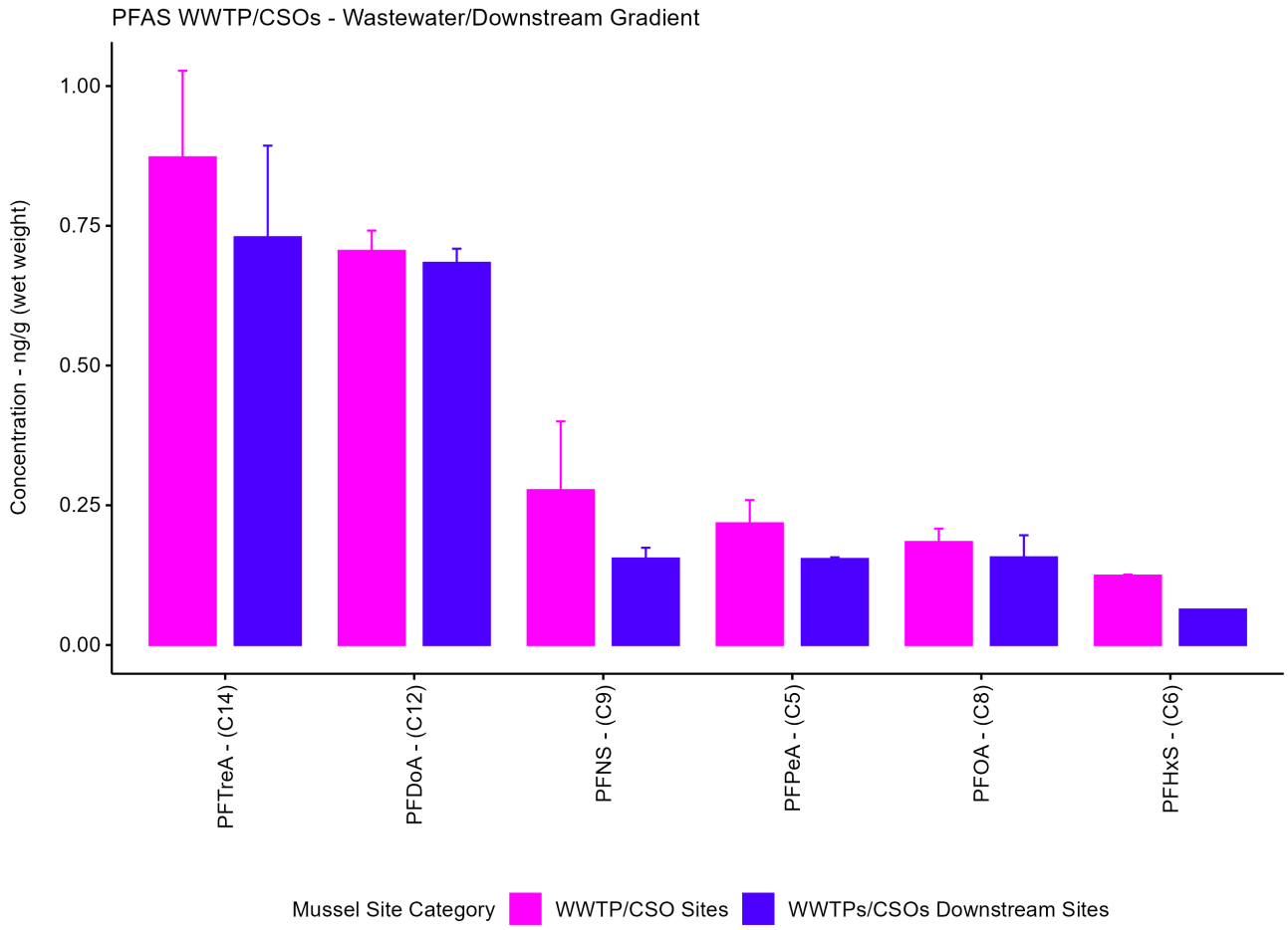

Fig. 21. Barplot depicting the transitory decrease/decline (from left to right, in order of decreasing ∑₆PFAS concentration) for individual long -and- short-chained ∑₆PFAS concentrations (ng/g wet weight) measured (> MDL) in mussels across sites sampled proximate to WWTPs/CSOs, and sites sampled downstream and along wastewater discharge zones/gradients between 2013 - 2018. The number between brackets represents the number of carbon atoms for individual ∑₆PFAS compounds. Collectively, the largest transitory decrease in PFAS concentration across sampled mussel WWTP/CSO-wastewater/downstream river gradient was observed for PFHxS (decrease: 49.2%), followed by PFNS (decrease: 41.5%), PFPeA (decrease: 40.3%), PFTreA (decrease: 24.1%), PFDoA (decrease: 15.6%), and PFOA (decrease: 5.77%), respectively. Additional information is provided in Table 13A and Table 13B.

3.6. Site Land-use Gradients PFAS Summary

A summary of $\sum_{19}$PFAS magnitude and environmental occurrence detected in mussels at predominant agriculture, developed, undeveloped (e.g., barren, forest, shrubs, and grassland), wetland, and open-water sites are presented in Fig. 22 and Table 14. Additional information on mussel PFAS sampling locations land-use and land cover estimates are presented in Table A3 (Appendix). Despite being slightly similar, higher mean concentrations were observed in mussels sampled from open-water sites (53 sites: mean; 0.658 ng/g wet weight), compared to mussels from developed (36 sites: mean; 0.657 ng/g wet weight), undeveloped (7 sites: mean; 0.587 ng/g wet weight), and agricultural sites (9 sites: mean; 0.503 ng/g wet weight; Fig. 22A and Table 14). Similarly, as shown in Fig. 22B and Fig. 23, $\sum_{19}$PFAS compounds composition and distribution remained heterogeneous across mussel sampling locations land-use categories. However, higher PFAS composition were detected in mussels sampled from open-water sites (94.7%; 18/19), followed by sites sampled adjacent to developed (84.2%; 16/19), agriculture (57.9%; 11/18) and undeveloped (15.8%; 3/18) sub-watersheds. In support of prior studies (Baker et al., 2022; Codling et al., 2018; George et al., 2023; Remucal, 2019), our results provide additional evidence that sub-watersheds (i.e., developed/urban, undeveloped, and agricultural), and land-use gradients adjacent to mussel sampling locations, are important emission sources, and environmental pathways for PFAS compounds detected within the Great Lakes aquatic environment.

Similar to results presented in prior studies (Brase et al., 2022; Munoz et al., 2022; Pickard et al., 2022; Tang et al., 2022), two $\sum_{2}$PFSA compounds, the long-chained (C_{11}) N-MeFOSAA (0.516 ng/g wet weight), and the short-chained (C_5) PFPeS (0.718 ng/g wet weight) were only detected (> MDL) in mussels from open-water sites in this study (Fig. 23). Similarly, the emerging long-chained (C_{10}) precursor 8:2 fluorotelomer sulfonic acid (8:2 FTS; 0.347 ng/g wet weight) was only detected in mussels from developed sites (Fig. 23). With known precursors such as PFOA and other terminal PFCA compounds (e.g., fluorotelomer aldehydes [FTALs], fluorotelomer carboxylic acids [FTCAs], and short-chained PFCAs [e.g., n ≥ C_4–C_6: PFHeA, PFHxA, PFBA, and PFHpA]; Berhanu et al., 2023), the detection of 8:2 FTS in mussels from developed sites, is indicative of their use in industrial and consumer-based products (Dewapriya et al., 2023; Xia et al., 2022), and subsequent emission in urban streams and surface water during urban water cycle processes (Link et al., 2024).

Additional correlation analysis revealed 8:2 FTS concentrations were significantly associated with site population estimates (Spearman's rho (ρ) = 0.70; $p < 0.001$), and mussel sampling locations developed land-use categories (Spearman's rho (ρ) = 0.535; $p < 0.01$; Fig. 11). In contrast, modest negative association was observed between 8:2 FTS concentration, and proximity to WWTP/CSO outfalls (Spearman's rho (ρ) = -0.416; $p < 0.05$), suggesting local usage, and urban wastewater treatment discharge are likely drivers for the detection of these contaminants at developed mussel sampling locations. Similarly, the correlation analysis also revealed the PFAS precursor N-MeFOSAA (Spearman's rho (ρ) = 0.367; $p < 0.05$), and PFPeS (Spearman's rho (ρ) = 0.612; $p < 0.001$; Fig. 11) concentrations were positively associated with mussel sampling locations open-water land-use categories, further suggesting sampling locations adjacent to open-water, and developed/urban land uses are likely sinks and hotspots for these PFAS contaminants in the Great Lakes Basin.

Overall, PFTreA, a long-chained C_{14}–PFCA (mean range; 0.975 - 1.60 ng/g wet weight) was measured at the highest mean concentration in mussels across examined mussel site land-use categories, followed by PFOSA (mean range; 0.618 - 1.46 ng/g wet weight), PFDS (mean range; 0.43 - 0.872 ng/g wet weight), PFDoA (mean range; 0.687 - 0.868 ng/g wet weight), PFTriA (mean range; 0.522 - 0.809 ng/g wet weight), PFBA (mean range; 0.726 - 0.771 ng/g wet weight), and PFOS (mean range; 0.238 - 0.72 ng/g wet weight). In addition, the concentration of several long-chained $\sum_{4}$PFCA compounds including PFTriA (0.714 - 0.903 ng/g wet weight), PFDoA (0.666 - 1.49 ng/g wet weight), PFTreA (0.638 - 3.02 ng/g wet weight), and PFOS (0.105 - 4.73 ng/g wet weight), were generally higher in mussels from developed sites, compared to open-water, agriculture, undeveloped and wetland sites. As reported in Lin et al. (2021) and Wang et al. (2014), the production of long-chained PFAS compounds (e.g., PFCA [n ≥ C_7–C_{14}] and PFSA [n ≥ C_6–C_{10}]) is limited. Hence, the detection of these PFAS compounds in mussels from developed and open-water sampling locations, is likely attributed to PFAS precursor degradation and transformation of PFSA and PFCA-based consumer products (e.g., PFOA, PFNA, and fluorotelomer-based products and derivatives; Giesy et al., 2006), occurring at these mussel sampling locations.

On average, PFAS compounds were detected frequently (DF > 20%) in mussels from sites sampled adjacent to developed land-use gradients (DF range; 22 - 78%), compared to open-water (DF range; 27 - 70%), undeveloped (DF range; 20 - 50%), and agricultural land-use types (DF range; 20 - 40%). Overall, PFOS was the most frequently detected (> 20%) compound in mussels examined across all mussel sampling location predominant land-use categories (DF range; 30 - 78%), followed by PFDS (DF range; 30 - 56%), PFDoA (DF range; 20 - 50%), and the short-chained (C_4) carboxilic acid PFBA (DF range; 32 - 40%). Moreover, PFDoA (DF = 33%), PFBA (DF = 44%), PFDS (DF = 56%), and PFOS (DF = 78%), were detected at higher frequency in mussels from developed sites, compared to the other dominant mussel land-use categories assessed in this study, suggesting adjacent mussel sampling locations land-use gradients are likely hotspots

and sinks for these PFAS compounds currently detected at Great Lakes mussel sampling locations. Our results further highlight the ubiquity, and persistence of these long -and- short chained PFAS compounds detected in mussels across the Great Lakes Basin. More so, our results also highlight the ecological risk these contaminants pose to aquatic communities, and organisms adjacent to mussel developed/urban and open-water sampling locations.

Across predominant agricultural, undeveloped, and wetland mussel sampling locations, PFDoA (range; 0.747 - 0.789 ng/g wet weight), and PFOS (range; 0.777 - 0.816 ng/g wet weight) were detected at the highest concentrations in mussels. Interestingly, modest to significant ($P < 0.05$) negative associations were observed between the concentrations of several PFAS compounds including PFTreA (Spearman's rho (ρ) = -0.426 to -0.583, $p < 0.05$), PFDA (Spearman's rho (ρ) = -0.576 to -0.615, $p < 0.05$), PFPeS (Spearman's rho (ρ) = -0.473 to -0.633, $p < 0.05$), PFHpA (Spearman's rho (ρ) = -0.369 to -0.710, $p < 0.05$), PFPeA (Spearman's rho (ρ) = -0.647 to -0.719, $p < 0.05$), PFOA (Spearman's rho (ρ) = -0.452 to -0.756, $p < 0.05$), and PFOS (Spearman's rho (ρ) = -0.405 to -0.834, $p < 0.05$), and mussel sampling locations undeveloped, agriculture, and wetland land-use categories (Fig. 11). As demonstrated in prior studies, adjacent landscapes and sub-watersheds can act as sinks for PFAS compounds (Baker et al., 2022; Llewellyn et al., 2024; Rafiei and Nejadhashemi, 2023). Equally important, PFAS components used in pesticide formulations (e.g., biocides - active products in plants grow regulators [PGRs]; Gaines, 2022; Hamid et al., 2018; Panieri et al., 2022), and in commercially available biosolid-based soil amendments and organic fertilizers (e.g., composts and digestates; O'Connor et al., 2022) can easily diffuse in soil and sediment of adjacent sub-watersheds landscape (George et al., 2023; Llewellyn et al., 2024; Point et al., 2021). Thus, PFAS release and transport across highly utilized agricultural, urban, and undeveloped (e.g., natural forests and wetlands; Rafiei and Nejadhashemi, 2023) sub-watersheds landscape via leaching, weathering, surface runoff and drainage from amended agricultural fields, including those with land applied biosolids/sewage sludge (e.g., used as fertilizer and soil conditioner/amendment; Link et al., 2024), might be a phenomenon that is influencing PFAS and land-use association observed across the Great Lakes mussel sampling locations (George et al., 2023; Guo et al., 2016; Point et al., 2021). Additional correlational analysis did not reveal any notable association between mussel sampling location land-use types and other PFAS compound concentrations (Fig. 11).

On average, summed $\sum_{19}$PFAS concentrations measured in mussel tissue were shown to vary spatially across mussel sampling location land-use types (Fig. 24B). The highest total $\sum_{19}$PFAS concentrations (> 4 ng/g wet weight) were measured in mussels from predominant open-water and developed sites sampled in Lakes Erie and Michigan (Fig. 24B). Elevated $\sum_{19}$PFAS concentrations measured in mussels from open-water and developed sampling locations in Lakes Erie and Michigan, is likely attributed to input from the gradual leaching and weathering of PFAS compounds and materials from domestic sources (e.g., domestic waste streams containing food packaging and commercial household materials, oil and paints, electronics, pesticide formulations; O'Connor et al., 2022; Lalonde and Garron, 2022). Elevated PFAS release from urban water cycle pulses (e.g., CSOs, urban storm water, and wastewater sources), mainly driven by elevated anthropogenic pressures including higher residential/population density adjacent to mussel sampling locations, are also likely candidates influencing elevated $\sum_{19}$PFAS concentrations measured in mussels from open-water and developed sampling locations in Lakes Erie and Michigan (Lin et al., 2021). Overall, the spatial distribution of $\sum_{19}$PFAS compounds observed in mussels from developed, and open-water sampling locations in Lake Michigan and Lake Erie, were similar to the distribution of emerging contaminants such as PPCPs and other CECs observed in mussels from open-water sites, and sampling locations adjacent to developed land-use gradients and associated sub-watersheds in the Great Lakes Basin (Edwards et al., 2024; Fuller et al., 2023; Kimbrough et al., 2018).

Collectively, our results revealed similar spatial patterns and chemical signatures for some PFAS groups examined in mussels across the predominant land-use types assessed in this study. For example, PFAS compound groups including C_{10}–PFESAs (0.134 - 0.139 ng/g wet weight), C_4–C_7 PFCAs (1.03 - 1.22 ng/g wet weight), C_8–FASAs (3.63 - 3.97 ng/g wet weight), and C_8–C_{10} PFSAs (4.73 - 4.50 ng/g wet weight; Fig. 24C and Table 15), were detected at similar concentrations in mussels examined across developed and open-water land-use categories. Likewise, C_8–C_{12} PFCAs concentrations (0.747 - 0.885 ng/g wet weight) were higher in mussels across developed, open-water, and undeveloped mussel land-use types, thus highlighting the complexity of PFAS compound distribution and their concentration profile among various landscapes within the Great Lakes (Point et al., 2021; Silver et al., 2023).

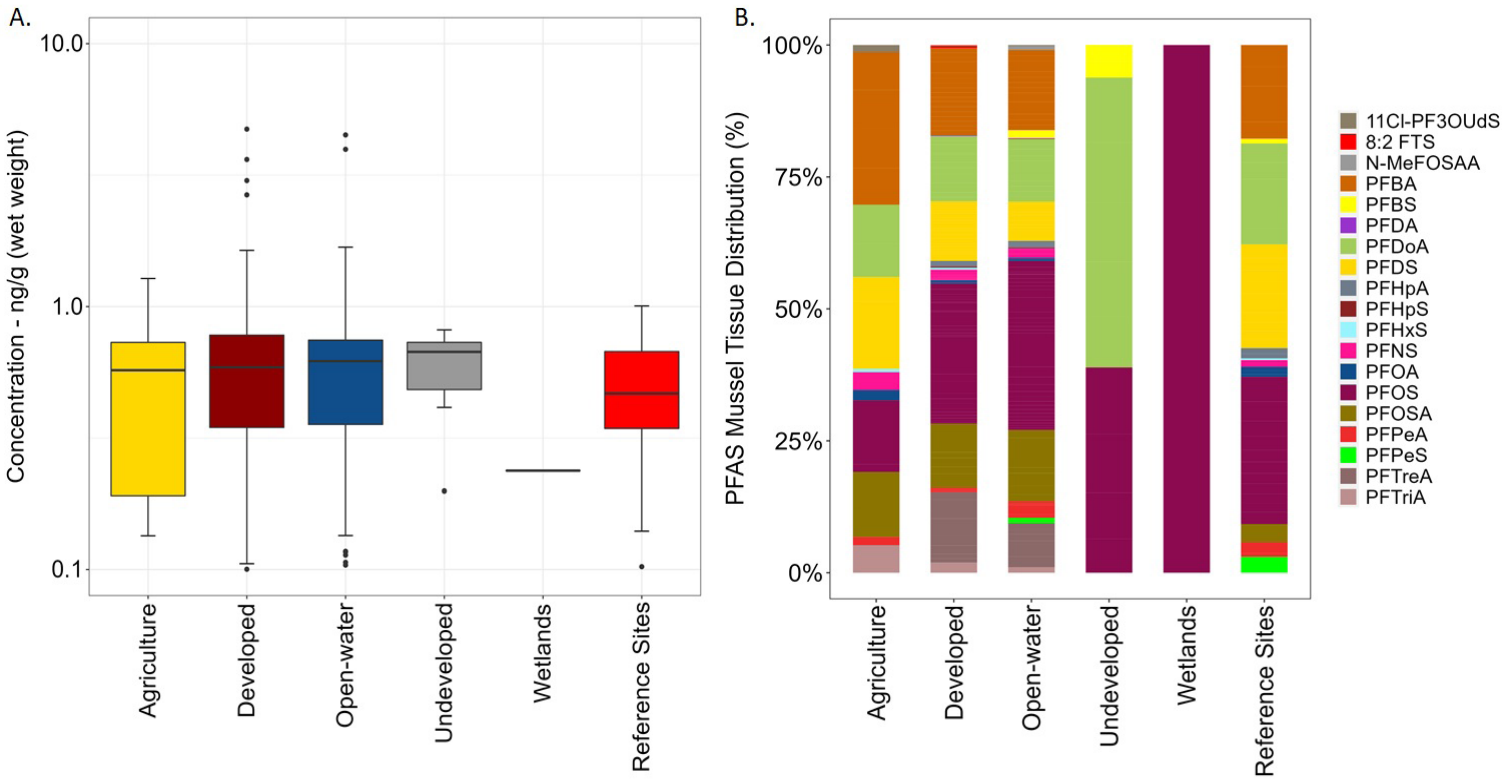

Fig. 22. A). Boxplots depicting overall ∑19PFAS concentration (ng/g wet weight) profile measured (> MDLs) in dreissenid mussels from predominant MWP site land-use categories (Agriculture, Developed, Undeveloped, Open-water, and Wetlands) during the 2013 - 2018 sampling period, and B), the percent composition (%) and relative distribution of ∑19PFAS recorded in mussel tissue from designated MWP land-use categories during the 2013 - 2018 sampling event. Reference sites provides perspective to the relative PFAS concentrations measured in mussel tissue from predominant MWP site land-use categories (Agriculture, Developed, Undeveloped, Open-water, and Wetlands).

Table 14. Summary of ∑19PFAS concentrations (ng/g wet weight) measured in dreissenid mussel tissue (> MDLs) from predominant agriculture, developed, open-water, undeveloped, and wetland sites between 2013 - 2018. Reference sites provides perspective to the relative PFAS concentrations measured in mussel tissue from predominant MWP site land-use categories (Agriculture, Developed, Undeveloped, Open-water, and Wetlands).

Category	(n)	Stdev	Min	Median	Mean	Max
Site Land-use Category			ng/g (ww)	ng/g (ww)	ng/g (ww)	ng/g (ww)
Agriculture	20	0.315	0.064	0.547	0.502	1.28
Developed	128	0.628	0.064	0.543	0.657	4.73
Open-water	107	0.591	0.078	0.616	0.658	4.50
Undeveloped	11	0.222	0.199	0.673	0.587	0.816
Wetlands	1	0	0.238	0.238	0.238	0.238
Reference Sites	45	0.23	0.073	0.46	0.477	1.01

Table 15. Summary of $\sum_{19}$PFAS compound group concentrations (ng/g wet weight) measured in dreissenid mussel tissue (> MDLs) from predominant agriculture, developed, open-water, undeveloped, and wetland sites between 2013 - 2018.

				Min	Median	Mean	Max
Site Land-use Category	PFAS Groups	(n)	Stdev	ng/g (ww)	ng/g (ww)	ng/g (ww)	ng/g (ww)
Developed	C4–C7 PFSAs	5	0.025	0.064	0.105	0.104	0.126
	C10 - PFESAs	1	0	0.139	0.139	0.139	0.139
	C10 - FTSAs	1	0	0.347	0.347	0.347	0.347
	C8–C10 PFSAs	62	0.602	0.098	0.404	0.532	4.73
	C4–C7 PFCAs	25	0.257	0.17	0.741	0.619	1.03
	C8–C12 PFCAs	15	0.371	0.139	0.759	0.728	1.49
	C8 - FASAs	8	0.985	0.605	0.927	1.273	3.63
	C13–C14 PFCAs	9	0.869	0.638	1.176	1.426	3.02
Agriculture	C4–C7 PFSAs	1	0	0.064	0.064	0.064	0.064
	C10 - PFESAs	1	0	0.134	0.134	0.134	0.134
	C8–C10 PFSAs	9	0.37	0.146	0.394	0.453	1.28
	C13–C14 PFCAs	1	0	0.522	0.522	0.522	0.522
	C8–C12 PFCAs	3	0.29	0.196	0.627	0.523	0.747
	C4–C7 PFCAs	5	0.255	0.157	0.72	0.612	0.742
	C8 - FASAs	2	0.064	0.573	0.618	0.618	0.664
Undeveloped	C4–C7 PFSAs	2	0.001	0.199	0.199	0.199	0.199
	C8–C10 PFSAs	4	0.176	0.414	0.64	0.627	0.816
	C8–C12 PFCAs	5	0.065	0.62	0.725	0.709	0.789
Wetlands	C8–C10 PFSAs	1	0	0.238	0.238	0.238	0.238
Open-water	C10 - PFESAs	1	0	0.136	0.136	0.136	0.136
	C4–C7 PFSAs	8	0.248	0.073	0.266	0.351	0.718
	C11 - FOSAAs	1	0	0.516	0.516	0.516	0.516
	C8–C12 PFCAs	24	0.251	0.103	0.664	0.552	0.885
	C8–C10 PFSAs	71	0.531	0.078	0.475	0.559	4.50
	C4–C7 PFCAs	33	0.312	0.135	0.69	0.565	1.22
	C13–C14 PFCAs	7	0.378	0.566	0.775	0.942	1.52
	C8 - FASAs	7	1.15	0.733	1.04	1.46	3.97

Results & Discussion

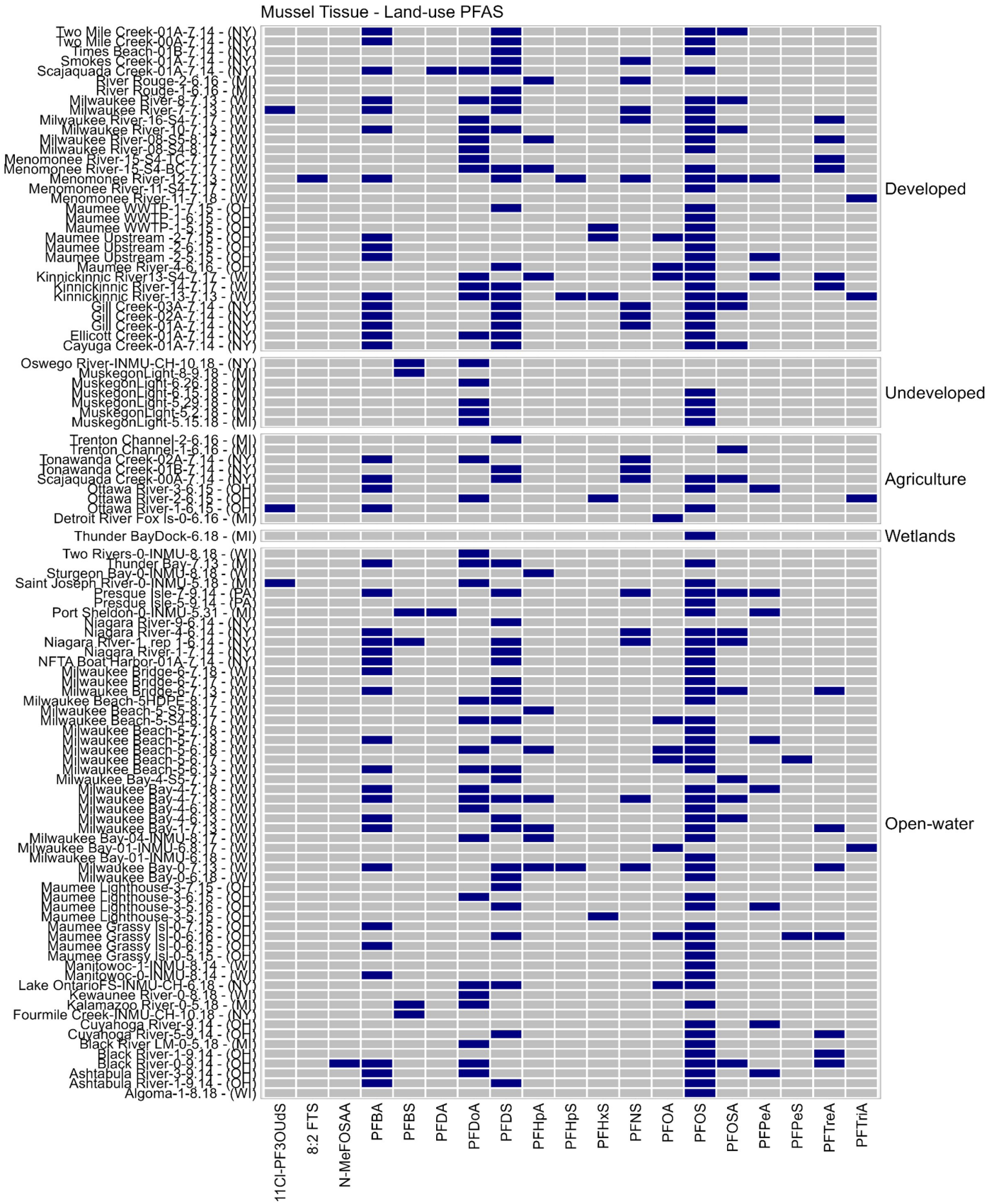

Fig. 23. Heat map depicting presence ( ) and absence ( ) of all $\sum_{19}$PFAS ccompounds measured in mussel tissue above the detection limit (> MDLs) from predominant MWP site land-use categories (Developed, Undeveloped, Agriculture, Wetlands, and Open-water) during the 2013 - 2018 sampling period. Individual sites are listed by their general location (associated riverine/lake region), state and month/year sampled.

Results & Discussion

Fig. 24. Barplot depicting A). mussel sampling locations predominant land-use category estimates (%), B), summed $\sum_{19}$PFAS concentrations (ng/g wet weight) measured (> MDL) in mussel tissue from predominant MWP site land-use categories/gradients, and C), the concentration profile (%) and relative distribution of predominant $\sum_{19}$PFAS groups (long and short-chained homologues) detected in mussels from predominant MWP site land-use categories/gradients during the 2013 - 2018 sampling period. Clusters 1-3 represents mussel sampling locations with measured low ( ), medium ( ), and high ( ) summed $\sum_{19}$PFAS concentrations. Individual sites are listed by their general location (associated riverine/lake region), state and month/year sampled.

3.7. Mussel Tissue PFAS Cluster Analysis

Multivariate analyses including unsupervised classification and cluster analysis were conducted to further identify mussel sampling locations with (dis)similar chemical patterns based on land-use types, discharge-types, PFAS composition and concentration profile. Results from our unsupervised classification and subsequent cluster analysis revealed three distinct clusters: cluster-1 (59 sites), cluster-2 (29 sites), and cluster-3 (18 sites; Fig. 25 and Fig. 26). Compositionally, $\sum_{19}$PFAS compounds remained spatially heterogeneous across clusters 1-3, with PFAS composition higher in mussels from sites sampled in cluster-1 (89.5%; 17/19), compared to cluster-2 (84.2%; 16/19) and cluster-3 (52.6%; 10/19), respectively (Fig. 27B, Fig. 28 and Fig. 29). On average, 9 $\sum_{9}$PFAS compounds (11Cl-PF3OUdS [Log K_{ow} = 6.58], PFNS [Log K_{ow} = 5.16], PFPeA [Log K_{ow} = 3.43], PFHpA [Log K_{ow} = 4.67], PFBS [Log K_{ow} = 3.90], PFDS [LLog K_{ow} = 5.83], PFDoA [Log K_{ow} = 7.49], PFTreA [Log K_{ow} = 8.83], and PFOS [Log K_{ow} = 6.43]), were consistently found co-occurring in mussels across all three clusters (Fig. 26 and Fig. 28). Furthermore, the long-chained perfluoroalkane sulfonamido acetic acid (C_{11}-N-MeFOSAA), and the short-chained perfluoro-1-pentanesulfonic acid (C_5-PFPeS) were only detected in mussels from sites sampled in cluster-1. In addition, several PFAS compounds including PFTreA, PFOSA, PFNS, PFDoA, PFBA, PFDS, and PFOS were frequently detected (DF: > 30%) in mussels across all three clusters, indicative of the ubiquity and persistence of these contaminants across the Great Lakes Basin.

In regards to mussel tissue concentration levels, of the 19 $\sum_{19}$PFAS compounds examined across clusters 1-3, relatively higher mean $\sum_{19}$PFAS levels were observed in mussels from cluster-3 (0.807 ng/g wet weight), compared to $\sum_{19}$PFAS concentrations measured in mussels from cluster-2 (0.63 ng/g wet weight) and cluster-1 (0.515 ng/g wet weight), respectively (Fig. 27A and Table 16). However, no statistically significant difference was observed between cluster 1-3 mean $\sum_{19}$PFAS concentrations (Kruskal-Wallis; $p > 0.05$). Similarly, the magnitude of individual $\sum_{19}$PFAS compounds were relatively higher concentrations detected in mussels from cluster-3 (n=56; 0.1 - 4.73 ng/g wet weight), compared to cluster-2 (n=136; 0.064- 3.97 ng/g wet weight), and cluster-1 (n= 120; 0.064 - 1.68 ng/g wet weight; Table 16). Additional examination of mussel PFAS concentration profile across clusters 1-3 revealed, several $\sum_{7}$PFAS compounds including PFBA (0.789 - 1.20 ng/g wet weight), PFPeA (0.232 - 1.22 ng/g wet weight), PFDS (0.477 - 1.28 ng/g wet weight), PFDoA (0.885 - 1.49 ng/g wet weight), PFTreA (0.893 - 3.02 ng/g wet weight), PFOSA (1.68 - 3.97 ng/g wet weight), and PFOS (1.07 - 4.73 ng/g wet weight), were consistently measured at higher concentrations in mussels across clusters 1-3.

A general assessment of $\sum_{19}$PFAS compounds examined across individual clusters revealed, elevated $\sum_{19}$PFAS composition and concentration observed in mussels from sites sampled in cluster-1, were mainly driven by detections at developed and open-water sampling locations in Lakes Michigan, and Erie, and the Niagara riverine system (Fig. 25 and Fig. 29). Interestingly, sites sampled from specific riverine systems, which are influenced by domestic and urban waste streams (e.g., municipal solid waste, urban wastewater system, storm water runoff), grouped distinctly from other mussel sampling locations in cluster-1. For example, as shown in Fig. 25, developed and open-water sites in Lake Michigan, especially sites sampled in the Milwaukee Estuary riverine system that are influenced by PFAS input from domestic and urban sources, generally group together (upper left quadrant) in cluster-1. Likewise, mussel sampling locations influenced by PFAS input from point (e.g., WWTPs and CSOs) and diffuse/fugitive sources in the western Lake Erie basin, and the Maumee and Ottawa riverine system, were shown to group together (left lower quadrant) in cluster-1. Similar spatial groupings were also observed in cluster-1 for sites sampled in Lake Erie (Black River, OH, and Cuyahoga River, OH), and the Niagara riverine system, that shared similar PFAS chemical signatures (cluster-1; upper right quadrant). Previous studies have also highlighted similar PFAS contamination patterns for sites sampled in Lake Michigan/Milwaukee Estuary, Lake Erie/Maumee River, and the Niagara riverine system (Remucal, 2019; Custer et al., 2020; Custer et al, 2024; Lin et al., 2021).

Additional site-site assessment revealed, summed $\sum_{17}$PFAS concentrations were similar for most mussel sampling locations examined across cluster-1. However, elevated $\sum_{17}$PFAS concentrations were mainly detected in mussels from agricultural, open-water, and developed sites (e.g., sites sampled adjacent to urban clusters) sampled in the Lake Erie (0.073 - 4.46 ng/g wet weight), compared to open-water, developed, and agricultural sites sampled in Lake Michigan (0.156 - 2.90 ng/g wet weight), Niagara River (0.399 - 1.51 ng/g wet weight), Detroit River (0.196 - 1.28 ng/g wet weight), and Lake Ontario (0.229 - 0.988 ng/g wet weight; Fig 29A and Fig. 29B). In addition, similar chemical signatures were also observed for the following short-chained PFSA (n ≥ C_4–C_7; 0.064 - 0.718 ng/g wet weight), and long-chained PFCA groups (n ≥ C_8–C_{12}: 0.103 - 0.885 ng/g wet weight; n ≥ C_{13}–C_{14}: 0.522 - 0.903 ng/g wet weight), measured in mussels across cluster-1 (Table. 17). Similar patterns were also observed for short-chained PFCA (n ≥ C_4–C_7; 0.135 - 1.22 ng/g wet weight), long-chained PFSA (n ≥ C_8–C_{10}; 0.078 - 1.28 ng/g wet weight), and long chained FASA groups (n ≥ C_8; 0.664 - 1.68 ng/g wet weight) examined in mussels across cluster-1 (Fig. 29C and Table 17), which suggests similarity in PFAS emission source and attenuation occurring at these sampling locations.

In regards to cluster-2, with the exception of sites sampled in Lake Erie (LEPB-7-9.14, LEAR-1-9.14), and Lake Huron (TBHS5-7.13), sampling locations assessed in cluster-2 represented a mix of mainly developed, and open-water sites sampled in Lake Michigan/Milwaukee Bay, WI, and the Niagara riverine system (Fig. 25 and Fig. 29). Specifically, developed and open-water sites in Niagara River, and Lake Michigan were observed to group together, or separated individually into different quadrants, based on (dis)similarity in their composition and concentration profile. For example, sites sampled from downstream developed/urban gradients in Niagara River, NY (Gill Creek-01A-7.14; Cayuga Creek-01A-7.14), Milwaukee River, WI (LMMB-10-7.13; LMMB-8-7.13) that depicted similar chemical signatures, tend to group together in cluster-2. Thus, mussels from developed and open-water sites in Niagara River and Lake Michigan that display high degrees of similarity in PFAS concentration and composition profile, may subsequently share similar PFAS fate and transport characteristics (Christensen et al., 2022; Dávila-Santiago, et al., 2022). Similarly, sites sampled proximal to point sources (e.g., WWTPs) in Lake Michigan (Milwaukee Bridge, WI [LMMB-6-7.13]), and Lake Erie (Ashtabula River, OH [LEAR-1-9.14]), were shown to group separately from other sampling locations, which suggests similar input and emission sources, with distinct PFAS chemical signatures likely occurring at these sampling locations.

Spatially, summed $\sum_{16}$PFAS concentrations were found to be higher (> 3.5 ng/g wet weight) in mussels across predominant developed (3.48 - 5.34 ng/g wet weight) and open-water sites (3.78 - 6.34 ng/g wet weight) sampled in Lake Michigan, Niagara River, and Lake Erie (Fig. 29B). Elevated $\sum_{16}$PFAS concentrations observed in mussels from sites sampled in cluster-2, were shown to be indicative of their proximity to localized anthropogenic sources, including point source discharge (e.g., WWTPs, CSOs), and their location downstream and along PFAS wastewater discharge gradients, resulting in elevated PFAS detection and chemical signatures. Similar spatial patterns were also observed for several $\sum$PFAS groups including short-chained PFCAs ($n \geq C_4$–C_7; 0.14 - 1.20 ng/g wet weight), and the following long-chained PFAS groups; PFSA ($n \geq C_8$–C_{10}; 0.107 - 1.23 ng/g wet weight), PFCA ($n \geq C_8$–C_{12}; 0.666 - 1.32 ng/g wet weight), and PFCA ($n \geq C_{13}$–C_{14}; 0.714 - 1.52 ng/g wet weight), examined in mussels across cluster-2 sampling locations (Figure 30C and Table 18). Interestingly, compared to clusters 1 and 3, perfluoroalkane sulfonamide (FASAs) compounds were mainly detected in mussels across developed and open-water sites in cluster-2 (Fig. 29C). In addition, C_8–FASA concentrations (0.573 - 3.97 ng/g wet weight) measured in mussels from sites sampled in cluster-2 were approximately 2 magnitudes higher, compared to PFSAs and PFCAs groups assessed in mussels across cluster-2 (Table 17), suggesting a likely "hotspot" and elevated C_8–FASA contamination and exposure to mussels and other lower-trophic level organisms occurring at these sampling locations.

Prior studies have reported, perfluoroalkane sulfonamide (FASAs) compounds including the long-chained C_8-PFOSA (a homologue of PFBSA [C_4], and also a precursor of PFOS; Silver et al., 2023) is widely used during industrial processes (Chen et al., 2022), in food packaging and other consumer products (e.g., teflon coating in cooking utensils, fabrics, food packaging, fire-fighting foams, and mechanical lubrication), and as an intermediate ingredient in the pesticide Sulfluramid (N-EtFOSAA; Lin et al., 2021; Boulanger et al., 2005). Moreover, the insecticide Sulfluramid (N-EtFOSAA) has been used in most Great Lakes residential/urban areas as bait stations for the control of insects (Lin et al., 2021). PFOSA is also considered equally toxic as the widely studied PFOA and PFOS compounds, with reported induce immunotoxicity, endocrine toxicity, and developmental toxicity among the known toxicological endpoints at environmentally relevant concentrations (Dasgupta et al., 2020; Liu et al., 2022). The detection of FASA PFAS compounds including PFOSA in mussels from developed sampling locations in Niagara River, NY, and Milwaukee Estuary, WI (Fig. 29C), is indicative of extensive domestic and urban use, and subsequent emission and runoff into urban surface water (De a Miranda et al., 2023; Remucal, 2019). Equally important, our findings suggest open-water, and developed/urban land-use gradients adjacent to mussel sampling locations are likely sinks and hotspots for these potent developmental toxicants (Dasgupta et al., 2020; Starkov, 2002).

In regards to cluster-3, with the exception of an open-water/offshore mussel sampling location in Lake Ontario (LOFO-INMU-CH-6.18), sampling locations examined across cluster-3 primarily represented a mix of undeveloped, developed, and open-water sites sampled in Lake Michigan (Fig. 25 and Fig. 29). Spatially, mussel sampling locations either grouped together, or separated individually across cluster-3 based on their geographic location. For example, mussels sampled from predominant undeveloped (Muskegon, MI; MUS-5.2.18, MUS-5.15.18, and MUS-5.29.18), and open-water sites (Black River, MI [LMBR-0-5.18]; St. Joseph River, MI [LMSJ-0-INMU-5.18]; and Kalamazoo River, MI [LMKZ-0-5.18]) on the eastern side of Lake Michigan were shown to group or separate individually across cluster-3. Similarly, mussels sampled from open-water and developed sites on the western side of Lake Michigan (Milwaukee Estuary, WI), were also shown to group or separate individually across cluster-3, indicative of different potential PFAS emission sources between the western and eastern sides of the Lake Michigan basin. Contaminant pattern detected in mussels from sites sampled on the western and eastern sides of Lake Michigan (Fig. 9), highly reflect PFAS compounds that are associated with emission from localized, as well as anthropogenic sources including input from conventional wastewater systems, as well as input from urban surface and stormwater runoff. Similar patterns were observed in prior PFAS studies conducted within the

Milwaukee Estuary, WI (Custer et al., 2024). Results from previous studies have also identified runoff events from a range of developed/urban sub-watershed types (e.g., low-density suburban housing developments, high-density urban mixed-use areas, commercial shopping districts, industrial areas and zones, and impervious [paved] surfaces), as important vectors and environmental pathways for PFAS input to urban streams and surface water (Houtz and Sedlak, 2012b; Nguyen et al., 2016; Zhang et al., 2016; Zushi and Masunaga, 2009).

As shown in Fig. 29B, summed $\sum_{10}$PFAS concentrations were significantly higher (Kruskal-Wallis; $p > 0.05$) in mussels from developed sites sampled in cluster-3 (1.65 - 9.83 ng/g wet weight), compared to mussels sampled from open-water (0.228 - 5.46 ng/g wet weight), and undeveloped sampling locations (1.15 - 1.44 ng/g wet weight). On average, the highest summed $\sum_{10}$PFAS concentrations were measured in mussels from a mix of open-water and developed sites sampled in the Milwaukee River (2.86 ng/g wet weight), Menomonee River (3.13 ng/g wet weight), Kalamazoo River, MI (5.46 ng/g wet weight) and the Kinnickinnic River (9.83 ng/g wet weight; Fig. 29B). Our finding is consistent with results from previous studies that reported elevated PFAS levels in WWTP effluent from sites sampled in the Kalamazoo River, MI (Helmer et al., 2022), and in tree swallow (*Tachycineta bicolor*) tissue from sites sampled in the Milwaukee, Menomonee, and Kinnickinnic Rivers (Milwaukee Estuary, WI; Custer et al., 2024). Interestingly, additional assessment revealed summed $\sum_{10}$PFAS concentrations (2.54 ng/g wet weight) measured in mussels from an offshore Lake Ontario site (Lake OntarioFS-INMU-CH-6.18; Fig. 29B) in cluster-3, was similar or equal to PFAS chemical signatures observed across some inshore sampling locations examined in clusters 1-3. Moreover, this finding is consistent with results from prior studies that reported elevated PFAS levels at offshore sites in Lake Ontario (Remucal, 2019; Ren et al., 2022; Yeung et al., 2013).

Elevated PFAS concentrations observed in mussels at offshore/open-water lake sampling locations in Lake Ontario, which are well beyond major pollution source (> 5Km), is indicative of PFAS compounds persistence, active offshore contaminant transport, and extended hydraulic residence time (e.g., hydraulic residence time: Lake Michigan = 62 years, Lake Huron = 21 years, Lake Erie = 2.7 years, Lake Ontario = 7.5 years; Jasechko et al., 2014; Quinn, 1992), in the Great Lakes Basin (Codling et al., 2018; Muir and Miaz, 2021; Point et al., 2021; Remucal, 2019). In regards to PFAS compound groups, the predominant $\sum_{10}$PFAS groups measured in mussels across cluster-3 included both long-chained ($n \geq C_8$–C_{12}) PFCA, and ($n \geq C_8$ - C_{10}) PFSA compounds (Table 17). Similarly, both long-chained PFCA ($n \geq C_{13}$ - C_{14}: 0.638 - 3.02 ng/g wet weight), and PFSA ($n \geq C_8$ - C_{10}: 0.1 - 4.73 ng/g wet weight) compounds were measured at the highest concentration in mussels across cluster-3. Comparatively, similar chemical patterns were observed for the following short-chained PFSA ($n \geq C_4$–C_7; 0.302 ng/g wet weight), PFCA ($n \geq C_4$–C_7; 0.244 ng/g wet weight), and long-chained PFESA (C_{10}; 0.244 ng/g wet weight), compound groups measured in mussels across sites sampled in cluster-3 (Fig. 29C and Table. 17).

In general, the results from the unsupervised classification and cluster analysis suggest, the composition and chemical profile for $\sum_{19}$PFAS compounds detected in mussel tissue basin-wide vary independently among mussel sampling locations. This may be attributed to several factors including intensity of PFAS input from adjacent sampling locations land-use gradients and discharge-types, proximity to PFAS contaminant source and their environmental pathways, detected PFAS compounds unique properties (e.g., PFAS functional groups, long vs. short-chained, and hydrophobicity vs. lipophobicity; Balgooyen and Remucal, 2022; Buck et al., 2021), as well as the environmental behavior of detected PFAS compounds (e.g., dilution and attenuation capacity; Kolpin et al., 2021; Sardiña et al., 2019). Our PFAS results further highlight the importance of adjacent mussel sampling locations land-use gradients and discharge-types, in contributing to elevated PFAS and other emerging contaminants runoff and loading within the Great Lakes Basin (Edwards et al., 2024).

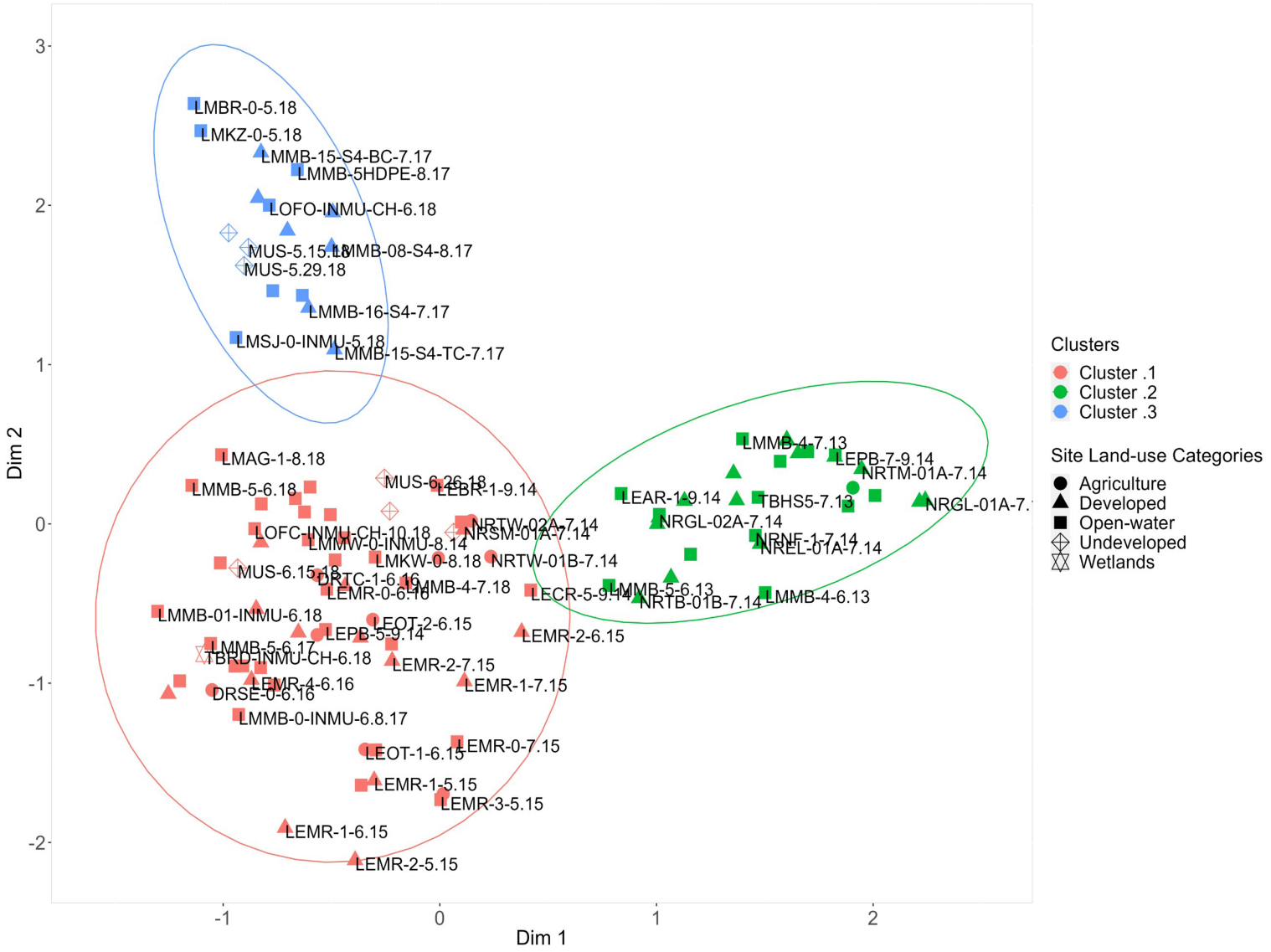

Fig. 25. Clusters and spatial grouping for predominant agriculture, developed, undeveloped (e.g., barren, forest, shrubs, and grassland), wetland, and open-water mussel sampling locations, resulting from unsupervised random forest classification and cluster analysis. Ellipse represents the 95% confidence intervals for each cluster. The unsupervised classification and subsequent cluster analysis results represents three major clusters (cluster 1-3) based on ∑PFAS compounds (> MDLs) presence/absence (1/0), and their composition profile measured in mussels across the Great Lakes between 2013-2018. Individual sites are listed by their site code which include the Great Lake or connecting channel sampled, as well as the year sampled. Some site names (codes) were removed from the cluster analysis plot due to space constraints. Additional information on MWP site codes and acronyms used in this study is provided in Table A1 and Table A3 (Appendix).

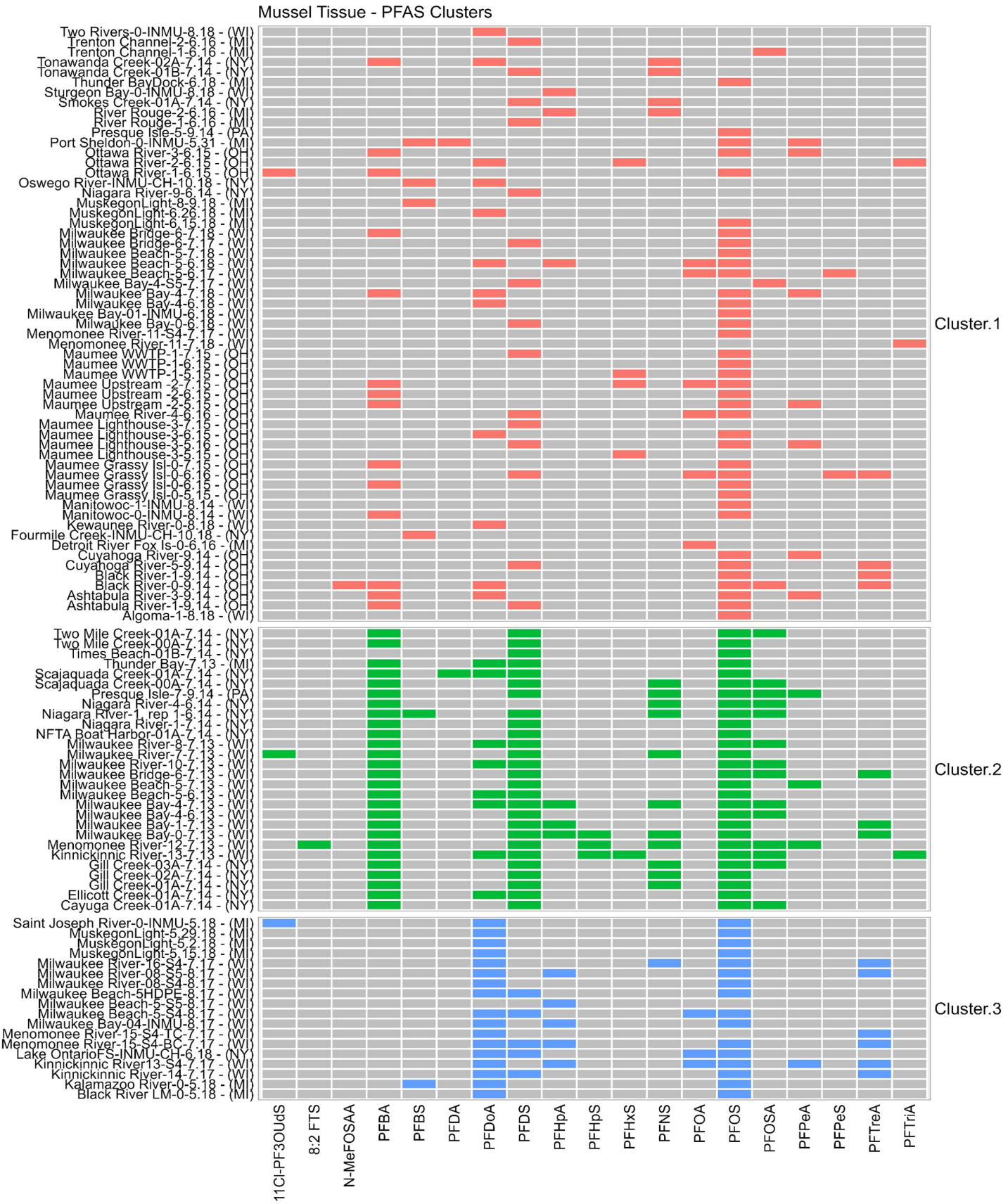

Fig. 26. Heat map depicting spatial grouping and clusters for Great Lakes MW PFAS sampling locations resulting from random forest (RF) unsupervised classification and cluster analyses. Heatmap depicts the absence ( ) and presence of $\sum_{19}$PFAS compounds measured (> MDLs) in mussels across cluster-1 ( ), cluster-2 ( ), and cluster-3 ( ) mussel sampling locations. Individual sites are listed by their general location (associated riverine/lake region), state and month/year sampled.

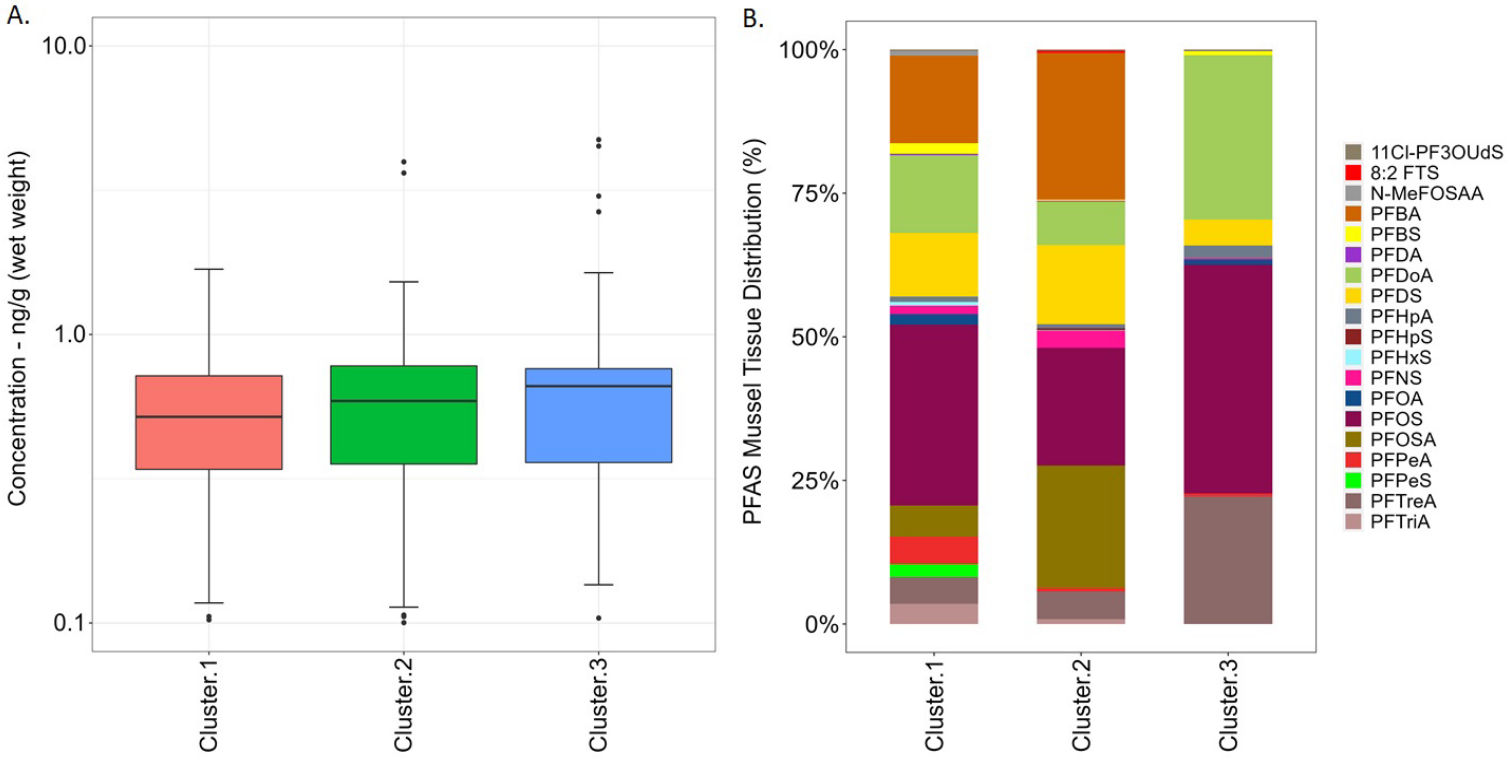

Fig. 27. A). Boxplot depicting ∑19PFAS concentration (ng/g wet weight) profile for compounds observed in individual clusters (clusters 1-3) derived from unsupervised random forest classification and cluster analysis, and B), the percent composition (%) and distribution of ∑19PFAS compounds recorded in mussel tissue from sites sampled across cluster-1 ( ), cluster-2, ( ), and cluster-3 ( ), during the 2013 - 2018 sampling event.

Table 16. Summary of ∑19PFAS concentrations (ng/g wet weight) measured in dreissenid mussel tissue (> MDLs) from individual clusters (clusters 1-3) derived from unsupervised random forest classification and cluster analysis.

Category	(n)	Stdev	Min	Median	Mean	Max
PFAS Clusters			ng/g (ww)	ng/g (ww)	ng/g (ww)	ng/g (ww)
Cluster.1	120	0.296	0.064	0.486	0.515	1.68
Cluster.2	136	0.496	0.064	0.583	0.63	3.97
Cluster.3	56	0.92	0.1	0.654	0.807	4.73

Table 17. Summary of $\sum_{19}$PFAS compound groups concentration (ng/g wet weight) measured in dreissenid mussel tissue (> MDLs) from sites sampled in clusters 1-3.

				Min	Median	Mean	Max
PFAS Clusters	PFAS Groups	(n)	Stdev	ng/g (ww)	ng/g (ww)	ng/g (ww)	ng/g (ww)
Cluster-1	C10 - PFESAs	1	0	0.134	0.134	0.134	0.134
	C11 - FOSAAs	1	0	0.516	0.516	0.516	0.516
	C13 - C14 PFCAs	7	0.149	0.522	0.748	0.725	0.903
	C4 - C7 PFSAs	10	0.245	0.064	0.199	0.291	0.718
	C4 - C7 PFCAs	23	0.281	0.135	0.69	0.564	1.22
	C8 - C10 PFSAs	56	0.267	0.078	0.408	0.488	1.28
	C8 - C12 PFCAs	19	0.275	0.103	0.627	0.501	0.885
	C8 - FASAs	3	0.516	0.664	1.04	1.13	1.68
Cluster-2	C10 - FTSAs	1	0	0.347	0.347	0.347	0.347
	C10 - PFESAs	1	0	0.139	0.139	0.14	0.139
	C13 - C14 PFCAs	4	0.361	0.714	1.30	1.21	1.52
	C4 - C7 PFSAs	5	0.047	0.064	0.105	0.115	0.192
	C4 - C7 PFCAs	34	0.253	0.14	0.738	0.676	1.20
	C8 - C10 PFSAs	69	0.229	0.107	0.438	0.465	1.23
	C8 - C12 PFCAs	8	0.22	0.666	0.713	0.805	1.32
	C8 - FASAs	14	1.08	0.573	0.907	1.31	3.97
Cluster-3	C10 - PFESAs	1	0	0.136	0.136	0.136	0.136
	C13 - C14 PFCAs	6	0.983	0.638	1.50	1.67	3.02
	C4 - C7 PFSAs	1	0	0.302	0.302	0.302	0.302
	C4 - C7 PFCAs	6	0.037	0.152	0.222	0.207	0.244
	C8 - C10 PFSAs	22	1.24	0.1	0.445	0.914	4.73
	C8 - C12 PFCAs	20	0.292	0.104	0.702	0.667	1.49

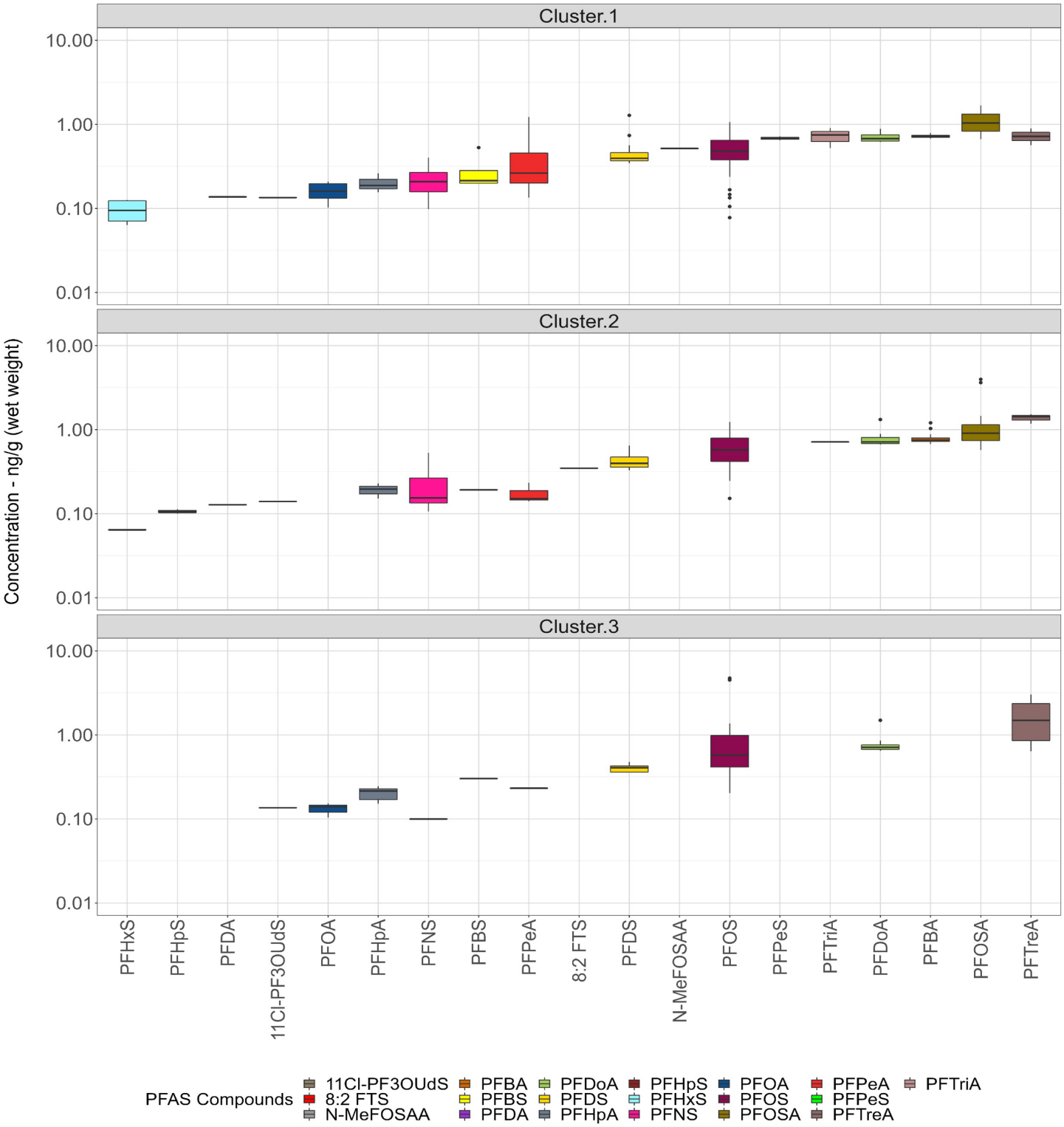

Fig. 28. Boxplots showing ∑19PFAS concentration (ng/g wet weight) profile for compounds observed in individual clusters derived from unsupervised classification and cluster analysis. ∑19PFAS compounds are ordered from left to right by lowest to highest mean concentration in each cluster. Cluster 1 and cluster 2 represents clusters with the most predominant ∑19PFAS mixtures and chemical composition.

Results & Discussion

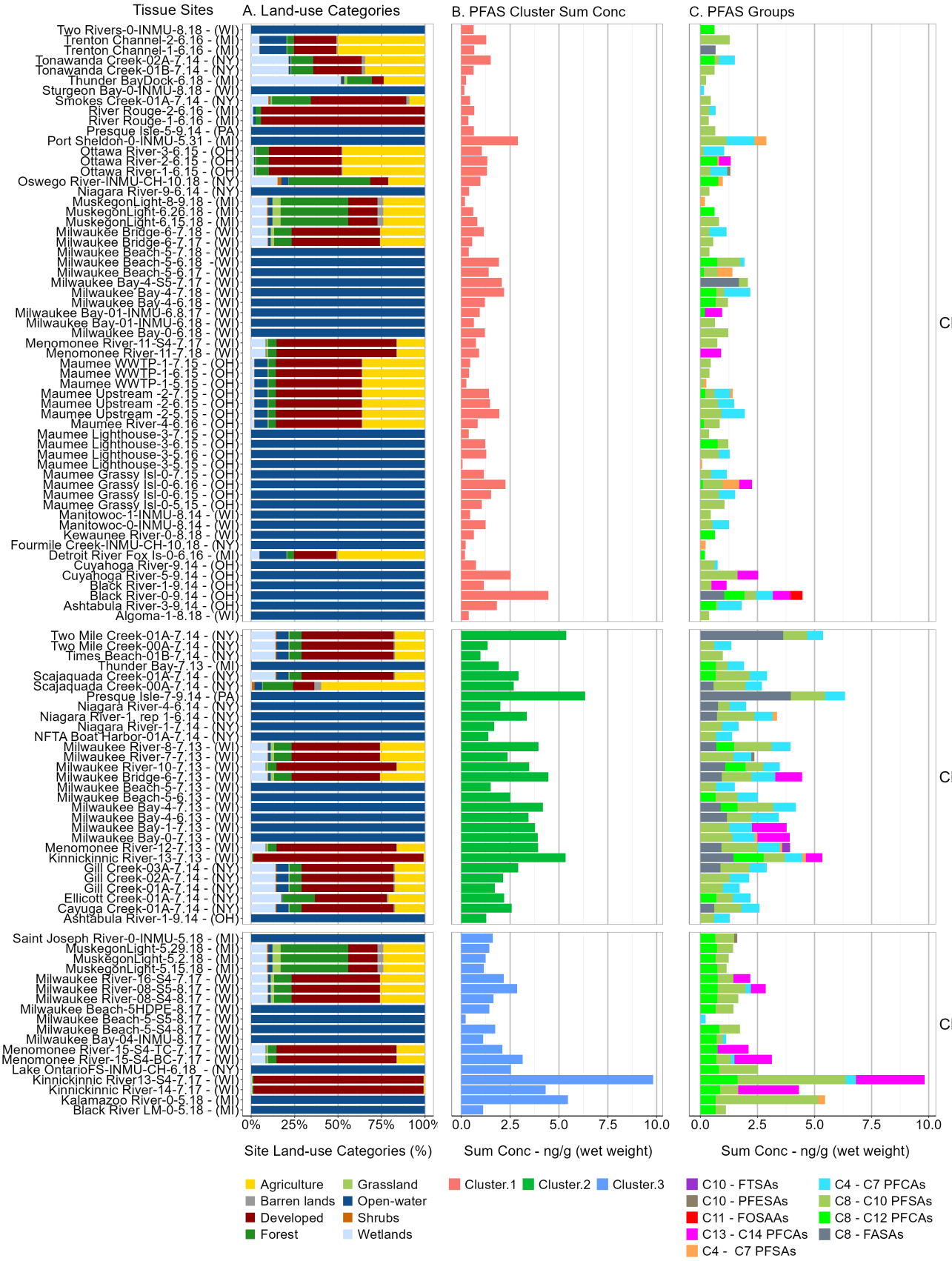

Fig. 29. Barplot depicting A). mussel sampling locations predominant land-use category estimates (%), B), spatial grouping and summed $\sum_{19}$PFAS concentrations (ng/g wet weight) for $\sum_{19}$PFAS compounds measured in mussels across cluster-1 ( ), cluster-2 ( ), and cluster-3 ( ), resulting from unsupervised classification and cluster analyses, and C), the distribution and concentration profile of predominant $\sum_{19}$PFAS compound groups detected in mussels across clusters 1-3. Individual sites are listed by their general location (associated riverine/lake region), state and month/year sampled.

3.8. PFAS Ecological Risk Assessment

The hazard quotient (HQ) results for $\sum_{19}$PFAS compounds measured (> MDL) across Great Lakes mussel sampling locations is presented in Fig. 30 and Table 18. An ecological risk threshold of HQ > 0.1 (medium or moderate risk), was used in the present study as a conservative risk-effects value for screening and prioritizing PFAS compounds measured in mussel tissue samples. As shown in Table 18, 2 $\sum_{2}$PFAS compounds (PFBS, and PFNS) were below the HQ < 0.01 threshold value, suggesting these compounds pose negligible to low risk to lower-trophic level aquatic organisms. Similarly, 3 $\sum_{3}$PFAS compounds (8:2 FTS, PFBA, and PFHxS) were below the HQ < 0.1 threshold value, suggesting low risk or minimal adverse effects to aquatic biota. Overall, these 5 $\sum_{5}$PFAS compounds were below the threshold risk-effects screening level (HQ > 0.1), and were removed from further discussion. Here, the discussion focuses on only the 14 $\sum_{14}$PFAS compounds that were detected in mussels above the HQ > 0.1 and HQ > 1 threshold criterion. Of the 14 compounds, 11 of these $\sum_{11}$PFAS compounds (11Cl-PF3OUdS [C_{10}], N-MeFOSAA [C_{11}], PFDA [C_{10}], PFDoA [C_{12}], PFDS [C_{10}], PFHpA [C_7], PFHpS [C_7], PFPeS [C_5], PFTreA [PFTeDA; C_{14}], PFTriA [PFTrDA; C_{13}], and PFPeA [C_5]) were identified exceeding the HQ > 0.1 threshold (Fig. 29). Further, 3 $\sum_{3}$PFAS compounds (PFOA, PFOSA [FOSA], and PFOS) were identified as exceeding the HQ > 1 threshold, indicating potential higher risk, and the possibility of adverse biological effects for mussels, and other aquatic organisms across mussel sampling locations (Table 18).

The distribution and number of $\sum_{14}$PFAS compounds exceeding the HQ > 0.1, and HQ > 1 threshold across mussel sampling locations is illustrated in Fig. 31 and Fig 32. Basin-wide, impacted mussel sampling locations with two or more PFAS compounds exceeding the HQ > 0.1, and HQ > 1 threshold were primarily recorded at developed, and open-water sites adjacent to sub-watersheds with larger population densities and industrial centers. As shown in Fig. 31 and Fig. 32, mussel sampling locations with the most compound exceedances were recorded at sites in Lake Michigan (Milwaukee River, Menomonee River, Kinnickinnic River, and Milwaukee Bay, WI; 4-6 compounds), Lake Erie (Black River, OH [LEBR-0-9.14; 5 compounds]; Cuyahoga River [LECR-5-9.14] and Maumee River [LEMR-4-6.16; LEMR-0-6.16]; 3-5 compounds), Lake Ontario (LOFO-INMU-CH-6.18; 4 compounds), and the Niagara riverine system (Cayuga Creek, Ellicott Creek, and Scajaquada Creek, NY 1-4 compounds). Conversely, sampling locations with the lowest number of HQ > 0.1, and HQ > 1 compounds exceedance were recorded for impacted sites sampled in Detroit River, and Lake Huron.

The ecological risks for individual $\sum_{11}$PFAS compounds exceeding the HQ > 0.1 threshold are ordered as follows (from low to high HQ values): PFDA > N-MeFOSAA > PFHpS > PFPeA > PFPeS > 11Cl-PF3OUdS > PFTriA > PFHpA > PFTreA > PFDoA > PFDS (Table 18). Basin-wide, PFDS was identified with the highest number of HQ > 0.1 threshold exceedances across Great Lakes mussel sampling locations (47 sites), followed by PFDoA (37 sites), PFTreA (13 sites) and PFHpA (11 sites; Fig. 31). Long-chained (n ≥ C_7–C_{14}) PFAS compounds contribution to PFAS exposures and elevated threshold exceedances across mussel sampling locations were not surprising. On average, long-chained compounds represented an average of 73.7% of the total PFAS compounds measured (> MDL) in mussel tissue during the 2013-2018 sampling period. Previous studies have shown long-chained (n ≥ C_7–C_{14}) PFAS compounds have similar physicochemical properties, and are used in similar industrial processes and consumer applications, which may explain their co-occurrence and threshold exceedances in this study (Gagliano et al., 2020; Goodrow et al., 2020; Wen et al., 2023). Compared to PFSA compounds, previous studies have shown due to their high octanol/water partition coefficient (log K_{ow} > 4; Table A2 Appendix), longer chained PFCA compounds have a higher tendency to bioaccumulate in tissue of aquatic organisms (Byns et al., 2024; Capozzi et al., 2023; George et al., 2023; Gomis et al., 2015; Koch et al., 2019).

Interestingly, the long-chained PFAS compounds PFDoA (C_{12}-PFCA), and PFDS (C_{10}-PFSA) followed similar pattern in PFAS HQ > 0.1 exceedance across the Great Lakes mussel sampling locations. Similarity in PFDoA and PFDS exceedance pattern across mussel sampling locations, is likely attributed to multiple factors including similar bioaccumulation mechanisms ocurring in mussel tissue (Munoz et al., 2022; Wen et al., 2019), exposure to similar contamination and emission sources (e.g., local direct emission and input from conventional wastewater systems, domestic, and industrial uses; Codling et al., 2018; George et al., 2023), and similar environmental behavior of these PFAS compounds within the Great Lakes aquatic environments (Remucal, 2019; Codling et al., 2018). In addition, input from atmospheric deposition (e.g., air–water exchange, wet deposition, and dry deposition; Xia et al., 2024), domestic and on-site wastewater treatment systems (Garcia et al., 2013; Subedi et al., 2015), are also likely contributors to PFDoA and PFDS elevated composition and exceedances detected in mussel's basin-wide. PFHpA (C_7-PFCA) and PFTreA (C_{14}-PFCA) also followed similar pattern in PFAS exceedance across the Great Lakes sampling locations. However, PFHpA and PFTreA (PFTeDA) were primarily recorded exceeding the HQ > 0.1 threshold at developed, and open-water sites in Lake Michigan (Kinnickinnic River, Menomonee River, Milwaukee River, and Milwaukee Bay, WI), and Lake Erie (Black River, OH [LEBR-0-9.14 and LEBR-1-9.14]; Cuyahoga River, OH [LECR-5-9.14], and Maumee River, OH [LEMR-0-6.16]; Fig. 31). The detection of long-chained PFAS compounds in mussel tissue at developed and open-water sites in the Great Lakes are of concern, as several studies have shown that most long-chained PFCAs (n ≥ C_7–C_{14}) are identified as either; persistent, bio-accumulative and toxic

(PBT), or very persistent and very bio-accumulative (vPvB) substances (Giesy et al., 2006b; Wang et al., 2014). Furthermore, the potetial toxic effects and apical endpoints (e.g., cytotoxic, genotoxic, mutagenic, and teratogenic effects) for most PFAS compounds detected within the Great Lakes Basin lower-trophic aquatic communities, at environmentally low concentration is relatively unknown.

In regards to short-chained PFAS compounds (n ≥ C_5–C_7; PFPeA, PFPeS, and PFHpA: Log K_{ow} = 2.49 - 4.67), their contribution to mussel PFAS exposures and HQ > 0.1 threshold exceedances were unexpected. Prior studies have shown short-chained PFAS compounds are highly soluble, and less bio-accumulative in aquatic organisms, relative to long-chained PFAS compounds (Conder et al., 2008; Lewis et al., 2022). PFPeA, PFPeS, and PFHpA are used as replacement compounds for PFOS, and PFOA, and can be found in a host of industrial and consumer products including surfactants, carpets, outdoor textiles, gloves, nanosprays, leather, ski wax, food packaging, cleaning products, stain-resistant fabrics, fire-fighting foams, and outdoor textiles (Kotthoff et al., 2015). Hence, short-chained PFAS compounds exceedance detected across mussel sampling locations, likely reflects the production/voluntary phase-outs and transition from long-chained PFAS compounds, resulting in increased use and emission of short-chained replacement PFAS compounds in the Great Lakes aquatic systems (Koban et al., 2024b; Teunen et al., 2021b). Furthermore, short-chained PFAS exceedances observed in this study, most likely reflects elevated composition and concentration in surrounding Great Lakes surface water column (Baker et al., 2022; Xia et al., 2024b), resulting in high exposure from local sources of these emerging contaminants to mussels at Great Lakes MWP sampling locations. Overall, short-chained PFPeA, and PFPeS were shown to exceed the HQ > 0.1 threshold at sites sampled primarily in Lake Michigan (Port Sheldon, MI [LMPS-0-INMU-5.31], and Milwaukee Beach, WI [LMMB-5-6.18]), and Lake Erie (Maumee River [LEMR-0-6.15]). Similarly, PFHpA exceeded the HQ > 0.1 threshold at one site sampled in Detroit River (Rouge River-2-6-16), and at 10 sites sampled in Lake Michigan (Fig. 31). Compared to long-chained PFAS compounds, further research is required to determine the bioconcentration potential and apical endpoints of these novel short-chained PFAS compounds in Great Lakes invertebrates and lower trophic-level organisms.

Additional mussel PFAS HQ results revealed, PFOA, PFOSA, and PFOS were the only compounds to exceed the HQ > 1 threshold, thus representing the $\sum_3$PFAS compounds posing the highest ecological risk to aquatic organisms across the Great Lakes mussel sampling locations. PFAS compounds exceeding the HQ > 1 threshold is ordered as follows (from low to high HQ values): PFOA > PFOSA > PFOS. On average, PFOA ($PNEC_{Tissue}$; 0.101 µg/kg ww), PFOSA ($PNEC_{Tissue}$; 0.701 µg/kg ww), and PFOS ($PNEC_{Tissue}$; 0.025 µg/kg ww) high HQ threshold values could be attributed to their low $PNEC_{Tissue}$ values (Table 18). Overall, PFOS and PFOA high mussel tissue HQ score is of environmental significance. The detection of PFOS and PFOA in aquatic environments has been shown to be a major concern, due to their sub-lethal effects and biological endpoints in aquatic biota. PFOS and PFOA are known environmental toxicants, linked to various deleterious and toxicological endpoints such as liver damage, cancer, developmental toxicity, immune system suppression, tumor induction, endocrine disruption, and obesity (Fenton et al., 2020; Mokra, 2021; Wee and Aris, 2023b).

As displayed in Fig. 30, clear differences can be observed in the spatial distribution of PFOA, PFOSA, and PFOS HQ exceedance across the Great Lakes mussel sampling locations. Spatially, PFOS exceedances were more widespread than PFOA, PFOSA, and was found to exceed the HQ > 1 threshold at one or more land-use categories, and major discharge-types assessed in this study. On average, PFOS exceeded the HQ > 1 threshold at 77.4% (82/106) of the sites assessed across the Great Lakes Basin. In contrast, PFOA and PFOSA were shown to exceed the HQ > 1 threshold at 8.49% (9/106), and 12.3% (13/106) of the sites assessed during the 2013-2018 sampling period. Overall, impacted mussel sampling locations with two or more PFAS compounds exceeding the HQ > 1 threshold, were primarily recorded at developed, and open-water sites in Lakes Michigan, Erie, and the Niagara riverine system (Fig. 32 and Fig. 33). The co-occurrence of PFOA, PFOSA, and PFOS across developed, and open-water sampling locations suggest, the combined toxicity and sub-lethal effects of these three compounds might be greater at these sampling locations. For developed, and open-water sites sampled in Lakes Michigan, Erie, and the Niagara riverine system, input and emission via urban water cycle to urban streams and surface water is viewed as important anthropogenic drivers contributing to elevated PFOA, PFOSA, and PFOS composition and exceedances observed at these sampling locations (Baker et al., 2022; George et al., 2023; Llewellyn et al., 2024; Myers t al., 2012).

Besides the traditional emission sources (i.e., point sources), runoff from agricultural and urban landscapes containing pesticide residues with PFAS formulations, are also likely environmental pathways and emission sources contributing to PFOA, PFOSA, and PFOS exceedances observed across Great Lakes mussel agricultural, developed/urban, and open-water sampling locations. Popular pesticides such as permanone 30-30 (30% permethrin; mosquito insecticide), Anvil 10+10 (Sumithrin; an insecticide), sulfentrazone (a broad-spectrum herbicide), bifenthrin (synthetic pyrethroid insecticide),

novaluron (insect growth regulators [IGR]), imidacloprid (a systemic neonicotinoid insecticide), abamectin (also called avermectin B1, a widely used insecticide), spiromesifen (a miticide insecticide), Intrepid 2F® (widely used insecticide), and malathion (a commercial broad-spectrum organophosphorus pesticide; Wu et al., 2021), have been shown to contain varying degree of PFOS and PFOA formulations (Lasee et al., 2022; Llewellyn et al., 2024; Maine Department of Agriculture, Conservation and Forestry, 2022). Currently, malathion is registered for use in both the US and Canada, and is used extensively in agricultural and non-agricultural areas of the Great Lakes Basin (Baldwin et al., 2016; Hull et al., 2015; Klečka et al., 2010). Therefore, PFOA and PFOS exceedances detected in mussels from sites sampled in the Maumee (LEMR-0-6.16, LEMR-2-7.15, and LEMR-4-6.16), and the Detroit (DRSE-0-6.16; Fig. 30) riverine systems, likely reflect both the historical, and continual use of pesticides containing PFAS-precursor formulations, and as a result their subsequent detection within these mixed Great Lakes agricultural and developed/urban sub-watersheds (Chu and Letcher, 2017; Link et al., 2024; Llewellyn et al., 2024). In addition, proximity to potential PFAS sources including runoff from municipal solid waste landfills (MSWLF) containing consumer and industrial products (Coffin et al.,2023), and agricultural fields containing amended land-applied sewage sludge and biosolids, are also likely important environmental pathways and emission sources for PFAS elevated exceedances within these areas of the Great Lakes Basin (Baker et al., 2022; Helmer et al., 2022; Point et al., 2021).

PFOSA (Perfluorooctane sulfonamide), is also an important intermediate and active ingredient used in the pesticide Sulfluramid (N-EtFOSAA, also used in ant and roach insecticides; Guida et al., 2023; Lasee et al., 2022; Lin et al., 2021; Nguyen et al., 2016). Sulfluramid is currently used in most Great Lakes urban and residential areas as bait stations for the control of insects (Lin et al., 2021). As such, it is plausible that PFOSA exceedances observed at developed/urban, and open-water sites sampled in Lake Michigan, Lake Erie, and the Niagara riverine system (Fig. 30), could be attributed to the continued use of these pesticides containing PFAS formulations, as well as their transformation and incomplete elimination during conventional wastewater treatment processes (Leung et al., 2022; Houtz, et al., 2012; Kolpin et al., 2021; Lin et al., 2021; Nguyen et al., 2016). With mounting evidence of adverse biological outcomes and effects in fish and mammalian models, health advisories for PFAS compounds currently detected in this study including PFOS, PFOA, PFDS, PFBS, PFDoA, PFHpS, PFHxS, PFOSA, PFTreA (PFTeDA), and PFTriA (PFTrDA) continue to be revised downward by the USEPA for fish and shellfish (USEPA, 2024). Based on these concerns, ample opportunities exist for biomonitoring programs such as the MWP and others in the Laurentian Great Lakes to be at the forefront of this impending ecological storm. Continued bio-monitoring efforts utilizing both basin-wide surveillance and placed techniques can be used to address ecosystem concerns as it pertains to these novel PFAS compounds emergence in lower -and- upper trophic-level organisms, as well as providing Great Lakes resource managers and stakeholders with adequate information on these contaminants environmental fate, risk of exposure, and apical endpoints in making informed management decisions.

Credit: NOAA Great Lakes MWP

Results & Discussion

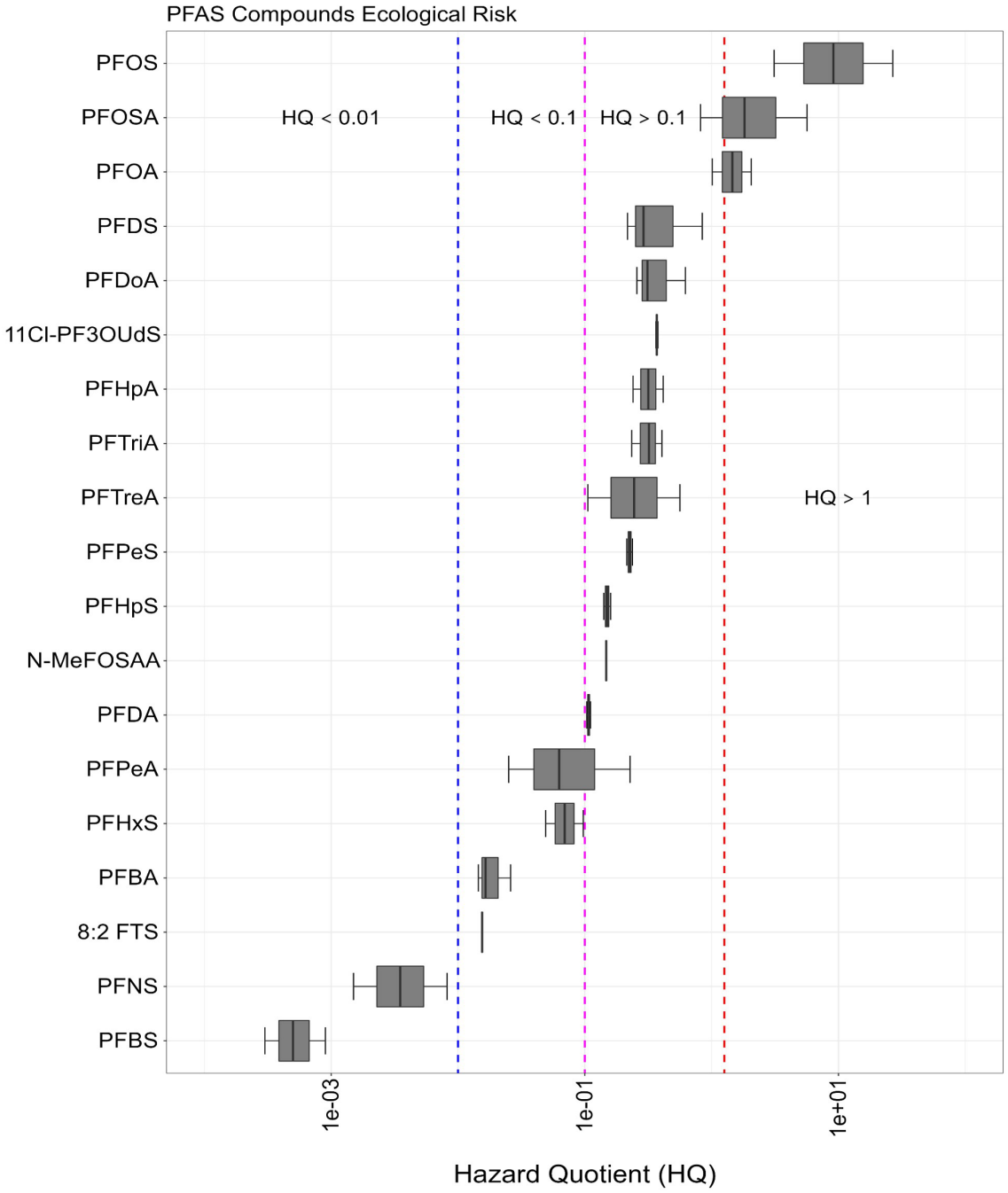

Fig. 30. Boxplot showing calculated hazard quotients (HQ; on a logarithmic scale) for individual $\sum_{19}$PFAS compounds detected in dreissenid mussels from Great Lakes mussel sampling locations between 2013-2018. $\sum_{19}$PFAS compounds are ordered from left to right by lowest to highest hazard quotient (HQ) threshold value. Dashed blue line represents HQ threshold values below < 0.01 (HQ < 0.01), while dashed magenta line represents HQ threshold values between 0.1 ≤ HQ > 0.1, and dashed red line represents HQ threshold values above > 1 (HQ > 1). Two $\sum_{2}$PFAS compounds (PFBS, and PFNS) were detected below HQ < 0.01 (no risk), while 3 $\sum_{3}$PFAS compounds (8:2 FTS, PFBA, and PFHxS) were detected below the HQ < 0.1 (low risk or minimal adverse effects) threshold. Eleven $\sum_{11}$PFAS compounds were detected above HQ > 0.1 threshold (PFDA, N-MeFOSAA, PFHpS, PFPeS, PFPeA, PFTreA, PFTriA, PFHpA, 11Cl-PF3OUdS, PFDoA, and PFDS) and were identified as posing moderate risk to aquatic organisms. Three long-chained (C_8) $\sum_{3}$PFAS compounds (PFOA, PFOSA, and PFOS) were detected above the HQ > 1 threshold, suggesting these compounds present significant or high risk to aquatic biota.

Table 18. Summary of $\sum_{19}$PFAS compounds min, mean, and max measured (> MDL) environmental concentrations ($MECs_{Tissue}$) in dreissenid mussels from Great Lakes sampling locations between 2013-2018. $\sum_{19}$PFAS compound summary also include predicted no-effect concentrations ($PNECs_{Tissue}$; Lowest PNEC Biota [mollusc]) values (µg/kg ww), and calculated min, mean, and max HQ (hazard quotient) threshold values for individual $\sum_{19}$PFAS compounds detected across Great Lakes mussel sampling locations. Compounds with their respective HQ threshold designation (HQ < 0.01, HQ < 0.1, HQ > 0.1, and HQ > 1) are also shown. Additional information on Norman bivalve tissue predicted no-effect concentrations ($PNECs_{Tissue}$; Lowest PNEC Biota [mollusc]) threshold values (µg/kg ww) used in this study to calculate hazard quotient (HQ) values is provided in Table A6 (Appendix).

PFAS Analytes	CASRN #	MEC - Min (ng/g ww)	MEC - Mean (ng/g ww)	MEC - Max (ng/g ww)	PNEC (µg/kg ww)	HQ - Min	HQ - Mean	HQ - Max	Hazard Quotients (HQs)
11Cl-PF3OUdS	83329-89-9/ 763051-92-9	0.134	0.136	0.139	0.370	0.363	0.369	0.377	HQ > 0.1
8:2 FTS	27619-96-1	0.347	0.347	0.347	22.4	0.016	0.016	0.016	HQ < 0.1
N-MeFOSAA	2355-31-9	0.516	0.516	0.516	3.5	0.148	0.148	0.148	HQ > 0.1
PFBA	375-22-4	0.673	0.763	1.20	46.3	0.015	0.017	0.026	HQ < 0.1
PFBS	375-73-5	0.192	0.275	0.529	585.7	3.00E-04	5.00E-04	9.00E-04	HQ < 0.01
PFDA	335-76-2	0.128	0.132	0.137	1.24	0.103	0.107	0.111	HQ > 0.1
PFDoA/(PFDoDA)	307-55-1	0.62	0.75	1.49	2.41	0.258	0.312	0.620	HQ > 0.1
PFDS	2806-15-7	0.329	0.441	1.28	1.52	0.217	0.291	0.844	HQ > 0.1
PFHpA	375-85-9	0.151	0.199	0.261	0.629	0.240	0.317	0.416	HQ > 0.1
PFHpS	375-92-8	0.1	0.106	0.113	0.711	0.141	0.150	0.160	HQ > 0.1
PFHxS	3871-99-6	0.064	0.09	0.126	1.29	0.049	0.069	0.097	HQ < 0.1
PFNS	98789-57-2	0.098	0.223	0.529	64.2	0.002	0.004	0.008	HQ < 0.01
PFOA	335-67-1	0.103	0.153	0.208	0.101	1.01	1.46	2.05	HQ >1
PFOS	1763-23-1	0.078	0.671	4.73	0.025	3.11	26.8	189.3	HQ >1
PFOSA/(FOSA)	754-91-6	0.573	1.275	3.97	0.701	0.817	1.82	5.65	HQ >1
PFPeA/(PFPA)	2706-90-3	0.135	0.336	1.2	5.36	0.025	0.063	0.228	HQ > 0.1
PFPeS	630402-22-1	0.647	0.682	0.718	3.02	0.214	0.226	0.238	HQ > 0.1
PFTreA/(PFTeDA)	376-06-7	0.566	1.313	3.02	5.36	0.106	0.245	0.563	HQ > 0.1
PFTriA/(PFTrDA)	72629-94-8	0.522	0.722	0.903	2.23	0.234	0.320	0.406	HQ > 0.1

Results & Discussion

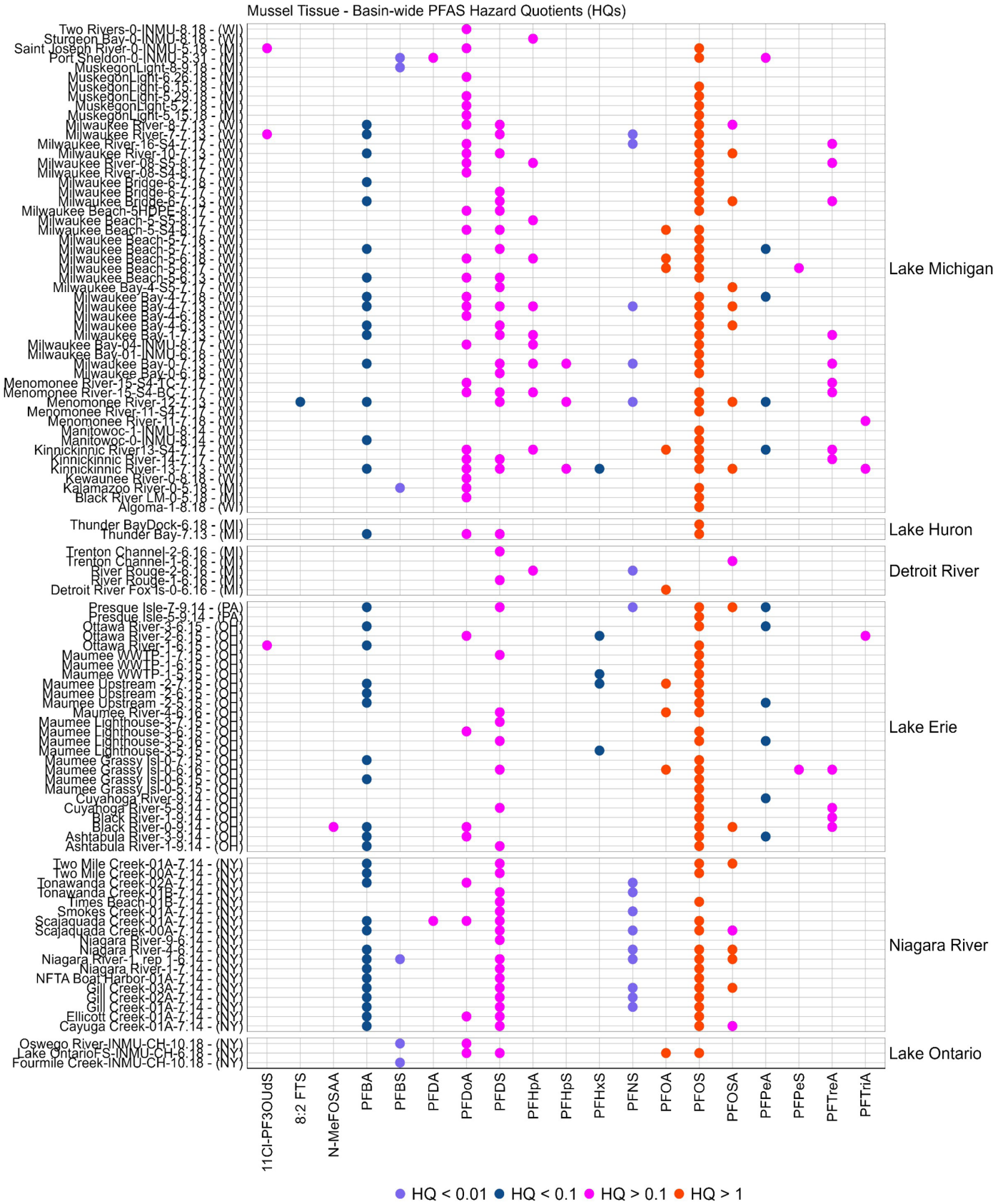

Fig. 31. Heat map depicting individual $\sum_{19}$PFAS compounds hazard quotient (HQs) threshold exceedances across the Great Lakes mussel sampling locations. HQ < 0.01 (●), and HQ < 0.1 (●) represents PFAS compounds posing no risk to low or minimal adverse effects, while HQ > 0.1 (●), and HQ > 1 (●) signify compounds posing moderate to high risk to aquatic biota. Mussel sampling locations are arranged from west (Lake Michigan) to east (Lake Ontario), and are listed by their general location (associated riverine/lake region), state and month/year sampled.

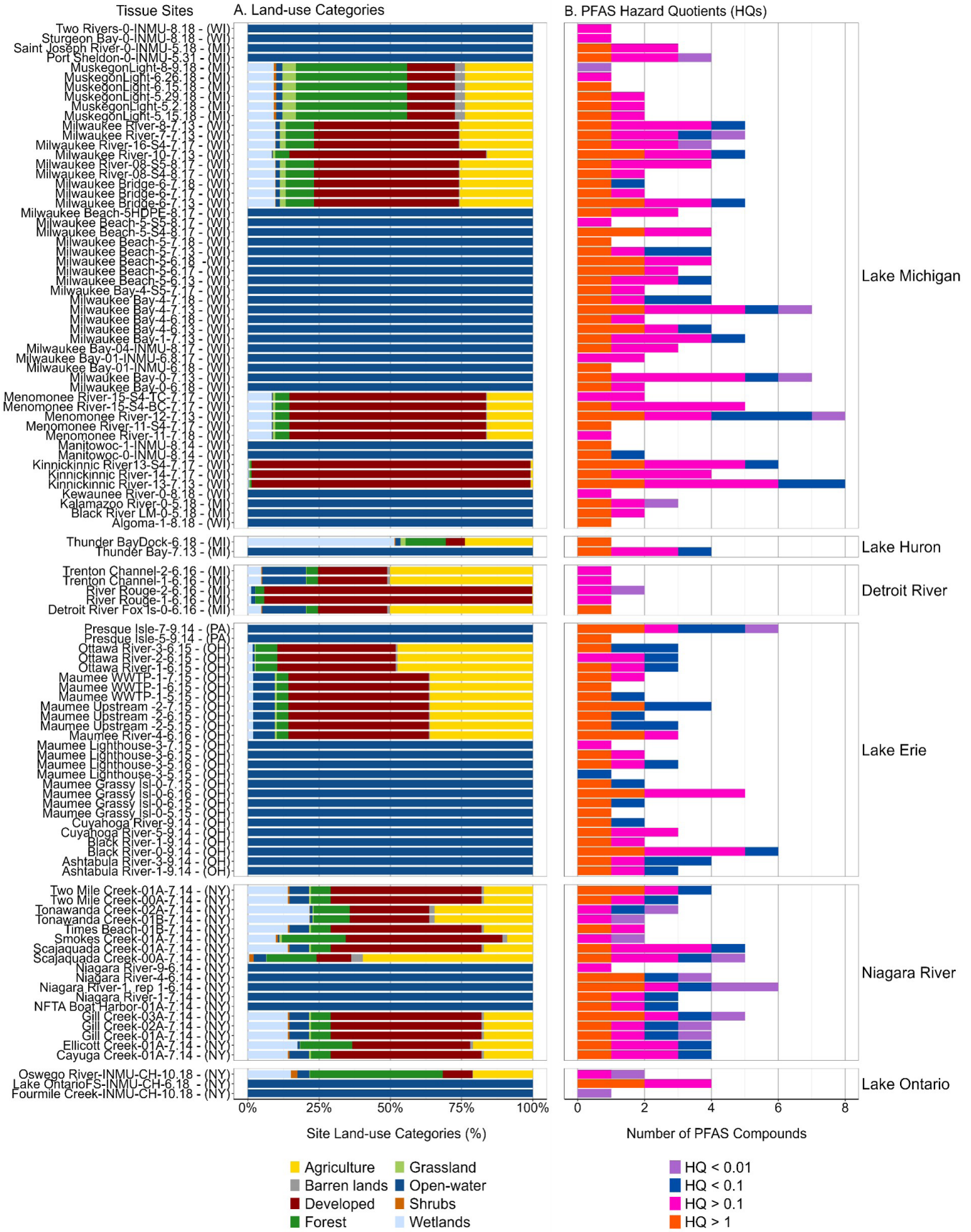

Fig. 32. Barplot depicting A), mussel sampling locations predominant land-use category estimates (%), and B), number of ∑PFAS compound exceedances (HQ > 0.1, and HQ > 1 threshold) detected across Great Lakes mussel sampling locations. Mussel sampling locations are arranged from west (Lake Michigan) to east (Lake Ontario), and are listed by their general location (associated riverine/ lake region), state and month/year sampled.

Results & Discussion

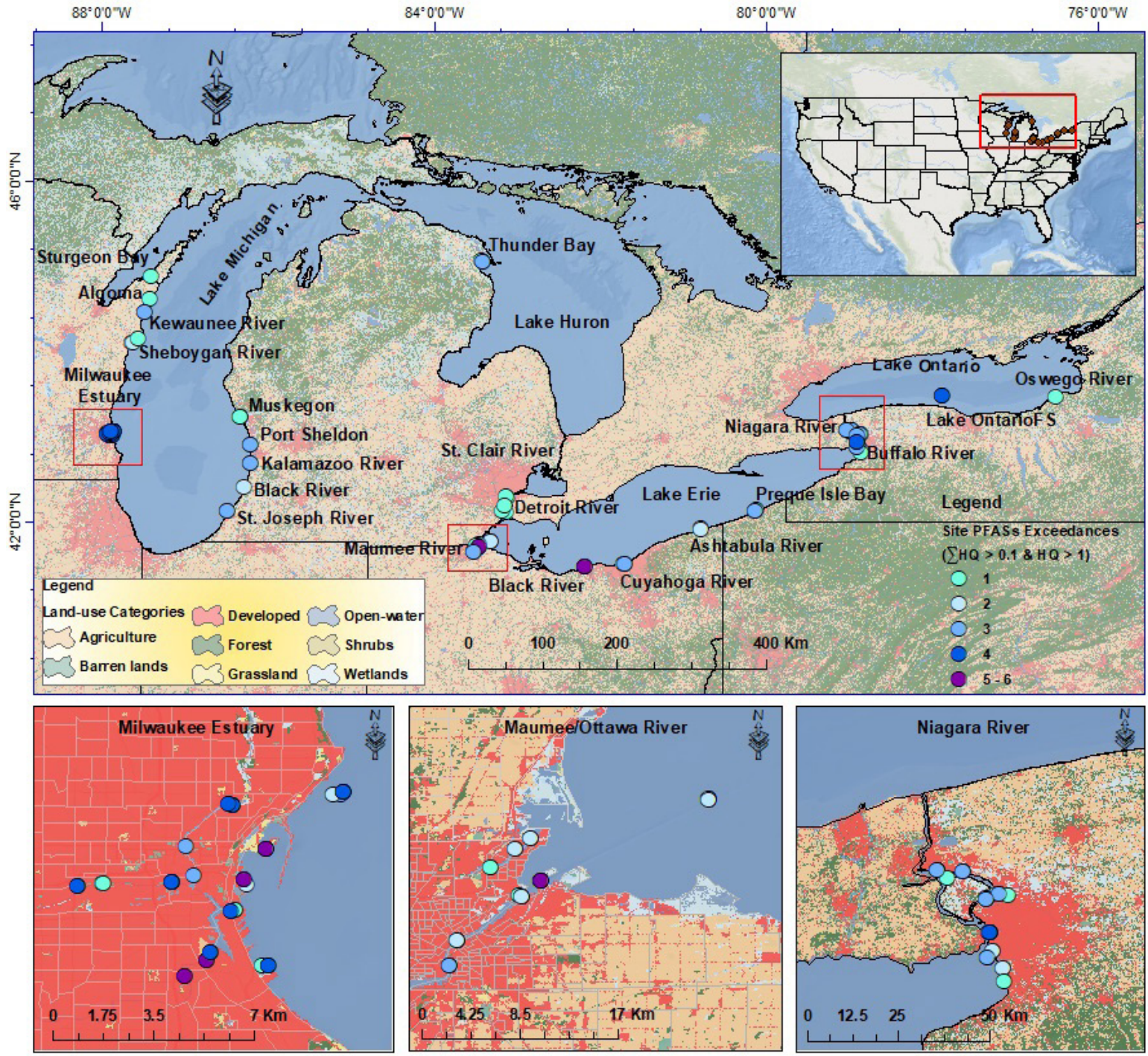

Fig. 33. Map depicting the spatial variation and number of PFAS compound exceedances (HQ > 0.1, and HQ > 1 threshold) detected across Great Lakes mussel sampling locations. The highest number of PFAS HQ > 0.1 exceedances were recorded for sites sampled in Lake Michigan, followed by sites sampled in Niagara River, and Lake Erie. Conversely, the lowest number of PFAS HQ > 0.1 exceedances were recorded for sites sampled in Detroit River, Lake Ontario, and Lake Huron. Impacted mussel sampling locations with two or more PFAS compounds HQ >1 exceedance, were recorded mainly at developed, and open-water sites sampled in Lakes Michigan, Erie, and the Niagara riverine system.

3.9. PFAS Ecotoxicological Implications

While the sub-lethal effects for $\sum_{14}$PFAS compounds exceeding the HQ > 0.1, and HQ > 1 threshold have been documented primarily in traditional fish models, limited or no toxicity information exist for some PFAS compounds biological effects and apical endpoints in lower-trophic organisms/biota (e.g., dreissenid mussels). Of the 11 compounds identified exceeding the HQ > 0.1 threshold, PFPeS (estimated serum half-life [$t_{1/2}$], 230 days; Xu et al., 2020), PFPeA (PFPA), and PFHpA were among the short-chained compounds identified as posing moderate risk to aquatic biota. PFPeS is used as a PFAS replacement for PFOA and PFOS in additives, chemical coatings and surface treatments (Hamid et al., 2024). Developmental neurotoxicity studies conducted by Gaballah et al. (2020) revealed, zebrafish (*Danio rerio*) larvae exposed to PFPeS (0.0 - 100.0µM) resulted in apical developmental endpoints that was generally characterized by abnormal ventroflexion of the tail and failed swim bladder inflation. In addition, Gaballah et al. (2020) further demonstrated that zebrafish (*Danio rerio*) larvae exposure to PFPeS was quite potent for developmental toxicity (EC_{50} = 48.8 µM; LOEC = 56.0 µM), relative to PFHpS (EC_{50} = 168.1 µM; LOEC = 31.4 µM), another PFAS compound identified in this study exceeding the HQ > 0.1 toxicity criterion. Equally important, the results from Gaballah et al. (2020) neurotoxicity studies further suggests, PFPeS was nearly as potent as PFOS (0.04 - 80.0µM), which was considered the most potent chemical evaluated in their study.

Hoke et al. (2012b) demonstrated in a short-term freshwater toxicity test (48, 72 and 96-h exposure; EC/LC_{50} typically between 1 and >100 mg L^{-1}), that PFPeA was the most toxic compound to fish (96-h LC_{50}; 31.8 mg L^{-1}). Similarly, in a short-chained developmental toxicity study, zebrafish embryos exposed to PFPeA (exposures at 8 h post-fertilization [hpf]; 1–100 µM), with morphological and behavioral apical endpoints assessed at 24 and 120 hpf, was shown to induce apical endpoints including abnormal behavior response (e.g., hypo -and- hyper active larval photo motor response) during light (e.g., PFPeA exposure induced hypoactivity), and dark phases (e.g., PFPeA exposure induced hyperactivity; Rericha et al., 2022). PFHpA (estimated serum half-life [$t_{1/2}$], 62 days - 1.2 years; Weatherly et al., 2023; Zhang et al., 2013) is also a short-chained replacement for PFOA and PFOS, widely found in additives such as firefighting foams, chemical coatings and surface treatments (Hamid et al., 2024). Huang et al. (2023) reported reduced locomotor activity in developing zebrafish (*Danio rerio*) exposed to PFHpA (0.1 µM), and decreased ATP-linked respiration of zebrafish (*Danio rerio*) embryos when exposed to 200 µM PFHpA, during a series of sub-lethal toxicity test including visual motor response test. Rericha et al. (2021) also reported, zebrafish (*Danio rerio*) exposed to PFHpA in developmental toxicity test, elicited abnormal behavior including inducing hypoactivity at 100 µM, while causing hyperactivity at 2.5 and 6.5 µM, respectively. In addition, Menger et al. (2020) also reported significant apical endpoints including altered swimming behavior, and locomotor activity impairment in zebrafish (*Danio rerio*) embryos and larvae exposed to PFHpA (89 µM; BCF = 18).

Prior studies (Brendel et al., 2018; Buck et al., 2011; Coy et al, 2022c) have also demonstrated aquatic organisms exposed to long-chained PFAS compounds elicited a wide variety of adverse apical events (e.g., reproductive and endocrine disruption, induce hepatotoxicity, developmental toxicity, growth inhibition, immune toxicity, and neuronal system disruption). Liu et al. (2008), and Guo et al. (2018) evaluated PFDoA (PFDoDA or PFDOA: estimated serum half-life [$t_{1/2}$], 230 days; Xu et al., 2020), PFTriA (PFTrDA or PFTrA), and PFDA (PFDeA: estimated serum half-life [$t_{1/2}$], 4.0 - 7.1 years; Zhang et al., 2013b), toxicity and adverse biological effects on female zebrafish (*Danio rerio*). Significant malformations including histopathological liver damage, swollen hepatocytes, vacuolar degeneration, and nuclei pycnosis female zebrafish (*Danio rerio*) resulted from exposure to all 3 $\sum_{3}$PFAS compounds. In addition, female Japanese medaka (*Oryzias latipes*) exposed to PFTriA was shown to stimulate the growth of the gonads and inhibited egg production (Ma et al., 2023). Similarly, Ma et al. (2022b) in a series of bivalve toxicity studies found dose-dependent and bioaccumulation-correlated oxidative damage (e.g., alteration of SOD activity and short-term changes in GSH, MDA, and GSH content in the coat and visceral mass), as well as DNA damage (e.g., DNA strand breaks and fragmentation, chromosomal breaks, and apoptosis), membrane instability, and reduced body weight in green mussels (*P. viridis*) exposed to PFDA (96-hr LC_{50} of 68.3 mg/L). In addition, Jo et al. (2014) demonstrated long-term exposure to PFDA and PFTriA modulated sex steroid hormone production and related gene transcription of the HPG axis in a sex-dependent manner in zebrafish (*D. rerio*). Rericha et al. (2021) further reported, PFDA and PFTriA elicited hyperactivity at 2.5 and 10.0 µM, while inducing hypoactivity at 16.4, and 35.0 µM in zebrafish (*Danio rerio*) during a series of developmental toxicity test. Furthermore, Ulhaq et al. (2013) reported zebrafish embryos exposed to PFDA (test range: 0.1- 30mg/L, 6-d EC_{50}: 5.0 mg/L, 6-d LC_{50} (postfertilization): 8.4 mg/L) elicited similar toxicity and developmental effects (e.g., spinal malformation) to PFOS. These studies suggest the effects from PFAS binary and complex mixtures can cause deleterious, as well as species-specific effects and endpoints in aquatic organisms.

Previous PFAS exposure studies have highlighted PFHpS (estimated serum half-life [$t_{1/2}$], 1.0 - 7.4 years; Nilsson et al.,

toxicity, and their risk and apical endpoints in aquatic organisms. For example, Gaballah et al. (2020), and Ma et al. (2023) found PFHpS (EC_{50} = 168.1µM; LOEC = 31.4µM) shared toxicity phenotype effects similar to other PFAS compounds (e.g., containing five or more fluorinated carbons) in zebrafish (*Danio rerio*), characterized by apical endpoints such as abnormal ventroflexion of the tail, body axis, and swim bladder defects in a series of developmental toxicity and developmental neurotoxicity tests. In addition, Kadlec et al. (2023) found changes in freshwater invertebrates Ceriodaphnia dubia (*C. dubia*), and Hyalella azteca (*H. Azteca*) reproduction (decrease *C. dubia* reproduction by 22% relative to controls [p = 0.038], and H. azteca growth by 18% relative to controls [p = 0.085;]), following single concentration PFDS exposure studies. Kadlec et al. (2023) further suggest, based on additional median and 20% effect concentration exposure results that, PFDS might be more toxic to freshwater invertebrates including C. dubia (EC_{50}: >0.85*, and EC_{20}: >0.85* [*ECx greater than solubility limit]), and H. Azteca (EC_{50}: > 0.85*, and EC_{20}: > 0.85* [*ECx greater than solubility limit]), compared to similar PFAS compounds such as PFOS and PFNS. Mahoney et al. (2022), and Zhang et al. (2018) further reported thyroid function disruption and transcriptional changes including upregulation of genes like thyrotropin-releasing hormone, corticotropin-releasing hormone, and iodothyronine deiodinase 2 (a gene that codes enzymes important for the activation and de-activation of thyroid hormones) in zebrafish following exposure to PFDoA. Similarly, female and larvae zebrafish (*Danio rerio*) exposed to PFDoA resulted in hatching delay, reduced heart rate and body length, as well as decreased locomotor speed, induced developmental neurotoxicity, increased deformity and death rates, pericardial edema, and other teratogenic endpoints (Guo et al., 2018; Liu et al., 2008).

The long-chained PFTreA (C_{14}; PFTeDA, PFTeA, or PFTA), is found in a variety of industrial and commercial products including firefighting foams, detergents, photographic films, and insecticides (Patel et al., 2022). Zebrafish (*Danio rerio*) exposed to PFTreA (0.03 mg/L) during freshwater invertebrate toxicity testing, was shown to induce pericardial edema (PE), and spinal lordosis (SL), followed by yolk sac edema (YSE) deformity during early developmental stages (Kim et al., 2021). In similar studies, zebrafish (*Danio rerio*) larvae exposed to PFTreA (10 µM) was shown to induce reactive oxygen species (ROS) levels, coinciding with increased transcription of antioxidant defense genes, suggesting PFTreA may induce overexpression of antioxidant enzymes in lower -and- higher-trophic organisms, which is required to counteract when ROS is being produced during exposure to environmental toxicants (Patel et al., 2022). Patel et al. (2022) also reported mitochondrial-related genes (cox1 and mt-nd3) and oxidative stress-related genes (cat, hsp70, and hsp90a) expression levels were increased in larval zebrafish (*Danio rerio*) exposed to PFTreA (10 µM, over a 7-day exposure period).

Limited data exist on N-MeFOSAA (MeFOSAA, NMeFOSA or N-Me-FOSA: estimated serum half-life [$t_{1/2}$], 4.59 years; Lin et al., 2021), and 11Cl-PF3OUdS (11-ClPF3OUdS, F-53B Minor, or 8:2 Cl-PFESA: estimated serum half-life [$t_{1/2}$], 15.3 years; Pan et al., 2020) toxicity to lower trophic-level aquatic organisms (i.e., dreissenid mussels). However, in vivo studies conducted on zebrafish (*Danio rerio*) larvae exposed to 11Cl-PF3OUdS (7-day separate exposure; 1 µmol/L) reported significant hepatic steatosis (fatty acid circulation), evidenced by pathological micro/macro vacuolation, which contributed to excess lipid accumulation, a result of overloaded triglyceride (TG) level (Yi et al., 2019). Results from the in vivo studies also suggest, 11Cl-PF3OUdS might disrupt the lipid homeostasis (e.g., impede the excretion or export of lipid [LDL/VLDL] out of hepatocytes) in aquatic organisms. Massarsky et al. (2022) also investigated the toxicity thresholds for apical endpoints (e.g., sensitive acute and chronic endpoints) for N-MeFOSAA, and 11Cl-PF3OUdS, using the ECOSAR tool for certain freshwater species (e.g., fish, and water flea [daphnid; *C. dubia*]). The results suggest, the predicted median acute toxicity threshold values for N-MeFOSAA were: LC_{50} 0.208 mg/L for fish, and 0.167 mg/L for water flea (*C. dubia*). Similarly, N-MeFOSAA predicted median chronic toxicity values were 0.031 mg/L for fish, and 0.042 mg/L for water flea (*C. dubia*). The predicted median acute toxicity threshold values for 11Cl-PF3OUdS were: LC_{50} 0.398 mg/L for fish, and 0.345 mg/L for water flea (*C. dubia*). Likewise, the predicted median chronic toxicity values for N-MeFOSAA were 0.064 mg/L for fish, and 0.109 mg/L for water flea (*C. dubia*).

Of the 3 $\sum_3$PFAS compounds exceeding the HQ > 1 threshold level, numerous studies have demonstrated PFOA (estimated serum half-life [$t_{1/2}$]: 3.5 - 5 years; Nilsson et at., 2022; Olsen et al., 2007) and PFOS (estimated serum half-life [$t_{1/2}$]: 7.8 - 8.5 years; Nilsson et at., 2022; Olsen et al., 2007) acute and chronic toxicity to a variety of aquatic organisms (Mojiri et al., 2023; Zhang et al., 2023b). In a series of bioaccumulation kinetics test (1–1,000 µg/L; 10-day exposure), zebra mussels (*Dreissena polymorpha*) exposed to both PFOA and PFOS were shown to affect oxygen consumption and mutixenobiotic resistance (MXR) mechanisms (Fernández-Sanjuan et al., 2013). Another study also comfirmed Mediterranean mussels (*Mytilus galloprovincialis*) exposed to PFOS during a (48 h) bivalve embryo toxicity test, experienced a decline in normal larval development (Fabbri et al., 2014b). Likewise, green mussels (*P. viridis*) exposed to PFOS (96 h LC_{50}: 68.3 mg/L) was shown to induce oxidative stress, including alteration of SOD activity and short-term changes in GSH, MDA, and GSH content in the coat and visceral mass (Wang et al., 2012). Similarly, Liu et al. (2014) demonstrated green mussels (*P. viridis*) exposed to PFOS (33 µg/L), and PFOA (594 µg/L), experienced related genetic injuries and endpoints.

Ding et al. (2013) also investigated the binary effects of PFOS and PFOA to zebrafish (*Danio rerio*) embryos. A series of complex biological and interactive effects including: from synergistic effect → to antagonistic effect → to synergic effect again (with increased variable molar ratios of PFOS [1:1, 1:3, 1:6, and 1:10] in the mixture), was observed in zebrafish (*Danio rerio*) embryos exposed to PFOS and PFOA (Ding et al., 2013). Similarly, Logeshwaran et al. (2021) examined the combined effects and toxicological interactions of PFOA and PFOS on Daphnia carinata, during acute and chronic toxicity tests using similar combination-index method. Daphnia carinata, exposed to PFOA (LC_{50}/48 h; 78.2 mg/L) and PFOS (LC_{50}/48 h; 8.8 mg/L), depicted various apical endpoints including induced gene aberrations. Equally important, Daphnia carinata exposed to PFOS (0.001 mg/L) during chronic exposure tests, showed sub-lethal endpoints including mortality and reproductive defects (Logeshwaran et al., 2021). These results suggest that combined and transgenerational effects on aquatic invertebrates is evident for some non-targeted species that is continously exposed to binary or complex mixtures of environmentally relevant legacy PFAS concentrations.

PFOSA (FOSA: estimated serum half-life [$t_{1/2}$], 3.3 years; Gebbink et at., 2015) is widely used in the manufacturing industry to synthesize PFOS during industrial processes, such as surfactants, carpets, and textile production (Chen et al., 2022). Previous studies have shown that PFOSA (a potent mitochondrial toxicant; Starkov and Wallace, 2002), can readily pass-through cell membranes (e.g., placenta and blood-brain barrier), relative to other PFAS compounds (Slotkin et al., 2008), thus inducing endocrine disrupting effects, developmental malformations, and neurotoxicity (Olufsen ad Arukwe, 2014). Additional toxicological studies have also shown that PFOSA (30-50 µM) elicited a greater degree of oxidative stress, evoking cell enlargement and cell loss, increase in cell membrane/total protein ratio, and altered neural cell differentiation relative to PFOS and perfluorooctanoate (PFOA) in mammalian systems (Slotkin and Seidler, 2010). Few studies have investigated the ecotoxicological effects of PFOSA exposure in aquatic invertebrates. In a recent study that screened 38 PFAS compounds (including PFOS and PFOA) for developmental toxicity using zebrafish (*Danio rerio*) embryos revealed, PFOSA (exposure 6.25, 12.5, 25, and 50 µM) was the most potent developmental toxicant following exposure post fertilization (6 to 24 hours post-fertilization [hpf], and 6 to 72 hours post-fertilization [hpf]), inducing mortality, and elevated developmental abnormalities including induced embryonic toxicity and developmental delay (6 to 72 hpf, 50 µM; Dasgupta et al., 2020). In addition, zebrafish embryos early exposure to PFOSA adversely impacted embryogenesis, by disrupting and altering pathways related to hepatotoxicity (e.g., liver development impairment), and lipid transport (Dasgupta et al., 2020). Similarly, Chen et al. (2022) further revealed zebrafish (*Danio rerio*) exposed to PFOSA, induced sub-lethal effects including abnormal cardiac morphology, disordered heartbeat signals, as well as reduced heart rate and cardiac output following exposure of 0.1, 1, 10, or 100 µg/L PFOSA.

Taken together, these findings suggest, for $\sum_{14}$PFAS compounds assessed in this study with threshold exceedances above HQ > 0.1 and HQ > 1, these compounds pose moderate to significant risk for sub-lethal toxic effects and endpoints to Great Lakes aquatic biota. The above finding further suggests replacement short-chained fluorinated PFAS compounds share similar toxicity profiles to long-chained compounds, and are just as toxic and potent to freshwater aquatic organisms. Equally important, with these legacy and emerging contaminants currently detected in mussels as complex mixtures, and with mussels being viewed as transfer vectors for these potent environmental toxicants across the Great Lakes food-web, the cumulative risk of long-term PFAS exposure to upper trophic-level organisms (e.g., Lake trout [*Salvelinus namaycush*], Smallmouth bass [*Micropterus dolomieu*], Walleye [*Sander vitreus*], Yellow perch [*Perca flavescens*], Rainbow trout or steelhead [*Oncorhynchus mykiss*], Coho salmon [*Oncorhynchus kisutch*], and Chinook salmon [*Oncorhynchus tshawytscha*]) cannot be ignored. Hence, continued monitoring efforts should be conducted to assess the risk these contaminants pose across the Great Lakes food-web, and whether lower-trophic level organisms are affected by the continuous release and long-term exposure to these potentially harmful contaminants across the Great Lakes Basin.

Conclusion

Credit: NOAA Great Lakes MWP

4.0 CONCLUSION

In this retrospective study, a suite of legacy and novel PFAS compounds were assessed and characterized to gain a better understanding of their environmental occurrence, magnitude, and spatial distribution across the Great Lakes inshore (harbors, rivers, tributaries) and offshore mussel sampling locations. Our results revealed, of the 28 $\sum_{28}$PFAS analyzed in this study, 19 $\sum_{19}$PFAS compounds were detected at least once in dreissenid mussels (> MDLs), with concentrations ranging from 0.064 to 4.73 ng/g (wet weight). Of the 19 $\sum_{19}$PFAS compounds quantified in mussels, PFTreA, a long-chained PFCA was detected at the highest mean concentration, followed by PFOSA, PFBA, PFDoA, PFTriA, PFPeS, PFOS, and the precursor N-MeFOSAA. Similarly, PFTreA, PFPeA, PFOSA, PFDoA, PFDS, PFBA, and PFOS were the largest contributors to the total $\sum_{19}$PFAS concentration measured (> MDL) in mussel tissue basin-wide, comprising approximately 36.8% of the total $\sum_{19}$PFAS compounds detected in mussel tissue during the 2013 -2018 study period. For other PFAS compounds quantified in mussel tissue, approximately 58% were measured at low mean concentrations, suggesting either low uptake or low bioaccumulation potential for some contaminants, likely resulting from low affinity binding occurring in dreissenid mussels. Despite the detection of these PFAS compounds in mussel tissue at environmentally low concentrations, their potential to exert sub-lethal and biological endpoints (e.g., population-level effects) in Great Lakes lower-trophic aquatic communities and food-web cannot be ignored.

The results from our study confirm PFAS compounds are widely distributed and bioavailable within the Great Lakes aquatic environment, with various long -and- short-chained PFAS compounds among those detected frequently (DF > 30%) in mussel tissue. Thus, our study highlight the ubiquity of these contaminants within the Great Lakes Basin. Overall, long-chained PFAS compounds were more persistent and more widely detected across mussel sampling locations major discharge-types, and predominant land-use types. Long-chained (n ≥ C_7–C_{11}, C_{12}, C_{13} and C_{14}) PFAS homologues were detected ~2 times higher in mussel tissue, compared to short-chained PFAS homologues assessed in this study. However, since short-chained PFAS compounds are widely used as alternatives to long-chained PFASs, and with some short-chained compounds shown to be more persistent than their long-chained counterparts (Chambers et al., 2021; Li et al., 2020), harmful levels of these replacement compounds could be reached across the Great Lakes Basin sometime soon. With this looming ecological storm, the need for continued monitoring and prioritization of these emerging contaminants may be warranted, since information regarding short-chained PFAS compounds chemical pressure, toxicity, fate, and potential for biomagnification across the Great Lakes food web is lacking.

While previous studies have shown short-chained PFAS compounds tend to be less bioaccumulative than long-chained PFASs in aquatic organisms (Hamid et al., 2024), our study have demonstrated and shown where several short-chained compounds including PFBS, PFBA, PFPeS, PFPeA, PFHxS, PFHpS, and PFHpA were readily detected in mussel tissue, thus highlighting the bioaccumulation potential of some short-chained PFAS compounds in Great Lakes aquatic biota. While partly filling an important data gap for short-chained PFAS compounds bioaccumulation potential in Great Lakes lower trophic-level organisms, the present study further highlights the need to assess these PFAS compounds, since mussels are shown to act as transfer vectors of various contaminants including PFAS to higher trophic-level organisms (i.e., fish), and humans in the Great Lakes Basin (Apeti and Lauenstein, 2006; Ghedotti et al., 1995; Murphy et al., 2012; Pagnucco et al., 2015).

Between-lakes and connecting channels comparison revealed, PFAS compounds (> MDL) were detected at 106 sites (out of 120), mainly as complex mixtures, with 2 to 8 compounds detected in mussels at 76.4% (81/106) of the sites sampled between 2013 and 2018. Summed $\sum_{19}$PFAS concentrations remained spatially heterogenous across mussel sampling locations, with higher $\sum_{19}$PFAS concentrations primarily detected in mussels from sites sampled in Lake Michigan, compared to mussels sampled from other Great Lakes and connecting channel sites assessed in this study. Basin-wide, our results showed where patterns and spatial variations in elevated mussel PFAS contaminant body burden levels closely matched sites sampled adjacent to urban rivers and tributaries, with larger population densities and industrial centers in Lakes Michigan, Erie, Ontario, and the Detroit and Niagara River connecting channels, compared to other sites sampled basin-wide in this study. In addition, our study further revealed PFAS composition was highest at non WWTP sites, compared to other discharge-types assessed in this study, thus confirming the importance of non-point/diffuse sources as important transport and environmental pathways for PFAS compounds detected within the Great Lakes Basin.

Similarly, our results revealed higher PFAS composition was detected in mussels sampled from open-water sites, followed by sites sampled adjacent to developed, agriculture, and undeveloped sub-watersheds, thus providing additional evidence that sub-watersheds and land-use gradients (i.e., developed/urban, undeveloped, and agricultural) adjacent to open-water mussel sampling locations are important emission source, and transport pathways for PFAS compounds detected within the Great Lakes. Of equal importance, significant correlations were observed between several PFAS groups and mussel sampling locations dominant land-use categories, site population estimates, point source, and

Conclusion

wastewater parameters. While the results presented in this study does not demonstrate among others, a cause and effect between PFAS compounds and mussel sampling locations dominant land-use categories, site discharge-types, and wastewater parameters, our results do suggest the cumulative risk of long-term PFAS exposure to both lower -and-upper-trophic level organisms originating from these emission sources are of importance, and additional monitoring may be warranted at some Great Lakes inshore and offshore sampling locations.

For $\sum_{14}$PFAS compounds identified in this study exceeding the HQ > 0.1 and HQ > 1 threshold, ecotoxicological data for freshwater lower trophic-level aquatic invertebrates including dreissenid mussels are lacking for most. With most PFAS compounds HQ > 0.1 and HQ > 1 exceedance detected in mussels as complex mixtures across the Great Lakes mussel sampling locations, it is plausible that a variety of these contaminants can contribute to many overlapping apical effects and biological endpoints. Even for PFAS compounds with HQs less than 0.1 (HQ < 0.1), there is a potential for adverse biological effects, which have been shown in prior studies to be attributable to factors such as PFAS exposure at environmentally relevant concentrations over time (e.g., low-dose - chronic exposure), PFAS binary mixture, as well as PFAS complex mixture effects with other organic and inorganic contaminants (Goodrum et al., 2020; Labine et al., 2022; Luo et al., 2021). As such, continued bio-monitoring and assessment of the ecotoxicological effects resulting from co-exposure to PFAS chemical mixtures to lower trophic-level organisms is also of particular importance. Further, the findings from our ecological risk assessment suggests, replacement short-chained fluorinated PFAS compounds share similar toxicity profiles to long-chained compounds (Chambers et al., 2021; Li et al., 2020), and have been shown in previous studies to be just as potent as some long-chained PFAS compounds to freshwater aquatic organisms (Gaballah et al., 2020; Rericha et al., 2022b).

Overall, our monitoring data and results highlight the importance of bio-monitoring programs such as the MWP, and ongoing bio-monitoring studies such as this in sampling and assessing legacy, as well as emerging chemicals of mutual concern (CMCs) on a larger spatial scale, to better understand the magnitude and distribution of these contaminants in large freshwater systems such as the Laurentian Great Lakes. Future PFAS bio-monitoring efforts and studies should incorporate a multi-matrix approach, utilizing both passive sampling devices (PSDs) such as Polar Organic Integrative Samplers (POCIS), and co-located dreissenid mussels (*Dreissena spp*.) in characterizing PFAS chemical exposure, and assessing PFAS bioavailability and toxicity pattern in lower trophic-level aquatic organisms. These sampling techniques can be used to support a “weight of evidence” approach in combination with basin-wide surveillance sampling techniques, to compare the occurrence and concentrations of PFAS compounds that are readily detected in surface water, and those compounds that are proteinophilic, and commonly found in aquatic biota tissue. More so, these sampling techniques can also be used in identifying sampling locations and study areas with elevated PFAS concentrations, and where further monitoring and investigation is required in implementing management actions across the Great Lakes Basin.

Credit: NOAA Great Lakes MWP

PFAS Characterization & Result Highlights

- Only PFAS compounds recorded above the method detection limit (> MDL), and found at ten (10) or more sites are summarized in this section.
- Mussel tissue PFAS data obtained between 2013-2018, provides a detailed perspective of PFAS contamination in dreissenid mussels across the Great Lakes Basin.
- Mussel PFAS concentrations from inshore (e.g., tributary, river, and harbor), nearshore, offshore/open lake zones, and reference sites, provides an assessment of bioavailable PFAS compounds quantified in mussel tissue, and help in providing perspective to the extent of PFAS contamination across the Great Lakes mussel sampling locations.
- PFAS comparison across mussel sampling locations discharge-types, and predominant land-use categories, provides needed information and data that fill knowledge gaps surrounding these contaminants emission source and environmental pathways within the Great Lakes Basin.
- PFAS compounds are summarized as follows:
  - General Observations/Findings
  - Basin-wide Highlights
  - Inshore/offshore Highlights
  - Major Discharge-types Highlights
  - Land-use Highlights

Credit: NOAA Great Lakes MWP

PFBA (Perfluoro-n-butanoic acid)

PFBA: (Perfluoro-n-butanoic acid) Summary

General Observations/Findings:

- PFBA: (Perfluoro-n-butanoic acid) was detected (> MDL) in dreissenid mussels at 41 sites (DF: detection frequency of 38%).
- PFBA was detected (> MDL) in mussel tissue at concentrations ranging from 0.673 - 1.20 ng/g wet weight during the 2013-2018 sampling event.
  - Minimum concentration (0.673 ng/g wet weight) detected at site Ashtabula River-1-9.14 (LEAR-1-9.14).
  - Maximum concentration (1.20 ng/g wet weight) detected at site Milwaukee Bay-4-6.13 (LMMB-4-6.13).

Basin-wide Highlights

- Highest PFBA mean concentrations (0.816 ng/g wet weight) measured in mussels from Lake Michigan.
- Basin-wide, PFBA mean concentrations measured in mussel decreased in order from Lake Michigan (0.816 ng/g wet weight) > Reference Sites (0.762 ng/g wet weight) > Niagara River (0.745 ng/g wet weight) > Lake Erie (0.722 ng/g wet weight).

Inshore/offshore Highlights

- The highest PFBA mean concentration (0.781 ng/g wet weight) was found in mussel tissue from designated harbor sites.
- PFBA mean concentrations measured in mussel tissue from inshore (tributary, river, and harbor) and offshore (nearshore and open-lake) sampling locations decreased in order from harbor (0.781 ng/g wet weight) > offshore (0.765 ng/g wet weight) > river (0.754 ng/g wet weight) > tributary (0.754 ng/g wet weight) sites.

Major Discharge-types Highlights

- The highest PFBA mean concentration (0.809 ng/g wet weight) measured was found in mussel tissue from sites sampled in proximity to WWTPs.
- PFBA mean concentrations measured in mussel tissue from sampled discharge-types locations decreased in order from WWTPs (0.809 ng/g wet weight) > non-WWTPs (0.785 ng/g wet weight) > WWTP Gradient (0.738 ng/g wet weight) > WWTPs/CSOs (0.723 ng/g wet weight) sites.

Land-use Highlights

- The highest PFBA mean concentration (0.771 ng/g wet weight) was measured in mussel tissue from developed dominan sites.
- PFBA mean concentration measured in mussel tissue from designated site land-use categories trended downward from developed (0.771 ng/g wet weight) > open-water (0.764 ng/g wet weight) > agriculture (0.726 ng/g wet weight) sites.

PFAS Characterization & Result Highlights

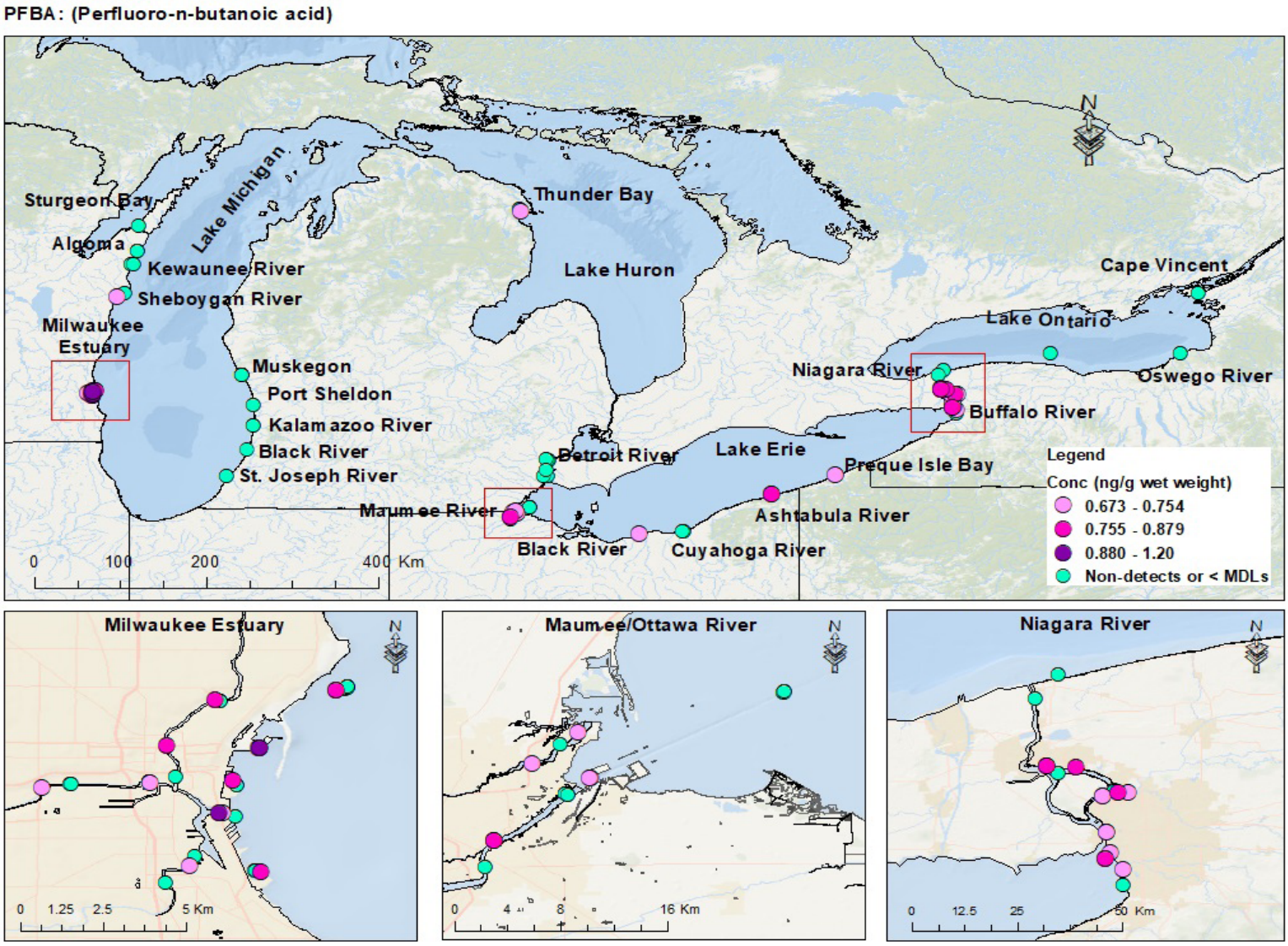

Fig.34. Map of Great Lakes Mussel Watch PFAS sampling locations, highlighting PFAS compounds detected (> MDL) in mussel tissue during the 2013-2018 sampling event.

Concentration table: Summary of basin-wide PFAS concentrations (ng/g wet weight) measured (> MDL) in dreissenid mussel tissue from Lakes Michigan, Huron, Erie, Ontario, and Detroit and Niagara River connecting channels (*) sampling locations between 2013 - 2018.

			Min	Mean	Max
Category	(n)	Stdev	ng/g (ww)	ng/g (ww)	ng/g (ww)
Lake Michigan	13	0.144	0.689	0.816	1.20
Lake Huron	0	0	0	0	0
Detroit River (*)	0	0	0	0	0
Lake Erie	11	0.036	0.673	0.722	0.789
Niagara River (*)	12	0.049	0.693	0.745	0.859
Lake Ontario	0	0	0	0	0
Reference Sites	5	0.076	0.686	0.762	0.879

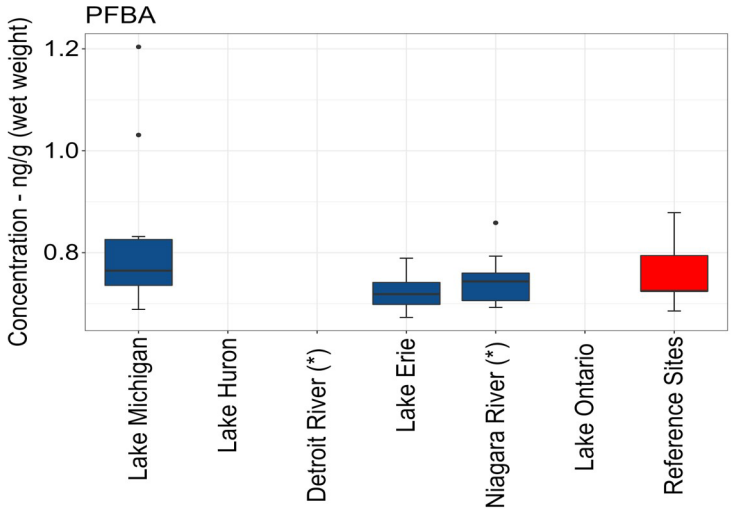

Boxplot: PFAS concentrations (ng/g wet weight) measured in dreissenid mussel tissue basin-wide between 2013-2018. Reference sites provides perspective to the relative PFAS concentrations found in mussel tissue basin-wide.

PFAS Characterization & Result Highlights

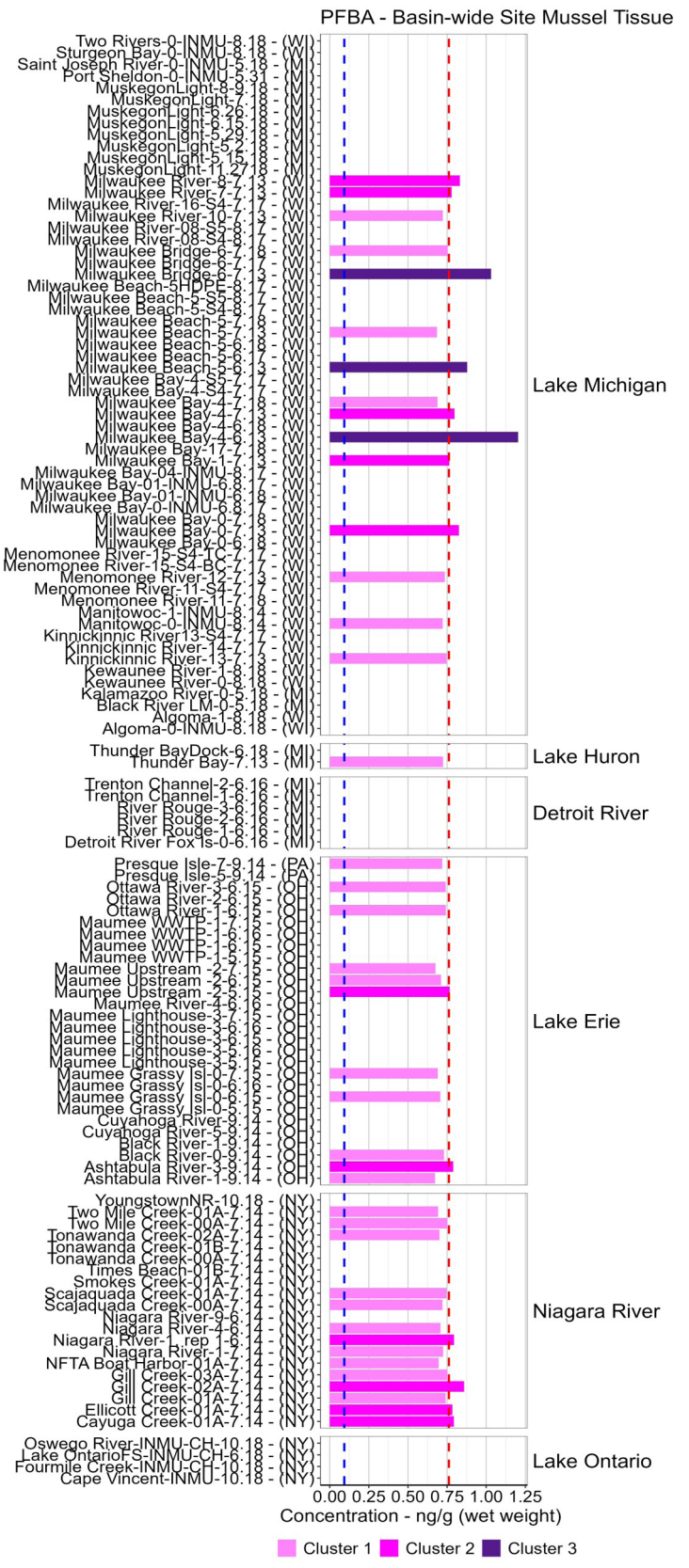

Basin-wide site tissue bar chart: PFAS contaminant concentration results (ng/g wet weight) measured (> MDL) in mussel tissue basin-wide during 2013-2018. Clusters 1-3 represents sites with low, medium and high PFAS concentrations. Blue dashed line represents concentration method detection limit (MDL). Reference line (red dashed line) represent mean reference sites concentration.

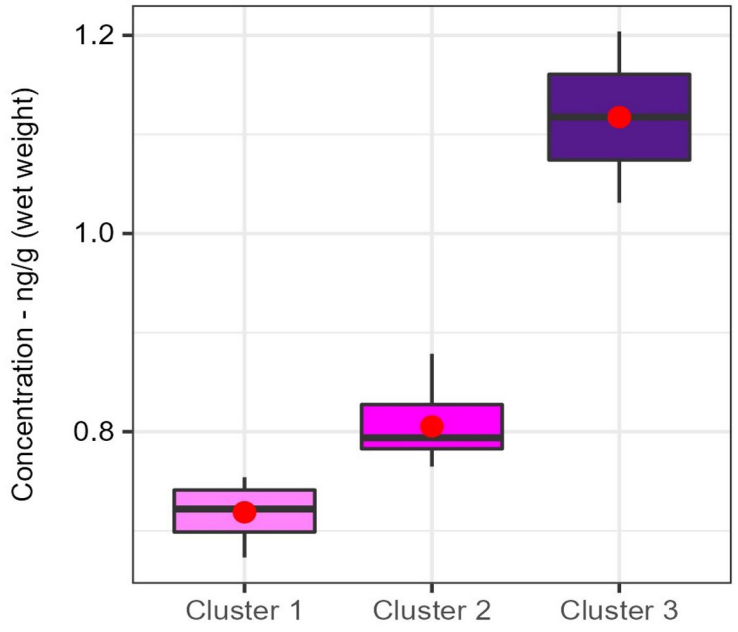

Boxplot: PFAS concentration results detected in dreissenid mussels during 2013-2018. Mean values are plotted as red points. Clusters 1-3 represent low, medium and high PFAS concentrations, respectively.

Total PFBA Concentration (ng/g wet weight)		
	Low	0.673 - 0.754
	Medium	0.755 - 0.879
	High	0.880 - 1.20

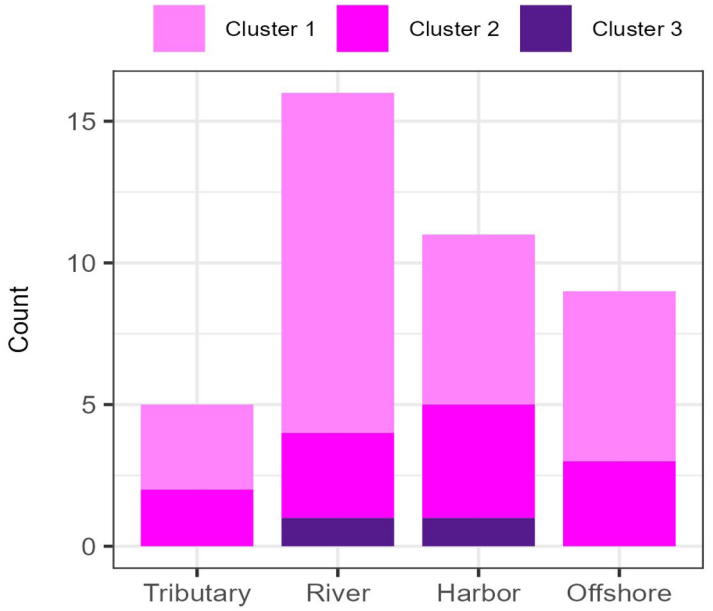

Tissue inshore - offshore bar chart: Measured PFAS composition profile detected in dreissenid mussels across inshore (tributary, river, harbor) and offshore (e.g., open-lake) Great Lakes complexes. Counts (y-axis) represents number of PFAS samples found in mussel tissue across inshore and offshore sampling locations during the 2013-2018 period.

PFAS Characterization & Result Highlights

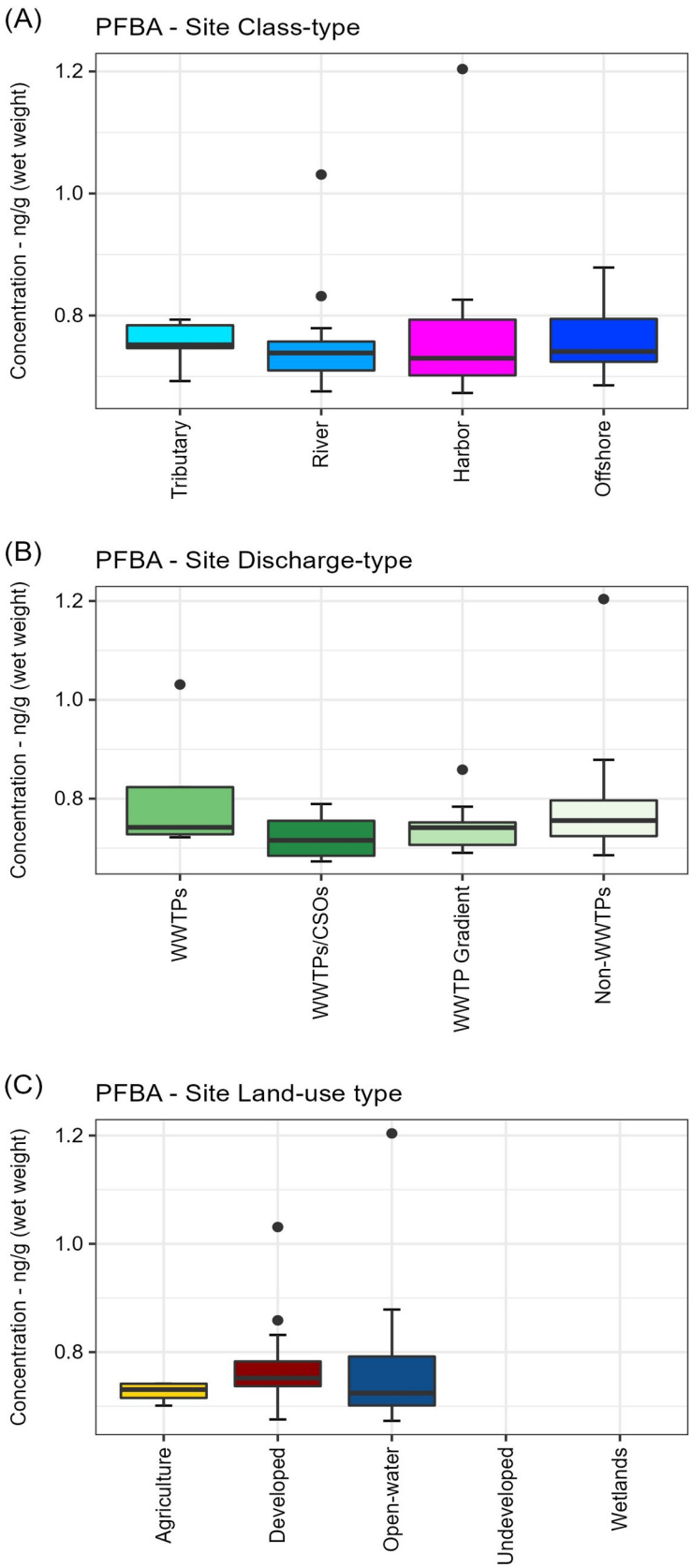

Boxplots: PFAS concentrations measured (> MDL) in mussel tissue at A) inshore and offshore sampling locations, B) designated MWP site discharge-types, and C) predominant site land-use categories/ gradients. Only compounds found at ten or more sites were included in PFAS concentration summary. Plots provide perspective on the most commonly found PFAS in mussel tissue, and their relative concentrations across various Great Lakes environmental matrices.

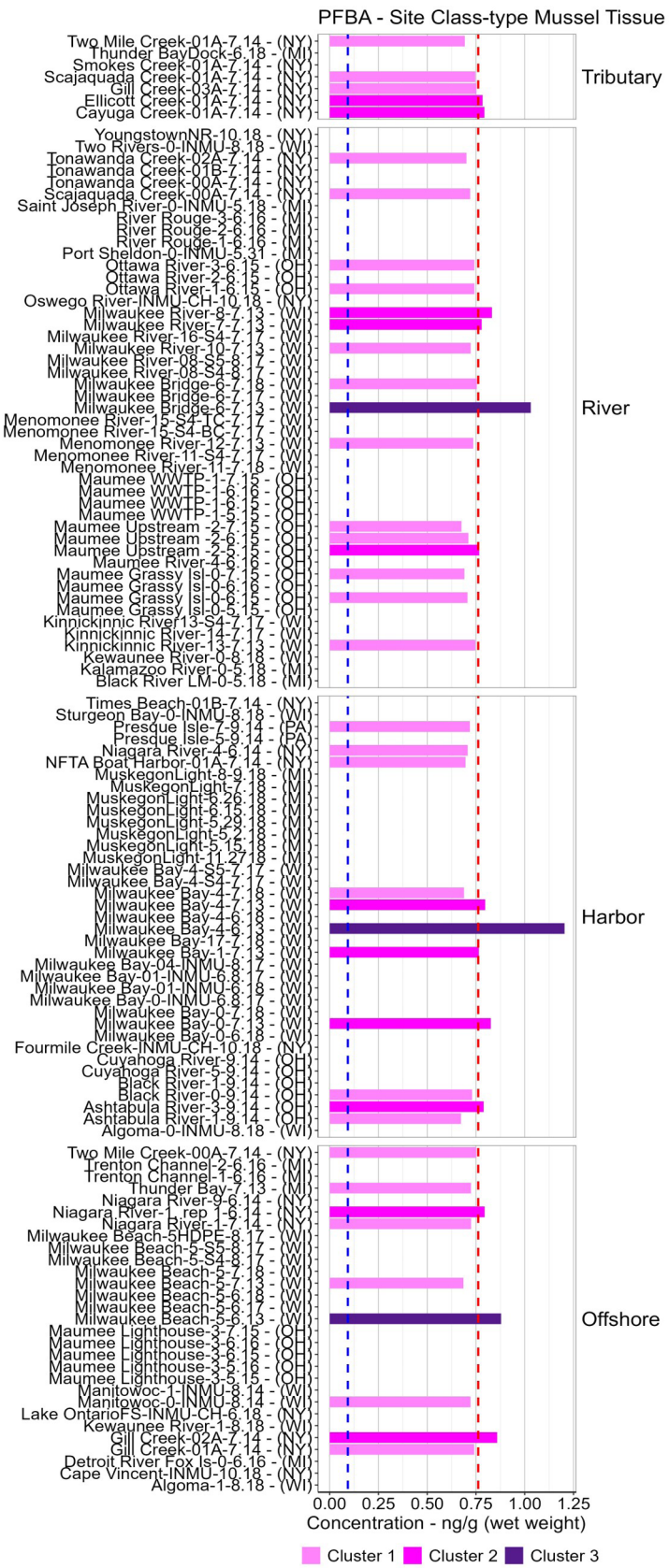

Site class-type tissue bar chart: PFAS contaminant concentration results (ng/g wet weight) measured (> MDL) in dreissenid mussels during 2013-2018 sampling event. Clusters 1-3 represents sites with low, medium and high PFAS concentrations. Blue dashed line represents concentration method detection limit (MDL). Reference line (red dashed line) represent mean reference sites concentration.

PFAS Characterization & Result Highlights

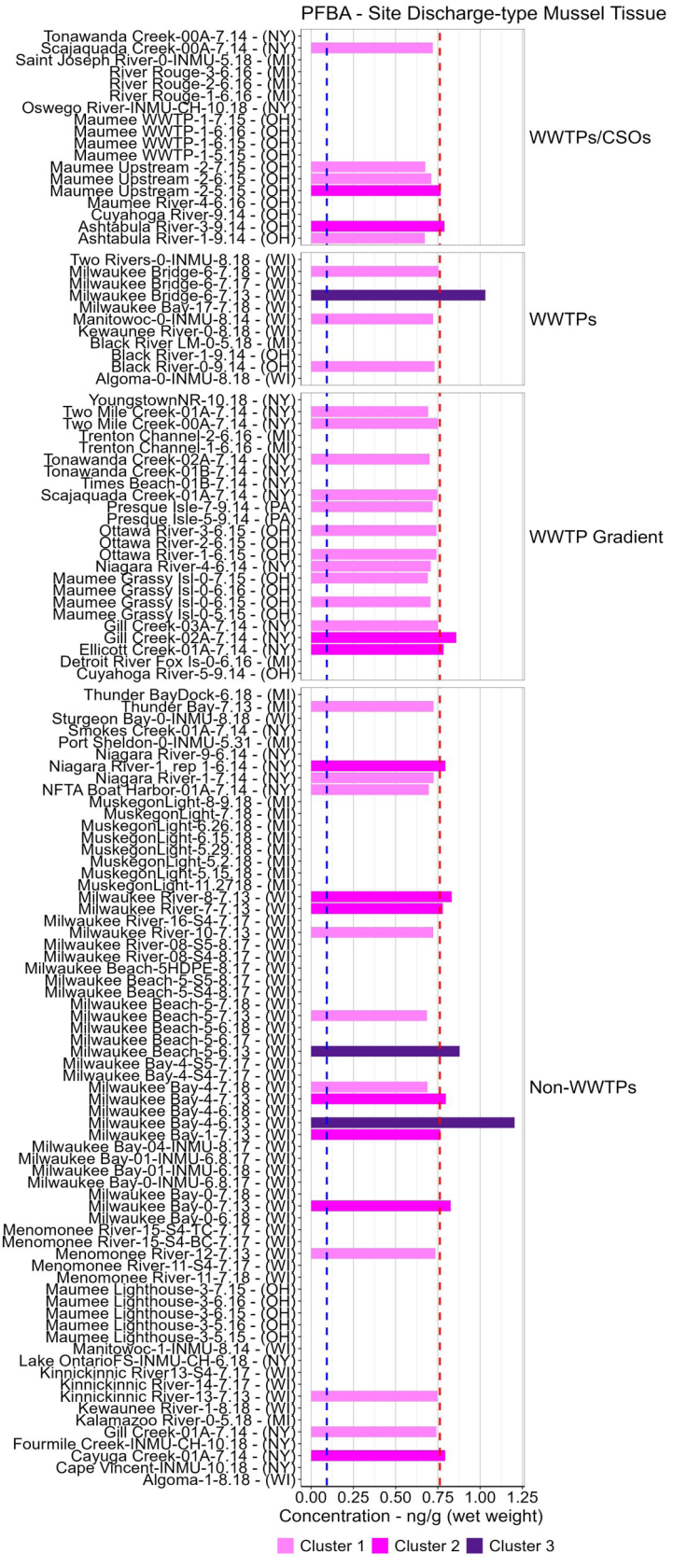

Site discharge-type tissue bar chart: PFAS contaminant concentration results (ng/g wet weight) measured (> MDL) in dreissenid mussels during 2013-2018 sampling event. Clusters 1-3 represents sites with low, medium and high PFAS concentrations. Blue dashed line represents concentration method detection limit (MDL). Reference line (red dashed line) represent mean reference sites concentration.

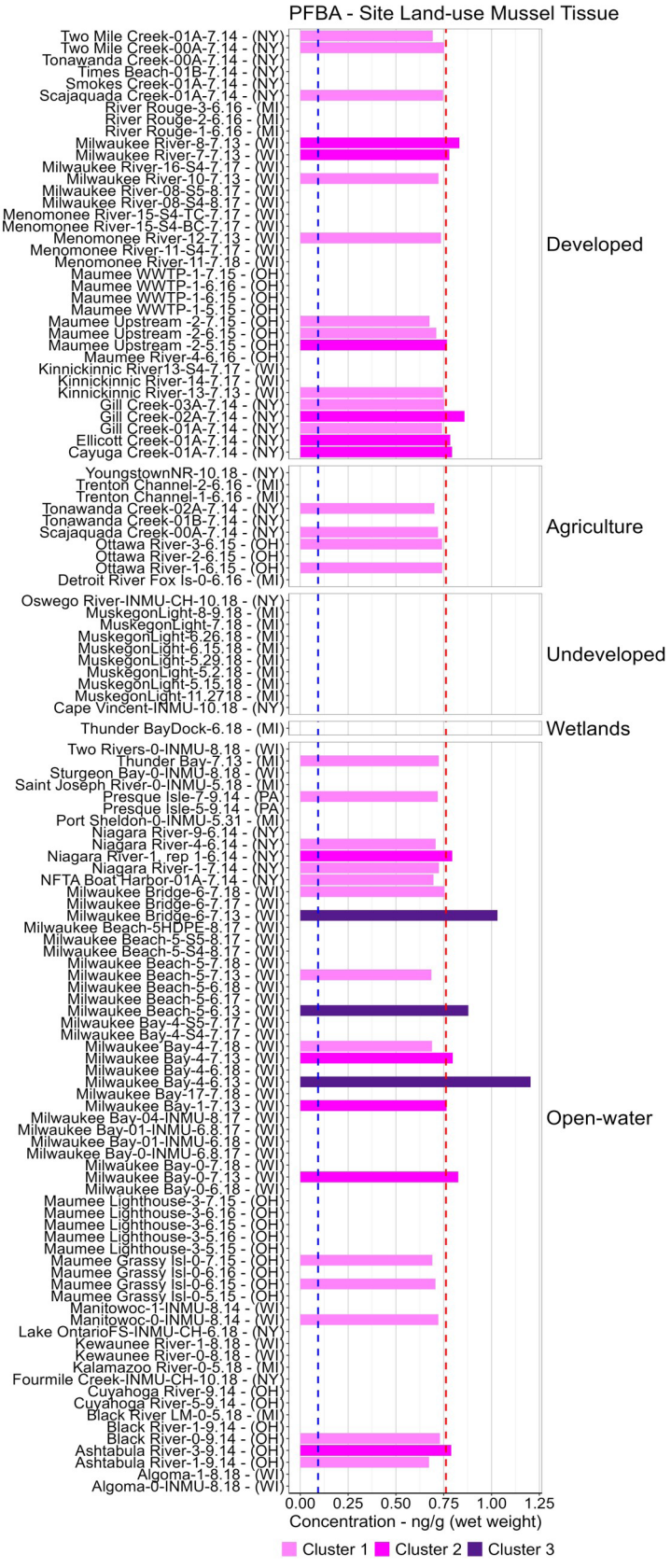

Site land-use tissue bar chart: PFAS contaminant concentration results (ng/g wet weight) measured (> MDL) in dreissenid mussels during 2013-2018 sampling event. Clusters 1-3 represents sites with low, medium and high PFAS concentrations. Blue dashed line represents concentration method detection limit (MDL). Reference line (red dashed line) represent mean reference sites concentration.

PFDoA (Perfluoro-n-dodecanoic acid)

PFDoA: (Perfluoro-n-dodecanoic acid) Summary

General Observations/Findings:

- PFDoA: (Perfluoro-n-dodecanoic acid) was detected (> MDL) in dreissenid mussels at 37 sites (DF: detection frequency of 34%).
- PFDoA was detected (> MDL) in mussel tissue at concentrations ranging from 0.62 - 1.49 ng/g wet weight during the 2013-2018 sampling event.
  - Minimum concentration (0.62 ng/g wet weight) detected at site MuskegonLight-6.26.18 (MUS-6.26.18).
  - Maximum concentration (1.49 ng/g wet weight) detected at site Kinnickinnic River13-S4-7.17 (LMMB-13-S4-7.17).

Basin-wide Highlights

- Highest PFDoA mean concentrations (0.777 ng/g wet weight) measured in mussels from Lake Michigan.
- Basin-wide, PFDoA mean concentrations measured in mussel decreased in order from Lake Michigan (0.777 ng/g wet weight) > Lake Erie (0.773 ng/g wet weight) > Lake Ontario (0.748 ng/g wet weight) > Reference Sites (0.683 ng/g wet weight) > Niagara River (0.663 ng/g wet weight).

Inshore/offshore Highlights

- The highest PFDoA mean concentration (0.803 ng/g wet weight) was found in mussel tissue from designated river sites.
- PFDoA mean concentrations measured in mussel tissue from inshore (tributary, river, and harbor) and offshore sampling locations decreased in order from river (0.803 ng/g wet weight) > harbor (0.714 ng/g wet weight) > off shore (0.687 ng/g wet weight) > tributary (0.681 ng/g wet weight) sites.

Major Discharge-types Highlights

- The highest PFDoA mean concentration (0.773 ng/g wet weight) measured was found in mussel tissue from non-WWTP sites.
- PFDoA mean concentrations measured in mussel tissue from sampled major discharge-types locations decreased in order from non-WWTP (0.773 ng/g wet weight) > WWTPs/CSOs (0.707 ng/g wet weight) > WWTP (0.704 ng/g wet weight) > WWTP Gradient (0.684 ng/g wet weight) sites.

Land-use Highlights

- The highest PFDoA mean concentration (0.868 ng/g wet weight) was found in mussel tissue from developed dominant sites.
- PFDoA mean concentration measured in mussel tissue from designated site land-use categories trended downward from developed (0.868 ng/g wet weight) > undeveloped (0.709 ng/g wet weight) > open-water (0.69 ng/g wet weight) > agriculture (0.687 ng/g wet weight) sites.

PFAS Characterization & Result Highlights

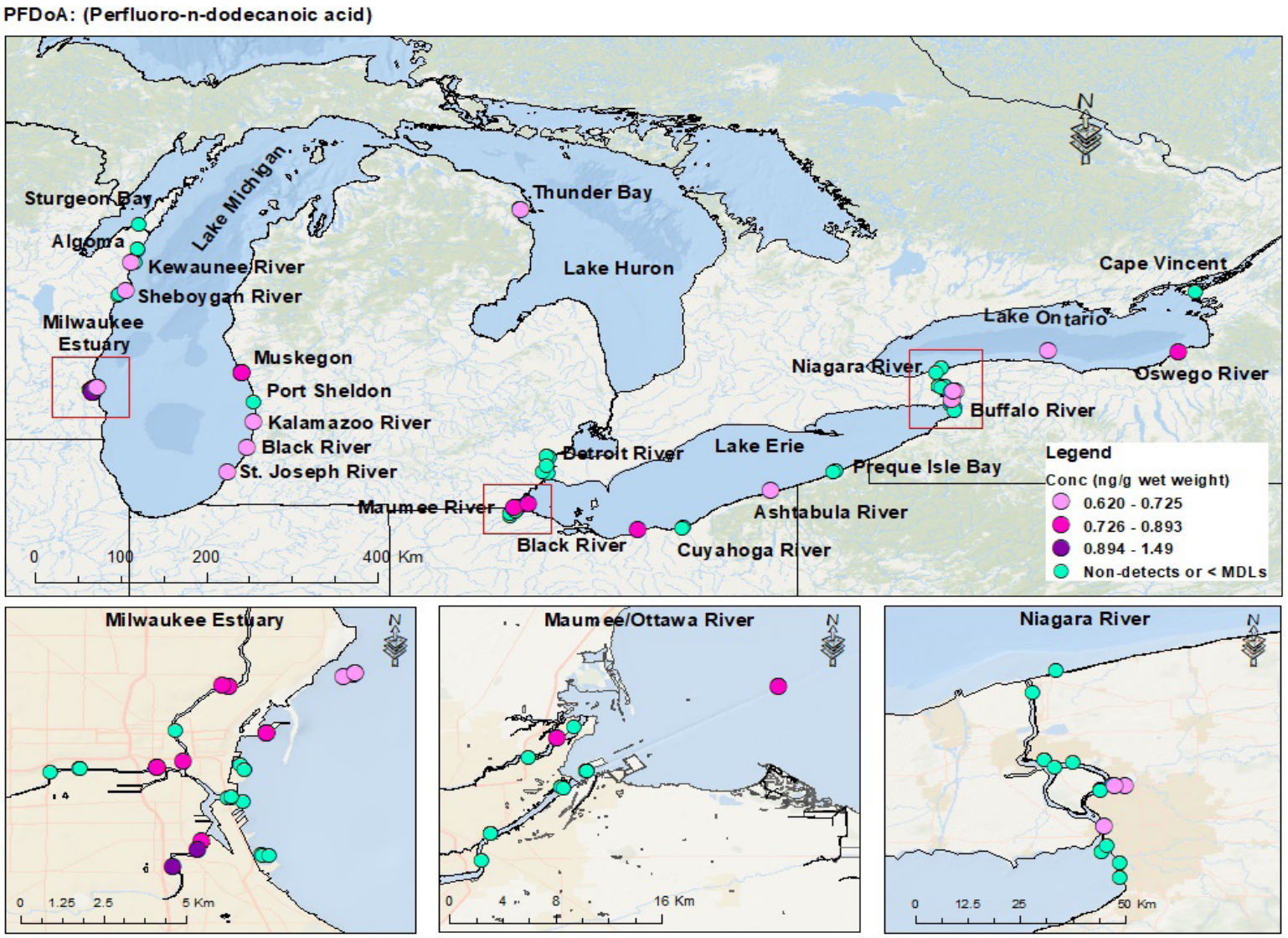

Fig.35. Map of Great Lakes Mussel Watch PFAS sampling locations, highlighting PFAS compounds detected (> MDL) in mussel tissue during the 2013-2018 sampling event.

Concentration table: Summary of basin-wide PFAS concentrations (ng/g wet weight) measured (> MDL) in dreissenid mussel tissue from Lakes Michigan, Huron, Erie, Ontario, and Detroit and Niagara River connecting channels (*) sampling locations between 2013 - 2018.

			Min	Mean	Max
Category	(n)	Stdev	ng/g (ww)	ng/g (ww)	ng/g (ww)
Lake Michigan	23	0.211	0.62	0.777	1.49
Lake Huron	0	0	0	0	0
Detroit River (*)	0	0	0	0	0
Lake Erie	3	0.102	0.686	0.773	0.885
Niagara River (*)	3	0.034	0.627	0.663	0.695
Lake Ontario	2	0.058	0.707	0.748	0.789
Reference Sites	6	0.042	0.633	0.683	0.761

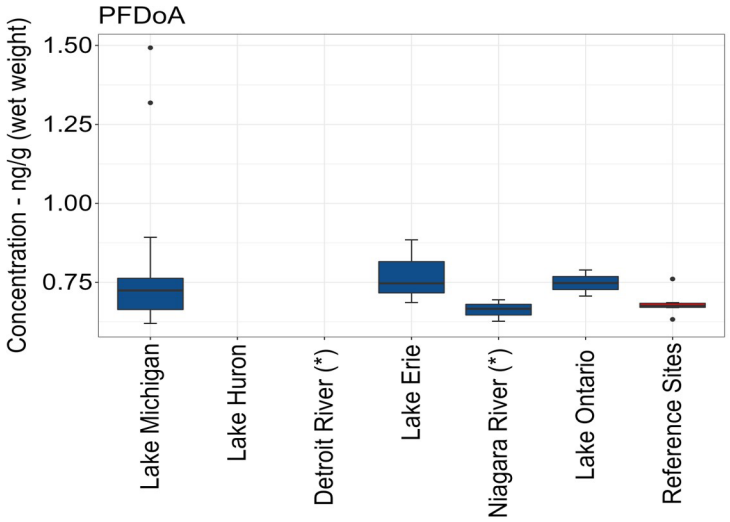

Boxplot: PFAS concentrations (ng/g wet weight) measured in dreissenid mussel tissue basin-wide between 2013 - 2018. Reference sites provides perspective to the relative PFAS concentrations found in mussel tissue basin-wide.

PFAS Characterization & Result Highlights

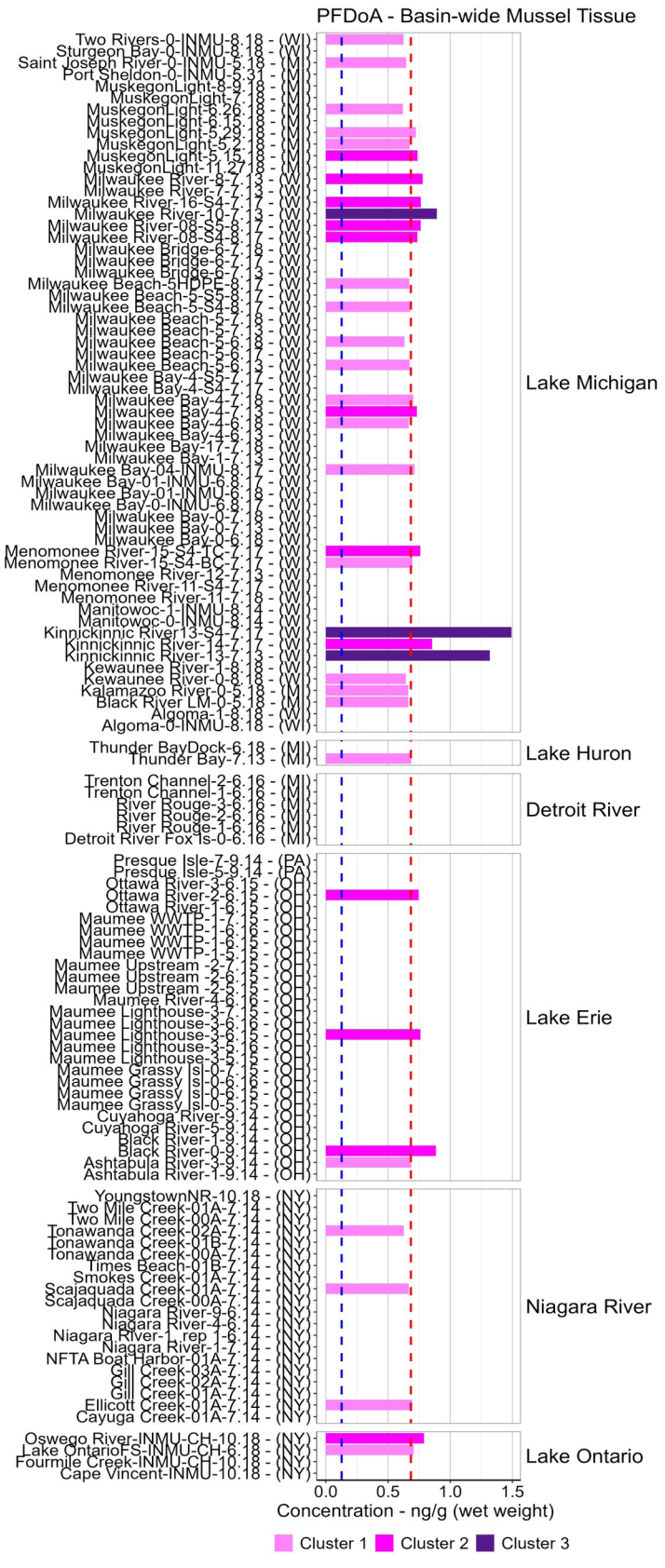

Basin-wide site tissue bar chart: PFAS contaminant concentration results (ng/g wet weight) measured (> MDL) in mussel tissue basin-wide during 2013-2018. Clusters 1-3 represents sites with low, medium and high PFAS concentrations. Blue dashed line represents concentration method detection limit (MDL). Reference line (red dashed line) represent mean reference sites concentration.

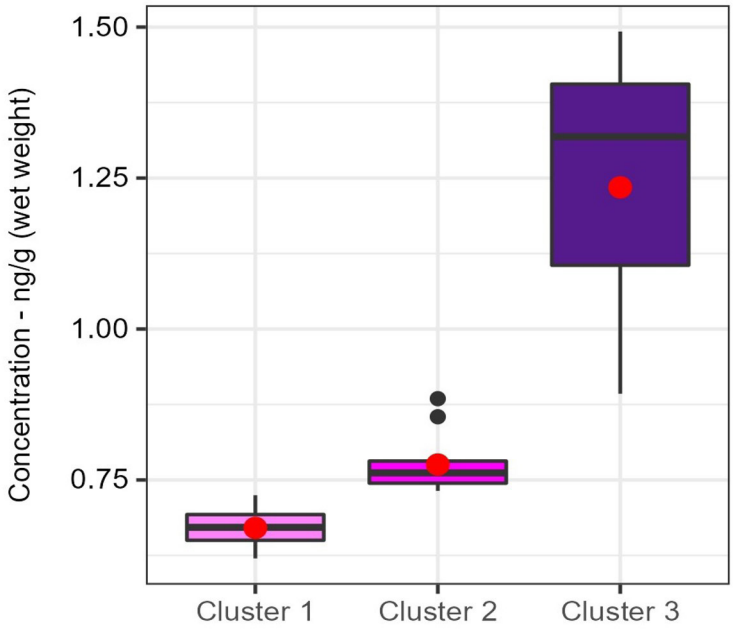

Boxplot: PFAS concentration results detected in dreissenid mussels during 2013-2018. Mean values are plotted as red points. Clusters 1-3 represent low, medium and high PFAS concentrations, respectively.

Total PFDoA Concentration (ng/g wet weight)		
	Low	0.620 - 0.725
	Medium	0.726 - 0.893
	High	0.894 - 1.49

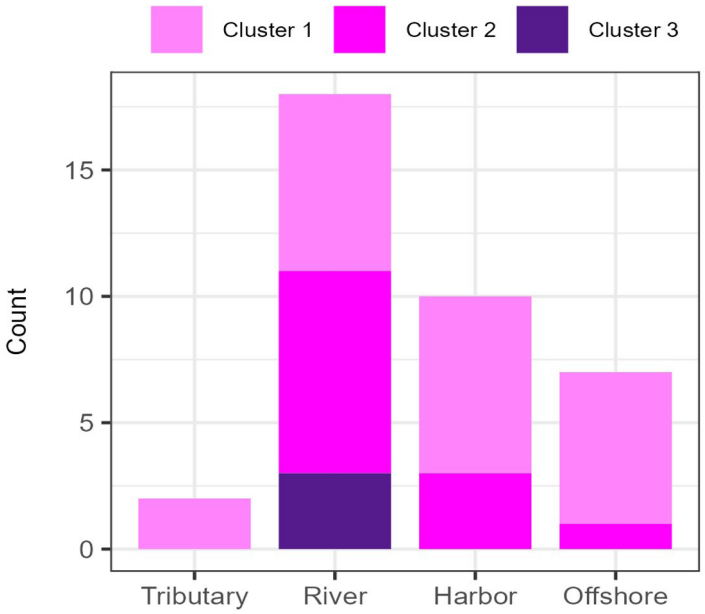

Tissue inshore - offshore bar chart: Measured PFAS composition profile detected in dreissenid mussels across inshore (tributary, river, harbor) and offshore (e.g., open-lake) Great Lakes complexes. Counts (y-axis) represents number of PFAS samples found in mussel tissue across inshore and offshore sampling locations during the 2013-2018 period.

PFAS Characterization & Result Highlights

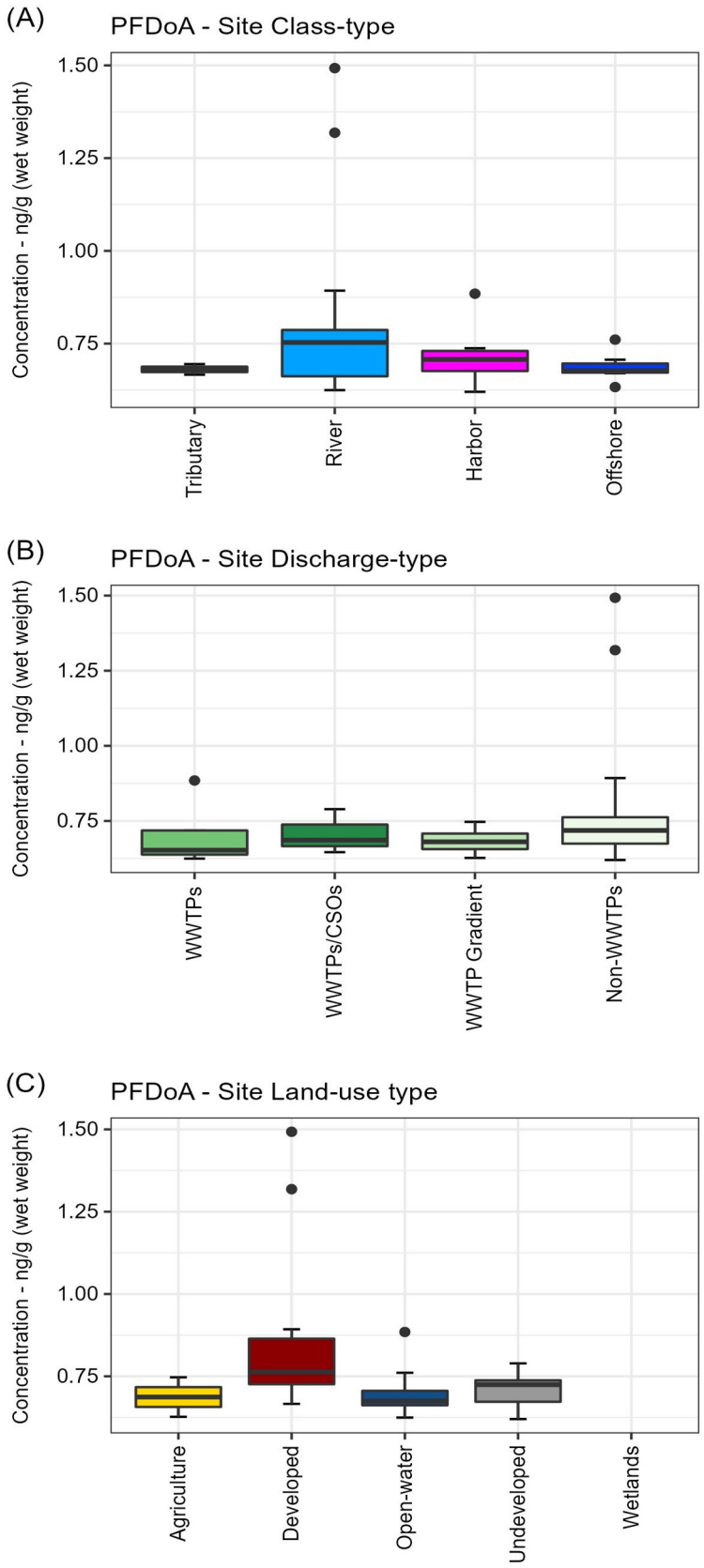

Boxplots: PFAS concentrations measured (> MDL) in mussel tissue at A) inshore and offshore sampling locations, B) designated MWP site discharge-types, and C) predominant site land-use categories/ gradients. Only compounds found at ten or more sites were included in PFAS concentration summary. Plots provide perspective on the most commonly found PFAS in mussel tissue, and their relative concentrations across various Great Lakes environmental matrices.

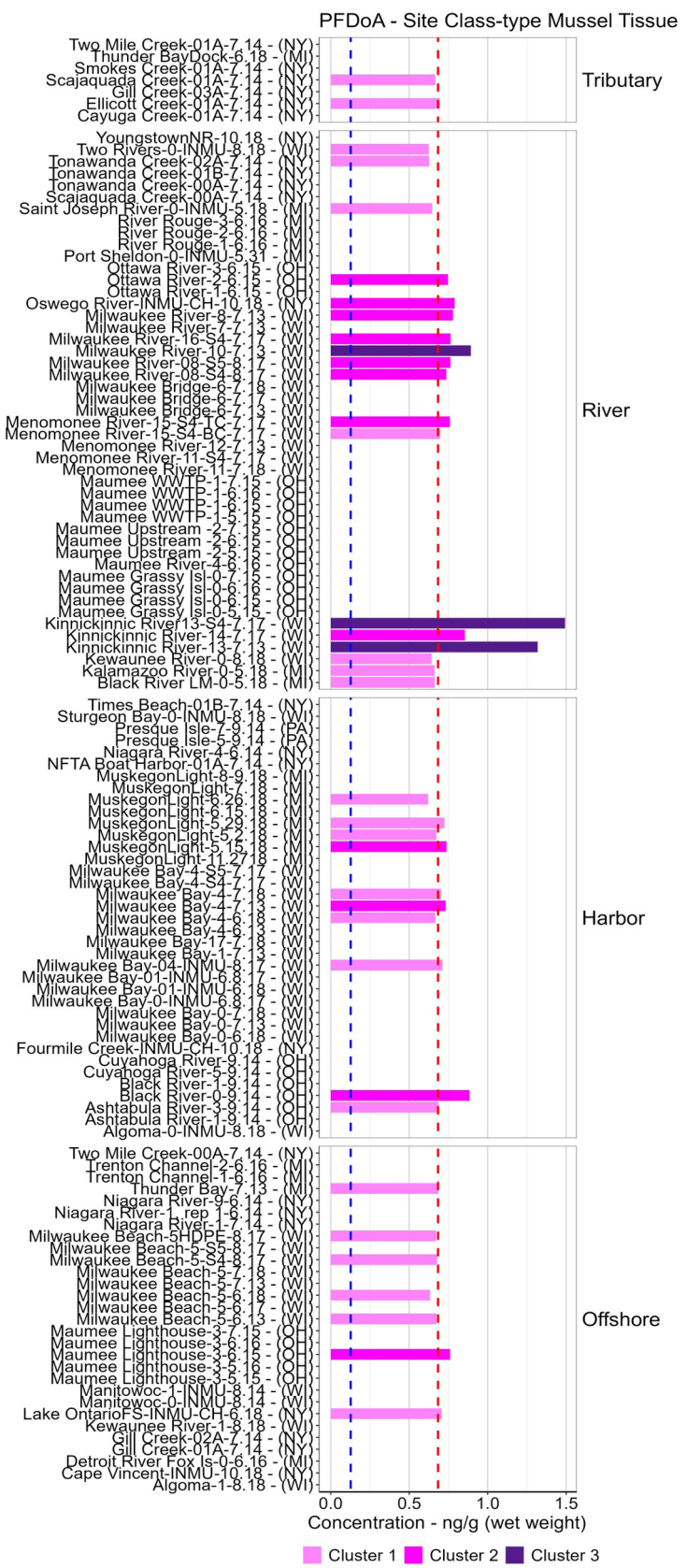

Site class-type tissue bar chart: PFAS contaminant concentration results (ng/g wet weight) measured (> MDL) in dreissenid mussels during 2013-2018 sampling event. Clusters 1-3 represents sites with low, medium and high PFAS concentrations. Blue dashed line represents concentration method detection limit (MDL). Reference line (red dashed line) represent mean reference sites concentration.

PFAS Characterization & Result Highlights

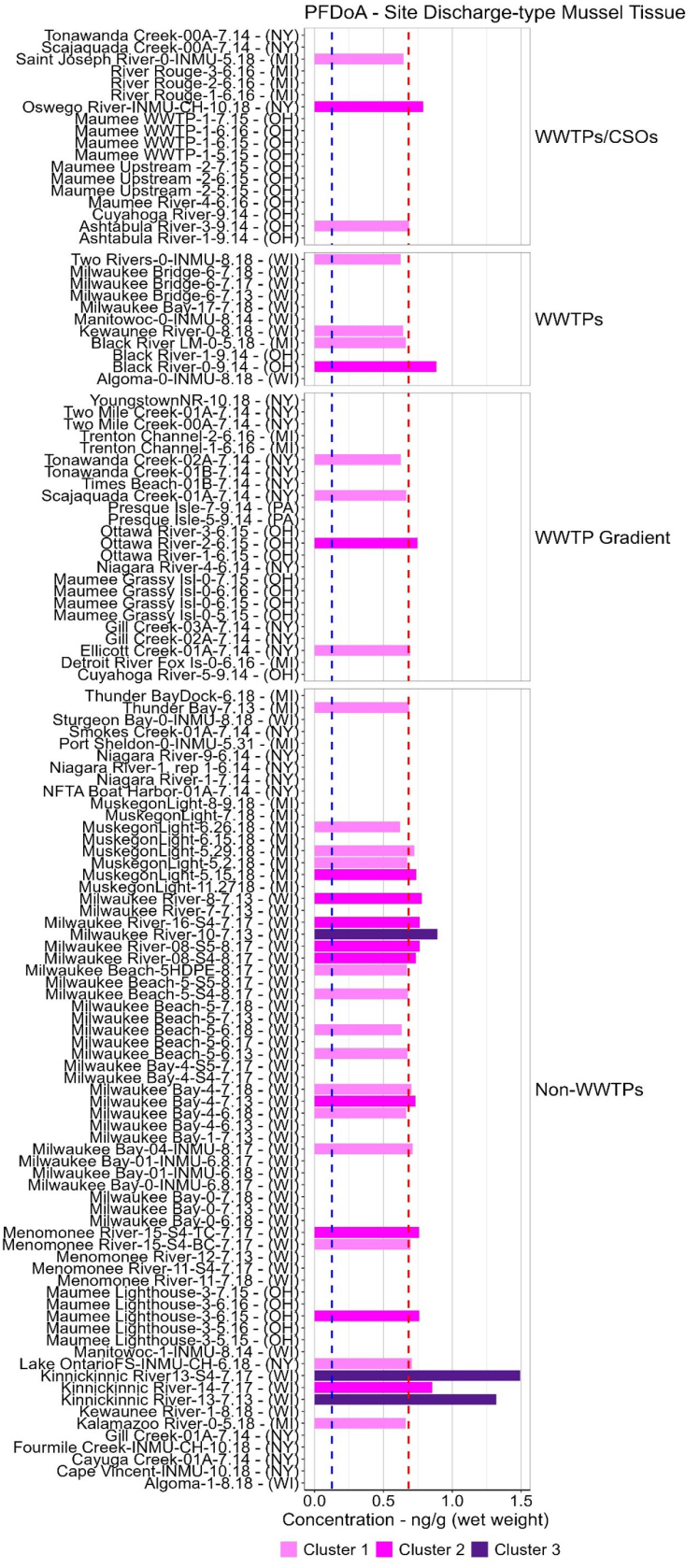

Site discharge-type tissue bar chart: PFAS contaminant concentration results (ng/g wet weight) measured (> MDL) in dreissenid mussels during 2013-2018 sampling event. Clusters 1-3 represents sites with low, medium and high PFAS concentrations. Blue dashed line represents concentration method detection limit (MDL). Reference line (red dashed line) represent mean reference sites concentration.

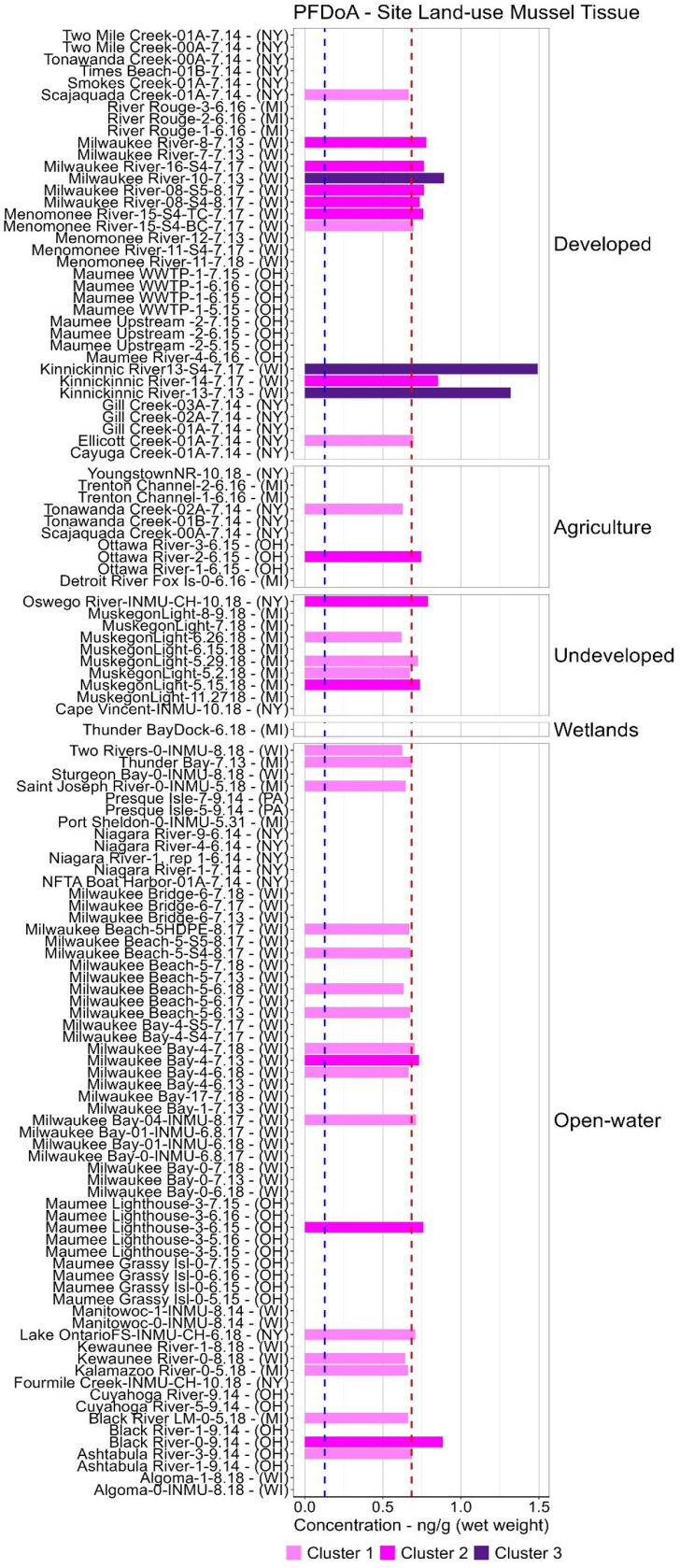

Site land-use tissue bar chart: PFAS contaminant concentration results (ng/g wet weight) measured (> MDL) in dreissenid mussels during 2013-2018 sampling event. Clusters 1-3 represents sites with low, medium and high PFAS concentrations. Blue dashed line represents concentration method detection limit (MDL). Reference line (red dashed line) represent mean reference sites concentration.

PFDS (Perfluoro-1-decanesulfonic acid)

PFDS: (Perfluoro-1-decanesulfonic acid) Summary

General Observations/Findings:

- PFDS: (Perfluoro-1-decanesulfonic acid) was detected (> MDL) in dreissenid mussels at 47 sites (DF: detection frequency of 44%).
- PFDS was detected (> MDL) in mussel tissue at concentrations ranging from 0.329 - 1.28 ng/g wet weight during the 2013-2018 sampling event.
  - Minimum concentration (0.329 ng/g wet weight) detected at site Ashtabula River-1-9.14 (LEAR-1-9.14).
  - Maximum concentration (1.28 ng/g wet weight) detected at site Trenton Channel-2-6.16 (DRTC-2-6.16).

Basin-wide Highlights

- Highest PFDS mean concentrations (0.822 ng/g wet weight) measured in mussels from Detroit River.
- Basin-wide, PFDS mean concentrations measured in mussel decreased in order from Detroit River (0.822 ng/g wet weight) > Lake Michigan (0.438 ng/g wet weight) > Reference Sites (0.422 ng/g wet weight) > Niagara River (0.417 ng/g wet weight) > Lake Erie (0.414 ng/g wet weight) > Lake Ontario (0.359 ng/g wet weight).

Inshore/offshore Highlights

- The highest PFDS mean concentration (0.468 ng/g wet weight) was found in mussel tissue from designated offshore sites
- PFDS mean concentrations measured in mussel tissue from inshore (tributary, river, and harbor) and offshore sampling locations decreased in order from offshore (0.468 ng/g wet weight) > harbor (0.453 ng/g wet weight) > tributary (0.428 ng/g wet weight) > river (0.409 ng/g wet weight) sites.

Major Discharge-types Highlights

- The highest PFDS mean concentration (0.519 ng/g wet weight) measured was found in mussel tissue from WWTP discharge zones/Gradient sites.
- PFDS mean concentrations measured in mussel tissue from sampled major discharge-types locations decreased in order from WWTP discharge zones/Gradient (0.519 ng/g wet weight) > non-WWTPs (0.421 ng/g wet weight) > WWTPs (0.418 ng/g wet weight) > WWTPs/CSOs (0.37 ng/g wet weight) sites.

Land-use Highlights

- The highest PFDS mean concentration (0.872 ng/g wet weight) was found in mussel tissue from agriculture dominant sites.
- PFDS concentration measured in mussel tissue from designated site land-use categories trended downward from Agriculture (0.872 ng/g wet weight) > Open-water (0.43 ng/g wet weight) > Developed (0.413 ng/g wet weight) sites.

PFAS Characterization & Result Highlights

PFDS: (Perfluoro-1-decanesulfonic acid)

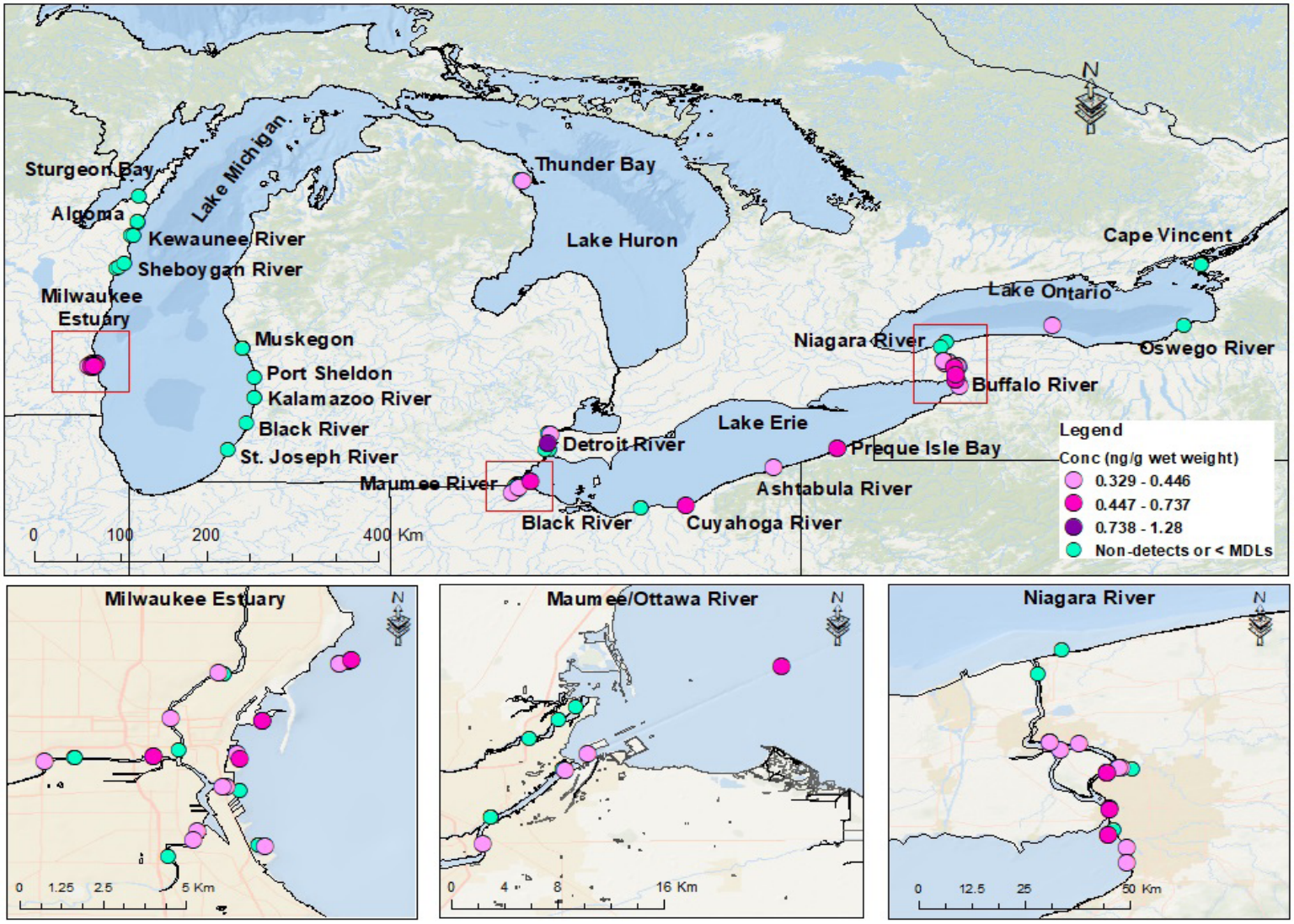

Fig.36. Map of Great Lakes Mussel Watch PFAS sampling locations, highlighting PFAS compounds detected (> MDL) in mussel tissue during the 2013-2018 sampling event.

Concentration table: Summary of basin-wide PFAS concentrations (ng/g wet weight) measured (> MDL) in dreissenid mussel tissue from Lakes Michigan, Huron, Erie, Ontario, and Detroit and Niagara River connecting channels (*) sampling locations between 2013 - 2018.

			Min	Mean	Max
Category	(n)	Stdev	ng/g (ww)	ng/g (ww)	ng/g (ww)
Lake Michigan	15	0.103	0.336	0.438	0.737
Lake Huron	0	0	0	0	0
Detroit River (*)	2	0.646	0.365	0.822	1.28
Lake Erie	6	0.101	0.329	0.414	0.562
Niagara River (*)	13	0.082	0.355	0.417	0.645
Lake Ontario	1	0	0.359	0.359	0.359
Reference Sites	10	0.074	0.336	0.422	0.566

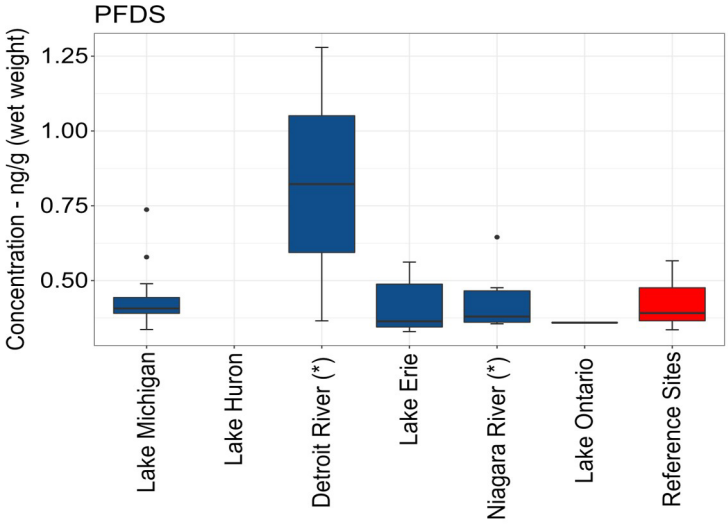

Boxplot: PFAS concentrations (ng/g wet weight) measured in dreissenid mussel tissue basin-wide between 2013 - 2018. Reference sites provides perspective to the relative PFAS concentrations found in mussel tissue basin-wide.

PFAS Characterization & Result Highlights

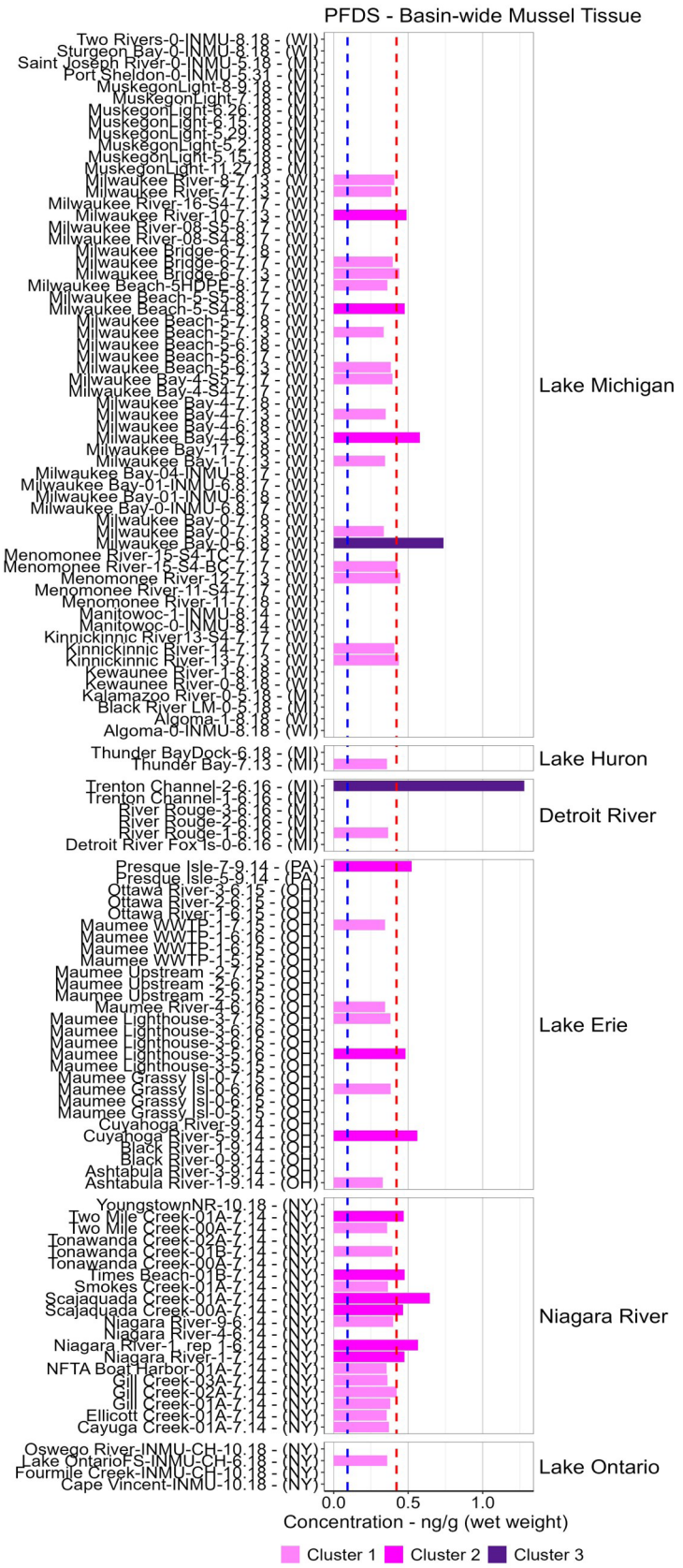

Basin-wide site tissue bar chart: PFAS contaminant concentration results (ng/g wet weight) measured (> MDL) in mussel tissue basin-wide during 2013-2018. Clusters 1-3 represents sites with low, medium and high PFAS concentrations. Blue dashed line represents concentration method detection limit (MDL). Reference line (red dashed line) represent mean reference sites concentration.

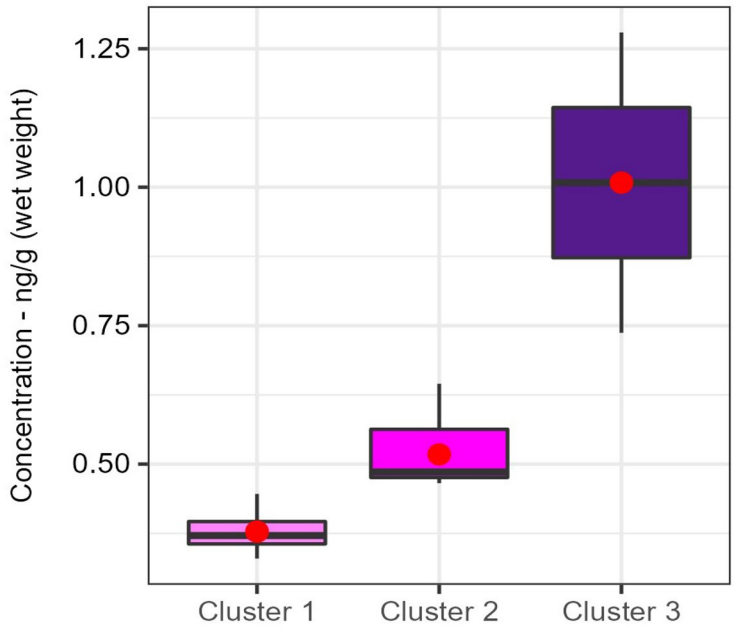

Boxplot: PFAS concentration results detected in dreissenid mussels during 2013-2018. Mean values are plotted as red points. Clusters 1-3 represent low, medium and high PFAS concentrations, respectively.

Total PFDS Concentration (ng/g wet weight)		
	Low	0.329 - 0.446
	Medium	0.447 - 0.737
	High	0.738 - 1.28

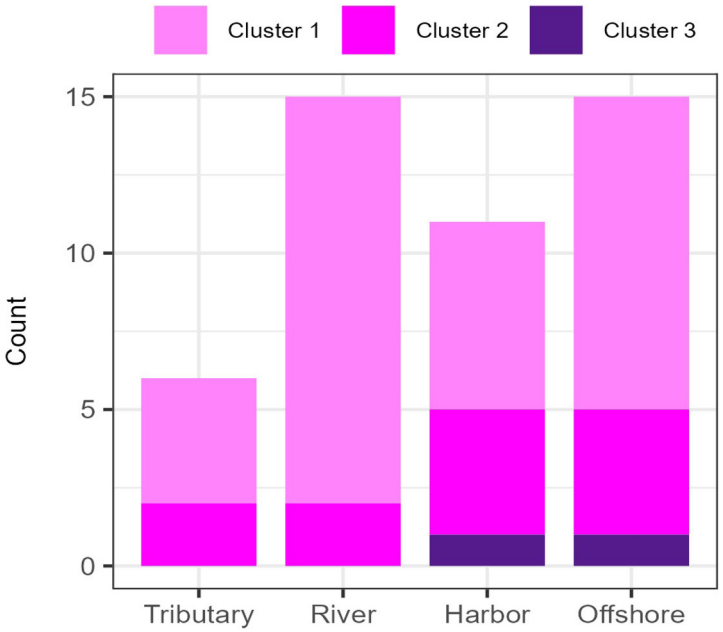

Tissue inshore - offshore bar chart: Measured PFAS composition profile detected in dreissenid mussels across inshore (tributary, river, harbor) and offshore (e.g., open-lake) Great Lakes complexes. Counts (y-axis) represents number of PFAS samples found in mussel tissue across inshore and offshore sampling locations during the 2013-2018 period.

PFAS Characterization & Result Highlights

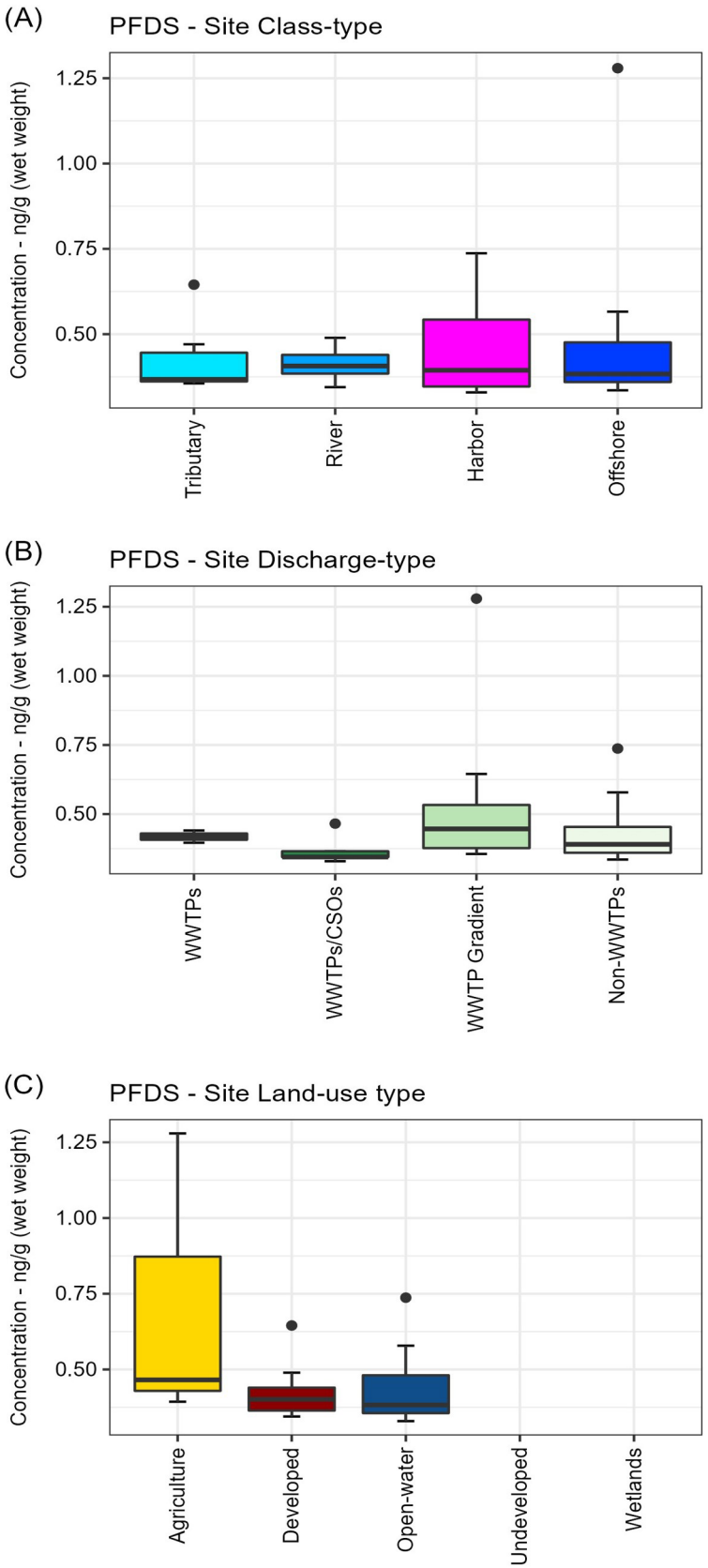

Boxplots: PFAS concentrations measured (> MDL) in mussel tissue at A) inshore and offshore sampling locations, B) designated MWP site discharge-types, and C) predominant site land-use categories/ gradients. Only compounds found at ten or more sites were included in PFAS concentration summary. Plots provide perspective on the most commonly found PFAS in mussel tissue, and their relative concentrations across various Great Lakes environmental matrices.

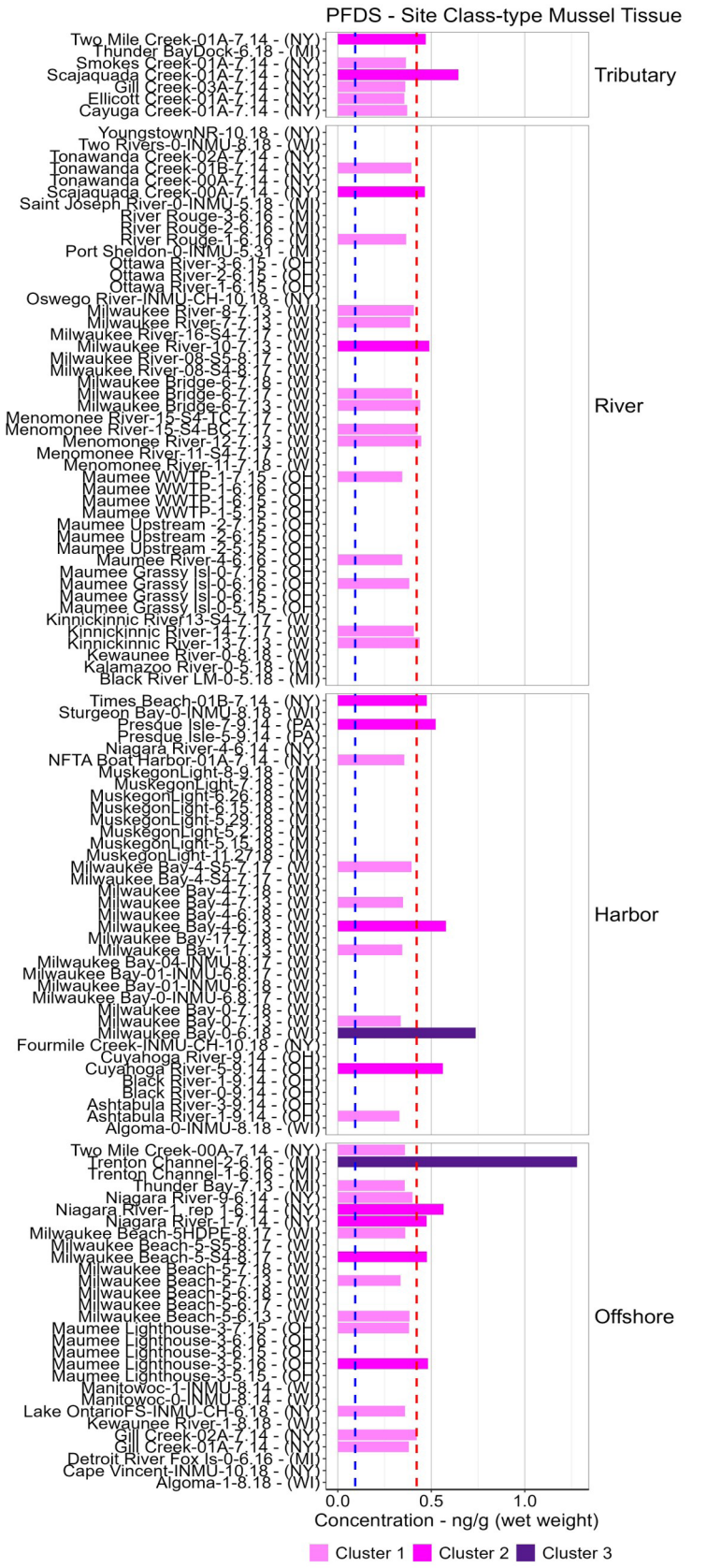

Site class-type tissue bar chart: PFAS contaminant concentration results (ng/g wet weight) measured (> MDL) in dreissenid mussels during 2013-2018 sampling event. Clusters 1-3 represents sites with low, medium and high PFAS concentrations. Blue dashed line represents concentration method detection limit (MDL). Reference line (red dashed line) represent mean reference sites concentration.

PFAS Characterization & Result Highlights

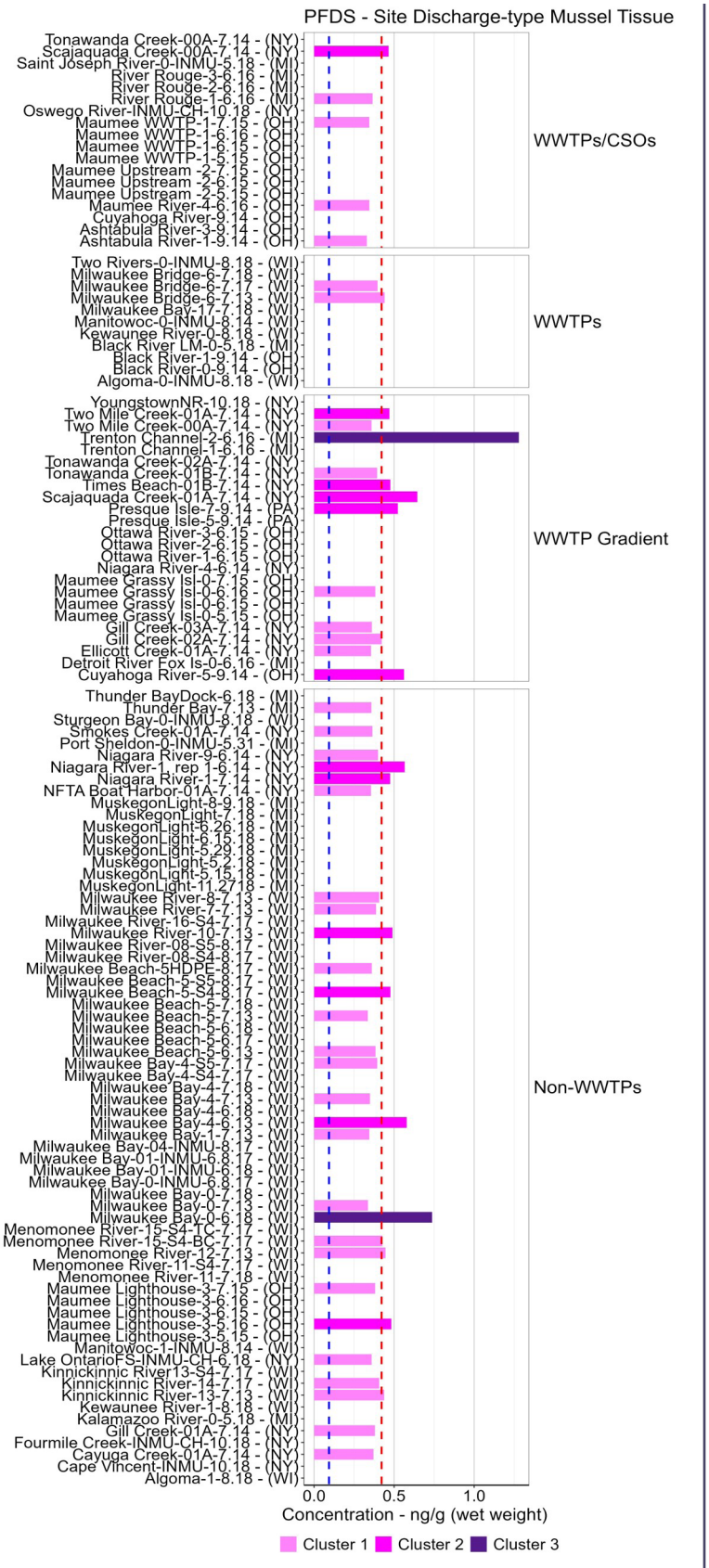

Site discharge-type tissue bar chart: PFAS contaminant concentration results (ng/g wet weight) measured (> MDL) in dreissenid mussels during 2013-2018 sampling event. Clusters 1-3 represents sites with low, medium and high PFAS concentrations. Blue dashed line represents concentration method detection limit (MDL). Reference line (red dashed line) represent mean reference sites concentration.

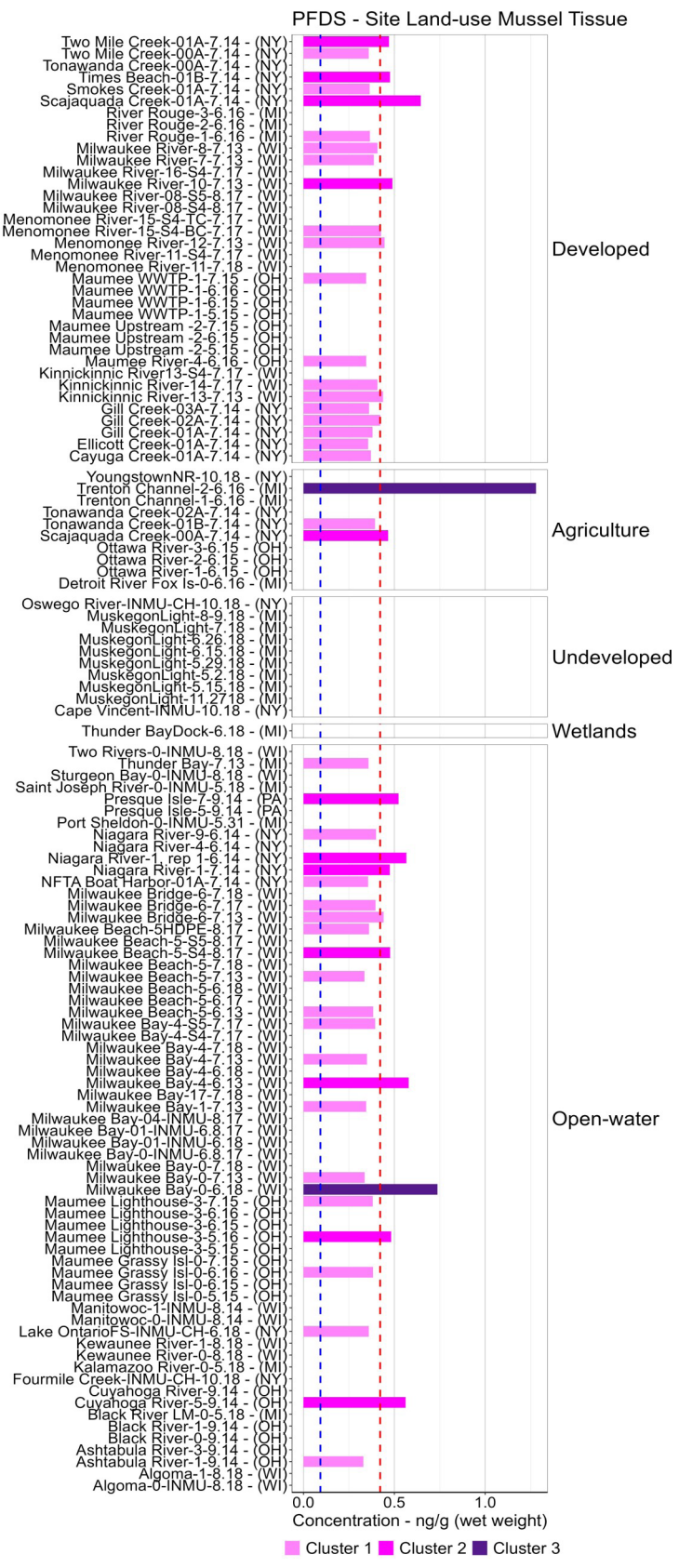

Site land-use tissue bar chart: PFAS contaminant concentration results (ng/g wet weight) measured (> MDL) in dreissenid mussels during 2013-2018 sampling event. Clusters 1-3 represents sites with low, medium and high PFAS concentrations. Blue dashed line represents concentration method detection limit (MDL). Reference line (red dashed line) represent mean reference sites concentration.

PFHpA (Perfluoro-n-heptanoic acid)

PFHpA: (Perfluoro-n-heptanoic acid) Summary

General Observations/Findings:

- PFHpA: (Perfluoro-n-heptanoic acid) was detected (> MDL) in dreissenid mussels at 11 sites (DF: detection frequency of 10%).
- PFHpA was detected (> MDL) in mussel tissue at concentrations ranging from 0.151 - 0.261ng/g wet weight during the 2013-2018 sampling event.
  - Minimum concentration (0.151 ng/g wet weight) detected at site Milwaukee Bay-0-7.13 (LMMB-0-7.13).
  - Maximum concentration (0.261 ng/g wet weight) detected at site River Rouge-2-6.16 (DRRR-2-6.16).

Basin-wide Highlights

- Highest PFHpA mean concentrations (0.261 ng/g wet weight) measured in mussels from Detroit River.
- Basin-wide, PFHpA mean concentrations measured in mussel decreased in order from Detroit River (0.261 ng/g wet weight) > reference sites (0.208 ng/g wet weight) > Lake Michigan (0.189 ng/g wet weight).

Inshore/offshore Highlights

- The highest PFHpA mean concentration (0.223 ng/g wet weight) was found in mussel tissue from designated river sites.
- PFHpA mean concentrations measured in mussel tissue from inshore (tributary, river, and harbor) and offshore sampling locations decreased in order from river (0.223 ng/g wet weight) > offshore (0.208 ng/g wet weight) > harbor (0.177 ng/g wet weight) sites.

Major Discharge-types Highlights

- The highest PFHpA mean concentration (0.261 ng/g wet weight) measured was found in mussel tissue from WWTPs/CSO sites.
- PFHpA mean concentrations measured in mussel tissue from sampled major discharge-types locations decreased in order from WWTPs/CSOs (0.261 ng/g wet weight) > non-WWTPs (0.193 ng/g wet weight) sites.

Land-use Highlights

- The highest PFHpA mean concentration (0.223 ng/g wet weight) was found in mussel tissue from developed dominant sites.
- PFHpA mean concentration measured in mussel tissue from designated site land-use categories trended downward from Developed (0.223 ng/g wet weight) > Open-water (0.186 ng/g wet weight) sites.

PFAS Characterization & Result Highlights

PFHpA: (Perfluoro-n-heptanoic acid)

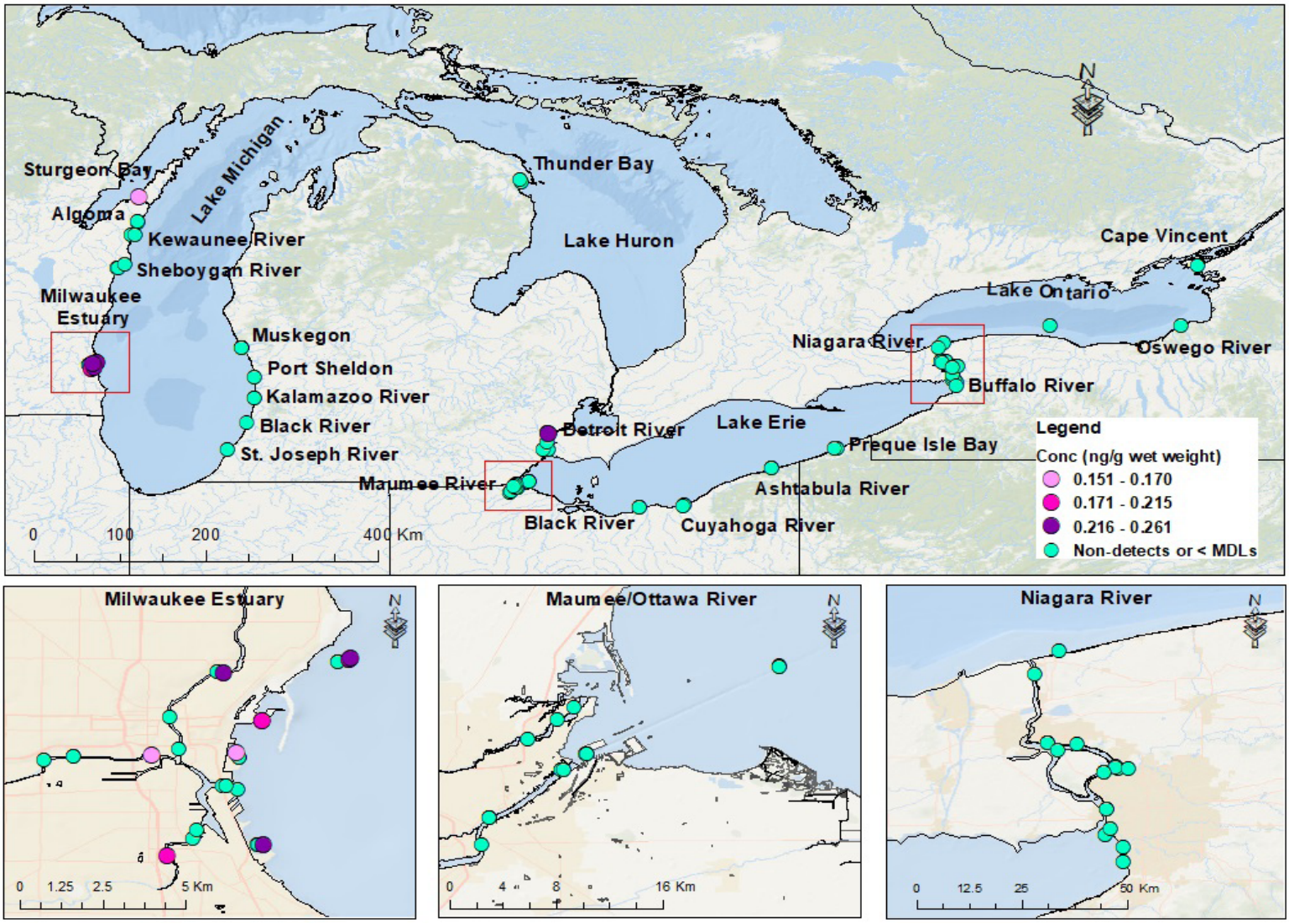

Fig.37. Map of Great Lakes Mussel Watch PFAS sampling locations, highlighting PFAS compounds detected (> MDL) in mussel tissue during the 2013-2018 sampling event.

Concentration table: Summary of basin-wide PFAS concentrations (ng/g wet weight) measured (> MDL) in dreissenid mussel tissue from Lakes Michigan, Huron, Erie, Ontario, and Detroit and Niagara River connecting channels (*) sampling locations between 2013 - 2018.

			Min	Mean	Max
Category	(n)	Stdev	ng/g (ww)	ng/g (ww)	ng/g (ww)
Lake Michigan	8	0.037	0.151	0.189	0.244
Lake Huron	0	0	0	0	0
Detroit River (*)	1	0	0.261	0.261	0.261
Lake Erie	0	0	0	0	0
Niagara River (*)	0	0	0	0	0
Lake Ontario	0	0	0	0	0
Reference Sites	2	0.029	0.188	0.208	0.228

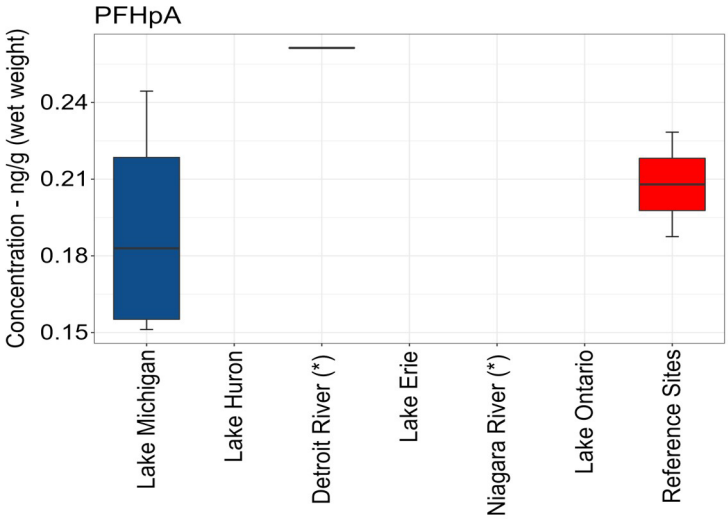

Boxplot: PFAS concentrations (ng/g wet weight) measured in dreissenid mussel tissue basin-wide between 2013 - 2018. Reference sites provides perspective to the relative PFAS concentrations found in mussel tissue basin-wide.

PFAS Characterization & Result Highlights

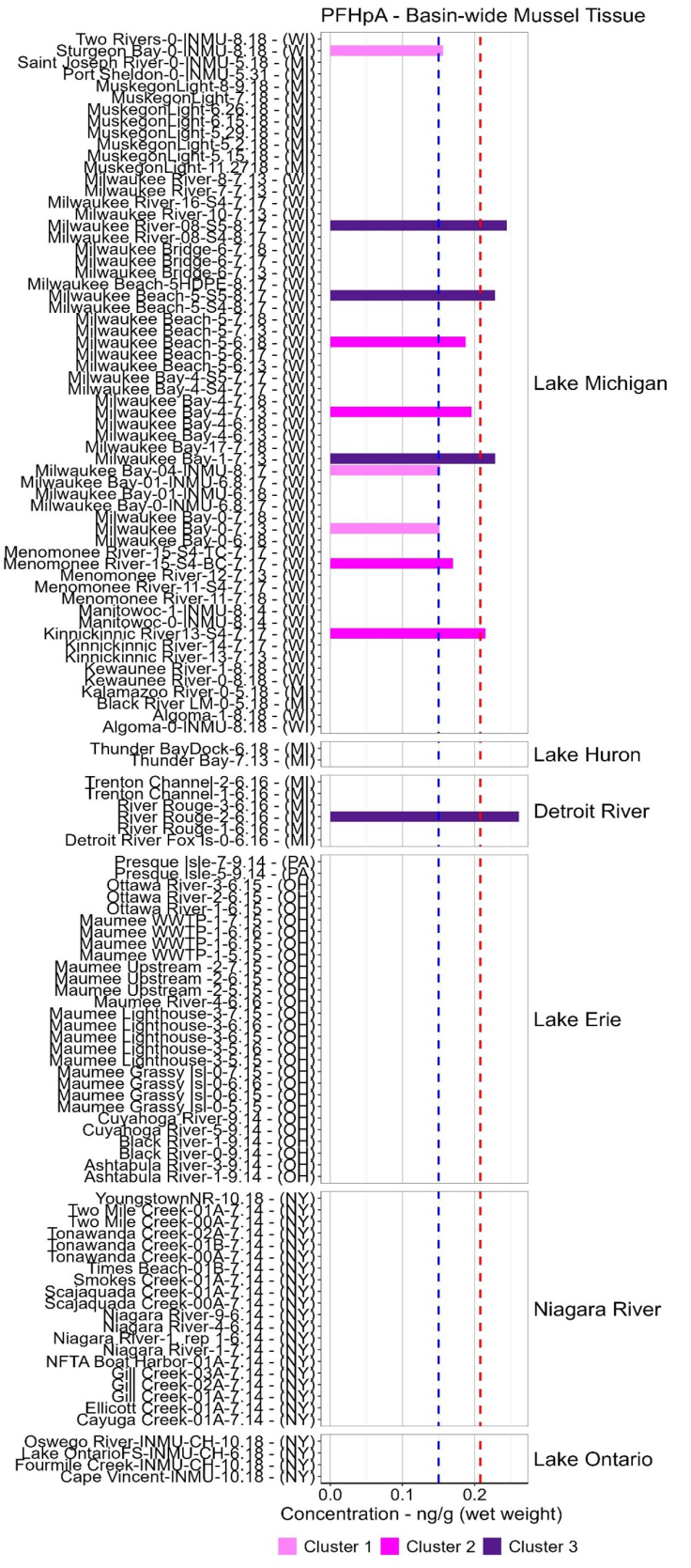

Basin-wide site tissue bar chart: PFAS contaminant concentration results (ng/g wet weight) measured (> MDL) in mussel tissue basin-wide during 2013-2018. Clusters 1-3 represents sites with low, medium and high PFAS concentrations. Blue dashed line represents concentration method detection limit (MDL). Reference line (red dashed line) represent mean reference sites concentration.

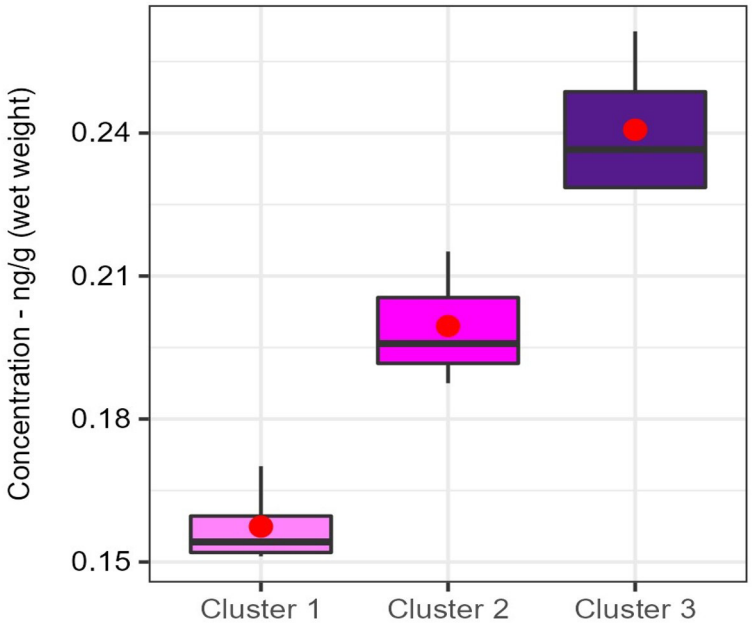

Boxplot: PFAS concentration results detected in dreissenid mussels during 2013-2018. Mean values are plotted as red points. Clusters 1-3 represent low, medium and high PFAS concentrations, respectively.

Total PFHpA Concentration (ng/g wet weight)		
	Low	0.151 - 0.170
	Medium	0.171 - 0.215
	High	0.216 - 0.261

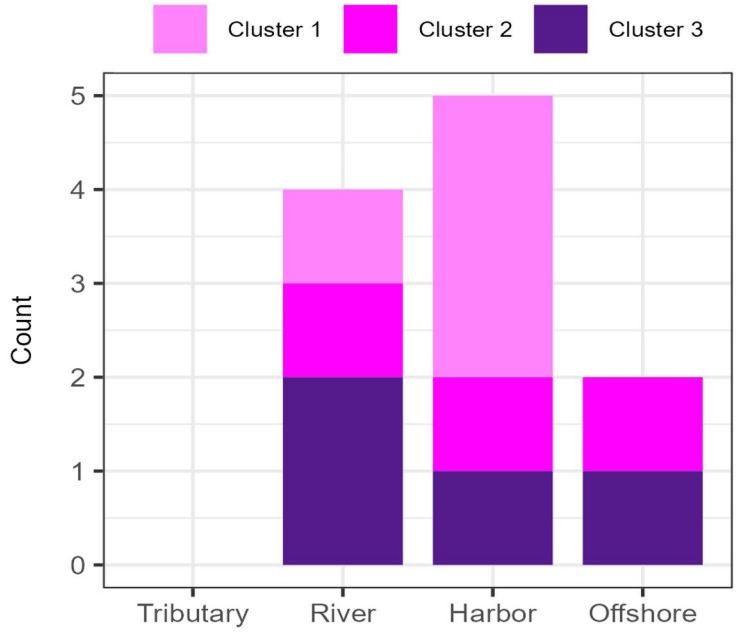

Tissue inshore - offshore bar chart: Measured PFAS composition profile detected in dreissenid mussels across inshore (tributary, river, harbor) and offshore (e.g., open-lake) Great Lakes complexes. Counts (y-axis) represents number of PFAS samples found in mussel tissue across inshore and offshore sampling locations during the 2013-2018 period.

PFAS Characterization & Result Highlights

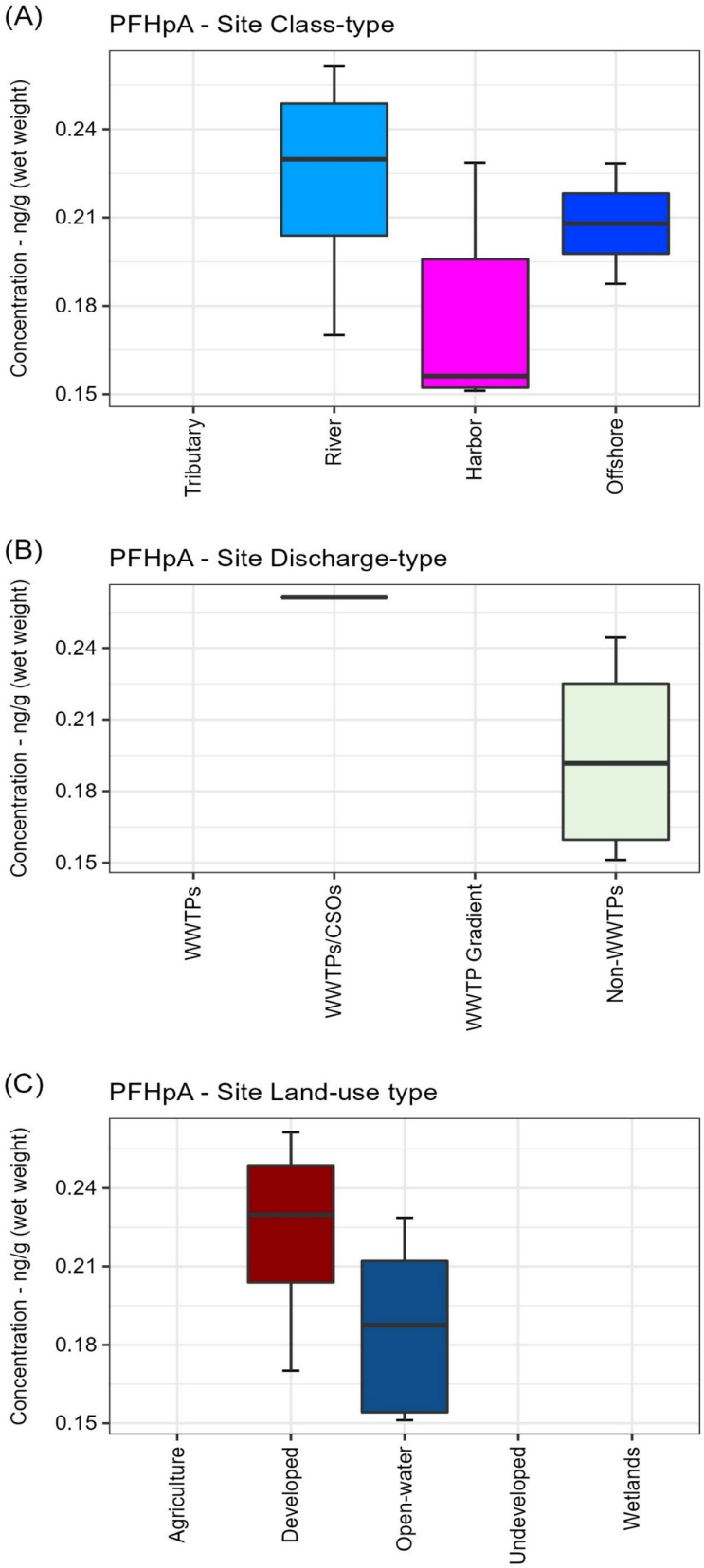

Boxplots: PFAS concentrations measured (> MDL) in mussel tissue at A) inshore and offshore sampling locations, B) designated MWP site discharge-types, and C) predominant site land-use categories/ gradients. Only compounds found at ten or more sites were included in PFAS concentration summary. Plots provide perspective on the most commonly found PFAS in mussel tissue, and their relative concentrations across various Great Lakes environmental matrices.

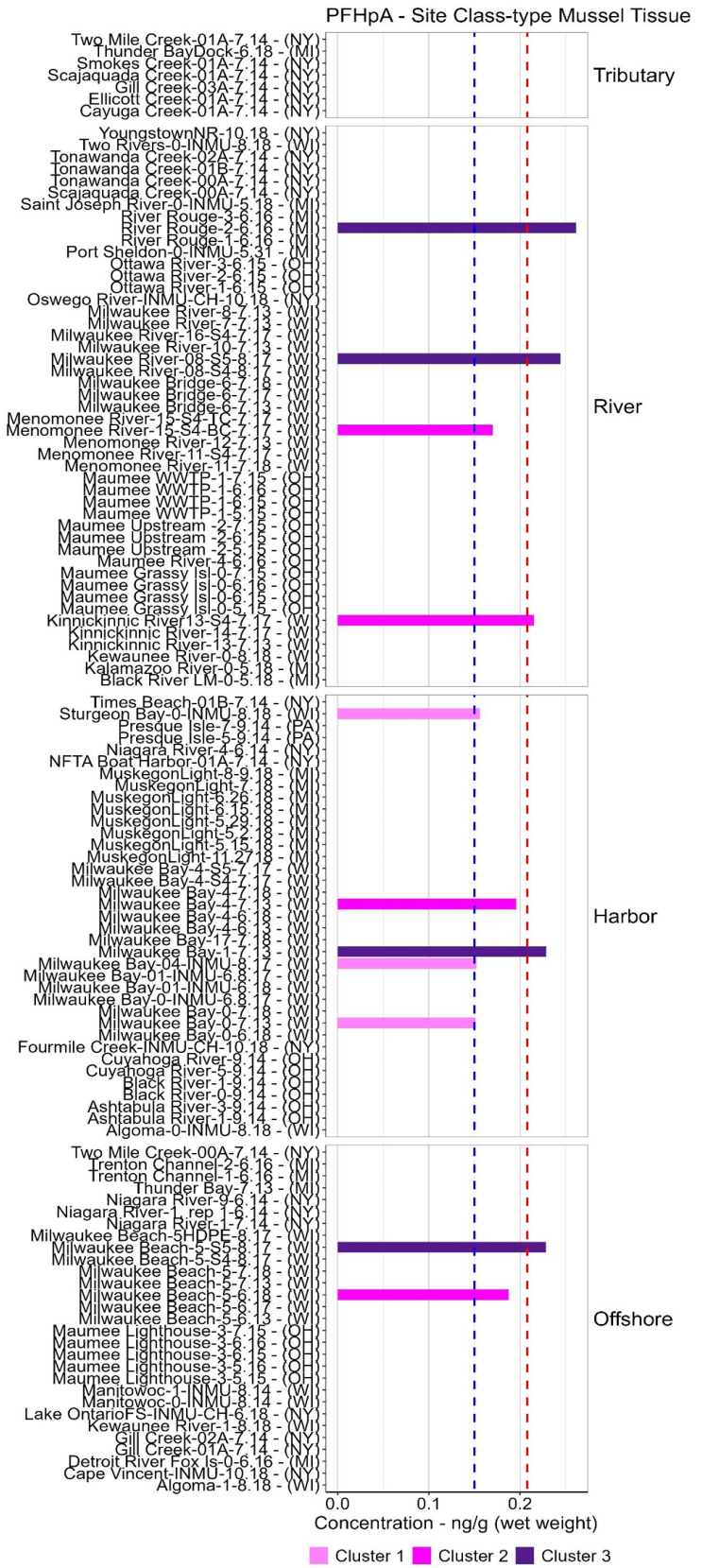

Site class-type tissue bar chart: PFAS contaminant concentration results (ng/g wet weight) measured (> MDL) in dreissenid mussels during 2013-2018 sampling event. Clusters 1-3 represents sites with low, medium and high PFAS concentrations. Blue dashed line represents concentration method detection limit (MDL). Reference line (red dashed line) represent mean reference sites concentration.

PFAS Characterization & Result Highlights

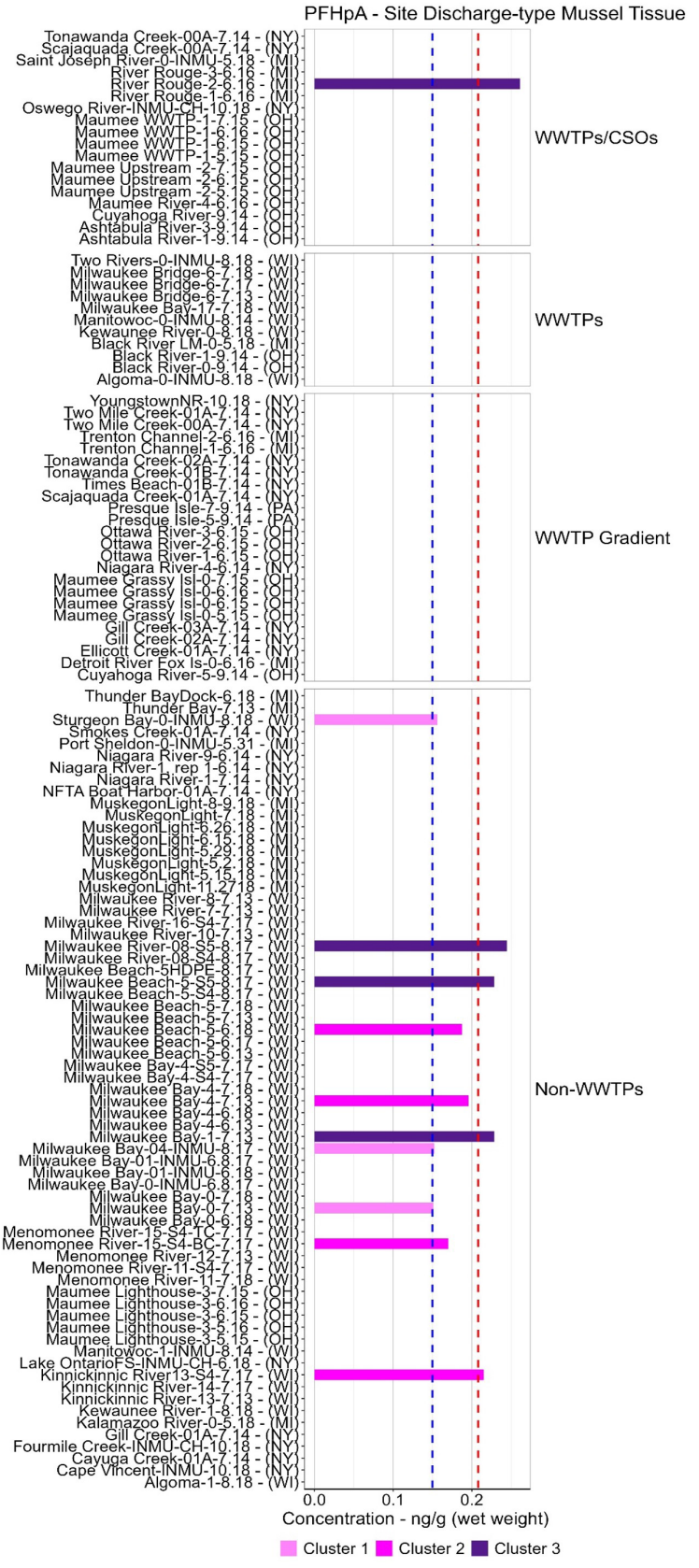

Site discharge-type tissue bar chart: PFAS contaminant concentration results (ng/g wet weight) measured (> MDL) in dreissenid mussels during 2013-2018 sampling event. Clusters 1-3 represents sites with low, medium and high PFAS concentrations. Blue dashed line represents concentration method detection limit (MDL). Reference line (red dashed line) represent mean reference sites concentration.

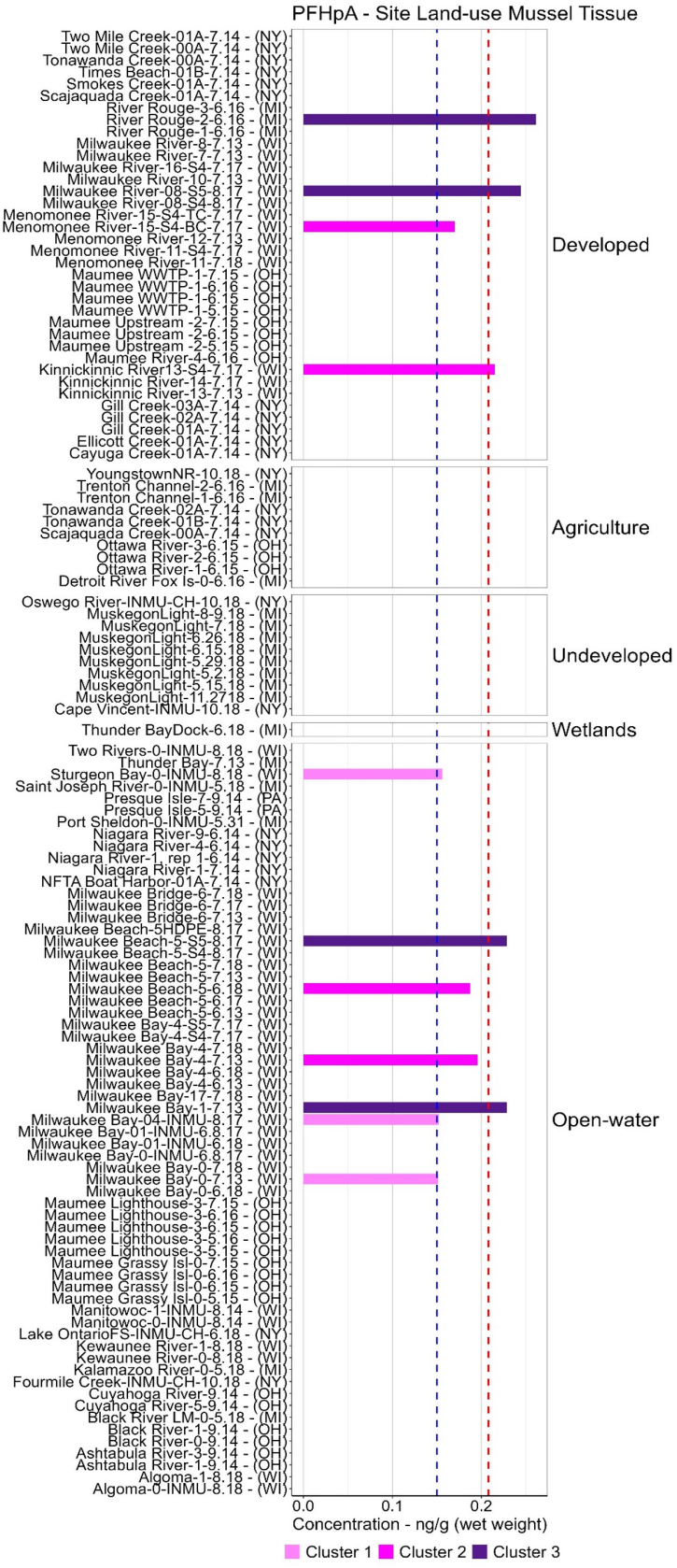

Site land-use tissue bar chart: PFAS contaminant concentration results (ng/g wet weight) measured (> MDL) in dreissenid mussels during 2013-2018 sampling event. Clusters 1-3 represents sites with low, medium and high PFAS concentrations. Blue dashed line represents concentration method detection limit (MDL). Reference line (red dashed line) represent mean reference sites concentration.

PFNS (Perfluoro-1-nonanesulfonic acid)

PFNS: (Perfluoro-1-nonanesulfonic acid) Summary

General Observations/Findings:

- PFNS: (Perfluoro-1-nonanesulfonic acid) was detected (> MDL) in dreissenid mussels at 16 sites (DF: detection frequency of 15%).
- PFNS was detected (> MDL) in mussel tissue at concentrations ranging from 0.098 - 0.529 ng/g wet weight during the 2013-2018 sampling event.
  - Minimum concentration (0.098 ng/g wet weight) detected at site Smokes Creek-01A-7.14 (NRSM-01A-7.14).
  - Maximum concentration (0.529 ng/g wet weight) detected at site Milwaukee Bay-4-7.13 (LMMB-4-7.13).

Basin-wide Highlights

- Highest PFNS mean concentration (0.317 ng/g wet weight) measured in mussels Detroit River, MI.
- Basin-wide, PFNS mean concentration measured in mussel decreased in order from Detroit River (0.4 ng/g wet weight) > Lake Michigan (0.317 ng/g wet weight) > Reference Sites (0.273 ng/g wet weight) > Niagara River (0.149 ng/g wet weight) > Lake Erie (0.117 ng/g wet weight).

Inshore/offshore Highlights

- The highest PFNS mean concentration (0.319 ng/g wet weight) was found in mussel tissue from designated harbor sites.
- PFNS mean concentrations measured in mussel tissue from inshore (tributary, river, and harbor) and offshore sampling locations decreased in order from harbor (0.319 ng/g wet weight) > river (0.215 ng/g wet weight) > offshore (0.181 ng/g wet weight) > tributary (0.123 ng/g wet weight) sites.

Major Discharge-types Highlights

- The highest PFNS mean concentration (0.277 ng/g wet weight) measured was found in mussel tissue from WWTPs/CSO sites.
- PFNS mean concentrations measured in mussel tissue from sampled major discharge-types locations decreased in order from WWTPs/CSOs (0.277 ng/g wet weight) > non-WWTPs (0.261 ng/g wet weight) > WWTP discharge zones/Gradient (0.155 ng/g wet weight) sites.

Land-use Highlights

- The highest PFNS mean concentration (0.31 ng/g wet weight) was found in mussel tissue from open-water dominant site.
- PFNS mean concentration measured in mussel tissue from designated site land-use categories trended downward from Open-water (0.31 ng/g wet weight) > Developed (0.187 ng/g wet weight) > Agriculture (0.17 ng/g wet weight) sites.

PFAS Characterization & Result Highlights

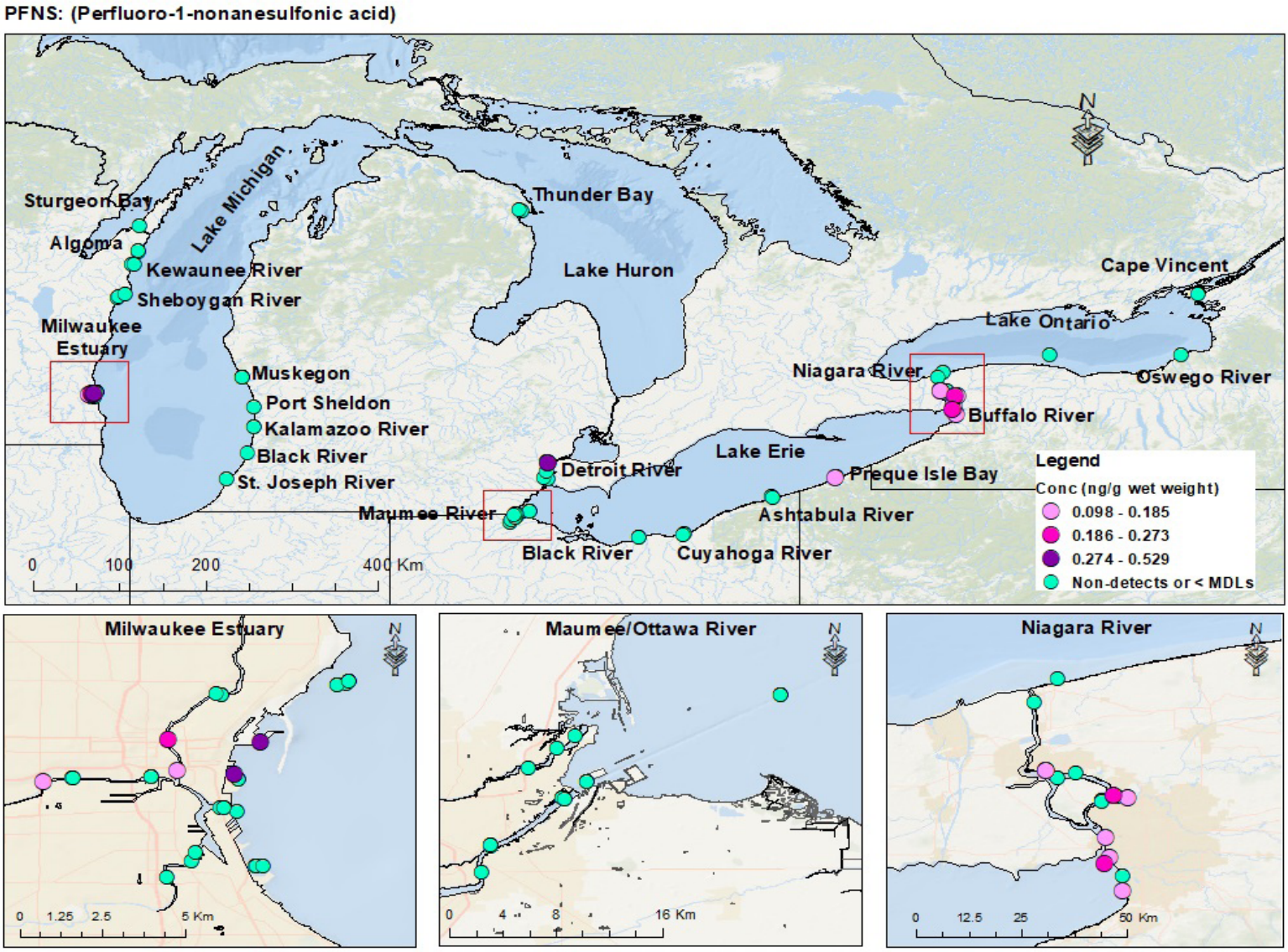

Fig.38. Map of Great Lakes Mussel Watch PFAS sampling locations, highlighting PFAS compounds detected (> MDL) in mussel tissue during the 2013-2018 sampling event.

Concentration table: Summary of basin-wide PFAS concentrations (ng/g wet weight) measured (> MDL) in dreissenid mussel tissue from Lakes Michigan, Huron, Erie, Ontario, and Detroit and Niagara River connecting channels (*) sampling locations between 2013 - 2018.

			Min	Mean	Max
Category	(n)	Stdev	ng/g (ww)	ng/g (ww)	ng/g (ww)
Lake Michigan	5	0.2	0.1	0.317	0.529
Lake Huron	0	0	0	0	0
Detroit River (*)	1	0	0.4	0.4	0.4
Lake Erie	1	0	0.117	0.117	0.117
Niagara River (*)	8	0.044	0.098	0.149	0.234
Lake Ontario	0	0	0	0	0
Reference Sites	1	0	0.273	0.273	0.273

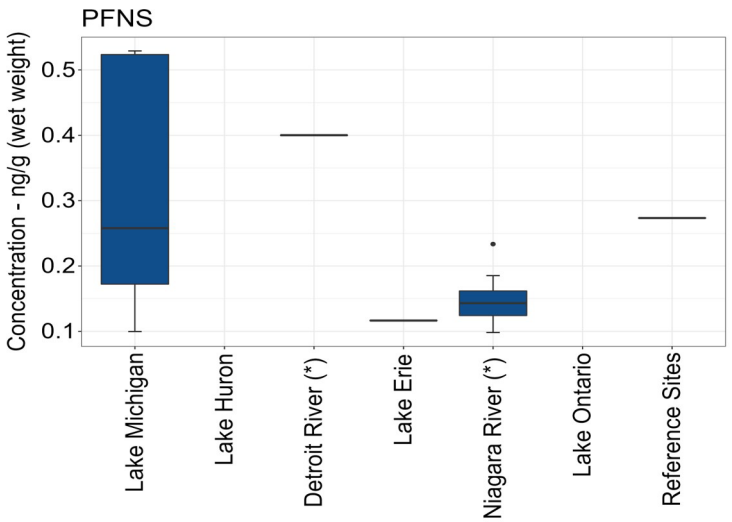

Boxplot: PFAS concentrations (ng/g wet weight) measured in dreissenid mussel tissue basin-wide between 2013 - 2018. Reference sites provides perspective to the relative PFAS concentrations found in mussel tissue basin-wide.

PFAS Characterization & Result Highlights

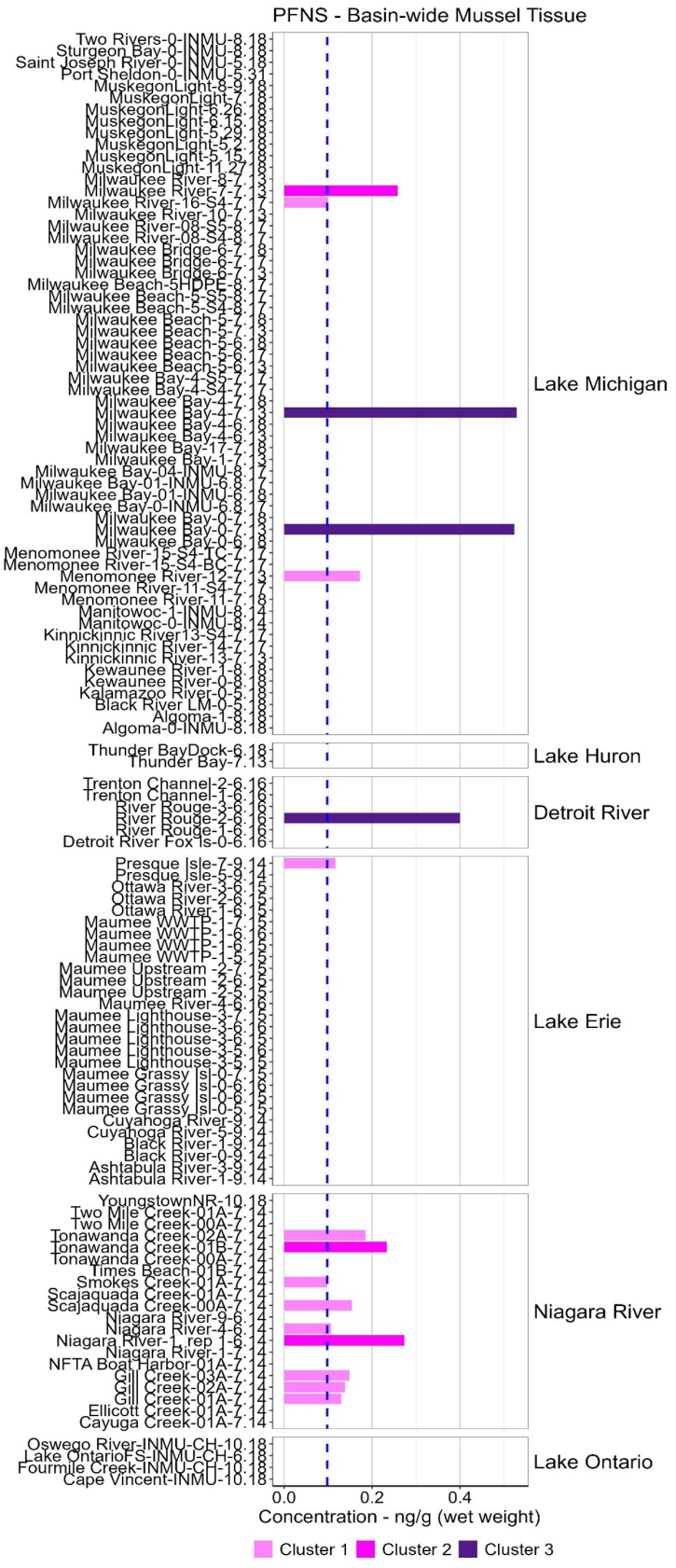

Basin-wide site tissue bar chart: PFAS contaminant concentration results (ng/g wet weight) measured (> MDL) in mussel tissue basin-wide during 2013-2018. Clusters 1-3 represents sites with low, medium and high PFAS concentrations. Blue dashed line represents concentration method detection limit (MDL). Reference line (red dashed line) represent mean reference sites concentration.

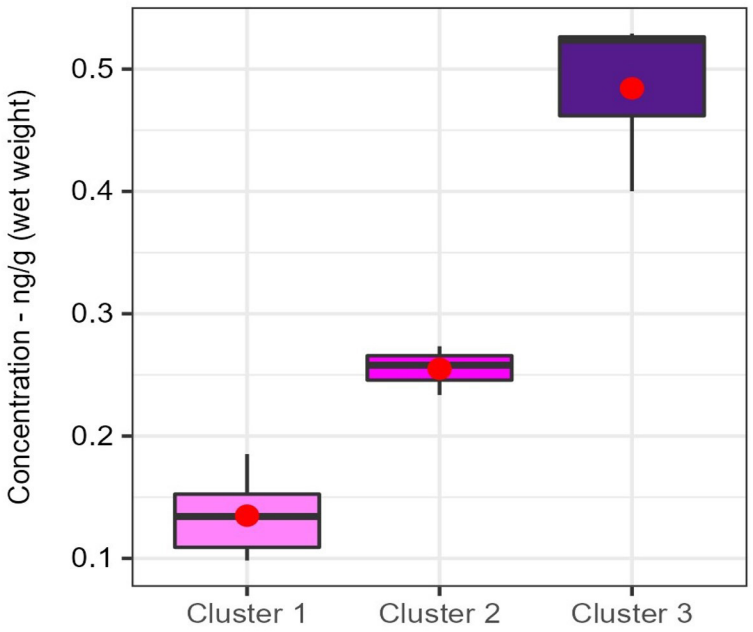

Boxplot: PFAS concentration results detected in dreissenid mussels during 2013-2018. Mean values are plotted as red points. Clusters 1-3 represent low, medium and high PFAS concentrations, respectively.

Total PFNS Concentration (ng/g wet weight)		
	Low	0.098 - 0.185
	Medium	0.186 - 0.273
	High	0.274 - 0.529

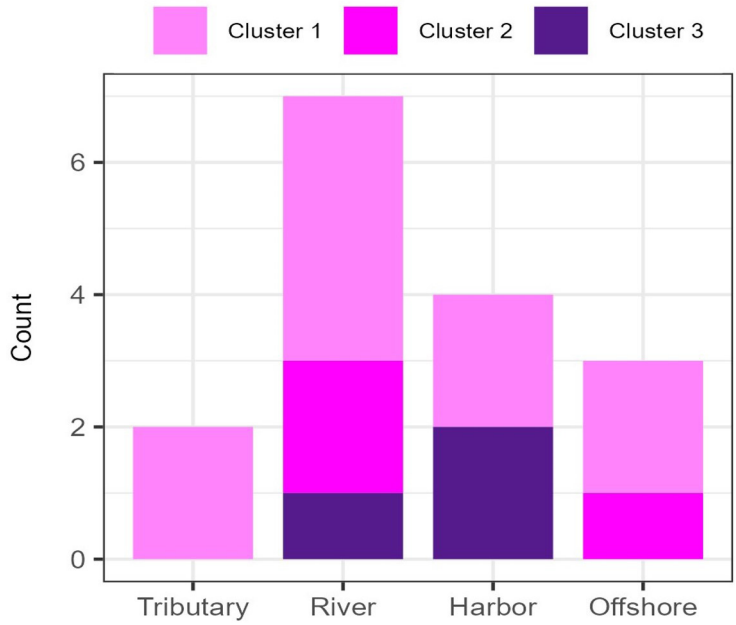

Tissue inshore - offshore bar chart: Measured PFAS composition profile detected in dreissenid mussels across inshore (tributary, river, harbor) and offshore (e.g., open-lake) Great Lakes complexes. Counts (y-axis) represents number of PFAS samples found in mussel tissue across inshore and offshore sampling locations during the 2013-2018 period.

PFAS Characterization & Result Highlights

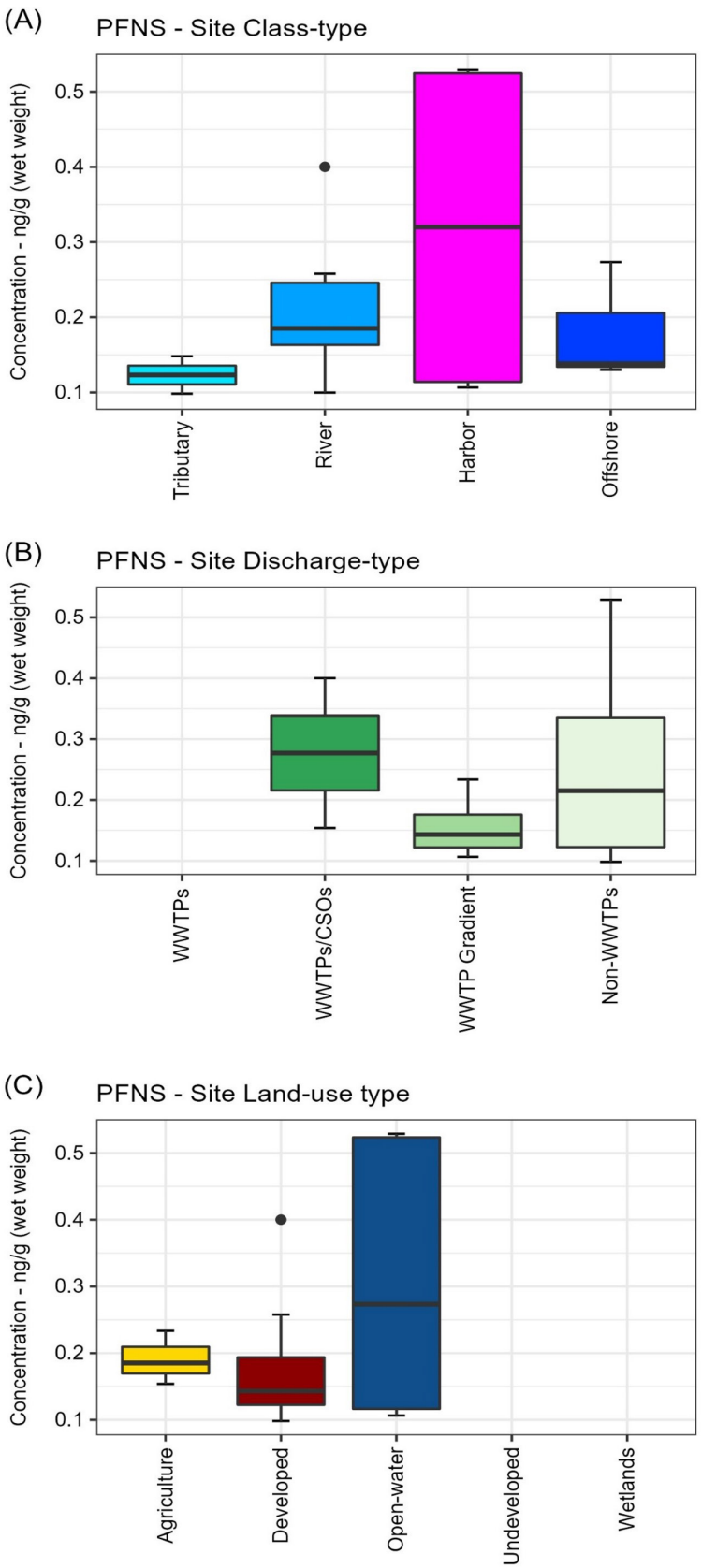

Boxplots: PFAS concentrations measured (> MDL) in mussel tissue at A) inshore and offshore sampling locations, B) designated MWP site discharge-types, and C) predominant site land-use categories/ gradients. Only compounds found at ten or more sites were included in PFAS concentration summary. Plots provide perspective on the most commonly found PFAS in mussel tissue, and their relative concentrations across various Great Lakes environmental matrices.

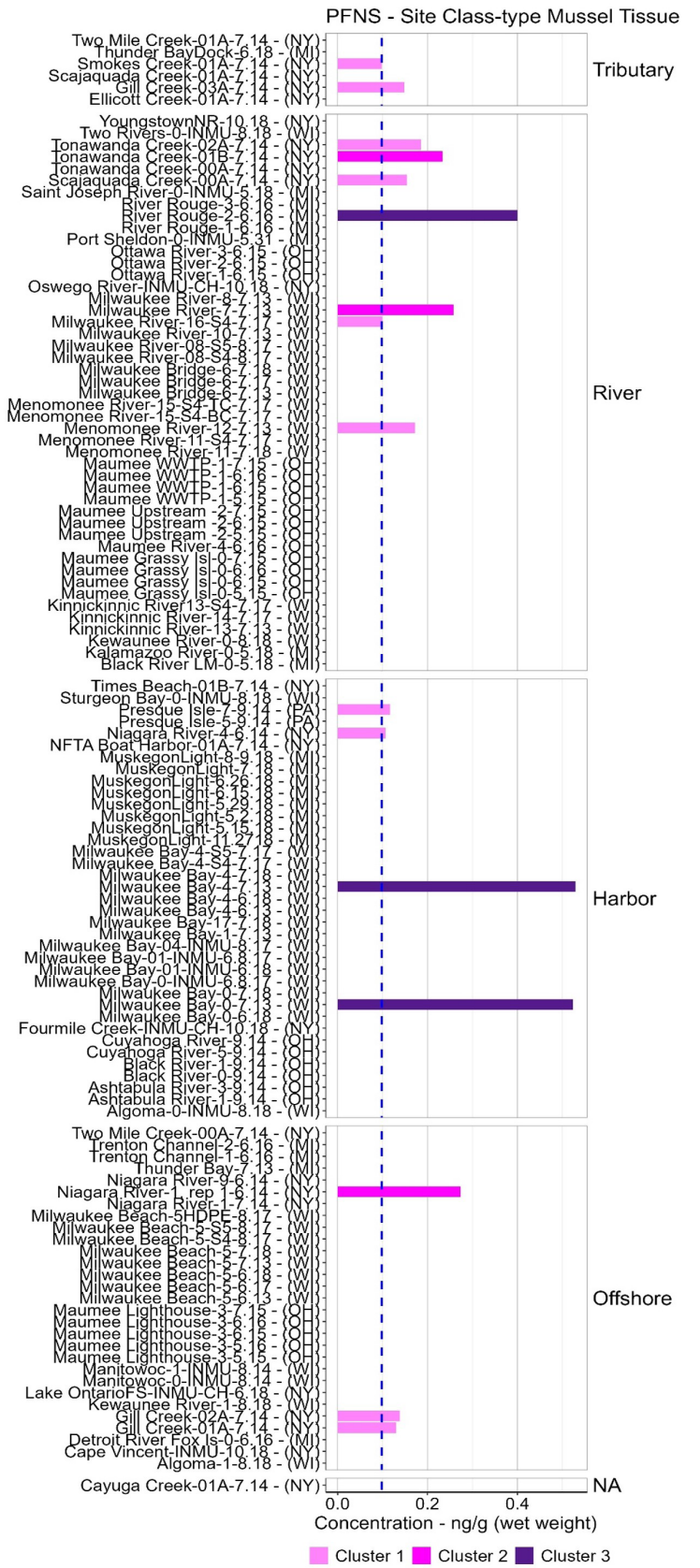

Site class-type tissue bar chart: PFAS contaminant concentration results (ng/g wet weight) measured (> MDL) in dreissenid mussels during 2013-2018 sampling event. Clusters 1-3 represents sites with low, medium and high PFAS concentrations. Blue dashed line represents concentration method detection limit (MDL). Reference line (red dashed line) represent mean reference sites concentration.

PFAS Characterization & Result Highlights

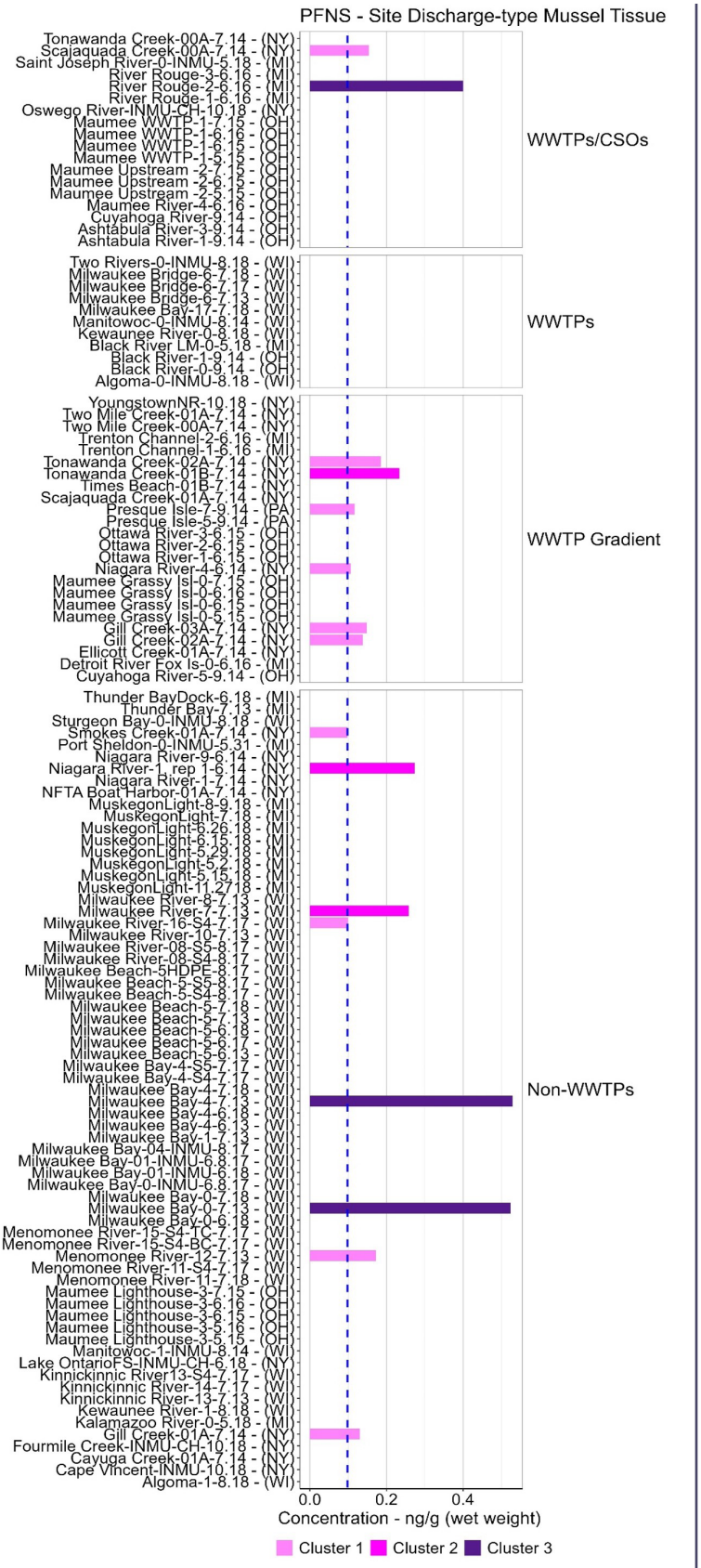

Site discharge-type tissue bar chart: PFAS contaminant concentration results (ng/g wet weight) measured (> MDL) in dreissenid mussels during 2013-2018 sampling event. Clusters 1-3 represents sites with low, medium and high PFAS concentrations. Blue dashed line represents concentration method detection limit (MDL). Reference line (red dashed line) represent mean reference sites concentration.

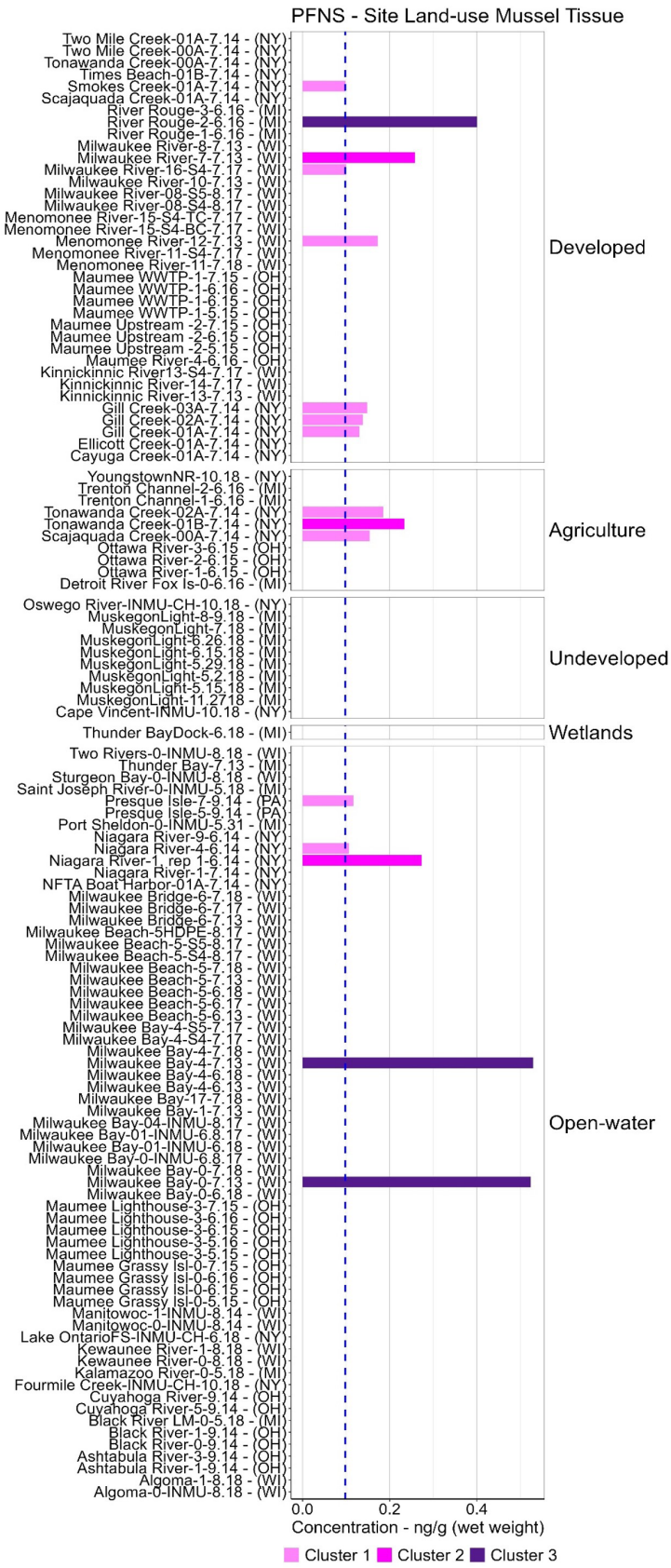

Site land-use tissue bar chart: PFAS contaminant concentration results (ng/g wet weight) measured (> MDL) in dreissenid mussels during 2013-2018 sampling event. Clusters 1-3 represents sites with low, medium and high PFAS concentrations. Blue dashed line represents concentration method detection limit (MDL). Reference line (red dashed line) represent mean reference sites concentration.

PFOA (Perfluoro-n-octanoic acid)

PFOA: (Perfluoro-n-octanoic acid) Summary

General Observations/Findings:

- PFOA: (Perfluoro-n-octanoic acid) was detected (> MDL) in dreissenid mussels at 9 sites (DF: detection frequency of 8%).
- PFOA was detected (> MDL) in mussel tissue at concentrations ranging from 0.103 - 0.208 ng/g wet weight during the 2013-2018 sampling event.
  - Minimum concentration (0.103 ng/g wet weight) detected at site Milwaukee Beach-5-6.18 (LMMB-5-6.18).
  - Maximum concentration (0.208 ng/g wet weight) detected at site Maumee Upstream -2-7.15 (LEMR-2-7.15).

Basin-wide Highlights

- Highest PFOA mean concentrations (0.196 ng/g wet weight) measured in mussels from Detroit River.
- Basin-wide, PFOA mean concentrations measured in mussel decreased in order from Detroit River (0.196 ng/g wet weight) > Lake Michigan (0.168 ng/g wet weight) > Lake Erie (0.162 ng/g wet weight) > Reference Sites (0.135 ng/g wet weight) > Lake Ontario (0.104 ng/g wet weight).

Inshore/offshore Highlights

- The highest PFOA mean concentration (0.197 ng/g wet weight) was found in mussel tissue from harbor sites.
- PFOA mean concentrations measured in mussel tissue from inshore (tributary, river, and harbor) and offshore sampling locations decreased in order from harbor (0.197 ng/g wet weight) > river (0.156 ng/g wet weight) > offshore (0.141 ng/g wet weight) sites.

Major Discharge-types Highlights

- The highest PFOA mean concentration (0.184 ng/g wet weight) measured was found in mussel tissue from WWTPs/CSO sites.
- PFOA mean concentrations measured in mussel tissue from sampled major discharge-type locations decreased in order from sites proximate to WWTPs/CSOs (0.184 ng/g wet weight) > WWTP Gradient (0.157 ng/g wet weight) > non-WWTP (0.141 ng/g wet weight) sites.

Land-use Highlights

- The highest PFOA mean concentration (0.196 ng/g wet weight) was found in mussel tissue from agriculture dominant site.
- PFOA mean concentration measured in mussel tissue from designated site land-use categories trended downward from Agriculture (0.196 ng/g wet weight) > Developed (0.169 ng/g wet weight) > Open-water (0.137 ng/g wet weight) sites.

PFAS Characterization & Result Highlights

PFOA: (Perfluoro-n-octanoic acid)

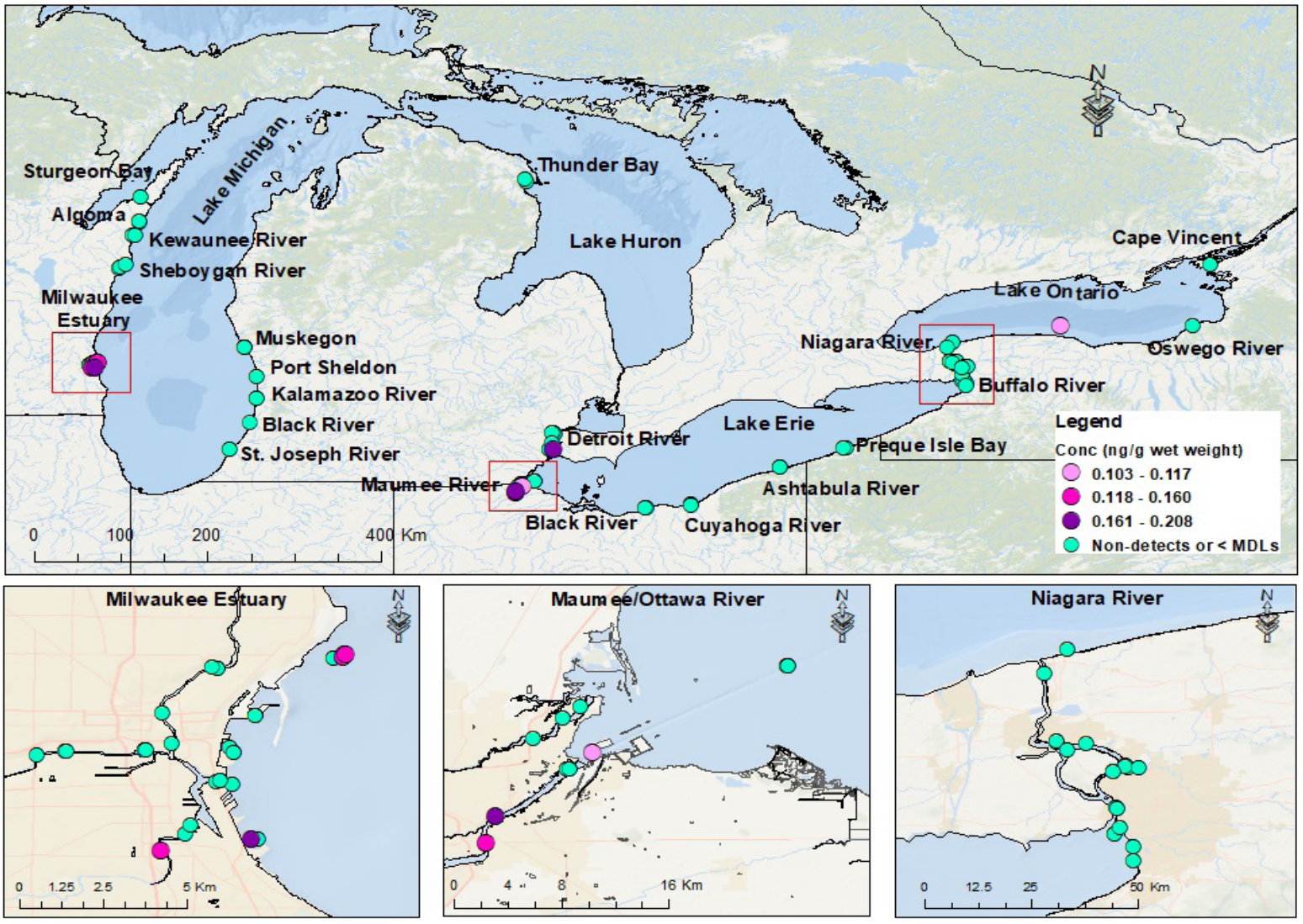

Fig.39. Map of Great Lakes Mussel Watch PFAS sampling locations, highlighting PFAS compounds detected (> MDL) in mussel tissue during the 2013-2018 sampling event.

Concentration table: Summary of basin-wide PFAS concentrations (ng/g wet weight) measured (> MDL) in dreissenid mussel tissue from Lakes Michigan, Huron, Erie, Ontario, and Detroit and Niagara River connecting channels (*) sampling locations between 2013 - 2018.

			Min	Mean	Max
Category	(n)	Stdev	ng/g (ww)	ng/g (ww)	ng/g (ww)
Lake Michigan	2	0.041	0.139	0.168	0.197
Lake Huron	0	0	0	0	0
Detroit River (*)	1	0	0.196	0.196	0.196
Lake Erie	3	0.045	0.117	0.162	0.208
Niagara River (*)	0	0	0	0	0
Lake Ontario	1	0	0.104	0.104	0.104
Reference Sites	3	0.028	0.103	0.135	0.153

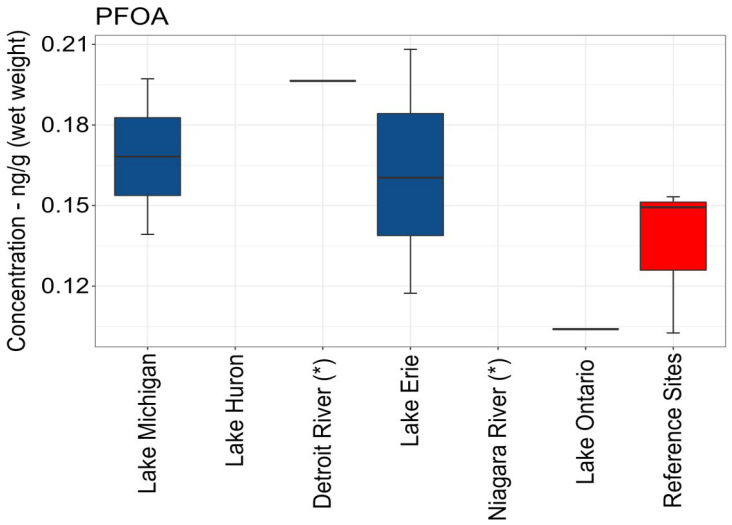

Boxplot: PFAS concentrations (ng/g wet weight) measured in dreissenid mussel tissue basin-wide between 2013 - 2018. Reference sites provides perspective to the relative PFAS concentrations found in mussel tissue basin-wide.

PFAS Characterization & Result Highlights

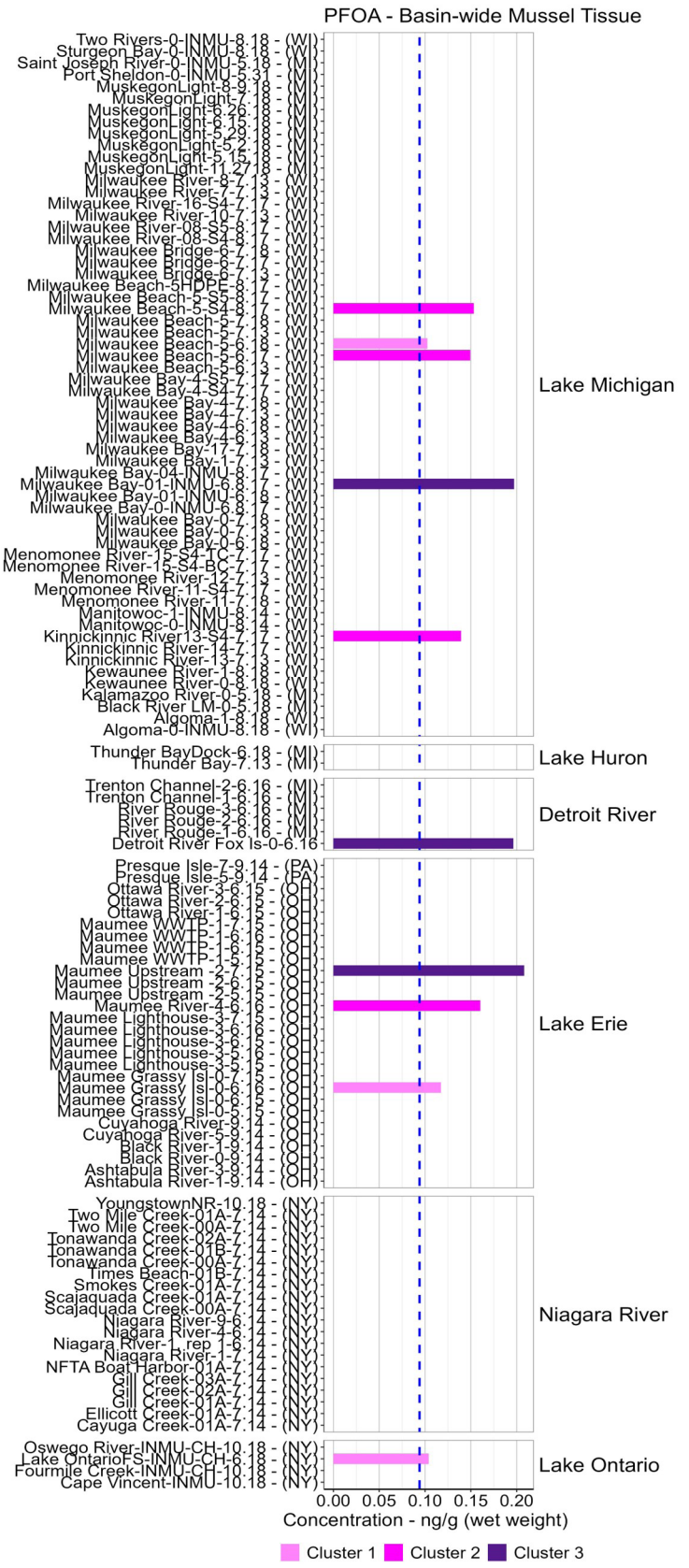

Basin-wide site tissue bar chart: PFAS contaminant concentration results (ng/g wet weight) measured (> MDL) in mussel tissue basin-wide during 2013-2018. Clusters 1-3 represents sites with low, medium and high PFAS concentrations. Blue dashed line represents concentration method detection limit (MDL). Reference line (red dashed line) represent mean reference sites concentration.

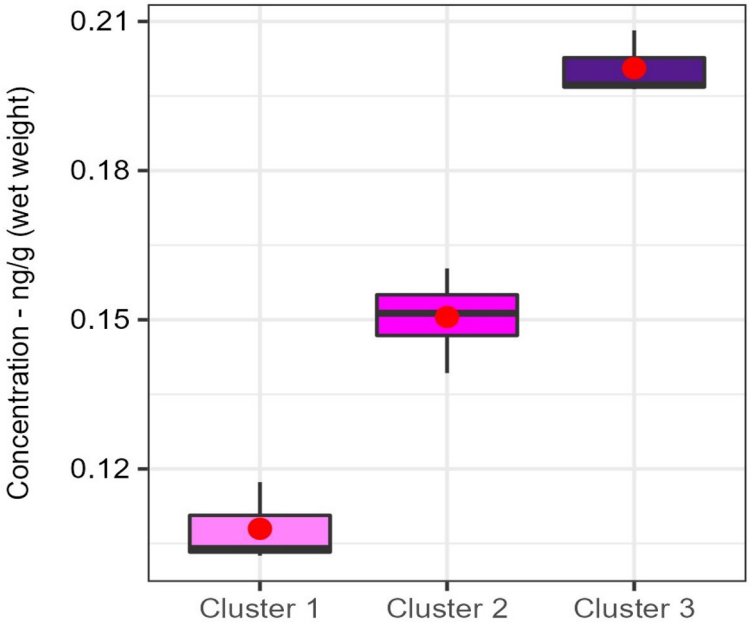

Boxplot: PFAS concentration results detected in dreissenid mussels during 2013-2018. Mean values are plotted as red points. Clusters 1-3 represent low, medium and high PFAS concentrations, respectively.

Total PFOA Concentration (ng/g wet weight)		
	Low	0.103 - 0.117
	Medium	0.118 - 0.160
	High	0.161 - 0.208

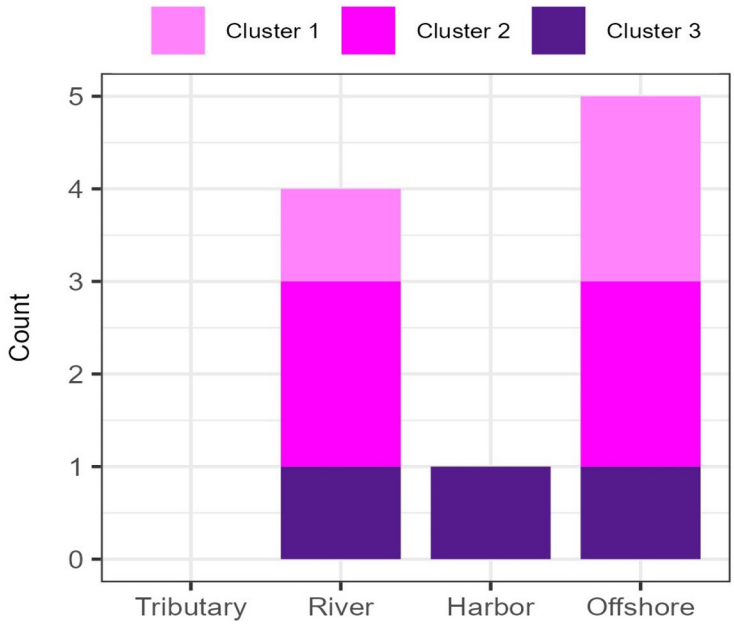

Tissue inshore - offshore bar chart: Measured PFAS composition profile detected in dreissenid mussels across inshore (tributary, river, harbor) and offshore (e.g., open-lake) Great Lakes complexes. Counts (y-axis) represents number of PFAS samples found in mussel tissue across inshore and offshore sampling locations during the 2013-2018 period.

PFAS Characterization & Result Highlights

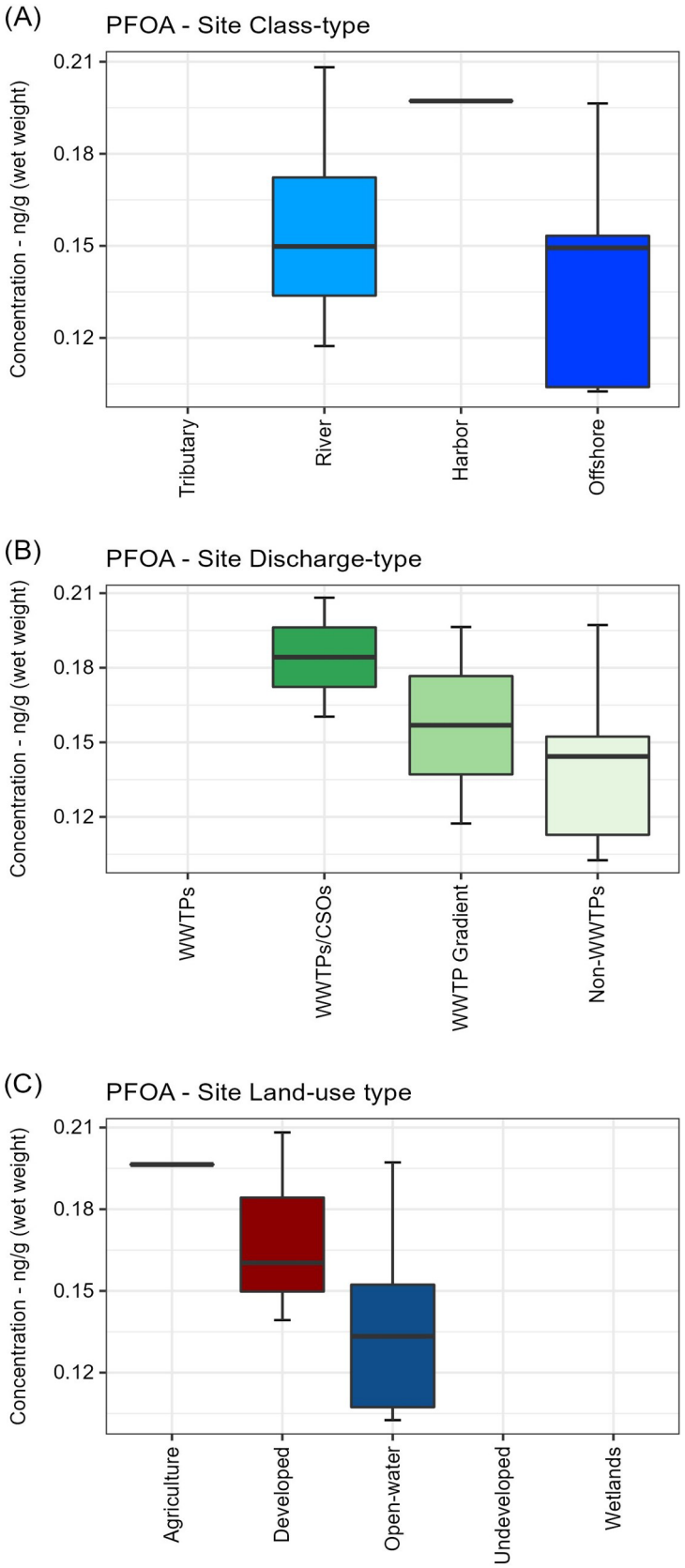

Boxplots: PFAS concentrations measured (> MDL) in mussel tissue at A) inshore and offshore sampling locations, B) designated MWP site discharge-types, and C) predominant site land-use categories/ gradients. Only compounds found at ten or more sites were included in PFAS concentration summary. Plots provide perspective on the most commonly found PFAS in mussel tissue, and their relative concentrations across various Great Lakes environmental matrices.

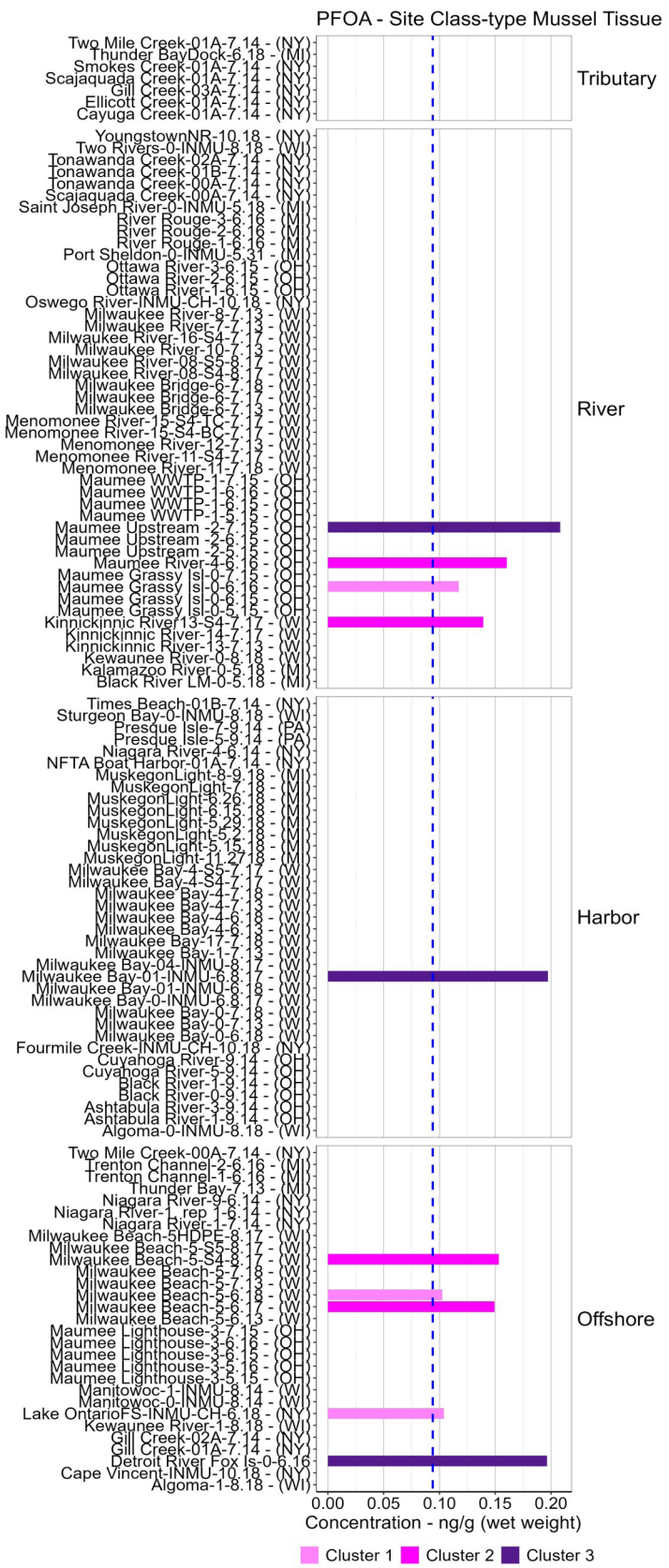

Site class-type tissue bar chart: PFAS contaminant concentration results (ng/g wet weight) measured (> MDL) in dreissenid mussels during 2013-2018 sampling event. Clusters 1-3 represents sites with low, medium and high PFAS concentrations. Blue dashed line represents concentration method detection limit (MDL). Reference line (red dashed line) represent mean reference sites concentration.

PFAS Characterization & Result Highlights

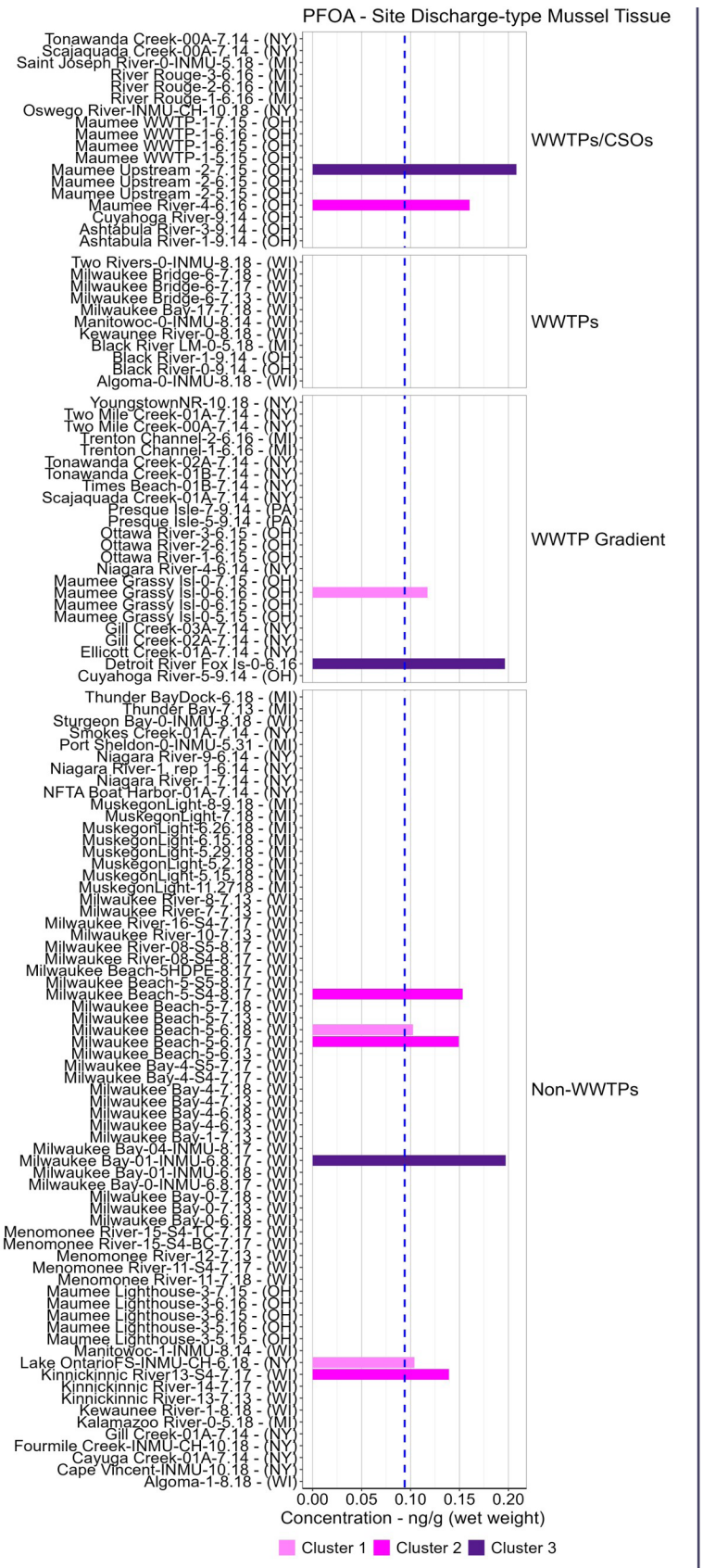

Site discharge-type tissue bar chart: PFAS contaminant concentration results (ng/g wet weight) measured (> MDL) in dreissenid mussels during 2013-2018 sampling event. Clusters 1-3 represents sites with low, medium and high PFAS concentrations. Blue dashed line represents concentration method detection limit (MDL). Reference line (red dashed line) represent mean reference sites concentration.

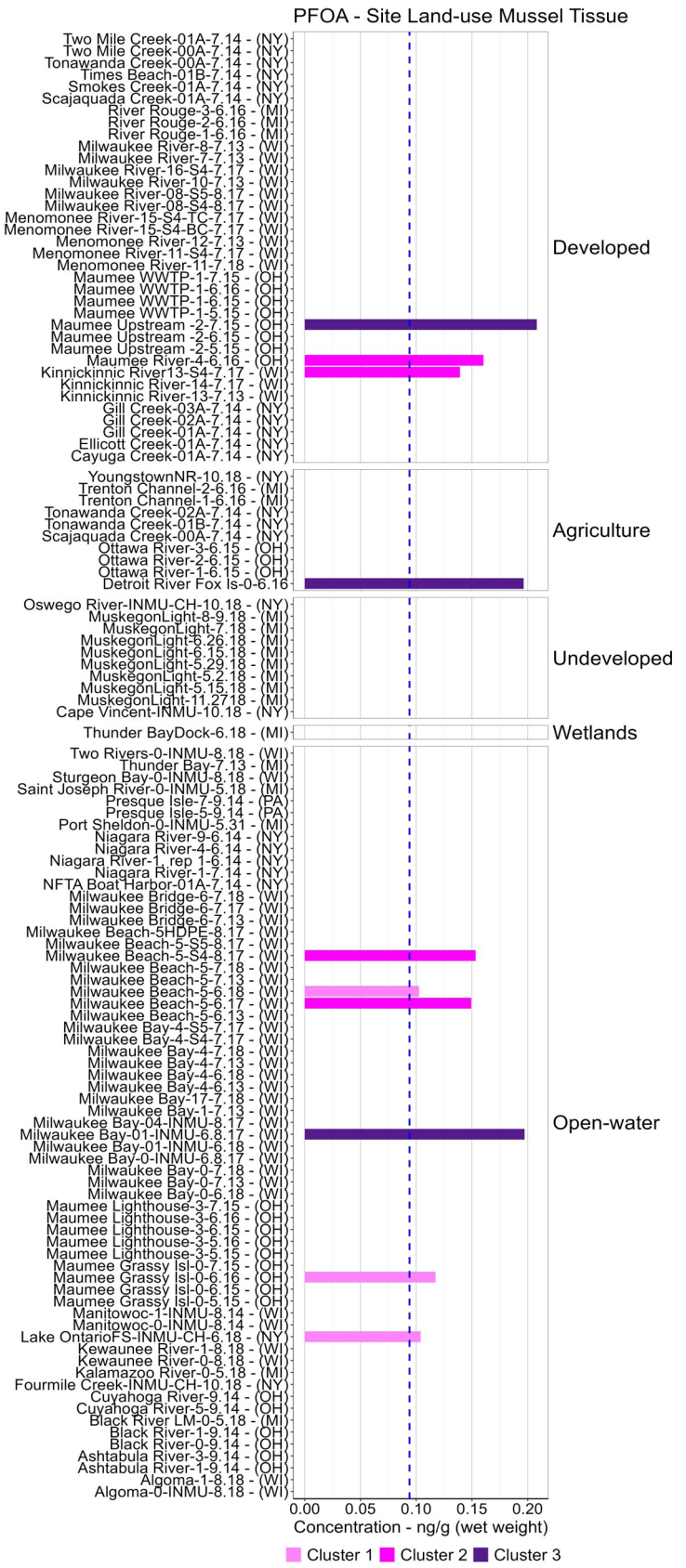

Site land-use tissue bar chart: PFAS contaminant concentration results (ng/g wet weight) measured (> MDL) in dreissenid mussels during 2013-2018 sampling event. Clusters 1-3 represents sites with low, medium and high PFAS concentrations. Blue dashed line represents concentration method detection limit (MDL). Reference line (red dashed line) represent mean reference sites concentration.

PFOS (Perfluoro-1-octanesulfonic acid)

PFOS: (Perfluoro-1-octanesulfonic acid) Summary

General Observations/Findings:

- PFOS: (Perfluoro-1-octanesulfonic acid) was detected (> MDL) in dreissenid mussels at 82 sites (DF: detection frequency of 76%).
- PFOS was detected (> MDL) in mussel tissue at concentrations ranging from 0.078 - 4.73 ng/g wet weight during the 2013-2018 sampling event.
  - Minimum concentration (0.078 ng/g wet weight) detected at site Ashtabula River-3-9.14 (LEAR-3-9.14).
  - Maximum concentration (4.73 ng/g wet weight) detected at site Kinnickinnic River13-S4-7.17 (LMMB-13-S4-7.17).

Basin-wide Highlights

- Highest PFOS mean concentration (1.37 ng/g wet weight) measured in mussels from Lake Ontario.
- Basin-wide, PFOS mean concentrations measured in mussel decreased in order from > Lake Ontario (1.37 ng/g wet weight) > Lake Michigan (0.845 ng/g wet weight) > Niagara River (0.563 ng/g wet weight) > Lake Erie (0.526 ng/g wet weight) Reference Sites (0.499 ng/g wet weight) > Lake Huron (0.238 ng/g wet weight).

Inshore/offshore Highlights

- The highest PFOS mean concentration (0.851 ng/g wet weight) was found in mussel tissue from designated river sites.
- PFOS mean concentrations measured in mussel tissue from inshore (tributary, river, and harbor) and offshore sampling locations decreased in order from River (0.851 ng/g wet weight) > Tributary (0.587 ng/g wet weight) > Harbor (0.551 ng/g wet weight) > Offshore (0.534 ng/g wet weight) sites.

Major Discharge-types Highlights

- The highest PFOS mean concentration (0.773 ng/g wet weight) measured was found in mussel tissue from non-WWTP sites.
- PFOS mean concentrations measured in mussel tissue from sampled major discharge-types locations decreased in order from non-WWTPs (0.773 ng/g wet weight) > WWTP discharge zones/Gradient (0.609 ng/g wet weight) > WWTPs (0.49 ng/g wet weight) > WWTPs/CSOs (0.472 ng/g wet weight) sites.

Land-use Highlights

- The highest PFOS mean concentration (0.72 ng/g wet weight) was found in mussel tissue from Developed dominant site.
- PFOS concentration measured in mussel tissue from designated site land-use categories trended downward from Developed (0.72 ng/g wet weight) > Open-water (0.664 ng/g wet weight) > Undeveloped (0.627 ng/g wet weight) > Agriculture (0.454 ng/g wet weight) > Wetland (0.238 ng/g wet weight) sites.

PFAS Characterization & Result Highlights

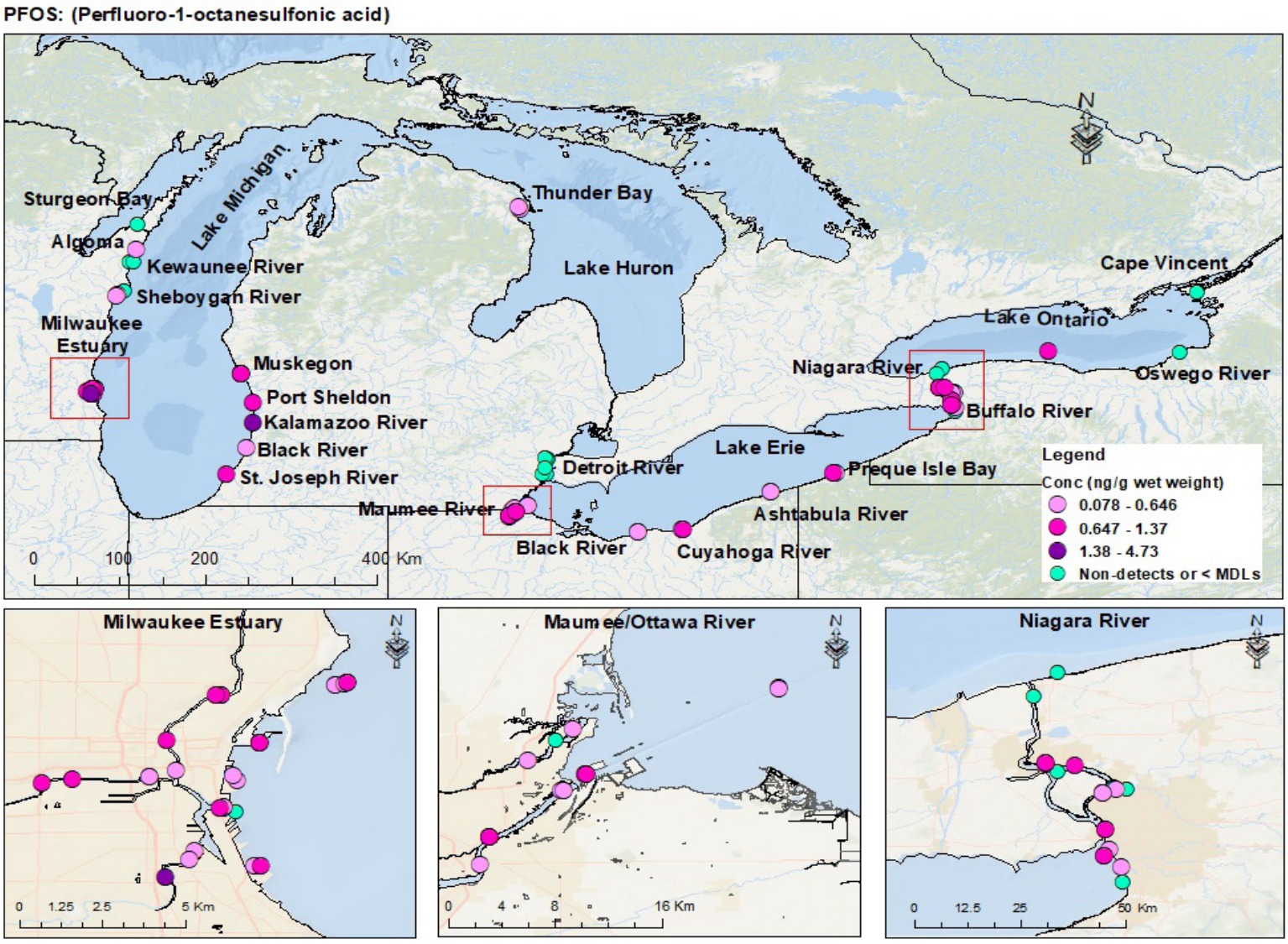

Fig.34. Map of Great Lakes Mussel Watch PFAS sampling locations, highlighting PFAS compounds detected (> MDL) in mussel tissue during the 2013-2018 sampling event.

Concentration table: Summary of basin-wide PFAS concentrations (ng/g wet weight) measured (> MDL) in dreissenid mussel tissue from Lakes Michigan, Huron, Erie, Ontario, and Detroit and Niagara River connecting channels (*) sampling locations between 2013 - 2018.

			Min	Mean	Max
Category	(n)	Stdev	ng/g (ww)	ng/g (ww)	ng/g (ww)
Lake Michigan	35	0.979	0.167	0.845	4.73
Lake Huron	1	0	0.238	0.238	0.238
Detroit River (*)	0	0	0	0	0
Lake Erie	21	0.302	0.078	0.526	1.07
Niagara River (*)	12	0.2	0.246	0.563	0.818
Lake Ontario	1	0	1.37	1.37	1.37
Reference Sites	12	0.225	0.152	0.499	1.01

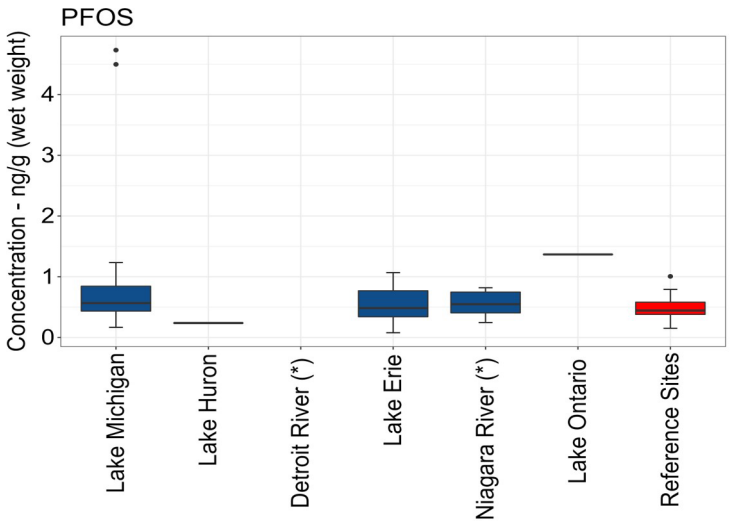

Boxplot: PFAS concentrations (ng/g wet weight) measured in dreissenid mussel tissue basin-wide between 2013 - 2018. Reference sites provides perspective to the relative PFAS concentrations found in mussel tissue basin-wide.

PFAS Characterization & Result Highlights

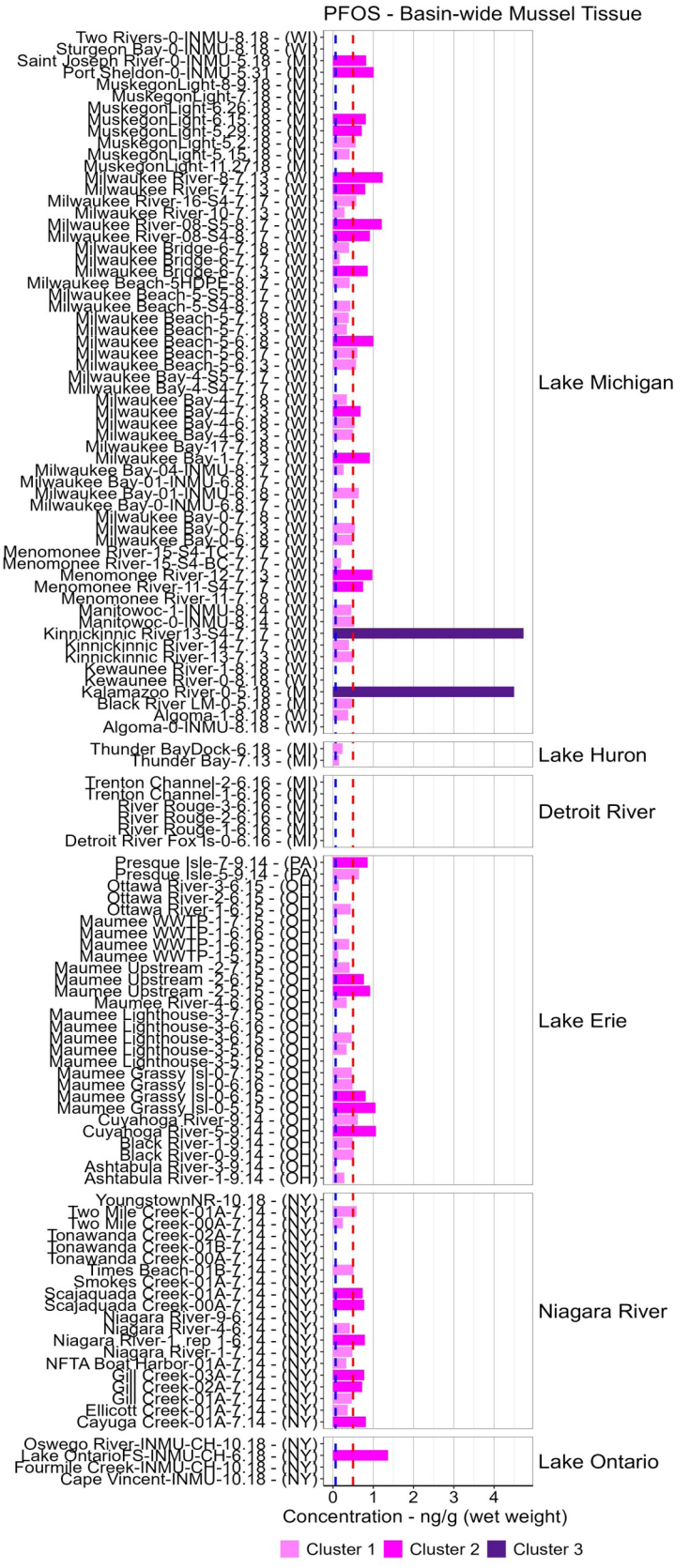

Basin-wide site tissue bar chart: PFAS contaminant concentration results (ng/g wet weight) measured (> MDL) in mussel tissue basin-wide during 2013-2018. Clusters 1-3 represents sites with low, medium and high PFAS concentrations. Blue dashed line represents concentration method detection limit (MDL). Reference line (red dashed line) represent mean reference sites concentration.

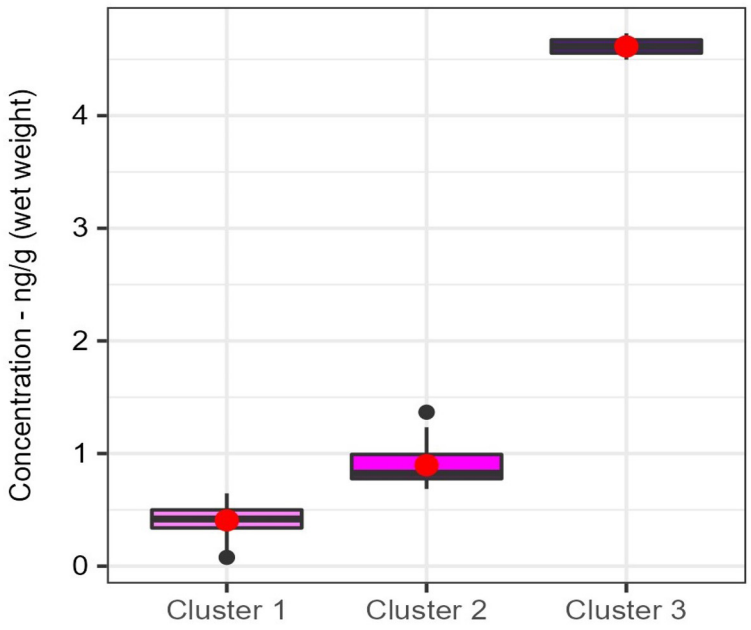

Boxplot: PFAS concentration results detected in dreissenid mussels during 2013-2018. Mean values are plotted as red points. Clusters 1-3 represent low, medium and high PFAS concentrations, respectively.

Total PFOS Concentration (ng/g wet weight)		
	Low	0.078 - 0.646
	Medium	0.647 - 1.37
	High	1.38 - 4.73

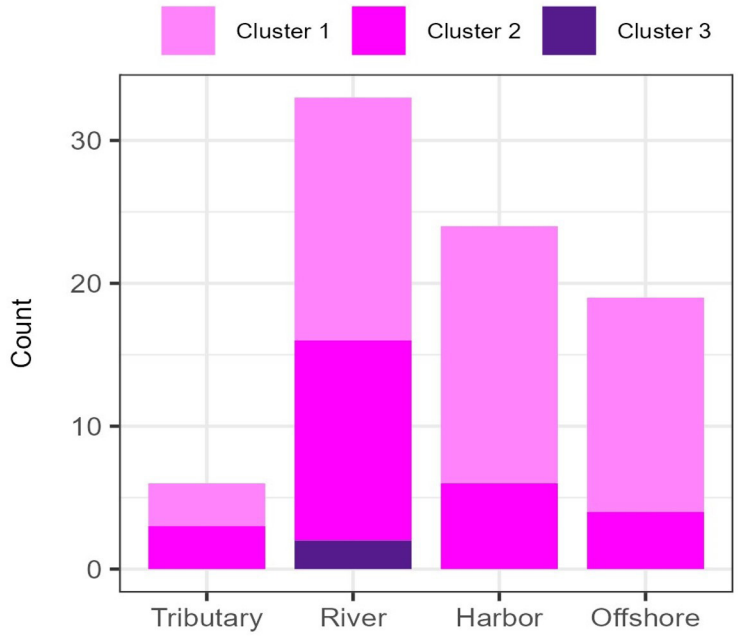

Tissue inshore - offshore bar chart: Measured PFAS composition profile detected in dreissenid mussels across inshore (tributary, river, harbor) and offshore (e.g., open-lake) Great Lakes complexes. Counts (y-axis) represents number of PFAS samples found in mussel tissue across inshore and offshore sampling locations during the 2013-2018 period.

PFAS Characterization & Result Highlights

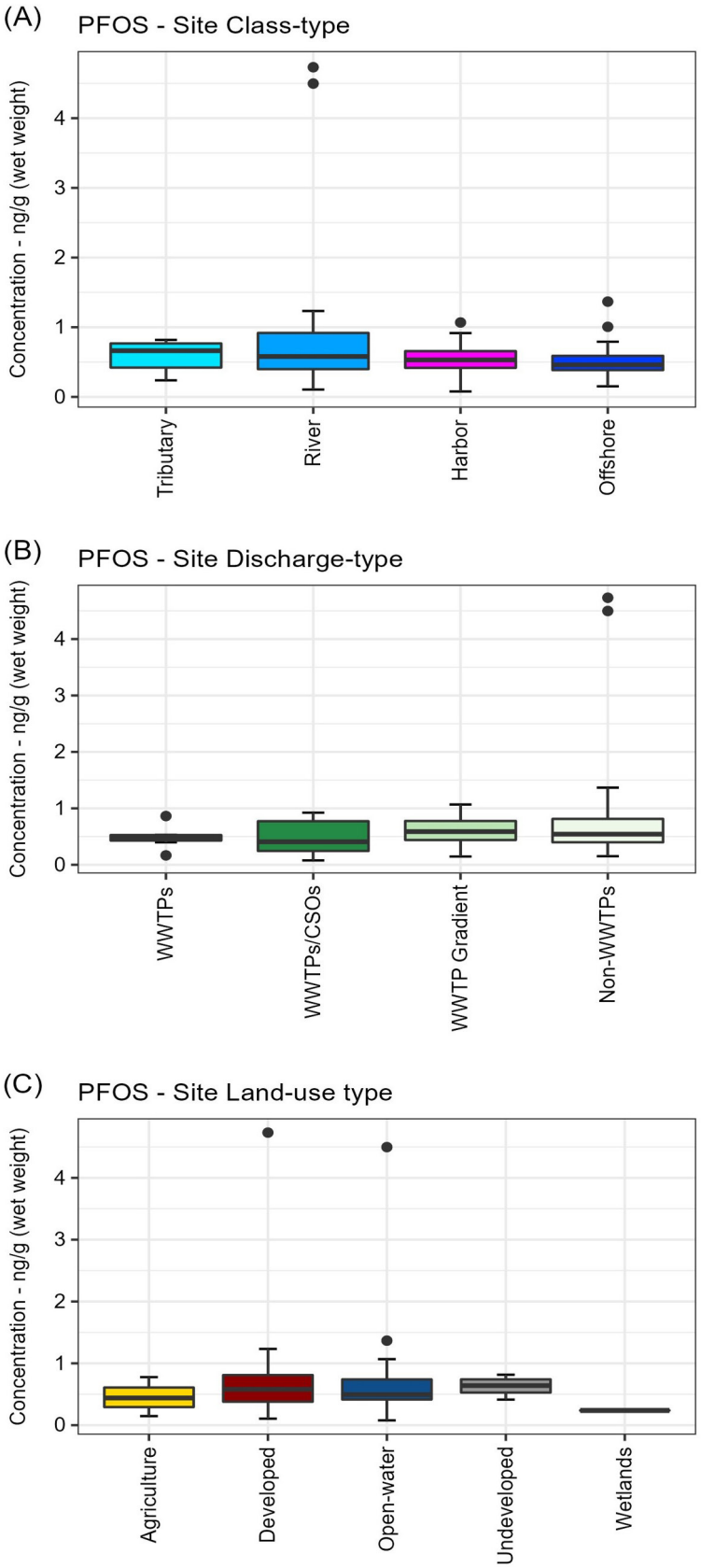

Boxplots: PFAS concentrations measured (> MDL) in mussel tissue at A) inshore and offshore sampling locations, B) designated MWP site discharge-types, and C) predominant site land-use categories/ gradients. Only compounds found at ten or more sites were included in PFAS concentration summary. Plots provide perspective on the most commonly found PFAS in mussel tissue, and their relative concentrations across various Great Lakes environmental matrices.

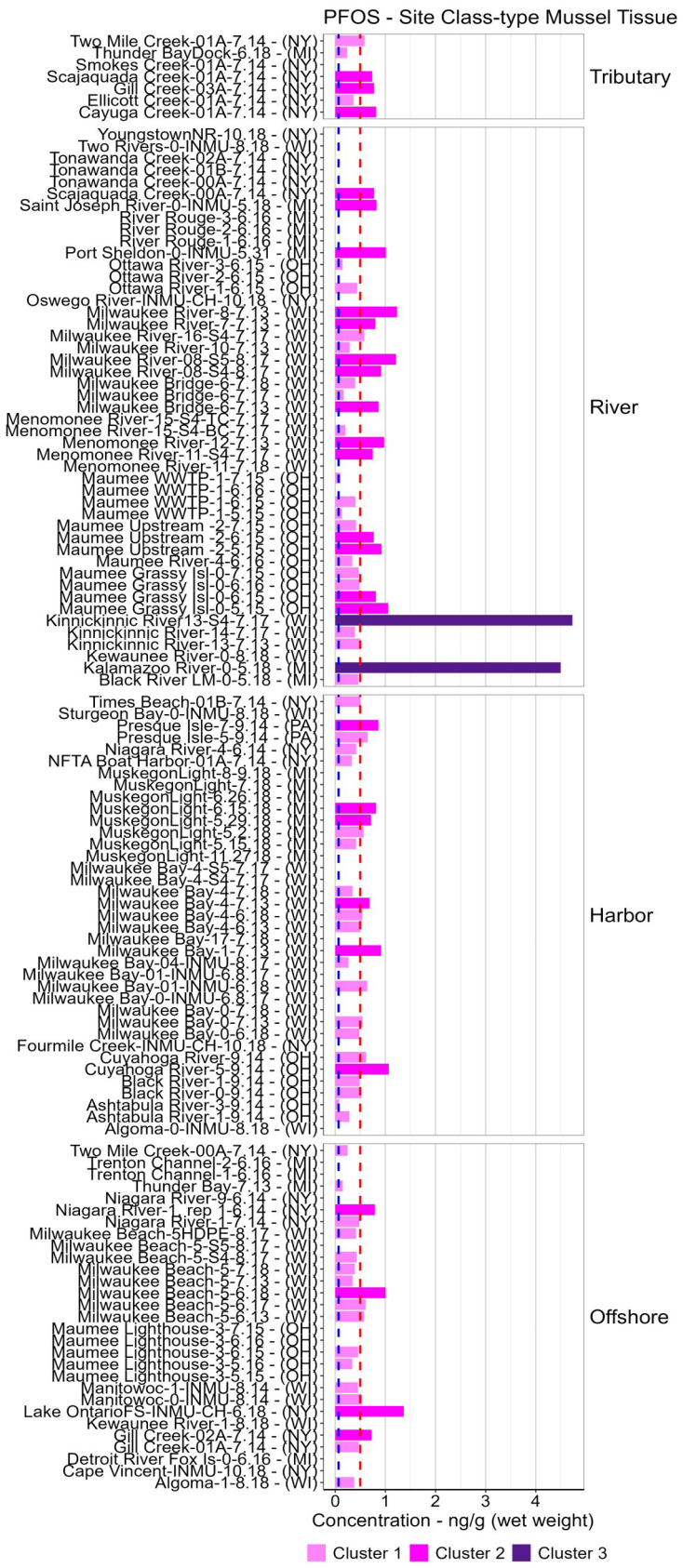

Site class-type tissue bar chart: PFAS contaminant concentration results (ng/g wet weight) measured (> MDL) in dreissenid mussels during 2013-2018 sampling event. Clusters 1-3 represents sites with low, medium and high PFAS concentrations. Blue dashed line represents concentration method detection limit (MDL). Reference line (red dashed line) represent mean reference sites concentration.

PFAS Characterization & Result Highlights

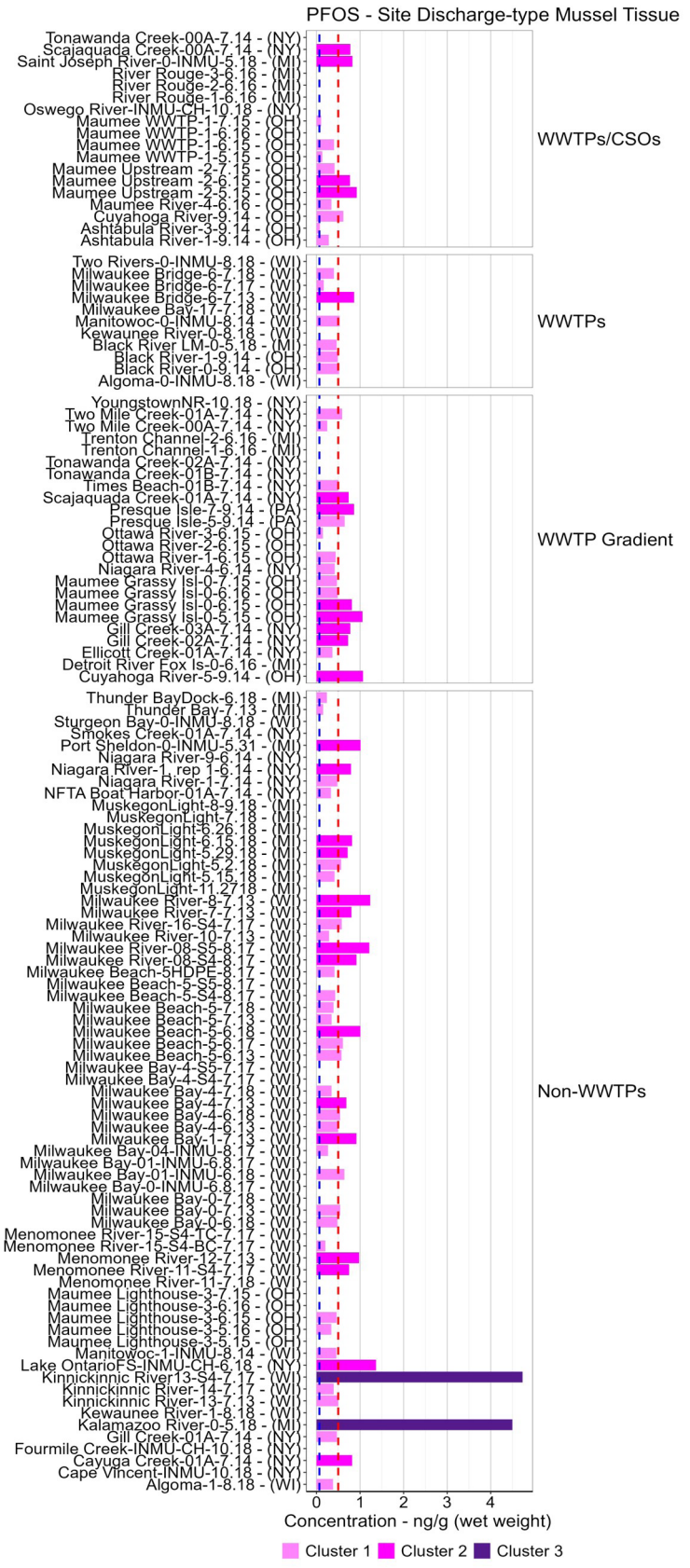

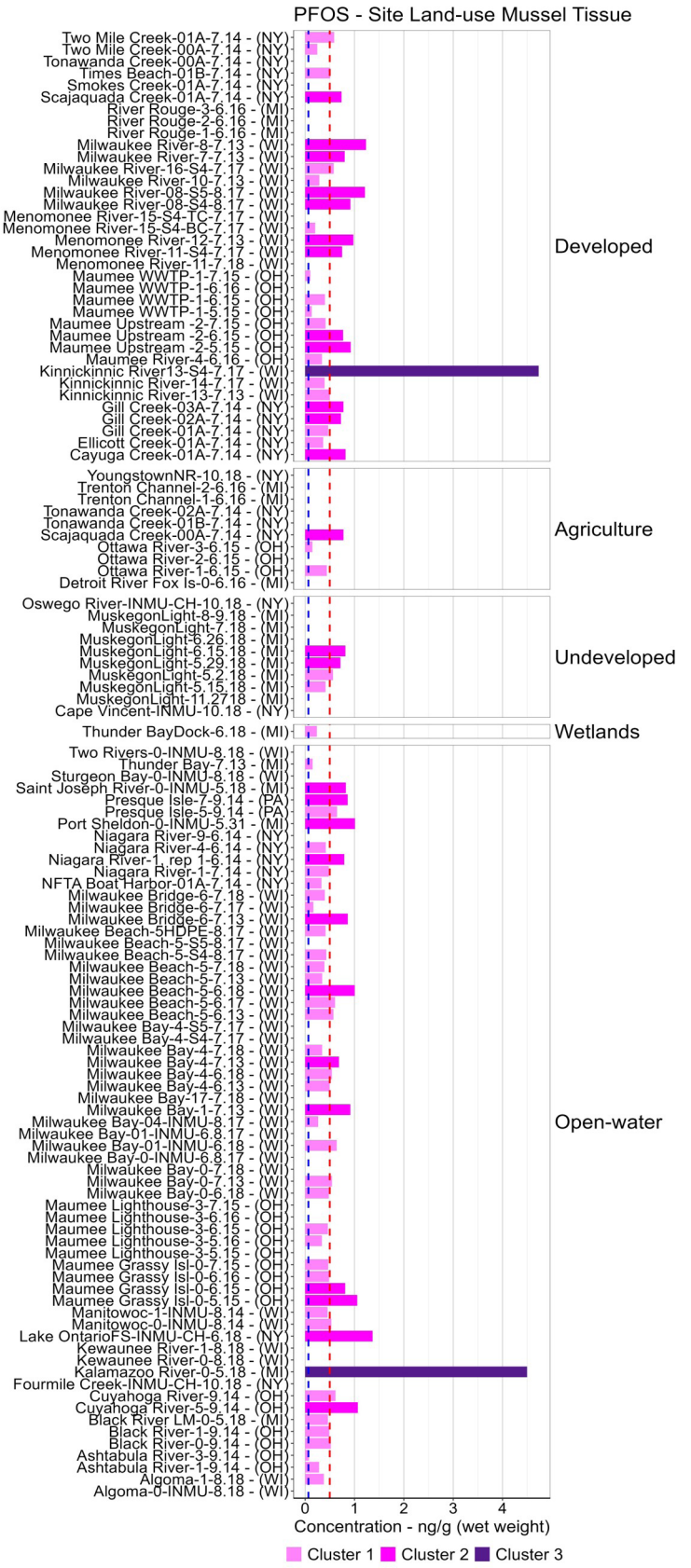

Site discharge-type tissue bar chart: PFAS contaminant concentration results (ng/g wet weight) measured (> MDL) in dreissenid mussels during 2013-2018 sampling event. Clusters 1-3 represents sites with low, medium and high PFAS concentrations. Blue dashed line represents concentration method detection limit (MDL). Reference line (red dashed line) represent mean reference sites concentration.

Site land-use tissue bar chart: PFAS contaminant concentration results (ng/g wet weight) measured (> MDL) in dreissenid mussels during 2013-2018 sampling event. Clusters 1-3 represents sites with low, medium and high PFAS concentrations. Blue dashed line represents concentration method detection limit (MDL). Reference line (red dashed line) represent mean reference sites concentration.

PFOSA (Perfluorooctane sulfonamide)

PFOSA: (Perfluorooctane sulfonamide) Summary

General Observations/Findings:

- PFOSA: (Perfluorooctane sulfonamide) was detected (> MDL) in dreissenid mussels at 17 sites (DF: detection frequency of 16%).
- PFOSA was detected (> MDL) in mussel tissue at concentrations ranging from 0.573 - 3.97 ng/g wet weight during the 2013-2018 sampling event.
  - Minimum concentration (0.573 ng/g wet weight) detected at site Scajaquada Creek-00A-7.14 (NRSC-00A-7.14).
  - Maximum concentration (3.97 ng/g wet weight) detected at site Presque Isle-7-9.14 (LEPB-7-9.14).

Basin-wide Highlights

- Highest PFOSA mean concentrations (2.50 ng/g wet weight) measured in mussels from Lake Erie.
- Basin-wide, PFOSA mean concentrations measured in mussel decreased in order from Lake Erie (2.50 ng/g wet weight) > Niagara River (1.29 ng/g wet weight) > Lake Michigan (1.10 ng/g wet weight) > Reference Sites (0.733 ng/g wet weight) > Detroit River (0.664 ng/g wet weight).

Inshore/offshore Highlights

- The highest PFOSA mean concentration (1.7 ng/g wet weight) was found in mussel tissue from designated tributary sites.
- PFOSA mean concentrations measured in mussel tissue from inshore (tributary, river, and harbor) and offshore sampling locations decreased in order from Tributary (1.7 ng/g wet weight) > Harbor (1.59 ng/g wet weight) > River (0.943 ng/g wet weight) > Offshore (0.698 ng/g wet weight) sites.

Major Discharge-types Highlights

- The highest PFOSA mean concentration (1.98 ng/g wet weight) measured was found in mussel tissue from WWTP discharge zones/Gradient sites.
- PFOSA mean concentrations measured in mussel tissue from sampled major discharge-types locations decreased in order from WWTP discharge zones/Gradient (1.98 ng/g wet weight) > non-WWTPs (1.03 ng/g wet weight) > WWTPs (0.989 ng/g wet weight) > WWTPs/CSOs (0.573 ng/g wet weight) sites.

Land-use Highlights

- The highest PFOSA mean concentration (1.46 ng/g wet weight) was found in mussel tissue from open-water sites.
- PFOSA mean concentration measured in mussel tissue from designated site land-use categories trended downward from Open-water (1.46 ng/g wet weight) > Developed (1.27 ng/g wet weight) > Agriculture (0.618 ng/g wet weight) sites.

PFAS Characterization & Result Highlights

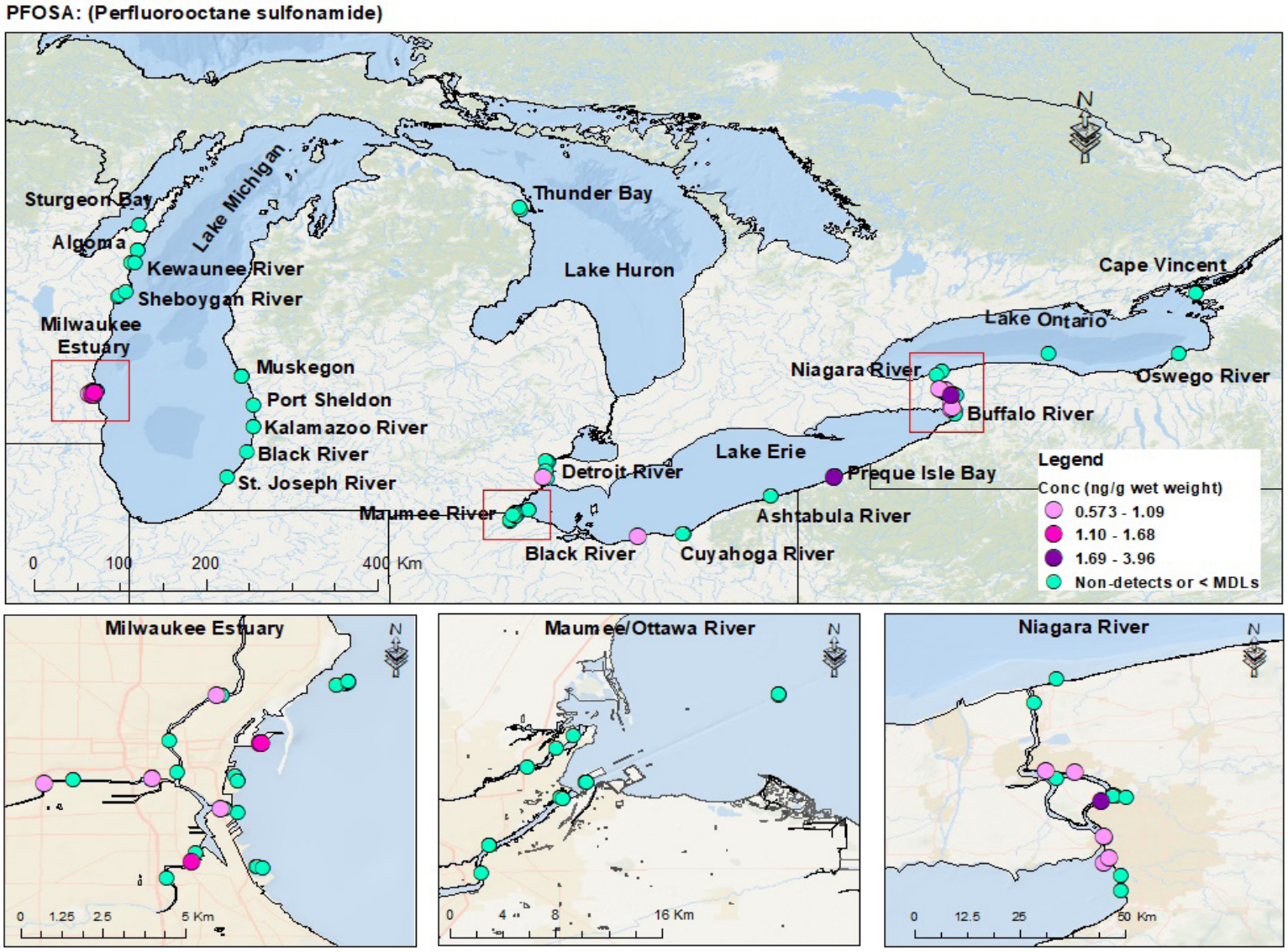

Fig.41. Map of Great Lakes Mussel Watch PFAS sampling locations, highlighting PFAS compounds detected (> MDL) in mussel tissue during the 2013-2018 sampling event.

Concentration table: Summary of basin-wide PFAS concentrations (ng/g wet weight) measured (> MDL) in dreissenid mussel tissue from Lakes Michigan, Huron, Erie, Ontario, and Detroit and Niagara River connecting channels (*) sampling locations between 2013 - 2018.

			Min	Mean	Max
Category	(n)	Stdev	ng/g (ww)	ng/g (ww)	ng/g (ww)
Lake Michigan	8	0.323	0.695	1.104	1.68
Lake Huron	0	0	0	0	0
Detroit River (*)	1	0	0.664	0.664	0.664
Lake Erie	2	2.07	1.038	2.501	3.97
Niagara River (*)	5	1.313	0.573	1.288	3.63
Lake Ontario	0	0	0	0	0
Reference Sites	1	0	0.733	0.733	0.733

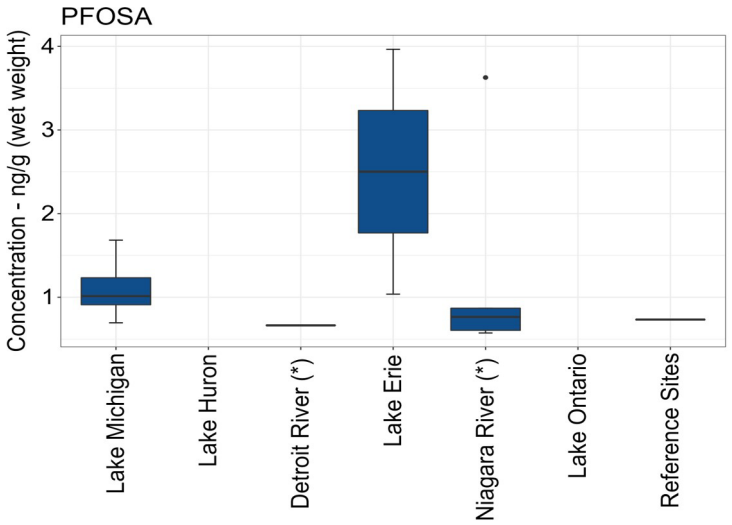

Boxplot: PFAS concentrations (ng/g wet weight) measured in dreissenid mussel tissue basin-wide between 2013 - 2018. Reference sites provides perspective to the relative PFAS concentrations found in mussel tissue basin-wide.

PFAS Characterization & Result Highlights

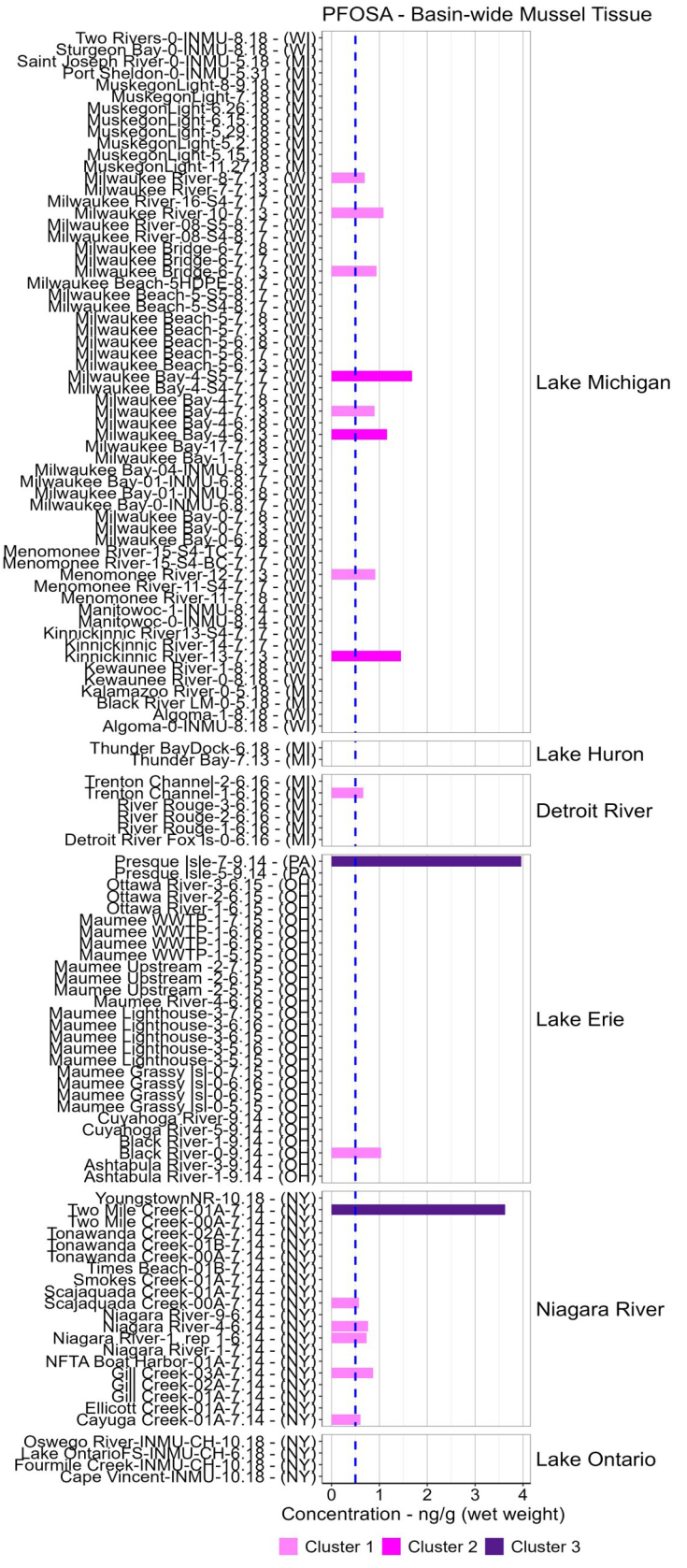

Basin-wide site tissue bar chart: PFAS contaminant concentration results (ng/g wet weight) measured (> MDL) in mussel tissue basin-wide during 2013-2018. Clusters 1-3 represents sites with low, medium and high PFAS concentrations. Blue dashed line represents concentration method detection limit (MDL). Reference line (red dashed line) represent mean reference sites concentration.

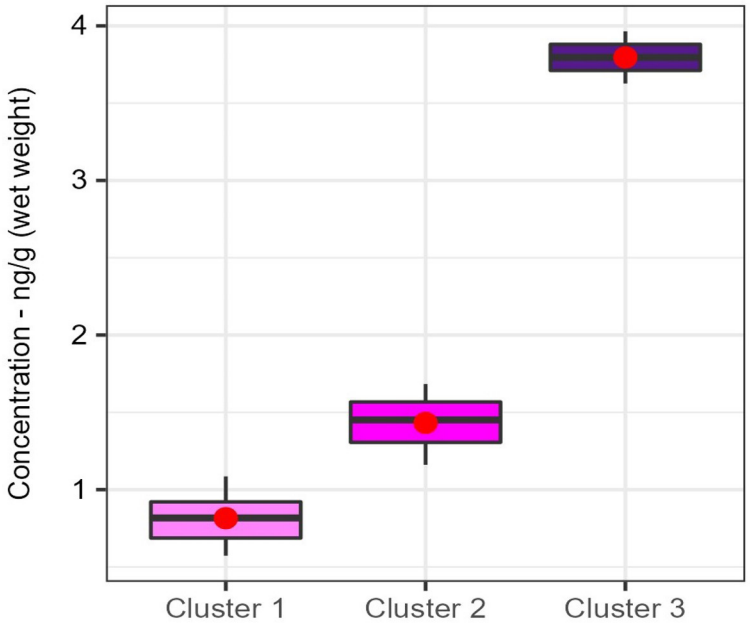

Boxplot: PFAS concentration results detected in dreissenid mussels during 2013-2018. Mean values are plotted as red points. Clusters 1-3 represent low, medium and high PFAS concentrations, respectively.

Total PFOSA Concentration (ng/g wet weight)		
	Low	0.573 - 1.09
	Medium	1.10 - 1.68
	High	1.69 - 3.96

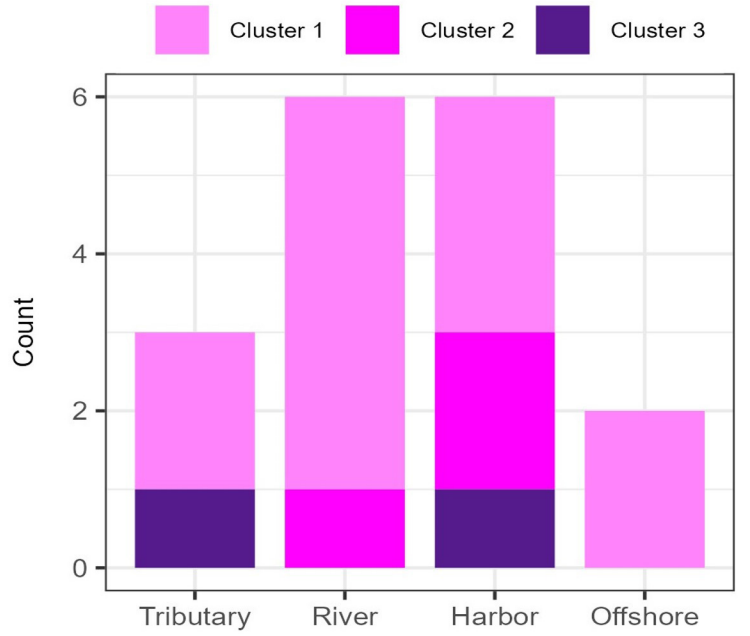

Tissue inshore - offshore bar chart: Measured PFAS composition profile detected in dreissenid mussels across inshore (tributary, river, harbor) and offshore (e.g., open-lake) Great Lakes complexes. Counts (y-axis) represents number of PFAS samples found in mussel tissue across inshore and offshore sampling locations during the 2013-2018 period.

PFAS Characterization & Result Highlights

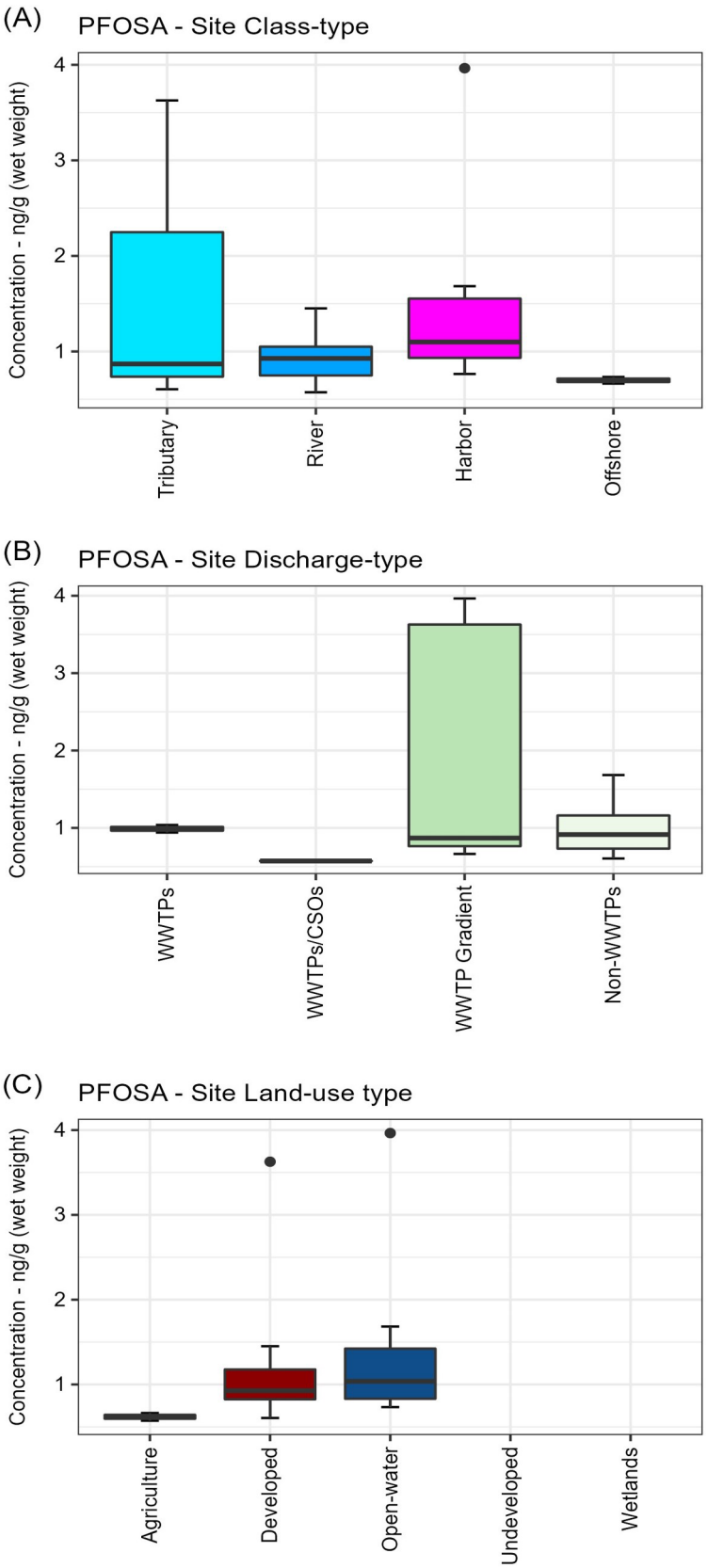

Boxplots: PFAS concentrations measured (> MDL) in mussel tissue at A) inshore and offshore sampling locations, B) designated MWP site discharge-types, and C) predominant site land-use categories/ gradients. Only compounds found at ten or more sites were included in PFAS concentration summary. Plots provide perspective on the most commonly found PFAS in mussel tissue, and their relative concentrations across various Great Lakes environmental matrices.

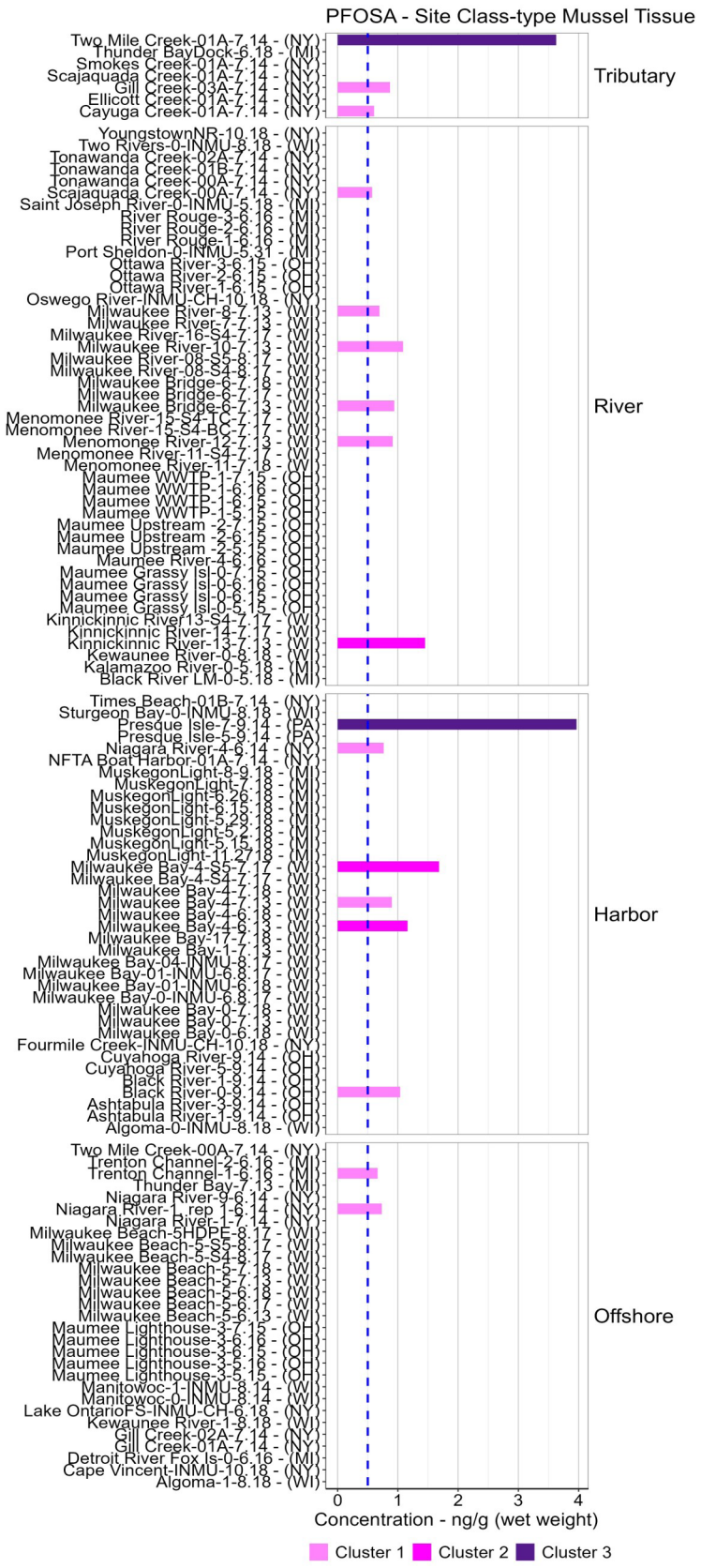

Site class-type tissue bar chart: PFAS contaminant concentration results (ng/g wet weight) measured (> MDL) in dreissenid mussels during 2013-2018 sampling event. Clusters 1-3 represents sites with low, medium and high PFAS concentrations. Blue dashed line represents concentration method detection limit (MDL). Reference line (red dashed line) represent mean reference sites concentration.

PFAS Characterization & Result Highlights

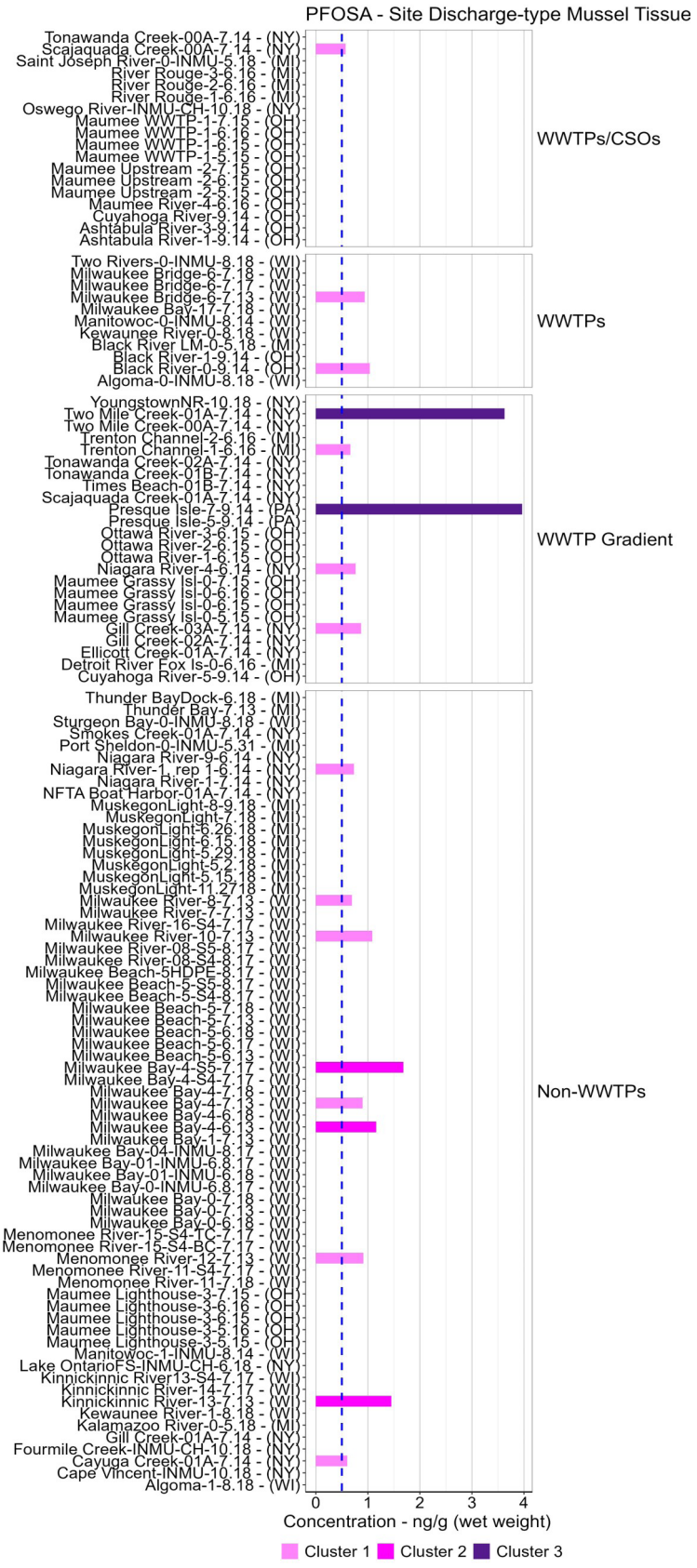

Site discharge-type tissue bar chart: PFAS contaminant concentration results (ng/g wet weight) measured (> MDL) in dreissenid mussels during 2013-2018 sampling event. Clusters 1-3 represents sites with low, medium and high PFAS concentrations. Blue dashed line represents concentration method detection limit (MDL). Reference line (red dashed line) represent mean reference sites concentration.

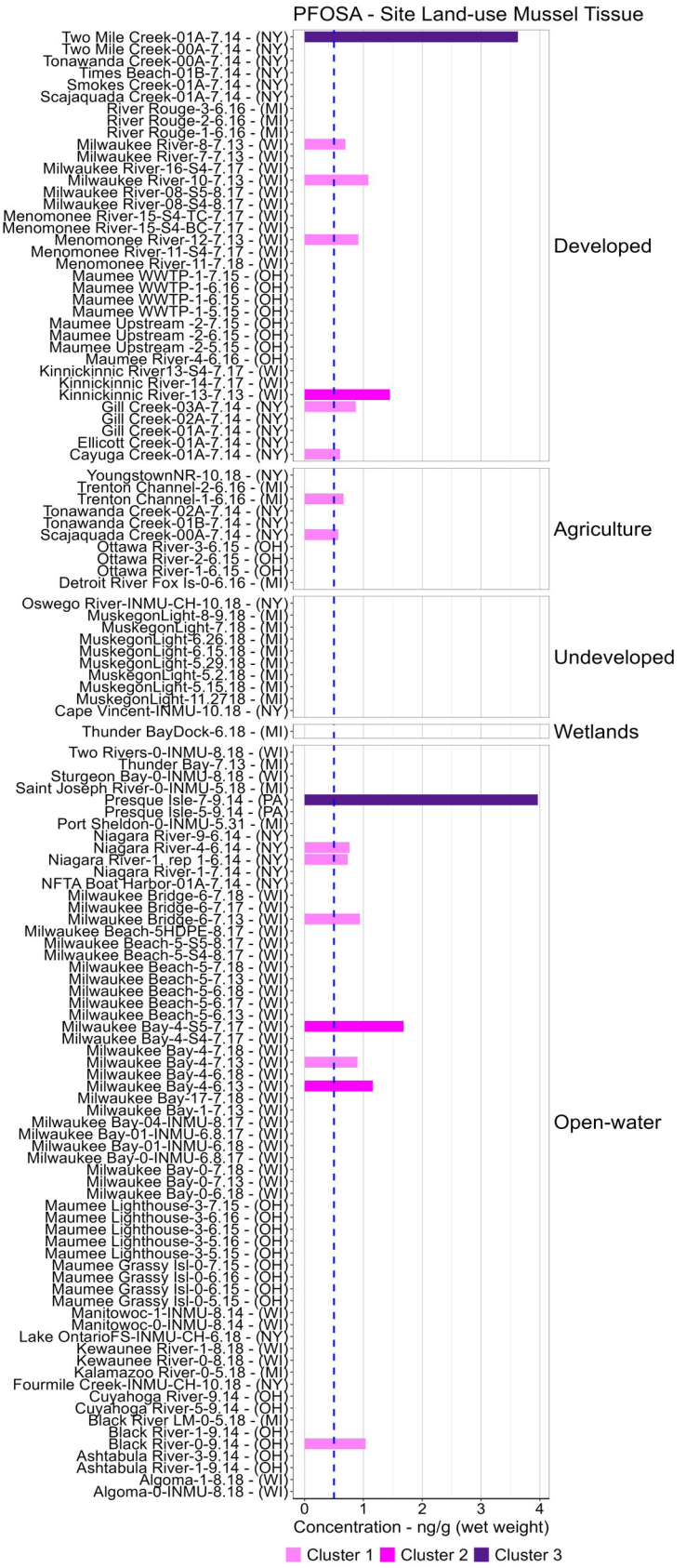

Site land-use tissue bar chart: PFAS contaminant concentration results (ng/g wet weight) measured (> MDL) in dreissenid mussels during 2013-2018 sampling event. Clusters 1-3 represents sites with low, medium and high PFAS concentrations. Blue dashed line represents concentration method detection limit (MDL). Reference line (red dashed line) represent mean reference sites concentration.

PFPeA (Perfluoro-n-pentanoic acid)

PFPeA: (Perfluoro-n-pentanoic acid) Summary

General Observations/Findings:

- PFPeA: (Perfluoro-n-pentanoic acid) was detected (> MDL) in dreissenid mussels at 11 sites (DF: detection frequency of 10%).
- PFPeA was detected (> MDL) in mussel tissue at concentrations ranging from 0.135 - 1.22 ng/g wet weight during the 2013-2018 sampling event.
  - Minimum concentration (0.135 ng/g wet weight) detected at site Cuyahoga River-9.14 (LECR-9.14).
  - Maximum concentration (1.22 ng/g wet weight) detected at site Port Sheldon-0-INMU-5.31 (LMPS-0-INMU-5.31).

Basin-wide Highlights

- Highest PFPeA mean concentrations (0.536 ng/g wet weight) measured in mussels from Lake Michigan.
- Basin-wide, PFPeA mean concentrations measured in mussel decreased in order from Lake Michigan (0.536 ng/g wet weight) > Reference Sites (0.297 ng/g wet weight) > Lake Erie (0.192 ng/g wet weight).

Inshore/offshore Highlights

- The highest PFPeA mean concentration (0.42 ng/g wet weight) was found in mussel tissue from designated river sites.
- PFPeA mean concentrations measured in mussel tissue from inshore (tributary, river, and harbor) and offshore sampling locations decreased in order from River (0.42 ng/g wet weight) > Offshore (0.297 ng/g wet weight) > Harbor (0.251 ng/g wet weight) sites.

Major Discharge-types Highlights

- The highest PFPeA mean concentration (0.456 ng/g wet weight) measured was found in mussel tissue from non-WWTP sites.
- PFPeA mean concentrations measured in mussel tissue from sampled major discharge-types locations decreased in order from non-WWTPs (0.456 ng/g wet weight) > WWTPs/CSOs (0.218 ng/g wet weight) > WWTP Gradient (0.154 ng/g wet weight) sites.

Land-use Highlights

- The highest PFPeA mean concentration (0.403 ng/g wet weight) was found in mussel tissue from Open-water dominant sites.
- PFPeA mean concentration measured in mussel tissue from designated site land-use categories trended downward from Open-water (0.403 ng/g wet weight) > Developed (0.24 ng/g wet weight) > Agriculture (0.157 ng/g wet weight) sites.

PFAS Characterization & Result Highlights

PFPeA: (Perfluoro-n-pentanoic acid)

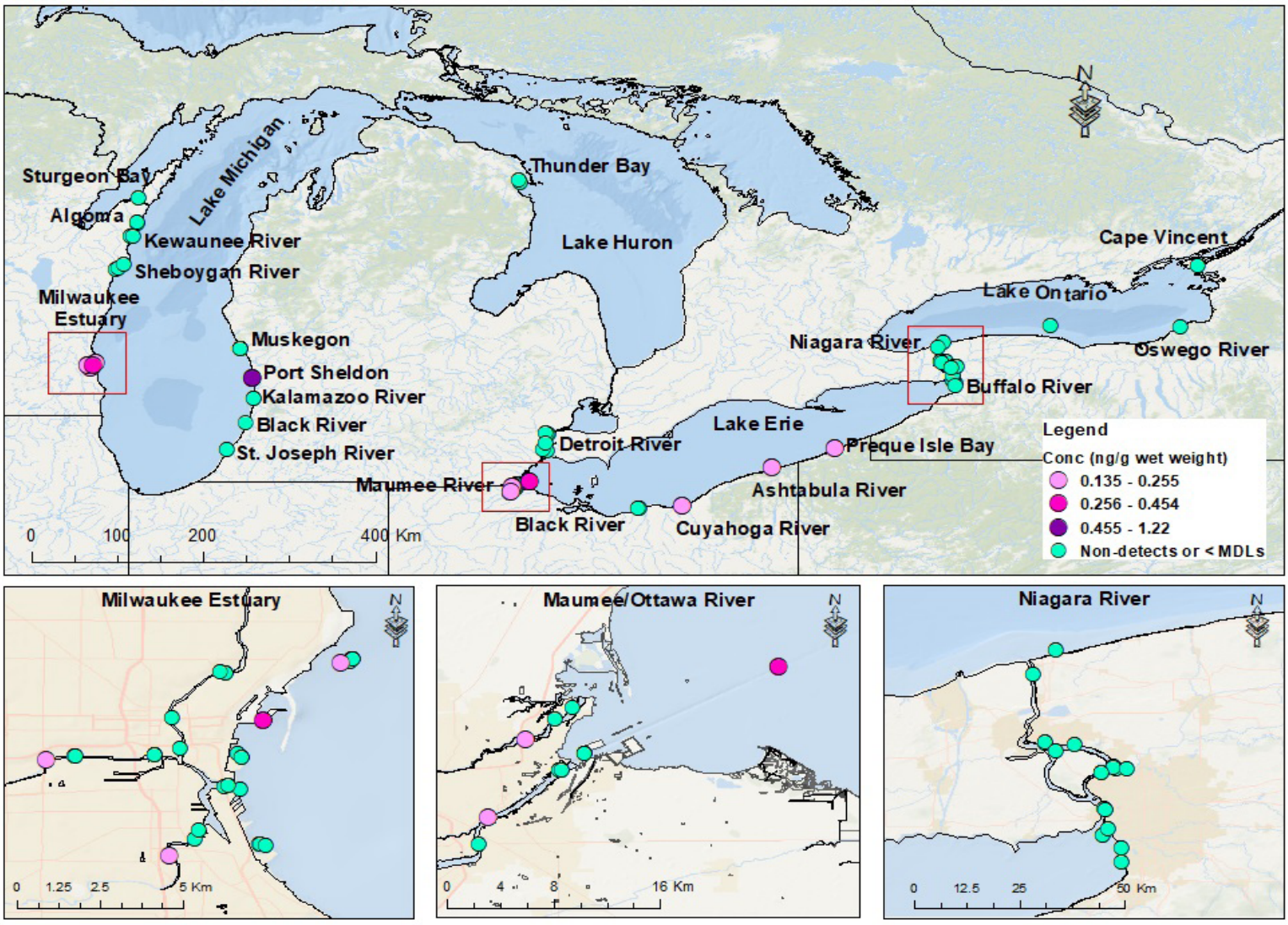

Fig.42. Map of Great Lakes Mussel Watch PFAS sampling locations, highlighting PFAS compounds detected (> MDL) in mussel tissue during the 2013-2018 sampling event.

Concentration table: Summary of basin-wide PFAS concentrations (ng/g wet weight) measured (> MDL) in dreissenid mussel tissue from Lakes Michigan, Huron, Erie, Ontario, and Detroit and Niagara River connecting channels (*) sampling locations between 2013 - 2018.

			Min	Mean	Max
Category	(n)	Stdev	ng/g (ww)	ng/g (ww)	ng/g (ww)
Lake Michigan	4	0.469	0.232	0.536	1.22
Lake Huron	0	0	0	0	0
Detroit River (*)	0	0	0	0	0
Lake Erie	5	0.062	0.135	0.192	0.263
Niagara River (*)	0	0	0	0	0
Lake Ontario	0	0	0	0	0
Reference Sites	2	0.222	0.14	0.297	0.454

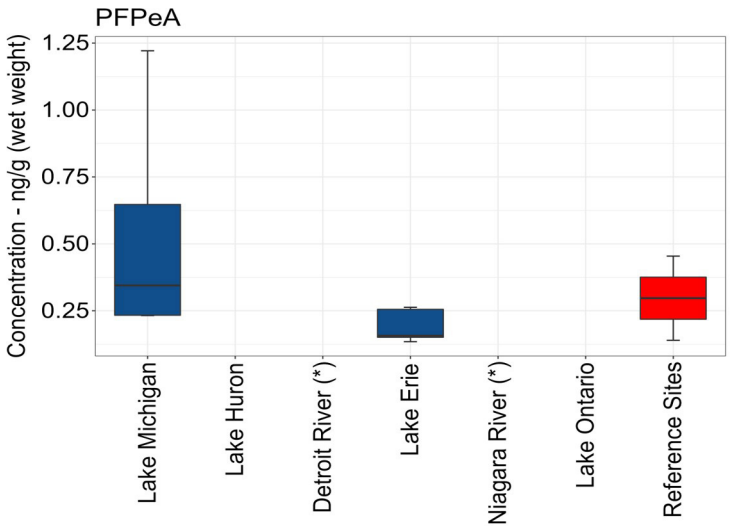

Boxplot: PFAS concentrations (ng/g wet weight) measured in dreissenid mussel tissue basin-wide between 2013 - 2018. Reference sites provides perspective to the relative PFAS concentrations found in mussel tissue basin-wide.

PFAS Characterization & Result Highlights

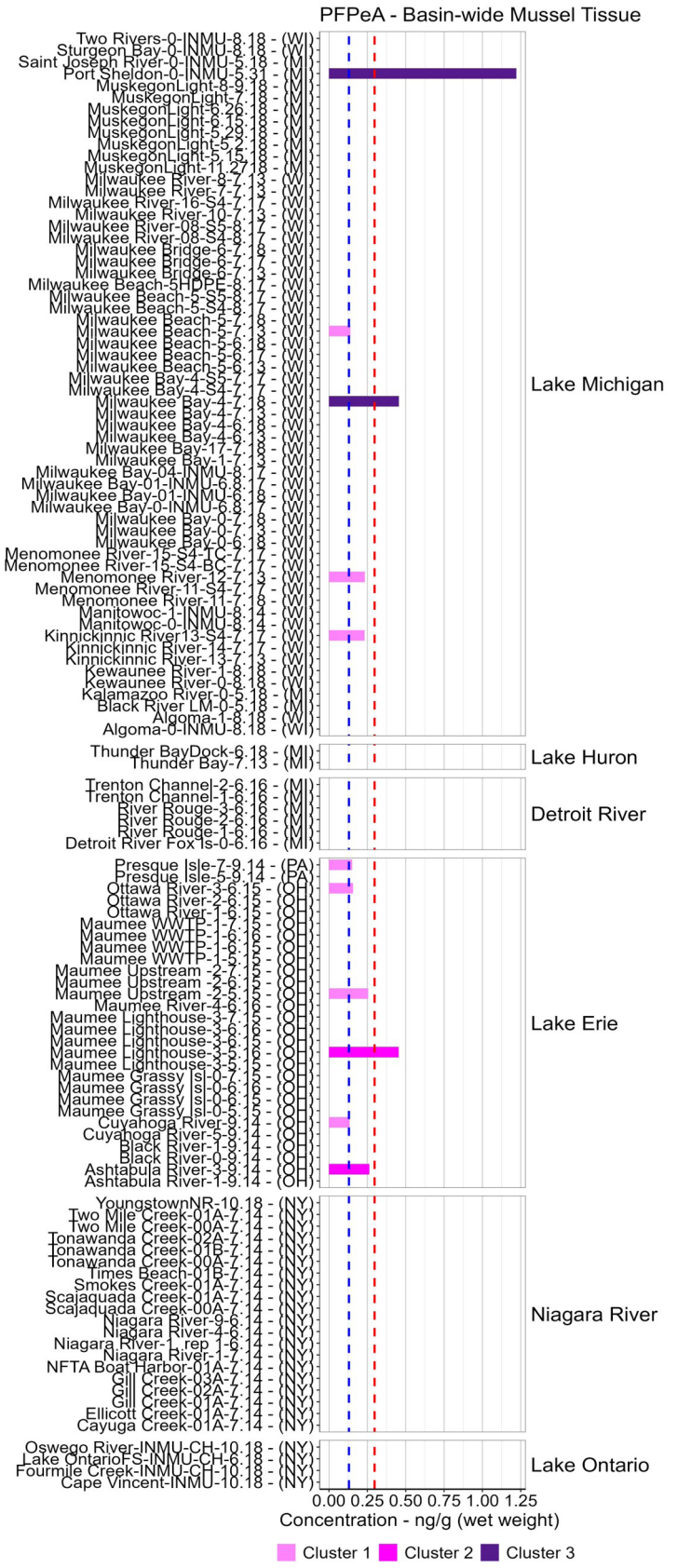

Basin-wide site tissue bar chart: PFAS contaminant concentration results (ng/g wet weight) measured (> MDL) in mussel tissue basin-wide during 2013-2018. Clusters 1-3 represents sites with low, medium and high PFAS concentrations. Blue dashed line represents concentration method detection limit (MDL). Reference line (red dashed line) represent mean reference sites concentration.

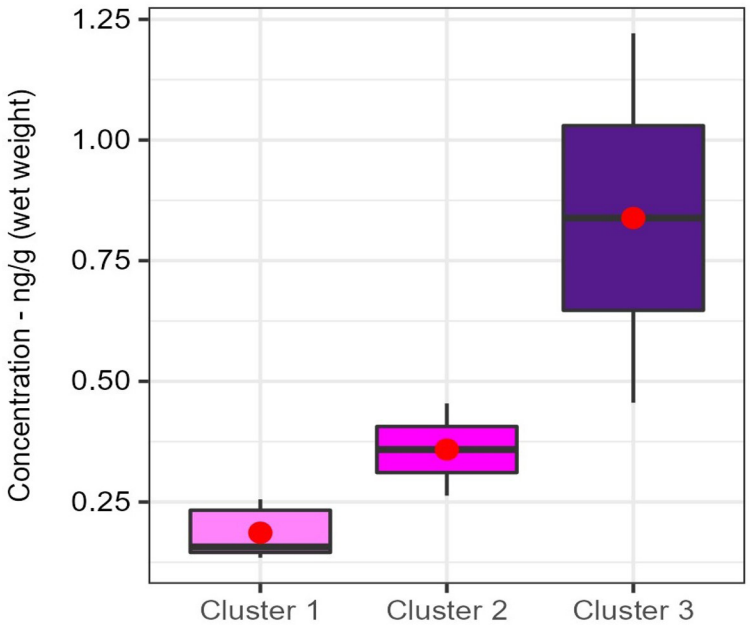

Boxplot: PFAS concentration results detected in dreissenid mussels during 2013-2018. Mean values are plotted as red points. Clusters 1-3 represent low, medium and high PFAS concentrations, respectively.

Total PFPeA Concentration (ng/g wet weight)		
	Low	0.135 - 0.255
	Medium	0.256 - 0.454
	High	0.455 - 1.22

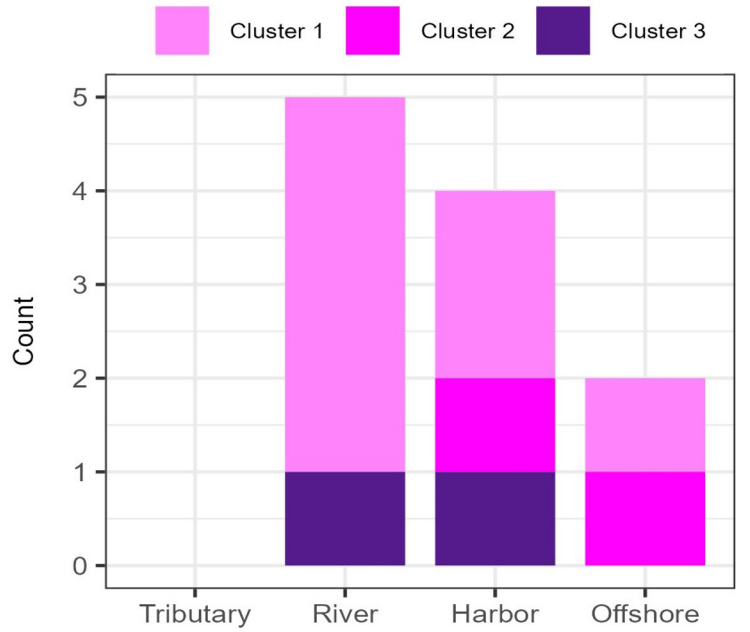

Tissue inshore - offshore bar chart: Measured PFAS composition profile detected in dreissenid mussels across inshore (tributary, river, harbor) and offshore (e.g., open-lake) Great Lakes complexes. Counts (y-axis) represents number of PFAS samples found in mussel tissue across inshore and offshore sampling locations during the 2013-2018 period.

PFAS Characterization & Result Highlights

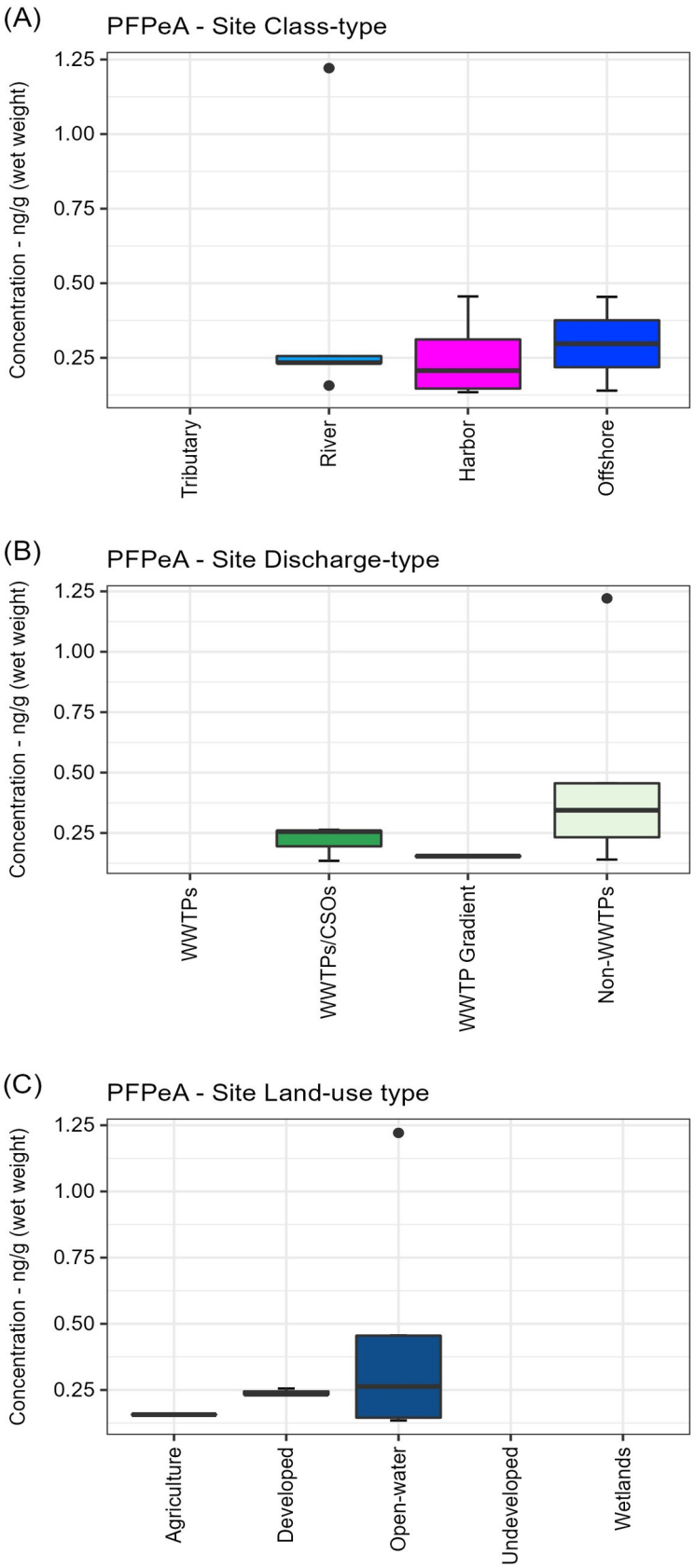

Boxplots: PFAS concentrations measured (> MDL) in mussel tissue at A) inshore and offshore sampling locations, B) designated MWP site discharge-types, and C) predominant site land-use categories/ gradients. Only compounds found at ten or more sites were included in PFAS concentration summary. Plots provide perspective on the most commonly found PFAS in mussel tissue, and their relative concentrations across various Great Lakes environmental matrices.

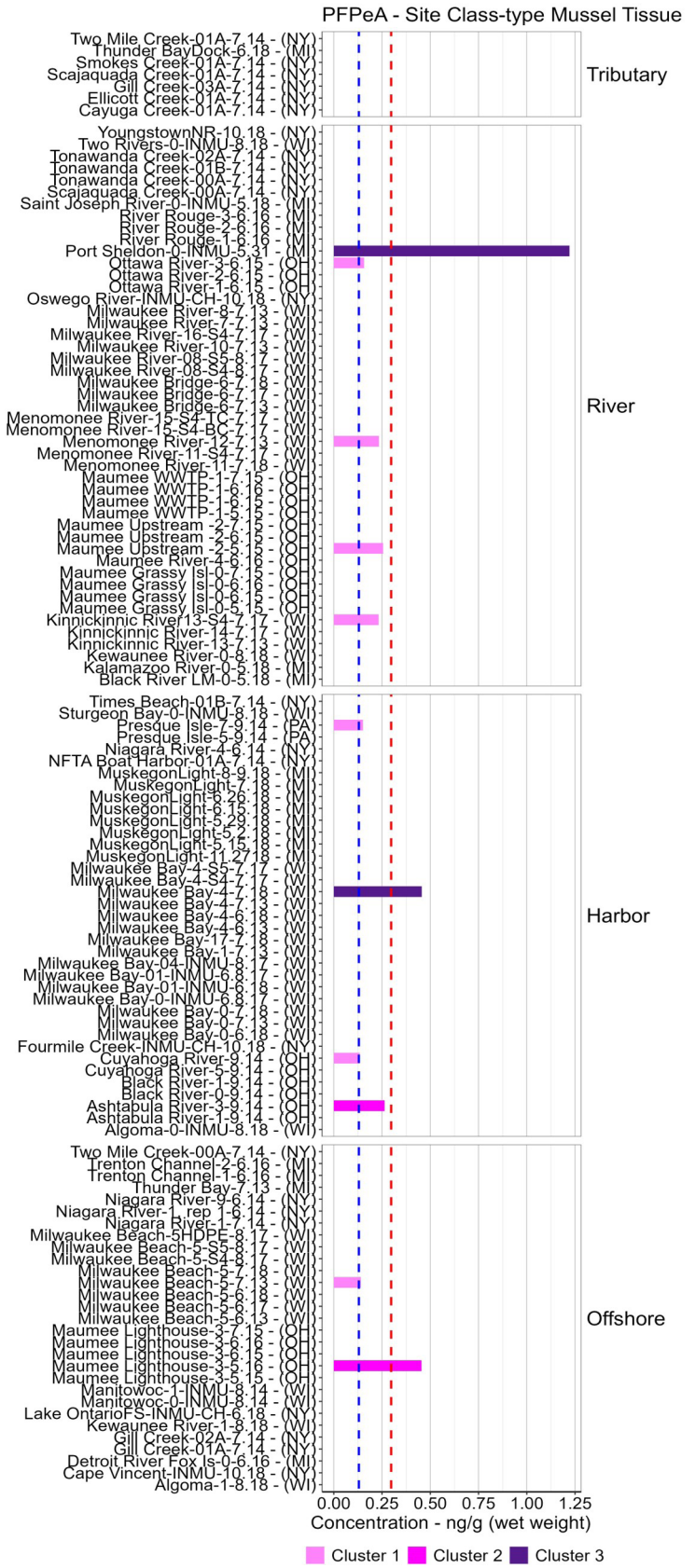

Site class-type tissue bar chart: PFAS contaminant concentration results (ng/g wet weight) measured (> MDL) in dreissenid mussels during 2013-2018 sampling event. Clusters 1-3 represents sites with low, medium and high PFAS concentrations. Blue dashed line represents concentration method detection limit (MDL). Reference line (red dashed line) represent mean reference sites concentration.

PFAS Characterization & Result Highlights

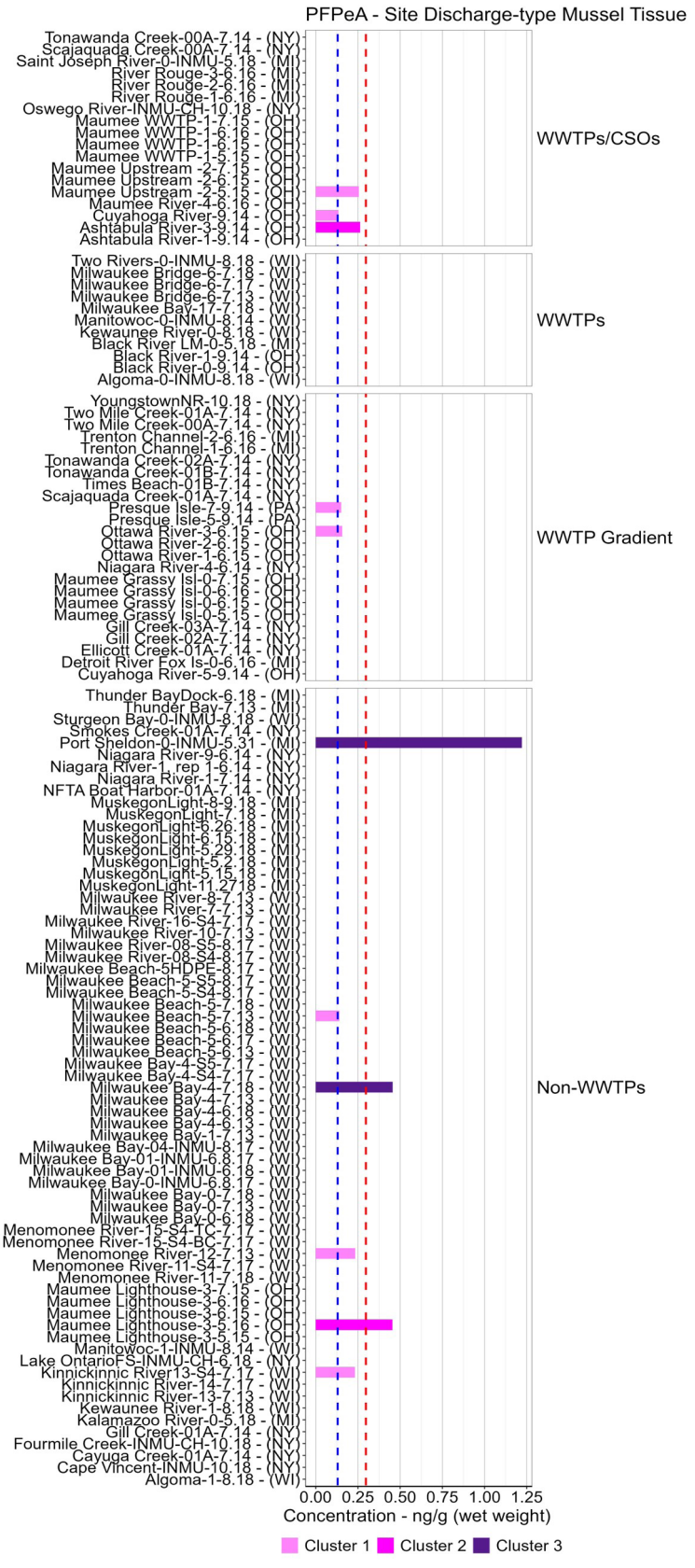

Site discharge-type tissue bar chart: PFAS contaminant concentration results (ng/g wet weight) measured (> MDL) in dreissenid mussels during 2013-2018 sampling event. Clusters 1-3 represents sites with low, medium and high PFAS concentrations. Blue dashed line represents concentration method detection limit (MDL). Reference line (red dashed line) represent mean reference sites concentration.

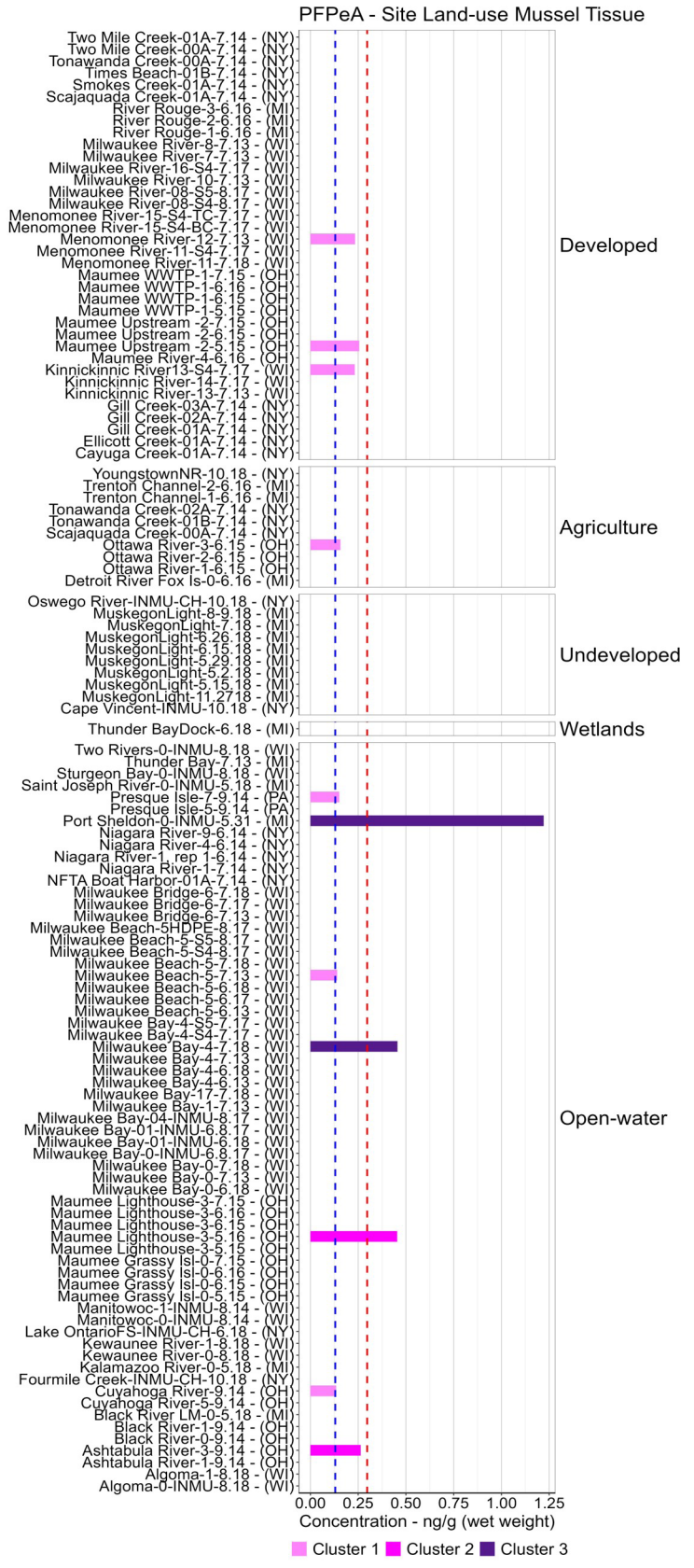

Site land-use tissue bar chart: PFAS contaminant concentration results (ng/g wet weight) measured (> MDL) in dreissenid mussels during 2013-2018 sampling event. Clusters 1-3 represents sites with low, medium and high PFAS concentrations. Blue dashed line represents concentration method detection limit (MDL). Reference line (red dashed line) represent mean reference sites concentration.

PFTreA (Perfluoro-n-tetradecanoic acid)

PFTreA: (Perfluoro-n-tetradecanoic acid) Summary

General Observations/Findings:

- PFTreA: (Perfluoro-n-tetradecanoic acid) was detected (> MDL) in dreissenid mussels at 13 sites (DF: detection frequency of 12%).
- PFTreA was detected (> MDL) in mussel tissue at concentrations ranging from 0.566 - 3.02 ng/g wet weight during the 2013-2018 sampling event.
  - Minimum concentration (0.566 ng/g wet weight) detected at site Maumee Grassy Isl-0-6.16 (LEMR-0-6.16).
  - Maximum concentration (3.02 ng/g wet weight) detected at site Kinnickinnic River13-S4-7.17 (LMMB-13-S4-7.17).

Basin-wide Highlights

- Highest PFTreA mean concentrations (1.57 ng/g wet weight) measured in mussels from Lake Michigan.
- Basin-wide, PFTreA mean concentrations measured in mussel decreased in order from Lake Michigan (1.57 ng/g wet weight) > Lake Erie (0.725 ng/g wet weight).

Inshore/offshore Highlights

- The highest PFTreA mean concentration (1.47 ng/g wet weight) was found in mussel tissue from designated river sites.
- PFTreA mean concentrations measured in mussel tissue from inshore (tributary, river, and harbor) and offshore sampling locations decreased in order from River (1.47 ng/g wet weight) > Harbor (1.06 ng/g wet weight) sites.

Major Discharge-types Highlights

- The highest PFTreA mean concentration (1.62 ng/g wet weight) measured was found in mussel tissue from non-WWTP sites..
- PFTreA mean concentrations measured in mussel tissue from sampled major discharge-types locations decreased in order from non-WWTPs (1.62 ng/g wet weight) > WWTPs (0.872 ng/g wet weight) > WWTP Gradient (0.73 ng/g wet weight) sites.

Land-use Highlights

- The highest PFTreA mean concentration (1.60 ng/g wet weight) was found in mussel tissue from Developed dominant site.
- PFTreA concentration measured in mussel tissue from designated site land-use categories trended downward from Developed (1.60 ng/g wet weight) > Open-water (0.975 ng/g wet weight) sites.

PFAS Characterization & Result Highlights

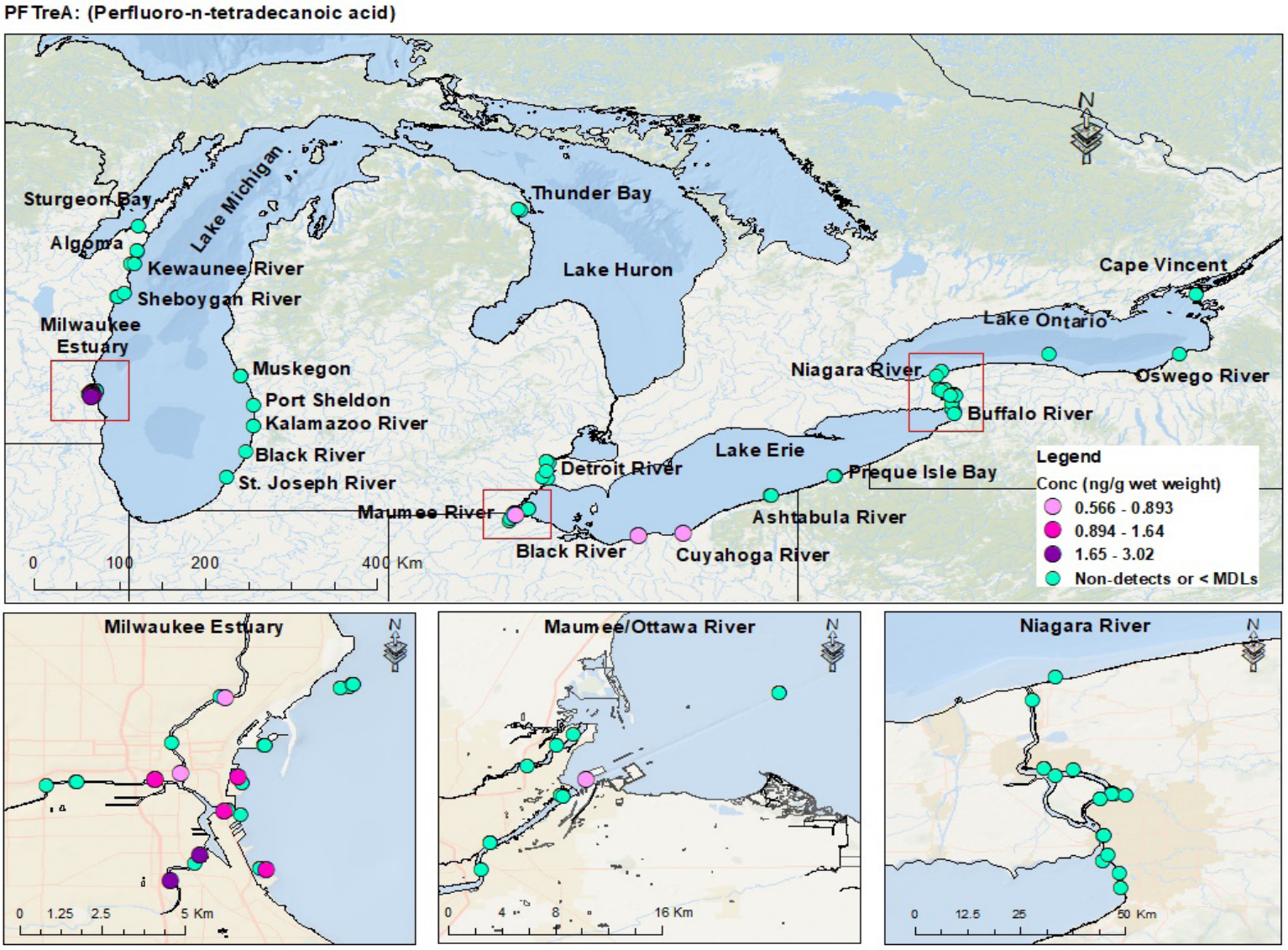

Fig.43. Map of Great Lakes Mussel Watch PFAS sampling locations, highlighting PFAS compounds detected (> MDL) in mussel tissue during the 2013-2018 sampling event.

Concentration table: Summary of basin-wide PFAS concentrations (ng/g wet weight) measured (> MDL) in dreissenid mussel tissue from Lakes Michigan, Huron, Erie, Ontario, and Detroit and Niagara River connecting channels (*) sampling locations between 2013 - 2018.

			Min	Mean	Max
Category	(n)	Stdev	ng/g (ww)	ng/g (ww)	ng/g (ww)
Lake Michigan	9	0.797	0.638	1.574	3.02
Lake Huron	0	0	0	0	0
Detroit River (*)	0	0	0	0	0
Lake Erie	4	0.141	0.566	0.725	0.893
Niagara River (*)	0	0	0	0	0
Lake Ontario	0	0	0	0	0
Reference Sites	0	0	0	0	0

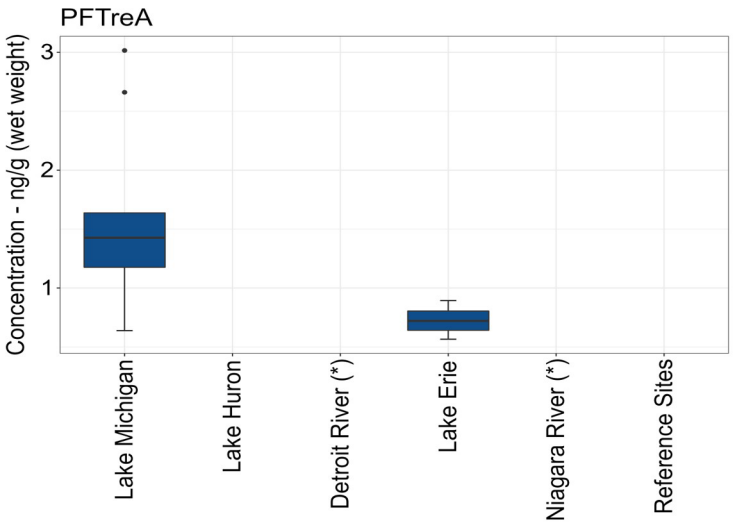

Boxplot: PFAS concentrations (ng/g wet weight) measured in dreissenid mussel tissue basin-wide between 2013 - 2018. Reference sites provides perspective to the relative PFAS concentrations found in mussel tissue basin-wide.

PFAS Characterization & Result Highlights

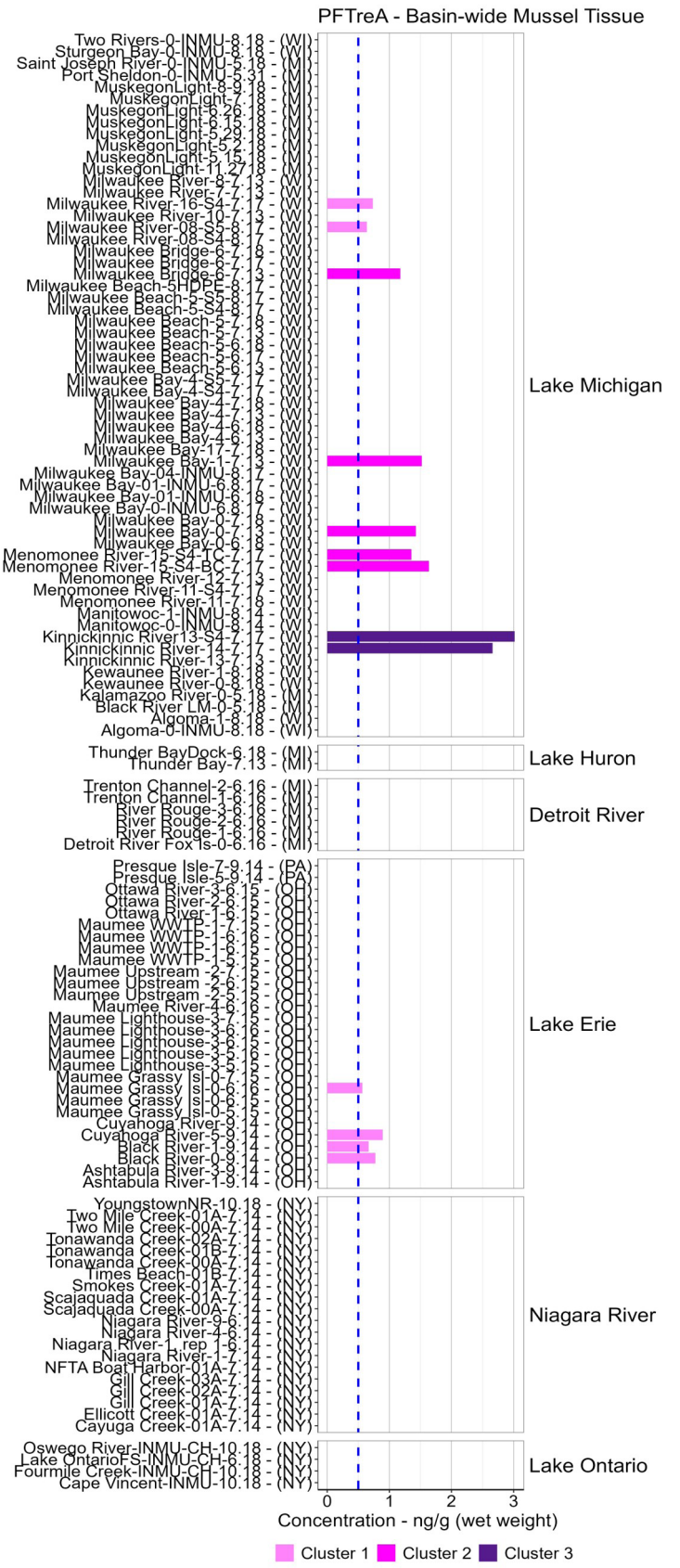

Basin-wide site tissue bar chart: PFAS contaminant concentration results (ng/g wet weight) measured (> MDL) in mussel tissue basin-wide during 2013-2018. Clusters 1-3 represents sites with low, medium and high PFAS concentrations. Blue dashed line represents concentration method detection limit (MDL). Reference line (red dashed line) represent mean reference sites concentration.

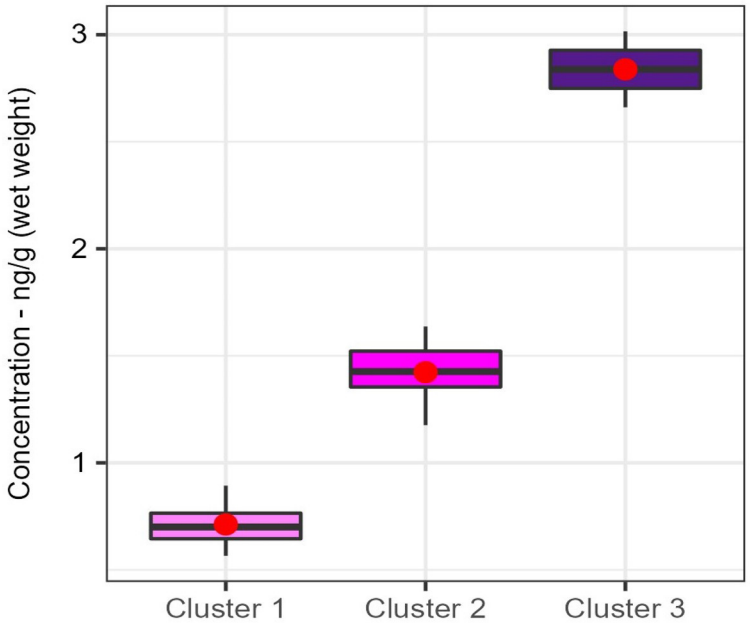

Boxplot: PFAS concentration results detected in dreissenid mussels during 2013-2018. Mean values are plotted as red points. Clusters 1-3 represent low, medium and high PFAS concentrations, respectively.

Total PFTreA Concentration (ng/g wet weight)	
Low	0.566 - 0.893
Medium	0.894 - 1.64
High	1.65 - 3.02

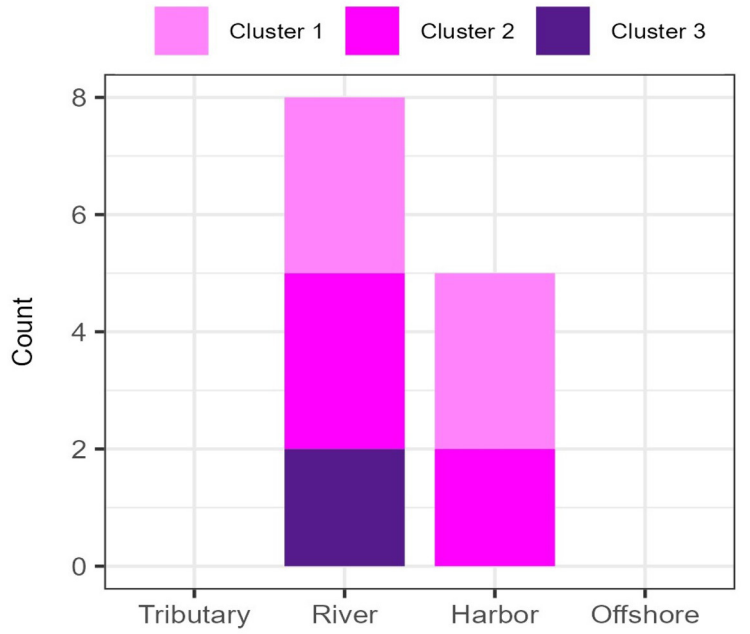

Tissue inshore - offshore bar chart: Measured PFAS composition profile detected in dreissenid mussels across inshore (tributary, river, harbor) and offshore (e.g., open-lake) Great Lakes complexes. Counts (y-axis) represents number of PFAS samples found in mussel tissue across inshore and offshore sampling locations during the 2013-2018 period.

PFAS Characterization & Result Highlights

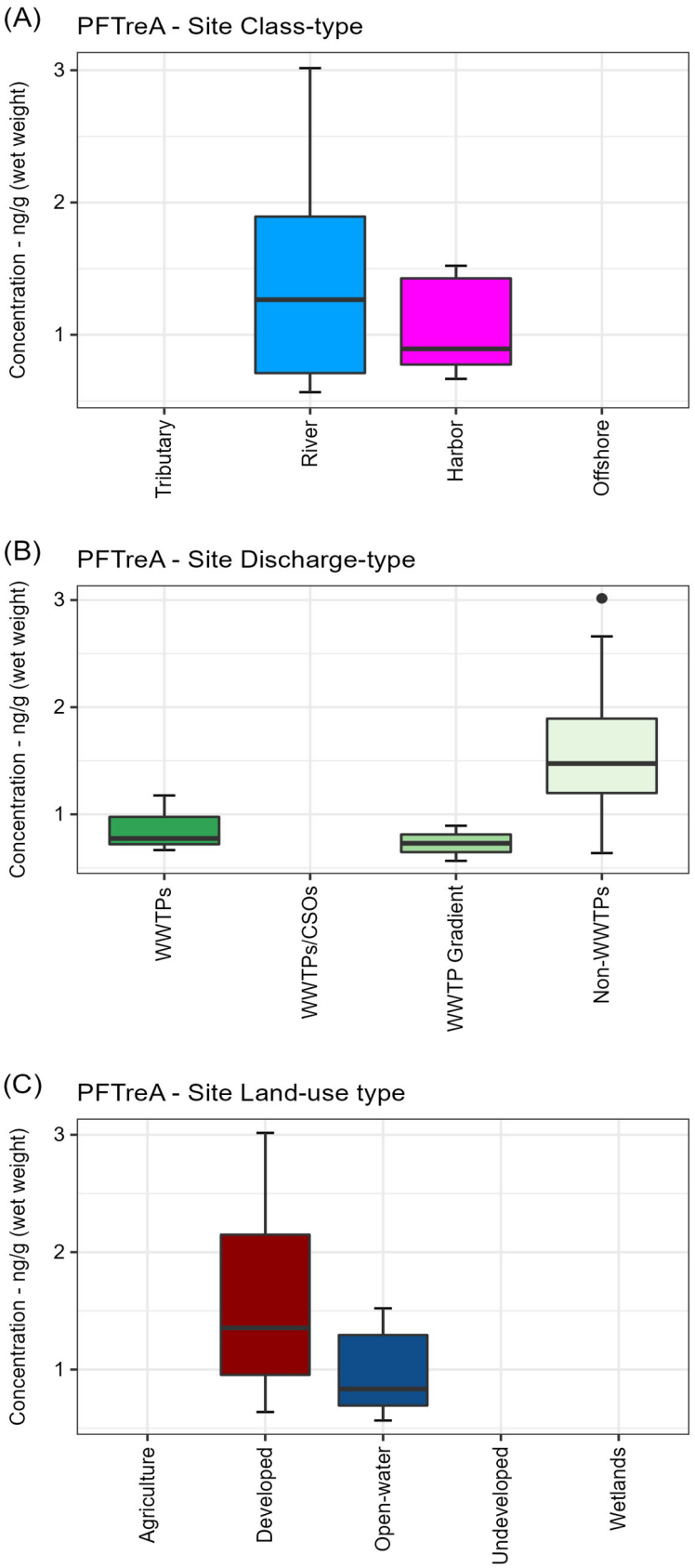

Boxplots: PFAS concentrations measured (> MDL) in mussel tissue at A) inshore and offshore sampling locations, B) designated MWP site discharge-types, and C) predominant site land-use categories/ gradients. Only compounds found at ten or more sites were included in PFAS concentration summary. Plots provide perspective on the most commonly found PFAS in mussel tissue, and their relative concentrations across various Great Lakes environmental matrices.

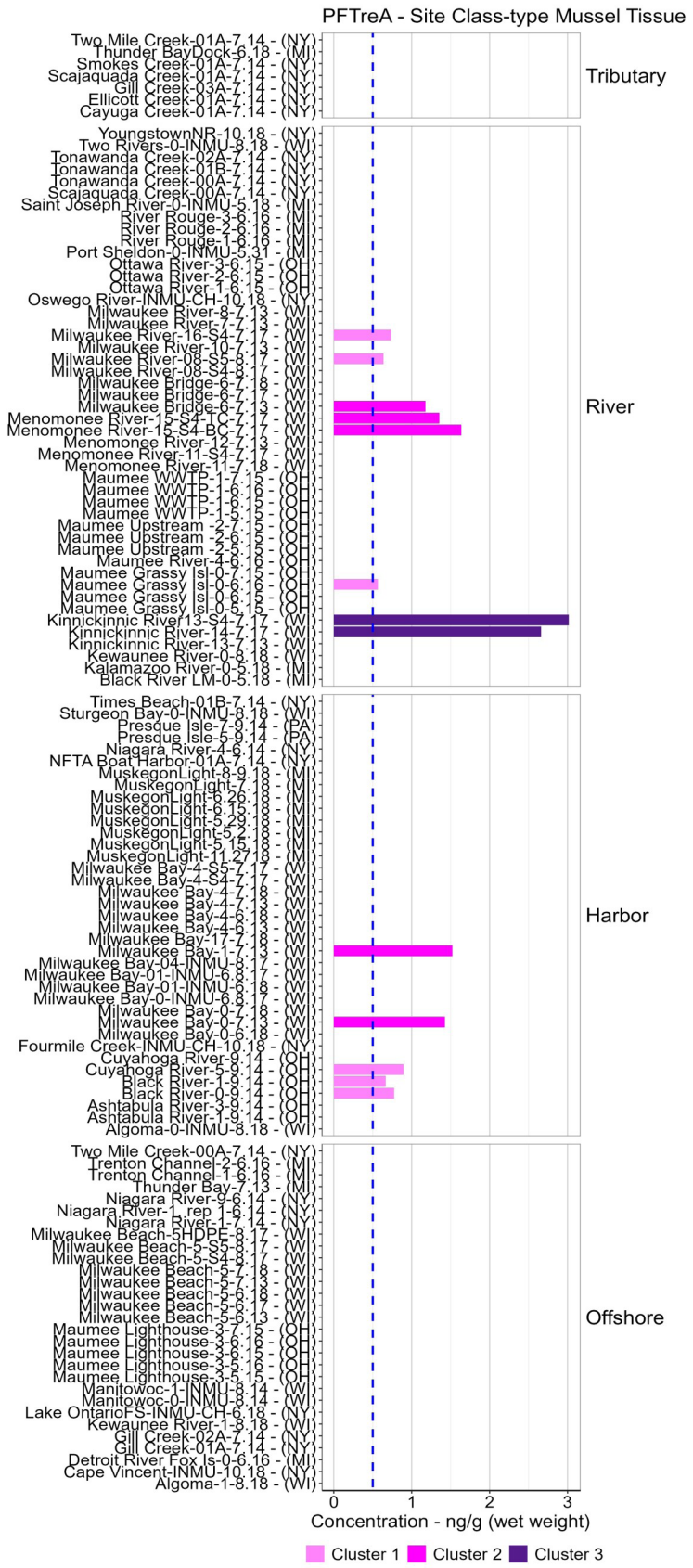

Site class-type tissue bar chart: PFAS contaminant concentration results (ng/g wet weight) measured (> MDL) in dreissenid mussels during 2013-2018 sampling event. Clusters 1-3 represents sites with low, medium and high PFAS concentrations. Blue dashed line represents concentration method detection limit (MDL). Reference line (red dashed line) represent mean reference sites concentration.

PFAS Characterization & Result Highlights

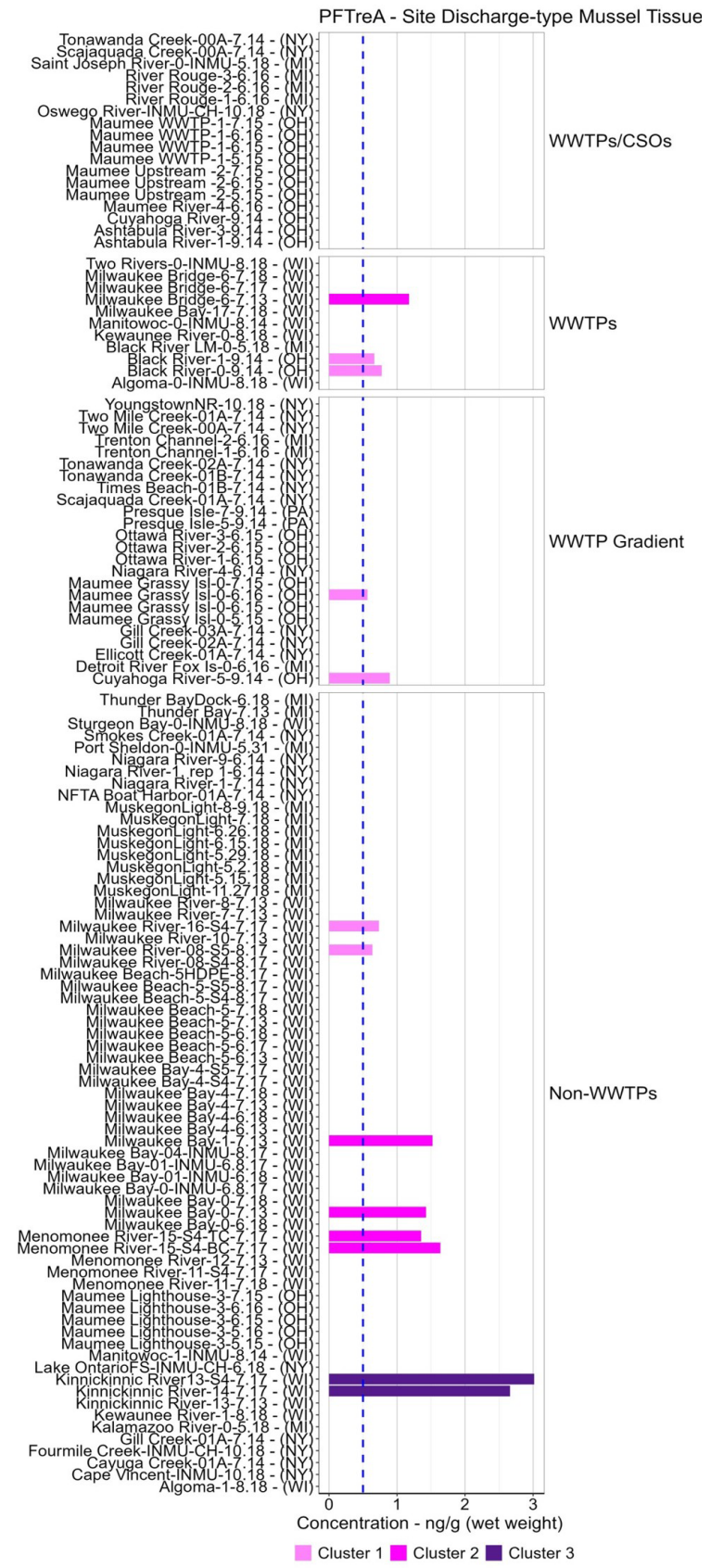

Site discharge-type tissue bar chart: PFAS contaminant concentration results (ng/g wet weight) measured (> MDL) in dreissenid mussels during 2013-2018 sampling event. Clusters 1-3 represents sites with low, medium and high PFAS concentrations. Blue dashed line represents concentration method detection limit (MDL). Reference line (red dashed line) represent mean reference sites concentration.

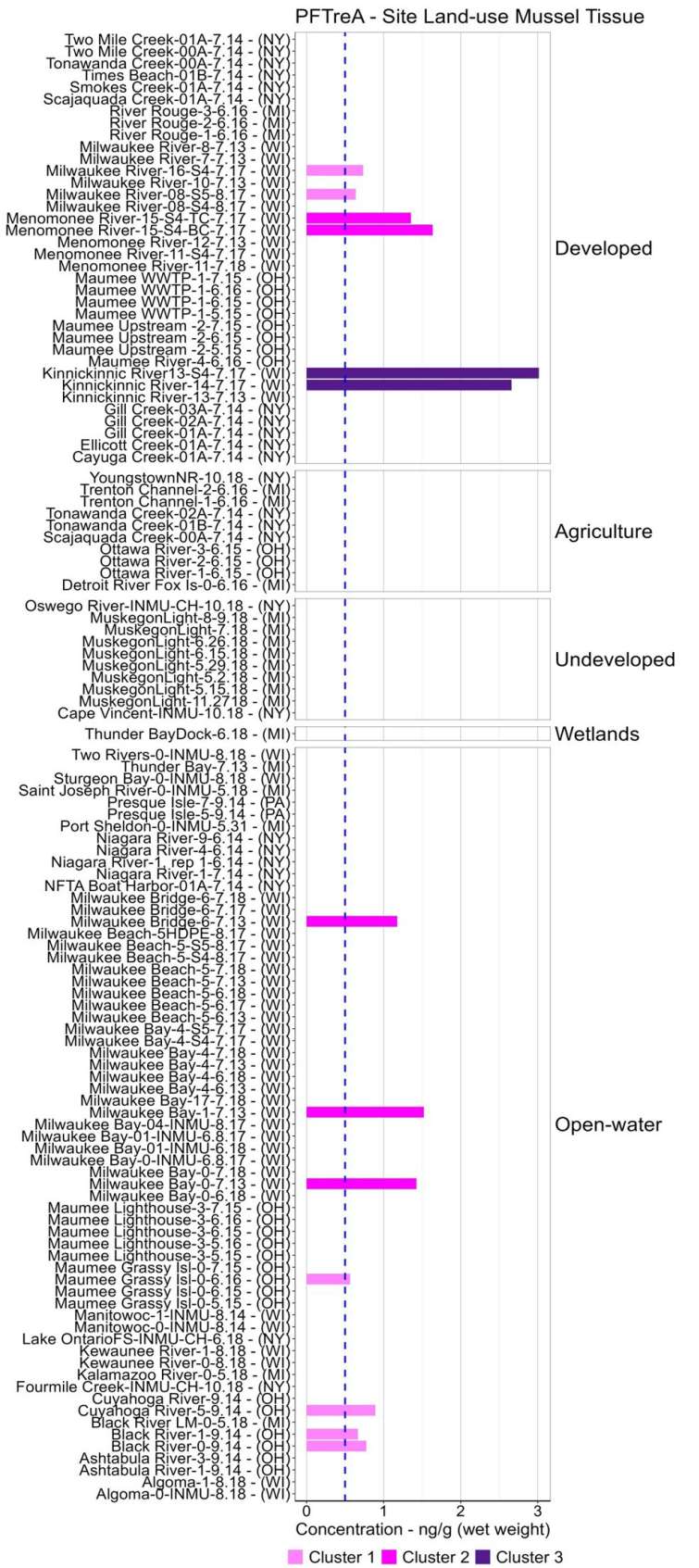

Site land-use tissue bar chart: PFAS contaminant concentration results (ng/g wet weight) measured (> MDL) in dreissenid mussels during 2013-2018 sampling event. Clusters 1-3 represents sites with low, medium and high PFAS concentrations. Blue dashed line represents concentration method detection limit (MDL). Reference line (red dashed line) represent mean reference sites concentration.

PFAS Characterization & Result Highlights

References

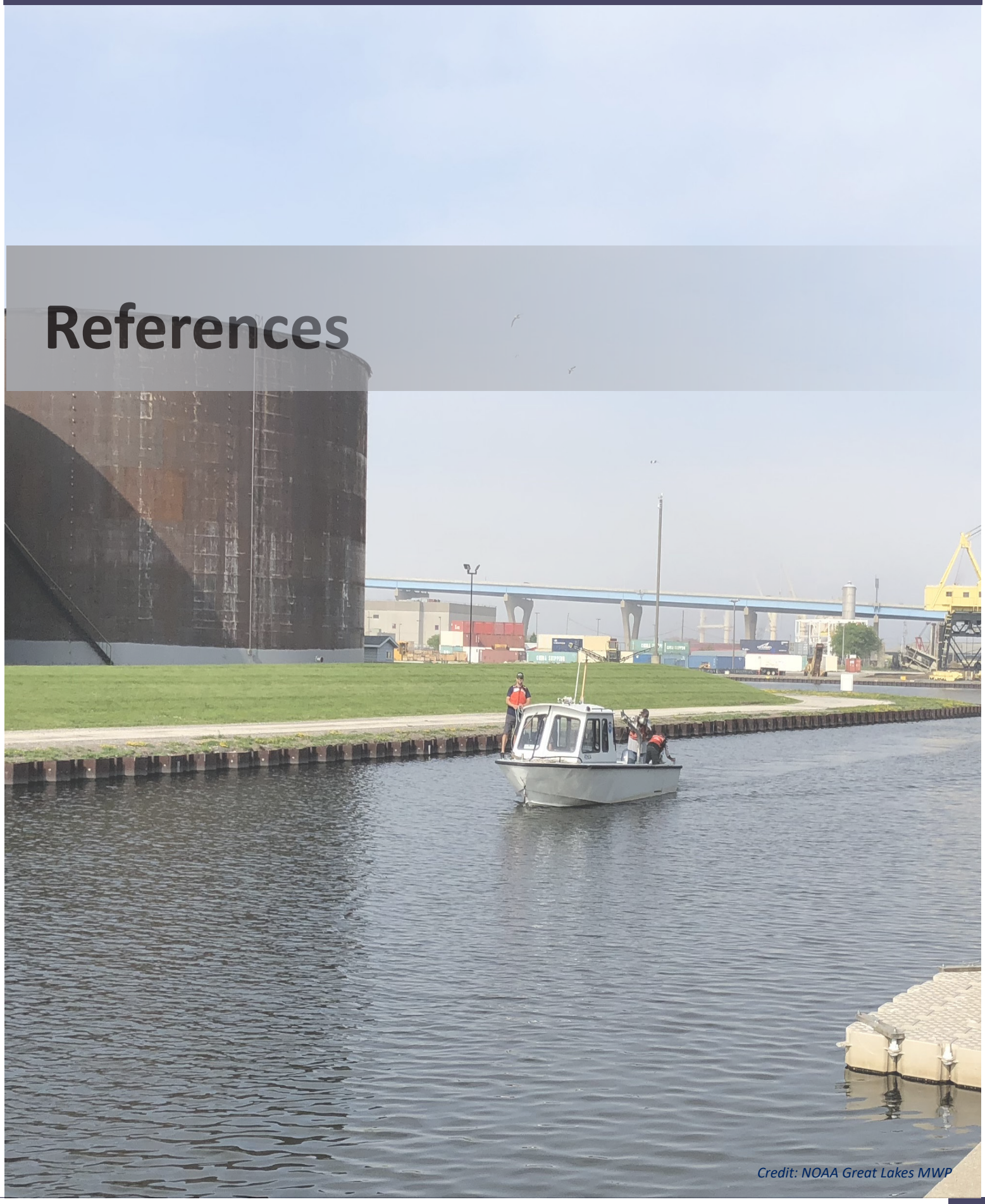

Credit: NOAA Great Lakes MWP

References

REFERENCES

Anderson J., Hardy, E. E., Roach, J. T., & Witmer, R. E. (1976). A land use and land cover classification system for use with remote sensor data. U.S.D.O.I., Geological survey professional paper 964.US Dept of Interior, Washington, DC, 1–65.

Ankley, G. T., Cureton, P., Hoke, R. A., Houde, M., Kumar, A., Kurias, J., Lanno, R., McCarthy, C., Newsted, J., Salice, C. J., Sample, B. E., Sepúlveda, M. S., Steevens, J., & Valsecchi, S. (2020). Assessing the ecological risks of per- and polyfluoroalkyl substances: current state-of-the science and a proposed Path forward. Environmental Toxicology and Chemistry, 40(3), 564–605. https://doi.org/10.1002/etc.4869

Apeti, D. A., & Lauenstein, G. G. (2006). An Assessment of Mirex Concentrations along the Southern Shorelines of the Great Lakes, USA. American Journal of Environmental Sciences, 2(3), 95–103. https://doi.org/10.3844/ajessp.2006.95.103

Awad, R., Zhou, Y., Nyberg, E., Namazkar, S., Wu, Y., Xiao, Q., Sun, Y., Zhu, Z., Bergman, Å., & Benskin, J. P. (2020). Emerging per- and polyfluoroalkyl substances (PFAS) in human milk from Sweden and China. Environmental Science: Processes & Impacts, 22(10), 2023–2030. https://doi.org/10.1039/d0em00077a

Baker, B. B., Haimbaugh, A., Sperone, F. G., Johnson, D., & Baker, T. R. (2022). Persistent contaminants of emerging concern in a great lakes urban-dominant watershed. Journal of Great Lakes Research, 48(1), 171–182. https://doi.org/10.1016/j.jglr.2021.12.001

Baldwin, A. K., Corsi, S. R., De Cicco, L. A., Lenaker, P. L., Lutz, M. A., Sullivan, D. J., & Richards, K. D. (2016). Organic contaminants in Great Lakes tributaries: Prevalence and potential aquatic toxicity. Science of the Total Environment, 554–555, 42–52. https://doi.org/10.1016/j.scitotenv.2016.02.137

Balgooyen, S., & Remucal, C. K. (2022). Tributary loading and sediment desorption as sources of PFAS to receiving waters. ACS ES & T Water, 2(3), 436–445. https://doi.org/10.1021/acsestwater.1c00348

Barber, L. B., Pickard, H. M., Alvarez, D. A., Bečanová, J., Keefe, S. H., LeBlanc, D. R., Lohmann, R., Steevens, J. A., & Vajda, A. M. (2023). Uptake of Per- and Polyfluoroalkyl Substances by Fish, Mussel, and Passive Samplers in Mobile-Laboratory Exposures Using Groundwater from a Contamination Plume at a Historical Fire Training Area, Cape Cod, Massachusetts. Environmental Science & Technology, 57(14), 5544–5557. https://doi.org/10.1021/acs.est.2c06500

Barbiero, R. P., Lesht, B. M., Hinchey, E. K., & Nettesheim, T. G. (2018). A brief history of the U.S. EPA Great Lakes National Program Office's water quality survey. Journal of Great Lakes Research, 44(4), 539–546. https://doi.org/10.1016/j.jglr.2018.05.011

Barron, M. G., Otter, R. R., Connors, K. A., Kienzler, A., & Embry, M. R. (2021). Ecological Thresholds of Toxicological Concern: a review. Frontiers in Toxicology, 3. https://doi.org/10.3389/ftox.2021.640183

Berhanu, A., Mutanda, I., Taolin, J., Qaria, M. A., Yang, B., & Zhu, D. (2023). A review of microbial degradation of per- and polyfluoroalkyl substances (PFAS): Biotransformation routes and enzymes. Science of the Total Environment, 859, 160010. https://doi.org/10.1016/j.scitotenv.2022.160010

Blagrave, K., Bailey, K., Basu, A., Benoit, N., Howell, T., & Sharma, S. (2023). Spatial heterogeneity in water quality across the northern nearshore regions of the Laurentian Great Lakes. Journal of Great Lakes Research, 49(6), 102231. https://doi.org/10.1016/j.jglr.2023.09.002

Blair, B. D., Crago, J. P., Hedman, C. J., & Klaper, R. D. (2013). Pharmaceuticals and personal care products found in the Great Lakes above concentrations of environmental concern. Chemosphere, 93(9), 2116–2123. https://doi.org/10.1016/j.chemosphere.2013.07.057

Borthakur, A., Wang, M., He, M., Ascencio, K., Blotevogel, J., Adamson, D. T., Mahendra, S., & Mohanty, S. K. (2021). Perfluoroalkyl acids on suspended particles: Significant transport pathways in surface runoff, surface waters, and subsurface soils. Journal of Hazardous Materials, 417, 126159. https://doi.org/10.1016/j.jhazmat.2021.126159

References

Boulanger, B., Vargo, J. D., Schnoor, J. L., & Hornbuckle, K. C. (2005). Evaluation of perfluorooctane surfactants in a wastewater treatment system and in a commercial surface protection product. Environmental Science & Technology, 39(15), 5524–5530. https://doi.org/10.1021/es050213u

Brase, R. A., Schwab, H. E., Li, L., & Spink, D. C. (2022). Elevated levels of per- and polyfluoroalkyl substances (PFAS) in freshwater benthic macroinvertebrates from the Hudson River Watershed. Chemosphere, 291, 132830. https://doi.org/10.1016/j.chemosphere.2021.132830

Brendel, S., Fetter, É., Staude, C., Vierke, L., & Biegel-Engler, A. (2018). Short-chained perfluoroalkyl acids: environmental concerns and a regulatory strategy under REACH. Environmental Sciences Europe, 30(1). https://doi.org/10.1186/s12302-018-0134-

Buck, R. C., Franklin, J. M., Berger, U., Conder, J. M., Cousins, I. T., De Voogt, P., Jensen, A. A., Kannan, K., Mabury, S. A., & Van Leeuwen, S. (2011). Perfluoroalkyl and polyfluoroalkyl substances in the environment: Terminology, classification, and origins. Integrated Environmental Assessment and Management, 7(4), 513–541. https://doi.org/10.1002/ieam.258

Buck, R. C., Korzeniowski, S. H., Laganis, E., & Adamsky, F. (2021). Identification and classification of commercially relevant per- and poly-fluoroalkyl substances (PFAS). Integrated Environmental Assessment and Management, 17(5), 1045–1055. https://doi.org/10.1002/ieam.4450

Byns, C., Groffen, T., & Bervoets, L. (2024). Aquatic macroinvertebrate community responses to pollution of perfluoroalkyl substances (PFAS): Can we define threshold body burdens? Science of the Total Environment, 917, 170611. https://doi.org/10.1016/j.scitotenv.2024.170611

Campo, J., Pérez, F., Masiá, A. R., Picó, Y., Farré, M., & Barceló, D. (2015). Perfluoroalkyl substance contamination of the Llobregat River ecosystem (Mediterranean area, NE Spain). Science of the Total Environment, 503–504, 48–57. https://doi.org/10.1016/j.scitotenv.2014.05.094

Capozzi, S. L., Xia, C., Shuwal, M., Miller, G. Z., Gearhart, J., Bloom, E., Gehrenkemper, L., & Venier, M. (2023). From watersheds to dinner plates: Evaluating PFAS exposure through fish consumption in Southeast Michigan. Chemosphere, 345, 140454. https://doi.org/10.1016/j.chemosphere.2023.140454

Carere, M., Antoccia, A., Buschini, A., Frenzilli, G., Marcon, F., Andreoli, C., Gorbi, G., Suppa, A., Montalbano, S., Prota, V., De Battistis, F., Guidi, P., Bernardeschi, M., Palumbo, M., Scarcelli, V., Colasanti, M., D'Ezio, V., Persichini, T., Scalici, M., . . . Mancini, L. (2021). An integrated approach for chemical water quality assessment of an urban river stretch through Effect-Based Methods and emerging pollutants analysis with a focus on genotoxicity. Journal of Environmental Management, 300, 113549. https://doi.org/10.1016/j.jenvman.2021.113549

Carvalho, J., Garrido-Maestu, A., Azinheiro, S., Fuciños, P., Barros-Velázquez, J., De Miguel, R. J., Gros, V., & Prado, M. (2021). Faster monitoring of the invasive alien species (IAS) Dreissena polymorpha in river basins through isothermal amplification. Scientific Reports, 11(1). https://doi.org/10.1038/s41598-021-89574-w

Chambers, W. S., Hopkins, J. G., & Richards, S. M. (2021). A review of per- and Polyfluorinated alkyl Substance Impairment of Reproduction. Frontiers in Toxicology, 3. https://doi.org/10.3389/ftox.2021.732436

Chen, H., Zheng, Y., Yang, X., Chen, F., Chen, J., Tang, L., Zhong, H., Magnuson, J. T., Chen, K., & Xu, E. G. (2022). Perfluorooctane sulfonamide (PFOSA) induces cardiotoxicity via aryl hydrocarbon receptor activation in zebrafish. Environmental Science & Technology, 56(12), 8438–8448. https://doi.org/10.1021/acs.est.1c08875

Choy, S. J., Annis, M. L., Banda, J, Bowman, S. R., Brigham, M. E., Elliott, S. M.,Gefell, D. J., Jankowski, M. D., Jorgenson, Z. G., Lee, K. E., Moore, J. N., & Tucker, W. A. (2017). Contaminants of Emerging Concern in the Great Lakes Basin: A report on Sediment, Water, and Fish Tissue Chemistry Collected in 2010-2012. U.S. Fish and Wildlife Service, Biological Technical Publication BTP-R3017-2013, 80 p. Retrieved from https://digitalmedia.fws.gov/digital/ collection/document/id/2192

Christensen, E. R., Wang, Y., Huo, J., & Li, A. (2022). Properties and fate and transport of persistent and mobile polar organic water pollutants: A review. Journal of Environmental Chemical Engineering, 10(2), 107201. https://doi.org/10.1016/j.jece.2022.107201

References

Chu, S., & Letcher, R. J. (2017). Side-chain fluorinated polymer surfactants in aquatic sediment and biosolid-augmented agricultural soil from the Great Lakes basin of North America. Science of the Total Environment, 607–608, 262–270. https://doi.org/10.1016/j.scitotenv.2017.06.252

Codling, G., Sturchio, N. C., Rockne, K. J., Liu, A., Peng, H., Tse, T. J., Jones, P. D., & Giesy, J. P. (2018). Spatial and temporal trends in poly- and per-fluorinated compounds in the Laurentian Great Lakes Erie, Ontario and St. Clair. Environmental Pollution, 237, 396–405. https://doi.org/10.1016/j.envpol.2018.02.013

Coffin, E. S., Reeves, D. M., & Cassidy, D. P. (2023). PFAS in municipal solid waste landfills: Sources, leachate composition, chemical transformations, and future challenges. Current Opinion in Environmental Science & Health, 31, 100418. https://doi.org/10.1016/j.coesh.2022.100418

Conder, J. M., Hoke, R. A., De Wolf, W., Russell, M. H., & Buck, R. C. (2008c). Are PFCAs Bioaccumulative? A Critical Review and Comparison with Regulatory Criteria and Persistent Lipophilic Compounds. Environmental Science & Technology, 42(4), 995–1003. https://doi.org/10.1021/es070895g

Cordner, A., De La Rosa, V. Y., Schaider, L. A., Rudel, R. A., Richter, L., & Brown, P. (2019). Guideline levels for PFOA and PFOS in drinking water: the role of scientific uncertainty, risk assessment decisions, and social factors. Journal of Exposure Science and Environmental Epidemiology, 29(2), 157–171. https://doi.org/10.1038/s41370-018-0099-9

Cordner, A., Goldenman, G., Birnbaum, L. S., Brown, P., Miller, M. F., Mueller, R., Patton, S., Salvatore, D. H., & Trasande, L. (2021). The true cost of PFAS and the benefits of acting now. Environmental Science & Technology, 55(14), 9630–9633. https://doi.org/10.1021/acs.est.1c03565

Cousins, I. T., Johansson, J., Salter, M., Sha, B., & Scheringer, M. (2022). Outside the safe operating space of a new planetary boundary for per- and polyfluoroalkyl substances (PFAS). Environmental Science & Technology, 56(16), 11172–11179. https://doi.org/10.1021/acs.est.2c02765

Coy, C. O., Steele, A. N., Abdulelah, S. A., Belanger, R. M., Crile, K. G., Stevenson, L. M., & Moore, P. A. (2022b). Differing behavioral changes in crayfish and bluegill under short- and long-chained PFAS exposures: Field study in Northern Michigan, USA. Ecotoxicology and Environmental Safety, 247, 114212. https://doi.org/10.1016/j.ecoenv.2022.114212

Custer, C. M., Custer, T. W., Delaney, R., Dummer, P. M. H., Schultz, S. L., & Karouna-Renier, N. K. (2019). Perfluoroalkyl contaminant exposure and effects in tree swallows nesting at Clarks Marsh, Oscoda, Michigan, USA. Archives of Environmental Contamination and Toxicology, 77(1), 1–13. https://doi.org/10.1007/s00244-019-00620-1

Custer, C. M., Custer, T. W., Dummer, P. M. H., Schultz, S. L., Tseng, C. Y., Karouna-Renier, N. K., & Matson, C. W. (2020). Legacy and contaminants of emerging concern in tree swallows along an agricultural to industrial gradient: Maumee River, Ohio. Environmental Toxicology and Chemistry (Print), 39(10), 1936–1952. https://doi.org/10.1002/etc.4792

Custer, C. M., Custer, T. W., Dummer, P. M. H., Schultz, S. L., Karouna-Renier, N. K., Tseng, C. Y., & Matson, C. W. (2024). Exposure to and biomarker responses from legacy and emerging contaminants along three drainages in the Milwaukee Estuary, Wisconsin, USA. Environmental Toxicology and Chemistry. https://doi.org/10.1002/etc.5822

Danz, N. P., Niemi, G. J., Regal, R. R., Hollenhorst, T., Johnson, L. B., Hanowski, J. M., Axler, R. P., Ciborowski, J. J. H., Hrabik, T., Brady, V. J., Kelly, J. R., Morrice, J. A., Brazner, J. C., Howe, R. W., Johnston, C. A., & Host, G. E. (2007). Integrated measures of anthropogenic stress in the U.S. Great Lakes Basin. Environmental Management, 39(5), 631–647. https://doi.org/10.1007/s00267-005-0293-0

Dasgupta, S., Reddam, A., Li, Y., Liu, J., & Volz, D. C. (2020). High-content screening in zebrafish identifies perfluorooctanesulfonamide as a potent developmental toxicant. Environmental Pollution, 256, 113550. https://doi.org/10.1016/j.envpol.2019.113550

Dávila-Santiago, E., Shi, C., Mahadwar, G., Medeghini, B., Insinga, L., Hutchinson, R., Good, S. P., & Jones, G. D. (2022). Machine learning applications for chemical fingerprinting and environmental source tracking using non-target chemical data. Environmental Science & Technology, 56(7), 4080–4090. https://doi.org/10.1021/acs.est.1c06655

References

De a Miranda, D., Zachritz, A. M., Whitehead, H. D., Cressman, S. R., Peaslee, G. F., & Lamberti, G. A. (2023). Occurrence and biomagnification of perfluoroalkyl substances (PFAS) in Lake Michigan fishes. Science of the Total Environment, 895, 164903. https://doi.org/10.1016/j.scitotenv.2023.164903

De Silva, A. O., Spencer, C., Scott, B., Backus, S., & Muir, D. C. (2011). Detection of a cyclic perfluorinated acid, perfluoroethylcyclohexane sulfonate, in the Great Lakes of North America. Environmental Science & Technology, 45(19), 8060–8066. https://doi.org/10.1021/es200135c

Desgens-Martin, V., Li, W., Medina, T., & Keller, A. A. (2023). Estimated influent PFAS loads to wastewater treatment plants and ambient concentrations in downstream waterbodies: case study in southern and Central California. ACS ES & T Water, 3(8), 2219–2228. https://doi.org/10.1021/acsestwater.3c00022

Dewapriya, P., Chadwick, L. E., Gorji, S. G., Schulze, B., Valsecchi, S., Samanipour, S., Thomas, K. V., & Kaserzon, S. (2023). Per- and polyfluoroalkyl substances (PFAS) in consumer products: Current knowledge and research gaps. Journal of Hazardous Materials Letters, 4, 100086. https://doi.org/10.1016/j.hazl.2023.100086

Di Nisio, A., Šabovic, I., Valente, U., Tescari, S., Rocca, M. S., Guidolin, D., Dall'Acqua, S., Acquasaliente, L., Pozzi, N., Plebani, M., Garolla, A., & Foresta, C. (2018). Endocrine disruption of androgenic activity by perfluoroalkyl substances: clinical and experimental evidence. The Journal of Clinical Endocrinology & Metabolism, 104(4), 1259–1271. https://doi.org/10.1210/jc.2018-01855

Ding, G., Zhang, J., Chen, Y., Wang, L., Wang, M., Xiong, D., & Sun, Y. (2013). Combined Effects of PFOS and PFOA on Zebrafish (Danio rerio) Embryos. Archives of Environmental Contamination and Toxicology, 64(4), 668–675. https://doi.org/10.1007/s00244-012-9864-2

Dong, H., Lu, G., Wang, X., Zhang, P., Yang, H., Yan, Z., Liu, J., & Jiang, R. (2023). Tissue-specific accumulation, depuration, and effects of perfluorooctanoic acid on fish: Influences of aqueous pH and sex. Science of the Total Environment, 861, 160567. https://doi.org/10.1016/j.scitotenv.2022.160567

ECHO, 2022. Enforcement and Compliance History Online Exporter Version 2.0. United States Environmental Protection Agency. Data Retrieved September 18, 2022. https://echo.epa.gov/(2022).

Edwards, M. A., Jacob, A., Kimbrough, K., Johnson, W., & Davenport, E. D. (2016). Great lakes mussel watch sites land-use characterization and assessment. In NOAA Technical memorandum NOS NCCOS (Vol. 208, p. 138). https://repository.library.noaa.gov/view/noaa/12942

Edwards, M. A., Kimbrough, K. L., Fuller, N. W., Davenport, E. D., Rider, M., Freitag, A., Regan, S. D., Leight, A. K., K., Burkart, H., Jacob, A., & Johnson, E. W. (2024). An assessment and characterization of pharmaceuticals and personal care products (PPCPs) within the Great Lakes Basin: Mussel Watch Program (2013–2018). Environmental Monitoring and Assessment (Print), 196(4). https://doi.org/10.1007/s10661-023-12119-3

Elgin, A., Johnson, W. E., Davenport, E., Jacob, A.,Fuller, N., Schock, T., Baylees, A., Jaruga, P. 2023. Temporal Changes in the Dreissenid Mussel Metabolome and Other Biomarkers in Relation to Environmental and Biological Factors. NOAA Technical Memorandum NOS NCCOS XXX. Silver Spring, MD. XXX pp. DOI XXX.

Elliott, S. M., Brigham, M. E., Lee, K. E., Banda, J. A., Choy, S. J., Gefell, D. J., Minarik, T. A., Moore, J. N., & Jorgenson, Z. G. (2017). Contaminants of emerging concern in tributaries to the Laurentian Great Lakes: I Patterns of Occurrence. Plos One, 12(9), e0182868. https://doi.org/10.1371/journal.pone.0182868

Eriksson, U., Haglund, P., & Kärrman, A. (2017). Contribution of precursor compounds to the release of per- and polyfluoroalkyl substances (PFASs) from waste water treatment plants (WWTPs). Journal of Environmental Sciences (China), 61, 80–90. https://doi.org/10.1016/j.jes.2017.05.004

Fraley, C., Raftery, A. E., Murphy, T. B., & Scrucca, L. (2012). Mclust version 4 for R: Normal mixture modelling for model-based clustering, classification, and density estimation. In Technical report no. 597. Department of Statistics, University of Washington. https://stat.uw.edu/sites/default/files/files/reports/2012/tr597.pdf

References

Fenton, S. E., Ducatman, A., Boobis, A., DeWitt, J. C., Lau, C., Ng, C., Smith, J. S., & Roberts, S. M. (2020). Per- and Polyfluoroalkyl Substance Toxicity and Human Health Review: Current State of Knowledge and Strategies for Informing Future Research. Environmental Toxicology and Chemistry, 40(3), 606–630. https://doi.org/10.1002/etc.4890
Fields, S. (2005). Great Lakes resource at risk. Environmental Health Perspectives, 113(3). https://doi.org/10.1289/ehp.113-a164

Fuller, N., Kimbrough, K. L., Davenport, E., Edwards, M.E., and Johnson W. E. 2023. A comparison of dreissenid mussels and passive samplers as monitors of contaminants of emerging concern and polycyclic aromatic hydrocarbons in the great lakes. NOAA Technical Memorandum NOS NCCOS 317 Silver Spring, MD. 40 pp. DOI 10.25923/kk5w-3r94.

Gaballah, S., Swank, A., Sobus, J. R., Howey, X. M., Schmid, J., Catron, T., McCord, J., Hines, E., Strynar, M., & Tal, T. (2020). Evaluation of developmental toxicity, developmental neurotoxicity, and tissue dose in zebrafish exposed to GenX and other PFAS. Environmental Health Perspectives, 128(4). https://doi.org/10.1289/ehp5843

Gagliano, E., Sgroi, M., Falciglia, P. P., Vagliasindi, F. G., & Roccaro, P. (2020). Removal of poly- and perfluoroalkyl substances (PFAS) from water by adsorption: Role of PFAS chain length, effect of organic matter and challenges in adsorbent regeneration. Water Research, 171, 115381. https://doi.org/10.1016/j.watres.2019.115381
Gaines, L. G. T. (2022). Historical and current usage of per- and polyfluoroalkyl substances (PFAS): A literature review. American Journal of Industrial Medicine, 66(5), 353–378. https://doi.org/10.1002/ajim.23362

Garcia, S. N., Clubbs, R. L., Stanley, J. K., Scheffe, B., Yelderman, J. C., & Brooks, B. W. (2013). Comparative analysis of effluent water quality from a municipal treatment plant and two on-site wastewater treatment systems. Chemosphere, 92(1), 38–44. https://doi.org/10.1016/j.chemosphere.2013.03.007
Gebbink, W. A., Glynn, A., & Berger, U. (2015). Temporal changes (1997–2012) of perfluoroalkyl acids and selected precursors (including isomers) in Swedish human serum. Environmental Pollution, 199, 166–173. https://doi.org/10.1016/j.envpol.2015.01.024

George, S. E., Baker, T. R., & Baker, B. B. (2023). Nonlethal detection of PFAS bioaccumulation and biomagnification within fishes in an urban- and wastewater-dominant Great Lakes watershed. Environmental Pollution, 321, 121123. https://doi.org/10.1016/j.envpol.2023.121123

Gewurtz, S. B., Bradley, L., Backus, S., Dove, A., McGoldrick, D. J., Hung, H., & Dryfhout-Clark, H. (2019). Perfluoroalkyl acids in great lakes precipitation and surface water (2006–2018) indicate response to phase-outs, regulatory action, and variability in fate and transport processes. Environmental Science & Technology, 53(15), 8543–8552. https://doi.org/10.1021/acs.est.9b01337

Ghedotti, M. J., Smihula, J. C., & Smith, G. R. (1995). Zebra mussel predation by round gobies in the laboratory. Journal of Great Lakes Research, 21(4), 665–669. https://doi.org/10.1016/s0380-1330(95)71076-0

Giesy, J. P., Mabury, S. A., Martin, J. W., Kannan, K., Jones, P. D., Newsted, J. L., & Coady, K. (2006). Perfluorinated compounds in the Great Lakes. In Springer eBooks (pp. 391–438). https://doi.org/10.1007/698_5_046
Giffard, N., Gitlin, S. A., Rardin, M., Petali, J., Chen, C. Y., & Romano, M. E. (2022). Occurrence and risks of per- and polyfluoroalkyl substances in shellfish. Current Environmental Health Reports, 9(4), 591–603. https://doi.org/10.1007/s40572-022-00379-z

Goodrum, P. E., Anderson, J. K., Luz, A. L., & Ansell, G. K. (2020). Application of a Framework for Grouping and Mixtures Toxicity Assessment of PFAS: A Closer Examination of Dose-Additivity Approaches. Toxicological Sciences, 179(2), 262–278. https://doi.org/10.1093/toxsci/kfaa123

Goodrow, S. M., Ruppel, B., Lippincott, R. L., Post, G. B., & Procopio, N. A. (2020). Investigation of levels of perfluoroalkyl substances in surface water, sediment and fish tissue in New Jersey, USA. Science of the Total Environment, 729, 138839. https://doi.org/10.1016/j.scitotenv.2020.138839

Gomis, M., Wang, Z., Scheringer, M., & Cousins, I. T. (2015). A modeling assessment of the physicochemical properties and environmental fate of emerging and novel per- and polyfluoroalkyl substances. Science of the Total Environment, 505, 981–991. https://doi.org/10.1016/j.scitotenv.2014.10.062

References

Guida, Y., Torres, F. B. M., Barizon, R. R. M., Assalin, M. R., & Rosa, M. A. (2023). Confirming sulfluramid (EtFOSA) application as a precursor of perfluorooctanesulfonic acid (PFOS) in Brazilian agricultural soils. Chemosphere, 325, 138370. https://doi.org/10.1016/j.chemosphere.2023.138370

Guo, R., Megson, D., Myers, A. L., Helm, P. A., Märvin, C. H., Crozier, P. W., Mabury, S. A., Bhavsar, S. P., Tomy, G. T., Simcik, M. F., McCarry, B. E., & Reiner, E. J. (2016). Application of a comprehensive extraction technique for the determination of poly- and perfluoroalkyl substances (PFASs) in Great Lakes Region sediments. Chemosphere, 164, 535–546. https://doi.org/10.1016/j.chemosphere.2016.08.126

Guo, X., Zhang, S., Lu, S., Zheng, B., Xie, P., Chen, J., Li, G., Liu, C., Wu, Q., Cheng, H., & Sang, N. (2018). Perfluorododecanoic acid exposure induced developmental neurotoxicity in zebrafish embryos. Environmental Pollution, 241, 1018–1026. https://doi.org/10.1016/j.envpol.2018.06.013

Hamid, H., Li, L. Y., & Grace, J. R. (2018). Review of the fate and transformation of per- and polyfluoroalkyl substances (PFASs) in landfills. Environmental Pollution (1987), 235, 74–84. https://doi.org/10.1016/j.envpol.2017.12.030

Hamid, N., Junaid, M., Sultan, M., Yoganandham, S. T., & Chuan, O. M. (2024). The untold story of PFAS alternatives: Insights into the occurrence, ecotoxicological impacts, and removal strategies in the aquatic environment. Water Research, 250, 121044. https://doi.org/10.1016/j.watres.2023.121044

Hartig, J. H., Krantzberg, G., & Alsip, P. (2020). Thirty-five years of restoring Great Lakes Areas of Concern: Gradual progress, hopeful future. Journal of Great Lakes Research, 46(3), 429–442. https://doi.org/10.1016/j.jglr.2020.04.004

Hedgespeth, M. L., Taylor, D., Balint, S., Schwartz, M., & Cantwell, M. G. (2023). Ecological characteristics impact PFAS concentrations in a U.S. North Atlantic food web. Science of the Total Environment, 880, 163302. https://doi.org/10.1016/j.scitotenv.2023.163302

Helmer, R. W., Reeves, D. M., & Cassidy, D. P. (2022). Per- and Polyfluorinated Alkyl Substances (PFAS) cycling within Michigan: Contaminated sites, landfills and wastewater treatment plants. Water Research, 210, 117983. https://doi.org/10.1016/j.watres.2021.117983

Hladik, M. L., Corsi, S. R., Kolpin, D. W., Baldwin, A. K., Blackwell, B. R., & Cavallin, J. E. (2018b). Year-round presence of neonicotinoid insecticides in tributaries to the Great Lakes, USA. Environmental Pollution, 235, 1022–1029. https://doi.org/10.1016/j.envpol.2018.01.013

Hoke, R. A., Bouchelle, L. D., Ferrell, B. D., & Buck, R. C. (2012b). Comparative acute freshwater hazard assessment and preliminary PNEC development for eight fluorinated acids. Chemosphere, 87(7), 725–733. https://doi.org/10.1016/j.chemosphere.2011.12.066

Houtz, E., & Sedlak, D. L. (2012). Oxidative conversion as a means of detecting precursors to perfluoroalkyl acids in urban runoff. Environmental Science & Technology, 46(17), 9342–9349. https://doi.org/10.1021/es302274g

Hu, W., Zhang, M., Liu, L., Zhang, Z., & Guo, Y. (2023). Perfluoroalkyl and polyfluoroalkyl substances (PFASs) crossing the blood-cerebrospinal fluid barrier: Their occurrence in human cerebrospinal fluid. Journal of Hazardous Materials, 442, 130003. https://doi.org/10.1016/j.jhazmat.2022.130003

Hull, R. N., Kleywegt, S., & Schroeder, J. (2015). Risk-based screening of selected contaminants in the Great Lakes Basin. Journal of Great Lakes Research, 41(1), 238–245. https://doi.org/10.1016/j.jglr.2014.11.013

Hu, X. C., Dassuncao, C., Zhang, X., Grandjean, P., Weihe, P., Webster, G. M., Nielsen, F., & Sunderland, E. M. (2018). Can profiles of poly- and Perfluoroalkyl substances (PFASs) in human serum provide information on major exposure sources? Environmental Health, 17(1). https://doi.org/10.1186/s12940-018-0355-4

Huang, M., Ivantsova, E., Konig, I., Patel, N., English, C., Souders, C. L., & Martyniuk, C. J. (2023). Developmental and mitochondrial toxicity assessment of perfluoroheptanoic acid (PFHpA) in zebrafish (Danio rerio). Environmental Toxicology and Pharmacology, 97, 104037. https://doi.org/10.1016/j.etap.2022.104037

References

Jasechko, S., Gibson, J. J., & Edwards, T. W. (2014). Stable isotope mass balance of the Laurentian Great Lakes. Journal of Great Lakes Research, 40(2), 336–346. https://doi.org/10.1016/j.jglr.2014.02.020

Jetoo, S., & Krantzberg, G. (2014). A SWOT Analysis of the Great Lakes Water Quality Protocol 2012: The Good, the Bad and the Opportunity. Electronic Green Journal, 1(37). https://doi.org/10.5070/g313724071

Jo, A., Ji, K., & Choi, K. (2014). Endocrine disruption effects of long-term exposure to perfluorodecanoic acid (PFDA) and perfluorotridecanoic acid (PFTrDA) in zebrafish (Danio rerio) and related mechanisms. Chemosphere, 108, 360–366. https://doi.org/10.1016/j.chemosphere.2014.01.080

Joensen, U. N., Bossi, R., Leffers, H., Jensen, A. A., Skakkebæk, N. E., & Jørgensen, N. (2009). Do perfluoroalkyl compounds impair human semen quality? Environmental Health Perspectives, 117(6), 923–927. https://doi.org/10.1289/ehp.0800517

Johnson, G. R. (2022). PFAS in soil and groundwater following historical land application of biosolids. Water Research, 211, 118035. https://doi.org/10.1016/j.watres.2021.118035

Kannan, K., Lin, T., Sinclair, E., Pastva, S. D., Jude, D. J., & Giesy, J. P. (2005). Perfluorinated compounds in aquatic organisms at various trophic levels in a great lakes food chain. Archives of Environmental Contamination and Toxicology, 48(4), 559–566. https://doi.org/10.1007/s00244-004-0133-x

Khairy, M. A., Muir, D. C., Teixeira, C., & Lohmann, R. (2014). Spatial trends, sources, and Air–Water exchange of organochlorine pesticides in the Great Lakes basin using low density polyethylene passive samplers. Environmental Science & Technology, 48(16), 9315–9324. https://doi.org/10.1021/es501686a

Kiesling, R. L., Elliott, S. M., Kammel, L. E., Choy, S. J., & Hummel, S. L. (2019). Predicting the occurrence of chemicals of emerging concern in surface water and sediment across the U.S. portion of the Great Lakes Basin. Science of the Total Environment, 651, 838–850. https://doi.org/10.1016/j.scitotenv.2018.09.201

Kiesling, R. L., Elliott, S. M., Kennedy, J. L., & Hummel, S. L. (2022). Validation of a vulnerability index of exposure to chemicals of emerging concern in surface water and sediment of Great Lakes tributaries of the United States. Science of the Total Environment, 830, 154618. https://doi.org/10.1016/j.scitotenv.2022.154618

Kimbrough, K, L., Johnson, W, E., Jacob, A, P., and Lauenstein, G, G., (2013). Contaminant Concentrations in Dreissenid Mussels from the Laurentian Great Lakes: A Summary of Trends from the Mussel Watch Program. In CRC Press eBooks (pp. 297–310). https://doi.org/10.1201/b15437-26

Kimbrough, K., Johnson, W. E., Jacob, A., Edwards, M., Davenport, E., Lauenstein, G., Nalepa, T., Fulton, M., & Pait, A. (2014). Mussel watch great lakes contaminant monitoring and assessment: Phase 1. In Silver Spring, MD. NOAA technical memorandum NOS NCCOS 180, 113 pp. https://repository.library.noaa.gov/view/noaa/4834

Kimbrough, K., Johnson, W. E., Jacob, A., Edwards, M., & Davenport, E. (2018). Great Lakes mussel watch: Assessment of contaminants of emerging concern. In NOAA technical memorandum NOS NCCOS 249 (p. 66). https://doi.org/10.25923/2jp9-pn57

Klečka, G., Persoon, C., & Currie, R. (2010). Chemicals of emerging concern in the Great Lakes Basin: An analysis of environmental exposures. In Reviews of environmental contamination and toxicology (pp. 1–93). https://doi.org/10.1007/978-1-4419-6406-9_1

Kleywegt, S., Raby, M., McGill, S., & Helm, P. A. (2020). The impact of risk management measures on the concentrations of per- and polyfluoroalkyl substances in source and treated drinking waters in Ontario, Canada. Science of the Total Environment, 748, 141195. https://doi.org/10.1016/j.scitotenv.2020.141195

Knox, S. S., Jackson, T., Javins, B., Frisbee, S. J., Shankar, A., & Ducatman, A. M. (2011). Implications of early menopause in women exposed to perfluorocarbons. The Journal of Clinical Endocrinology and Metabolism/Journal of Clinical Endocrinology & Metabolism, 96(6), 1747–1753. https://doi.org/10.1210/jc.2010-2401

References

Koban, L. A., King, T., Huff, T. B., Furst, K. E., Nelson, T. R., Pfluger, A. R., Kuppa, M., & Fowler, A. E. (2024b). Passive biomonitoring for Per- and Polyfluoroalkyl substances using invasive clams, C. fluminea. Journal of Hazardous Materials, 134463. https://doi.org/10.1016/j.jhazmat.2024.134463

Koch, A., Kärrman, A., Yeung, L. W. Y., Jonsson, M., Ahrens, L., & Wang, T. (2019). Point source characterization of per- and polyfluoroalkyl substances (PFASs) and extractable organofluorine (EOF) in freshwater and aquatic invertebrates. Environmental Science. Processes & Impacts, 21(11), 1887–1898. https://doi.org/10.1039/c9em00281b

Kolpin, D. W., Hubbard, L., Cwiertny, D. M., Meppelink, S. M., Thompson, D. A., & Gray, J. L. (2021). A comprehensive statewide spatiotemporal stream assessment of per- and polyfluoroalkyl substances (PFAS) in an agricultural region of the United States. Environmental Science & Technology Letters, 8(11), 981–988. https://doi.org/10.1021/acs.estlett.1c00750

Kotthoff, M., Müller, J., Jürling, H., Schlummer, M., & Fiedler, D. (2015). Perfluoroalkyl and polyfluoroalkyl substances in consumer products. Environmental Science and Pollution Research International, 22(19), 14546–14559. https://doi.org/10.1007/s11356-015-4202-7

Kurwadkar, S., Dane, J., Kanel, S. R., Nadagouda, M. N., Cawdrey, R. W., Ambade, B., Struckhoff, G. C., & Wilkin, R. T. (2022). Per- and polyfluoroalkyl substances in water and wastewater: A critical review of their global occurrence and distribution. Science of the Total Environment, 809, 151003. https://doi.org/10.1016/j.scitotenv.2021.151003

Labine, L. M., Pereira, E. a. O., Kleywegt, S., Jobst, K. J., Simpson, A. J., & Simpson, M. J. (2022). Comparison of sub-lethal metabolic perturbations of select legacy and novel perfluorinated alkyl substances (PFAS) in Daphnia magna. Environmental Research, 212, 113582. https://doi.org/10.1016/j.envres.2022.113582

Laitta, M. T. (2016). Waste water treatment plants in the Great Lakes. Retrieved May 16, 2024, from: https://usgs.maps.arcgis.com/home/item.html?id=e4a5b201232944c2a671eb96621274dd

Lalonde, B., & Garron, C. (2022). Perfluoroalkyl substances (PFASs) in the Canadian freshwater environment. Archives of Environmental Contamination and Toxicology, 82(4), 581–591. https://doi.org/10.1007/s00244-022-00922-x

Langberg, H. A., Arp, H. P. H., Breedveld, G. D., Slinde, G. A., Høisæter, Å., Grønning, H. M., Jartun, M., Rundberget, T., Jenssen, B. M., & Hale, S. E. (2021). Paper product production identified as the main source of per- and polyfluoroalkyl substances (PFAS) in a Norwegian lake: Source and historic emission tracking. Environmental Pollution, 273, 116259. https://doi.org/10.1016/j.envpol.2020.116259

Larson, J. H., Trebitz, A. S., Steinman, A. D., Wiley, M. J., Mazur, M. C., Pebbles, V., Braun, H. A., & Seelbach, P. W. (2013). Great Lakes rivermouth ecosystems: Scientific synthesis and management implications. Journal of Great Lakes Research, 39(3), 513–524. https://doi.org/10.1016/j.jglr.2013.06.002

Lasee, S., McDermett, K., Kumar, N., Guelfo, J., Payton, P., Zhao, Y., & Anderson, T. A. (2022). Targeted analysis and Total Oxidizable Precursor assay of several insecticides for PFAS. Journal of Hazardous Materials Letters, 3, 100067. https://doi.org/10.1016/j.hazl.2022.100067

Lee, J. W., Lee, H., Lim, J. M., & Moon, H. (2020). Legacy and emerging per- and polyfluoroalkyl substances (PFASs) in the coastal environment of Korea: Occurrence, spatial distribution, and bioaccumulation potential. Chemosphere, 251, 126633. https://doi.org/10.1016/j.chemosphere.2020.126633

Lee, Y., Lee, J., Kim, M., Yang, H., Lee, J., Son, Y., Kho, Y., Choi, K., & Zoh, K. (2020). Concentration and distribution of per- and polyfluoroalkyl substances (PFAS) in the Asan Lake area of South Korea. Journal of Hazardous Materials, 381, 120909. https://doi.org/10.1016/j.jhazmat.2019.120909

Leung, S. C. E., Shukla, P., Chen, D., Eftekhari, E., An, H., Zare, F., Ghasemi, N., Zhang, D., Nguyen, N., & Q, L. (2022). Emerging technologies for PFOS/PFOA degradation and removal: A review. Science of the Total Environment, 827, 153669. https://doi.org/10.1016/j.scitotenv.2022.153669

References

Lewis, A. J., Yun, X., Spooner, D. E., Kurz, M. J., McKenzie, E. R., & Sales, C. M. (2022). Exposure pathways and bioaccumulation of per- and polyfluoroalkyl substances in freshwater aquatic ecosystems: Key considerations. Science of the Total Environment, 822, 153561. https://doi.org/10.1016/j.scitotenv.2022.153561

Li, F., Duan, J., Tian, S., Ji, H., Zhu, Y., Wei, Z., & Zhao, D. (2020). Short-chained per- and polyfluoroalkyl substances in aquatic systems: Occurrence, impacts and treatment. Chemical Engineering Journal, 380, 122506. https://doi.org/10.1016/j.cej.2019.122506

Lin, Y., Capozzi, S. L., Li, L., & Rodenburg, L. A. (2021). Source apportionment of perfluoroalkyl substances in Great Lakes fish. Environmental Pollution, 290, 118047. https://doi.org/10.1016/j.envpol.2021.118047

Link, G. W., Reeves, D. M., Cassidy, D. P., & Coffin, E. S. (2024). Per- and polyfluoroalkyl substances (PFAS) in final treated solids (Biosolids) from 190 Michigan wastewater treatment plants. Journal of Hazardous Materials, 463, 132734. https://doi.org/10.1016/j.jhazmat.2023.132734

Liu, Y., Wang, J., Wei, Y., Zhang, H., Xu, M., & Dai, J. (2008). Induction of time-dependent oxidative stress and related transcriptional effects of perfluorododecanoic acid in zebrafish liver. Aquatic Toxicology, 89(4), 242–250. https://doi.org/10.1016/j.aquatox.2008.07.009

Liu, C., Chang, V. W., Gin, K. Y., & Nguyen, V. T. (2014). Genotoxicity of perfluorinated chemicals (PFCs) to the green mussel (Perna viridis). Science of the Total Environment, 487, 117–122. https://doi.org/10.1016/j.scitotenv.2014.04.017

Liu, X., Liu, S., Qiu, W., Magnuson, J. T., Liu, Z., Yang, G., Chen, H., Liu, Y., Xu, X., & Chen, K. (2022). Cardiotoxicity of PFOA, PFOS, and PFOSA in early life stage Zebrafish: Molecular changes to behavioral-level response. Sustainable Horizons, 3, 100027. https://doi.org/10.1016/j.horiz.2022.100027

Llewellyn, M. J., Griffin, E. K., Caspar, R. J., Timshina, A. S., Bowden, J. A., Miller, C. J., Baker, B. B., & Baker, T. R. (2024). Identification and quantification of novel per- and polyfluoroalkyl substances (PFAS) contamination in a Great Lakes urban-dominated watershed. Science of the Total Environment, 173325. https://doi.org/10.1016/j.scitotenv.2024.173325

Logeshwaran, P., Sivaram, A. K., Surapaneni, A., Kannan, K., Naidu, R., & Megharaj, M. (2021). Exposure to perfluorooctanesulfonate (PFOS) but not perfluorooctanoic acid (PFOA) at ppb concentration induces chronic toxicity in Daphnia carinata. Science of the Total Environment, 769, 144577. https://doi.org/10.1016/j.scitotenv.2020.144577

Longpré, D., Lorusso, L., Levicki, C., Carrier, R., & Cureton, P. (2020). PFOS, PFOA, LC-PFCAS, and certain other PFAS: A focus on Canadian guidelines and guidance for contaminated sites management. Environmental Technology and Innovation, 18, 100752. https://doi.org/10.1016/j.eti.2020.100752

Luo, K., Liu, X., Nian, M., Wang, Y., Qiu, J., Yu, H., Chen, X., & Zhang, J. (2021). Environmental exposure to per- and polyfluoroalkyl substances mixture and male reproductive hormones. Environment International, 152, 106496. https://doi.org/10.1016/j.envint.2021.106496

Ma, T., Ye, C., Wang, T., Li, X., & Luo, Y. (2022b). Toxicity of per- and polyfluoroalkyl substances to aquatic invertebrates, planktons, and microorganisms. International Journal of Environmental Research and Public Health/International Journal of Environmental Research and Public Health, 19(24), 16729. https://doi.org/10.3390/ijerph192416729

Ma, T., Wu, P., Wang, L., Li, Q., Li, X., & Luo, Y. (2023). Toxicity of per- and polyfluoroalkyl substances to aquatic vertebrates. Frontiers in Environmental Science, 11. https://doi.org/10.3389/fenvs.2023.1101100

Mahoney, H., Xie, Y., Brinkmann, M., & Giesy, J. P. (2022). Next generation per- and poly-fluoroalkyl substances: Status and trends, aquatic toxicity, and risk assessment. Eco-environment & Health, 1(2), 117–131. https://doi.org/10.1016/j.eehl.2022.05.002

Maine Department of Agriculture, Conservation and Forestry. (2022). PFAS Container Contamination Updates. https://www.maine.gov/dacf/php/pesticides/documents2/bd_mtgs/Oct22/3a-2022%20PFAS%20October%20Memo%20Tox.pdf. Accessed 6.1.2024.

References

Menger, F., Pohl, J., Ahrens, L., Carlsson, G., & Örn, S. (2020). Behavioural effects and bioconcentration of per- and polyfluoroalkyl substances (PFASs) in zebrafish (Danio rerio) embryos. Chemosphere, 245, 125573. https://doi.org/10.1016/j.chemosphere.2019.125573

Miranda, D. A., Zachritz, A. M., Whitehead, H. D., Cressman, S. R., Peaslee, G. F., & Lamberti, G. A. (2023b). Occurrence and biomagnification of perfluoroalkyl substances (PFAS) in Lake Michigan fishes. Science of the Total Environment, 895, 164903. https://doi.org/10.1016/j.scitotenv.2023.164903

Mokra, K. (2021). Endocrine Disruptor Potential of Short- and Long-chained Perfluoroalkyl Substances (PFASs)—A Synthesis of Current Knowledge with Proposal of Molecular Mechanism. International Journal of Molecular Sciences, 22(4), 2148. https://doi.org/10.3390/ijms22042148

Morrice, J. A., Danz, N. P., Regal, R. R., Kelly, J. R., Niemi, G. J., Reavie, E. D., Hollenhorst, T., Axler, R. P., Trebitz, A. S., Cotter, A. M., & Peterson, G. S. (2007). Human influences on water quality in Great Lakes coastal wetlands. Environmental Management, 41(3), 347–357. https://doi.org/10.1007/s00267-007-9055-5

Muir, D., & Miaz, L. T. (2021). Spatial and temporal trends of perfluoroalkyl substances in global ocean and coastal waters. Environmental Science & Technology, 55(14), 9527–9537. https://doi.org/10.1021/acs.est.0c08035

Munoz, G., Budzinski, H., Babut, M., Drouineau, H., Lauzent, M., Ménach, K. L., Lobry, J., Selleslagh, J., Simonnet-Laprade, C., & Labadie, P. (2017). Evidence for the trophic transfer of perfluoroalkylated substances in a temperate macrotidal estuary. Environmental Science & Technology, 51(15), 8450–8459. https://doi.org/10.1021/acs.est.7b02399

Munoz, G., Mercier, L., Duy, S. V., Liu, J., Sauvé, S., & Houde, M. (2022). Bioaccumulation and trophic magnification of emerging and legacy per- and polyfluoroalkyl substances (PFAS) in a St. Lawrence River food web. Environmental Pollution (1987), 309, 119739. https://doi.org/10.1016/j.envpol.2022.119739

Munschy, C., Marchand, P., Vénisseau, A., Veyrand, B., & Zendong, Z. (2013). Levels and trends of the emerging contaminants HBCDs (hexabromocyclododecanes) and PFCs (perfluorinated compounds) in marine shellfish along French coasts. Chemosphere, 91(2), 233–240. https://doi.org/10.1016/j.chemosphere.2012.12.063

Munschy, C., Bely, N., Pollono, C., & Aminot, Y. (2019). Perfluoroalkyl substances (PFASs) in the marine environment: Spatial distribution and temporal profile shifts in shellfish from French coasts. Chemosphere, 228, 640–648. https://doi.org/10.1016/j.chemosphere.2019.04.205

Murphy, C. A., Bhavsar, S. P., & Gandhi, N. (2012). Contaminants in Great Lakes fish: historic, current, and emerging concerns. In: Great Lakes Fisheries Policy and Management: A Binational Perspective. 2nd ed. Taylor WW, Lynch AJ, Leonard NJ, eds. East Lansing, MI:Michigan State University Press, 203-258.

Myers, A. L., Crozier, P. W., Helm, P. A., Brimacombe, C., Furdui, V. I., Reiner, E. J., Burniston, D., & Märvin, C. H. (2012). Fate, distribution, and contrasting temporal trends of perfluoroalkyl substances (PFASs) in Lake Ontario, Canada. Environment International, 44, 92–99. https://doi.org/10.1016/j.envint.2012.02.002

Ng, K., Alygizakis, N., Androulakakis, A., Galani, A., Aalizadeh, R., Thomaidis, N. S., & Slobodnik, J. (2022). Target and suspect screening of 4777 per- and polyfluoroalkyl substances (PFAS) in river water, wastewater, groundwater and biota samples in the Danube River Basin. Journal of Hazardous Materials, 436, 129276. https://doi.org/10.1016/j.jhazmat.2022.129276

Nguyen, T. V., Reinhard, M., Chen, H., & Gin, K. Y. (2016). Fate and transport of perfluoro- and polyfluoroalkyl substances including perfluorooctane sulfonamides in a managed urban water body. Environmental Science and Pollution Research, 23(11), 10382–10392. https://doi.org/10.1007/s11356-016-6788-9

Nilsson, S., Smurthwaite, K., Aylward, L., Kay, M., Toms, L., King, L., Marrington, S., Barnes, C., Kirk, M., Mueller, J., & Bräunig, J. (2022). Serum concentration trends and apparent half-lives of per- and polyfluoroalkyl substances (PFAS) in Australian firefighters. International Journal of Hygiene and Environmental Health, 246, 114040. https://doi.org/10.1016/j.ijheh.2022.114040

References

O'Connor, J. T., Bolan, N., Kumar, M., Nital, A. S., Ahmed, M. B., Vithanage, M., Rinklebe, J., Mukhopadhyay, R., Srivastava, P., Sarkar, B., Bhatnagar, A., Wang, H., Siddique, K. H. M., & Kirkham, M. (2022). Distribution, transformation and remediation of poly- and per-fluoroalkyl substances (PFAS) in wastewater sources. Process Safety and Environmental Protection/Transactions of the Institution of Chemical Engineers. Part B, Process Safety and Environmental Protection/Chemical Engineering Research and Design/Chemical Engineering Research & Design, 164, 91–108. https://doi.org/10.1016/j.psep.2022.06.002

Ogunbiyi, O. D., Massenat, N., & Quinete, N. (2024). Dispersion and stratification of Per-and polyfluoroalkyl substances (PFAS) in surface and deep-water profiles: A case study of the Biscayne Bay area. Science of the Total Environment, 909, 168413. https://doi.org/10.1016/j.scitotenv.2023.168413

Olsen, G. W., Chang, S., Noker, P. E., Gorman, G. S., Ehresman, D. J., Lieder, P. H., & Butenhoff, J. L. (2009). A comparison of the pharmacokinetics of perfluorobutanesulfonate (PFBS) in rats, monkeys, and humans. Toxicology, 256(1–2), 65–74. https://doi.org/10.1016/j.tox.2008.11.008

Olufsen, M., & Arukwe, A. (2014). Endocrine, biotransformation, and oxidative stress responses in salmon hepatocytes exposed to chemically induced hypoxia and perfluorooctane sulfonamide (PFOSA), given singly or in combination. Environmental Science and Pollution Research International, 22(22), 17350–17366. https://doi.org/10.1007/s11356-014-3847-y

Pagnucco, K. S., Maynard, G. A., Fera, S. A., Yan, N. D., Nalepa, T. F., & Ricciardi, A. (2015). The future of species invasions in the Great Lakes-St. Lawrence River basin. Journal of Great Lakes Research, 41, 96–107. https://doi.org/10.1016/j.jglr.2014.11.004

Panieri, E., Baralić, K., Đukić-ćosić, D., Đorđević, A., & Saso, L. (2022). PFAS molecules: a major concern for the human health and the environment. Toxics, 10(2), 44. https://doi.org/10.3390/toxics10020044

Masoner, J. R., Kolpin, D. W., Cozzarelli, I. M., Smalling, K. L., Bolyard, S. C., Field, J. A., Furlong, E. T., Gray, J. L., Lozinski, D., Reinhart, D. R., Rodowa, A. E., & Bradley, P. M. (2020). Landfill leachate contributes per-/poly-fluoroalkyl substances (PFAS) and pharmaceuticals to municipal wastewater. Environmental Science. Water Research & Technology (Print), 6(5), 1300–1311. https://doi.org/10.1039/d0ew00045k

Panieri, E., Baralić, K., Đukić-ćosić, D., Đorđević, A., & Saso, L. (2022). PFAS molecules: a major concern for the human health and the environment. Toxics, 10(2), 44. https://doi.org/10.3390/toxics10020044

Pepper, I. L., Kelley, C., & Brusseau, M. L. (2023). Is PFAS from land applied municipal biosolids a significant source of human exposure via groundwater? Science of the Total Environment, 864, 161154. https://doi.org/10.1016/j.scitotenv.2022.161154

Pfotenhauer, D., Sellers, E., Olson, M. A., Praedel, K., & Shafer, M. M. (2022). PFAS concentrations and deposition in precipitation: An intensive 5-month study at National Atmospheric Deposition Program – National trends sites (NADP-NTN) across Wisconsin, USA. Atmospheric Environment, 291, 119368. https://doi.org/10.1016/j.atmosenv.2022.119368

Pickard, H. M., Ruyle, B. J., Thackray, C. P., Chovancova, A., Dassuncao, C., Bečanová, J., Vojta, Š., Lohmann, R., & Sunderland, E. M. (2022). PFAS and precursor bioaccumulation in freshwater recreational fish: Implications for fish advisories. Environmental Science & Technology, 56(22), 15573–15583. https://doi.org/10.1021/acs.est.2c03734

Pizzorno, J. (2024). Fluorocarbons (PFAS)-The forever chemicals. PubMed, 22(6), 6–10. https://pubmed.ncbi.nlm.nih.gov/38404606

Point, A. D., Holsen, T. M., Fernando, S., Hopke, P. K., & Crimmins, B. S. (2021). Trends (2005–2016) of perfluoroalkyl acids in top predator fish of the Laurentian Great Lakes. Science of the Total Environment, 778, 146151. https://doi.org/10.1016/j.scitotenv.2021.146151

Pütz, K. W., Namazkar, S., Plassmann, M., & Benskin, J. P. (2022). Are cosmetics a significant source of PFAS in Europe? product inventories, chemical characterization and emission estimates. Environmental Science. Processes & Impacts, 24(10), 1697–1707. https://doi.org/10.1039/d2em00123c

References

Quinn, F. H. (1992). Hydraulic residence times for the Laurentian Great Lakes. Journal of Great Lakes Research, 18(1), 22–28. https://doi.org/10.1016/s0380-1330(92)71271-4

R Core Team. (2020). R: A language and environment for statistical computing. R Foundation for Statistical Computing. http://www.R-project.org/

Rafiei, V., & Nejadhashemi, A. P. (2023). Watershed scale PFAS fate and transport model for source identification and management implications. Water Research, 240, 120073. https://doi.org/10.1016/j.watres.2023.120073

Rao, Y. R., & Schwab, D. J. (2007). Transport and Mixing Between the Coastal and Offshore Waters in the Great Lakes: a Review. Journal of Great Lakes Research, 33(1), 202–218. https://doi.org/10.3394/0380-1330(2007)33

Remucal, C. K. (2019). Spatial and temporal variability of perfluoroalkyl substances in the Laurentian Great Lakes. Environmental Science: Processes & Impacts, 21(11), 1816–1834. https://doi.org/10.1039/c9em00265k

Ren, J., Point, A., Baygi, S. F., Fernando, S., Hopke, P. K., Holsen, T. M., Lantry, B., Weidel, B., & Crimmins, B. S. (2022). Bio accumulation of perfluoroalkyl substances in a Lake Ontario food web. Journal of Great Lakes Research, 48(2), 315–325. https://doi.org/10.1016/j.jglr.2021.08.013

Ren, J., Point, A. D., Baygi, S. F., Fernando, S., Hopke, P. K., Holsen, T. M., & Crimmins, B. S. (2022a). Bioaccumulation of perfluoroalkyl substances in the Lake Erie Food web. Social Science Research Network. https://doi.org/10.2139/ssrn.4224037

Ren, J., Point, A. D., Baygi, S. F., Fernando, S., Hopke, P. K., Holsen, T. M., & Crimmins, B. S. (2022). Bioaccumulation of polyfluoroalkyl substances in the Lake Huron aquatic food web. Science of the Total Environment, 819, 152974. https://doi.org/10.1016/j.scitotenv.2022.152974

Ren, J., Point, A. D., Baygi, S. F., Fernando, S., Hopke, P. K., Holsen, T. M., & Crimmins, B. S. (2023). Bioaccumulation of perfluoroalkyl substances in the Lake Erie food web. Environmental Pollution, 317, 120677. https://doi.org/10.1016/j.envpol.2022.120677

Rericha, Y., Cao, D., Truong, L., Simonich, M., Field, J. A., & Tanguay, R. L. (2021). Behavior effects of structurally diverse per- and polyfluoroalkyl substances in zebrafish. Chemical Research in Toxicology, 34(6), 1409–1416. https://doi.org/10.1021/acs.chemrestox.1c00101

Rericha, Y., Cao, D., Truong, L., Simonich, M. T., Field, J. A., & Tanguay, R. L. (2022). Sulfonamide functional head on short-chained perfluorinated substance drives developmental toxicity. iScience, 25(2), 103789. https://doi.org/10.1016/j.isci.2022.103789

Rosenblum, J. S., Liethen, A., & Miller-Robbie, L. (2024). Prioritization and risk ranking of regulated and unregulated chemicals in US drinking water. Environmental Science & Technology. https://doi.org/10.1021/acs.est.3c08745
Salvatore, D., Mok, K., Garrett, K. K., Poudrier, G., Brown, P., Birnbaum, L. S., Goldenman, G., Miller, M. F., Patton, S.,

Poehlein, M., Varshavsky, J., & Cordner, A. (2022). Presumptive contamination: A new approach to PFAS contamination based on likely sources. Environmental Science & Technology Letters, 9(11), 983–990. https://doi.org/10.1021/acs.estlett.2c00502

Sardiña, P., Leahy, P., Metzeling, L., Stevenson, G., & Hinwood, A. (2019). Emerging and legacy contaminants across land-use gradients and the risk to aquatic ecosystems. Science of the Total Environment, 695, 133842. https://doi.org/10.1016/j.scitotenv.2019.133842

Savoca, D., & Pace, A. (2021). Bioaccumulation, biodistribution, toxicology and biomonitoring of organofluorine compounds in aquatic organisms. International Journal of Molecular Sciences, 22(12), 6276. https://doi.org/10.3390/ijms22126276

Scully-Engelmeyer, K. M., & Granek, E. F. (2022b). Predicting springtime herbicide exposure across multiple scales in pacific coastal drainages (Oregon, USA). Ecological Indicators, 142, 109195. https://doi.org/10.1016/j.ecolind.2022.109195

References

Siddiqui, S., Conkle, J. L., Scarpa, J., & Sadovski, A. L. (2020). An analysis of U.S. wastewater treatment plant effluent dilution ratio: Implications for water quality and aquaculture. Science of the Total Environment, 721, 137819. https://doi.org/10.1016/j.scitotenv.2020.137819

Silver, M., Phelps, W. L., Masarik, K., Burke, K., Zhang, C., Schwartz, A. T., Wang, M., Nitka, A., Schutz, J., Trainor, T. P., Washington, J. W., & Rheineck, B. D. (2023). Prevalence and source tracing of PFAS in shallow groundwater used for drinking water in Wisconsin, USA. Environmental Science & Technology, 57(45), 17415–17426. https://doi.org/10.1021/acs.est.3c02826

Sinclair, E., Mayack, D. T., Roblee, K. J., Yamashita, N., & Kannan, K. (2006). Occurrence of Perfluoroalkyl Surfactants in Water, Fish, and Birds from New York State. Archives of Environmental Contamination and Toxicology, 50(3), 398–410. https://doi.org/10.1007/s00244-005-1188-z

Sinclair, E., & Kannan, K. (2006). Mass loading and fate of perfluoroalkyl surfactants in wastewater treatment plants. Environmental Science & Technology, 40(5), 1408–1414. https://doi.org/10.1021/es051798v

Sinclair, G. M., Long, S. M., & Jones, O. A. (2020). What are the effects of PFAS exposure at environmentally relevant concentrations? Chemosphere, 258, 127340. https://doi.org/10.1016/j.chemosphere.2020.127340

Slotkin, T. A., MacKillop, E. A., Melnick, R. L., Thayer, K. A., & Seidler, F. J. (2008). Developmental neurotoxicity of perfluorinated chemicals modeled in vitro. Environmental Health Perspectives, 116(6), 716–722. https://doi.org/10.1289/ehp.11253

Slotkin, T. A., & Seidler, F. J. (2010). Oxidative stress from diverse developmental neurotoxicants: Antioxidants protect against lipid peroxidation without preventing cell loss. Neurotoxicology and Teratology, 32(2), 124–131. https://doi.org/10.1016/j.ntt.2009.12.001

Sponberg, A. F. (2009). Great Lakes: Sailing to the forefront of national water policy? BioScience, 59(5), 372–372. https://doi.org/10.1525/bio.2009.59.5.4

Spyrakis, F., & Dragani, T. A. (2023). The EU's Per- and Polyfluoroalkyl Substances (PFAS) Ban: A Case of Policy over Science. Toxics, 11(9), 721. https://doi.org/10.3390/toxics11090721

Stahl, L. L., Snyder, B. D., Olsen, A. R., Kincaid, T. M., Wathen, J. B., & McCarty, H. B. (2014). Perfluorinated compounds in fish from U.S. urban rivers and the Great Lakes. Science of the Total Environment, 499, 185–195. https://doi.org/10.1016/j.scitotenv.2014.07.126

Starkov, A. A. (2002). Structural Determinants of Fluorochemical-Induced mitochondrial dysfunction. Toxicological Sciences, 66(2), 244–252. https://doi.org/10.1093/toxsci/66.2.244

Starkov, A. A, and Wallace, K. B, (2002b). Structural Determinants of Fluorochemical-Induced mitochondrial dysfunction. Toxicological Sciences, 66(2), 244–252. https://doi.org/10.1093/toxsci/66.2.244

Subedi, B., Codru, N., Dziewulski, D. M., Wilson, L. R., Xue, J., Yun, S., Braun-Howland, E., Minihane, C., & Kannan, K. (2015). A pilot study on the assessment of trace organic contaminants including pharmaceuticals and personal care products from on-site wastewater treatment systems along Skaneateles Lake in New York State, USA. Water Research, 72, 28–39. https://doi.org/10.1016/j.watres.2014.10.049

Sun, J., Letcher, R. J., Eens, M., Covaci, A., & Fernie, K. J. (2020). Perfluoroalkyl acids and sulfonamides and dietary, biological and ecological associations in peregrine falcons from the Laurentian Great Lakes Basin, Canada. Environmental Research, 191, 110151. https://doi.org/10.1016/j.envres.2020.110151

Swam, L.M., M.M. Rider, D.A. Apeti, and E. Pisarski. 2023. A 2017 Assessment of Contaminants of Emerging Concern in the Gulf of Mexico. NOAA Technical Memorandum NOS NCCOS 323. Silver Spring, MD. 70 pp. DOI 10.25923/d1j6-e075.

Swam, L.M., M.M. Rider, and D.A. Apeti. 2024. A 2017 Assessment of Legacy Organic Contaminants in the Gulf of Mexico. NOAA Technical Memorandum NOS NCCOS 326. Silver Spring, MD. 72 pp. DOI 10.25923/k49q-6398.

References

Tang, A., Zhang, X., Li, R., Tu, W., Guo, H., Zhang, Y., Li, Z., Liu, Y., & Mai, B. (2022). Spatiotemporal distribution, partitioning behavior and flux of per- and polyfluoroalkyl substances in surface water and sediment from Poyang Lake, China. Chemosphere, 295, 133855. https://doi.org/10.1016/j.chemosphere.2022.133855

Teunen, L., Bervoets, L., Belpaire, C., De Jonge, M., & Groffen, T. (2021b). PFAS accumulation in indigenous and translocated aquatic organisms from Belgium, with translation to human and ecological health risk. Environmental Sciences Europe, 33(1). https://doi.org/10.1186/s12302-021-00477-z

Thompson, K. A., Mortazavian, S., González, D., Bott, C., Hooper, J., Schaefer, C. E., & Dickenson, E. (2022). Poly- and perfluoroalkyl substances in municipal wastewater treatment plants in the United States: Seasonal Patterns and Meta-Analysis of Long-Term Trends and Average Concentrations. ACS ES&T Water, 2(5), 690–700. https://doi.org/10.1021/acsestwater.1c00377

Ulhaq, M., Carlsson, G., Örn, S., & Norrgren, L. (2013). Comparison of developmental toxicity of seven perfluoroalkyl acids to zebrafish embryos. Environmental Toxicology and Pharmacology, 36(2), 423–426. https://doi.org/10.1016/j.etap.2013.05.004

USEPA (2020) Announcement of Preliminary Regulatory Determinations for Contaminants on the Fourth Drinking Water Contaminant Candidate List, 85 FR 14098. Accessed 6.20.24

USEPA (2021) Multi-Industry Per- and Polyfluoroalkyl Substances (PFAS) Study –2021 Preliminary Report: https://www.epa.gov/system/files/documents/2021-09/multi-industry-pfas-study_preliminary-2021-report_508_2021.09.08.pdf. Accessed 4.10.24

USEPA (2024). Contaminants to Monitor in Fish and Shellfish Advisory Programs: https://www.epa.gov/system/files/documents/2024-06/contaminants-monitor-fish-factsheet-july2024.pdf. Accessed 7.12.24

VanNijnatten, D., & Johns, C. (2020). The International Joint Commission and the Evolution of the Great Lakes Water Quality Agreement: Accountability, progress Reporting, and Measuring Performance. In University of Calgary Press eBooks (pp. 395–430). https://doi.org/10.1515/9781773851099-017

Wang, Z., Cousins, I. T., Scheringer, M., Buck, R. C., & Hungerbühler, K. (2014). Global emission inventories for C4–C14 perfluoroalkyl carboxylic acid (PFCA) homologues from 1951 to 2030, Part I: production and emissions from quantifiable sources. Environment International, 70, 62–75. https://doi.org/10.1016/j.envint.2014.04.013

Wang H.W., Ma S.W., Zhang Z., Chen H.G., Huang Z.F., Gong X.Y., Cai W.G., Jia X.P. (2012). Effects of perfluorooctanesulfonate (PFOS) exposure on antioxidant enzymes of Perna viridis. Asian J. Ecotoxicol.7:508–516.

Wang, Z., Liu, S., Huang, P., & Xu, Y. (2021). Mixture predicted no-effect concentrations derived by independent action model vs concentration addition model based on different species sensitivity distribution models. Ecotoxicology and Environmental Safety, 227, 112898. https://doi.org/10.1016/j.ecoenv.2021.112898

Weatherly, L. M., Shane, H. L., Lukomska, E., Baur, R., & Anderson, S. E. (2023). Systemic toxicity induced by topical application of perfluoroheptanoic acid (PFHpA), perfluorohexanoic acid (PFHxA), and perfluoropentanoic acid (PFPeA) in a murine model. Food and Chemical Toxicology, 171, 113515. https://doi.org/10.1016/j.fct.2022.113515

Wee, S. Y., & Aris, A. Z. (2023b). Environmental impacts, exposure pathways, and health effects of PFOA and PFOS. Ecotoxicology and Environmental Safety, 267, 115663. https://doi.org/10.1016/j.ecoenv.2023.115663

Wen, W., Xia, X., Zhou, D., Wang, H., Zhai, Y., Lin, H., Chen, J., & Hu, D. (2019). Bioconcentration and tissue distribution of shorter and longer chain perfluoroalkyl acids (PFAAs) in zebrafish (Danio rerio): Effects of perfluorinated carbon chain length and zebrafish protein content. Environmental Pollution, 249, 277–285. https://doi.org/10.1016/j.envpol.2019.03.003

Wen, W., Xiao, L., Hu, D., Zhang, Z., Xiao, Y., Jiang, X., Zhang, S., & Xia, X. (2023). Fractionation of perfluoroalkyl acids (PFAAs) along the aquatic food chain promoted by competitive effects between longer and shorter chain PFAAs. Chemosphere, 318, 137931. https://doi.org/10.1016/j.chemosphere.2023.137931

References

Westreich, P., Mimna, R., Brewer, J., & Forrester, F. (2018). The removal of short-chain and long-chain perfluoroalkyl acids and sulfonates via granular activated carbons: A comparative column study. Remediation, 29(1), 19–26. https://doi.org/10.1002/rem.21579

Wolter, P. T., Johnston, C. A., & Niemi, G. J. (2006). Land use land cover change in the U.S. Great Lakes Basin 1992 to 2001. Journal of Great Lakes Research, 32(3), 607–628. https://doi.org/10.3394/0380-1330(2006)32[607:LULCCI]2.0.CO;2

Worley, R. R., Moore, S. M., Tierney, B. C., Ye, X., Calafat, A. M., Campbell, S., Woudneh, M. B., & Fisher, J. (2017). Per- and polyfluoroalkyl substances in human serum and urine samples from a residentially exposed community. Environment International, 106, 135–143. https://doi.org/10.1016/j.envint.2017.06.007

Wu, Y., Simon, K. L., Best, D. A., Bowerman, W. W., & Venier, M. (2020). Novel and legacy per- and polyfluoroalkyl substances in bald eagle eggs from the Great Lakes region. Environmental Pollution, 260, 113811. https://doi.org/10.1016/j.envpol.2019.113811

Wu, H., Wu, J., Wang, H., Liu, Y., Han, G., & Zou, P. (2021). Sensitive and label-free chemiluminescence detection of malathion using exonuclease-assisted dual signal amplification and G-quadruplex/hemin DNAzyme. Journal of Hazardous Materials, 411, 124784. https://doi.org/10.1016/j.jhazmat.2020.124784

Xia, C., Diamond, M. L., Peaslee, G. F., Peng, H., Blum, A., Wang, Z., Shalin, A., Whitehead, H. D., Green, M., Schwartz-Narbonne, H., Yang, D., & Venier, M. (2022). Per- and polyfluoroalkyl substances in North American school uniforms. Environmental Science & Technology, 56(19), 13845–13857. https://doi.org/10.1021/acs.est.2c02111

Xia, C., Capozzi, S. L., Romanak, K. A., Lehman, D. C., Dove, A., Richardson, V., Greenberg, T., McGoldrick, D., & Venier, M. (2024c). The ins and outs of per- and polyfluoroalkyl substances in the Great Lakes: the role of atmospheric deposition. Environmental Science & Technology. https://doi.org/10.1021/acs.est.3c10098

Xu, Y., Fletcher, T., Pineda, D., Lindh, C. H., Nilsson, C., Glynn, A., Vogs, C., Norström, K., Lilja, K., Jakobsson, K., & Li, Y. (2020). Serum Half-Lives for Short- and Long-chained Perfluoroalkyl Acids after Ceasing Exposure from Drinking Water Contaminated by Firefighting Foam. Environmental Health Perspectives, 128(7). https://doi.org/10.1289/ehp6785

Xu, K., Huang, J., Zhang, Y., Wu, X., Cai, D., Hu, G., Li, Y., Ni, Z., Lin, Q., Wang, S., & Qiu, R. (2024). Crop Contamination and Human Exposure to Per- and Polyfluoroalkyl Substances around a Fluorochemical Industrial Park in China. Toxics, 12(4), 269. https://doi.org/10.3390/toxics12040269

Xuan, R., Qiu, X., Wang, J., Liu, S., Magnuson, J. T., Xu, B., Qiu, W., & Chen, K. (2024). Hepatotoxic response of perfluorooctane sulfonamide (PFOSA) in early life stage zebrafish (Danio rerio) is greater than perfluorooctane sulfonate (PFOS). Journal of Hazardous Materials, 461, 132552. https://doi.org/10.1016/j.jhazmat.2023.132552

Yeung, L. W. Y., De Silva, A. O., Loi, E. I. H., Märvin, C. H., Taniyasu, S., Yamashita, N., Mabury, S. A., Muir, D. C., & Lam, P. K. (2013). Perfluoroalkyl substances and extractable organic fluorine in surface sediments and cores from Lake Ontario. Environment International, 59, 389–397. https://doi.org/10.1016/j.envint.2013.06.026

Yi, S., Chen, P., Yang, L., & Zhu, L. (2019). Probing the hepatotoxicity mechanisms of novel chlorinated polyfluoroalkyl sulfonates to zebrafish larvae: Implication of structural specificity. Environment International, 133, 105262. https://doi.org/10.1016/j.envint.2019.105262

Yu, C. H., Weisel, C. P., Alimokhtari, S., Georgopoulos, P. G., & Fan, Z. (2021). Biomonitoring: A tool to assess PFNA body burdens and evaluate the effectiveness of drinking water intervention for communities in New Jersey. International Journal of Hygiene and Environmental Health, 235, 113757. https://doi.org/10.1016/j.ijheh.2021.113757

Yun, X., Lewis, A. J., Stevens-King, G., Sales, C. M., Spooner, D. E., Kurz, M. J., Suri, R., & McKenzie, E. R. (2023). Bioaccumulation of per- and polyfluoroalkyl substances by freshwater benthic macroinvertebrates: Impact of species and sediment organic carbon content. Science of the Total Environment, 866, 161208. https://doi.org/10.1016/j.scitotenv.2022.161208

Yurista, P. M., Kelly, J. R., & Scharold, J. V. (2016). Great Lakes nearshore–offshore: Distinct water quality regions. Journal of Great Lakes Research, 42(2), 375–385. https://doi.org/10.1016/j.jglr.2015.12.002

References

Zhang, Y., Beesoon, S., Zhu, L., & Martin, J. W. (2013). Biomonitoring of perfluoroalkyl acids in human urine and estimates of biological Half-Life. Environmental Science & Technology, 47(18), 10619–10627. https://doi.org/10.1021/es401905e

Zhang, X., Lohmann, R., Dassuncao, C., Hu, X. C., Weber, A. K., Vecitis, C. D., & Sunderland, E. M. (2016). Source Attribution of Poly- and Perfluoroalkyl Substances (PFASs) in Surface Waters from Rhode Island and the New York Metropolitan Area. Environmental Science & Technology Letters, 3(9), 316–321. https://doi.org/10.1021/acs.estlett.6b00255

Zhang, S., Guo, X., Lu, S., Sang, N., Li, G., Xie, P., Liu, C., Zhang, L., & Xing, Y. (2018). Exposure to PFDoA causes disruption of the hypothalamus-pituitary-thyroid axis in zebrafish larvae. Environmental Pollution, 235, 974–982. https://doi.org/10.1016/j.envpol.2018.01.015

Zhang, Y., Ding, T., Huang, Z., Liang, H., Du, S., Zhang, J., & Li, H. (2023). Environmental exposure and ecological risk of perfluorinated substances (PFASs) in the Shaying River Basin, China. Chemosphere, 339, 139537. https://doi.org/10.1016/j.chemosphere.2023.139537

Zhang, J., Xie, Y., Zhang, J., Ye, M., Diao, J., Wang, J., Sun, Q., & Wang, T. (2024). Perfluoroalkyl substances in the environment and biota from the coasts of the South China Sea: profiles, sources, and potential risks. Frontiers in Environmental Science, 12. https://doi.org/10.3389/fenvs.2024.1380232

Zhao, Y., Wan, H. T., Wong, M. H., & Wong, C. K. C. (2014). Partitioning behavior of perfluorinated compounds between sediment and biota in the Pearl River Delta of South China. Marine Pollution Bulletin, 83(1), 148–154. https://doi.org/10.1016/j.marpolbul.2014.03.060

Zhao, Y., Lee, C. K., Wang, Z., Wang, J., Gu, Y., Xie, J., Law, Y. K., Song, G., Bonebrake, T. C., Yang, X., Nelson, B. W., & Wu, J. (2022). Evaluating fine-scale phenology from PlanetScope satellites with ground observations across temperate forests in eastern North America. Remote Sensing of Environment, 283, 113310. https://doi.org/10.1016/j.rse.2022.113310

Zhou, Y., Lin, X., Xing, Y., Zhang, X., Lee, H. K., & Huang, Z. (2023). Per- and polyfluoroalkyl substances in personal hygiene products: the implications for human exposure and emission to the environment. Environmental Science & Technology, 57(23), 8484–8495. https://doi.org/10.1021/acs.est.2c08912

Zushi, Y., & Masunaga, S. (2009). Identifying the nonpoint source of perfluorinated compounds using a geographic information system based approach. Environmental Toxicology and Chemistry, 28(4), 691–700. https://doi.org/10.1897/08-194.1

Credit: NOAA Great Lakes MWP

Appendix

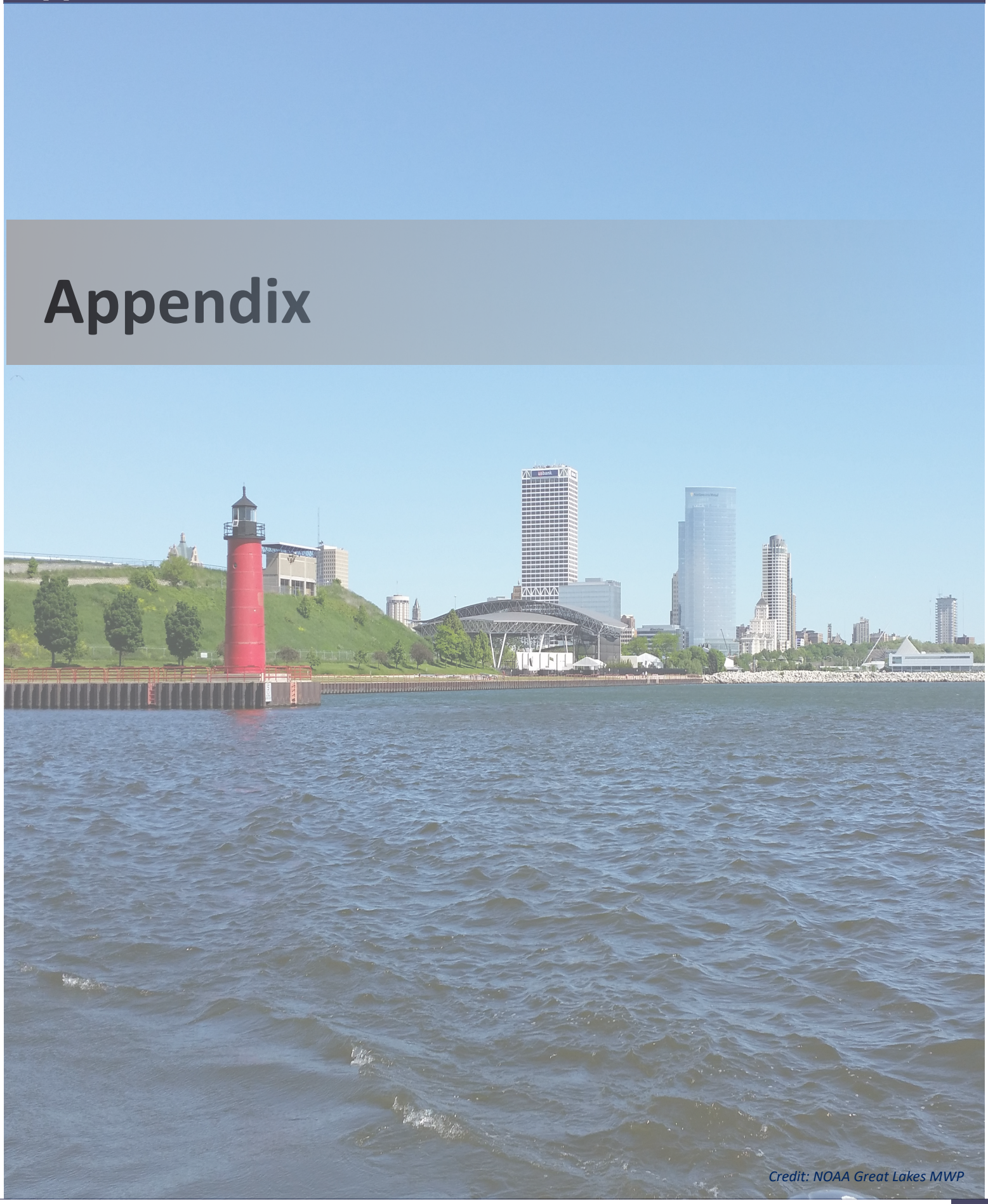

Credit: NOAA Great Lakes MWP

Appendix

Table A1. Great Lakes Mussel Watch 2013 - 2018 PFAS sampling locations. Individual sites are listed by their general location (associated river/lake region) and year sampled, while (*) signifies reference sites. (WI - Wisconsin, MI - Michigan, OH - Ohio, PA - Pennsylvania, NY – New York). Additional information on MWP PFAS sampling locations are provided in Table A3.

Site Name	Site Code	State	General Location	Latitude	Longitude	Sample Type	Year Sampled
Algoma-0-INMU-8.18	LMAG-0-INMU-8.18	WI	Algoma	44.6072	-87.4305	Monitoring/Surveillance	2018
Algoma-1-8.18	LMAG-1-8.18	WI	Lake Michigan	44.5982	-87.4293	Monitoring/Surveillance	2018
Ashtabula River-1-9.14	LEAR-1-9.14	OH	Ashtabula River	41.9123	-80.7935	Monitoring/Surveillance	2014
Ashtabula River-3-9.14	LEAR-3-9.14	OH	Ashtabula River	41.9120	-80.7900	Monitoring/Surveillance	2014
Black River LM-0-5.18	LMBR-0-5.18	MI	Black River/Lake Michigan	42.6766	-86.2147	Monitoring/Surveillance	2018
Black River-0-9.14	LEBR-0-9.14	OH	Black River/Lake Erie	41.4741	-82.1810	Monitoring/Surveillance	2014
Black River-1-9.14	LEBR-1-9.14	OH	Black River/Lake Erie	41.4736	-82.1822	Monitoring/Surveillance	2014
Cape Vincent-INMU-10.18	LOCV-INMU-10.18	NY	Cape Vincent	44.1323	-76.3308	Place-based/Caged	2018
Cayuga Creek-01A-7.14	NRCY-01A-7.14	NY	Cayuga Creek	43.0750	-78.9639	Place-based/Caged	2014
Cuyahoga River-5-9.14	LECR-5-9.14	OH	Cuyahoga River	41.5042	-81.7114	Monitoring/Surveillance	2014
Cuyahoga River-9.14	LECR-9.14	OH	Cuyahoga River	41.4984	-81.7201	Monitoring/Surveillance	2014
Detroit River Fox Is-0-6.16	DRSE-0-6.16	MI	Detroit River	42.1069	-83.1356	Place-based/Caged	2016
Ellicott Creek-01A-7.14	NREL-01A-7.14	NY	Ellicott Creek	43.0203	-78.8754	Place-based/Caged	2014
Fourmile Creek-INMU-CH-10.18	LOFC-INMU-CH-10.18	NY	Fourmile Creek	43.2840	-79.0020	Monitoring/Surveillance	2018
Gill Creek-01A-7.14	NRGL-01A-7.14	NY	Niagara River	43.0781	-79.0267	Place-based/Caged	2014
Gill Creek-02A-7.14	NRGL-02A-7.14	NY	Niagara River	43.0783	-79.0259	Place-based/Caged	2014
Gill Creek-03A-7.14	NRGL-03A-7.14	NY	Niagara River	43.0788	-79.0258	Place-based/Caged	2014
Kalamazoo River-0-5.18	LMKZ-0-5.18	MI	Kalamazoo River	42.6766	-86.2147	Monitoring/Surveillance	2018
Kewaunee River-0-8.18	LMKW-0-8.18	WI	Kewaunee River	44.4590	-87.4989	Monitoring/Surveillance	2018
Kewaunee River-01-8.18	LMKW-01-8.18	WI	Kewaunee River	44.4584	-87.4654	Monitoring/Surveillance	2018
Kinnickinnic River-13-7.13	LMMB-13-7.13	WI	Kinnickinnic River	43.0095	-87.9067	Place-based/Caged	2013
Kinnickinnic River13-S4-7.17	LMMB-13-S4-7.17	WI	Kinnickinnic River	43.0047	-87.9134	Place-based/Caged	2017
Kinnickinnic River-14-7.17	LMMB-14-7.17	WI	Kinnickinnic River	43.0120	-87.9055	Place-based/Caged	2017
Lake OntarioFS-INMU-CH-6.18	LOFO-INMU-CH-6.18	NY	Lake Ontario	43.4684	-77.8820	Monitoring/Surveillance	2018
Manitowoc-0-INMU-8.14	LMMW-0-INMU-8.14	WI	Manitowoc	44.0933	-87.6451	Monitoring/Surveillance	2014
Manitowoc-1-INMU-8.14	LMMW-1-INMU-8.14	WI	Manitowoc	44.1037	-87.6271	Monitoring/Surveillance	2014
Maumee Grassy Isl-0-5.15	LEMR-0-5.15	OH	Maumee River	41.7004	-83.4601	Place-based/Caged	2015
Maumee Grassy Isl-0-6.15	LEMR-0-6.15	OH	Maumee River	41.7005	-83.4601	Place-based/Caged	2015
Maumee Grassy Isl-0-6.16	LEMR-0-6.16	OH	Maumee River	41.7006	-83.4596	Place-based/Caged	2016
Maumee Grassy Isl-0-7.15	LEMR-0-7.15	OH	Maumee River	41.7006	-83.4601	Place-based/Caged	2015
Maumee Lighthouse-3-5.15 (*)	LEMR-3-5.15	OH	Lake Erie	41.7618	-83.3290	Place-based	2015
Maumee Lighthouse-3-5.16 (*)	LEMR-3-5.16	OH	Lake Erie	41.7623	-83.3290	Place-based/Caged	2016
Maumee Lighthouse-3-6.15 (*)	LEMR-3-6.15	OH	Lake Erie	41.7617	-83.3289	Place-based	2015
Maumee Lighthouse-3-6.16 (*)	LEMR-3-6.16	OH	Lake Erie	41.7623	-83.3289	Place-based/Caged	2016
Maumee Lighthouse-3-7.15 (*)	LEMR-3-7.15	OH	Lake Erie	41.7617	-83.3291	Place-based/Caged	2015
Maumee Upstream-02-5.15	LEMR-2-5.15	OH	Maumee River	41.6553	-83.5251	Place-based/Caged	2015

(*) – Reference sites

Appendix

Table A1 (cont). Great Lakes Mussel Watch 2013 - 2018 PFAS sampling locations. Individual sites are listed by their general location (associated river/lake region) and year sampled, while (*) signifies reference sites. (WI - Wisconsin, MI - Michigan, OH - Ohio, PA - Pennsylvania, NY – New York). Additional information on MWP PFAS sampling locations are provided in Table A3.

Site Name	Site Code	State	General Location	Latitude	Longitude	Sample Type	Year Sampled
Maumee Upstream -2-6.15	LEMR-2-6.15	OH	Maumee River	41.6553	-83.5251	Place-based/Caged	2015
Maumee Upstream -2-7.15	LEMR-2-7.15	OH	Maumee River	41.6557	-83.5249	Place-based/Caged	2015
Maumee River-4-6.16	LEMR-4-6.16	OH	Maumee River	41.6361	-83.5311	Place-based/Caged	2016
Maumee WWTP-1-5.15	LEMR-1-5.15	OH	Maumee River	41.6890	-83.4751	Place-based/Caged	2015
Maumee WWTP-1-6.15	LEMR-1-6.15	OH	Maumee River	41.6886	-83.4749	Place-based/Caged	2015
Maumee WWTP-1-6.16	LEMR-1-6.16	OH	Maumee River	41.6891	-83.4768	Place-based/Caged	2016
Maumee WWTP-1-7.15	LEMR-1-7.15	OH	Maumee River	41.6885	-83.4749	Place-based/Caged	2015
Menomonee River-11-7.18	LMMB-11-7.18	WI	Menomonee River	43.0329	-87.9390	Place-based/Caged	2018
Menomonee River-11-S4-7.17	LMMB-11-S4-7.17	WI	Menomonee River	43.0329	-87.9388	Place-based/Caged	2017
Menomonee River-12-7.13	LMMB-12-7.13	WI	Menomonee River	43.0318	-87.9469	Place-based/Caged	2013
Menomonee River-15-S4-BC-7.17	LMMB-15-S4-BC-7.17	WI	Menomonee River	43.0334	-87.9176	Place-based/Caged	2017
Menomonee River-15-S4-TC-7.17	LMMB-15-S4-TC-7.17	WI	Menomonee River	43.0334	-87.9176	Place-based/Caged	2017
Milwaukee Bay-01-INMU-6.18	LMMB-01-INMU-6.18	WI	Milwaukee Bay	43.0079	-87.8891	Place-based/Insitu	2018
Milwaukee Bay-01-INMU-6.8.17	LMMB-01-INMU-6.8.17	WI	Milwaukee Bay	43.0079	-87.8888	Place-based/Insitu	2017
Milwaukee Bay-04-INMU-8.17	LMMB-04-INMU-8.17	WI	Milwaukee Bay	43.0432	-87.8878	Place-based/Insitu	2017
Milwaukee Bay-0-6.18	LMMB-0-6.18	WI	Milwaukee Bay	43.0327	-87.8940	Place-based/Caged	2018
Milwaukee Bay-0-7.13	LMMB-0-7.13	WI	Milwaukee Bay	43.0339	-87.8948	Place-based/Caged	2013
Milwaukee Bay-0-7.18	LMMB-0-7.18	WI	Milwaukee Bay	43.0325	-87.8939	Place-based/Caged	2018
Milwaukee Bay-0-INMU-6.8.17	LMMB-0-INMU-6.8.17	WI	Milwaukee Bay	43.0329	-87.8938	Place-based/Insitu	2017
Milwaukee Bay-1-7.13	LMMB-1-7.13	WI	Milwaukee Bay	43.0078	-87.8872	Place-based/Caged	2013
Milwaukee Bay-17-7.18	LMMB-17-7.18	WI	Milwaukee Bay	43.0234	-87.8943	Place-based/Caged	2018
Milwaukee Bay-4-6.13	LMMB-4-6.13	WI	Milwaukee Bay	43.0431	-87.8878	Place-based/Caged	2013
Milwaukee Bay-4-6.18	LMMB-4-6.18	WI	Milwaukee Bay	43.0431	-87.8879	Place-based/Caged	2018
Milwaukee Bay-4-7.13	LMMB-4-7.13	WI	Milwaukee Bay	43.0431	-87.8878	Place-based/Caged	2013
Milwaukee Bay-4-7.18	LMMB-4-7.18	WI	Milwaukee Bay	43.0431	-87.8879	Place-based/Caged	2018
Milwaukee Bay-4-S4-7.17	LMMB-4-S4-7.17	WI	Milwaukee Bay	43.0432	-87.8878	Place-based/Caged	2017
Milwaukee Bay-4-S5-7.17	LMMB-4-S5-7.17	WI	Milwaukee Bay	43.0432	-87.8878	Place-based/Caged	2017
Milwaukee Beach-5-6.13 (*)	LMMB-5-6.13	WI	Lake Michigan	43.0596	-87.8670	Place-based/Insitu	2013
Milwaukee Beach-5-6.17 (*)	LMMB-5-6.17	WI	Lake Michigan	43.0599	-87.8645	Place-based/Insitu	2017
Milwaukee Beach-5-6.18 (*)	LMMB-5-6.18	WI	Lake Michigan	43.0605	-87.8639	Place-based/Caged	2018
Milwaukee Beach-5-7.13 (*)	LMMB-5-7.13	WI	Lake Michigan	43.0596	-87.8670	Place-based/Caged	2013
Milwaukee Beach-5-7.18 (*)	LMMB-5-7.18	WI	Lake Michigan	43.0605	-87.8639	Place-based/Caged	2018
Milwaukee Beach-5HDPE-8.17 (*)	LMMB-5HDPE-8.17	WI	Lake Michigan	43.0607	-87.8638	Place-based/Caged	2017
Milwaukee River-08-S4-8.17	LMMB-08-S4-8.17	WI	Milwaukee River	43.0568	-87.8983	Place-based/Caged	2017
Milwaukee River-08-S5-8.17	LMMB-08-S5-8.17	WI	Milwaukee River	43.0568	-87.8983	Place-based/Caged	2017
Milwaukee Bridge-6-7.13	LMMB-6-7.13	WI	Milwaukee Bay	43.0244	-87.8986	Place-based/Caged	2013

(*) – Reference sites

Table A1 (cont). Great Lakes Mussel Watch 2013 - 2018 PFAS sampling locations. Individual sites are listed by their general location (associated river/lake region) and year sampled, while (*) signifies reference sites. (WI - Wisconsin, MI - Michigan, OH - Ohio, PA - Pennsylvania, NY – New York). Additional information on MWP PFAS sampling locations are provided in Table A3.

Site Name	Site Code	State	General Location	Latitude	Longitude	Sample Type	Year Sampled
Milwaukee Bridge-6-7.17	LMMB-6-7.17	WI	Milwaukee Bay	43.0246	-87.8976	Place-based/Caged	2017
Milwaukee Bridge-6-7.18	LMMB-6-7.18	WI	Milwaukee Bay	43.0247	-87.8975	Place-based/Caged	2018
Milwaukee River-08-S4-8.17	LMMB-08-S4-8.17	WI	Milwaukee River	43.0568	-87.8983	Place-based/Caged	2017
Milwaukee River-08-S5-8.17	LMMB-08-S5-8.17	WI	Milwaukee River	43.0568	-87.8983	Place-based/Caged	2017
Milwaukee River-10-7.13	LMMB-10-7.13	WI	Milwaukee River	43.0333	-87.9176	Place-based/Caged	2013
Milwaukee River-16-S4-7.17	LMMB-16-S4-7.17	WI	Milwaukee River	43.0351	-87.9105	Place-based/Caged	2017
Milwaukee River-7-7.13	LMMB-7-7.13	WI	Milwaukee River	43.0440	-87.9129	Place-based/Caged	2013
Milwaukee River-8-7.13	LMMB-8-7.13	WI	Milwaukee River	43.0570	-87.8997	Place-based/Caged	2013
MuskegonLight-11.2718	MUS-11.27.18	MI	Muskegon	43.2266	-86.3415	Place-based/Insitu	2018
MuskegonLight-5.15.18	MUS-5.15.18	MI	Muskegon	43.2266	-86.3415	Place-based/Insitu	2018
MuskegonLight-5.2.18	MUS-5.2.18	MI	Muskegon	43.2266	-86.3415	Place-based/Insitu	2018
MuskegonLight-5.29.18	MUS-5.29.18	MI	Muskegon	43.2266	-86.3415	Place-based/Insitu	2018
MuskegonLight-6.15.18	MUS-6.15.18	MI	Muskegon	43.2266	-86.3415	Place-based/Insitu	2018
MuskegonLight-6.26.18	MUS-6.26.18	MI	Muskegon	43.2266	-86.3415	Place-based/Insitu	2018
MuskegonLight-7.18	MUS-7.18	MI	Muskegon	43.2266	-86.3415	Place-based/Insitu	2018
MuskegonLight-8-9.18	MUS-8-9.18	MI	Muskegon	43.2266	-86.3415	Place-based/Insitu	2018
NFTA Boat Harbor-01A-7.14	NRHP-01A-7.14	NY	NFTA Boat Harbor	42.8442	-78.8644	Place-based/Caged	2014
Niagara River-1, rep 1-6.14 (*)	NRNF-1, rep 1-6.14	NY	Niagara River	42.8708	-78.9022	Place-based	2014
Niagara River-1-7.14 (*)	NRNF-1-7.14	NY	Niagara River	42.8708	-78.9022	Place-based/Caged	2014
Niagara River-4-6.14	NRNF-4-6.14	NY	Niagara River	42.8845	-78.8908	Place-based/Insitu	2014
Niagara River-9-6.14 (*)	NRNF-9-6.14	NY	Niagara River	43.0612	-79.0028	Place-based/Insitu	2014
Oswego River-INMU-CH-10.18	LOOR-INMU-CH-10.18	NY	Oswego River	43.4649	-76.5157	Monitoring/Surveillance	2018
Milwaukee Beach-5-6.13 (*)	LMMB-5-6.13	WI	Lake Michigan	43.0596	-87.8670	Place-based/Insitu	2013
Milwaukee Beach-5-6.17 (*)	LMMB-5-6.17	WI	Lake Michigan	43.0599	-87.8645	Place-based/Insitu	2017
Milwaukee Beach-5-6.18 (*)	LMMB-5-6.18	WI	Lake Michigan	43.0605	-87.8639	Place-based/Caged	2018
Milwaukee Beach-5-7.13 (*)	LMMB-5-7.13	WI	Lake Michigan	43.0596	-87.8670	Place-based/Caged	2013
Milwaukee Beach-5-7.18 (*)	LMMB-5-7.18	WI	Lake Michigan	43.0605	-87.8639	Place-based/Caged	2018
Milwaukee Beach-5HDPE-8.17 (*)	LMMB-5HDPE-8.17	WI	Lake Michigan	43.0607	-87.8638	Place-based/Caged	2017
Milwaukee River-08-S4-8.17	LMMB-08-S4-8.17	WI	Milwaukee River	43.0568	-87.8983	Place-based/Caged	2017
Milwaukee River-08-S5-8.17	LMMB-08-S5-8.17	WI	Milwaukee River	43.0568	-87.8983	Place-based/Caged	2017
Milwaukee Bridge-6-7.13	LMMB-6-7.13	WI	Milwaukee Bay	43.0244	-87.8986	Place-based/Caged	2013
Milwaukee Bridge-6-7.17	LMMB-6-7.17	WI	Milwaukee Bay	43.0246	-87.8976	Place-based/Caged	2017
Milwaukee Bridge-6-7.18	LMMB-6-7.18	WI	Milwaukee Bay	43.0247	-87.8975	Place-based/Caged	2018
Milwaukee River-08-S4-8.17	LMMB-08-S4-8.17	WI	Milwaukee River	43.0568	-87.8983	Place-based/Caged	2017
Milwaukee River-08-S5-8.17	LMMB-08-S5-8.17	WI	Milwaukee River	43.0568	-87.8983	Place-based/Caged	2017
Milwaukee River-10-7.13	LMMB-10-7.13	WI	Milwaukee River	43.0333	-87.9176	Place-based/Caged	2013

(*) – Reference sites

Appendix

Table A1 (cont). Great Lakes Mussel Watch 2013 - 2018 PFAS sampling locations. Individual sites are listed by their general location (associated river/lake region) and year sampled, while (*) signifies reference sites. (WI - Wisconsin, MI - Michigan, OH - Ohio, PA - Pennsylvania, NY – New York). Additional information on MWP PFAS sampling locations are provided in Table A3.

Site Name	Site Code	State	General Location	Latitude	Longitude	Sample Type	Year Sampled
Milwaukee River-16-S4-7.17	LMMB-16-S4-7.17	WI	Milwaukee River	43.0351	-87.9105	Place-based/Caged	2017
Milwaukee River-7-7.13	LMMB-7-7.13	WI	Milwaukee River	43.0440	-87.9129	Place-based/Caged	2013
Milwaukee River-8-7.13	LMMB-8-7.13	WI	Milwaukee River	43.0570	-87.8997	Place-based/Caged	2013
MuskegonLight-11.2718	MUS-11.27.18	MI	Muskegon	43.2266	-86.3415	Place-based/Insitu	2018
MuskegonLight-5.15.18	MUS-5.15.18	MI	Muskegon	43.2266	-86.3415	Place-based/Insitu	2018
MuskegonLight-5.2.18	MUS-5.2.18	MI	Muskegon	43.2266	-86.3415	Place-based/Insitu	2018
MuskegonLight-5.29.18	MUS-5.29.18	MI	Muskegon	43.2266	-86.3415	Place-based/Insitu	2018
MuskegonLight-6.15.18	MUS-6.15.18	MI	Muskegon	43.2266	-86.3415	Place-based/Insitu	2018
MuskegonLight-6.26.18	MUS-6.26.18	MI	Muskegon	43.2266	-86.3415	Place-based/Insitu	2018
MuskegonLight-7.18	MUS-7.18	MI	Muskegon	43.2266	-86.3415	Place-based/Insitu	2018
MuskegonLight-8-9.18	MUS-8-9.18	MI	Muskegon	43.2266	-86.3415	Place-based/Insitu	2018
NFTA Boat Harbor-01A-7.14	NRHP-01A-7.14	NY	NFTA Boat Harbor	42.8442	-78.8644	Place-based/Caged	2014
Niagara River-1, rep 1-6.14 (*)	NRNF-1, rep 1-6.14	NY	Niagara River	42.8708	-78.9022	Place-based	2014
Niagara River-1-7.14 (*)	NRNF-1-7.14	NY	Niagara River	42.8708	-78.9022	Place-based/Caged	2014
Niagara River-4-6.14	NRNF-4-6.14	NY	Niagara River	42.8845	-78.8908	Place-based/Insitu	2014
Niagara River-9-6.14 (*)	NRNF-9-6.14	NY	Niagara River	43.0612	-79.0028	Place-based/Insitu	2014
Oswego River-INMU-CH-10.18	LOOR-INMU-CH-10.18	NY	Oswego River	43.4649	-76.5157	Monitoring/Surveillance	2018
Ottawa River-1-6.15	LEOT-1-6.15	OH	Ottawa River	41.7329	-83.4682	Place-based/Caged	2015
Ottawa River-2-6.15	LEOT-2-6.15	OH	Ottawa River	41.7247	-83.4798	Place-based/Caged	2015
Ottawa River-3.6.15	LEOT-3-6.15	OH	Ottawa River	41.7106	-83.4994	Place-based/Caged	2015
Port Sheldon-0-INMU-5.31.18	LMPS-0-INMU-5.31.18	MI	Port Sheldon	42.9016	-86.2155	Monitoring/Surveillance	2018
Presque Isle-5-9.14	LEPB-5-9.14	PA	Presque Isle	42.1304	-80.1132	Monitoring/Surveillance	2014
Presque Isle-7-9.14	LEPB-7-9.14	PA	Presque Isle	42.1233	-80.1320	Monitoring/Surveillance	2014
River Rouge-1-6.16	DRRR-1-6.16	MI	River Rouge	42.2801	-83.1225	Place-based/Caged	2016
River Rouge-2-6.16	DRRR-2-6.16	MI	River Rouge	42.2859	-83.1394	Place-based/Caged	2016
River Rouge-3-6.16	DRRR-3-6.16	MI	River Rouge	42.2951	-83.1491	Place-based/Caged	2016
St. Joseph River-0-INMU-5.18	LMSJ-0-INMU-5.18	MI	St. Joseph River	42.1160	-86.4937	Monitoring/Surveillance	2018
Scajaquada Creek-00A-7.14	NRSC-00A-7.14	NY	Scajaquada Creek	42.9300	-78.8999	Place-based/Caged	2014
Scajaquada Creek-01A-7.14	NRSC-01A-7.14	NY	Scajaquada Creek	42.9291	-78.8985	Place-based/Caged	2014
Smokes Creek-01A-7.14	NRSM-01A-7.14	NY	Smokes Creek	42.8113	-78.8637	Place-based/Caged	2014
Sturgeon Bay-0-INMU-8.18	LMSB-0-INMU-8.18	WI	Sturgeon Bay	44.8798	-87.4172	Monitoring/Surveillance	2018
Thunder Bay-7.13 (*)	TBHS5-7.13	MI	Thunder Bay	45.0461	-83.4156	Monitoring/Surveillance	2013
Thunder BayDock-6.18	TBRD-INMU-CH-6.18	MI	Thunder Bay River	45.0671	-83.4346	Monitoring/Surveillance	2018
Times Beach-01B-7.14	NRTB-01B-7.14	NY	Times Beach	43.0112	-78.9061	Place-based/Caged	2014
Tonawanda Creek-00A-7.14	NRTW-00A-7.14	NY	Tonawanda Creek	43.0247	-78.8815	Place-based/Caged	2014
Tonawanda Creek-01B-7.14	NRTW-01B-7.14	NY	Tonawanda Creek	43.0223	-78.8812	Place-based/Caged	2014

(*) – Reference sites

Appendix

Table A1 (cont). Great Lakes Mussel Watch 2013 - 2018 PFAS sampling locations. Individual sites are listed by their general location (associated river/lake region) and year sampled, while (*) signifies reference sites. (WI - Wisconsin, MI - Michigan, OH - Ohio, PA - Pennsylvania, NY – New York). Additional information on MWP PFAS sampling locations are provided in Table A3.

Site Name	Site Code	State	General Location	Latitude	Longitude	Sample Type	Year Sampled
Tonawanda Creek-02A-7.14	NRTW-02A-7.14	NY	Tonawanda Creek	43.0195	-78.8530	Place-based/Caged	2014
Trenton Channel-1-6.16	DRTC-1-6.16	MI	Trenton Channel	42.1165	-83.1806	Monitoring/Surveillance	2016
Trenton Channel-2-6.16	DRTC-2-6.16	MI	Trenton Channel	42.1861	-83.1502	Monitoring/Surveillance	2016
Two Mile Creek-00A-7.14	NRTM-00A-7.14	NY	Two Mile Creek	43.0112	-78.9062	Place-based/Caged	2014
Two Mile Creek-01A-7.14	NRTM-01A-7.14	NY	Two Mile Creek	43.0108	-78.9064	Place-based/Caged	2014
Two Rivers-0-INMU-8.18	LMTR-0-INMU-8.18	WI	Two Rivers	44.1431	-87.5623	Monitoring/Surveillance	2018
YoungstownNR-10.18	NRYT-INMU-CH-10.18	NY	Youngstown	43.2313	-79.0518	Monitoring/Surveillance	2018

(*) – Reference sites

Appendix

Table A2. Information on individual per- and polyfluoroalkyl substances (PFAS), analyte abbreviations (acronym), and analyte groups measured in dreissenid mussel tissue 2013-2018. [CASRN, Chemical Abstracts Service Registry Number].

Chemical Name	Acronym	CASRN #	PFAS Group	Carbon Number	LogKow	Molecular Formula	Molecular Weight
4,8-dioxa-3H-perfluorononanoic acid	ADONA	958445-44-8	Per- and polyfluoroalkyl ether carboxylic acids (PFECAs)	C7	3.56[b]	$C_7H_2F_{12}O_4$	378.1
Hexafluoropropylene oxide dimer acid (Gen-X)	HFPO-DA (GenX)	13252-13-6	Per- and polyfluoroalkyl ether acids (PFEAs)	C6	3.36[b]	$C_6HF_{11}O_3$	330.1
N-Ethylperfluorooctanesulfonamidoacetic acid	N-EtFOSAA	2991-50-6	Perfluoroalkane sulfonamido acetic acids (FOSAAs)	C12	6.22[b]	$C_{12}H_8F_{17}NO_4S$	527.2
N-Methylperfluorooctanesulfonamidoacetic acid	N-MeFOSAA	2355-31-9	Perfluoroalkane sulfonamido acetic acids (FOSAAs)	C11	5.73[b]	$C_{11}H_6F_{17}NO_4S$	571.2
Perfluoro-n-butanoic acid	PFBA	375-22-4	Perfluoroalkyl carboxylic acids (PFCAs)	C4	2.82[a]	$C_4HF_7O_2$	214.0
Perfluoro-1-butanesulfonic acid	PFBS	375-73-5	Perfluoroalkane sulfonic acids (PFSAs)	C4	3.90[a]	$C_4HF_9O_3S$	300.1
Perfluoro-n-decanoic acid	PFDA	335-76-2	Perfluoroalkyl carboxylic acids (PFCAs)	C10	6.50[a]	$C_{10}HF_{19}O_2$	514.1
Perfluoro-n-dodecanoic acid	PFDoA	307-55-1	Perfluoroalkyl carboxylic acids (PFCAs)	C12	7.49[b]	$C_{12}HF_{23}O_2$	614.1
Perfluoro-1-decanesulfonic acid	PFDS	2806-15-7	Perfluoroalkane sulfonic acids (PFSAs)	C10	5.83[b]	$C_{10}F_{21}O_3S$	600.1
Perfluoro-n-heptanoic acid	PFHpA	375-85-9	Perfluoroalkyl carboxylic acids (PFCAs)	C7	4.67[a]	$C_7HF_{13}O_2$	364.1
Perfluoro-1-heptanesulfonic acid	PFHpS	375-92-8	Perfluoroalkane sulfonic acids (PFSAs)	C7	3.82[b]	$C_7F_{15}SO_3$	450.1
Perfluoro-n-hexanoic acid	PFHxA	307-24-4	Perfluoroalkyl carboxylic acids (PFCAs)	C6	4.06[a]	$C_6HF_{11}O_2$	314.1
Perfluoro-1-hexanesulfonic acid	PFHxS	3871-99-6	Perfluoroalkane sulfonic acids (PFSAs)	C6	5.17[a]	$C_6HF_{13}O_3S$	400.1
Perfluoro-n-nonanoic acid	PFNA	375-95-1	Perfluoroalkyl carboxylic acids (PFCAs)	C9	5.92[a]	$C_9HF_{17}O_2$	464.1
Perfluoro-1-nonanesulfonic acid	PFNS	98789-57-2	Perfluoroalkane sulfonic acids (PFSAs)	C9	5.16[b]	$C_9F_{19}SO_3-$	550.1
Perfluoro-n-octanoic acid	PFOA	335-67-1	Perfluoroalkyl carboxylic acids (PFCAs)	C8	5.30[a]	$C_8HF_{15}O_2$	414.1
Perfluoro-1-octanesulfonic acid	PFOS	1763-23-1	Perfluoroalkane sulfonic acids (PFSAs)	C8	6.43[a]	$C_8HF_{17}O_3S$	500.1
Perfluorooctane sulfonamide	PFOSA	754-91-6	Perfluoroalkane sulfonamide (FASA)	C8	5.8[b]	$C_8H_2F_{17}NO_2S$	499.1
Perfluoro-n-pentanoic acid	PFPeA	2706-90-3	Perfluoroalkyl carboxylic acids (PFCAs)	C5	3.43[a]	$C_5HF_9O_2$	264.0
Perfluoro-1-pentanesulfonic acid	PFPeS	630402-22-1	Perfluoroalkane sulfonic acids (PFSAs)	C5	2.49[b]	$C_5HF_{11}O_2S$	350.1
Perfluoro-n-tetradecanoic acid	PFTreA	376-06-7	Perfluoroalkyl carboxylic acids (PFCAs)	C14	8.83[b]	$C_{14}HF_{27}O_2$	714.1
Perfluoro-n-tridecanoic acid	PFTriA	72629-94-8	Perfluoroalkyl carboxylic acids (PFCAs)	C13	8.16[b]	$C_{13}HF_{25}O_2$	664.1
Perfluoro-n-undecanoic acid	PFUnA	2058-94-8	Perfluoroalkyl carboxylic acids (PFCAs)	C11	7.15[a]	$C_{11}HF_{21}O_2$	564.1
11-chloroeicosafluoro-3-oxaundecane-1-sulfonic acid	11Cl-PF3OUdS	83329-89-9	Per- and polyfluoroalkyl ether acids (PFESAs)	C10	6.58[b]	$C_{10}HClF_{20}O_4S$	632.6
1H,1H,2H,2H-perfluoro-1-hexanesulfonic acid	4:2 FTS	27619-93-8	Fluorotelomer sulfonic acids (FTSAs)	C6	3.21[a]	$C_6H_5F_9O_3S$	328.2
1H,1H,2H,2H-perfluoro-1-octanesulfonic acid	6:2 FTS	27619-94-9	Fluorotelomer sulfonic acids (FTSAs)	C8	4.44[a]	$C_8H_5F_{13}O_3S$	428.2
1H,1H,2H,2H-perfluoro-1-decanesulfonic acid	8:2 FTS	27619-96-1	Fluorotelomer sulfonic acids (FTSAs)	C10	5.66[a]	$C_{10}H_5F_{17}O_3S$	529.2
9-chlorohexadecafluoro-3-oxanone-1-sulfonic acid	9Cl-PF3ONS	73606-19-6	Per- and polyfluoroalkyl ether acids (PFESAs)	C8	5.24[b]	$C_8HClF_{16}O_4S$	532.6

a: Yun et al., 2023.

b: USEPA EPI Suite - (EPI Suite™ v4.10).

Appendix

Table A3. List of Great Lakes dreissenid mussel study sites sub-watersheds (HUC-10), and land-use category estimates (%). Mussel sites are listed by their site category (predominant land-use category), general location (associated riverine/lake region), and month/year sampled, while mussel site code provides an abbreviated listing of mussel sampling locations (lakes and connecting channels), and month/year sampled.

					Mussel site land-use categories							
					Barren	Developed	Forest	Grassland	Open-water	Agriculture	Shrubs	Wetlands
Site Code	Site Name	Site Category	HUC Name	HUC-10	(%)	(%)	(%)	(%)	(%)	(%)	(%)	(%)
LMAG-0-INMU-8.18	Algoma-0-INMU-8.18	Open-water	Lake Michigan	0	0	0	0	0	1	0	0	0
LMAG-1-8.18	Algoma-1-8.18	Open-water	Lake Michigan	0	0	0	0	0	1	0	0	0
LEAR-1-9.14	Ashtabula River-1-9.14	Open-water	Lake Erie	0	0	0	0	0	1	0	0	0
LEAR-3-9.14	Ashtabula River-3-9.14	Open-water	Lake Erie	0	0	0	0	0	1	0	0	0
LMBR-0-5.18	Black River LM-0-5.18	Open-water	Lake Michigan	0	0	0	0	0	1	0	0	0
LEBR-0-9.14	Black River-0-9.14	Open-water	Lake Erie	0	0	0	0	0	1	0	0	0
LEBR-1-9.14	Black River-1-9.14	Open-water	Lake Erie	0	0	0	0	0	1	0	0	0
LOCV-IN-10-INMU-10.18	Cape Vincent-INMU-10.18	Undeveloped	Headwaters St. Lawrence River	0415030900	0.0315	0.0519	0.3982	0.0187	0.2495	0.2125	0.0202	0.0176
NRCY-01A-7.14	Cayuga Creek-01A-7.14	Developed	Niagara River	0412010406	0.0077	0.5297	0.0692	0.0065	0.0689	0.1720	0.0055	0.1407
LECR-5-9.14	Cuyahoga River-5-9.14	Open-water	Lake Erie	0	0	0	0	0	1	0	0	0
LECR-9.14	Cuyahoga River-9.14	Open-water	Lake Erie	0	0	0	0	0	1	0	0	0
DRSE-0-6.16	Detroit River Fox Is-0-6.16	Agriculture	Detroit	0409000400	0.0095	0.2419	0.0405	0.0025	0.1538	0.5016	0.0027	0.0472
NREL-01A-7.14	Ellicott Creek-01A-7.14	Developed	Ellicott Creek	0412010404	0.0101	0.4131	0.1829	0.0019	0.0072	0.2099	0.0012	0.1736
LOFC-IN-INMU-CH-10.18	Fourmile Creek-INMU-CH-10.18	Open-water	Lake Ontario	0	0	0	0	0	1	0	0	0
NRGL-01A-7.14	Gill Creek-01A-7.14	Developed	Niagara River	0412010406	0.0077	0.5297	0.0692	0.0065	0.0689	0.1720	0.0055	0.1407
NRGL-02A-7.14	Gill Creek-02A-7.14	Developed	Niagara River	0412010406	0.0077	0.5297	0.0692	0.0065	0.0689	0.1720	0.0055	0.1407
NRGL-03A-7.14	Gill Creek-03A-7.14	Developed	Niagara River	0412010406	0.0077	0.5297	0.0692	0.0065	0.0689	0.1720	0.0055	0.1407
LMKZ-0-5.18	Kalamazoo River-0-5.18	Open-water	Lake Michigan	0	0	0	0	0	1	0	0	0
LMKW-0-8.18	Kewaunee River-0-8.18	Open-water	Lake Michigan	0	0	₀	0	0	1	0	0	0
LMKW-1-8.18	Kewaunee River-1-8.18	Open-water	Lake Michigan	0	0	0	0	0	1	0	0	0
LMMB-13-7.13	Kinnickinnic River-13-7.13	Developed	Kinnickinnic River	0404000305	0.0008	0.9785	0.0054	0.0036	0.0018	0.0071	0.0001	0.0027
LMMB-13-S4-7.17	Kinnickinnic River13-S4-7.17	Developed	Kinnickinnic River	0404000305	0.0008	0.9785	0.0054	0.0036	0.0018	0.0071	0.0001	0.0027

Table A3 (cont)**.** List of Great Lakes dreissenid mussel study sites sub-watersheds (HUC-10), and land-use category estimates (%). Mussel sites are listed by their site category (predominant land-use category), general location (associated riverine/lake region), and month/year sampled, while mussel site code provides an abbreviated listing of mussel sampling locations (lakes and connecting channels), and month/year sampled.

					Mussel site land-use categories							
					Barren	Developed	Forest	Grassland	Open-water	Agriculture	Shrubs	Wetlands
Site Code	Site Name	Site Category	HUC Name	HUC-10	(%)	(%)	(%)	(%)	(%)	(%)	(%)	(%)
LMMB-14-7.17	Kinnickinnic River-14-7.17	Developed	Kinnickinnic River	0404000305	0.0008	0.9785	0.0054	0.0036	0.0018	0.0071	0.0001	0.0027
LOFO-INMU-CH-6.18	Lake OntarioFS-INMU-CH-6.18	Open-water	Lake Ontario	0	0	0	0	0	1	0	0	0
LMMW-0-INMU-8.14	Manitowoc-0-INMU-8.14	Open-water	Lake Michigan	0	0	0	0	0	1	0	0	0
LMMW-1-INMU-8.14	Manitowoc-1-INMU-8.14	Open-water	Lake Michigan	0	0	0	0	0	1	0	0	0
LEMR-0-5.16	Maumee Grassy Isl-0-5.16	Open-water	Lake Erie	0	0	0	0	0	1	0	0	0
LEMR-0-6.15	Maumee Grassy Isl-0-6.15	Open-water	Lake Erie	0	0	0	0	0	1	0	0	0
LEMR-0-6.16	Maumee Grassy Isl-0-6.16	Open-water	Lake Erie	0	0	0	0	0	1	0	0	0
LEMR-0-7.15	Maumee Grassy Isl-0-7.15	Open-water	Lake Erie	0	0	0	0	0	1	0	0	0
LEMR-3-5.15	Maumee Lighthouse-3-5.15	Open-water	Lake Erie	0	0	0	0	0	1	0	0	0
LEMR-3-5.16	Maumee Lighthouse-3-5.16	Open-water	Lake Erie	0	0	0	0	0	1	0	0	0
LEMR-3-6.15	Maumee Lighthouse-3-6.15	Open-water	Lake Erie	0	0	0	0	0	1	0	0	0
LEMR-3-6.16	Maumee Lighthouse-3-6.16	Open-water	Lake Erie	0	0	0	0	0	1	0	0	0
LEMR-3-7.15	Maumee Lighthouse-3-7.15	Open-water	Lake Erie	0	0	0	0	0	1	0	0	0
LEMR-4-6.16	Maumee River-4-6.16	Developed	Grassy Creek-Maumee River	0410000909	0.0037	0.4934	0.0407	0.0062	0.0764	0.3611	0.0002	0.0183
LEMR-2-5.16	Maumee Upstream -2-5.15	Developed	Grassy Creek-Maumee River	0410000909	0.0037	0.4934	0.0407	0.0062	0.0764	0.3611	0.0002	0.0183
LEMR-2-6.16	Maumee Upstream -2-6.15	Developed	Grassy Creek-Maumee River	0410000909	0.0037	0.4934	0.0407	0.0062	0.0764	0.3611	0.0002	0.0183
LEMR-2-7.15	Maumee Upstream -2-7.15	Developed	Grassy Creek-Maumee River	0410000909	0.0037	0.4934	0.0407	0.0062	0.0764	0.3611	0.0002	0.0183
LEMR-1-5.15	Maumee WWTP-1-5.15	Developed	Grassy Creek-Maumee River	0410000909	0.0037	0.4934	0.0407	0.0062	0.0764	0.3611	0.0002	0.0183

Table A3 (cont)**.** List of Great Lakes dreissenid mussel study sites sub-watersheds (HUC-10), and land-use category estimates (%). Mussel sites are listed by their site category (predominant land-use category), general location (associated riverine/lake region), and month/year sampled, while mussel site code provides an abbreviated listing of mussel sampling locations (lakes and connecting channels), and month/year sampled.

					Mussel site land-use categories							
					Barren	Developed	Forest	Grassland	Open-water	Agriculture	Shrubs	Wetlands
Site Code	Site Name	Site Category	HUC Name	HUC-10	(%)	(%)	(%)	(%)	(%)	(%)	(%)	(%)
LEMR-1-6.15	Maumee WWTP-1-6.15	Developed	Grassy Creek-Maumee River	0410000909	0.0037	0.4934	0.0407	0.0062	0.0764	0.3611	0.0002	0.0183
LEMR-1-6.16	Maumee WWTP-1-6.16	Developed	Grassy Creek-Maumee River	0410000909	0.0037	0.4934	0.0407	0.0062	0.0764	0.3611	0.0002	0.0183
LEMR-1-7.15	Maumee WWTP-1-7.15	Developed	Grassy Creek-Maumee River	0410000909	0.0037	0.4934	0.0407	0.0062	0.0764	0.3611	0.0002	0.0183
LMMB-11-7.18	Menomonee River-11-7.18	Developed	Menomonee River	0404000304	0.0034	0.6904	0.0492	0.0087	0.0027	0.1608	0.0015	0.0832
LMMB-11-S4-7.17	Menomonee River-11-S4-7.17	Developed	Menomonee River	0404000304	0.0034	0.6904	0.0492	0.0087	0.0027	0.1608	0.0015	0.0832
LMMB-12-7.13	Menomonee River-12-7.13	Developed	Menomonee River	0404000304	0.0034	0.6904	0.0492	0.0087	0.0027	0.1608	0.0015	0.0832
LMMB-15-S4-BC-7.17	Menomonee River-15-S4-BC-7.17	Developed	Menomonee River	0404000304	0.0034	0.6904	0.0492	0.0087	0.0027	0.1608	0.0015	0.0832
LMMB-15-S4-TC-7.17	Menomonee River-15-S4-TC-7.17	Developed	Menomonee River	0404000304	0.0034	0.6904	0.0492	0.0087	0.0027	0.1608	0.0015	0.0832
LMMB-01-IN-6.18	Milwaukee Bay-01-INMU-6.18	Open-water	Lake Michigan	0	0	0	0	0	1	0	0	0
LMMB-01-IN-6.8.17	Milwaukee Bay-01-INMU-6.8.17	Open-water	Lake Michigan	0	0	0	0	0	1	0	0	0
LMMB-04-IN-8.17	Milwaukee Bay-04-INMU-8.17	Open-water	Lake Michigan	0	0	0	0	0	1	0	0	0
LMMB-0-6.18	Milwaukee Bay-0-6.18	Open-water	Lake Michigan	0	0	0	0	0	1	0	0	0
LMMB-12-7.13	Milwaukee Bay-0-7.13	Open-water	Lake Michigan	0	0	0	0	0	1	0	0	0
LMMB-0-7	Milwaukee Bay-0-7.18	Open-water	Lake Michigan	0	0	0	0	0	1	0	0	0
LMMB-0-IN-6	Milwaukee Bay-0-INMU-6.8.17	Open-water	Lake Michigan	0	0	0	0	0	1	0	0	0
LMMB-1-7.13	Milwaukee Bay-1-7.13	Open-water	Lake Michigan	0	0	0	0	0	1	0	0	0
LMMB-17-7.18	Milwaukee Bay-17-7.18	Open-water	Lake Michigan	0	0	0	0	0	1	0	0	0
LMMB-17-7	Milwaukee Bay-17-7.18	Open-water	Lake Michigan	0	0	0	0	0	1	0	0	0

Table A3 (cont)**.** List of Great Lakes dreissenid mussel study sites sub-watersheds (HUC-10), and land-use category estimates (%). Mussel sites are listed by their site category (predominant land-use category), general location (associated riverine/lake region), and month/year sampled, while mussel site code provides an abbreviated listing of mussel sampling locations (lakes and connecting channels), and month/year sampled.

					Mussel site land-use categories							
					Barren	Developed	Forest	Grassland	Open-water	Agriculture	Shrubs	Wetlands
Site Code	Site Name	Site Category	HUC Name	HUC-10	(%)	(%)	(%)	(%)	(%)	(%)	(%)	(%)
LMMB-4-7.13	Milwaukee Bay-4-7.13	Open-water	Lake Michigan	0	0	0	0	0	1	0	0	0
LMMB-4-7	Milwaukee Bay-4-7.18	Open-water	Lake Michigan	0	0	0	0	0	1	0	0	0
LMMB-4-S4	Milwaukee Bay-4-S4-7.17	Open-water	Lake Michigan	0	0	0	0	0	1	0	0	0
LMMB-4-S5	Milwaukee Bay-4-S5-7.17	Open-water	Lake Michigan	0	0	0	0	0	1	0	0	0
LMMB-5-6.13	Milwaukee Beach-5-6.13	Open-water	Lake Michigan	0	0	0	0	0	1	0	0	0
LMMB-5-6.17	Milwaukee Beach-5-6.17	Open-water	Lake Michigan	0	0	0	0	0	1	0	0	0
LMMB-5-6.18	Milwaukee Beach-5-6.18	Open-water	Lake Michigan	0	0	0	0	0	1	0	0	0
LMMB-5-7.13	Milwaukee Beach-5-7.13	Open-water	Lake Michigan	0	0	0	0	0	1	0	0	0
LMMB-5-7.18	Milwaukee Beach-5-7.18	Open-water	Lake Michigan	0	0	0	0	0	1	0	0	0
LMMB-5-8	Milwaukee Beach-5HDPE-8.17	Open-water	Lake Michigan	0	0	0	0	0	1	0	0	0
LMMB-08-S4	Milwaukee Beach-5-S4-8.17	Open-water	Lake Michigan	0	0	0	0	0	1	0	0	0
LMMB-08-S5	Milwaukee Beach-5-S5-8.17	Open-water	Lake Michigan	0	0	0	0	0	1	0	0	0
LMMB-6-7.13	Milwaukee Bridge-6-7.13	Developed	Lower Milwaukee River-Frontal Lake Michigan	0404000306	0.0028	0.5079	0.1002	0.0207	0.0139	0.2567	0.0023	0.0955
LMMB-6-7.17	Milwaukee Bridge-6-7.17	Developed	Lower Milwaukee River-Frontal Lake Michigan	0404000306	0.0028	0.5079	0.1002	0.0207	0.0139	0.2567	0.0023	0.0955
LMMB-6-7.18	Milwaukee Bridge-6-7.18	Developed	Lower Milwaukee River-Frontal Lake Michigan	0404000306	0.0028	0.5079	0.1002	0.0207	0.0139	0.2567	0.0023	0.0955
LMMB-08-S4	Milwaukee River-08-S4-8.17	Developed	Lower Milwaukee River-Frontal Lake Michigan	0404000306	0.0028	0.5079	0.1002	0.0207	0.0139	0.2567	0.0023	0.0955

Table A3 (cont)**.** List of Great Lakes dreissenid mussel study sites sub-watersheds (HUC-10), and land-use category estimates (%). Mussel sites are listed by their site category (predominant land-use category), general location (associated riverine/lake region), and month/year sampled, while mussel site code provides an abbreviated listing of mussel sampling locations (lakes and connecting channels), and month/year sampled.

					Mussel site land-use categories							
					Barren	Developed	Forest	Grassland	Open-water	Agriculture	Shrubs	Wetlands
Site Code	Site Name	Site Category	HUC Name	HUC-10	(%)	(%)	(%)	(%)	(%)	(%)	(%)	(%)
LMMB-08-S5	Milwaukee River-08-S5-8.17	Developed	Lower Milwaukee River-Frontal Lake Michigan	0404000306	0.0028	0.5079	0.1002	0.0207	0.0139	0.2567	0.0023	0.0955
LMMB-10-7.13	Milwaukee River-10-7.13	Developed	Lower Milwaukee River-Frontal Lake Michigan	0404000306	0.0028	0.5079	0.1002	0.0207	0.0139	0.2567	0.0023	0.0955
LMMB-16-S4	Milwaukee River-16-S4-7.17	Developed	Lower Milwaukee River-Frontal Lake Michigan	0404000306	0.0028	0.5079	0.1002	0.0207	0.0139	0.2567	0.0023	0.0955
LMMB-7-7.13	Milwaukee River-7-7.13	Developed	Lower Milwaukee River-Frontal Lake Michigan	0404000306	0.0028	0.5079	0.1002	0.0207	0.0139	0.2567	0.0023	0.0955
LMMB-8-7.13	Milwaukee River-8-7.13	Developed	Lower Milwaukee River-Frontal Lake Michigan	0404000306	0.0028	0.5079	0.1002	0.0207	0.0139	0.2567	0.0023	0.0955
MUS-11.27	MuskegonLight-11.2718	Undeveloped	Stony Creek-Frontal Lake Michigan	0406010110	0.0355	0.1673	0.3895	0.0475	0.0223	0.2387	0.0081	0.0910
MUS-5.15	MuskegonLight-5.15.18	Undeveloped	Stony Creek-Frontal Lake Michigan	0406010110	0.0355	0.1673	0.3895	0.0475	0.0223	0.2387	0.0081	0.0910
MUS-5.2	MuskegonLight-5.2.18	Undeveloped	Stony Creek-Frontal Lake Michigan	0406010110	0.0355	0.1673	0.3895	0.0475	0.0223	0.2387	0.0081	0.0910
MUS-5.29	MuskegonLight-5.29.18	Undeveloped	Stony Creek-Frontal Lake Michigan	0406010110	0.0355	0.1673	0.3895	0.0475	0.0223	0.2387	0.0081	0.0910
MUS-6.15	MuskegonLight-6.15.18	Undeveloped	Stony Creek-Frontal Lake Michigan	0406010110	0.0355	0.1673	0.3895	0.0475	0.0223	0.2387	0.0081	0.0910
MUS-6.26	MuskegonLight-6.26.18	Undeveloped	Stony Creek-Frontal Lake Michigan	0406010110	0.0355	0.1673	0.3895	0.0475	0.0223	0.2387	0.0081	0.0910

Table A3 (cont)**.** List of Great Lakes dreissenid mussel study sites sub-watersheds (HUC-10), and land-use category estimates (%). Mussel sites are listed by their site category (predominant land-use category), general location (associated riverine/lake region), and month/year sampled, while mussel site code provides an abbreviated listing of mussel sampling locations (lakes and connecting channels), and month/year sampled.

					Mussel site land-use categories							
					Barren	Developed	Forest	Grassland	Open-water	Agriculture	Shrubs	Wetlands
Site Code	Site Name	Site Category	HUC Name	HUC-10	(%)	(%)	(%)	(%)	(%)	(%)	(%)	(%)
MUS-7.19	MuskegonLight-7.18	Undeveloped	Stony Creek-Frontal Lake Michigan	0406010110	0.0355	0.1673	0.3895	0.0475	0.0223	0.2387	0.0081	0.0910
MUS-8-9	MuskegonLight-8-9.18	Undeveloped	Stony Creek-Frontal Lake Michigan	0406010110	0.0355	0.1673	0.3895	0.0475	0.0223	0.2387	0.0081	0.0910
NRHP-01A-7.15	NFTA Boat Harbor-01A-7.14	Open-water	Lake Erie	0	0	0	0	0	1	0	0	0
NRNF-1, rep 1-6.15	Niagara River-1, rep 1-6.14	Open-water	Lake Erie	0	0	0	0	0	1	0	0	0
NRNF-1-7.15	Niagara River-1-7.14	Open-water	Lake Erie	0	0	0	0	0	1	0	0	0
NRNF-4-6.15	Niagara River-4-6.14	Open-water	Lake Erie	0	0	0	0	0	1	0	0	0
NRNF-9-6.15	Niagara River-9-6.14	Open-water	Lake Erie	0	0	0	0	0	1	0	0	0
LOOR-IN-10	Oswego River-INMU-CH-10.18	Undeveloped	Oswego River	0414020302	0.0018	0.1041	0.4666	0.0025	0.0415	0.2096	0.0222	0.1516
LEOT-01	Ottawa River-1-6.15	Agriculture	Ottawa River-Frontal Lake Erie	0410000103	0.0066	0.4158	0.0758	0.0038	0.0071	0.4745	0.0002	0.0165
LEOT-02	Ottawa River-2-6.15	Agriculture	Ottawa River-Frontal Lake Erie	0410000103	0.0066	0.4158	0.0758	0.0038	0.0071	0.4745	0.0002	0.0165
LEOT-03	Ottawa River-3-6.15	Agriculture	Ottawa River-Frontal Lake Erie	0410000103	0.0066	0.4158	0.0758	0.0038	0.0071	0.4745	0.0002	0.0165
LMPS-IN-0	Port Sheldon-0-INMU-5.31	Open-water	Lake Michigan	0	0	0	0	0	1	0	0	0
LEPB-5-9.15	Presque Isle-5-9.14	Open-water	Lake Erie	0	0	0	0	0	1	0	0	0
LEPB-7-9.15	Presque Isle-7-9.14	Open-water	Lake Erie	0	0	0	0	0	1	0	0	0
DRRR-1-6.17	River Rouge-1-6.16	Developed	River Rouge	0409000404	0.0004	0.9416	0.0307	0.0006	0.0134	0.0012	0	0.0121
DRRR-2-6.17	River Rouge-2-6.16	Developed	River Rouge	0409000404	0.0004	0.9416	0.0307	0.0006	0.0134	0.0012	0	0.0121
DRRR-3-6.17	River Rouge-3-6.16	Developed	River Rouge	0409000404	0.0004	0.9416	0.0307	0.0006	0.0134	0.0012	0	0.0121

Table A3 (cont)**.** List of Great Lakes dreissenid mussel study sites sub-watersheds (HUC-10), and land-use category estimates (%). Mussel sites are listed by their site category (predominant land-use category), general location (associated riverine/lake region), and month/year sampled, while mussel site code provides an abbreviated listing of mussel sampling locations (lakes and connecting channels), and month/year sampled.

					Mussel site land-use categories							
					Barren	Developed	Forest	Grassland	Open-water	Agriculture	Shrubs	Wetlands
Site Code	Site Name	Site Category	HUC Name	HUC-10	(%)	(%)	(%)	(%)	(%)	(%)	(%)	(%)
LMSJ-IN-0	Saint Joseph River-0-INMU-5.18	Open-water	Lake Michigan	0	0	0	0	0	1	0	0	0
NRSC-00A-7.15	Scajaquada Creek-00A-7.14	Agriculture	Niagara River	0412010406	0.0401	0.1216	0.1755	0.0023	0.0435	0.5968	0.0157	0.0045
NRSC-01A-7.15	Scajaquada Creek-01A-7.14	Developed	Niagara River	0412010406	0.0077	0.5297	0.0692	0.0065	0.0689	0.1720	0.0055	0.1407
NRSM-01A-7.15	Smokes Creek-01A-7.14	Developed	Smoke Creek-Frontal Lake Erie	0412010304	0.0173	0.5500	0.2240	0.0096	0.0042	0.0893	0.0070	0.0986
LMSB-IN-0	Sturgeon Bay-0-INMU-8.18	Open-water	Lake Michigan	0	0	0	0	0	1	0	0	0
TBHS5-7.13	Thunder Bay-7.13	Open-water	Lake Huron	0	0	0	0	0	1	0	0	0
TBRD-IN-6	Thunder BayDock-6.18	Wetlands	Thunder Bay River	0407000606	0.0007	0.0667	0.1415	0.0184	0.0164	0.2379	0.0034	0.5150
NRTB-01B-7.15	Times Beach-01B-7.14	Developed	Niagara River	0412010406	0.0077	0.5297	0.0692	0.0065	0.0689	0.1720	0.0055	0.1407
NRTW-00A-7.15	Tonawanda Creek-00A-7.14	Developed	Niagara River	0412010406	0.0077	0.5297	0.0692	0.0065	0.0689	0.1720	0.0055	0.1407
NRTW-01B-7.15	Tonawanda Creek-01B-7.14	Agriculture	Lower Tonawanda Creek	0412010405	0.0186	0.2785	0.1267	0.0050	0.0089	0.3450	0.0013	0.2160
NRTW-02A-7.15	Tonawanda Creek-02A-7.14	Agriculture	Lower Tonawanda Creek	0412010405	0.0186	0.2785	0.1267	0.0050	0.0089	0.3450	0.0013	0.2160
DRTC-1-6.17	Trenton Channel-1-6.16	Agriculture	Detroit	0409000401	0.0095	0.2419	0.0405	0.0025	0.1538	0.5016	0.0027	0.0472
DRTC-2-6.17	Trenton Channel-2-6.16	Agriculture	Detroit	0409000401	0.0095	0.2419	0.0405	0.0025	0.1538	0.5016	0.0027	0.0472
NRTM-00A-7.15	Two Mile Creek-00A-7.14	Developed	Niagara River	0412010406	0.0077	0.5297	0.0692	0.0065	0.0689	0.1720	0.0055	0.1407
NRTM-01A-7.15	Two Mile Creek-01A-7.14	Developed	Niagara River	0412010406	0.0077	0.5297	0.0692	0.0065	0.0689	0.1720	0.0055	0.1407
LMTR-IN-0	Two Rivers-0-INMU-8.18	Open-water	Lake Michigan	0	0	0	0	0	1	0	0	0
NRYT-IN-10	YoungstownNR-10.18	Agriculture	Twelvemile Creek-Frontal Lake Ontario	0413000109	0.0401	0.1216	0.1755	0.0023	0.0435	0.5968	0.0157	0.0045

Appendix

Table A4. Summary of $\sum_{19}$PFAS sum concentration range (ng/g wet weight) measured (> MDL) in mussel tissue across the Great Lakes MWP sampling locations between 2013-2018. Individual sites are listed by their general location (associated river/lake region) and year sampled, while (*) signifies reference sites. (WI - Wisconsin, MI - Michigan, OH - Ohio, PA - Pennsylvania, NY – New York).

						Min	Mean	Max (SumConc)
Sampling Location	Site Name	Site Code	State	Dominant Land-use	#Compounds Detected (> MDL)	ng/g (ww)	ng/g (ww)	ng/g (ww)
Lake Michigan	Algoma-1-8.18	LMAG-1-8.18	WI	Open-water	1	0.379	0.379	0.379
	Black River LM-0-5.18	LMBR-0-5.18	MI	Open-water	2	0.461	0.562	1.12
	Kalamazoo River-0-5.18	LMKZ-0-5.18	WI	Open-water	3	0.302	1.82	5.46
	Kewaunee River-0-8.18	LMKW-0-8.18	WI	Open-water	1	0.643	0.643	0.643
	Kinnickinnic River-13-7.13	LMMB-13-7.13	WI	Developed	8	0.064	0.667	5.34
	Kinnickinnic River-14-7.17	LMMB-14-7.17	WI	Developed	4	0.394	1.08	4.32
	Kinnickinnic River13-S4-7.17	LMMB-13-S4-7.17	WI	Developed	6	0.139	1.64	9.83
	Manitowoc-0-INMU-8.14	LMMW-0-INMU-8.14	WI	Open-water	2	0.531	0.626	1.25
	Manitowoc-1-INMU-8.14	LMMW-1-INMU-8.14	WI	Developed	1	0.455	0.455	0.455
	Menomonee River-11-7.18	LMMB-11-7.18	WI	Developed	1	0.903	0.903	0.903
	Menomonee River-11-S4-7.17	LMMB-11-S4-7.17	WI	Developed	1	0.749	0.749	0.749
	Menomonee River-12-7.13	LMMB-12-7.13	WI	Developed	8	0.100	0.491	3.93
	Menomonee River-15-S4-BC-7.17	LMMB-15-S4-BC-7.17	WI	Developed	5	0.170	0.627	3.13
	Menomonee River-15-S4-TC-7.17	LMMB-15-S4-TC-7.17	WI	Developed	2	0.759	1.06	2.11
	Milwaukee Bay-0-6.18	LMMB-0-6.18	WI	Open-water	2	0.479	0.608	1.22
	Milwaukee Bay-0-7.13	LMMB-0-7.13	WI	Open-water	7	0.113	0.560	3.92
	Milwaukee Bay-0-INMU-6.8.17	LMMB-0-INMU-6.8.17	WI	Open-water	2	0.197	0.473	0.945
	Milwaukee Bay-01-INMU-6.18	LMMB-01-INMU-6.18	WI	Open-water	1	0.640	0.640	0.640
	Milwaukee Bay-04-INMU-8.17	LMMB-04-INMU-8.17	WI	Open-water	3	0.152	0.376	1.13
	Milwaukee Bay-1-7.13	LMMB-1-7.13	WI	Open-water	5	0.229	0.755	3.78
	Milwaukee Bay-4-6.13	LMMB-4-6.13	WI	Open-water	4	0.495	0.860	3.44
	Milwaukee Bay-4-6.18	LMMB-4-6.18	WI	Open-water	2	0.541	0.603	1.21
	Milwaukee Bay-4-7.13	LMMB-4-7.13	WI	Open-water	7	0.196	0.598	4.19
	Milwaukee Bay-4-7.18	LMMB-4-7.18	WI	Open-water	4	0.344	0.548	2.19
	Milwaukee Bay-4-S5-7.17	LMMB-4-S5-7.17	WI	Open-water	2	0.394	1.04	2.08
	Milwaukee Beach-5-6.13(*)	LMMB-5-6.13	WI	Open-water	4	0.383	0.627	2.51
	Milwaukee Beach-5-6.17 (*)	LMMB-5-6.17	WI	Open-water	3	0.149	0.468	1.40
	Milwaukee Beach-5-6.18 (*)	LMMB-5-6.18	WI	Open-water	4	0.103	0.482	1.93
	Milwaukee Beach-5-7.13 (*)	LMMB-5-7.13	WI	Open-water	4	0.140	0.377	1.51
	Milwaukee Beach-5-7.18 (*)	LMMB-5-7.18	WI	Open-water	1	0.390	0.390	0.390
	Milwaukee Beach-5-S4-8.17 (*)	LMMB-5-S4-8.17	WI	Open-water	4	0.153	0.434	1.74
	Milwaukee Beach-5-S5-8.17 (*)	LMMB-5-S5-8.17	WI	Open-water	1	0.228	0.228	0.228
	Milwaukee Beach-5HDPE-8.17 (*)	LMMB-5HDPE-8.17	WI	Open-water	3	0.361	0.481	1.44

(*) – Reference sites

Appendix

Table A4 (cont)**.** Summary of $\sum_{19}$PFAS sum concentration range (ng/g wet weight) measured (> MDL) in mussel tissue across the Great Lakes MWP sampling locations between 2013-2018. Individual sites are listed by their general location (associated river/lake region) and year sampled, while (*) signifies reference sites. (WI - Wisconsin, MI - Michigan, OH - Ohio, PA - Pennsylvania, NY – New York).

						Min	Mean	Max (SumConc)
Sampling Location	**Site Name**	**Site Code**	**State**	**Dominant Land-use**	**#Compounds Detected (> MDL)**	**ng/g (ww)**	**ng/g (ww)**	**ng/g (ww)**
Lake Michigan	Milwaukee Bridge-6-7.17	LMMB-6-7.17	WI	Developed	2	0.167	0.281	0.563
	Milwaukee Bridge-6-7.18	LMMB-6-7.18	WI	Developed	2	0.399	0.576	1.15
	Milwaukee River-08-S4-8.17	LMMB-08-S4-8.17	WI	Developed	2	0.736	0.827	1.65
	Milwaukee River-08-S5-8.17	LMMB-08-S5-8.17	WI	Developed	4	0.244	0.714	2.86
	Milwaukee River-10-7.13	LMMB-10-7.13	WI	Developed	5	0.288	0.696	3.48
	Milwaukee River-16-S4-7.17	LMMB-16-S4-7.17	WI	Developed	4	0.100	0.544	2.18
	Milwaukee River-7-7.13	LMMB-7-7.13	WI	Developed	5	0.139	0.473	2.37
	Milwaukee River-8-7.13	LMMB-8-7.13	WI	Developed	5	0.407	0.789	3.95
	MuskegonLight-5.15.18	MUS-5.15.18	MI	Undeveloped	2	0.414	0.576	1.15
	MuskegonLight-5.2.18	MUS-5.2.18	MI	Undeveloped	2	0.565	0.619	1.24
	MuskegonLight-5.29.18	MUS-5.29.18	MI	Undeveloped	2	0.715	0.720	1.44
	MuskegonLight-6.15.18	MUS-6.15.18	MI	Undeveloped	1	0.816	0.816	0.816
	MuskegonLight-6.26.18	MUS-6.26.18	MI	Undeveloped	1	0.620	0.620	0.620
	MuskegonLight-8-9.18	MUS-8-9.18	MI	Undeveloped	1	0.199	0.199	0.199
	Port Sheldon-0-INMU-5.31.18	LMPS-0-INMU-5.31.18	MI	Open-water	4	0.137	0.724	2.90
	Saint Joseph River-0-INMU-5.18	LMSJ-0-INMU-5.18	MI	Open-water	3	0.136	0.536	1.61
	Sturgeon Bay-0-INMU-8.18	LMSB-0-INMU-8.18	WI	Open-water	1	0.156	0.156	0.156
	Two Rivers-0-INMU-8.18	LMTR-0-INMU-8.18	WI	Open-water	1	0.625	0.625	0.625
Lake Huron	Thunder Bay-7.13(*)	TBHS5-7.13	MI	Open-water	4	0.152	0.480	1.92
	Thunder BayDock-6.18	TBRD-INMU-CH-6.18	MI	Wetlands	1	0.238	0.238	0.238
Detroit River	Detroit River Fox Is-0-6.16	DRSE-0-6.16	MI	Agriculture	1	0.196	0.196	0.196
	River Rouge-1-6.16	DRRR-1-6.16	MI	Developed	1	0.365	0.365	0.365
	River Rouge-2-6.16	DRRR-2-6.16	MI	Developed	2	0.261	0.331	0.661
	Trenton Channel-1-6.16	DRTC-1-6.16	MI	Agriculture	1	0.664	0.664	0.664
	Trenton Channel-2-6.16	DRTC-2-6.16	MI	Agriculture	1	1.28	1.28	1.28
Lake Erie	Ashtabula River-1-9.14	LEAR-1-9.14	OH	Open-water	3	0.282	0.428	1.29
	Ashtabula River-3-9.14	LEAR-3-9.14	OH	Open-water	4	0.078	0.454	1.82
	Black River-0-9.14	LEBR-0-9.14	OH	Open-water	6	0.516	0.744	4.46
	Black River-1-9.14	LEBR-1-9.14	OH	Open-water	2	0.488	0.577	1.15
	Cuyahoga River-5-9.14	LECR-5-9.14	OH	Open-water	3	0.562	0.841	2.52

(*) – Reference sites

Appendix

Table A4 (cont). Summary of $\sum_{19}$PFAS sum concentration range (ng/g wet weight) measured (> MDL) in mussel tissue across the Great Lakes MWP sampling locations between 2013-2018. Individual sites are listed by their general location (associated river/lake region) and year sampled, while (*) signifies reference sites. (WI - Wisconsin, MI - Michigan, OH - Ohio, PA - Pennsylvania, NY – New York).

						Min	Mean	Max (SumConc)
Sampling Location	**Site Name**	**Site Code**	**State**	**Dominant Land-use**	**#Compounds Detected (> MDL)**	**ng/g (ww)**	**ng/g (ww)**	**ng/g (ww)**
Lake Erie	Cuyahoga River-9.14	LECR-9.14	OH	Open-water	2	0.135	0.375	0.750
	Maumee Grassy Isl-0-5.15	LEMR-0-5.15	OH	Open-water	1	1.056	1.056	1.06
	Maumee Grassy Isl-0-6.15	LEMR-0-6.15	OH	Open-water	2	0.707	0.759	1.52
	Maumee Grassy Isl-0-6.16	LEMR-0-6.16	OH	Open-water	5	0.117	0.453	2.27
	Maumee Grassy Isl-0-7.15	LEMR-0-7.15	OH	Open-water	2	0.468	0.579	1.16
	Maumee Lighthouse-3-5.15 (*)	LEMR-3-5.15	OH	Open-water	1	0.073	0.073	0.073
	Maumee Lighthouse-3-5.16 (*)	LEMR-3-5.16	OH	Open-water	3	0.339	0.425	1.28
	Maumee Lighthouse-3-6.15 (*)	LEMR-3-6.15	OH	Open-water	2	0.460	0.610	1.22
	Maumee Lighthouse-3-7.15 (*)	LEMR-3-7.15	OH	Open-water	1	0.381	0.381	0.381
	Maumee River-4-6.16	LEMR-4-6.16	OH	Developed	3	0.160	0.282	0.847
	Maumee Upstream -2-6.15	LEMR-2-6.15	OH	Developed	3	0.255	0.648	1.95
	Maumee Upstream -2-7.15	LEMR-2-7.15	OH	Developed	2	0.711	0.740	1.48
	Maumee Upstream-02-5.15	LEMR-2-5.15	OH	Developed	4	0.122	0.355	1.42
	Maumee WWTP-1-5.15	LEMR-1-5.15	OH	Developed	2	0.126	0.130	0.260
	Maumee WWTP-1-6.15	LEMR-1-6.15	OH	Developed	1	0.402	0.402	0.402
	Maumee WWTP-1-7.15	LEMR-1-7.15	OH	Developed	2	0.105	0.225	0.450
	Ottawa River-1-6.15	LEOT-1-6.15	OH	Agriculture	3	0.134	0.439	1.32
	Ottawa River-2-6.15	LEOT-2-6.15	OH	Agriculture	3	0.064	0.444	1.33
	Ottawa River-3.6.15	LEOT-3-6.15	OH	Agriculture	3	0.146	0.348	1.05
	Presque Isle-5-9.14	LEPB-5-9.14	PA	Open-water	1	0.646	0.646	0.646
	Presque Isle-7-9.14	LEPB-7-9.14	PA	Open-water	6	0.117	1.056	6.34
Niagara River	Cayuga Creek-01A-7.14	NRCY-01A-7.14	NY	Developed	4	0.371	0.647	2.59
	Ellicott Creek-01A-7.14	NREL-01A-7.14	NY	Developed	4	0.356	0.550	2.20
	Gill Creek-01A-7.14	NRGL-01A-7.14	NY	Developed	4	0.130	0.429	1.72
	Gill Creek-02A-7.14	NRGL-02A-7.14	NY	Developed	4	0.138	0.536	2.14
	Gill Creek-03A-7.14	NRGL-03A-7.14	NY	Developed	5	0.148	0.581	2.91
	NFTA Boat Harbor-01A-7.14	NRHP-01A-7.14	NY	Open-water	3	0.331	0.461	1.38
	Niagara River-1-7.14 (*)	NRNF-1-7.14	NY	Open-water	3	0.475	0.560	1.68
	Niagara River-1, rep 1-6.14 (*)	NRNF-1, rep 1-6.14	NY	Open-water	6	0.192	0.558	3.35
	Niagara River-4-6.14	NRNF-4-6.14	NY	Open-water	4	0.107	0.499	1.99
	Niagara River-9-6.14 (*)	NRNF-9-6.14	NY	Open-water	1	0.399	0.399	0.399
	Scajaquada Creek-00A-7.14	NRSC-00A-7.14	NY	Agriculture	5	0.154	0.538	2.69

(*) – Reference sites

Table A4 (cont)**.** Summary of $\sum_{19}$PFAS sum concentration range (ng/g wet weight) measured (> MDL) in mussel tissue across the Great Lakes MWP sampling locations between 2013-2018. Individual sites are listed by their general location (associated river/lake region) and year sampled, while (*) signifies reference sites. (WI - Wisconsin, MI - Michigan, OH - Ohio, PA - Pennsylvania, NY – New York).

						Min	Mean	Max (SumConc)
Sampling Location	**Site Name**	**Site Code**	**State**	**Dominant Land-use**	**#Compounds Detected (> MDL)**	**ng/g (ww)**	**ng/g (ww)**	**ng/g (ww)**
Niagara River	Scajaquada Creek-01A-7.14	NRSC-01A-7.14	NY	Developed	5	0.128	0.585	2.92
	Smokes Creek-01A-7.14	NRSM-01A-7.14	NY	Developed	2	0.098	0.231	0.462
	Times Beach-01B-7.14	NRTB-01B-7.14	NY	Developed	2	0.476	0.491	0.983
	Tonawanda Creek-01B-7.14	NRTW-01B-7.14	NY	Agriculture	2	0.234	0.314	0.627
	Tonawanda Creek-02A-7.14	NRTW-02A-7.14	NY	Agriculture	3	0.185	0.504	1.51
	Two Mile Creek-00A-7.14	NRTM-00A-7.14	NY	Developed	3	0.246	0.452	1.36
	Two Mile Creek-01A-7.14	NRTM-01A-7.14	NY	Developed	4	0.470	1.345	5.38
Lake Ontario	Fourmile Creek-INMU-CH-10.18	LOFC-INMU-CH-10.18	NY	Open-water	1	0.229	0.229	0.229
	Lake OntarioFS-INMU-CH-6.18	LOFO-INMU-CH-6.18	NY	Open-water	4	0.104	0.634	2.54
	Oswego River-INMU-CH-10.18	LOOR-INMU-CH-10.18	NY	Undeveloped	2	0.199	0.494	0.988

(*) – Reference sites

Appendix

Table A5. Spearman's (ρ) correlation matrix depicting statistically significant correlation coefficients measured between $\sum_{19}$PFAS compounds detected in mussel tissue samples during the 2013-2018 sampling period.

	PFBS	PFOSA	PFDA	PFHpA	PFOS	PFTreA	8:2 FTS	PFBA	PFDS	PFHpS	PFNS	PFPeA	PFDoA	PFOA	PFTriA	N.MeFOSAA	PFHxS	PFPeS	11Cl-PF3OUdS
PFBS	1																		
PFOSA	-0.393*	1																	
PFDA	0.413*	0.194	1																
PFHpA	0.289	-0.302	0.332	1															
PFOS	0.440*	-0.174	0.457**	0.856***	1														
PFTreA	0.1	-0.147	0.345	0.925***	0.803***	1													
8:2 FTS	-0.420*	0.656***	0.379*	0.144	0.053	0.365*	1												
PFBA	-0.357*	0.894***	0.241	-0.327	-0.076	-0.217	0.506**	1											
PFDS	-0.508**	0.908***	0.071	-0.392*	-0.346	-0.217	0.677***	0.801***	1										
PFHpS	0.037	0.222	0.025	0.054	0.433*	-0.016	-0.104	0.527**	0.072	1									
PFNS	-0.155	0.695***	0.238	0.21	0.158	0.248	0.674***	0.628***	0.681***	0.155	1								
PFPeA	0.763***	0.045	0.790***	0.346	0.589***	0.223	-0.065	0.175	-0.147	0.301	0.183	1							
PFDoA	0.254	-0.506**	0.074	0.793***	0.644***	0.829***	0.014	-0.600***	-0.583***	-0.195	-0.15	0.056	1						
PFOA	0.332	-0.374*	0.459**	0.768***	0.769***	0.630***	-0.154	-0.283	-0.460**	0.176	-0.093	0.483**	0.485**	1					
PFTriA	0.092	-0.431*	0.216	0.690***	0.551**	0.789***	0.128	-0.510**	-0.526**	-0.259	-0.213	0.027	0.915***	0.485**	1				
N.MeFOSAA	-0.246	0.677***	0.397*	0.072	0.159	0.218	0.495**	0.592***	0.476**	0.203	0.326	0.217	-0.116	0.038	-0.008	1			
PFHxS	-0.533**	0.688***	0.09	-0.436*	-0.168	-0.291	0.365*	0.858***	0.633***	0.526**	0.309	-0.051	-0.576***	-0.231	-0.392*	0.436*	1		
PFPeS	0.306	-0.301	0.256	0.345	0.350*	0.13	-0.359*	-0.234	-0.293	0.142	-0.177	0.354*	0.011	0.736***	-0.042	-0.089	-0.257	1	
11Cl-PF3OUdS	-0.122	-0.345	-0.195	-0.195	-0.3	-0.267	-0.316	-0.242	-0.335	-0.225	-0.3	-0.213	-0.026	-0.183	0.097	-0.437*	-0.167	-0.12	1`

Significance codes: * $p < 0.05$, ** $p < 0.01$, *** $p < 0.001$, **** $p < 0.0001$.

Appendix

Table A6. List of NORMAN bivalve tissue $\sum_{28}$PFAS predicted no-effect concentrations (PNECs_Tissue; Lowest PNEC Biota [mollusc]) threshold values (µg/kg ww) used in this study to calculate hazard quotient (HQ) values for PFAS compounds detected (> MDLs) in mussels across the Great Lakes sampling locations.

Norman Database ID	Acronym	CASRN#	PNEC Biota (mollusc) (µg/kg ww)	Name	SMILES
NS00011374	ADONA	919005-14-4 /958445-44-8	2.36	4,8-Dioxa-3H-perfluorononanoic acid (ADONA)	O=C(O)C(F)(F)C(F)OC(F)(F)C(F)(F)C(F)(F)OC(F)(F)F
NS00011372	HFPO-DA	13252-13-6	2.12	Perfluoro-2-methyl-3-oxahexanoic acid (HFPO-DA)	O=C(C(OC(C(C(F)(F)F)(F)F)(F)F)(C(F)(F)F)F)O
NS00000428	N-EtFOSAA	2991-50-6	2.02	2-(N-Ethylperfluorooctanesulfonamido)acetic acid (EtFOSAA)	FC(F)(C(F)(F)C(F)(F)C(F)(F)C(F)(F)C(F)(F)C(F)(F)C(F)(F)C(F)(F)F)S(=O)(=O)N(CC(O)=O)CC
NS00000427	N-MeFOSAA	2355-31-9	3.5	2-(N-Methylperfluorooctanesulfonamido)acetic acid (MeFOSAA)	FC(F)(C(F)(F)C(F)(F)C(F)(F)C(F)(F)C(F)(F)C(F)(F)C(F)(F)C(F)(F)F)S(=O)(=O)N(C)CC(O)=O
NS00000364	PFBA	375-22-4	46.3	Perfluorobutanoic acid (PFBA)	O=C(O)C(F)(F)C(F)(F)C(F)(F)F
NS00010276	PFBS	375-73-5	585.7	Perfluorobutanesulfonic acid (PFBS)	C(C(C(F)(F)S(=O)(=O)O)(F)F)(C(F)(F)F)(F)F
NS00000369	PFDA	335-76-2	1.24	Perfluorodecanoic acid (PFDA)	O=C(O)C(F)(F)C(F)(F)C(F)(F)C(F)(F)C(F)(F)C(F)(F)C(F)(F)C(F)(F)C(F)(F)C(F)(F)C(F)(F)F
NS00009617	PFDoA/ (PFDoDA)	307-55-1	2.41	Perfluorododecanoic acid (PFDoA/PFDoDA)	OC(=O)C(F)(F)C(F)(F)C(F)(F)C(F)(F)C(F)(F)C(F)(F)C(F)(F)C(F)(F)C(F)(F)C(F)(F)C(F)(F)C(F)(F)C(F)(F)C(F)(F)C(F)(F)F
NS00011418	PFDS	335-77-3 / 2806-15-7	1.52	Perfluorodecane sulfonic acid (PFDS)	O=[S]([O-])(=O)C(F)(F)C(F)(F)C(F)(F)C(F)(F)C(F)(F)C(F)(F)C(F)(F)C(F)(F)C(F)(F)C(F)(F)C(F)(F)C(F)(F)C(F)(F)C(F)(F)F.[NH4+]
NS00000367	PFHpA	375-85-9	0.629	Perfluoroheptanoic acid (PFHpA)	O=C(O)C(F)(F)C(F)(F)C(F)(F)C(F)(F)C(F)(F)C(F)(F)C(F)(F)F
NS00011291	PFHpS	375-92-8	0.711	Perfluoroheptanesulfonic acid (PFHpS)	O=[S](=O)(O)C(F)(F)C(F)(F)C(F)(F)C(F)(F)C(F)(F)C(F)(F)C(F)(F)C(F)(F)F
NS00000366	PFHxA	307-24-4	191.5	Perfluorohexanoic acid (PFHxA)	O=C(O)C(F)(F)C(F)(F)C(F)(F)C(F)(F)C(F)(F)F
NS00010279	PFHxS	3871-99-6	1.29	Perfluorohexanesulfonic acid (PFHxS)	OS(=O)(=O)C(F)(F)C(F)(F)C(F)(F)C(F)(F)C(F)(F)C(F)(F)F
NS00000368	PFNA	375-95-1	1.24	Perfluorononanoic acid (PFNA)	O=C(O)C(F)(F)C(F)(F)C(F)(F)C(F)(F)C(F)(F)C(F)(F)C(F)(F)C(F)(F)C(F)(F)F
NS00011292	PFNS	17202-41-4 /98789-57-2	64.2	Perfluorononanesulfonic acid (PFNS)	O=[S](=O)(O)C(F)(F)C(F)(F)C(F)(F)C(F)(F)C(F)(F)C(F)(F)C(F)(F)C(F)(F)C(F)(F)C(F)(F)C(F)(F)C(F)(F)C(F)(F)F
NS00009389	PFOA	335-67-1	0.101	Perfluorooctanoic acid (PFOA)	OC(=O)C(F)(F)C(F)(F)C(F)(F)C(F)(F)C(F)(F)C(F)(F)C(F)(F)C(F)(F)F
NS00010280	PFOS	1763-23-1	0.025	Perfluorooctanesulfonic acid (PFOS)	C(C(C(C(C(F)(F)S(=O)(=O)O)(F)F)(F)F)(F)F)(C(C(C(F)(F)F)(F)F)(F)F)(F)F)(F)F
NS00010967	PFOSA	754-91-6	0.701	Perfluorooctanesulfonamide (PFOSA)	FC(F)(C(F)(F)C(F)(F)C(F)(F)C(F)(F)C(F)(C(F)(F)F)F)C(F)(F)S(=O)(N)=O
NS00000365	PFPeA	2706-90-3	5.36	Perfluoropentanoic acid (PFPeA)	O=C(O)C(F)(F)C(F)(F)C(F)(F)C(F)(F)F
NS00011290	PFPeS	2706-91-4 /630402-22-1	3.02	Perfluoropentanesulfonic acid (PFPeS)	O=[S](=O)(O)C(F)(F)C(F)(F)C(F)(F)C(F)(F)C(F)(F)C(F)(F)F
NS00011273	PFTreA/ (PFTeDA)	376-06-7	5.36	Perfluorotetradecanoic acid (PFTriA/PFTrDA)	O=C(C(C(C(C(C(C(C(C(C(C(C(C(C(C(F)(F)F)(F)F)(F)F)(F)F)(F)F)(F)F)(F)F)(F)F)(F)F)(F)F)(F)F)(F)F)(F)F)(F)F)O

Table A6 (cont). List of NORMAN bivalve tissue $\sum_{28}$PFAS predicted no-effect concentrations (PNECs_Tissue; Lowest PNEC Biota [mollusc]) threshold values (µg/kg ww) used in this study to calculate hazard quotient (HQ) values for PFAS compounds detected (> MDLs) in mussels across the Great Lakes sampling locations.

Norman Database ID	Acronym	CASRN#	PNEC Biota (mollusc) (µg/kg ww)	Name	SMILES
NS00011270	PFTriA/(PFTrDA)	72629-94-9/72629-94-8	2.23	Perfluorotridecanoic acid (PFTriA/PFTrDA)	O=C(O)C(F)(F)C(F)(F)C(F)(F)C(F)(F)C(F)(F)C(F)(F)C(F)(F)C(F)(F)C(F)(F)C(F)(F)C(F)(F)C(F)(F)C(F)(F)C(F)(F)C(F)(F)C(F)(F)C(F)(F)C(F)(F)F
NS00000370	PFUnA/(PFUdA)	2058-94-8	1.06	Perfluoroundecanoic acid (PFUnA/PFUdA)	OC(=O)C(F)(F)C(F)(F)C(F)(F)C(F)(F)C(F)(F)C(F)(F)C(F)(F)C(F)(F)C(F)(F)C(F)(F)C(F)(F)C(F)(F)C(F)(F)C(F)(F)C(F)(F)C(F)(F)F
NS00098603	11Cl-PF3OUdS	83329-89-9/ 763051-92-9	0.37	11Cl-PF3OUdS: 2-((8-Chloro-1,1,2,2,3,3,4,4,5,5,6,6,7,7,8,8-hexadecafluorooctyl) oxy)-1,1,2,2-tetrafluoroethanesulfonic acid	ClC(F)(C(F)(C(F)(C(F)(C(F)(C(F)(C(F)(C(F)(C(F)(OC(F)(C(F)(S(=O)(O)=O)F)F)F)F)F)F)F)F)F)F)F
NS00011094	4:2 FTS	27619-93-8/757124-72-4	4.72	4:2 Fluorotelomer sulfonic acid (4:2 FTS) : 2-(Perfluorobutyl)-1-ethanesulfonic acid	O=S(CCC(F)(C(F)(C(F)(C(F)(F)F)F)F)F)(O)=O
NS00010579	6:2 FTS	27619-94-9/27619-97-2	29.3	6:2 Fluorotelomer sulfonic acid (6:2 FTS)	FC(F)(CCS(=O)(=O)O)C(F)(F)C(F)(F)C(F)(F)C(F)(F)C(F)(F)C(F)(F)F
NS00011092	8:2 FTS	27619-96-1/ 39108-34-4	22.4	8:2 Fluorotelomer sulfonic acid	C([S](=O)(=O)O)CC(F)(F)C(F)(F)C(F)(F)C(F)(F)C(F)(F)C(F)(F)C(F)(F)C(F)(F)C(F)(F)C(F)(F)C(F)(F)C(F)(F)F
NS00019227	9Cl-PF3ONS	73606-19-6	0.444	9-chlorohexadecafluoro-3-oxanone-1-sulfonic acid	[K+].[O-]S(=O)(=O)C(F)(F)C(F)(F)OC(F)(F)C(F)(F)C(F)(F)C(F)(F)C(F)(F)C(F)(F)C(F)(F)C(F)(F)Cl

U.S. Department of Commerce
Gina M. Raimondo, *Secretary*

National Oceanic and Atmospheric Administration
Richard W. Spinrad, *Under Secretary for Oceans and Atmosphere*

National Ocean Service
Nicole LeBoeuf, *Assistant Administrator for Ocean Service and Coastal Zone Management*

The mission of the National Centers for Coastal Ocean Science is to provide managers with scientific information and tools needed to balance society's environmental, social and economic goals. For more information, visit: http://www.coastalscience.noaa.gov/